Downloaded from orbit.dtu.dk on: May 05, 2023

DTU Library

Mapping of secondary metabolites to their synthase genes in Aspergillus species

Klejnstrup, Marie Louise

Publication date:
2012

Document Version
Publisher's PDF, also known as Version of record

Link back to DTU Orbit

Citation (APA):
Klejnstrup, M. L. (2012). *Mapping of secondary metabolites to their synthase genes in Aspergillus species*. Department of Systems Biology, Technical University of Denmark.

General rights
Copyright and moral rights for the publications made accessible in the public portal are retained by the authors and/or other copyright owners and it is a condition of accessing publications that users recognise and abide by the legal requirements associated with these rights.

- Users may download and print one copy of any publication from the public portal for the purpose of private study or research.
- You may not further distribute the material or use it for any profit-making activity or commercial gain
- You may freely distribute the URL identifying the publication in the public portal

If you believe that this document breaches copyright please contact us providing details, and we will remove access to the work immediately and investigate your claim.

Mapping of secondary metabolites to their synthase genes in *Aspergillus* species



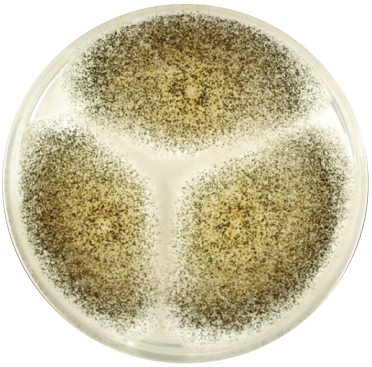

Marie Louise Klejnstrup
PhD Thesis
September 2012

Center for Microbial Biotechnology
Department of Systems Biology

Mapping of secondary metabolites to their synthase genes in *Aspergillus* species

Marie Louise Klejnstrup

PhD thesis

Center for Microbial Biotechnology

DTU Systems Biology

Center for Microbial Biotechnology
Department of Systems Biology

Copyright©: Marie Louise Klejnstrup
September 2012

Address: Center for Microbial Biotechnology
Department of Systems Biology
Technical University of Denmark
Søltofts Plads, Building 223
DK-2800 Kgs. Lyngby
Denmark
Phone: +45 4525 2525
Fax: +45 4588 4148
Web: www.cmb.dtu.dk

Print: J&R Frydenberg A/S
København
January 2013

ISBN: 978-87-91494-17-8

Preface

This thesis is submitted to the Technical University of Denmark in partial fulfillment of the requirements for the Degree of Doctor of Philosophy in Chemistry. The work has been carried out between June 2009 and June 2012, at the Center for Microbial Biotechnology at the Department of Systems Biology under the main supervision of associate professor Thomas Ostenfeld Larsen (CMB) with associate professors Charlotte Held Gotfredsen (Department of Chemistry, DTU) and Uffe Hasbro Mortensen (CMB) as co-supervisors. The project was funded by DTU, Novozymes A/S and FOBI (Research School for Biotechnology).

First I would like to thank my three supervisors for giving me the opportunity of working on this project and for their guidance and enthusiasm for the last three years. It has been a pleasure.

I would also like to thank the molecular biologists I have had the pleasure of working with for the past three years. Starting with Michael L. Nielsen who introduced me to the world of genetics, Morten T. Nielsen for picking up afterwards and last but not least for Jakob B. Nielsen for his patience with my endless stream of questions and for making evening and weekend work a pleasure.

A special thanks also goes to Christian Rank, Anita Iversen, Richard K. Phipps, Kristian F. Nielsen and Maria Månsson for taking time for discussions and helpful suggestions in the daily work.

Another thank goes to the technical staff at CMB, Hanne Jakobsen for running MS samples, Jesper Mogensen, Anne Hector and Ellen Kirstine Lyhne for helping when needed and especially Lisette Knoth-Nielsen for being an invaluable help in the lab.

During my PhD I had the privilege to spend three months at the University of Southern California with associate professor Clay C.C. Wang's group. I would like to thank Clay for letting me come and work at his lab and enjoy the sun of California. I also own the rest of his group a big thanks but especially CJ, Mike, Ken and Jim for helping me get settled and guiding me in the world of making mutants. I would also like to thank the Oticon and Otto Mønsted foundations financial support.

A big thanks also goes out to all my former and present officemates; Tanja, Richard, Anita, Olivera, Andreas, Christian, Lucas and Morten for creating a great atmosphere. A special thanks also goes out to the rest of CMB for the good times and to Paiman for all the trips to Mexibar and bringing strawberry cakes when needed.

Credit is also due to the Carlsberg laboratories for allowing me to use their 800 MHz NMR spectrometer.

Lastly I would like to thank my family and friends for their support over the past three years.

Summary

Secondary metabolites have for centuries been used as drugs and inspiring structural leads in the pursuit for new potent drugs. The main sources for secondary metabolites are marine and terrestrial plants, bacteria, and filamentous fungi. During the past decade the genomes of several filamentous fungi and bacteria have been sequenced opening new possibilities for further analysis of the secondary metabolite potential of the organisms, and directing the focus of natural product chemists towards the elucidation of biosynthetic pathways of the metabolites. Thereby, aiding in identifying the genes encoding for the enzymes responsible for constructing these complex molecules.

The aim of this Ph.D. study has been to explore the secondary metabolite potential of important filamentous fungi and link specific metabolites to their synthase genes and biosynthetic pathways. Throughout this study three important filamentous fungi have been examined; *Aspergillus oryzae*, *A. niger* and *A. nidulans*. *A. oryzae* and *A. niger* are used in the fermentation industry for production of various products such as sake, miso and soy sauce from *A. oryzae* and organic acids as well as enzymes for *A. oryzae*. At the same time *A. niger* is also an important contaminant of crops and feed due to the possibility of mycotoxins or other metabolites ending up in human and animal food. *A. nidulans* is a model organism for genetic studies and vast efforts have been used in the development of a molecular platform used for studying the genetic of the organism.

The work with *A. oryzae* and *A. niger* focused on discovery of the secondary metabolite potential of these two filamentous fungi. Several new metabolites were isolated and structure elucidated from *A. oryzae* including; 13-desoxypaxilline a tremorgenic intermediate of the aflatrem biosynthesis seen in *A. flavus*, dide- and 14-deacetyl parasiticolide A, and the novel non-ribosomal peptides ditryptoleucine and oryzamide $A_{1\text{-}2}$ which are variants of known *A. flavus* metabolites. From a strain of *A. niger* a new isomer of the mycotoxin group of fumonisins, fumonisin B_6 was isolated and characterized through NMR-spectroscopy.

Due to *A. nidulans*' role as a platform for genetic studies emphasis was put on identifying and linking metabolites to their synthase genes. To identify novel metabolites of *A. nidulans* several attempts, both chemical and genetic, were made to activate the secondary metabolites production. The study was initiated with the creation of a deletion library of 32 putative polyketide synthase genes encoding for the enzymes responsible for catalyzing the production polyketides. To initiate secondary metabolite production these strains were cultivated on several complex media. The study linked austinol and dehydroaustinol to their synthase gene as well as providing new insights into two already partly identified biosynthetic pathways; monodictyphenone and orsellinic acid.

To enhance secondary metabolite production in *A. nidulans* overexpression of a transcription factor belonging to a polyketide gene cluster identified in the deletion library resulted in the isolation of several metabolites including cichorine, nidulol, 4-hydroxy-3,6-dimethyl-2-pyrone and the novel metabolites cichonidulol and demethylcichonidulol. A deletion study of the surrounding genes led to a proposed biosynthetic pathway towards these 3-methylorsellinic acid derived metabolites.

A study which included another strain of *A. nidulans* and the deletion of a global regulator gene challenges on complex media resulted in the isolation of asperugin A and B, which through a deletion study were linked to their synthase gene, and nidubenzal A and B. The study ends with a report on the production of the insect juvenile hormones in *A. nidulans* provoked by the heterologous expression of a regulatory gene of *A. niger*.

In conclusion this PhD study has added to the knowledge of the chemical diversity of three important filamentous fungi through activation of silent genes through the use of complex media and genome modifications.

Sammenfatning

Sekundære metabolitter er i løbet af de sidste mange århundrede blevet brugt som medikamenter og som inspiration til syntese af nye biologisk potente stoffer, der kan bruges til ny medicin. Hovedkilderne til sekundære metabolitter i naturen er planter, bakterier og skimmelsvampe både fra land og marint ophav. Genomerne af flere skimmelsvampe og bakterier er gennem det sidste årti blevet sekventeret, hvilket har åbnet op for forskningen i potentialet af sekundære metabolitter i disse organismer. Dette har for naturstofkemikere medført et øget fokus på udredning af biosyntesen for disse metabolitter, og dertil identificering af generne som koder for de enzymer, der katalyserer konstruktionen af disse komplekse metabolitter.

Formålet med dette PhD studie var at udforske potentialet for en selektion af de vigtige skimmelsvampes produktion af sekundære metabolitter og kortlægge sammenhængen mellem identificerede metabolitter og syntesegenerne. Igennem dette studie er *Aspergillus oryzae*, *A. niger*, og *A. nidulans* blevet undersøgt. *A. oryzae* og *A. niger* bliver brugt i fermenteringsindustrien til produktion af diverse produkter, bl.a. sake, misu og sojasovs for *A. oryzaes* og organiske syrer samt enzymer for *A. nigers* vedkommende. Derudover er *A. niger* også en udbredt kontaminant af både foder og afgrøder, hvilket øger risikoen for at mykotoksiner og andre metabolitter kan ende i både mennesker og dyr. *A. nidulans* bliver brugt som en modelorganisme til genetiske og biologiske studier via en stor og mangeårig indsats, der har muliggjort effektiv genetisk transformation i denne og nu også andre Aspergilli.

Fokus i arbejdet med *A. niger* og *A. oryzae* har været på udforskning af potentialet af sekundære metabolitter i disse to skimmelsvampe. Hertil er flere nye metabolitter fra *A. oryzae* blevet oprenset og strukturbestemt, blandt andre 13-desoxypaxilline, som er et mellemprodukt i biosyntesen af den tremorgene metabolit aflatrem, dide- og 14-deacetyl parasiticolide A, der er mellemprodukter fra biosyntesen af parasiticolide A samt ditryptoleucine og oryzamid $A_{1\text{-}2,}$ varianter af kendte metabolitter fra *A. flavus*. Derudover er en ny isomer fra fumonisin mykotoksingruppen fundet og strukturbestemt ud fra en *A. niger* stamme.

Med henblik på *A. nidulans*' rolle som modelorganisme for genetiske studier, blev hovedvægten lagt på at identificere nye metabolitter og efterfølgende koble dem til gener. Både kemiske og genetiske metoder er blevet anvendt til at aktivere produktionen af sekundære metabolitter. Studiet startede med konstruktionen af et deletionsbibliotek for de 32 gener, der via bioinformatiske studier var blevet forudsagt til at kode for polyketidsyntase enzymer, der syntetiserer polyketider, en stor og vigtig gruppe inden for naturstoffer. For at få en varieret produktion af polyketider blev stammerne dyrket på forskellige komplekse vækstmedier. I dette studie blev austinol og dehydroaustinol koblet til deres syntasegen, og flere nye aspekter blev tilføjet til de allerede delvist beskrevne biosynteseveje: monodictyphenon og orsellinsyre.

I forsøget på at øge produktionen af metabolitter i en interessant biosyntese gengruppe i *A. nidulans*, blev et regulatorisk gen overudtrykt. Dette medførte en øget produktion af flere metabolitter inklusiv cichorine, nidulol, 4-hydroxy-3,6-dimethyl-2-pyrone og de nye metabolitter cichonidulol og demethylcichonidulol. Ved hjælp af en stor serie gendeletioner, og efterfølgende kemisk analyse af mutanterne, kunne vi opstille et forslag til biosyntesen af de 3-methylorsellinsyre afledte metabolitter. Et andet studie afrapporteret i denne afhandling

inkluderede et vildtypeisolat af *A. nidulans*, og her blev de to nye metabolitter nidubenzal A og B isoleret og strukturbestemt. Derudover blev asperugin A og B gennem et nyt gendeletionsstudie, der påvirkede tilgængeligheden i kromatin, koblet til et syntasegen. Afhandlingen slutter med et studie, hvori produktionen af juvenile hormone III blev aktiveret ved heterolog ekspression af et regulatorisk gen fra *A. niger* kombineret med dyrkning på komplekse medier.

Dette PhD studie har bidraget til viden om den kemiske diversitet af tre, på hver sin måde vigtige, skimmelsvampe, og arbejdet demonstrerer hvorledes avanceret kemisk analyse og effektive gensplejsningsværktøj sammenspiller til at kortlægge den fascinerende sekundære metabolisme i skimmelsvampe.

List of papers and other publications

Paper 1 **ML Klejnstrup**, RJN Frandsen, DK Holm, MT Nielsen, UH Mortensen, TO Larsen, JB Nielsen; "**Genetics of polyketide metabolism in *Aspergillus nidulans***", Metabolites 2, 100-133 (2012).

Paper 2 C Rank and **ML Klejnstrup** (Joint 1st author), LM Petersen, S Kildgaard, JC Frisvad, CH Gotfredsen, TO Larsen; "**Comparative chemistry of *Aspergillus oryzae* (RIB40) and *A. flavus* (NRRL 3357)**", Metabolites 2, 39-56 (2012).

Paper 3 M Månsson, **ML Klejnstrup**, RK Phipps, KF Nielsen, JC Frisvad, CH Gotfredsen, TO Larsen; "**Isolation and NMR characterization of fumonisin B_2 and a new fumonisin B_6 from *Aspergillus niger***", J. Agric. Food Chem. 58, 949-953 (2010).

Paper 4 ML Nielsen, JB Nielsen, C Rank, **ML Klejnstrup**, DK Holm, KH Brogaard, BG Hansen, JC Frisvad, TO Larsen, UH Mortensen; "**A genome-wide polyketide synthase deletion library uncovers novel genetic links to polyketides and meroterpenoids in *Aspergillus nidulans***", FEMS Microbiol. Lett. 321, 157-166 (2011).

Paper 5 JB Nielsen and **ML Klejnstrup** (joint 1st author), P Khorsand-Jamal, DK Holm, A Kabat, ML Nielsen, JC Frisvad, CH Gotfredsen, TO Larsen, UH Mortensen; "**Characterization of the *A. nidulans* 3-methylorsellinic acid gene cluster**" Manuscript in preparation.

Paper 6 **ML Klejnstrup**, MT Nielsen, JB Nielsen, JC Frisvad, CH Gotfredsen, UH Mortensen, TO Larsen; "**A combined genetic and multi medium approach reveals new secondary metabolites of *Aspergillus nidulans***". Rough draft.

Paper 7 MT Nielsen and **ML Klejnstrup** (Joint 1st author), CH Gotfredsen, MR Andersen, BG Hansen, UH Mortensen, TO Larsen; "**A regulatory protein from *Aspergillus niger* induces juvenile hormones upon heterologous expression in *A. nidulans***", Submitted to PLoS ONE – under revision.

Conference proceeding:

ML Klejnstrup, MT Nielsen, JC Frisvad, UH Mortensen, TO Larsen; **A combined genetic and multi medium approach reveals new secondary metabolites in *Aspergillus nidulans*.** Poster at Eight International *Aspergillus* meeting Asperfest 8 and 26th fungal genetics conference, Asilomar, California, USA. March 14th – 20th 2011.

Abbreviations

ACP	Acyl Carrier Protein
AT	acyltransferase
BPC	Base Peak Chromatogram
CLC	Claisen Cyclase
CMB	Center for Microbial Biotechnology
CY20	Czapek Yeast sucrose
CYA	Czapek Yeast Agar
CYAs	Czapek Yeast Agar salt
DAD	Diode Array Detection
DH	Dehydratase
DMSO	Dimethyl sulfoxide
DQF-COSY	Double-quantum filtered correlated spectroscopy
DTU	Technical University of Denmark
ESI	Extracted Ion Chromatogram
ER	Enoyl Reductase
H2BC	Heteronuclear two bond correlation
HMBC	Heteronuclear multiple bond correlation
HR	Highly Reduced
HSQC	Heteronuclear single quantum coherence
iPKS	iterative Polyketide synthase
KR	β-ketoreductase
KS	β-ketosynthase
MM	Minimal medium
MS	Mass Spectrometry
MS/MS	Tandem Mass Spectrometry
MT	Methyl transferase
NMR	Nuclear Magnetic Resonance
NR	Non-Reduced
NRP	Non-Ribosomal Peptide
NRPS	Non-Ribosomal Peptide Synthetase
Oex	Overexpression
OSMAC	One Strain Many Compounds
PK	Polyketide
PKS	Polyketide Synthase
PR	Partially Reduced
PT	Product Template
qRT-PCR	quantitative Reverse Transcription Polymerase Chain Reaction
RT	Raulin-Thom
RTO	Raulin-Thom Oatmeal
SAM	S-adenosylmethionine
SAT	Starter-unit ACP Transacylase
TE	Thioesterase

TOF	Time of Flight
UHPLC	Ultra High Pressure Liquid Chromatography
UV	Ultra Violet
YE	Yeast Extract
YES	Yeast Extract Sucrose

Table of contents

1 Background

Natural products (or secondary metabolites) have for centuries been used as drugs or inspiring structural leads in the pursuit for new potent drugs. The main sources for secondary metabolites are marine and terrestrial plants, bacteria, and filamentous fungi. Secondary metabolites are classified depending on their structural scaffold. These classes include among others polyketides (PKs), non-ribosomal peptides (NRPs), terpenoids, alkaloids and hybrid metabolites of the different classes. The function of secondary metabolites in their hosts has not yet been exploited to its fullest; however, they seem to have several functions including defense, communication, and signaling (Calvo 2002, Fox 2008, Kempken 2010, Rohlfs 2010). Secondary metabolites have, especially after the discovery of the penicillins in 1929 (Fleming 1929), been used as inspiration in the discovery of new pharmaceutical candidates. In fact, a study by Newman and Cragg showed that 34 % of all small-molecule new chemical entries between 1981 and 2010 were natural products or derived thereof and further 25 % were mimics of natural products (Newman 2012).

The filamentous fungi within the *Aspergillus* family are important due to both their vast uses as industrial workhorses (*A. niger*) (Schuster 2002) and as model organisms for genetic studies (*A. nidulans*) (Pontecorvo 1953, Chiang 2010a), but also due to their prevalence as food contaminants (*A. niger*) (Perrone 2007, Nielsen 2009). *A. niger* is both an industrial workhorse for the production of citric acid and various enzymes (Schuster 2002) as well as a contaminant of food and feeds on which it can produce the mycotoxins ochratoxin and the fumonisins (Perrone 2007, Nielsen 2009). The *Aspergillus* section includes other mycotoxin and drug producing species such as *A. flavus* (aflatoxin) and *A. terreus* (lovastatin (mevinolin)), respectively (Hoffmeister 2007).

Table 1.1 Overview of fully genome sequenced *Aspergillus* species

Species	Strain	References
A. aculeatus	ATCC 16872	DOE Joint Genome Institute 2012a
A. awamori	IFO 4308	NCBI 2012a
A. carbonarius	ITEM 5010	DOE Joint Genome Institute 2012b
A. clavatus	NRRL 1	Fedorova 2008
A. fischerianus	NRRL 181	Fedorova 2008
A. flavus	NRRL 3357	Center for Integrated Fungal Research 2012
A. fumigatus	Af293	Nierman 2005
A. fumigatus	A1163	Fedorova 2008
A. nidulans	FGSC A4	Galagan 2005
A. niger	CBS 513.88	Pel 2007
A. niger	ATCC 1015	Baker 2006, Andersen 2011
A. oryzae	RIB40	Machida 2005
A. sojae	NBRC 4239	NCBI 2012b
A. terreus	NIH 2624	Broad Institute 2012

During the past decade, the genome of several *Aspergillus* species have been fully sequenced and become available for the public, table 1.1. The availability of genome sequences have led to a shift in natural product research from discovery of new drug-like metabolites to linking metabolites to the responsible genes as well as further elucidation of biosynthetic pathways (Walsh 2010). Detailed information on the genetic and enzymatic work in an organism enable the possibility of

production of specifically designed metabolites and chemical scaffolds (synthetic biology), provide information for the optimization of fungi as cell factories and enable heterologous expression of genes (Fisch 2011, Heneghan 2011, Liu 2011, Pickens 2011, Wong 2012).

Genome sequences have, through bioinformatics studies, revealed that the number of secondary metabolite synthase genes far exceeds the number of metabolites known. For example, *A. nidulans* appears to contain as many as 32 polyketide synthases (PKSs) of which, until recently, only nine gene clusters have been identified and linked to metabolites (paper 1). The information from the bioinformatic studies reveals that the secondary metabolite potential by far exceeds the known secondary metabolite pool. This huge, untapped potential for secondary metabolite production has led to collaborations between molecular biologists and natural product chemists to explore the full potential of filamentous fungi through genome mining, optimized chemical screening, and other advanced techniques towards activation of silent genes (Sanchez 2012).

The aim of this Ph.D. study has been to explore the secondary metabolite potential of important filamentous fungi, to link specific metabolites to their synthase genes and elucidate the biosynthetic pathways. The work presented in the following chapters includes exploring the chemistry of *A. oryzae* (paper 2) by comparison of the metabolic profiles to *A. flavus* and isolation and characterization of several new metabolites. This is followed by isolation and characterization of a new fumonisin analogue isolated from *A. niger* (paper 3). To discover the hidden secondary metabolic potential of *A. nidulans* attempts have been performed to activate the silent genes through both media variation and genetic modifications. The activation of genes has led to the identification of several new metabolites being identified, isolated and structure elucidated (paper 4-7). Several of these metabolites have been linked to their biosynthetic genes. An overview over the genes which at the time had been linked to polyketides in *A. nidulans* is given in paper 1.

Altogether this thesis consists of 6 chapters where chapter 1 gives background information for the Ph.D. study. Chapter 2 gives a general introduction to production of secondary metabolites in filamentous fungi and ways of activating silent genes. Chapter 3 gives an overview of the experimental work and a short introduction to experimental procedures used throughout the work. In chapter 4 the results are presented and discussed and chapter 5 is an overall discussion and conclusions of the work presented. The references are in chapter 6. The papers presented in this thesis are in the accompanying appendix (paper 1-7) where paper 5 and 6 are rough drafts.

2 Production of secondary metabolites in filamentous fungi

This section will focus on the production of secondary metabolites in filamentous fungi including biosynthesis, regulation and activation of genes.

2.1 Biosynthesis of secondary metabolites

Secondary metabolites are divided into classes according to their biosynthetic origin. The following sections will describe some of the general biosynthetic features of three main classes of secondary metabolites including examples of metabolites from *A. nidulans*. The focus will be on PKs, however, general characteristics on NRPs, terpenoids and examples of hybrid metabolites will be described.

2.1.1 Polyketides

PKs are one of the most important classes of secondary metabolites and are produced by several terrestrial and marine organisms including bacteria, plants and fungi. Though the structures of PKs are highly diverse they share a common biosynthetic origin of the carbon skeleton which is synthesized from small activated carboxylic acids such as acetate, propionate and butyrate. The carbon skeleton is biosynthesized by polyketide synthases (PKSs). PKSs can be divided into three types, type I, II, and III based on their catalytic organization; however, only the iterative type I PKS (iPKS) has been reported in *A. nidulans*. The iPKS repeat the use of a single module, containing several catalytic domains, until the growing chain has reached the desired length.

Fungal PKSs are generally type I iPKSs. The fungal iPKSs can, based on their catalytic domains, be divided into three classes: non-reducing (NR), highly reducing (HR) and partially reducing (PR) (Bingle 1999, Nicholson 2001, Kroken 2003). The difference between the three classes reflects their ability to reduce the β-keto carbon of the growing carbon chain. The reduction occurs in the catalytic domains of the iPKS-enzymes.

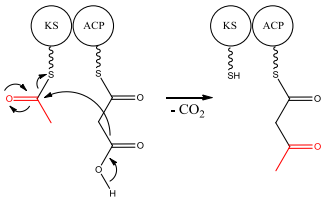

Figure 2.1 Chain extension of the PK chain in iPKSs through Claisen-like condensations of the extender and starter unit. The synthesis is started by binding a starter unit, here acetyl-CoA, to the KS domain and loading of the extender unit, here malonyl-CoA, to the ACP domain, releasing the CoA. The KS catalyzes the claisen-like condensation extending the polyketide chain by an acetate unit (marked in red) whereby CO_2 is released. To start another extension the polyketide chain is transferred back to the KS domain and the ACP domain is loaded with a new extender unit. Abbreviations: KS: β-ketosynthase, ACP: Acyl carrier protein.

Three fundamental domains are in general found in all filamentous fungal iPKSs; β-ketosynthase (KS), acyltransferase (AT) and the acyl carrier protein (ACP). The KS catalyzes the C-C bond formation through Claisen-type condensations. The ACP domain is responsible for transiently

holding the growing acyl chain, hereby allowing the loading of the extender units. AT recognizes the acyl extender units which are transferred from CoA onto KS and transferred to the growing PK chain through Claisen-like condensations catalyzed by KS, figure 2.1. The iterative use of the three domains results in a NR-PK.

In partially reduced and highly reduced PKSs, reduction occurs through the β-ketoreductase (KR) domain that reduces the β-ketone to a hydroxyl group. Loss of the hydroxyl group can occur by the elimination of water through the dehydratase (DH) domain which can be followed by hydrogenation catalyzed by the enoyl reductase (ER), figure 2.2a.

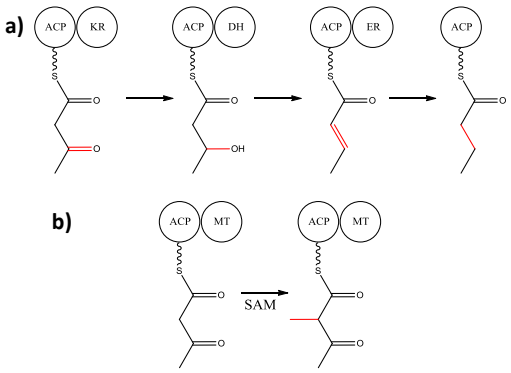

Figure 2.2 Functional domains which may be present in a PKS. The reaction schemes show examples of the general reactions of the PKS domains **a)** reduction of ketone to saturation catalyzed by the KR, DH, ER domains. **b)** methylation catalyzed by the MT domain. Abbreviations: ACP: Acyl carrier protein, KR: ketoreductase, DH: dehydratase, ER: enoyl reductase, MT: methyltransferase, SAM: S-adenosylmethionine

Another domain which can be present in the reducing PKSs is the methyltransferase domain (MT) which is responsible for C-methylation of the growing PK chain, using S-adenosylmethionine (SAM) as a carbon-donor. The degree of eventual reductions and modifications, and their positions in the PK product, is always the same for the individual PKSs; however, it is presently unknown how deployment of the basic modifying domains are programmed into the PKS.

The NR-PKSs do not contain the reducing domains, however, they contain an *N*-terminal starter unit-ACP transacylase (SAT) domain, which is responsible for selecting the starter unit (Crawford 2008a), and an internal product template (PT) domain, which is responsible for folding and cyclization of the NR-PK backbone (Crawford 2008b, Crawford 2009, Crawford 2010). The number of iterations within the PKS and thereby the display of functional groups and size of the final product is likely determined by the size of the active site cavity in the iPKS (Yadav 2009). The iterative nature of the iPKSs makes it difficult to predict the structure of the final product of the iPKSs both with respect to the degree of saturation, methylation pattern and size; however, domain swapping experiments by Fisch and co-workers (Fisch 2011) are starting to reveal the programming of the iPKSs (Fisch 2011).

Once the final length of the PK backbone has been achieved, the PK chain is released from the PKS, catalyzed by either a thioesterase (TE), a Claisen cyclase (CLC) or by other accessory enzymes (Du 2010).

The product coming directly from the PKS rarely seems to be the only product in the biosynthesis, but usually undergoes further modifications by tailoring enzymes which can range from small changes (methylations, reductions, oxidations) to large modifications including ring formation and condensations with other metabolites. The PKS genes tend to reside in gene clusters where the genes responsible for further modifications, e.g. genes encoding monooxygenases, O-methyltransferase, dehydrogenases, are present.

For a more detailed description on polyketides than the one given here, reviews by Cox (Cox 2007), Hertweck (Hertweck 2009) and Crawford (Crawford, 2010) can be consulted.

An example of a complex PK biosynthesis found in several *Aspergillus* species including *A. nidulans* is sterigmatocystin (Rank 2011). Sterigmatocystin is an intermediate in the biosynthesis of the aflatoxins which are among the most carcinogenic mycotoxins. Research into the biosynthesis and biological function of aflatoxin and sterigmatocystin intensified with the Turkey X disease caused by aflatoxins in the middle of the last century (Blount 1961) and it is therefore one of the most extensively studied biosynthesic pathways and there are several reviews for further reading (Yu 2004, Yabe 2004). The proposed biosynthesis of sterigmatocystin in *A. nidulans* can be seen in figure 2.3. The gene cluster consists of 27 genes (Brown 1996) where *stcA* is a NR-PKS which codes for the enzyme that catalyzes the condensation of the starting unit hexanoyl-CoA and seven malonyl-CoA extender units into the PK backbone, which is followed by cyclization and release of norsolorinic acid anthrone (Yu 1995). Several enzymatic steps are required for converting norsolorinic acid anthrone to sterigmatocystin which include oxidations, reductions, O-methylations and Bayer-Villiger oxidation (Yabe 1993, Yabe 1991, Keller 1994, Trail 1994, Keller 1995, Kelkar 1996, Silva 1996, Kelkar 1997, Chang 2000, Keller 2000, Watanabe 2002, Sakuno 2003, Chang 2004, Ehrlich 2005, Henry 2005, McDonald 2005, Cary 2006, Ehrlich 2010). For a more detailed description see paper 1.

Even though the biosynthesis of sterigmatocystin has been studied extensively all the biosynthetic steps are still not accounted for. This highlights that the biosynthesis of secondary metabolites can be very complex and difficult to decipher.

2.1.2 Non-ribosomal peptides

NRPs are another large group of secondary metabolites produced in microorganisms. They are made up of amino acids which are linked by a non-ribosomal peptide synthethase (NRPS) through condensations. The NRPSs are single multimodular enzymes where each module includes several catalytic domains. The modules contain the necessary domains; adenylation, peptidyl carrier protein and condensation. The adenylation domain is specific for each amino acid which is recognized, adenylated, and loaded onto the peptidyl carrier protein domain where the condensation domain catalyzes the formation of the peptide bond between the two amino acids. The number of modules corresponds to the number of amino acids in the final product and their order in the metabolite follows the order of the adenylation domains. Other catalytic functions that may be present in an NRPS includes epimerization, peptide cyclization and *N*-methylation domains. The amino acids are produced from two pathways. The aliphatic amino acids are produced from the central carbon metabolism whereas the aromatic amino acids are derived

from shikimic acid, figure 2.4. Shikimic acid can also be incorporated into secondary metabolites and may be recognized for the substitution pattern of the three hydroxyl-groups on the ring.

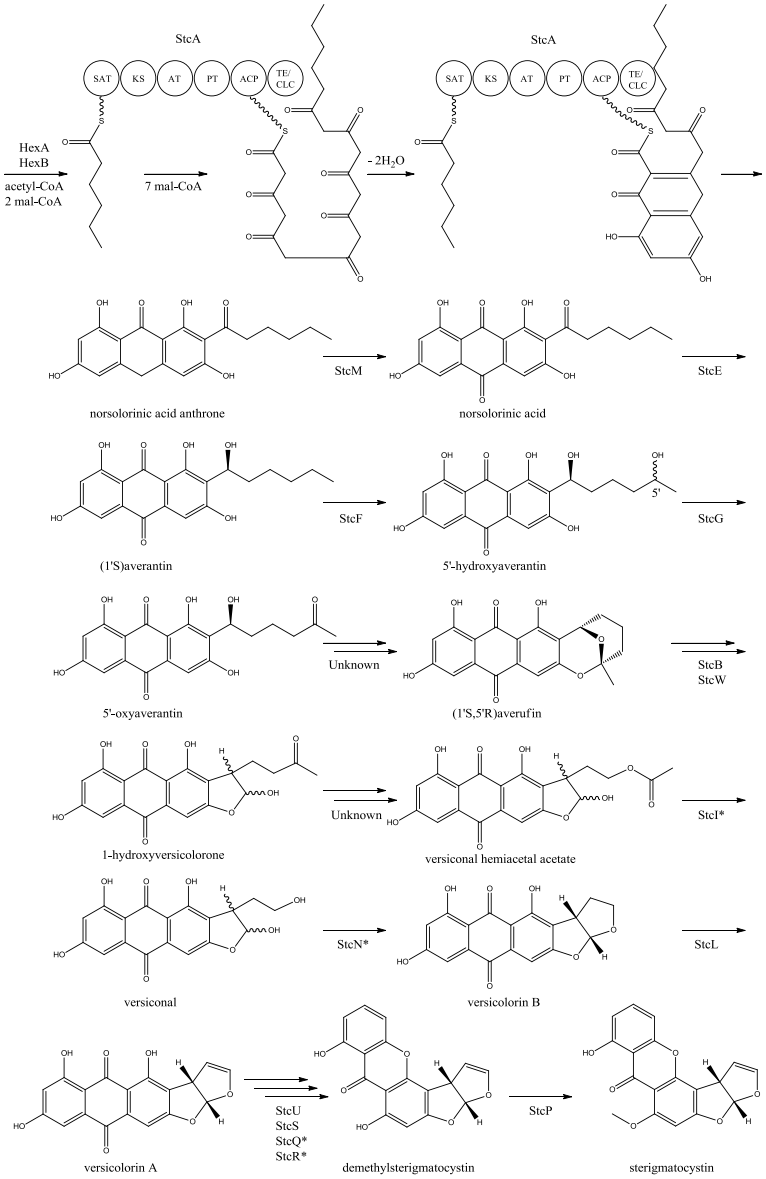

Figure 2.3 Proposed biosynthesis taken from Klejnstrup 2012 (paper 1). StcA contains SAT, KS, AT, PT, ACP and TE/CLC domains. *Indicates a proposed, but not confirmed, enzyme. Multiple arrows indicate that the number of enzymatic steps is unknown.

The emericellamides, figure 2.7 are examples of secondary metabolites of a combined PKS and NRPS origin produced by *A. nidulans*. The product of the PKS is loaded onto the NRPS which consist of five modules each responsible for addition of an amino acid (glycine, valine, isoleucine,

alanine and alanine) to the metabolite backbone followed by release and cyclization (Chiang 2008).

Beside NRPS genes there are also NRPS-like genes present in the genomes. These genes share the catalytic domains found in NRPSs but are missing the condensation domain necessary for peptide-bond formation (von Döhren 2009). So far products of two NRPS-like genes in *A. nidulans* have been identified, terrequinone A (Bok 2006, Balibar 2007, Schneider 2008), which does not have a peptide bond in its structure, and microperfuranone, without a nitrogen atom in its structure (Yeh 2012), figure 2.4.

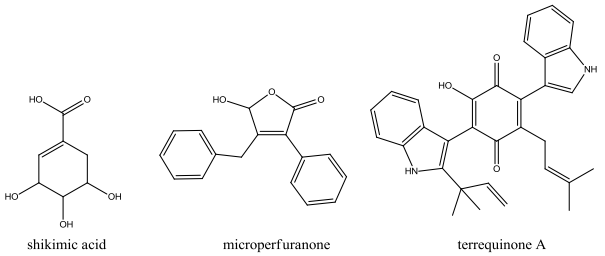

Figure 2.4 Structures of shikimic acid, microperfuranone and terrequinone A

For reviews on the biosynthesis of NRPs and the shikimic pathway please see reviews by Fischbach (Fischbach 2006), Koglin (Koglin 2009), Du (Du 2010), and Matthias (Matthias 2010) and Dewick and Knaggs respectively (Dewick 1998, Knaggs 2003).

2.1.3 Terpenoids

Terpenoids is a group of natural products made up of activated C_5 isoprene units; dimethylallyl diphosphate (DMAPP) and isopentenyl diphosphate (IPP), which are condensed in a head to tail fashion, figure 2.5, in the terpene synthases. These carbon-chains can then undergo several modifications like cyclization, reduction or oxidations to reach the final product. DMAPP and IPP are derived by the mevalonate (Miziorko 2011) and the methylerythritol phosphate pathways (Rohmer 2008).

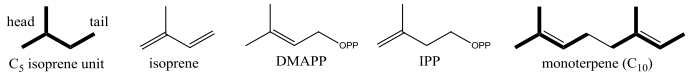

Figure 2.5 Structure of an isoprene unit and example of linking of two isoprene units in a head to tail fashion. The two isoprene units in the monoterpene is highlighted in bold.

The biosynthetic potential of terpenoids in *A. nidulans* has not yet been exploited to its fullest. In fact, only one terpene, *ent*-pimara-8(14),15-diene, have, so far, been identified and linked to a gene cluster which includes a putative geranylgeranyl-diphosphate (GGPP) synthase, AN1593, and a pimaradiene synthase, AN1594 (figure 2.6) (Broman 2012). The DDPP-synthase is responsible for the formation of geranylgeranyl-PP formation and AN1594 catalyzes the cyclization reactions

into the final product (Broman 2012). In the figure the head to tail linking of the isoprene backbone can be seen.

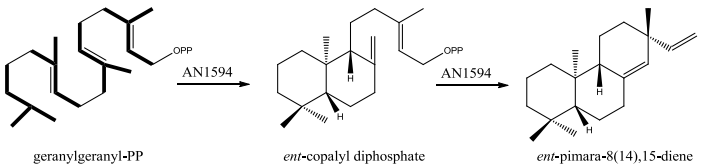

Figure 2.6 Folding and cyclization of the terpene *ent*-pimara-8(14),15-diene as proposed by Broman and co-workers (Broman 2012). The four isoprene units in geranylgeranyl-PP is highlighted in bold.

For further reading of the details of the biosynthesis of terpenoids please consult review by Dewick (Dewick 2002) and Oldfield (Oldfield 2012).

2.1.4 Hybrid metabolites

Hybrid metabolites are metabolites where different parts of the molecule originate from different biosynthetic routes. In *A. nidulans* both the emericellamides and the aspyridones, figure 2.7 are hybrid metabolites which have a PK and NRP part they are; however, produced by different types of enzymes. Aspyridone is a PK-NRP which is assembled from the activity of a single fusion enzyme, whereas the biosynthesis of the emericellamides requires a PKS and a NRPS where the product from the PKS acts as the starter unit in the NRPS (Bergmann 2007, Chiang 2008). A further discussion of the biosynthesis of the emericellamides and aspyridones can be found in paper 1.

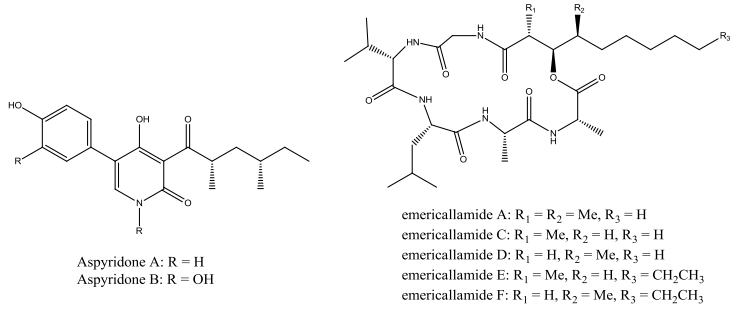

Figure 2.7 The structures of aspyridone A and B and emericellamide A, C, D, E and F produced by *A. nidulans*.

Meroterpenoids is another group of natural products of mixed biosynthetic origin where one or more parts are derived from terpenoids. The meroterpenoids can be divided into two main classes, PK-terpenoids and non-PK-terpenoids. As the name indicates this division is based on whether the non-terpenoid part of the molecule is PK derived or derived from other biosynthetic routes, e.g. from the shikimate route (Geris 2009).

In *A. nidulans* austinol and dehydroaustinol are examples of PK-meroterpenoids. The biosynthesis of 3,5-dimethylorsellinic acid, the PK, is catalyzed by AusA and then prenylated by the

prenyltransferase AusN (Nielsen 2011, Lo 2012). The meroterpenoid then undergoes several modifications to the products austinol and dehydroaustinol, figure 2.8 (Lo 2012).

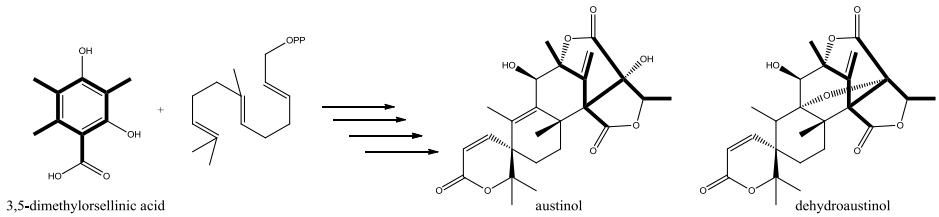

Figure 2.8 The structures of 3,5-dimethylorsellinic acid, austinol and dehydroaustinol. The carbon skeleton of 3,5-dimethylorsellinic acid incorporated into austinol and dehydroaustinol is presented in bold.

Isoprene units can be linked to PKs and NRPs by a prenyltransferase (dimethylallyl tryptophan synthases DMAT) through either O-C or C-C bonds. Emericellin, figure 2.9 is a mixed terpenoid and PK metabolite which is produced in the monodictyphenone pathway in *A. nidulans*. The origin of the two isoprene units arise from two separate prenyltransferases, XptA and XptB, and are coupled to the PK through a C-O and a C-C bond, respectively (Sanchez 2011).

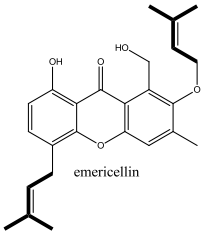

Figure 2.9 Structure of emericellin. The carbon skeleton of the two isoprene units is highlighted in bold.

2.2 Genetics of secondary metabolite biosynthesis

To understand the biosynthesis of secondary metabolites, one of the important tasks is to target genes encoding the enzymes that catalyze steps within the biosynthetic pathways. Due to the availability of fungal genome sequences, the search for genes coding for these enzymes can be intensified among the thousands of genes, e.g. the 11223 genes in the *A. nidulans* genome (Arnaud 2012). In this section the prediction of gene function, regulation and activation of genes related to secondary metabolite biosynthesis in filamentous fungi will be introduced with a focus on *A. nidulans*.

2.2.1 Prediction of gene function

It is possible to identify putative secondary metabolite genes within genome sequences, through computational analysis. Automated annotations and manual validations of predictions are already present for several of the *Aspergillus* genomes. Therefore Blast analysis on amino acid sequences of predicted protein activities will offer a list of homologous targets and their respective loci, especially due to their functional domains which can be highly homologous. As the gene function prediction is based on available knowledge on genes and protein activity, it is important to stress

that these predictions need to be confirmed through follow-up experiments, unless sequence homology and coverage of sequence is high. Still sequence analysis of the genomes gives a qualified putative overview of the gene functions. In table 2.1 the number of secondary metabolite synthase genes which have been predicted in the literature for the fully genome sequenced strains of *A. niger*, *A. oryzae*, *A. flavus* and *A. nidulans*, using a BlastP analysis approach. The total amount of synthase genes exceeds the number of known biosynthetic pathways. For example *A. nidulans* are predicted to contain 32 PKS genes (Nielsen 2011) of which 17 have been linked to metabolites (Brown 1996, Watanabe 1998, Watanabe 1999, Bergmann 2007, Chiang 2008, Szewczyk 2008, Bok 2009, Chiang 2009a, Schroeckh 2009, Nielsen 2011, Ahuja 2012) indicating a large potential for new metabolites, even in one of the most studied fungi.

Table 2.1: Overview of the predicted number of synthase genes in the fully genome sequenced strains of *A. flavus*, *A. nidulans*, *A. oryzae*, and *A. niger*. *These numbers includes NRPS- or PKS-like genes.

Species	PKS*	NRPS*	Hybrid	Reference
A. flavus	28	32	2	Cleveland 2009
A. nidulans	32	27	1	von Döhren 2009, Nielsen 2011
A. niger (ATCC 1015)	33	15	9	Sanchez 2012
A. niger (CBS 513.88)	39	33	7	Sanchez 2012
A. oryzae	27	32	2	Cleveland 2009

In filamentous fungi genes linked to biosynthesis of a given secondary metabolite tend to cluster, which enables the discovery of genes encoding tailoring enzymes both through Blast analysis but also the use of techniques like microarray and qRT-PCR (quantitative reverse transcription polymerase chain reaction) can assist in discovering connections between the expression of genes and gene clustering in the genome. Microarray is applicable for the overview of the expression level of genes in a genome under specific conditions. The data can be used to analyze whether genes are downregulated, unaltered, or upregulated at certain conditions or between different strains. Hereby, it is possible to establish connections between large groups of genes at the same time. In qRT-PCR, the strength is the ease of measuring for example relative expression of a gene in a mutant strain compared to the expression in a reference strain, or in one strain at different growth parameters. In the latter case, the overview is limited to genes chosen for the study.

Due to the fact that the total amount of synthase genes and thereby biosynthetic pathways far exceeds the number of known genes different terms to distinguish between unknown and not expressed genes and pathways has been developed. Orphan biosynthetic genes are defined as biosynthetic loci for which the corresponding metabolite(s) is/are unknown whereas silent pathways are pathways where the genes are not expressed under the given growth conditions (Gross 2007).

2.2.2 Activation of silent genes

With the recent recognition of the high percentage of orphan secondary metabolite genes several different techniques of activating biosynthetic genes have been explored. In this section some of the activation techniques, with relations to the methods used in this thesis, will be described with emphasis on *A. nidulans*. These approaches include the One Strain MAny Compounds (OSMAC) method, epigenome manipulations, gene regulation, and co-cultivation.

2.2.2.1 One strain – many compounds

One classic way to activate the production of secondary metabolites is to vary the growth conditions. The principle behind the method, named one strain – many compounds (OSMAC) by Zeeck and co-workers, is to expose the microorganism to other cultivating conditions than the standards used in laboratories (Fuchser 1997, Schiewe 1999, Höfs 2000, Bode 2002). There are several factors which can be altered for example temperature, pH, culture vessel, aeration, cultivation time, light intensity and media composition including carbon and nitrogen sources and salt concentration. All these factors can influence the biosynthesis of secondary metabolites in several places including transcription, translation and enzyme inhibition or activation (figure 2.10), however, the understanding of the exact mechanisms for the change in metabolic profile due to change in culture conditions is usually not completely understood and therefore difficult to predict (Bode 2002).

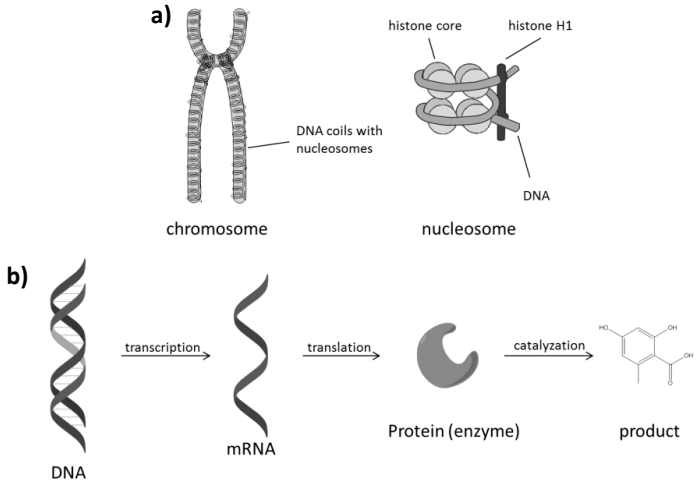

Figure 2.10. Storage of information in the cells. **a)** DNA is folded up on the histones into nucleosomes which coil up and are packed into the chromosome. **b)** The DNA is transcriped into mRNA which is translated into proteins which in the case of PKS and NRPSs are enzymes catalyzes the formation of a product.

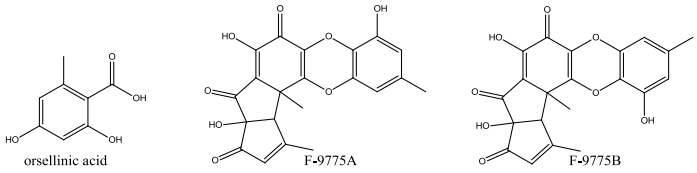

Figure 2.11 Structure of orsellinic acid, F-9775A and F-9775B.

The use of the OSMAC approach which included 20 different culture conditions of an *A. nidulans* strain, led to the activation of the orsellinic acid cluster resulting in the production of orsellinic acid and compounds derived thereof including F-9775A and F-9775B, figure 2.11 (Sanchez 2010). In another study by Scherlach and co-workers an *A. nidulans* strain was cultivated under 45

different culture conditions, which resulted in the isolation of two novel metabolites, aspernidine A and B, figure 2.12 (Scherlach 2010).

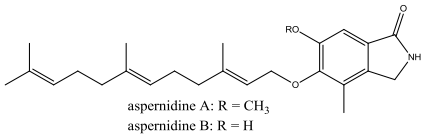

Figure 2.12 The structure of aspernidine A and B.

Interestingly these two examples of the use of the OSMAC approach have cultivated the strains used many conditions to activate the production of these metabolites. In 2011 Nielsen and co-workers showed the metabolic profile of an *A. nidulans* reference strain grown on seven complex media displayed large differences in the production of metabolites including the orsellinic acid derived compounds (Nielsen 2011).

2.2.2.2 Discovery of secondary metabolites through genome mining

The elucidation of the secondary metabolite production potential can, as stated above, be initiated through genome mining. This strategy is confined to genome sequenced species, and involves the search in the genome for genes which are predicted to have enzymatic activities that are associated with production of secondary metabolites. This enables subsequent systematic genetic manipulations and validation through chemical analysis. This includes deletion and/or overexpression of genes in connection to secondary metabolite gene clusters or regulatory genes. The regulatory genes can act globally within the fungus or within a single secondary metabolite gene cluster.

Epigenetic manipulations of global regulatory genes

The presence and possibilities of manipulation techniques of global regulators have been a vast challenge; however, several advances have increased the interest in epigenetic manipulations where examples of some of these manipulations will be described below (Keller 2005, Yu 2005a , Cichewicz 2009, Scherlach 2009).

The presence of secondary metabolite clusters in silent areas of the chromosomes, e.g. near telomeres and centromeres, suggests that chromatin remodeling factors can influence the expression of genes responsible for secondary metabolite production. Regulation of gene expression by chromatin regulation is directed by modifications of the histones through e.g. methylation, which closes, and acetylation, which opens the histones, since it is thought that histone modifications may control interactions of histones with transcriptional activators and repressors (Jenuwein 2001).

In 2004 Bok and Keller reported the LaeA protein, a putative methyl transferase with homology to histone methyltransferases, as a global regulator of secondary metabolism in *Aspergillus* species, however, the mechanism of gene activation remains elusive (Bok 2004, Bayram 2012). Deletion of *laeA* resulted in a significantly decreased production of secondary metabolites in *A. nidulans* including sterigmatocystin and penicillin (Bok 2004). The importance of LaeA was further

strengthened as it was shown to be part of the conserved velvet complex, which is a major factor for regulation of fungal development hereby coupling the triggering of secondary metabolism to central fungal biology (Bayram 2008).

Another example of chromatin regulated gene expression came from the deletion of a histone deacetylase, *hdaA*, which led to significant increase in production of penicillin and norsolorinic acid (intermediate in sterigmatocystin biosynthesis, figure 2.3) (Shwab 2007).

The SUMO protein is also a chromatin regulating gene which has been shown to have an effect on secondary metabolism. It is an ubiquitin-like protein which is added to many proteins including histones posttranslationally (reviewed in Verger 2003, Gill 2004, Johnson 2004). *A. nidulans* contains one *sumO* encoding gene (Wong 2008) which upon deletion was shown to give a decrease in the production of secondary metabolites such as austinol, dehydroaustinol and sterigmatocystin as well as an increase in asperthecin production (Szewczyk 2008). Ten NR-PKSs were identified by genome mining and a deletion series of these in the *sumO*Δ background was performed and the PKS for asperthecin biosynthesis was identified (Szewczyk 2008).

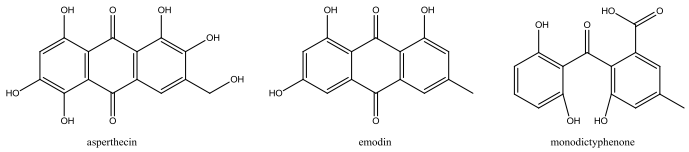

Figure 2.13 Structures of asperthecin, emodin and monodictyphenone.

Investigation of other possible chromatin-level regulation of secondary metabolite biosynthesis in *A. nidulans* led Bok and co-workers to delete *cclA*, an ortholog to the *BRE2* yeast gene, encoding an enzyme partner of the COMPASS transcriptional regulator complex conserved in eukaryotes, which both falicilitate and represses chromatin-mediating processes through methylation of the histone tails (Bok 2009). Deletion of *cclA* showed an altered chemical profile compared to the reference strain where two secondary metabolite gene clusters were activated and afterwards identified through deletions studies of *mdpG* and *orsA* which catalyzed the biosynthesis of monodictyphenone, figure 2.13, and several emodin analogs, as well as F9775A and F9775B, respectively (Bok 2009).

Transcription factor manipulations

Secondary metabolite gene clusters share common regulation of its member genes that can be activated or repressed by transcriptional regulators. Therefore activation or repression of the transcriptional regulators for example transcription factor offers a convenient way to control the expression of whole cluster by one genetic operation. Thus in studies based on mining genomes, the presence of a transcription factor within the cluster has been the driver in characterizing the gene cluster. Asperfuranone and the aspyridones are examples of metabolites discovered through genome mining in *A. nidulans* followed by activation of transcription factors (Bergmann 2007, Chiang 2009a). Chiang and co-workers noticed that a NR-PKS encoding gene, *afoE*, and *afoG* a gene coding for a HR-PKS were located close to each other on chromosome VIII. Since no product had ever been detected from activity of this locus, and due to the rare constellation of two

neighbor PKSs, the authors speculated whether a novel metabolite could be identified. A putative transcription activator, *afoA*, was found near the PKSs and the authors replaced the upstream sequence of *afoA*, estimated to be the native promoter, with an inducible promoter, *alcA*, which led to the production of asperfuranone (Chiang 2009a).

Bergmann and co-workers identified a putative transcription factor in the genome and overexpressed it under the control of an inducible promoter, *alcA*. They demonstrated by Northern blot analysis that six of the nearest neighbor genes were upregulated on inductive medium and detected the production of aspyridones and two intermediates (Bergmann 2007). In a recent study the promoters of the NR-PKS genes and other genes necessary for NR-PKS product formation or release were also replaced with *alcA*, leading to the identification of several NR-PKSs (Ahuja 2012).

The above mentioned studies illustrated the action of local acting transcription factors; however, it has also been reported that a transcription factor associated with a cluster can act on genes outside the cluster. Bergmann and co-workers showed that overexpression of a transcription factor on chromosome II of *A. nidulans* led to the activation of the asperfuranone gene cluster on chromosome VIII (Bergmann 2010). Another example is the transcription factor that regulates sterigmatocystin biosynthesis in *A. nidulans* and aflatoxin biosynthesis in *A. flavus* and *A. parasiticus*, *aflR*, also acts on genes outside the cluster (Price 2006).

For further reading on the regulation of secondary metabolite biosynthesis see reviews by Hoffmeister (Hoffmeister 2007), Palmer (Palmer 2010), Fox (Fox 2008), Strauss (Strauss 2011), Yin (Yin 2011).

2.2.2.3 Other methods and combinations of activation strategies

There are several other methods for activation of secondary metabolite production. One method is to mimic growth conditions resembling known natural environments. This is utilized in the OSMAC approach as described, and also in co-cultivation of microorganisms, which might induce the production of new secondary metabolites due to the influence of the different organisms to each other. The co-cultivation of *A. nidulans* with 58 soil-dwelling actinomycetes led to the activation of the orsellinic acid cluster resulting in the production of orsellinic acid and compounds derived thereof including F-9775A and F-9775B (Schroeckh 2009).

In section 2.2.2.2 molecular methods for altering the epigenome was presented. However, chemical methods which have similar effects are beginning to emerge. The research on chemical epigenetic modifiers focuses on the inhibition of DNA methyltransferases and histone deacetylase which modifies DNA and histones resulting in changes in the folding of DNA (Cichewicz 2010). A screening of nine DNA methyltransferase and histone deacetylase inhibitors against 12 fungal species, by Cichewicz and co-workers, led to production of new or enhanced levels of secondary metabolites in 11 species (Williams 2008). A study by the same group which tested inhibitors of a DNA methyl transferase (5-azacytidine) and a histone deacetylase (suberoylanilide hydroxamic acid) on *A. niger*, figure 2.14, led to increased transcriptional rates of all but seven of the total 55 PKSs, NRPSs and hybrid PKS-NRPSs clusters (Fisch 2009). One of the new metabolites identified was the novel metabolite nygerone A, figure 2.14 (Henrikson 2009).

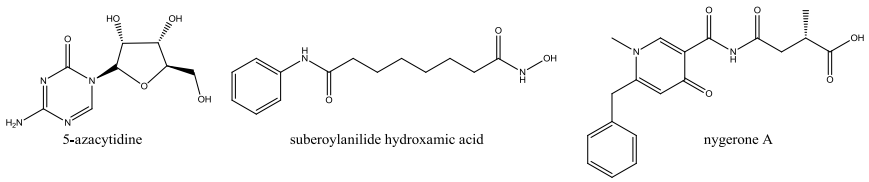

Figure 2.14 The structures of 5-azacytidine, suberoylanilide hydroxamic acid and nygerone A.

Several of the above mentioned strategies have an effect on the production of the same metabolites. As mentioned in the previous sections several orsellinic acid derived compounds were discovered in *A. nidulans* through both co-cultivation, histone-modification and the OSMAC approach (Bok 2009, Schroeckh 2009, Sanchez 2010, Nielsen 2011).

For further reading on activation of secondary metabolite gene clusters there are several reviews present in the literature (Gross 2007, Chiang 2009b, Scherlach 2009, Brakhage 2011, Chiang 2011, Winter 2011, Yin 2011).

3 Overview over experimental work

The figure below gives an overview of the experimental work performed over the past three years. The work in this thesis has been focused on *Aspergillus niger*, *A. oryzae* and *A. nidulans*. The results are presented and discussed in chapter 4 and the experimental sections can be found in the papers 2-7. The outcome of the work at the external stay at the University of Southern California was not as expected and is therefore not ready for publication yet. Since paper 1 is a review it is not listed in figure 3.1. Paper 5 and 6 are rough drafts; however, further experiments need to be conducted prior to submission.

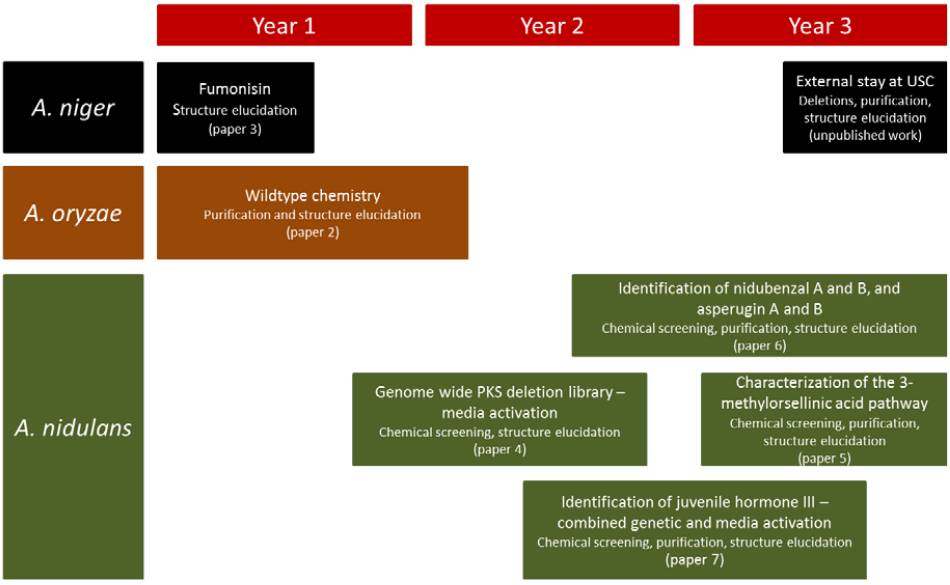

Figure 3.1 Experimental overview over the work for duration of the past three years. . Abbreviations: Oex: overexpression, PKS: polyketide synthase.

The aim of the work presented in this thesis has been to link secondary metabolites to genes; however, to do this several experiments and analysis needs to be performed. This includes bioinformatics, molecular biology, chemical analysis, isolation of metabolites and structure elucidation. My part of have consisted of the latter; chemical analysis, isolation and structure elucidation.

3.1 Linking of secondary metabolites to genes

This section will briefly outline the tools and instruments applied in the thesis. The experimental descriptions are presented in the paper 2-7; however, examples will be included in chapter 4.

3.1.1 Targeted genetic manipulations including deletions and over-expressions

Most of the strains analyzed in this work were genetically modified. The host strains used for genetic transformation in *A. nidulans* had been disrupted in the non-homologous end-joining pathway enabling efficient gene targeting (Nielsen 2008), referred to as the reference strain in this thesis. This was supported by the development of versatile tools to construct DNA substrates, e.g. fusion PCR and USER cloning technology. The mutant strains analyzed were gene deletions, point mutations or overexpressions where the gene of interest has been moved to an insertion site under the control of a constitutive or inducible promoter (Nielsen 2006, Nielsen 2008, Nielsen 2011, Hansen 2011).

3.1.2 Metabolome analysis

The chemical analysis of all the strains has been performed on three instruments. A UHPLC (Dionex RSLC Ultimate 3000) equipped with a Kinetex C_{18} column coupled with diode array dectection (DAD), throughout the thesis called UHPLC-DAD. Two TOF-MSs; a LCT oaTOF mass spectrometer (Micromass), equipped with a Phenomenex C_{18} column and diode array detection, and a MaXis 3G QTOF (Bruker Daltronics) coupled to a Dionex Ultimate 3000 UHPLC system equipped with a Kinetex C_{18} column, throughout the thesis called LC-TOF-MS (LC-DAD when DAD detection in reported) and UHPLC-TOF-MS respectively.

The approach in the metabolome analysis has been to compare mutant strains with the reference strain to detect metabolites either appearing or disappearing. Generally the strains have been analyzed in UHPLC-chromatograms (210 nm) and, in some cases, both positive and negative ionization mode, enabling the identification of metabolites which could only be detected in one of the techniques. When interesting peaks had been identified, the metabolite data was compared to the literature, and the metabolite database Antibase (Laatsch 2010) in order to identify already reported metabolites. The MaXis UHPLC-TOF-MS was acquired during the study and provided invaluable information on both the molecular formula and isotope pattern due to the high mass accuracy (1 ppm) .

3.1.3 Isolation and structure elucidation

The approach described above was done in micro-scale where plugs from a colony was extracted and analyzed (Frisvad 1987, Smedsgaard 1997). When the metabolome analysis of the mutants revealed new interesting metabolites the cultivations were scaled up to allow isolation and structure elucidation. The biomass was extracted and metabolites were isolated using different LC techniques with various column material including normal phase, reverse phase and size exclusion chromatography. The structures of the isolated metabolites were solved using 1D and 2D NMR-spectroscopy. The NMR spectra were acquired using standard experiments on either a Varian Unity Inova 500 MHz spectrometer placed at DTU Chemistry and/or on a Bruker Avance 800 MHz spectrometer at the Danish Instrument Center for NMR Spectroscopy of Biological Macromolecules.

4 Results and Discussion

The experimental work performed for the past three years have focused on the industrially important filamentous fungi; *A. oryzae* and *A. niger* and the genetic model organism *A. nidulans*. The results of the work will be presented in this section starting with the exploration of *A. oryzae* wildtype chemistry including several new metabolites and comparison of these to *A. flavus* metabolites (paper 2). The next section (4.2) will focus on the work done with *A. niger* where a new fumonisin analog was isolated and characterized through NMR spectroscopy (paper 3). Section 4.3 describes the results of the *A. nidulans* work. This included the analysis of a deletion library of 32 putative PKSs encoding genes including activation of genes using several complex media and linking of austinol and dehydroaustinol to their synthase gene (section 4.3.1, paper 4). This was followed by identification of several new *A. nidulans* metabolites through activation of a transcription factor, and a proposed biosynthetic pathway through deletion studies (section 4.3.2, paper 5). The last part of this section (4.3.3) focus on the novel metabolites, nidubenzal A and B and the linking of asperugin A and B to their PKS encoding gene (section 4.3.3.1, paper 6) and the juvenile hormones (section 4.3.3.2, paper 7) which were isolated after activation through genetic modifications combined with the use of complex media. The biosynthetic origin of asperugin A and B was identified by reference to the deletion library followed by genetic modifications.

4.1 *Aspergillus oryzae*

Aspergillus oryzae is one of industry's most used workhorses and has been used for centuries in food fermentation for the production of for example sake, miso, soy sauce and other traditional Asian foods (Machida 2008a). *A. oryzae* is also a widely used organism for production of amylase, lipases and proteases, and, more recently, also for heterologous expression of secondary metabolite genes and non-fungal proteins (Punt 2002, Meyer 2008, Fisch 2011). For many years, *A. oryzae*, has been suspected to be a domesticated form of *A. flavus*, a plant and mammalian pathogenic saprophyte, capable of producing some of the most carcinogenic compounds known, the aflatoxins, figure 4.1. Genetic work and subsequent genome sequencing of strains of both species have verified the tight link between the species (Geiser 1998, Geiser 2000, Machida 2005, Yu 2005b, Abe 2006, Kobayashi 2007, Machida 2008a).

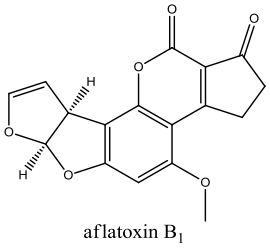

Figure 4.1 The structure of aflatoxin B_1.

The availability of the sequenced strains of *A. oryzae* (RIB40 (ATCC 42149)) (Machida 2005) and *A. flavus* (NRRL 3357) (Yu 2005b) have led to comparison of the two genomes. The comparison shows high homology: 99.5% genome homology and 98% at the protein level (Rokas 2007). The

high homology could lead one to expect *A. oryzae* to produce most of the metabolites found in *A. flavus* (Machida 2008a, Machida 2008b, Machida 2005, Payne 2006, Yu 2008) and the preliminary bioinformatics studies performed along with the genome sequencing reported roughly the same number of predicted genes: 28 PKSs, 32 NRPSs and 2 hybrid PKS-NRPSs for *A. flavus* and 27 PKSs, 32 NRPSs and 2 hybrid PKS-NRPS for *A. oryzae* with two NRPSs apparently unique for each strain (Cleveland 2009). However, published metabolic data indicated a very low chemical correlation between the two strains (Laatsch 2010). Most of the predicted genes for secondary metabolites of *A. oryzae* (or *A. flavus*) have not been linked to specific metabolic products. Only genes of the most important toxins: aflatoxin (Yu 2008, Lee 2006, Tominaga 2006), cyclopiazonic acid (Tokuoka 2008, Chang 2009) and aflatrem (Nicholson 2009) have been annotated in both species which leaves much to be explored.

The aim of the work in this section was to perform an initial comparative investigation of the small molecule chemistry from the two genome sequenced strains of *A. oryzae* (RIB40) and *A. flavus* (NRRL 3357) along with isolation and structure elucidation of new metabolites from *A. oryzae*, in order to get further insights into possible homologies in secondary metabolite production for these two important and related species. The results are described and discussed below and further experimental details can be found in paper 2.

4.1.1 Comparison of secondary metabolite profiles of *A. oryzae* and *A. flavus*

For the analysis of *A. oryzae* RIB40 (and *A. flavus* NRRL 3357) chemistry, we investigated a series of solid media cultivated at 25°C in the dark for 7 and 14 days followed by micro-scale extractions (Frisvad 1987, Smedsgaard 1997) and subsequently analysis with HPLC-DAD-MS for investigation of optimal secondary metabolite production conditions. The screening indicated the greatest chemodiversity and metabolite production from CYA, YES and WATM agar.

The comparison of the secondary metabolite profiles of the two strains showed a high degree of chemical difference on all media as illustrated in figure 4.2 for the WATM medium. The major metabolite repetitions between the two genome sequenced strains were merely kojic acid and ergosterol as well as a number of minor metabolites (not analyzed here), which seemed to be shared between the two strains. Altogether, this is in sharp contrast to the high gene homology; however, it reflects the difference in metabolic published data (Laatsch 2010).

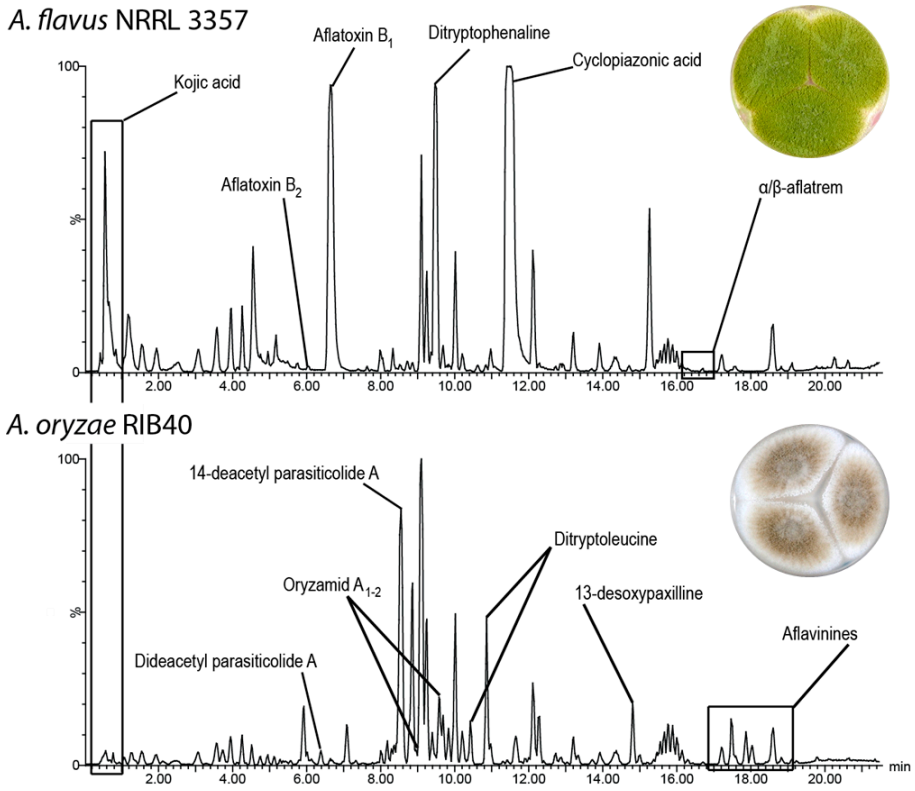

Figure 4.2 ESI+ (electrospray ionization) BPC (base peak chromatogram) of micro scale extract from WATM after seven days of incubation, bottom: *A. oryzae* RIB40, top: *A. flavus* NRRL3357. Besides kojic acid (shown in box) and analogues in the beginning of the chromatograms and ergosterol in the end (not shown), there are very few identical compounds between the genetically almost identical strains. Note that aspirochlorine is only detectable in negative ionization mode, and therefore not visible in these chromatograms. The oryzamides, ditryptoleucines and the parasiticolides are reported here. (figure taken from paper 2).

Several previously reported metabolites of *A. oryzae* were dereplicated and we found that the RIB40 strain did not produce detectable levels (LC-MS) of cyclopiazonic acid (Orth 1977) (as also noted by Tokuoka *et al.* (Tokuoka 2008)), asperfuran (Pfefferle 1990), sporogen AO1 (Tanaka 1984a, Tanaka 1984b), maltoryzine (Iizuka 1962) or aspergillomarasmine A (Robert 1962, Barbier 1963), under these growth conditions. The RIB40 strain did produce kojic acid (Manabe 1984, Bentley 2006) and aspirochlorin (Sakata 1982, Sakata 1983, Sakata 1987, Monti 1999, Klausmeyer 2005), figure 4.3 and a series of potentially new metabolites of which some were isolated and structure elucidated. These metabolites included the parasiticolites, ditryptoleucine, oryzamide $A_{1\text{-}2}$ and 13-desoxypaxilline.

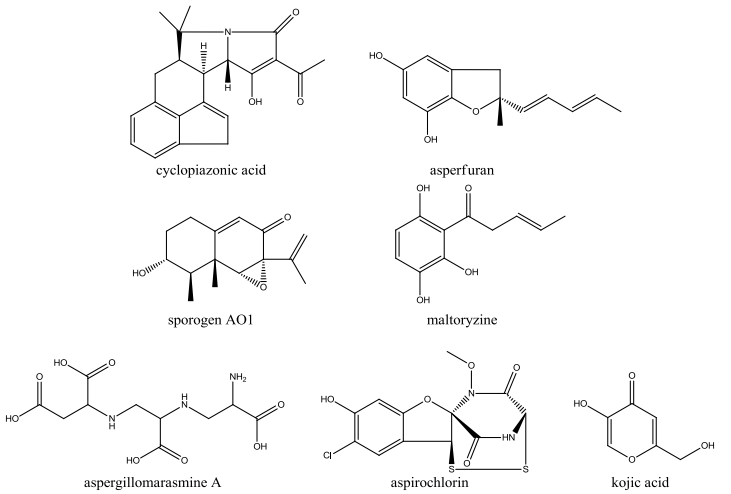

Figure 4.3 Structures of known metabolites from *A. oryzae*.

4.1.1.1 13-desoxypaxilline

During fermentation of the chemically potent RIB40 strain, we have been interested in the tremorgenic compounds, allegedly coupled to fungal sclerotia (Wicklow 1982, Gloer 1988, Gloer 1989, Staub 1992, Staub 1993, Tepaske 1989a, Tepaske 1989b, Tepaske 1990, Tepaske 1992) and whether these could be found in *A. oryzae* as they have been in *A. flavus*. The RIB40 strain produces large and abundant sclerotia, especially on WATM agar, a fact not widely announced in literature although sclerotia have been observed in *A. oryzae* sporadically (Raper 1965, Wicklow 2007, Jin 2010). No sclerotia were observable after 14 days on YES agar, but although these metabolites are often characterized as sclerotial metabolites, there is not a strict correlation between the biosynthesis of these metabolites and the formation of sclerotia, as also noted by Wilson (Wilson 1966), and this extract was used for the described isolations.

We isolated the aflatrem precursor 13-desoxypaxilline which was originally isolated from *Penicillium paxilli* (Springer 1975, Longland 2000, Bilmen 2002, Sabater-Vilar 2003, Sheehan 2009). Aflatrem is a known metabolite of *A. flavus* and was discovered by Wilson and Wilson in 1964 (Wilson 1964) and structure elucidated by Gallagher *et al.* (Gallagher 1978, Gallagher 1980). 13-desoxypaxilline was present in several media micro-scale extracts including YES, CYA, OAT and WATM. It was isolated from the above mentioned YES extract and the structure was confirmed by LC-MS, LC-MS/MS and NMR analysis. It was investigated through HPLC-DAD and LC-MS/MS whether alfatrem or other intermediates in the biosynthetic pathway were present in the extracts, however, none of the proposed intermediates towards aflatrem or aflatrem itself, figure 4.4 could be detected and only one sample (WATM, 7d) showed traces of paspaline, a precursor for 13-desoxypaxilline.

The discovery of 13-desoxypaxilline as the end-product of *A. oryzae* RIB40 is in agreement with the analysis of Nicholson *et al.*, who showed that a frameshift mutation in the *atmQ* gene presumably accounts for the 13-desoxypaxilline not being converted into paspalicine and paspalinine (Nicholson 2009). This mutation is therefore likely responsible for terminating the

aflatrem biosynthesis in RIB40 prematurely. Contrary to our discovery, Nicholson *et al*. did not find the aflatrem gene cluster of RIB40 to be transcribed during their fermentations (Nicholson 2009).

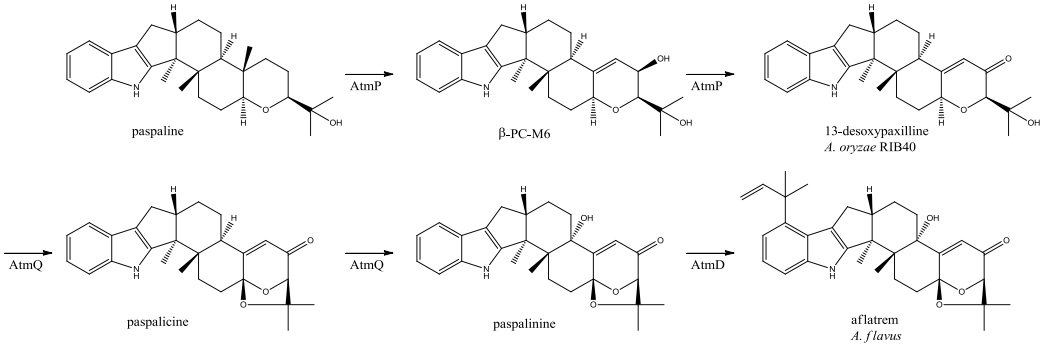

Figure 4.4 The final steps in the proposed biosynthesis of aflatrem (in *A. flavus*). *A. oryzae* RIB40 biosynthesis stops at 13-desoxypaxilline (Nicholson 2009).

A second extract was made from 100 plates of a 14 day old *A. oryzae* culture grown on WATM agar with abundant sclerotia formation to validate the findings from the YES extract. The analysis of the WATM extract showed 13-desoxypaxilline as a major metabolite alongside other sclerotium-related metabolites, such as aflavinines (based on UV – data not shown) which were unfortunately not isolated in pure and large enough quantities for NMR analysis.

The isolated 13-desoxypaxilline is a member of the paspalitrem tremorgens, a widely distributed group of metabolites that have been isolated from several genera: *Penicillium, Eupenicillium, Claviceps, Emericella, Aspergillus* and *Phomopsis* (Cole 1981, Steyn 1985, Bills 1992). Besides the tremorgenic activity in animals, these metabolites have been shown to be insecticides (Steyn 1985), which is believed to be their ecological function together with aflatoxin and cyclopiazonic acid for protection of the sclerotia against fungivorous insects (Wicklow 1982, Gloer 1988).

4.1.1.2 Parasiticolides

In addition to 13-desoxypaxilline, two new analogues of parasiticolide A were also isolated. The metabolites showed, through LC-MS and NMR analysis, to be dide- and 14-deacetyl analogues and are most likely precursors to the sesquiterpene parasiticolide A (also called astellolide A), figure 4.5. The shift values of all the parasiticolide analogues correlated with the published data for parasiticolide A, except for the missing signals of the acetate units and their minor influence on the chemical shift values of adjacent protons and carbons (see paper 2 for NMR details) (Hamasaki 1975, Gould 1981). Several different extraction procedures were tested to verify the correctness of the compounds as genuine metabolites and not *in vitro* degraded parasiticolide A products, but all samples showed only dide- and 14-deacetyl parasiticolide A and no traceable (LC-MS) levels of parasiticolide A ifself, even with different non-acidic extraction procedures. Parasiticolide A have been isolated from *A. flavus* var. *columnaris* once (Shiomi 2002) and was originally isolated and characterized from *A. parasiticus* (Fukuyama 1975, Ishikawa 1984) and later

also from a mutant of *Emericella variecolor* (Gould 1981). Recently parasiticolides have been detected in the newly described species *A. arachidicola* and *A. minisclerotigenes* (Pildain 2008). There have to our knowledge not been published any toxic studies on the parasiticolides, but the related peniopholides from the fungus *Peniophora polygonia* have been reported to have antifungal properties (Ayer 1992).

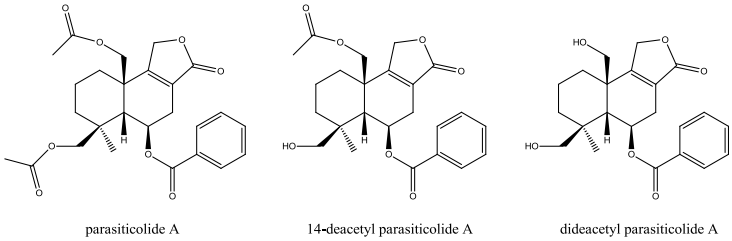

Figure 4.5 Structures of Parasiticolide A, and 14-deacetyl parasiticolide A, dideacetyl parasiticolide A.

According to our observations parasiticolides are more often detectable metabolites of *A. oryzae* than of *A. flavus* under the same fermentation conditions, suggesting that the pathway is partly silenced for *A. flavus* and may need to be activated under otherwise normal growth conditions. It is interesting that parasiticolide A is scarcely observed in *A. flavus*, when it is an important product of *A. oryzae* and also of *A. parasiticus*. We also isolated and elucidated a formyl variant of parasiticolide A; however, it was not possible to exclude the possibility of in vitro chemistry due to the formic acid added during the ethyl acetate extraction, so the correctness of this metabolite remains tentative (Hamasaki *et. al.* used benzene to extract parasiticolide A (Hamasaki 1975)).

To further verify these observations, a MS/MS method was used to analyze several different microscale extracts of *A. oryzae* RIB40 for parasiticolide A. Trace amounts of parasiticolide A could be measured, indicating a complete transformation into the end product. The small amount of parasiticolide A in RIB40 (roughly 1:1000 ratio compared to 14-deacetyl parasiticolide A, presuming the same response factor) might be the result of spontaneous acetylation involving the first acetylating enzyme. When the gene cluster responsible for the biosynthesis of these metabolites is mapped, it is likely that the gene responsible for the last (specific) acetylation will be found to be mutated.

4.1.1.3 Ditryptoleucine and oryzamide $A_{1\text{-}2}$

Four new *A. flavus* related NRP metabolites were also isolated from *A. oryzae* RIB40. The metabolites showed, through structure elucidating by ^{1}H, DQF-COSY, HSQC and HMBC NMR data, to be two isomeric metabolites named ditryptoleucine related to the ditryptophenalines (Springer 1977, Barrow 1993, Oleynek 1994, Barrow 1994), figure 4.6, and two indole-enamides named oryzamide $A_{1\text{-}2}$ (*cis*- and *trans*-isomers) structurally similar to the antibiotic miyakamide $B_{1\text{-}2}$ (Shiomi 2002), figure 4.7.

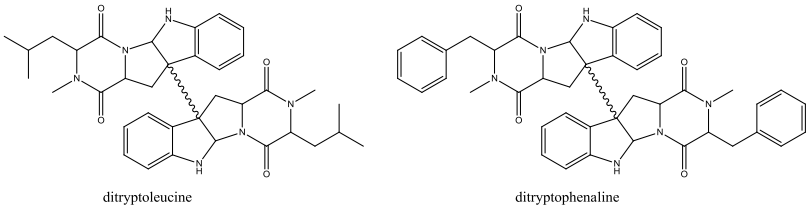

Figure 4.6 Structures of ditryptoleucine (*A. oryzae* metabolite) and ditryptophenaline (*A. flavus* metabolite).

The diketopeperazine ditryptoleucine was isolated in two variants with ^{1}H-NMR shifts varying around the C-C dimeric bond, but with the same base structure. This unspecific dimerization is in line with previously isolated compounds (Barrow 1994). A hybrid between the ditryptophenaline and ditryptoleucine was isolated from an *Aspergillus* sp. as WIN 64745, with both a phenylanaline and leucine moiety, but with no *N*-methylation (Barrow 1993). These compounds were tested and proved antagonistic against substance P at the NK1 receptor (Movassaghi 2008). Intriguingly, these new *A. oryzae* metabolites have apparently exchanged phenylalanine with leucine compared to the similar *A. flavus* metabolites, indicating either a common trait in the domestication process or coupling between the two pathways.

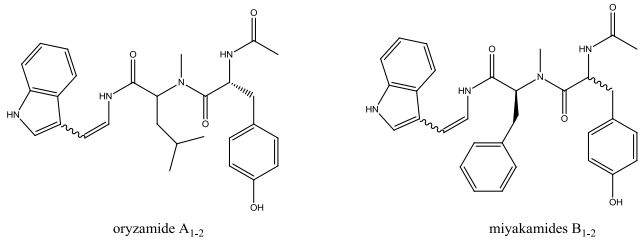

Figure 4.7 Structures of oryzamide A_{1-2} and the miyakamides B_{1-2}.

It proved difficult to unambiguously isolate the *cis*- and *trans*-isomers of oryzamide A in a pure form due to isomerization around the double bond. Due to this difficulty the structure elucidation has been performed on mixtures of compounds. It is evident from the structure elucidation that oryzamides A_{1-2} only differ in the configuration around the double bond of the enamine as evident from the size of the coupling constant. Marfey analysis of the amino acid derived compounds only established the presence of L-tyrosine in the oryzamides. The oryzamides A_{1-2} are variants of the miyakamides B_{1-2} (Shiomi 2002). The phenylalanine in the miyakamides has been substituted with leucine in the oryzamides. However, this exchange of phenylalanine and leucine has often been found for compounds produced within the same species. *Penicillium polonicum* produces both fructigenine A (also called puberulione and rugulosuvine A) containing phenylalanine and fructigenine B (also called verrucofortine) containing leucine (Arai 1989, Frisvad 2004a, Frisvad 2004b). We could also detect two slightly later eluting compounds in the *A. oryzae* RIB40 extracts likely to be further indole-enamides having phenylalanine incorporated instead of tyrosine as evident from LC-DAD-MS analysis (data not shown) as also seen for the miyakamides (Shiomi 2002).

4.1.2 Summary and part conclusion

The tremorgenic 13-desoxypaxilline have been isolated from *A. oryzae* RIB40 and verified under several different growth conditions contrary to previous studies. We believe that 13-desoxypaxilline is the end-product of the aflatrem biosynthesis for the RIB40 strain which correlated well with the results of Nicholson *et al.* (Nicholson 2009) who described a mutation in the gene responsible for further modifications of 13-desoxypaxilline in *A. oryzae* RIB40.

The new metabolites dide- and 14-deacetyl parasiticolide A were also found as genuine products from the RIB40 strain where parasiticolide A was only detected in trace amounts using a LC-MS/MS method. This indicates that a defective acetylation of the 14-deacetyl parasiticolide A and the small amount of parasiticolide A in RIB40 could be the result of spontaneous acetylation in the cell cytosol.

The new NRPs ditryptoleucine and oryzamide $A_{1\text{-}2}$ appear to be natural variants of known *A. flavus* metabolites. They share the exchange of a phenylalanine for a leucine, although they are believed to originate from two unrelated pathways. As for 13-desoxypaxilline, dide- and 14-deacetyl parasiticolide A are almost certainly products of a prematurely ended biosynthesis, here parasiticolide A. Further analysis of the genomes of *A. oryzae* and *A. flavus* could give possible candidates for the NRPS genes responsible for the production of ditryptoleucine and oryzamide $A_{1\text{-}2}$. After identification of the synthethase genes it could be interesting to investigate whether the aminoacid exchange is due to genetic mutations.

Altogether the finding contribute to understanding why the overall chemical profiles of *A. oryzae* (RIB40) and *A. flavus* (NRRL 3357) appear quite different since some of the end-products usually seen in *A. flavus* are apparently not reached in *A. oryzae* or the metabolites differ in one incorporated amino acid. Whether the different chemical profiles are merely the result of different regulation or are a result of genuine mutations, as with 13-desoxypaxilline, remains to be settled. *A. oryzae* RIB40 is clearly a chemically potent strain, and as more of its chemistry is unfolded it is likely to be revealed that most of the biosynthetic pathways of *A. flavus* will be found more or less functional which correlates to the high degree of homology between the two strains.

The findings above shows that genome comparisons are an important tool to explore the chemical potential of different strains, however, a regulatory difference or mutations (small or large) in the genome can lead to large chemical differences between species who seem alike.

4.2 *Aspergillus niger*

Aspergillus niger is another industrially important filamentous fungus used in the fermentation industry to produce organic acids such as citric acid and gluconic acid as well as enzymes such as amylases and lipases (Schuster 2002). Besides the uses in the fermentation industry *A. niger* is also a contaminant of crops and feed distributed worldwide, including corn, peanuts, onions, apples, grapes, raisins, mangos and dried meat products (Perrone 2007, Nielsen 2009).

Due to the vast importance of *A. niger*, both as contaminant and its uses in fermentations, the genome of two strains of *A. niger* have been sequenced (Baker 2006, Pel 2007) giving the

possibility of searching the genomes for secondary metabolites gene clusters. The next section describes how the genome sequences revealed the presence of a mycotoxin (fumonisin) gene cluster known from other species making researchers look for and report the production of fumonisins in *A. niger*. We have identified, isolated, and structure elucidated a new fumonisin isomer (paper 3).

4.2.1 Fumonisin production in *A. niger*

The sequencing of the genome of *A. niger* revealed the presence of a fumonisin-like gene cluster in two different isolates, ATCC 1015 (Baker 2006) and CBS 513.88 (Pel 2007). The fumonisins are a group of HR-PKs produced by *Fusarium verticilloides* and other Fusaria (Bezuidenhout 1988, Gelderblom 1988, Marin 2004). Several analogues of fumonisin have been reported, however, fumonisin B_1, B_2 and B_3 of the B-series are the most abundant in nature and are all carcinogenic (Gelderblom 1993, Rheeder 2002, Bartók 2006). The B-series analogues contain a terminal 2-amino-3-hydroxy motif on an eicosane backbone and two hydroxyl groups esterified with tricarboxylic acids. There had not, at the time of the publications of the genome sequences, been any reports of fumonisin production in *A. niger*. Therefore, after the discovery of the putative fumonisin gene cluster, Frisvad *et al.* (Frisvad 2007) investigated the possibility of fumonisin production in *A. niger*. They reported detection, through LC-MS comparisons to standards, of fumonisin B_2 (FB_2) from four strains of *A. niger* including the two fully genome sequenced strains (ATCC 1015 and CBS 513.88) and ATCC 9029 and NRRL 326 (Frisvad 2007) Later it was reported that *A. niger* could also produce fumonisin B_4 (Nielsen 2009, Noonim 2009). The ability of *A. niger* to produce fumonisins gave speculations to whether this could be an overlooked health risk, since *A. niger* is used in industrial fermentations and is a common contaminant of feed and foods due to the possibility of fumonisins ending up in the final products (Frisvad 2007).

4.2.1.1 Isolation and NMR characterization of fumonisin B_2 and B_6 from *A. niger*

Further analysis of the *A. niger* strains revealed the ability of *A. niger* to produce another isomer besides fumonisin B_2 and B_4 with the same elemental composition as fumonisin B_1 and *iso*-fumonisin B_1 but with a different retention time. We isolated and characterized this isomer, named fumonisin B_6, from *A. niger* NRRL 326, along with fumonisin B_2 which were NMR characterized to validate that fumonisin B_2 from *A. niger* is identical to that reported in several *Fusarium* species.

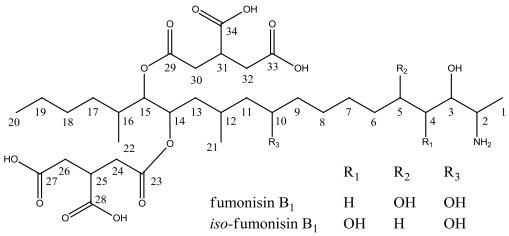

	R_1	R_2	R_3
fumonisin B_1	H	OH	OH
iso-fumonisin B_1	OH	H	OH
fumonisin B_2	H	OH	H
fumonisin B_3	H	H	OH
fumonisin B_4	H	H	H
fumonisin B_6	OH	OH	H

Figure 4.8 The structures of fumonisin B_1, *iso*-B_1, B_2, B_3, B_4 and B_6.

The structure of fumonisin B_6 were solved based on DQF-COSY, HSQC, HMBC and H2BC NMR experiments along with comparison to literature values of fumonisin B_1 (Savard 1994a) and *iso*-B_1 (MacKenzie 1998). Unambiguous assignment of the proton and carbon resonances of fumonisin B_6 could be obtained for most of the resonances. However due to spectral overlap individual assignment of C_7-C_9 was not possible. The two tricarboxylic acid side chains were assigned as two separate spin systems with only minor chemical shift differences. The attachment of the C_{29}-C_{34} side chain to the backbone structure were confirmed by the presence of an HMBC correlation between H_{15} and C_{29}, whereas the position of the C_{23}-C_{28} side chain is based on the chemical shifts of H_{14}/C_{14} and comparison with the assignment obtained from fumonisin B_1 and *iso*-B_1. The backbone fragments C_1-C_6 and C_{10}-C_{20} were unambiguously assigned and only showed minor deviations compared to fumonisin B_1 and *iso*-B_1. Fumonisin B_1 and *iso*-B_1 have OH-groups attached to C_3, C_5, and C_{10} and to C_3, C_4, and C_{10}, respectively, whereas fumonisin B_6 has OH-groups at C_3, C_4, and C_5 (figure 4.8). Chemical shift values of 1.25 ppm for H_{10} and 27.5 ppm for C_{10}, DQF-COSY connectivities from H_{11} to H_{10} and HMBC correlations from H_9 to C_{10} and from H_{10} to C_9, confirm that no OH-group is bound at this position due to the large upfield shift of the resonances when compared to fumonisin B_1, where H_{10} and C_{10} resonances at 3.62 and 69.8 ppm, respectively. DQF-COSY connectivities can be traced along the backbone from H_3 at 3.64 ppm, H_4 at 3.46 ppm, and H_5 at 3.71 ppm to H_6 at 1.53/1.59 ppm. In addition HMBC correlations can be seen from H_4 to C_2/C_5 and from H_3 to C_4, confirming the presence of the third OH-group at C_4 in the structure. The chemical shifts obtained for H_4/C_4 of 3.46 ppm/74.9 ppm compared to 3.65 ppm/72.2 ppm as seen in *iso*-fumonisin B_1 and equivalently for H_5/C_5 of 3.71 ppm/71.4 ppm compared to 3.84 ppm/68.4 ppm for fumonisin B_1 is in agreement with the proposed structure of fumonisin B_6.

The NMR data of the isolated fumonisin B_2 and the authentic standard from *Fusarium* were compared to establish whether they were identical. The chemical shifts were comparable except for the shifts of the two tricarboxylic acid side chains. The differences could be explained by a difference in the structural fold of the fumonisin B_2 between the two samples, likely to be caused by differences in pH and thereby overall level of protonation of the four carboxylic acid functionalities. The fact that fumonisin B_2 does have a unique globular folded structure has previously been addressed by Beier and Stanker (Beier 1997). The fumonisin B_2 from *A. niger* was purified on a cation exchange column and to ensure that the two samples had been subjected to the same purification protocol the standard fumonisin B_2 were also run over the column. The NMR spectra of the two fumonisins were now identical. The coupling constants for the protons in the amino terminal (C_2-C_5) and the attachment of the side chains (C_{14} and C_{15}) in the fumonisins from *A. niger* and *Fusarium* showed that they are of the same size, proving that the relative stereochemistry for these parts of the backbone are the same. The stereochemistry at position C_{12} and C_{16} could not be determined from the data due to chemical shifts overlap. The optical rotation of fumonisin B_2 from *A. niger* was similar to that known from *Fusarium*; however, with several stereocenters in the molecule this is not a direct proof of identical stereochemistry. The data points toward identical stereochemistry of the two fumonisins; however, a genetic comparison of the fumonisin gene cluster in the two genera revealed several differences in the placement and orientation of the different involved biosynthetic genes (Baker 2006) which could lead to differences in the stereochemistry in the final product.

4.2.3 Summary and part conclusion

Two fumonisin isomers were isolated and structure elucidated from an extract of *A. niger* where one was a new analogue. The absolute stereochemistry of both fumonisin B_2 and B_6 still needs to be determined either through crystallization or derivation studies. The production of fumonisins in *A. niger* is an example of how the genome sequences followed by the prediction of gene function revealed the possible production of a mycotoxin in a species, which is present in both food and feeds and which is used in the industry. The reason for the fumonisins not having been reported in *A. niger* before may be that it was not expected for them to be produced and that the extraction and detection methods are different from other mycotoxins.

4.3 *Aspergillus nidulans*

Aspergillus nidulans is one of the most significant biological model systems in the fungal kingdom. This was pioneered by Pontecorvos' (Pontecorvo 1953) work in the middle of the last century, which demonstrated that *A. nidulans*, in addition to the asexual state, also proliferate via sexual and parasexual life cycles giving an ideal platform for genetic studies. Due to the wide uses of *A. nidulans* as a model organism, efficient tools for targeted gene transformations have been developed (Nayak 2006, Nielsen 2006, Nielsen 2008) and the availability of the genome sequences has facilitated the possibilities of genome mining (Galagan 2005). Prior to the release of the genome sequence the research of secondary metabolism in *A. nidulans* was focused on a few biosynthetic pathways whereas the focus have now been shifted towards discovery and linking of metabolites to the silent genes.

The aim of the work in this section was to discover and link new secondary metabolites, especially PKs, of *A. nidulans* to their synthase genes. The strategies for activation of the secondary metabolite genes were the OSMAC approach, where the reference strain was grown on up to eight different media (section 4.3.1, paper 4), and through genetic modification (section 4.3.2, paper 5). These two approaches were combined and led in two studies to the discovery of metabolites not previously described from *A. nidulans* (section 4.3.3, paper 6 and 7). The results are described and further experimental details can be found in the papers.

4.3.1 Discovery and linking of polyketides to their PKS through a deletion library

As described in section 2.2.2 there are several ways to activate secondary metabolite genes in filamentous fungi. Due to previous experience at CMB with cultivating filamentous fungi at various media conditions we decided to use the OSMAC approach to possible enhance secondary metabolite production of *A. nidulans* (Frisvad 1981, Frisvad 1983, Filtenborg 1990, Frisvad 2007). Reports of novel metabolites from *A. nidulans* for example the aspoquinolones (Scherlach 2006) and aspernidine A and B (Scherlach 2010) indicated that this was a reasonable approach.

Three base media, Czapek yeast agar (CYA), Raulin-Thom (RT) and yeast extract (YE), were chosen and these were varied through the addition of salt (CYAs), sucrose (YES, CY20) and oatmeal (RTO). In addition a minimal media (MM) was used, giving eight different media in total. The media were selected based on the knowledge at CMB to ensure exploration of different growth conditions.

The reference strain, IBT29539 were cultivated on the eight media and inoculated for seven days at 37°C in the dark. Figure 4.9 show cultures of the strain on the different media.

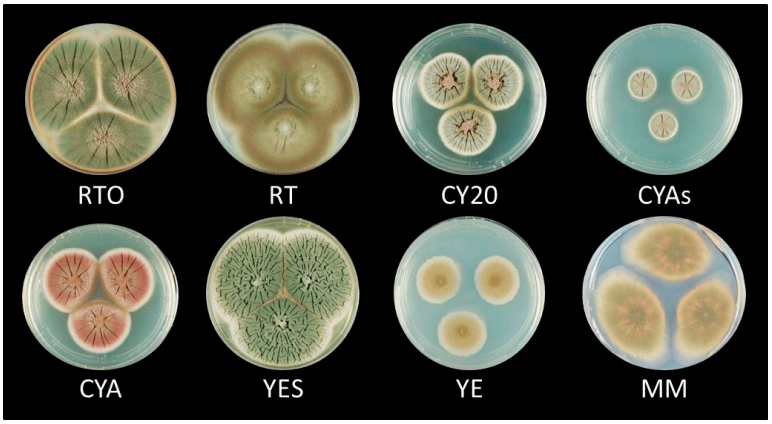

Figure 4.9 The reference strain cultivated on eight different media: RTO, RT, CY20, CYAs, CYA, YES, YE and MM.

The cultures appear quite different at the different cultivation conditions. To analyze the metabolite production micro-extraction was performed (Frisvad 1987, Smedsgaard 1997) and the extracts were analyzed by both UHPLC-DAD and LC-TOF-MS. The UHPLC analysis revealed a diverse production of secondary metabolites on the eight different media, figure 4.10.

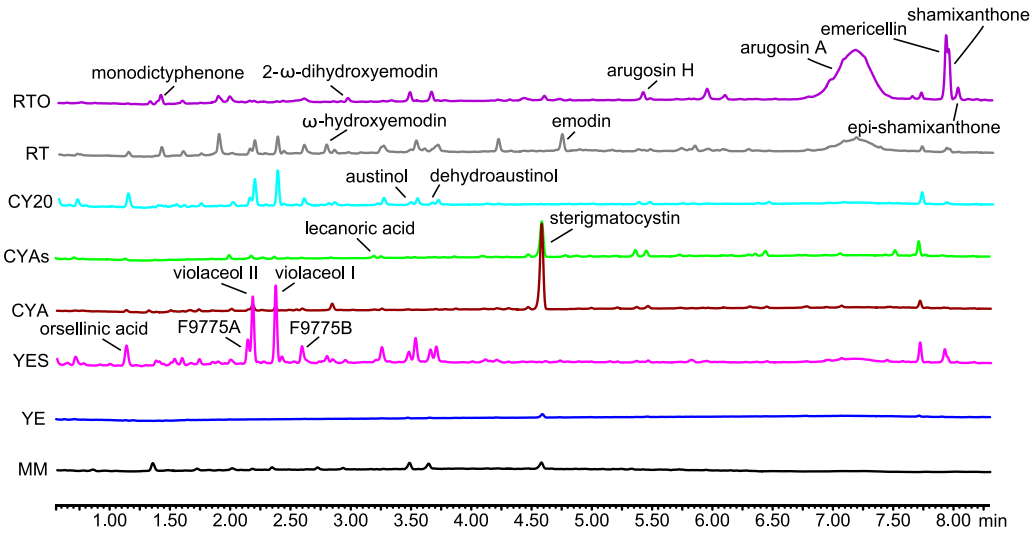

Figure 4.10 UHPLC-DAD chromatograms (210 nm) of extracts of the reference strain cultivated on eight different media compositions demonstrate the difference in secondary metabolite production. From bottom to top: MM, YE, YES, CYA, CYAs, CY20, RT and RTO. Note that the emericellamides are not visible in the UHPLC chromatogram (210 nm); however, they were detected in ESI+ and ESI- in all media except YE.

The secondary metabolite production was highly diverse and formed the basis for isolation and characterization of several metabolites which will be elaborated on the following sections. The metabolic profiles of MM and YE were considered to be redundant and these two media were therefore not used for further screening.

To investigate whether any of the metabolites in figure 4.10 were PKs we decided on a strategy to make a global deletion library where all 32 putative PKS encoding genes, as defined from the annotation of the genome databases at the Broad Institute of Harvard and MIT and the *Aspergillus* Genome Database at Stanford (Arnaud 2012), were deleted leaving us with 32 strains to be analyzed on the six chosen media. The deletion samples were prepared using the same micro-extraction procedure as for the reference strain. Since the deletion of a PKS gene should abolish the production of the metabolite, we hypothesized that comparison of a deletion strain to the reference would show missing peaks. To verify the approach we included deletions of genes which had already been linked, by others, to metabolites. Figure 4.11 show the UHPLC chromatogram of the reference strain compared to a deletion of *stcA* which is the PKS gene responsible for the biosynthesis of the sterigmatocystin backbone (Yu 1995). It is seen that the large peak at 4.6 minutes disappears. To confirm this result the same strains are analyzed with LC-TOF-MS where an extracted ion chromatogram of the $[M+H]^+$ of sterigmatocystin, 325 (±0.5 Da), disappeared in the deletion strain (data not shown).

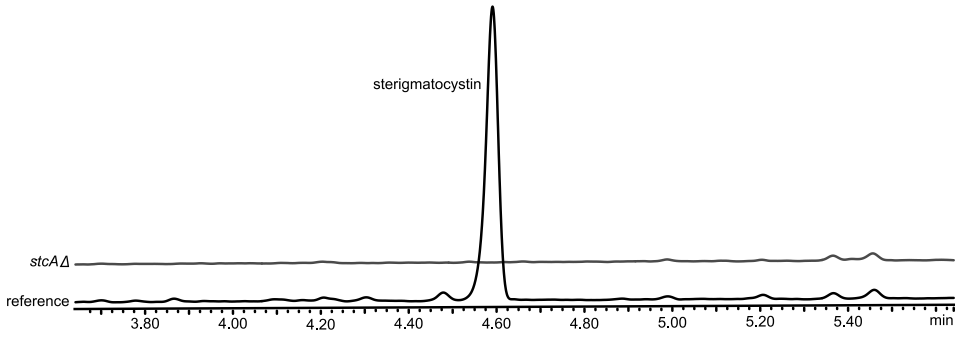

Figure 4.11 UHPLC chromatogram of the *stcA*Δ strain compared to the reference strain on CYA.

This analysis was also performed on the remaining eight PKS encoding genes which, at the time, had been linked to metabolites. Metabolites representing three, beside sterigmatocystin, of the eight gene clusters could be detected: monodictyphenone, orsellinic acid and emericellamide. In agreement with previously published data the metabolites were absent in the corresponding single PKS gene deletion mutant strains; *mdpG* (Bok 2009), *orsA* (Schroeckh 2009) and *easB* (Chiang 2008), respectively (data not shown). Beside the secondary metabolite effect seen in these four strains, the strain carrying the *wA*Δ mutation formed white conidiospores, figure 4.12. Formation of the white spores occurred as it fails to produce the naphthopyrone, YWA1, the precursor of green conidial pigment (Watanabe 1998, Watanabe 1999).

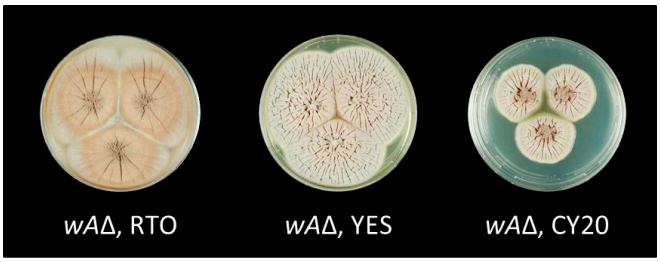

Figure 4.12 The *wA*Δ strain on RTO, YES and CY20 medium.

The compounds resulting from the remaining three PKS gene clusters were originally identified through activation of the gene clusters by controlled expression of the transcription factor gene (Bergmann 2007, Chiang 2009) or by deletion of the *sumO* gene (Szewczyk 2008) and were not expressed under our growth conditions.

The metabolic profiles of the remaining 24 strains were compared to the reference strain on all media to uncover novel genetic links between PKS genes and PKs. The UHPLC-DAD chromatograms were first compared and the interesting peaks were afterwards identified on the LC-TOF-MS. The measured *m/z* was used to perform dereplication by use of the natural product database AntiBase (Laatsch 2010) which contains around 37000 metabolites. The hits were subsequently sorted based on the UV-data and reports in the literature. The novel and linked metabolites were isolated and structure elucidated through NMR analysis. UHPLC-DAD was chosen as the initial analysis based on the conjugated nature of PKs and better separation of metabolites than on the LC-TOF-MS. When a metabolite had been identified in the reference strain and corresponding peak was missing in a deletion strain, it was confirmed by HR-MS data through an extracted ion chromatogram. Through the comparison, several PKs which could be linked to PKS genes were identified; arugosin and shamixanthones (*mdpG*), orsellinic acid (AN7903 and *orsA*) as well as austinol and dehydroaustinol (AN8383) as described in detail below.

4.3.1.1. Identification of the austinol/dehydroaustinol synthase gene

The meroterpenoids austinol and dehydroaustinol and related metabolites were first isolated from *A. ustus* by Simpson and co-workers in 1982 (Simpson 1982) and reported from *A. nidulans* in 2007 (Márquez-Fernández 2007). Austinol and dehydroaustinol are examples of a group of meroterpenoids which Simpson and co-workers through labeling studies showed to be derived from the polyketide 3,5-dimethylorsellinic acid (Simpson 1981, Scott 1986, Geris 2009), however, the genes responsible for the production was not identified.

In this study production of austinol and dehydroaustinol was observed on all the six media used for screening of the deletion library. The structures of austinol and dehydroaustinol were confirmed through LC-TOF-MS and for dehydroaustinol through extraction, purification and NMR analysis. Interestingly we noticed that on RTO five of the single PKS deletion strains, AN0523Δ, *pkbA*Δ (AN6448Δ), AN7022Δ, *ausA*Δ (AN8383Δ) and *adpA*Δ did not produce austinol and dehydroaustinol, figure 4.13 indicating a cross regulation of austinol and dehydroaustinol production involving these five genes. When the rest of the media was examined it was only *ausA* which failed to produce austinol and dehydroaustinol, see figure 4.13 for YES medium.

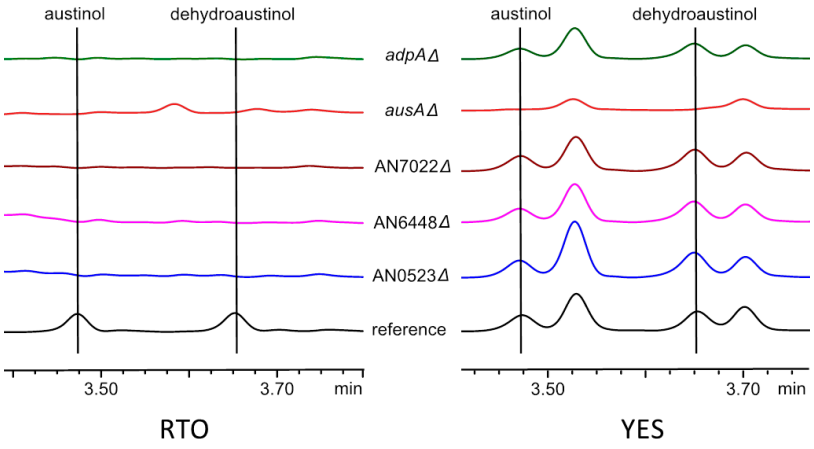

Figure 4.13 UHPLC-DAD chromatograms (210 nm) showing the presence of austinol and dehydroaustinol in AN0523Δ, *pkbA*Δ (AN6448Δ), AN7022Δ, *ausA*Δ (AN8383Δ) and *adpA*Δ compared to the reference strain on RTO and YES medium.

To confirm that the loss of austinol and dehydroaustinol production was directly due to the *ausA* deletion rather than to silencing of another gene caused by chromatin changes provoked by the *orsA* deletion, a point mutation which has been shown to disrupt the enzymatic activity of the PKS production was created (Evans 2008). Like with the *ausA*Δ strain the production of austinol and dehydroaustinol was completely abolished on all six media (data not shown) showing that AusA is directly involved in the production of austinol and dehydroaustinol. To identify the product of AusA we overexpressed the gene by creating a strain which expressed *ausA* controlled by an inducible promoter, *alcA*, in integration site I (Hansen 2011). On inductive medium the LC-TOF-MS analysis showed a large peak eluting at around 6 minutes which was also present in the reference strain in small amounts but not produced in the deletion strain, figure 4.14.

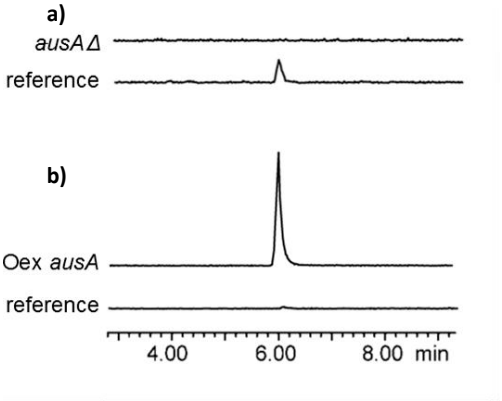

Figure 4.14 Extracted ion chromatograms of 3,5-dimethylorsellinic acid (*m/z* 195 (±0.5 Da) $[M-H]^-$) of **a)** the reference strain and *ausAΔ* on RTO medium and **b)** the reference strain and the *ausA* overexpression strain (Oex) on induction medium (glycerol with threonine).

The metabolite was purified and the structure was elucidated by NMR to be 3,5-dimethylorsellinic acid which is therefore believed to be the first step in the biosynthesis of austinol and dehydroaustinol as shown in figure 2.8 in section 2. This result confirms the results of the labeling experiments performed by Simpson and co-workers 30 years ago (Simpson 1981, Scott 1986). After our publication Lo and co-workers have shown that the conversion of 3,5-dimethylorsellinic acid into austinol and dehydroaustinol is catalyzed by enzymes whose genes are present in two separately located gene clusters (Lo 2012).

4.3.1.2 Linking of arugosin to the monodictyphenone gene cluster

The deletion which gave the most prominent change in metabolite profile was *mdpG*Δ which, in an earlier study by Bok and co-workers, had been activated through epigenetic modulation of the chromatin landscape by the deletion of *cclA* resulting in the linking of eight emodin analogues to *MdpG* (Bok 2009, Chiang 2010b). Figure 4.15 show a segment of the UHPLC chromatogram of *mdpG*Δ and the reference strain on RTO medium where the largest differences are observed.

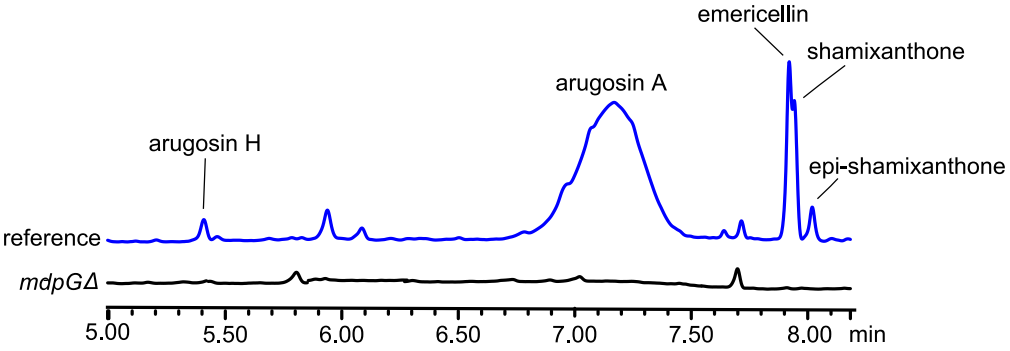

Figure 4.15 UHPLC-DAD chromatogram (210 nm) from four to eight minutes of the reference strain (bottom) and *mdpG*Δ (top) on RTO medium. The deletion eliminates the production of arugosin H, arugosin A, emericellin, shamixanthone and epi-shamixanthone as well as some unidentified peaks.

Several peaks disappeared, the most prominent being the broad peak which elutes at 7.2 minutes. This compound had a characteristic UV-spectrum, figure 4.16a, and through analysis of the adducts present in the MS-spectrum, figure 4.16b, the peak was identified to have an *m/z* 425.214 for $[M+H]^+$. A search in the AntiBase database (Laatsch 2010) tentatively gave 32 possible hits based on the molecular ion. To narrow the possible number of candidates the fragment pattern was investigated and an ion of *m/z* 357.161 was also observed which corresponds to $[M+H-C_5H_8]^+$ where C_5H_8 could correspond to a prenyl group. This information excluded metabolites of the 32 candidates to four, arugosin A, B, C and variecoxanthone C since they were the only compounds containing a labile prenyl group. The arugosins had the same UV-chromophore as reported in the literature (Ballantine 1970, Kawahara 1988a).

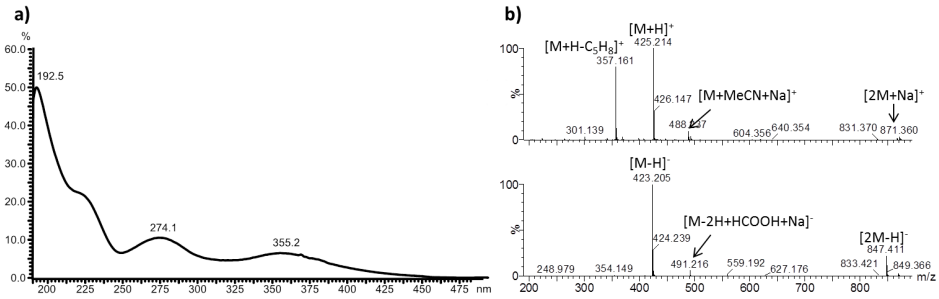

Figure 4.16 a) UV-spectrum of arugosin A **b)** MS-spectrum of arugosin A, top: ESI+ bottom: ESI-.

A large scale extraction of the reference strain on RTO medium was made for isolation of arugosin A. The NMR data were in agreement with the data reported in the literature (Kawahara 1988a) of the hemiacetal form of arugosin A except that in DMSO-d_6 the equilibrium is shifted completely to the open form. In contrast the NMR data, in methanol-d_4, figure 4.17, showed that arugosin A exists in an equilibrium between the open and closed form, explaining the broad peak observed in the UHPLC-chromatograms. Arugosin A had not previously been reported from *A. nidulans* but from *A. rugulosus* and *A. silvaticus* (Ballantine 1970, Kawahara 1988a).

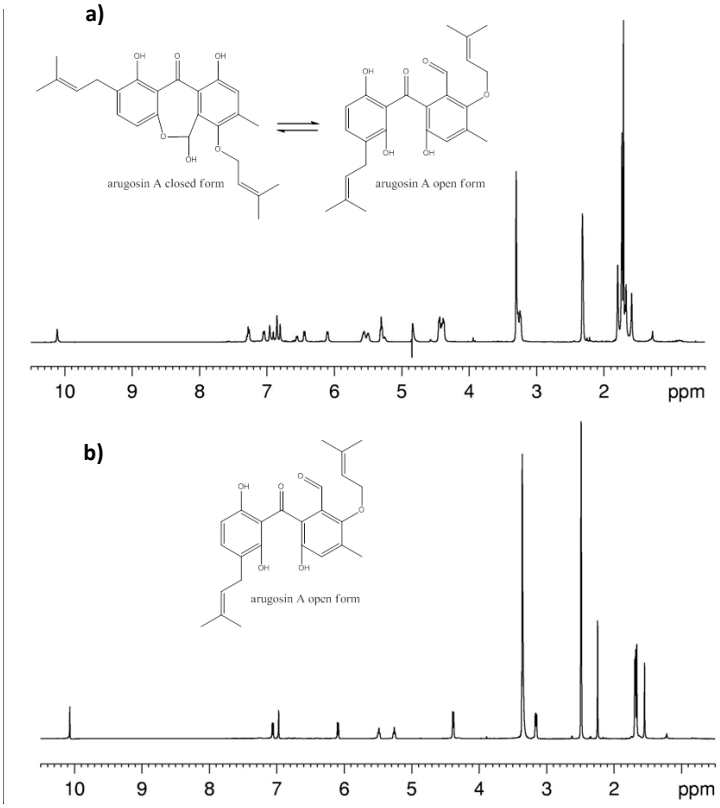

Figure 4.17 ^{1}H-NMR spectrum of arugosin A in **a)** methanol-d_4 and **b)** DMSO-d_6.

Further investigations of the metabolites disappearing in the *mdpG*Δ strain revealed a minor peak which could be assigned as a mono-prenylated arugosin with a $[M+H]^+$ of *m/z* 357.131, arugosin H, figure 4.18. The MS data did not show fragments due to loss of a prenyl, as in the case of arugosin A, indicating that the peak is a precursor to arugosin A and that arugosin H is C-prenylated since this is less labile than an O-prenyl. Arugosin H have along with arugosin G been reported from *Emericella nidulans* var. *acristata* (Krajl 2006) Emericellin and shamixanthone have previously been reported from *A. nidulans* (Márquez-Fernández 2007) and labeling studies have shown that the arugosins are precursors for emericellin and the shamixanthones but have not established a genetic link (Ahmed 1992), as done in this study. A recent paper of Simpson (Simpson 2012) have elaborated on the information published, both through chemical and genetic studies and proposed a biosynthesis of the shamixanthones combining recent findings with the information from the biosynthesis established through labeling studies 20 years ago (Ahmed 1992).

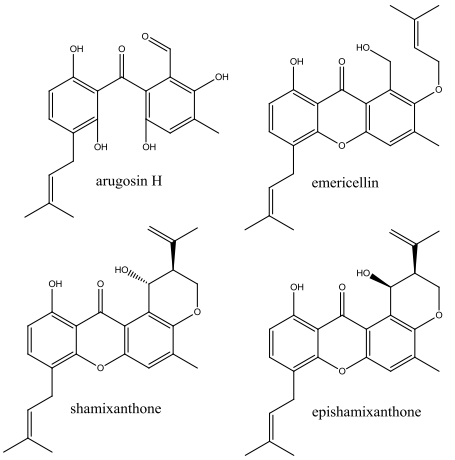

Figure 4.18 Structures of arugosin H, emericellin, shamixanthone and epishamixanthone.

The *mdpG* gene cluster is responsible for the biosynthesis of a family of structurally similar compounds which is not unusual (Walsh 2002, Kroken 2003, Frisvad 2004b, Amoutzias 2008).

4.3.1.3. Linking of orsellinic acid derived metabolites to the orsellinic acid gene cluster to and AN7903

One of the most studied PK families in *A. nidulans* is the products derived from the PK of the PKS encoding *orsA*, orsellinic acid. The metabolites F-9775A and F-9775B, lecanoric acid, gerfelin, C10-deoxy-gerfelin, diorcinol, orcinol cordyol C, violaceol I, violaceol II, sanghaspirodin A and sanghaspirodin B have all been shown to be linked to *orsA* (Bok 2009, Schroeckh 2009, Sanchez 2010, Nahlik 2010, Nützmann 2011, Scherlach 2011).

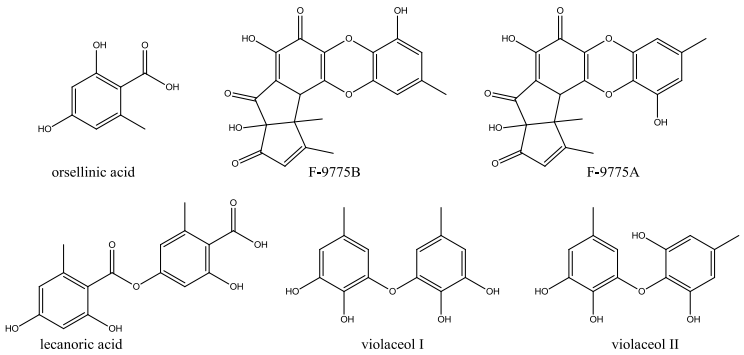

Figure 4.19 Structures of orsellinic acid, lecanoric acid, F-9775A, F9775B, violaceol I, and violaceol II.

In this study orsellinic acid, lecanoric acid, F-9775A, F-9775B, violaceol I and violaceol II, figure 4.19, were present in the extracts from the reference strains on the complex media and the production was abolished in the *orsA*Δ strain. Interestingly the metabolites which disappear in the *orsA*Δ strain also disappear in the AN7903Δ strain. This result does not contradict the original assignment of *orsA* as the PKS gene responsible for production of orsellinic acid. AN7903 is larger than *orsA* and contains a methyl-transferase domain, which is not required for orsellinic acid production. Schroeckh *et al.* (Schroeckh 2009) observed that both AN7903 and *orsA* were upregulated when orsellinic acid was induced by co-cultivation with *Streptomyces hygroscopicus*, which could indicate either cross-talk between the two clusters or induction of expression of both clusters due to interactions. What appears to be trace amounts of orsellinic acid could be detected in both the AN7903Δ and the *orsA*Δ strains. The source of the orsellinic acid remains elusive but could be produced by other PKSs. Ahuja and co-workers reported the production of orsellinaldehyde from PkfA (Ahuja 2012). It is interesting to note that in most of the strategies for activating secondary metabolite production through epigenetic modifications, both chemical and molecular, in *A. nidulans* the products of the orsellinic acid cluster seems to be activated.

4.3.2 Characterization of the 3-methylorsellinic acid gene cluster

Aspergillus nidulans has been shown to produce at least four variants of orsellinic acid; orsellinic acid (OrsA (Schroeckh 2009)), 3-methylorsellinic acid (Hansen 2011), 3,5-dimethylorsellinic acid (AusA (Nielsen 2011)) and orsellinic acid aldehyde (PkfA (Ahuja 2012)). The detection of 3-methylorsellinic acid reported by Hansen *et al.* (Hansen 2011) led us to examine the extracts of the reference strain used for creation of the PKS deletion library described in section 4.3.1. The extracts of the deletion library was analyzed on the LC-TOF-MS; however, due to the better mass accuracy and sensitivity of the newly acquired UHPLC-TOF-MS this instrument was used for the extract analysis. We found 3-methylorsellinic acid to be produced in trace amounts on CYA, CY20 and RT medium and of the 32 deletions it was only in AN6448Δ (*pkbA*Δ) that production failed. Figure 4.20 shows EICs of a 3-methylorsellinic acid $[M+H]^+$ (*m/z* 183.06483±0.001) standard, and the reference and *pkbA*Δ strains cultivated on CYA medium. This data corresponds to the recently published findings by Ahuja and co-workers that the PKS PkbA is required to produce 3-methylorsellenic acid along with cichorine (Ahuja 2012).

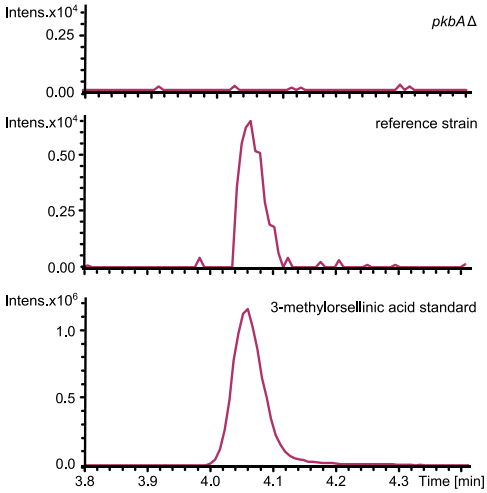

Figure 4.20 EIC of 3-methylorsellinic acid $[M+H]^+$ (calc. *m/z* 183.06483±0.001) (UHPLC-TOF-MS)) of a standard, the reference and *pkbAΔ* strains on CYA medium cultivated for seven days at 37°C.

As production of 3-methylorsellinic acid was relatively low under our cultivation conditions we searched the genome sequence for neighboring genes predicted to encode for transcriptional regulation. AN6446 was predicted to have DNA binding activity and we speculated that this could be a cluster-specific transcription factor and constructed an AN6446 overexpression strain (AN6446-Oex) in IS1 (Hansen 2011). The overexpression of AN6446 clearly had an effect on *A. nidulans*, since the AN6446-Oex compared to the reference displayed a decrease in pigmentation of conidia to a dusty green appearance and a light brown center of the colony after seven days growth on MM, figure 4.21.

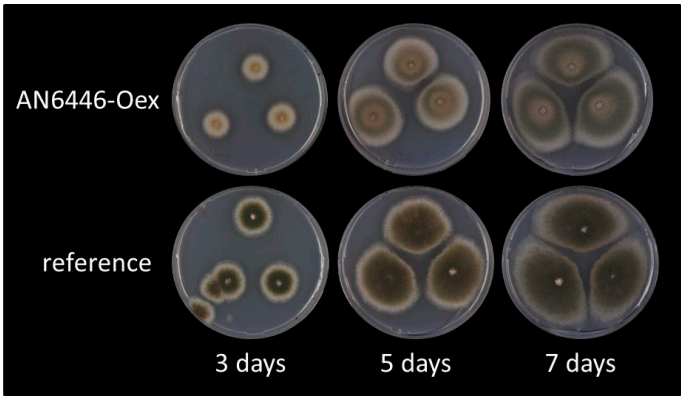

Figure 4.21 The reference strain compared to the AN6446-Oex strain cultivated on MM at 37°C for three, five days, and seven days.

To analyze the metabolite production micro-extraction was performed (Frisvad 1987, Smedsgaard 1997) and the extracts were analyzed by UHPLC-TOF-MS, figure 4.22. The strains were extracted

after three, five, and seven days to test the effect of growth time on the production of secondary metabolites.

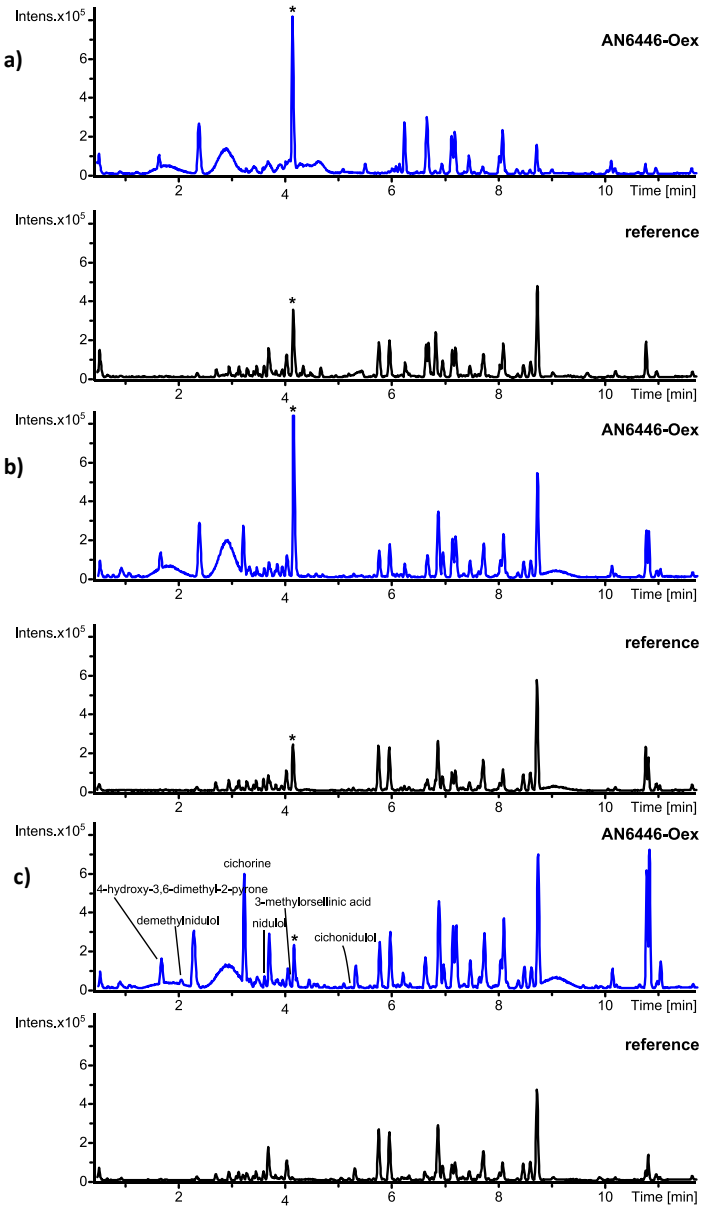

Figure 4.22 UHPLC-TOFMS ESI+ BPC of the micro-extracts of the reference and AN6446-Oex strains cultivated on MM media at 37°C for **a)** three, **b)** five, and **c)** seven days. The metabolites isolated in this study are marked. *This metabolite is the sideophore triacetylfusarine.

The UHPLC-TOF-MS analysis revealed several new peaks appearing on the AN6446-Oex strain compared to the reference indicating that the overexpression had indeed turned on the likely 3-methylorsellinic acid biosynthetic pathway. 3-methylorsellinic acid was present in trace amounts in the AN6446-Oex strain. The metabolic profile seemed to be rather similar for the three different days although new peaks were apparently more dominant after seven days and the peak at 4.1 which was identified to be the siderophore triacetylfusarine was less dominant. Consequently the strains were grown for seven days throughout the study. Moreover this showed that MM medium was a suitable growth medium for isolation of candidate metabolites.

A large scale extract of 200 petri dishes carrying the AN6446-Oex strain was thus prepared for isolation and structure elucidation of several metabolites. In figure 4.23, the UHPLC-TOF-MS ESI+ BPC of the large extract compared to the micro-extracts is shown.

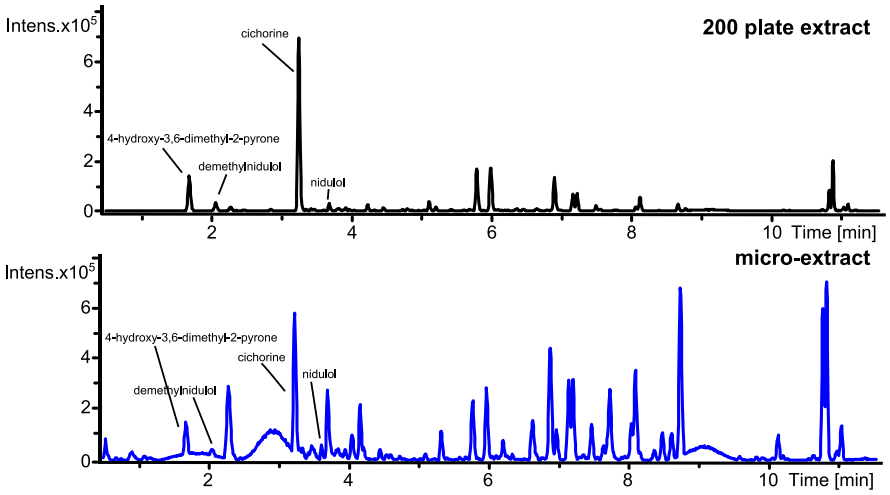

Figure 4.23 UHPLC-TOF-MS ESI+ BPC of the micro-extract (bottom) and 200 plate extract (top) of the overexpression of AN6446-Oex strain cultivated on MM medium for seven days at 37°C.

Sample preparations and cultivation conditions of a large number of plates could influence the loss of metabolites observed; however, further analysis revealed more metabolites than visible in the chromatogram as cichorine were present in very high concentrations. Isolation and structure elucidation revealed the presence of several metabolites; cichorine, demethylnidulol and 4-hydroxy-3,5-dimethyl-2-pyrone and two dimers of cichorine and nidulol/demethylnidulol, named cichonidulol and demethylcichonidulol figure 4.24. Throughout the study several deletion strains were constructed where some of these will not be mentioned further; however, nidulol and 3-methylorsellinic acid was isolated from two of these, AN6444Δ and AN6445Δ respectively. Cichorine and 3-methylorsellinic was recently reported to be the products of the overexpression of the AN6448 PKS (Ahuja 2012). Cichorine has previously been isolated from *A. silvaticus* (Kawahara 1988b) and *Alternaria cichorii* (Stierle 1993) whereas nidulol have been reported from *A. nidulans* (Aucamp 1968), *A. silvaticus* (Fujita 1984), and *Emericella desertorum* (Nozawa 1987).

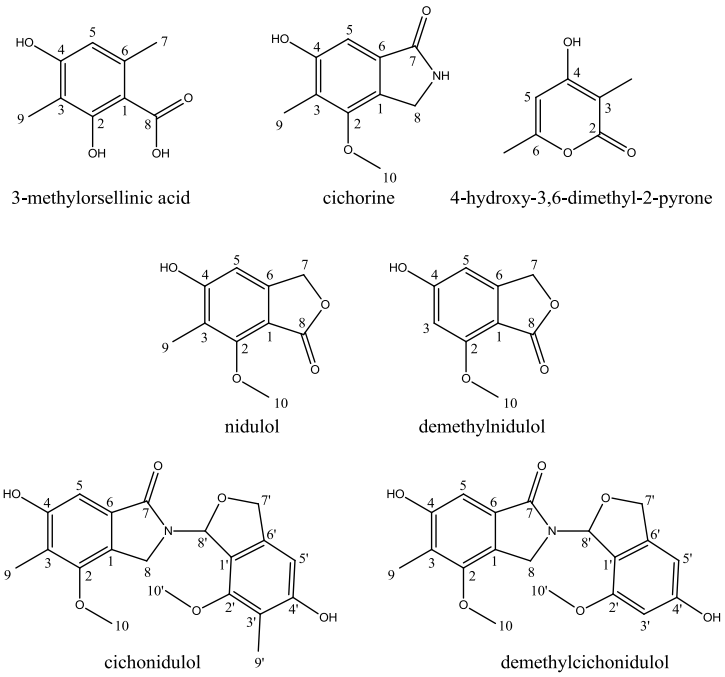

Figure 4.24 Structures of metabolites isolated and elucidated throughout this study. 3-methylorsellinic acid, cichorine, demethylcichorine, nidulol, demethylnidulol, cichonidulol, demethylcichonidulol, 4-hydroxy-3,6-dimethyl-2-pyrone.

The structures were elucidated using 2D NMR spectroscopy, where especially heteronuclear HSQC and HMBC spectra were extensively used due to the absence of proton-proton couplings and low proton density of the metabolites. For further details on NMR analysis and 1D spectra see paper 5. In addition the results were in accordance with chemical shift values reported in literature for cichorine (Monreau 2005), 3-methylorsellinic acid (Ahuja 2012), demethylnidulol (El-Feraly 1985), and 4-hydroxy-3,6-dimethyl-2-pyrone (Savard 1994b).

The resemblance of the molecular formulas of cichorine ($C_{10}H_{11}NO_3$) and nidulol ($C_{10}H_{10}O_4$) and initial comparison of the ^{1}H-spectra that suggested these metabolites could be related. The main issue in structure elucidation of these two metabolites was whether the carbonyl was situated on C_7 or C_8. The problem was solved by comparison of the carbon chemical shift of cichorine to the shifts reported in the literature obtained after total synthesis of cichorine (Moreau 2005). For all the metabolites key HMBC correlations from H_5 to C_7 and/or C_8 and from H_7/H_8 to the carbons present in the aromatic ring, figure 4.25, aided in the structure elucidation. A NOESY correlation between H_8 and H_{10} in cichorine which were missing in nidulol confirmed the difference in the two structures.

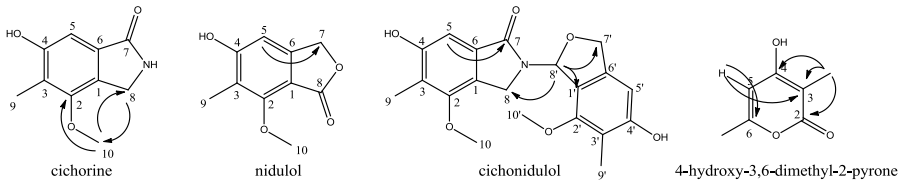

Figure 4.25 Key HMBC correlations of cichorine, nidulol, cichonidulol and 4-hydroxy-3,6-dimethyl-2-pyrone.

As these metabolites are biosynthetic derivatives of 3-methylorsellinic acid it was expected that the carbonyl would be present at C_8. These structures indicate that more enzymatic activities are involved in the biosynthesis due to the oxidations at C_7.

The UV spectrum of demethylnidulol was identical to the one of nidulol and the molecular formula $C_9H_8O_4$ showed that the difference between the two metabolites was a carbon and two protons. Through analysis of the NMR-spectra it was confirmed that the two metabolites were related and that the difference was the methylation of C_3 in nidulol which is not present in demethylnidulol.

Table 4.1 ^{13}C-chemical shifts (ppm) of 3-methylorsellinic acid, cichorine, nidulol, demethylnidulol, and cichonidulol. All data were obtained in DMSO-d_6 and referenced to the solvent peak at 39.5 ppm.

ID	3-methyl-orsellinic acid	Cichorine	Nidulol	Demethyl-nidulol	Cichonidulol
1/1'	103.7/-	123.1/-	107.2/-	92.9/-	121.3/116.1
2/2'	163.0/-	153.6/-	157.5/-	159.6/-	153.6/153.8
3/3'	107.7/-	118.9/-	117.5/-	101.1/-	120.5/115.3
4/4'	159.7/-	156.3/-	162.7/-	168.8/-	156.9/158.1
5/5'	109.9/-	102.9/-	103.0/-	103.2/-	103.4/102.4
6/6'	139.4/-	131.9/-	148.6/-	151.4/-	131.0/139.5
7/7'	23.4/-	169.8/-	68.2/-	66.9/-	167.1/71.7
8/8'	173.8/-	43.1/-	168.5/-	178.1/-	43.2/83.5
9/9'	7.9/-	9.1/-	8.2/-	-/-	9.3/8.6
10/10'	-/-	58.9/-	53.9/-	53.9/-	59.0/59.2

Through analysis of the large scale AN6446-Oex extract we noticed two small peaks eluting around five minutes which had UV-spectra that resembled those of nidulol and cichorine. These metabolites were present in small amounts in the large extract and based on the molecular formular of these metabolites $C_{20}H_{21}NO_6$ and $C_{19}H_{19}NO_6$ we speculated whether they could be dimers of cichorine, 3-methylorsellinic acid, nidulol or demethylnidulol through condensation and formation of e.g. an ester as seen with the formation of lecanoric acid in the orsellinic acid pathway (Schroeckh 2009). 2.0 mg of $C_{20}H_{21}NO_6$ and 0.6 mg of $C_{19}H_{19}NO_6$ were isolated from the extract and the structure of $C_{19}H_{19}NO_6$ was elucidated based on 2D NMR analysis to be a dimer of cichorine and nidulol, named cichonidulol. Analysis of the HMBC spectrum revealed that the link of the two molecules was not through an ester formation but interestingly through a C-N bond formed apparently with the loss of a carbonyl in nidulol. A search of the literature showed that cichonidulol and demethylnidulol were novel metabolites with a new base carbon skeleton. The metabolite which showed the closest resemblance was the plant metabolite, capaurine, which

contains the C-N condensation bond between two ringsystems; however, the nitrogen containing ring is a six membered ring and the substitution patterns of are quite different (Manske 1945).

Table 4.1 lists the ^{13}C-chemical shifts of the above mentioned isolated metabolites where it is seen that the largest differences in shift values occur around at C_1 and C_6 which differs depending on the position of the carbonyl.

The final metabolite isolated was 4-hydroxy-3,6-dimethyl-2-pyrone whose chemical shifts were in accordance with shifts reported in the literature (Savard 1994b). This metabolite is quite different from the above mentioned having a completely different carbon skeleton. Consequently this metabolite was either a product of *pkbA* or we could have activated another PKS encoding gene.

To verify that AN6446 had an activator effect on the surrounding genes, relative gene expression measurement by qRT-PCR analysis was performed. A deletion of AN6446, which displayed the same phonotype, as the reference was added to the analysis with the hypothesis that this would have the inverse effect from the overexpression strain minimizing the risk of picking false cluster members. AN6446-Oex and AN6446Δ strains compared to the reference strain was performed for all predicted genes in the range AN6435-AN6457, figure 4.26.

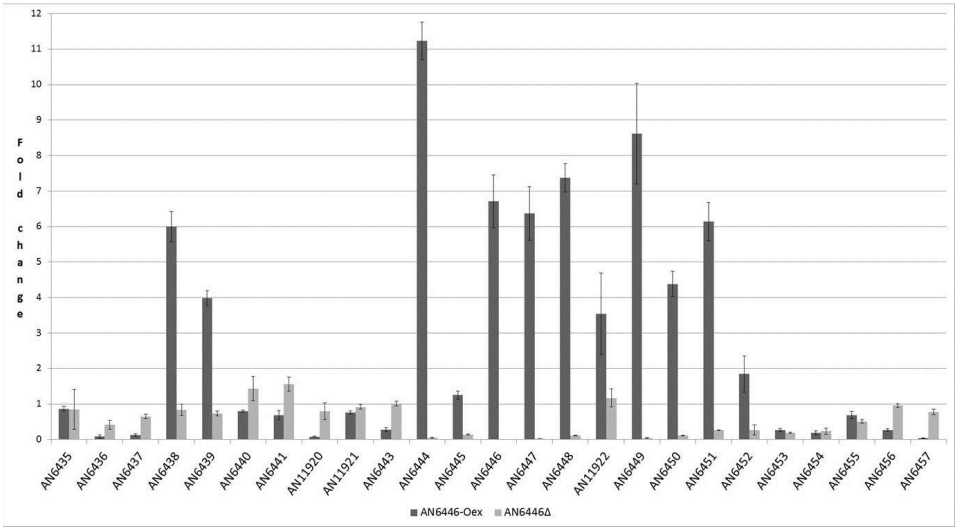

Figure 4.26 Results of the qRT-PCR analysis of AN6446-Oex and AN6446Δ on the genes from AN6435-AN6457 compared to the reference strain. An expression of 1 means unaltered expression, over 1 means higher expression and below 1 means lower expression. These data show that AN6444, AN6446, AN6447, AN6448, AN6449, AN6450 and AN6451 are upregulated in the overexpression strain and downregulated in the deletionstrain indicating that the *pkbA* cluster contains these genes.

The average fold change of three runs of all 25 genes in the AN6446Δ and AN6446-Oex strains compared to the reference is shown in figure 4.26. A level of one means unaltered expression whereas a level below means lower expression and above means higher. For a gene to be a putative cluster member one criterion was to have fold change above one for the AN6446-Oex

and close to zero for the AN6446Δ strains. Deviation from one or both of these criteria made us disregard the candidate as a cluster member based on the gene expression data.

Based on this analysis the values of the genes AN6444, AN6447, AN6448, AN6449, AN6450 and AN6451 along with AN6446 were considered as cluster candidates. To verify the results and to determine the biosynthetic role of the enzymes encoded by these genes we constructed deletions of all the 25 initial candidate genes in the AN6446-Oex background. The six most distant genes of AN6446 were deleted in triplets (AN6435-AN6437, AN6438-AN6440, AN6452-AN6454 and AN6455-AN6457) and the remaining as singular mutants.

To see whether AN6446 had regulatory effects on secondary metabolite production outside the cluster, a full cluster deletion (AN6435-AN6457) in the overexpression strain was constructed as well. Lastly to confirm the role of PkbA as the 3-methylorsellinic acid producing PKS an overexpression of this gene was constructed.

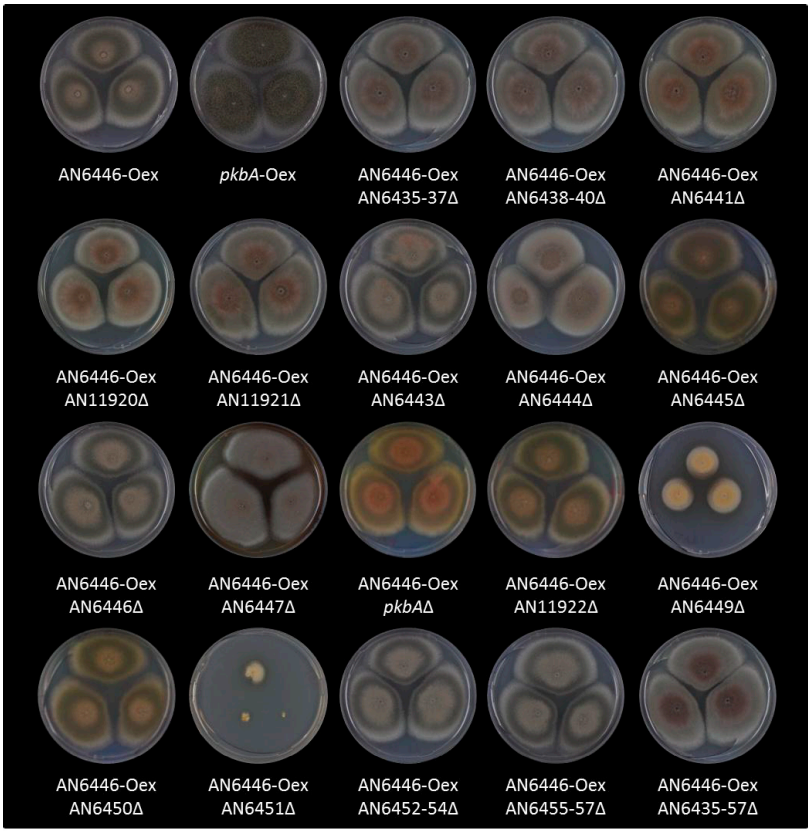

Figure 4.27 The appearance of the AN6446-Oex, *pkbA*-Oex, AN6446-Oex AN6435-6437Δ, AN6446-Oex AN6438-6440Δ, AN6446-Oex AN6441Δ, AN6446-Oex AN11920Δ, AN6446-Oex AN11921Δ, AN6446-Oex AN6443Δ, AN6446-Oex AN6444Δ, AN6446-Oex AN6445Δ, AN6446-Oex AN6446Δ, AN6446-Oex AN6447Δ, AN6446-Oex AN6448Δ, AN6446-Oex AN11922Δ, AN6446-Oex AN6449Δ, AN6446-Oex AN6450Δ, AN6446-Oex AN6451Δ, AN6446-Oex AN6452-6454Δ, AN6446-Oex AN6455-6457Δ and AN6446-Oex AN6435-6457Δ strains cultivated on MM medium for seven days at 37°C.

The phenotypes of the constructed strains can be compared in figure 4.27. The deletion of the genes, predicted to form the gene cluster of PkbA, indeed stood out from the others in the phenotype display. The phenotypes varied greatly, indicating altered metabolism in the respective strains. To investigate which metabolites originated from this cluster and if correlated with the phenotype of the mutant strains micro-extraction was performed (Frisvad 1987, Smedsgaard 1997) and the extracts were analyzed by UHPLC-TOF-MS. In figure 4.28, 4.29 and 4.30 ESI+ BPC of all the extracts can be seen.

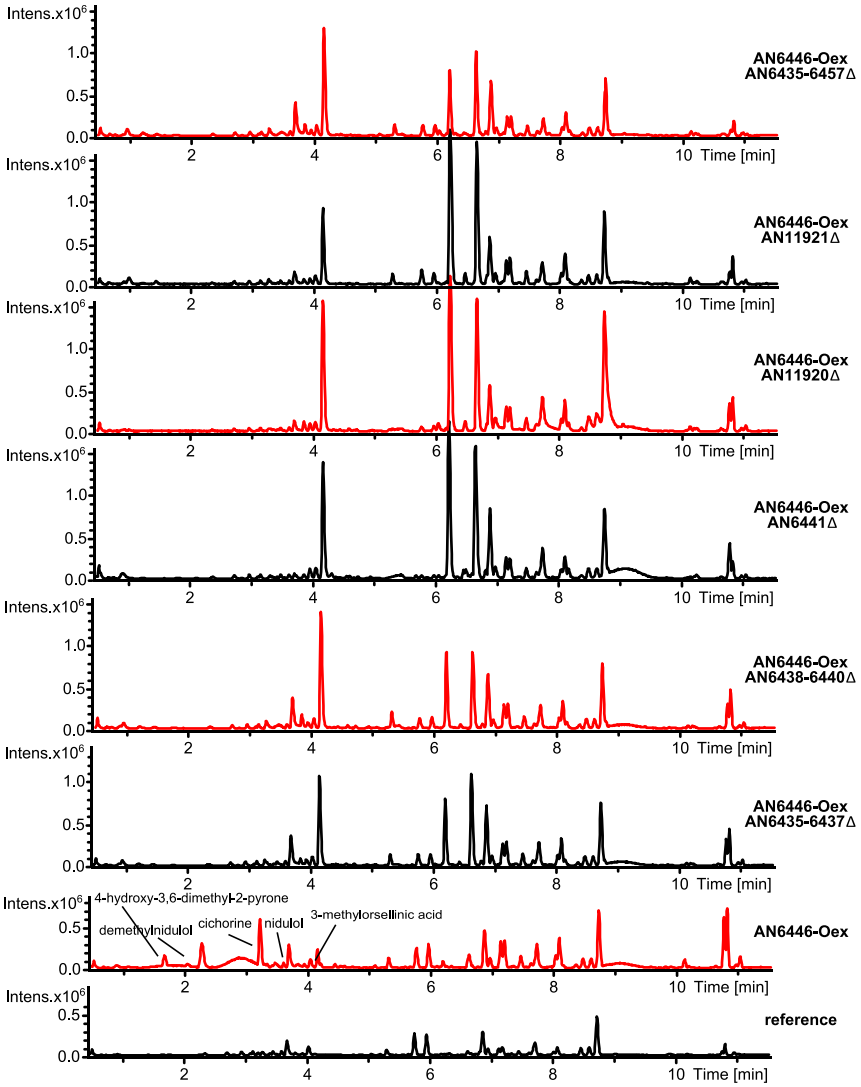

Figure 4.28 UHPLC-TOF-MS ESI+ BPC of the micro-extracts of the (from bottom to top) reference AN6446-Oex, AN6446-Oex AN6435-6437Δ, AN6446-Oex AN6438-6440Δ, AN6446-Oex AN6441Δ, AN6446-Oex AN11920Δ, AN6446-Oex AN11921Δ, AN6446-Oex AN6435-6457Δ strains cultivated on MM medium for seven days at 37°C. The metabolites identified in the AN6446-Oex strain are missing in all the deletions.

In figure 4.28 the strains where all the metabolites of the cluster had disappeared and the AN6446-Oex strain are depicted. In all the deletions from AN6435 to AN11921 all the key metabolites shown in the AN6446-Oex strain are missing. Since the qRT-PCR data did not support these belonging to the cluster we speculate that this links to local chromosomal aberration due to change in the strain. Inactivating one or some of these genes instead with point mutations would test this hypothesis.

Moreover, the phenotypes of these strains were very similar as the metabolic profiles were. The strains all showed the same differences from the reference strain, namely the massive production of the siderophore triacetylfusarinine.

In the whole cluster deletion strain, AN6446-Oex AN6435-6457Δ, all metabolite production is eliminated including 4-hydroxy-3,6-dimethyl-2-pyrone strongly indicating that this metabolite is also a product of the cluster. However, eliminated production may reflect the deletions of AN6435 to AN11921. A cluster deletion from AN6444 to AN6451 would be an alternative. A thorough investigation of the PKS deletion library described in section 4.3.1 revealed trace amounts of 4-hydroxy-3,6-dimethyl-2-pyrone on CYA medium in the reference strain. The 32 deletions on CYA medium were analyzed for 4-hydroxy-3,6-dimethyl-2-pyrone and it was only in *pkbA* that production failed.

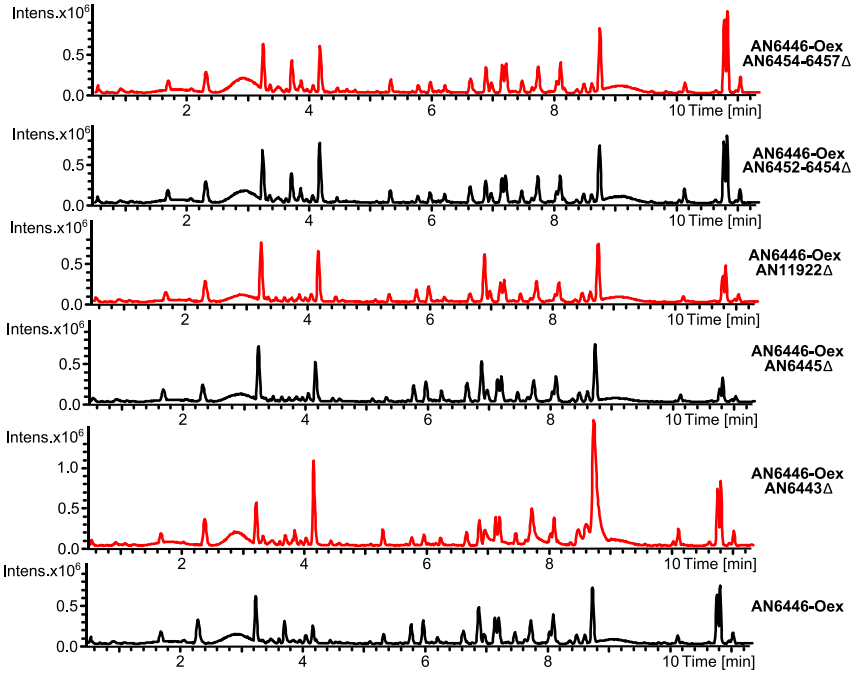

Figure 4.29 UHPLC-TOF-MS ESI+ BPC of the micro-extracts of the (from bottom to top) AN6446-Oex, AN6446-Oex AN6443Δ, AN6446-Oex AN6445Δ, AN6446-Oex AN11922Δ, AN6446-Oex AN6452-6454Δ, AN6446-Oex AN6454-6457Δ strains cultivated on MM medium for seven days at 37°C. The figure illustrates that these genes are not involved in the *pkbA* gene cluster in agreement with the qRT-PCR data.

The extracts depicted in figure 4.29 are the strains of which the chromatograms mimic the profile of AN6446-Oex. The colonies of these strains in figure 4.27 resembled the overexpression strain, and the results are in agreement with the qRT-PCR data, which excluded these genes to be part of the 3-methylorsellinic acid gene cluster.

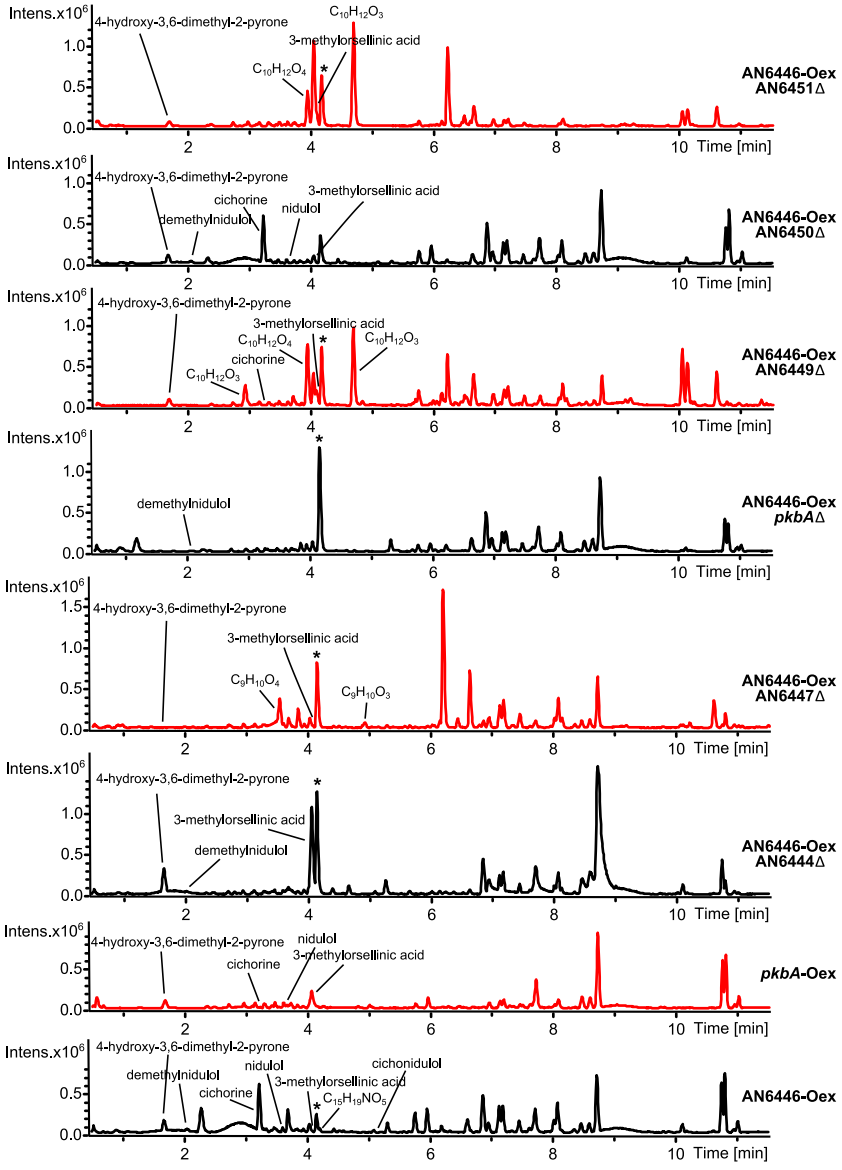

Figure 4.30 UHPLC-TOF-MS ESI+ BPC of the micro-extracts of the AN6446-Oxe, AN6448-Oex, AN6446-Oex AN6444Δ, AN6446-Oex AN6446Δ, AN6446-Oex AN6447Δ, AN6446-Oex *pkbA*Δ, AN6446-Oex AN6449Δ, AN6446-Oex AN6450Δ and AN6446-Oex AN6451Δ strains cultivated on MM medium for seven days at 37°C. *This metabolite is the sideophore triacetylfusarine. The figure illustrated that these genes indeed are part of the 3-methylorsellinic acid gene cluster.

The BPC chromatograms of the micro-extracts of the deletion strains predicted through the qRT-PCR analysis to belong to the 3-methylorsellinic acid cluster are depicted in figure 4.30. Detection of the metabolites isolated in this study are listed in table 4.2 along with there are several additional peaks appearing in the chromatograms; however, the structures of these have not yet been identified.

Table 4.2 Detection of metabolites (through EIC^+) in the micro-extracts of the deletion and overexpression strains constructed and identified as belonging to the 3-methylorsellinic clusters in this study; (from bottom to top) AN6446-Oex, AN6448-Oex, AN6446-Oex AN6444Δ, AN6446-Oex AN6447Δ, AN6446-Oex *pkbA*Δ, AN6446-Oex AN6449Δ, AN6446-Oex AN6450Δ, AN6446-Oex AN6451Δ. Parenthesis indicates that the metabolites are present in trace amounts. [a]strain having AN6446-Oex allele. *A metabolite eluting close to cichorine with a small mass difference makes further analysis needed for clarification.**Eluting at 2.9 minutes.***Eluting at 4.7 minutes.

Metabolite	AN6446 -Oex[a]	*pkbA* -Oex[a]	AN6444Δ[a]	AN6447Δ[a]	*pkbA*Δ[a]	AN6449Δ[a]	AN6450Δ[a]	AN6451Δ[a]
3-methyl-orsellinic acid	(+)	+	+	+	-	+	(+)	+
Cichorine*	+	+	-	-	-	-	+	-
Nidulol	+	+	-	-	-	-	+	-
Demethyl-nidulol	+	-	+	-	(+)	-	+	-
Cichonidulol	(+)	-	-	-	-	-	-	-
Demethyl-cichonidulol	-	-	-	-	-	-	-	-
4-hydroxy-3,6-dimethyl-2-pyrone	+	+	+	(+)	-	+	+	+
$C_9H_{10}O_3$	-	-	-	+	-	-	-	-
$C_9H_{10}O_4$	-	-	-	+	-	(+)	-	(+)
$C_{10}H_{12}O_3$**	-	-	-	-	-	+	-	-
$C_{10}H_{12}O_3$***	+	-	-	-	-	+	-	+
$C_{10}H_{12}O_4$	-	-	-	-	-	+	-	+
$C_{15}H_{19}NO_5$	+	(+)	-	-	-	+	+	-

In the deletion of *pkbA* in the AN6446-Oex strain the isolated metabolites are all, except demethylnidulol, missing confirming that these metabolites are part of the 3-methylorsellinic acid gene cluster. Demethylnidulol was detected in trace amount and could be due to the conversion of orsellinic acid into the product. A double deletion strain of *orsA* and *pkbA* could verify this hypothesis.

AN6450 is predicted to encode an oxidoreductase, and showed in the qRT-PCR analysis to be regulated by AN6446; however, the metabolite profile of AN6446-Oex AN6450Δ was equal to that of AN6446-Oex indicating that either it does not take part in the biosynthesis, or the product of this enzymatic step was undetected. Interestingly, AN6451 is predicted to encode a transporter of the Major Facilitator Superfamily and this deletion mutant is heavily impared in growth. This indicated that some compartmentalization of the biosynthesis may occur and failure to transport either 3-methylorsellinic acid or 4-hydroxy-3,6-dimethyl-2-pyrone, or even other products in the

pathway may be toxic for the fungus, at least under the artificial conditions that overexpression of AN6446 offers.

Table 4.3 Predicted function of the genes identified as belonging to the 3-methylorsellinic acid cluster.

Gene	Predicted function
AN6444	NRPS-like
AN6446	Transcription factor
AN6447	*O*-methyltransferase
pkbA	PKS
AN6449	Cytochrome P450
AN6450	Oxidoreductase
AN6451	Transporter

Based on the metabolic profile of the deletion strains a biosynthetic pathway from 3-methylorsellinic acid to cichonidulol is proposed, figure 4.31. 4-hydroxy-3,6-dimethyl-2-pyrone disappears in the AN6446-Oex *pkbA*Δ strain and are only present in trace amounts in the AN6446-Oex AN6447Δ strain. As oppose to 3-methylorsellinic acid the polyketide backbone seems to be C_6 and not C_8 and may be a shunt of PkbA. If the methylation pattern in the assembly of the polyketide backbones of 3-methylorsellinic acid and 4-hydroxy-3,6-dimethyl-2-pyrone were the same one would expect the latter to be methylated at C_5 and not C_3 as is observed based on careful investigation of the 2D NMR-spectra. This shows that there are several differences between the assembly of the two metabolites. Other metabolites with the same UV-spectrum as 4-hydroxy-3,6-dimethyl-2-pyrone were detected in the deletion strains but have not yet been isolated. Ahuja and co-workers (Ahuja 2012) isolated two products of the PkgA enzyme, dehydrocitreoisocoumarin and 6,8-dihydroxy-3-(2-oxopropyl)-isocoumarin where the difference of the polyketide backbone also was the incorporation of one less Mal-CoA in the latter.

The first step of the biosynthesis is likely to be oxidation and reduction of 3-methylorsellinic acid. The proposed intermediates are the 3-methylorsellinic acid in which the carboxylic acid has been reduced to an aldehyde ($C_9H_{10}O_3$) and the 6-methyl oxidized ($C_9H_{10}O_3$) compound. Due to the appearance of metabolites identified by LC-MS to have these molecular formulas in the AN6447Δ strain the next step is proposed to be *O*-methylation of the 2-OH catalyzed by the enzyme encoded by AN6447. This metabolite could then undergo ring closure to form nidulol. The C_7-carbonyl of nidulol, silvaticol, has also been reported in the literature isolated from *A. silvaticus* (Fujita 1984) and Kawahara and co-workers (Kawahara 1988b) suggest quadrilineatin as the intermediate before ring closure thereby explaining that both metabolites nidulol and silvaticol are present in *A. silvaticus*. Neither silvaticol nor quadrilineatin have been detected in any of the examined extracts yet.

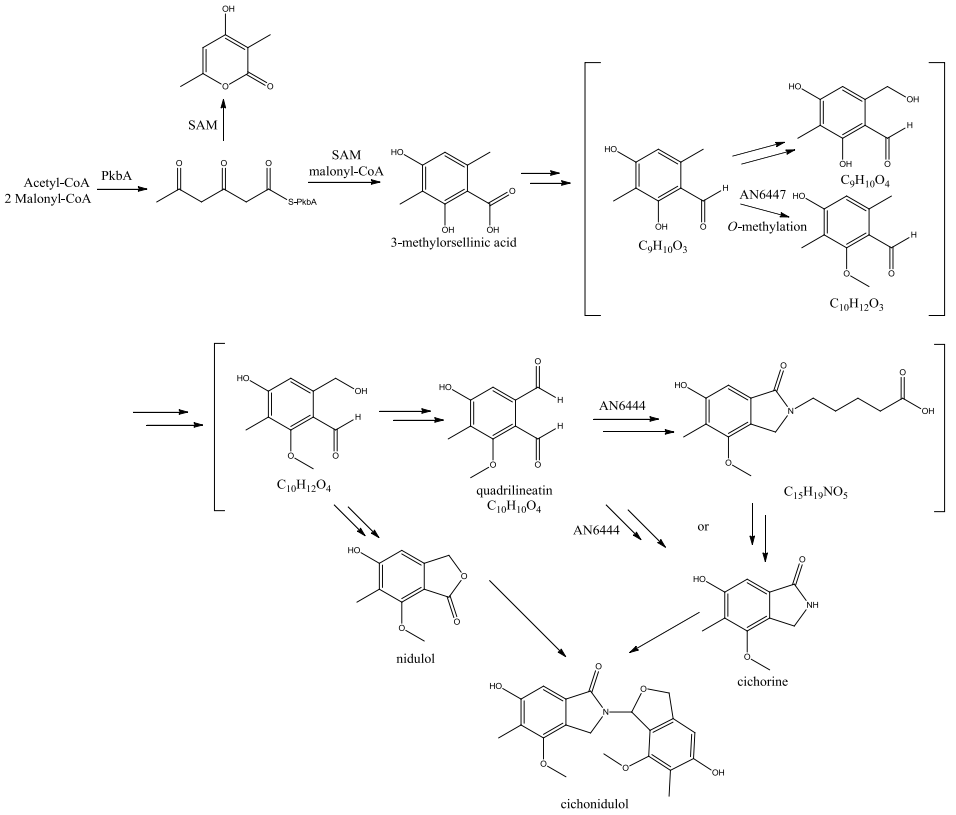

Figure 4.31 Proposed biosynthetic route of the elucidated metabolites of the *pkbA* cluster. The metabolites in brackets are proposed intermediates which have been detected through MS-analysis except for the dialdehyde ($C_{10}H_{10}O_4$) which have not been detected.

The metabolic profile of the AN6446-Oex AN6449Δ and AN6446-Oex AN6451Δ appear to be similar. Several peaks appear in these two deletions where the molecular formula for one of these is equal to the proposed methylated product of AN6447 ($C_{10}H_{12}O_4$) indicating that these enzymes are involved in the next steps of the biosynthesis. The roles for these two enzymes in the biosynthesis are still unknown but identification of the intermediates could provide helpful answers. AN6449 encodes for a cytochrome P450 which could be responsible for the oxidation of the $C_{10}H_{12}O_4$ to quadrilineatin proposed in figure 4.31 which could then undergo further modifications to cichorine.

In the AN6444Δ strain the production of several metabolites have terminated including cichorine and other nitrogen containing metabolites for example a metabolite eluding at 4.2 minutes with the molecular formular $C_{15}H_{19}NO_5$ (identified through UHPLC-TOF-MS). The role of AN6444 strongly indicates contribution of the nitrogen to the molecule and ring closure. As no new intermediates were detected in the extracts the exact role of the enzyme remains elusive. The nitrogen incorporated in the structure could arise from either transamination as seen in the biosynthesis of amino acids or from an amino acid which reacts with quadrilineatin. This reaction could yield a lactam where the rest of the amino acid is still attached to the nitrogen followed by

decarboxylation as seen for erinacerin A, figure 4.32, where the residual part of decarboxylated phenyalalanine is attached to the lactam-*N* (Yaoita 2005). The above mentioned metabolite, $C_{15}H_{19}NO_5$, which was present in the AN6446-Oex and AN6446-Oex AN6449Δ strains could indeed resemble the product, figure 4.32, of these reactions if the amino acid was 2-aminoadipic acid. Bioinformatic analysis of AN6444 supports this hypothesis since it predicts the adenylation domain of AN6444 to encode for 2-aminoadipic acid. This amino acid residue would then have to be cleaved from the molecule to reach cichorine. A way to test this hypothesis is to do feeding experiments with labeled 2-aminoadipic acid. Aspernidine A and B (not detected in these extracts) (figure 4.34) are two other metabolites reported from *A. nidulans* where a nitrogen is incorporated into aromatic part of the structure and is proposed to be derived from an orsellinic acid (Scherlach 2010). The nitrogen of these metabolites could also arise from AN6444 or other NRPS-like enzymes.

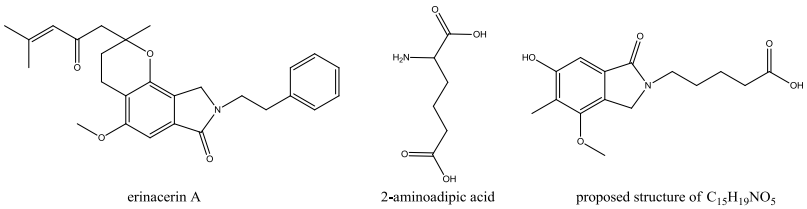

Figure 4.32 The structure of erinacerin A, 2-aminoadipic acid and proposed structure of $C_{15}H_{19}NO_5$.

It remains unknown whether the dimers, cichonidulol and demethylcichonidulol, were biosynthesized by an enzyme or the dimerization occurred non-enzymatically. Due to the small production of the metabolites in the overexpression strain the data obtained is not sufficient for identifying the potential enzyme.

Altogether this study has through qRT-PCR and subsequent chemical analysis identified the genes belonging to the 3-methylorsellinic acid gene cluster. Several metabolites have been isolated, structure elucidated and linked to the gene cluster e.g. nidulol, cichonidulol, demethylcichonidulol and 4-hydroxy-3,6-dimethyl-2-pyrone. The function of AN6447 has been shown to be *O*-methylation and data strongly suggests that AN6444 is involved in the incorporation of a nitrogen atom into the structure which might occur through an aminoadipic intermediate. Several interesting intermediates have been identified through UHPLC-TOF-MS analysis and remain to be isolated and structure elucidated to shed more light over the biosynthesis. A shunt product of the PKS have been identified and through analysis of the PKS deletion library and data of the strains constructed in this work it have been linked to PkbA.

4.3.3 Genetic activation with regulatory genes combined with complex media

The work in the previous sections indicated that it is possible to activate secondary metabolite production through both genetic and OSMAC approaches. However, as there were still a lot of silent genes we decided to look into combining these approaches of activation. In this section two examples of metabolites not previously reported from *A. nidulans* are described.

4.3.3.1 Identification and linking of *A. nidulans* metabolites to genes through a combined approach of complex media and genetic modifications

Due to the availability of the PKS deletion library, described in section 4.3.1 we wanted to identify possible PK candidates to isolate, structure elucidate and, if possible, link to their synthase genes. Linking of metabolites present in small quantities in the reference strain could be possible due to the possibility of comparison with an isolated standard. As seen in the previous study of the 3-methylorsellinic acid gene cluster the disappearing of a small peak helped identify a candidate for genetic studies, resulting in the discovery and linking of a family of both known and previously undescribed metabolites to their synthase genes. In the search of new secondary metabolites of *A. nidulans* we investigated the IBT culture collection at CMB.

The strain chosen for this study was IBT24909 which was cultivated on 200 plates of CYAs for 13 days at 25°C for optimal production of **1**, **2**, and **3**. The LC-DAD chromatogram at 210 nm of the extract can be seen in figure 4.33.

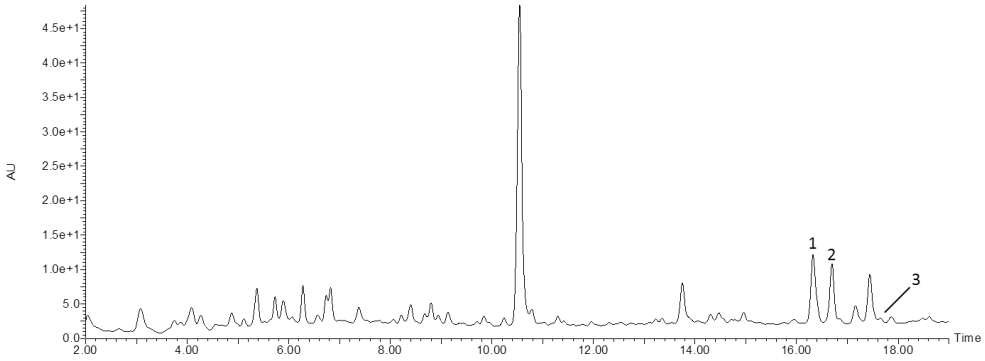

Figure 4.33 LC-DAD chromatogram (210 nm) of 200 plate extract of IBT24909 cultivated on CYAs for 13 days. The two peaks **1** and **2** were identified as potential PKs. The large peak at 10.5 minutes is sterigmatocystin.

After inspection of the chromatogram two rather large peaks, **1** and **2**, were identified as putative PKs based on their UV-spectra, figure 4.33, which had absorption maxima at wavelengths over 300 nm indicating that the metabolite or part of it contained a highly conjugated system.

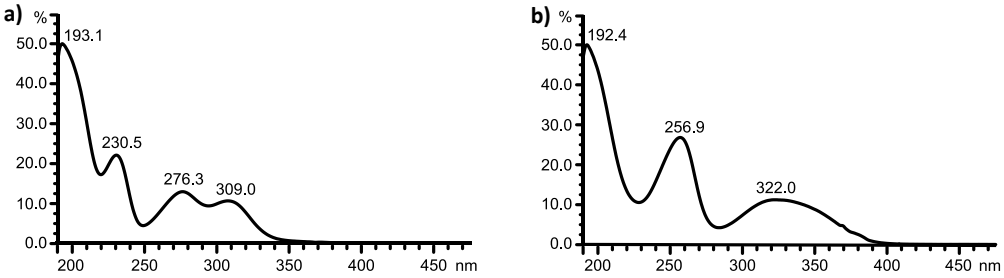

Figure 4.34 UV-spectra of **a) 1** and **b) 2**.

Analysis of the LC-TOF-MS data revealed an $[M+H]^+$ of 343.231 and 387.219 of **1** and **2**, respectively. A search of the Antibase database (Laatsch 2010) (tolerance ± 0.05 Da) gave 29 hits for **1** and 54 hits for **2** where several contained conjugated double bonds which could explain the absorption in the UV-spectra. So to be able to identify the metabolites they were isolated and structure elucidated by 2D NMR (DQF-COSY, HSQC, HMBC, H2BC and NOESY).

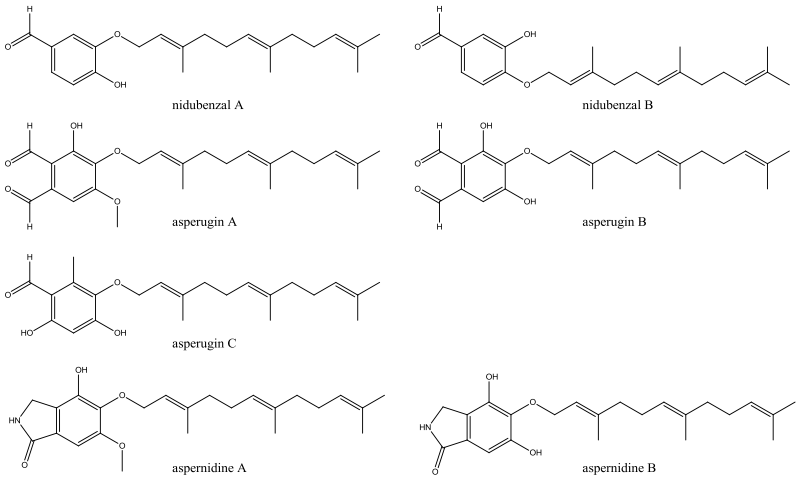

Figure 4.35 Structures of nidubenzal A and B (**1**), asperugin A, B (**2**), and C, and aspernidine A and B

NMR analysis of **1** revealed that two isomers, that we named nidubenzal A and B, figure 4.35, were present in the solution in a 5:1 ratio. The difference of the chemical shift values of the two isomers were small and only visible for H_1'/C_1' and in the aromatic moiety of the molecule, figure 4.36.

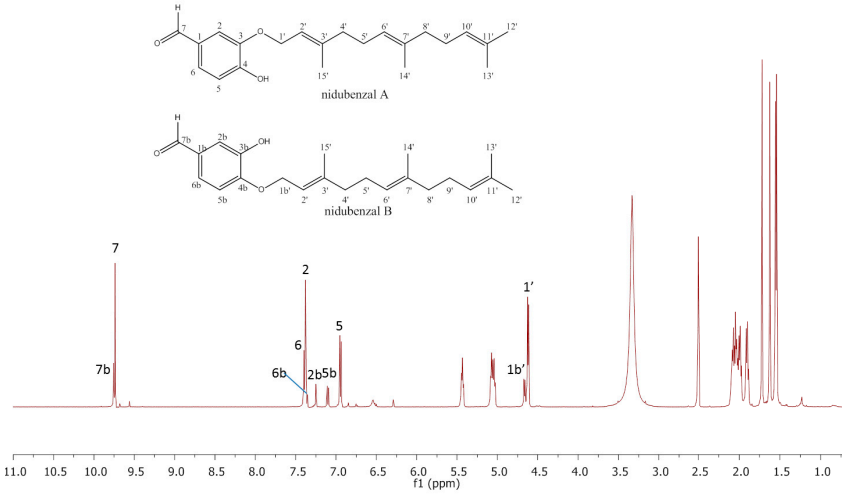

Figure 4.36 ^{1}H-NMR spectrum of nidubenzal A and B in DMSO-d_6. Which illustrates the two metabolites present in the solution.

The structure of the farnesyl side chain was deduced based on DQF-COSY, HSQC, HMBC and H2BC (for detailed NMR data see paper 6) correlations and comparison with literature data from the related structures aspernidine A and B (Scherlach 2010). The attachment of the farnesyl side chain to the two isomers was based on HMBC correlations of H_1' into the aromatic ring, figure 4.37. It had not been possible to see the two different isomers in any of the HPLC/UHPLC analysis due to co-elution; however, NMR analysis revealed the presence of them. Nidubenzal A has been reported in a synthetic screening library (Aurora Fine Chemicals LLC); however, neither nidubenzal A nor B has previously been reported from nature.

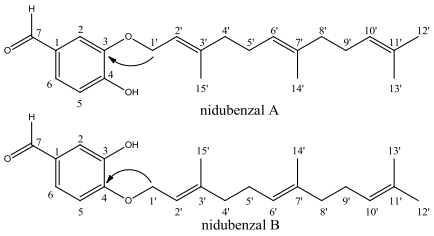

Figure 4.37 Key HMBC correlations of nidubenzal A and B

The structure of **2** was also solved through 2D-NMR analysis (DQF-COSY, HSQC, and HMBC) which identified it to be asperugin B a metabolite previously isolated from the related fungus *A. rugulosus* (Ballantine 1967). Two other asperugins, A and C, have been isolated from *A. rugulosus* (Ballantine 1964, 1965, and 1971) and through LC-TOF-MS-analysis we tentatively identified asperugin A (**3**), figure 4.33, but not asperugin C in the *A. nidulans* IBT24909 extract. We have not yet been able to isolate asperugin A in quantities sufficient for NMR-analysis. In 2005 An *et al.* (An 2005) reported production of asperugin A and B (also with B as the major product), as well as violaceol, in a strain where cosmid-size DNA from slow growing fungi was cloned and introduced into *A. nidulans*. During the course of this study Scherlach *et al*. reported the characterization of aspernidine A and B isolated from *A. nidulans* (Scherlach 2010); however, we were not able to trace these metabolites through LC-TOF-MS analysis of our extract.

All the isolated metabolites, nidubenzal A and B, asperugin A-C and the related aspernidines, seem to be hybrid metabolites which consist of a farnesyl side chain and an aromatic moiety, which may be of PK origin. The aromatic nature of the metabolites indicated that the pathway could be initiate with formation of a NR-PK catalyzed by a NR-PKS. The products of the NR-PKS could be orsellinic acid or even more likely orsellinaldehyde, figure 4.38, which have, just recently, been shown to be a metabolite of *A. nidulans* from the AN3230 (PkfA) NR-PKS (Ahuja 2012). The only difference between the aromatic part of asperugin A and B, and aspernidine A and B, are an O-methylation indicating that the two metabolites in each group are derived from the same biosynthetic pathway. Scherlach *et al.* (Scherlach 2010) suggests that the aspernidines are formed by either orsellinic acid or the corresponding aldehyde which traps ammonia nitrogen in an intermediary aldehyde, where oxidoreduction and condensation steps leads to the isoindolinone moiety as suggested for cichorine in the previous section. The precursor of the aromatic moiety of asperugin C could also be orsellinaldehyde which, in a shunt pathway, will be methylated instead of oxidated. The two new metabolites nidubenzal A and B differs in the aromatic moiety which containing seven carbons instead of the eight of the backbone of the other metabolites. This

could indicate a different biosynthetic pathway or a decarboxylation from a C_8-PK product. We speculated whether these metabolites might be a product of the shikimic acid pathway since the substitution pattern resembles protocatechuic acid, figure 4.38, a shunt product from the biosynthesis of shikimic acid, differing only by the aldehyde in the place of the carboxylic acid.

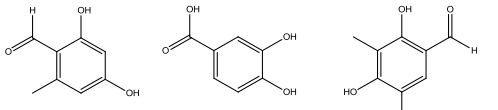

Figure 4.38 Structures of orsellinaldehyde, protocatechuic acid and 2-ethyl-4,6-dihydroxy-3,5-dimethylbenzaldehyde

Since the metabolites might be of PK origin we went back to the reference strain used in section 4.3.1 to see if whether trace amounts of the metabolites could be detected in EICs on any of the media.

Nidubenzal A and B were present in small quantities on the CYAs medium and analysis of the deletion library identified two PKS deletions, *ausA*Δ and AN11191Δ, where the production of nidubenzal A and B seemed to have been abolished.

Asperugin A could not be detected in any of the strains whereas asperugin B could be traced. The same procedure for identification of putative PKSs as for the nidubenzals was done and six PKS candidates were identified, AN0523 (*pkdA*), AN11191, AN3230 (*pkfA*), *ausA*, AN6791, and AN9005. Due to the small quantities of metabolites present in the extract it was, in some cases, difficult to determine the presence of the metabolites. It has recently been reported that AN3230 produces orsellinaldehyde and AN0523 2-ethyl-4,6-dihycroxy-3,5-dimethylbenzaldehyde, figure 4.38 (Ahuja 2012). *ausA*, *pkfA* and *pkdA* are NR-PKSs whereas AN11191, AN6791 and AN9005 are PR-PKSs (Sanchez 2012). These results gave several possible genes so we were not able to link the metabolites to their synthase genes.

At the same time as this study a strain where the *cclA* gene had been deleted activated the production of the asperugins and nidubenzals. It had already been shown that this deletion strain increased the production of secondary metabolites in *A. nidulans* (Bok 2009). We wanted to investigate whether challenging the *cclA*Δ strain on complex media could activate even more secondary metabolite production.

Figure 4.39 show the phenotypical appearance of the *cclA*Δ strain compared to the reference strain when grown on the same eight media as used initially in the deletion study. It is evident that the fungus was affected by the deletion, and as the reference strain it responded differently to the different medium conditions. Generally it seems that the *cclA*Δ strains grow slower than the reference. To analyze the metabolite production micro-extraction was performed (Frisvad 1987, Smedsgaard 1997) and the extracts were analyzed by both UHPLC-DAD and UHPLC-TOF-MS. The UHPLC analysis revealed a diverse and different production of secondary metabolites on the eight media compared to the reference strain, figure 4.40.

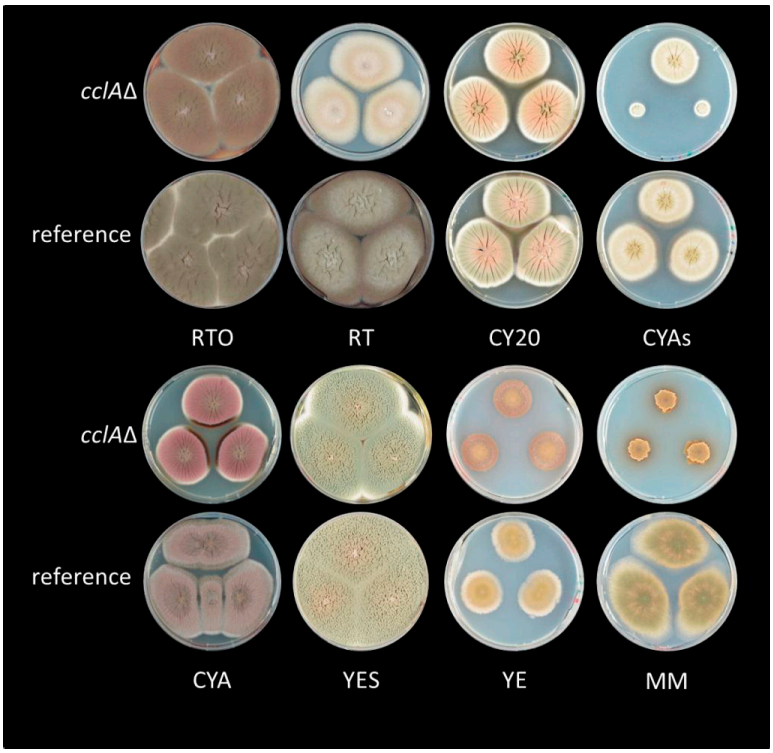

Figure 4.39 The reference strain compared to the *cclA*Δ strain cultivated for seven days at 37°C on RTO, RT, CY20. CYAs, CYA, YES, YE, and MM medium.

In all of the media except YE and CYAs there seemed to be an activation of secondary metabolite production. It was especially noticeable that many of the metabolites produced in the *cclA*Δ strain are derived from the orsellinic acid and monodictyphenone pathway, which was also the gene clusters activated by Bok *et al.* (Bok 2009). Arugosin A which was linked to the monodictyphenone pathway in section 4.3.1.2 seemed to disappear in the *cclA*Δ strain whereas intermediates in this pathway, for example emodin, seemed to accumulate. Most noticeable for our study, and what is focused on in this section, was the increased production of asperugin A and B as well as nidubenzal A and B on several of the media; YES, CY20, CYAs, CYA, RTO and MM, figure 4.41.

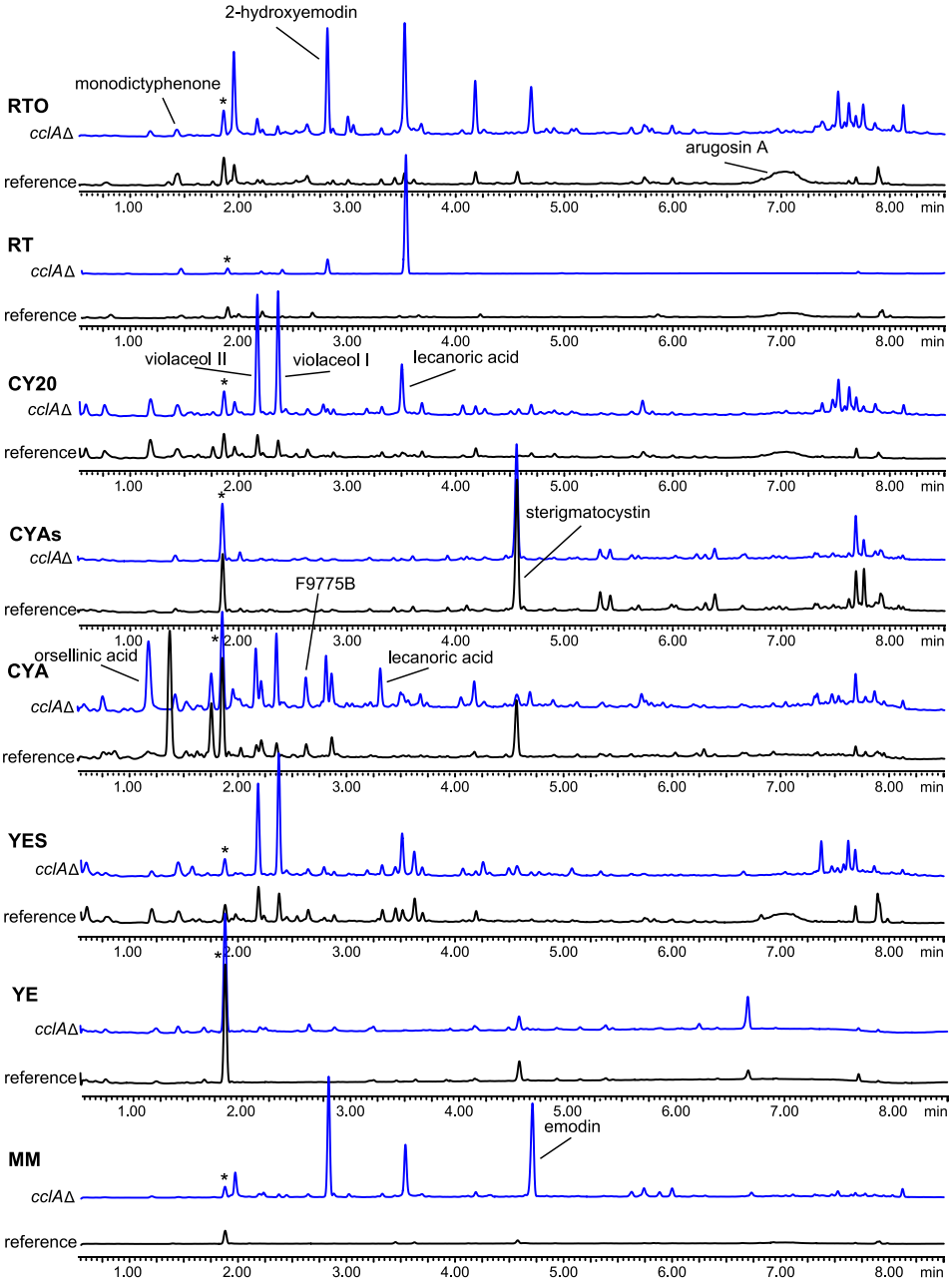

Figure 4.40 UHPLC-DAD chromatograms (210 nm) of micro-extracts of the *cclA*Δ strain cultivated on eight different media compositions for seven days at 37°C compared to the reference strain. From top to bottom RTO, RT, CY20, CYAs, CYA, YES, YE and MM.*This peak corresponds to an internal standard of chloroamphenicol added to the extracts. The concentration of chloroamphenicol is the same in all the samples. Metabolites were identified through comparison with standards or based on exact mass and UV-data.

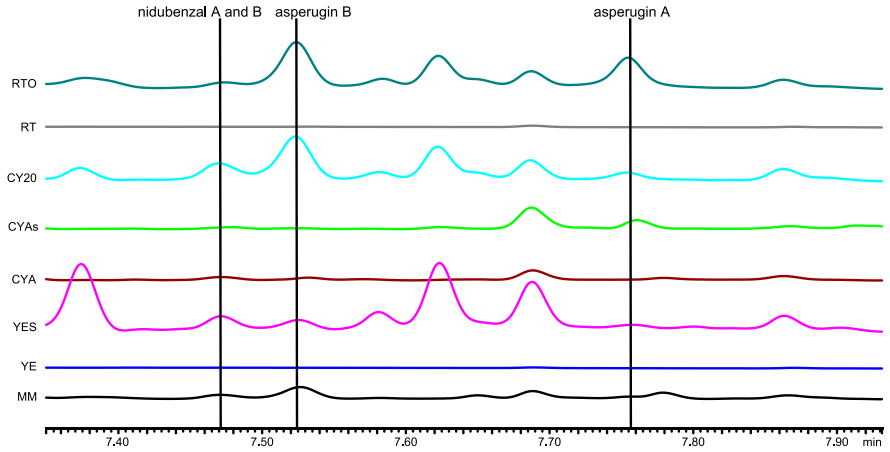

Figure 4.41 UHPLC-DAD chromatograms (210 nm) from seven to eight minutes of micro-extracts of the *cclA*Δ on the eight different media shows the production of nidubenzal A and B, and asperugin A and B. From top to bottom: RTO, RT, CY20, CYAs, CYA, YES, YE and MM.

The increased production of asperugin A and B, and nidubenzal A and B in this strain allowed for creating double deletions of *cclA* and the candidate PKS genes identified previously. Therefore *cclA* was deleted in the respective PKS gene deletions identified previously. Both the NR- and PR-PKSs were included in the study since they might have an effect on asperugin production. It was originally thought that these products could be derived from orsellinic acid, and due to the activation of several orsellinic acid derived metabolites in the *cclA*Δ strain, a deletion of *cclA* in *orsA*Δ was also constructed. As described previously we wondered whether nidubenzal A and B could be shikimic derived so a deletion of the *qutC* gene which has been shown to encode for an enzyme, dehydroshikimic acid dehydratase that catalyzes the production of protocatechius acid from 3-dehydroshikimic acid in *A. nidulans* were included in the study (Lamb 1992).

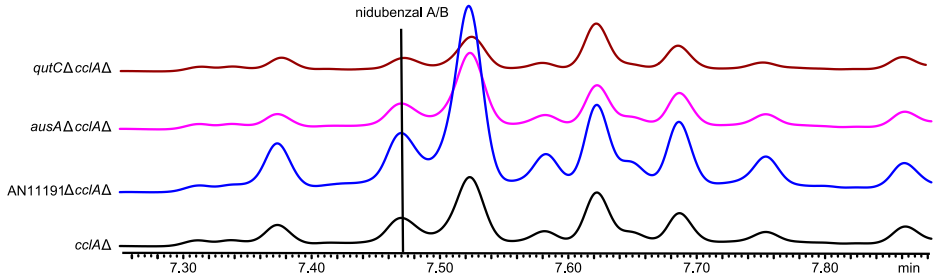

Figure 4.42 UHPLC chromatograms (210 nm) of micro-extracts of the *qutC*Δ*cclA*Δ, *ausA*Δ*cclA*Δ, AN11191Δ*cclA*Δ and *cclA*Δ strains after cultivation for seven days at 37°C on CY20 medium. The other parts of the chromatogram were also identical.

The double deletion mutants made were analyzed on both UHPLC-DAD and UHPLC-TOF-MS on all eight media. As seen in figure 4.42 nidubenzal A and B were present in all the deletion strains and on the different media; however, spore-PCR analysis of the AN11191Δ*cclA*Δ strain showed presence of WT AN11191 nuclei indicating this strain was not suited for analysis. A new double deletion based on the original confirmed AN11191Δ strain is in progress of being constructed. As

the *qutC*Δ*cclA*Δ strain also produced nidubenzal A and B it indicates that they are derived from either AN11191 or an alternative route to protocatechuic acid exists in *A. nidulans*.

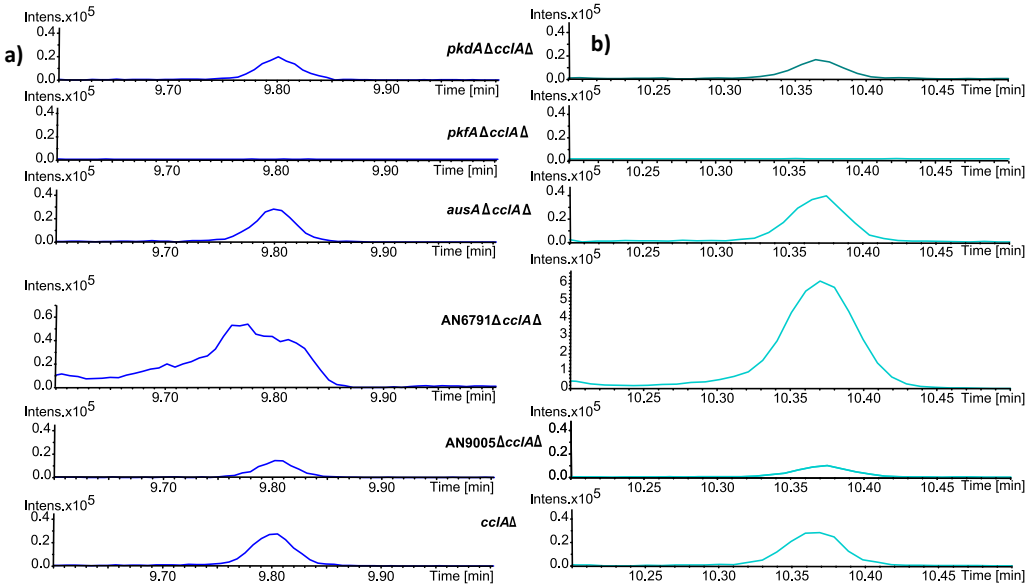

Figure 4.43 EIC of **a)** asperugin A (calc. $[M-H]^-$ 401.23225±0.002]) and **b)** asperugin B (calc. $[M+H]^+$ 387.21660±0.002]) of micro-extracts of the (from top to bottom) *pkdA*Δ*cclA*Δ, *pkfA*Δ*cclA*Δ, *ausA*Δ*cclA*Δ, AN6791Δ*cclA*Δ, AN9005Δ*cclA*Δ and *cclA*Δ strains after cultivation on CY20 medium for seven days at 37°C.

The EICs of asperugin A and B in the double deletion mutants and the reference strain can be seen in figure 4.43. As the AN11191Δ*cclA*Δ strain was not correct it have been removed from the study; however, a correct strain will be included in the analysis for the presence of the asperugins. As can be seen in the figure production of asperugin A and B are abolished in the *pkfA*Δ*cclA*Δ strain and this was consistent on the eight analyzed media. Ahuja *et al.* (Ahuja 2012) recently showed that overexpression of this PKS with an inducible promoter led to the production of orsellinaldehyde. Further biosynthesis of orsellinaldehyde to the asperugins would require several tailoring enzymes catalyzing oxidation of a methyl to an aldehyde, oxidation of the aromatic ring, a terpene synthase and an *O*-methyltransferase. As suggested by Scherlach *et al.* (Scherlach 2010) further modifications to the aromatic moiety of the metabolites could lead to the biosynthesis of the aspernidines. This biosynthetic pathway resembles in some ways the proposed biosynthesis of the cichorine gene cluster. Preliminary bioinformatics studies indicated the presence of *O*-methyltransferase, prenyltransferase, oxidase, cytochrome P450, and monooxidase enzymatic functions surrounding the *pkfA* gene. Construction of the double deletions of *cclA* and the surrounding genes to determine the biosynthetic pathway of these metabolites including identifying intermediates are ongoing. In the AN6791Δ*cclA*Δ stain it appears that the production of asperugin A and B have increased compared to the other strains. This is interesting due to the fact that the deletion was constructed based on analysis of the deletion library where the metabolites were missing in the single deletion strain, AN6791Δ. This phenomena is seen in

several media (YES, CY20, CYAs and MM); however, the reason for this apparently increase in production is so far unknown.

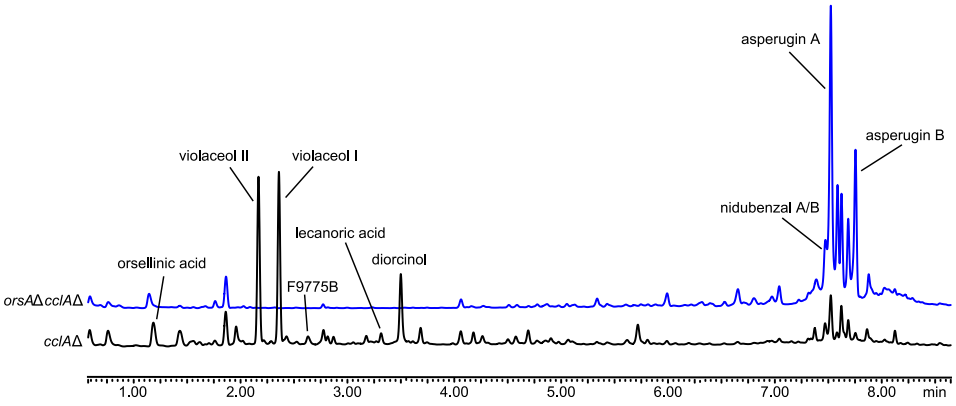

Figure 4.44 UHPLC chromatograms (210 nm) of micro-extracts of the *orsA*Δ*cclA*Δ strain compared to the *cclA*Δ strain on CY20 medium.

As mentioned a double deletion of *orsA* and *cclA* were included in the study. As seen from figure 4.44 the deletions did not abolish the production of the asperugins; however, the metabolites which have been shown to be derived from the orsellinic acid biosynthetic pathway were indeed absent in the double deletion strain (Bok 2009, Schroeckh 2009, Sanchez 2010, Nahlik 2010).

In this study two novel metabolites nidubenzal A and B have been isolated. Asperugin A and B have been linked to the PKS encoding gene AN3230. Deletions of the AN3230 gene cluster is underway and deletions to link nidubenzal A and B to a gene is undergoing.

4.3.3.2 Activation of juvenile hormone production in *A. nidulans*

As all the genetic modifications described so far have been in the *A. nidulans* genome we decided to investigate whether heterologous expression of regulatory genes from other filamentous fungi could induce secondary metabolite production in *A. nidulans*, using *A. niger* as a test case. As we have seen a significant difference in secondary metabolite production on different complex cultivation media we tested these strains on five media; MM, CYAs, RTO, YES and OAT (oatmeal agar).

The genes selected for expression was identified based on a collection of microarray experiments from *A. niger* grown under diverse conditions to identify regulatory genes associated with predicted secondary metabolite gene clusters using a local co-expression algorithm. Seven genes associated with predicted gene clusters containing either PKSs or NRPSs were identified. All seven genes belonged to the binuclear zinc finger class which is often associated with secondary metabolism in filamentous fungi (MacPherson 2006). The seven genes were expressed individually in *A. nidulans* (Hansen 2011) and incubated on the five media for seven days at 37°C and micro-extraction was performed (Frisvad 1987, Smedsgaard 1997) and the extracts were analyzed by both UHPLC-DAD and UHPLC-TOF-MS. Of the 35 combinations of strains and growth media only one strain, grown on CYAs, had a significant impact on secondary metabolite

production, resulting in an increased production of several metabolites not previously identified from *A. nidulans*, figure 4.45. The gene which was expressed in the strain was renamed (from est_fge1_pg_C_150220, Broad annotation) Secondary Metabolism associated Regulatory protein A (SmrA). BLAST analysis revealed that *smrA* did not have a potential ortholog in *A. nidulans*.

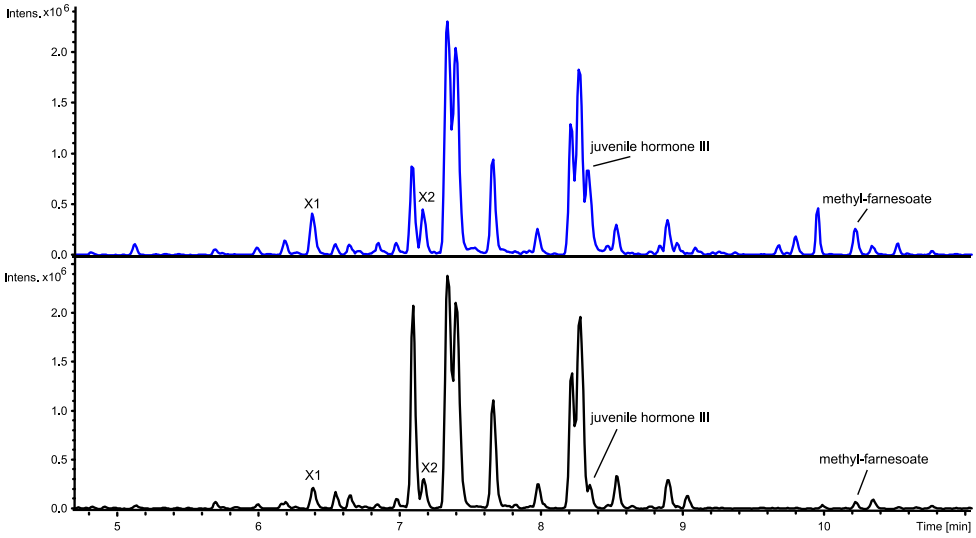

Figure 4.45 UHPLC-HRMS ESI+ BPC of the reference strain (bottom) and the strain where *smrA* (top) is expressed grown on CYAs at 37°C for seven days.

To purify the induced products we made a large extract and in this extract X2 was the dominant peak (data not shown). As X1 and X2 had a similar UV-chromatogram, a mass difference of 27.9948 (CO), and similar adduct patterns in their mass spectra, figure 4.46, it was speculated that these structures were related and both were purified.

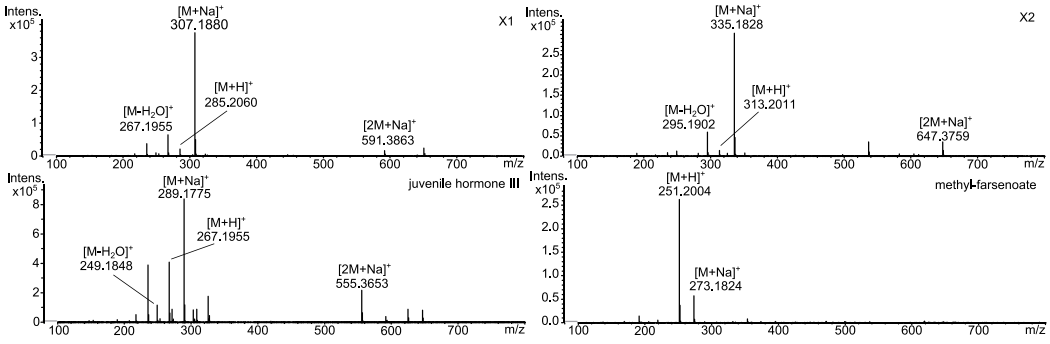

Figure 4.46 Mass spectra of X1, X2, JH-III and methyl-farnesoate.

The structures were elucidated using the following 2D NMR experiments; DQF-COSY, HSQC and HMBC. X1 was identified to be methyl (2E,6E)-10,11-epoxid-3,7,11-trimethyl-2,6-dodecadienoate (Kuhnz 1981) and X2 was indeed a formylated analogue of X1, figure 4.47. As formic acid was added to both the micro extraction and the large extract, a new micro extract was prepared

without formic acid. X2 was not produced in this extract and must therefore result from chemical modification resulting from the presence of formid acid in the extraction process.

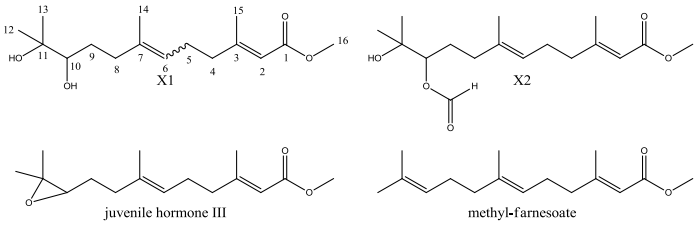

Figure 4.47 The structures of X1, X2, juvenile hormone III and methyl-farnesoate

The NMR data of X1 indicates that two diastereomers were present in the sample. The ^{1}H- and ^{13}C-chemical shifts differ most in the reduced end of X1 where a stereocenter (C_{10}) is present. The chemical shifts of H_1/C_1 to H_5/C_5 are identical. The difference of chemical shifts of the two methyl groups (H_{12}/C_{12} and H_{13}/C_{13}) and the two CH_2 groups next to the stereocenter are due to the presence of the chiral center. The two diastereomers present in the X1 solution must be due to the presence of X1 in both the *E*- and *Z*-conformation at the C_6 and C_7 double bond. The presence of both an *E* and a *Z* double bond conformation could a result from chemical modifications due to the presence of formic acid in the extraction process.

As the structure of X1 resembled juvenile hormone III, a hormone thought to be unique for insects with essential developmental roles (Wilson 2004, Gilbert 2000) and the crustacean hormone methyl-farnesoate (Nagaraju 2007) we searched for these metabolites in our extract. The two metabolites were putatively identified through extracted ion chromatograms of the calculated $[M+H]^+$ (juvenile hormone III: 267.1955 and methyl-farnesoate: 251.2006) of the metabolites and putatively identified both metabolites (juvenile hormone III: 267.1957 and methyl-farnesoate: 251.2007). The mass spectra of these two metabolites resembled the spectra of X1 and X2, figure 4.46; however, to confirm the structure of the metabolites an authentic sample of juvenile hormone III was compared to the extract and it confirmed that the metabolite was present. An attempt was made to purify both juvenile hormone III and methyl-farnesoate; however, obtaining sufficient amounts of methyl-farnesoate for NMR analysis was not possible and the juvenile hormone was unstable and had degraded before an NMR analysis was possible. As methyl-farnesoate was thought to be volatile we analyzed the production of volatiles in the mutant strain by GC-MS and were able to confirm the production of methyl-farnesoate through comparison with the Xcalibur software package (Thermo Scientific). Further GC-MS analysis of volatiles collected by the mutant strain showed that methyl-farnesoate was a major metabolite of the volatile fraction in both the *smrA* expression strain, and in the reference strain whereas juvenile hormone III and X1 were undetectable. Indicating that juvenile hormone III is retained in the fungus. The strongest metabolite induction was observed when *A. nidulans* was grown on CYAs (high salt concentration); however, data from the UHPLC-TOF-MS indicated presence of juvenile hormone III and increased levels of X1 production on YES media (data not shown).

The biological function of juvenile hormone III and methyl-farnesoate in *A. nidulans* have not yet been explored; however, they may serve as part of a defense strategy against insects and/or other predators since fungal secondary metabolites are known to play an important role in

fungal/insects interactions (Kempken 2010, Rohlfs 2011). As *A. nidulans* is generally believed to inhabit a variety of ecological niches, including dead plant materials, it is likely that competing insects will be part of the natural environment. However, it cannot be excluded that the metabolites can serve hormonal functions. It has been demonstrated that the juvenile hormone precursor farnesol (Cao 2009) in *Candida albicans* both regulates the transition from yeast to filamentous growth (Hornby 2001) and regulates induction of apoptosis in competing fungal species (Dinamarco 2011). To test the biological function of these metabolites it could be interesting to either feed the metabolites to the growing fungi or to test this new strain towards insects.

The biosynthetic origin of these metabolites is likely to be terpenoids with farnesol as the precursor where a methylation and oxidation occurs in one end of the molecule. Afterwards an epoxid, juvenile hormone III is produced, the ring is opened and the diol, X1, is formed. Bromann *et al*. have identified several putative terpene synthases in *A. nidulans* which could be involved in the production of these metabolites (Broman 2012). qRT-PCR of the putative terpene synthases and the *SmrA* strain could give an indication of possible biosynthetic origin which then could be followed up by deletion studies to determine the biosynthetic origin.

4.3.4 Summary and part conclusion

Cultivation of *A. nidulans* under different media compositions have led to the activation of several biosynthetic pathways, including austinol, monodictyphenone, and orsellinic acid. Through the creation of a deletion library austinol and dehydroaustinol was linked to the PKS *ausA* and several metabolites were contributed to the monodictyphenone (arugosin A and H) and orsellinic acid (violaceols) pathways.

Overexpression of a transcription factor led to the activation of a biosynthetic pathway where 3-methylorsellinic acid and several derivatives, nidulol, cichorine, cichonidulol, and demethylcichonidulol were produced. Through the qRT-PCR analysis and the creation of a deletion study a cluster of seven genes were identified. Based on metabolite screening a biosynthetic pathway of the metabolites have been proposed which includes a putative NRPS-like encoding gene that is suspected to be involved in the incorporation of a nitrogen atom to the structure.

Further analysis of *A. nidulans* cultivated on complex media led to the identification of asperugin A and B, and the novel metabolites; nidubenzal A and B. Through analysis of the PKS deletion library several PKSs were identified as putative synthase encoding genes. The combination deletion of the *cclA* gene and the putative PKS genes led to the linking of asperugin production to AN3230 where work is still in progress for the nidubenzals.

Heterologous expression of a transcription factor from *A. niger* led to the identification of the juvenile hormone III produced from *A. nidulans*. Clarification of the distribution of the juvenile hormones in filamentous fungi as well as their biological function in *A. nidulans* will improve our understanding of fungal/insect interactions. The finding that heterologous expression of transcription factors may influence secondary metabolism is of general relevance for activation of secondary metabolite production.

5 Overall discussion and conclusion

In summary the work performed during the last three years have contributed to the chemical knowledge of several important filamentous fungi including identifying several novel metabolites; oryzamid $A_{1\text{-}2}$, ditryptoleucine, fumonisin B_6, nidubenzal A and B, cichonidulol, and demethylcichonidulol as well as linking of several metabolites of *A. nidulans* to their synthase genes; austinol and dehydroaustinol, asperugin A and B, the arugosins, and finally elaboration on the biosynthetic pathway of cichorine and nidulol. The work have been an example of the advantages of the close collaboration of two fields; molecular biology and natural product chemistry, which have led to discoveries that neither could have achieved separately.

The study on the genetic important filamentous fungus *A. nidulans* has contributed to and elaborated on the understanding of secondary metabolism activation and biosynthesis. The availability of the genome of *A. nidulans* has changed the focus of research into the area of secondary metabolites from elucidation of the biosynthetic pathway of a few important metabolites to the search for new metabolites (Walsh 2009). Figure 5.1 shows the distribution of the 32 putative PKSs of *A. nidulans* on the eight chromosomes. The products of the PKSs marked in green were known at the beginning of this PhD study ((Brown 1996, Watanabe 1998, Watanabe 1999, Bergmann 2007, Chiang 2008, Szewczyk 2008, Bok 2009, Chiang 2009b, Schroeckh 2009, Nielsen 2011), the ones in black have been reported during the course of this PhD (Nielsen 2011, Ahuja 2012, Lo 2012), and the results of this study have contributed to the knowledge of the biosynthetic pathways of the clusters marked by black circles (papers 4-6). The products of the genes in red have not yet been identified.

As the figure shows, progress in mapping of the PKS encoding genes in *A. nidulans* has intensified in the recent years and many academic groups have added to the knowledge, illustrating the competitive nature of the field. Even though intense efforts have been made, there is still a lot of work to be performed before the complete potential of secondary metabolite biosynthesis of *A. nidulans* is elucidated. The results, both in this PhD and in the literature, indicate that attempts to affect gene regulation including the OSMAC approach and genetic modifications, have a tendency to activate some of the same gene clusters especially the orsellinic acid, monodictyphenone, and austinol clusters (Bok 2009, Schroeckh 2009, Chiang 2010b, Sanchez 2010, Nahlik 2010, Nielsen 2011, Nützmann 2011, Sanchez 2011, Scherlach 2011, Lo 2012). This may indicate that these metabolites are important to the fungus and a change from normal conditions (both cultivation and genetic) causes the fungus to react by producing other metabolites.

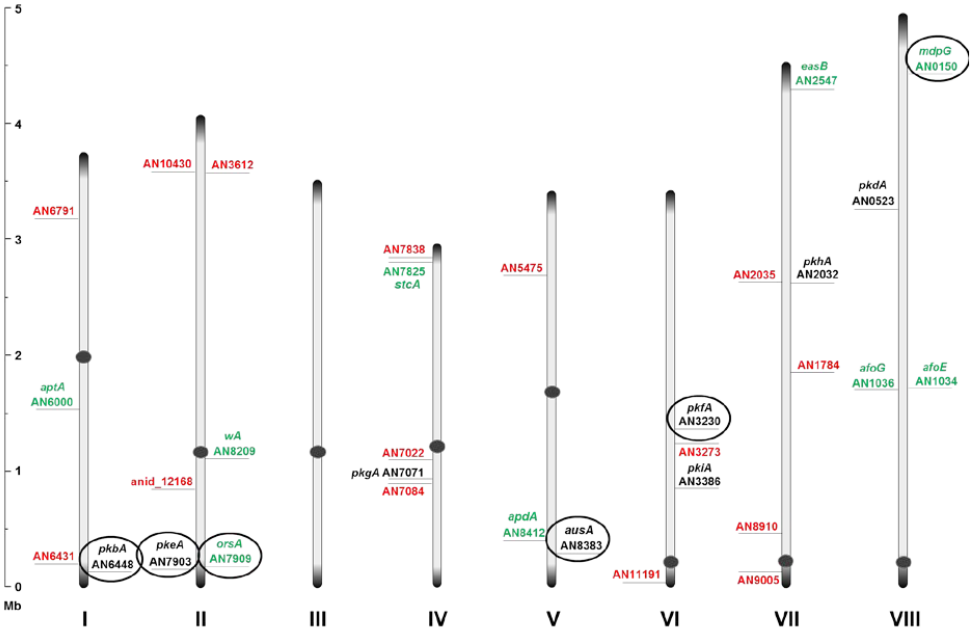

Figure 5.1 Overview of the distribution of the 32 putative PKSs in *A. nidulans*. The products of the genes shown in green were known when this study started, the once in black have been elucidated in the course of this study where results of this study have contributed to and/or discovered the once in the black circles. The products of the PKSs in red have not yet been identified. Dark grey circles and ends symbolize centromeric regions, respectively, and should not be considered to scale.

In this thesis the focus have been on combining genetic modifications with the OSMAC approach and through these attempts the discovery of several new metabolites have added to the chemical knowledge of these fungi. One of the more interesting results is the detection of the juvenile hormone III in *A. nidulans* (paper 7) which is known to have a biological function against insects and/or other predators. Further studies of the biological function of these and other secondary metabolites against the fungus itself could add to the knowledge of secondary metabolism and aid in the discovery process through cultivations under more natural conditions than the lab media (for example co-cultivation). Other metabolites which have been discovered in *A. nidulans* through the use of OSMAC in this thesis is the arugosins (Nielsen 2011), asperugin A and B (paper 6) and the novel metabolites nidubenzal A and B (paper 6). These results confirm the potential of challenging the fungus through differing of the cultivation conditions. Several methods of activation of silent genes have been reported in the literature. The individual exchange of the PKS promoters with an inducible promoter by Ahuja *et al.* have, recently, shown promising results both with respect to PKS and NRPSs (Ahuja 2012, Yeh 2012).

The discovery of new secondary metabolites has been focused on activation of silent genes and thereby, hopefully, new products can be formed. Even if the optimal strategies are found and even more effort is put into secondary metabolite discovery, it may not be possible to discover the products of all secondary metabolite synthase genes and clusters. This may be due to mutations in the genes which can have an effect on the transcription or translation of DNA and

RNA, respectively, in turn providing a non-functional enzyme. The mutations can have an effect on several steps in the assembly for example they may not be able to release the product, catch the substrate, or the folding may be incorrect. This was the case for *A. oryzae* where we showed that 13-desoxypaxilline was the final product in the biosynthetic cluster of aflatrem (paper 2) which confirmed the reports of Nicholson *et al.* (Nicholson 2009), who observed a mutation in the *atmQ* gene responsible for the next steps of the biosynthesis of aflatrem in *A. flavus*.

Another area which could be relevant to explore in the search for silent secondary metabolites is the extraction of the metabolites. Methods for secondary metabolite extraction have been developed and implemented as standard procedures in several laboratories. However, some metabolites, for example the fumonisins in *A. niger* (paper 3), went undetected because the extraction procedures are different from most other metabolites.

Even though a biosynthetic pathway is expressed it does not mean that the metabolites are detected. The detection of different metabolites depends of the analytical methods used. Two methods of combined separation and detection, UHLPC-DAD and HPLC-TOF-MS, were used throughout this study. In both methods some metabolites may not be detected. The emericellamides and the fumonisins does not absorb UV-light so they are not detected in a DAD detector whereas metabolites, which do not ionize, will not be detectable through LC-MS. During the course of this study, a new UHPLC-TOF-MS instrument was implemented which enhanced the detection of metabolites and provided valuable information, for example better predictions of the molecular formula due to improved mass accuracy and isotope pattern, in the identification of metabolites.

The discovery of the production of 3-methylorsellinic acid in *A. nidulans* was more prominent on the new instrument and it was not until this new data was available that the metabolite could be confirmed to be present in the reference strain. The availability of a more sensitive instrument also reveals the difficulty of determining whether a metabolite is present or production have been eliminated. This raises the question of the influence of the detection limit and if the metabolites, which cannot be detected, are due to the concentration falling below the detection limit of the instruments, or the loss of production. As in the case of nidubenzal A and B, several PKS candidates were identified even on the most sensitive instrument and it was not until a method of enhancing the metabolite production was found that it was possible to confirm the PKS gene AN3230 to be responsible for PK biosynthesis. Cichonidulol and demethylcichonidulol were isolated from a 200 plate extract in quantities sufficient for NMR analysis; however, only cichonidulol could be detected in the micro-scale extracts of the strain indicating that either the metabolites were produced in too small amount for detection, the cultivation conditions might have been slightly different in one of the experiments, or variations in extraction methods.

The availability of more sensitive and precise instruments also opens up to new methods of data analysis. Multivariate data analyses, which can decipher between co-eluting peaks and identify small variations in large amounts of date are tools which can be useful in future analysis (Toh 2010, Gao 2012, Tian 2012). However, for these programs to be able to give as correct results as possible it is important to be able to perform controlled experiments, especially, if data obtained over longer periods of time are compared. This is both in terms of variations of cultivation (media, temperature fluctuations, time), extraction procedures, and data acquisition. The sensitive TOF-

MS instruments are useful for these methods of data analysis and identification of small differences (for example appearance or disappearances of peaks); nonetheless, to confirm the metabolite structures a substantial amount of material is needed. Bioinformatic analysis can aid in the structure elucidation especially in the case of NRPs due to the modular nature of NRPSs (Koglin 2009, Matthias 2010); however, in the case of PKs it is still difficult to predict structures based on the iPKS (Crawford 2010). It is even more difficult when several tailoring enzymes are present in the secondary metabolite clusters due to the possibility of the biosynthesis of several isomers. Fragmentation patterns of metabolites can assist in the structure elucidation as seen in the example of arugosin A though further structural studies, for example NMR-spectroscopy or X-ray crystallography, may be necessary.

The identification of new secondary metabolites and linking these to genes have, especially since the availability of the genome sequences focused on creating conditions for activation of silent gene clusters in the fully genome sequences strain. Another approach could be to identify metabolites in other high-producer strains of the same species and afterwards use advanced data analysis programs to discover these metabolites in the genome sequenced strain. Since the genome sequenced strain of for example *A. nidulans* is a strain, which have been used in the lab for decades, the strain may have lost the ability to produce more secondary metabolites than needed due to the lack of natural competition in the surroundings. An example of the use of another strain of *A. nidulans* in this PhD has been the discovery of nidubenzal A and B, and asperugin A and B which were isolated from a strain from the IBT culture collection and afterwards found to be produced in trace amounts in the lab strain. Another advantage from this approach is the possibility to predict the steps in the biosynthetic pathway and thereby predict which functionalities the tailoiring enzymes should hold. Due to the clustering of the synthase and tailoring genes, genome mining could predict possible gene cluster candidates which could then be a target for genetic studies, thereby minimizing the amount of genetic work.

Discovery of the full biosynthetic potential of filamentous fungi can have several purposes. First, as many medical drugs are secondary metabolites or derivatives thereof (Newman 2012) the discovery of new structures enhances the possibilities of discovering new drugs. Second, the possibilities of synthetic biology where swapping of domains or genes can result in the production of designed metabolites. Third, it can help identify possible pathogenic species as the genes can reveal the possibility of mycotoxin production, as the example of fumonisin production of *A. niger* where a new analogue fumonisin B_6 which have not been reported from *Fusarium* was identified (paper 3). Fourth, for the filamentous fungi used for industrial purposes, it is easier to identify a new metabolite appearing in a process when the full potential is known. A lot of the genetic work performed on filamentous fungi has been focused on *A. nidulans*. The strategies and genetic tools developed in this fungus can be transferred into other organisms since the price of genome sequencing is decreasing and within the reach of individual laboratories (Nowrousian 2010).

Due to the vast interest in *A. nidulans* there are several groups working in this area. During this study several groups have published results of the same biosynthetic pathways, for example orsellinic acid (Bok 2009, Schroeckh 2009, Sanchez 2010, Nahlik 2010, Nützmann 2011, Scherlach 2011), austinol (Nielsen 2011, Lo 2012) and monodictyphenone (Bok 2009, Chiang 2010b, Sanchez 2011). Due to the complexity of the secondary metabolism it has been possible for the groups to contribute with new information on already discovered biosynthesis. For example three papers on

the monodictyphenone pathway in *A. nidulans* were published (Bok 2009, Chiang 2010b, Sanchez 2011) before the report of the arugosin intermediates was linked to *mpdG* as intermediates in the biosynthesis of the shamixanthones in this study (paper 4). The results of these works along with labeling studies (Ahmed 1992) have led to a detailed biosynthetic pathway proposed by Simpson (Simpson 2012). The examples above, illustrated, that even when the product of a PKS has been identified, the full potential of a biosynthetic pathway may not have been fully elucidated. Ahuja *et al.* reported linked the production of 3-methylorsellinic acid and cichorine to PkbA; however, overexpression of a transcription factor led the isolation of several metabolites including the two novel metabolites cichonidulol and demethylnidulol (paper 5).

The work in this thesis illustrates the enormous potential of secondary metabolism in filamentous fungi which gives discoveries of new metabolites of previously silent pathways and where new discoveries adds to the pool of knowledge, and at the same time, challenges researchers to go in different directions in the search of novel metabolites.

6 References

Abe, K.; Gomi, K.; Hasegawa, F.; Machida, M. Impact of *Aspergillus oryzae* genomics on industrial production of metabolites. *Mycopathologia* **2006**, *162*, 143-153.

Ahuja, M.; Chiang, Y.-M.; Chang, S.-L.; Praseuth, M.B.; Entwistle, R.; Sanchez, J.F.; Lo, H.-C.; Oakley, B.R.; Wang, C.C.C. Illuminating the diversity of aromatic polyketide synthases in *Aspergillus nidulans*. *J. Am. Chem. Soc.* **2012**, *134*, 8212-8221.

Ahmed, S.A.; Bardshiri, E.; McIntyre, C.R.; Simpson, T.J. Biosynthetic studies on tajixanthone and shamixanthone, polyketide hemiterpenoid metabolites of *Aspergillus variecolor*. *Aust. J. Chem.* **1992**, *45*, 249-274.

Amoutzias, G.D.; Van de Peer, Y.; Mossialos, D. Evolution and taxonomic distribution of nonribosomal peptides and polyketide synthases. *Future Microbiol.* **2008**, *3*, 361-370.

An, Z.; Harris, G.H.; Zink, D.; Giacobbe, R.; Lu, P.; Sangari, R.; Svetnik, V.; Gunter, B.; Liaw, A.; Masurekar, P.S.; Liesch, J.; Gould, S.; Strohl, W. Expression of cosmid-size DNA of slow-growing fungi in *Aspergillus nidulans* for secondary metabolite screening. In *Mycology series: Handbook of industrial mycology* (ed Bills, G.) **2005**, *22*, 167-186.

Andersen, M.R.; Salazar, M.P.; Schaap, P.J.; van de Vondervoort, P.J.I.; Culley, D.; Thykaer, J.; Frisvad, J.C.; Nielsen, K.F.; Albang, R.; Albermann, K.; Berka, R.M.; Braus, G.H.; Braus-Stromeyer, S.A.; Corrochano, L.M.; Dai, Z.; van Dijck, P.W.M.; Hofmann, G.; Lasure, L.L.; Magnuson, J.K.; Menke, H.; Meijer, M.; Meijerm S.L.; Nielsen, J.B.; Nielsen, M.L.; van Ooyen, A.J.J.; Pel, H.J.; Poulsen, L.; Samson, R.A.; Stam, H.; Tsang, A.; van den Brink, J.M.; Atkins, A.; Aerts, A.; Shapiro, H.; Pangilinan, J.; Salamov, A.; Lou, Y.; Lindquist, E.; Lucas, S.; Grimwood, J.; Grigoriev, I.V.; Kubicek, C.P.; Martinez, D.; van Peij, N.N.M.E.; Roubos, J.A.; Nielsen, J.; Baker, S.E. Comparative genomics of citric-acid-producing *Aspergillus niger* ATCC 1015 versus enzyme-producing CBS 513.88. *Genome Res.* **2011**, *21*, 885-897.

Arai, K.; Kimura, K.; Mushiroda, T.; Yamamoto, Y. Structures of fructigenies A and B, new alkaloids isolated from *Penicillium fructigenum* Takeuchi. *Chem. Pharm. Bull.* **1989**, *37*, 2937-2939.

Arnaud, M.B.; Binkley, J.; Chibucos, M.C.; Costanzo, M.C.; Crabtree, J.; Inglis, D.O.; Orvis, J.; Shah, P.; Skrzypek, M.S.; Binkley, G.; Miyasato, S.R.; Wortman, J.R.; Sherlock, G. *Aspergillus* Genome Database Avaliable online: http://www.aspgd.ord/ accessed June 9th 2012.

Aucamp, P.J.; Holzapfel, C.W. The constution of nidulol (5-hydroxy-7-methoxy-6-methylphthalide), a metabolic product of *Aspergillus nidulans* (Eidam) Wint. *J. S. Afr. Chem. I.* **1968**, *21*, 26-32.

Ayer, W.A.; Trifonov, L.S. Drimane sesquiterpene lactones from *Peniophora polygonia*. *J. Nat. Prod.* **1992**, *55*, 1454-1461.

Baker, S.E. *Aspergillus niger* genomics: past, present and into the future. *Med. Mycol.* **2006**, *44*, S17-S21.

Balibar, C.J.; Howard-Jones, A.R.; Walsh, C.T. Terrequinone A biosynthesis through *L*-tryptophan oxidation, dimerization and bisprenylation. *Nat. Chem. Bio.* **2007**, *3*, 584-592.

Ballantine, J.A.; Hassall, C.H.; Jones, G. Asperugin, a ,etabolite associated with abnormal morphology of *Aspergillus rugulosus*. *Tetrahedron Lett.* **1964**, *49*, 3739-3740.

Ballantine, J.A.; Hassall, C.H.; Jones, G. The biosynthesis of phenols. Part IX. Asperugin, a metabolic product of *Aspergillus rugulosus*. *J. Chem. Soc.* **1965**, 4672-4678.

Ballantine, J.A.; Hassall, C.H.; Jones, B.D.; Jones, G. The biosynthesis of phenols XII. Asperugin B, a metabolite of *Aspergillus rugulosus*. *Phytochem.* **1967**, *6*, 1157-1159.

Ballantine, J.A.; Francis, D.J.; Hassall, C.H.; Wright, J.L.C. The biosynthesis of phenols. Part XX1. The molecular structure of arugosin, a metabolite of a wild-type strain of *Aspergillus rugulosus*. *J. Chem. Soc. C* **1970**, *9*, 1175-1182.

Ballantine, J.A.; Ferrito, V.; Hassall, C.H. The biosynthesis of asperugin in *Aspergillus rugulosus*. *Phytochem.* **1971**, *10*, 1309-1313.

Barbier, M.; Vetter, W.; Bogdanov, D.; Lederer, E. Synthese und eigenschafgen eines analogen des lycomarasmins und der aspergillomarasmine. *Annalen der Chemie-Justus Liebig* **1963**, *668*, 132.

Barrow, C.J.; Cai, P.; Snyder, J.K.; Sedlock, D.M.; Sun, H.H.; Cooper, R. WIN 64821, a new competitive antagonist to substance P, isolated from an *Aspergillus* species: structure determination and solution conformation. *J. Org. Chem.* **1993**, *58*, 6016-6021.

Barrow, C.J.; Sedlock, D.M. 1'-(2-phenyl-ethylene)-ditryptophenaline, a new dimeric diketopiperazine from *Aspergillus flavus*. *J. Nat. Prod.* **1994**, *57*, 1239-1244.

Bartók, T.; Szécsi, Á.; Szekeres, A.; Mesterházy, Á.; Bartók, M. Detection of new fumonisin mycotoxins and fumonisin-like compounds by reversed-phase high-performance liquid chromatography/electrospray ionization ion trap mass spectrometry. *Rapid Commun. Mass Spectrom.* **2006**, *20*, 2447-2462.

Bayram, Ö.; Krappmann, S.; Ni, M.; Bok, J.W.; Helmstaedt, K.; Valerius, O.; Braus-Stromeyer, S.; Kwon, N.-J.; Keller, N.P.; Yu, J.-H.; Braus, G.H. VelB/VeA/LaeA complex coordinates light signal with fungal development and secondary metabolism. *Science* **2008**, *320*, 1504-1506.

Bayram, Ö, Braus, G.H. Coordination of secondary metabolism and development in fungi: the velvet family of regulatory proteins. *FEMS Microbiol. Rev.* **2012,** *36*, 1-24.

Beier, R.C.; Stanker, L.H. Molecular models for the stereochemical structures of fumonisin B_1 and B_2. *Arch. Environ. Contam. Toxicol.* **1997**, *33*, 1-8.

Bentley, R. From *miso, sake* and *shoyu* to cosmetics: a century of science for kojic acid. *Nat. Prod. Rep.* **2006**, *23*, 1046-1062.

Bergmann, S.; Schümann, J.; Scherlach, K.; Lange, C.; Brakhage, A.A.; Hertweck, C. Genomics-driven discovery of PKS-NRPS hybrid metabolites from *Aspergillus nidulans*. *Nat. Chem. Biol.* **2007**, *3*, 213-217.

Bergmann, S.; Funk, A.N.; Scherlach, K.; Schroeckh, V.; Shelest, E.; Horn, U.; Hertweck, C.; Brakhage, A.A. Activation of a silent fungal polyketide biosynthesis pathway through regulatory cross talk with a cryptic nonribosomal peptide synthetase gene cluster. *Appl. Environ. Microbiol.* **2010**, *76*, 8143-8149.

Bezuidenhout, S.C.; Gelderblom, W.C.A.; Gorst-Allman, C.P.; Horak, R.M.; Marasas, W.F.O.; Spiteller, G.; Vleggaar, R. Structure elucidation of the fumonisins, mycotoxins from *Fusarium moliforme*. *J. Chem. Soc. Chem. Commun.* **1988**, 743-745.

Bills, G.F.; Giacobbe, R.A.; Lee, S.H.; Peláez, F.; Tkacz, J.S. Tremorgenic mycotoxins, paspalitrem A and C, from a tropical *Phomopsis*. *Mycol. Res.* **1992**, *96*, 977-983.

Bilmen, J.G.; Wootton, L.L.; Michelangeli, F. The mechanism of inhibition of the sarco/endoplasmic reticulum Ca^{2+} ATPase by paxilline. *Arch. Biochem. Biophys.* **2002**, *406*, 55-64.

Bingle, L.E.H.; Simpson, T.J.; Lazarus, C.M. Ketosynthase domain probes identify two subclasses of fungal polyketide synthase genes. *Fungal Genet. Biol.* **1999**, *26*, 209-223.

Blount, W.P. Turkey "X" disease. *Turkeys* **1961**, *61*, 55-58.

Bode, H.B.; Bethe, B.; Höfs, R.; Zeeck, A. Big effects from small changes: possible ways to explore nature's chemical diversity. *ChemBioChem* **2002**, *3*, 619-627.

Bok, J.W.; Keller, N.P. LaeA, a regulator of secondary metabolism in *Aspergillus* spp. *Eukaryot. Cell.* **2004**, *3*, 527-535.

Bok, J.W.; Hoffmeister, D.; Maggio-Hall, L.A.; Murillo, R.; Glasner, J.D.; Keller, N.P. Genomic mining for *Aspergillus* natural products. *Chem. Biol.* **2006**, *13*, 31-37.

Bok, J.W.; Chiang, Y.-M.; Szewczyk, E.; Reyes-Domingez, Y.; Davidson, A.D.; Sanchez, J.F.; Lo, H.-C.; Watanabe, K.; Strauss, J.; Oakley, B.R.; Wang, C.C.C.; Keller, N.P. Chromatin-level regulation of biosynthetic gene clusters. *Nat. Chem. Biol.* **2009**, *5*, 462-464.

Brakhage, A.A.; Schroeckh, V. Fungal secondary metabolites – strategies to activate silent gene clusters. *Fungal. Genet. Biol.* **2011**, *48*, 15-22.

Broad Institute Aspergillus comparative database. **2012**. Available at: http://www.broadinstitute.org/annotation/genome/aspergillus_group/GenomeStats.html (accessed June 17th 2012).

Broman, K.; Toivari, M.; Viljanen, K.; Vouristo, A.; Ruohonen, L.; Nakari-Setälä, T. Identification and characterization of a novel diterpene gene cluster in *Aspergillus nidulans*. *PLoS ONE* **2012**, *7*, e35450.

Brown, D.W.; Yu, J.-H.; Kelkar, H.S.; Fernandes, M.; Nesbitt, T.C.; Keller, N.P.; Adams, T.H.; Leonard, T.J. Twenty-five coregulated transcripts define a sterigmatocystin gene cluster in *Aspergillus nidulans*. *Proc. Natl. Acad. Sci. USA* **1996**, *93*, 1418–1422.

Calvo, A.M.; Wilson, R.A.; Bok, J.W.; Keller, N.P. Relationship between secondary metabolism and fungal development. *Microbiol. Mol. Biol. Rev.* **2002**, *66*, 447-459.

Calvo , A.M. The VeA regulatory system and its role in morphological and chemical development in fungi. *Fungal Genet. Biol.* **2008**, *45*, 1053-1061

Cao, L.; Zhang, P.; Grant, D.F. An insect farnesyl phosphate homologous to the *N*-terminal domain of soluble epoxide hydrolase. *Biochem. Bioph. Res. Co.* **2009**, *380*, 188-192.

Cary, J.W.; Ehrlich, K.C.; Bland, J.M.; Montalbano, B.G. The aflatoxin biosynthesis cluster gene, *aflX*, encodes an oxidoreductase involved in conversion of versicolorin A to demethylsterigmatocystin. *Appl. Environ. Microbiol.* **2006**, *72*, 1096–1101.

Center for Integrated Fungal Research *Aspergillus flavus* genome sequencing project. 2012 Available at: http://aspergillusflavus.org/genomics/ (Accessed on June 17th 2012)

Chang, P.K.; Yu, J.; Ehrlich, K.C.; Boue, S.M.; Montalbano, B.G.; Bhatnagar, D.; Cleveland, T.E. *adhA* in *Aspergillus parasiticus* is involved in conversion of 5'-hydroxyaverantin to averufin. *Appl. Environ. Microbiol.* **2000**, *66*, 4715–4719.

Chang, P.-K.; Yabe, K.; Yu, J. The *Aspergillus parasiticus estA*-encoded esterase converts versiconal hemiacetal acetate to versiconal and versiconol acetate to versiconol in aflatoxin biosynthesis. *Appl. Environ. Microbiol.* **2004**, *70*, 3593–3599.

Chang, P.K.; Horn, B.W.; Dorner, J.W. Clustered genes involved in cyclopiazonic acid production are next to the aflatoxin biosynthesis gene cluster in *Aspergillus flavus*. *Fungal Genet. Biol.* **2009**, *46*, 176-182.

Chiang, Y.-M.; Szewczyk, E.; Nayak, T.; Davidson, A.D.; Sanchez, J.F.; Lo, H.-C.; Ho, W.-Y.; Simityan, H.; Kuo, E.; Praseuth, A.; Watanabe, K.; Oakley, B.R.; Wang, C.C.C. Molecular genetic mining of the *Aspergillus* secondary metabolome: discovery of the emericellamide biosynthetic pathway. *Chem. Biol.* **2008**, *15*, 527-532.

Chiang, Y.-M.; Szewczyk, E.; Davidson, A.D.; Keller, N.; Oakley, B.R.; Wang, C.C.C. A gene cluster containing two fungal polyketide synthases encodes the biosynthetic pathway for a polyketide, asperfuranone, in *Aspergillus nidulans*. *J. Am. Chem. Soc.* **2009a**, *131*, 2965-2970.

Chiang, Y.-M.; Lee, K.-H.; Sanchez, J.F.; Keller, N.P.; Wang, C.C.C. Unlocking fungal cryptic natural products. *Nat. Prod. Commun.* **2009b**, *4*, 1505-1510.

Chiang, Y.-M.; Oakley, B.R.; Keller, N.P.; Wang, C.C.C. Unraveling polyketide synthesis in menbers of the genus *Aspergillus*. *Appl. Environ. Microb*. **2010a**, *86*, 1719-1736.

Chiang, Y.-M.; Szewczyk, E.; Davidson, A.D.; Entwistle, R.; Keller, N.P.; Wang, C.C.C.; Oakley, B.R. Characterization of the *Aspergillus nidulans* monodictyphenone gene cluster. *Appl. Environ. Microbiol.* **2010b**, *76*, 2067-2074.

Chiang, Y.-M.; Chang, S.-L.; Oakley, B.R.; Wang, C.C.C. Recent advances in awakening silent biosynthetic gene clusters and linking orphan clusters to natural products in microorganisms. *Curr. Opin. Chem. Biol.* **2011**, *15*, 137-143.

Cichewicz, R.H. Epigenome manipulation as a pathway to new natural product scaffolds and their congeners. *Nat. Prod. Rep.* **2010**, *27*, 11-22.

Cleveland, T.E.; Yu, J.; Fedorova, N.; Bhatnagar, D.; Payne, G.A.; Nierman, W.C.; Bennett, J.W. Potential of *Aspergillus flavus* genomics for applications in biotechnology. *Trends Biotechnol.* **2009**, *27*, 151-157.

Cole, R.J.; Dorner, J.W.; Springer, J.W., Cox, R.H. Indole metabolites from a strain of *Aspergillus flavus*. *J. Agric. Food Chem.* **1981**, *29*, 293-295.

Cox, R.J. Polyketides, proteins and genes in fungi: programmed nano-machines begin to reveal their secrets. *Org. Biomol. Chem.* **2007**, *5*, 2010-2026.

Crawford, J.M; Vagstad, A.L.; Ehrlich, K.C.; Townsend, C.A. Starter unit specificity directs genome mining of polyketide synthase pathways in fungi. *Bioorg. Chem.* **2008a**, *36*, 16-22.

Crawford, J.M.; Thomas, P.M.; Scheerer, J.R.; Vagsted, A.L.; Kelleher, N.L.; Townsend, C.A. Deconstruction of iterative multidomain polyketide synthase function. *Science* **2008b**, *320*, 243-246.

Crawford, J.M.; Korman, T.P.; Labonte, J.W.; Vagstad, A.L.; Hill, E.A.; Kamari-Bidkorpeh, O.; Tsai, S.C.; Townsend, C.A. Structural basis for biosynthetic programming of fungal aromatic polyketide cyclization. *Nature* **2009**, *461*, 1139-1144.

Crawford J.M.; Townsend, C.A. New insights into the formation of fungal aromatic polyketides. *Nat. Rev. Microbiol.* **2010**, *8*, 879-889.

Dewick, P.M. The biosynthesis of shikimate metabolites. *Nat. Prod. Rep.* **1998**, *15*, 17-58.

Dewick, P.M. The biosynthesis of C_5-C_{25} terpenoid compounds. *Nat. Prod. Rep.* **2002**, *19*, 181-222.

Dinamarco, T.M.; Goldman, M.H.S.; Goldman, G.H. Farnesol-induced cell death in the filamentous fungus *Aspergillus nidulans*. *Biochem. Soc. T.* **2011**, *39*, 1544-1548.

DOE Joint Genome Institute *Aspergillus aculeatus* ATCC16872 Genome portal v.1.1. **2012a** Available at: http://genome.jgi-psf.org/Aspac1/Aspac1.home.html. (Accessed on June 17th 2012)

DOE Joint Genome Institute *Aspergillus carbonarius* ITEM 5010 Genome portal v.3. **2012b** Available at: http://genome.jgi-psf.org/Aspca3/Aspca3.home.html. (Accessed on June 17th 2012)

von Döhren, H. A survey of nonribosomal peptide synthetase (NRPS) genes in *Aspergillus nidulans*. *Fungal Genet. Biol.* **2009**, *46*, S45-S52.

Du, L.; Lou, L. PKS and NRPS release mechanisms. *Nat. Prod. Rep.* **2010**, *27*, 255-278.

Ehrlich, K.C.; Montalbano, B.; Boué, S.M.; Bhatnagar, D. An aflatoxin biosynthesis cluster gene encodes a novel oxidase required for conversion of versicolorin A to sterigmatocystin. *Appl. Environ. Microbiol.* **2005**, *71*, 8963–8965.

Ehrlich, K.C.; Li, P.; Scharfenstein, L.; Chang, P.-K. HypC, the anthrone oxidase involved in aflatoxin biosynthesis. *Appl. Environ. Microbiol.* **2010**, *76*, 3374–3377.

El-Feraly, F.S.; Cheatham, S.F.; McChesney, J.D. Total synthesis of notholaenic acid. *J. Nat. Prod.* **1985**, *48*, 293-298.

Evans, S.E.; Williams, C.; Arthur, C.J.; Burston, S.G.; Simpson, T.J.; Crosby, J.; Crump, M.P. An ACP structural switch: conformational differences between the apo and holo forms of the actinorhodin polyketide synthase acyl carrier protein. *ChemBioChem* **2008**, *9*, 2424-2432.

Fedorova, N.D.; Khaldi, N.; Joardar, V.S.; Maiti, R.; Amedeo, P.; Anderson, M.J.; Crabtree, J.; Silva, J.C.; Badger, J.H.; Albarraq, A.; Angiuoli, S.; Bussey, H.; Bowyer, P.; Cotty, P.J.; Dyer, P.S.; Egan, A.; Galens, K.; Fraser-Liggett, C.M.; Haas, B.J.; Inman, J.M.; Kent, R.; Lemieux, S.; Malavazi, I.; Orvis, J.; Roemer, T.; Ronning, C.M.; Sundaram, J.P.; Sutton, G.; Turner, G.; Venter, J.C.; White, O.R.; Whitty, B.R.; Youngman, P.; Wolfe, K.H.; Goldman, G.H.; Wortman, J.R.; Jiang, B.; Denning, D.W.; Nierman, W.C. Genomic islands in the pathogenic filamentous fungus *Aspergillus fumigatus*. *PLoS Genet.* **2008**, *4*, e1000046.

Filtenborg, O.; Frisvad, J.C.; Thrane, U. The significance of yeast extract composition on metabolite production in *Penicillium*. *Modern Concepts in Penicillium and Aspergillus classification* (Samson RA & Pitt JI, eds) **1990**, Plenum Press, New York, 433-440.

Fisch, K.M.; Gillaspy, A.F.; Gipson, M.; Henrikson, J.C.; Hoover, A.R.; Jackson, L.; Najar, F.Z.; Wägele, H.; Cichewicz, R.H. Chemical induction of silent biosynthetic pathway transcription in *Aspergillus niger*. *J. Ind. Microbiol. Biotechnol.* **2009**, *33*, 1199-1213.

Fisch, K.M.; Bakeer, W.; Yakasai, A.A.; Song, Z.; Pedricki, J.; Wasil, Z.; Bailey, A.M.; Lazarus, C.M.; Simpson, T.J.; Cox, R.J. Rational domain swaps decipher programming in fungal highly reducing polyketide synthases and resurrect an extinct metabolite. *J. Am. Chem. Soc.* **2011**, *133*, 16635-16641.

Fischbach, M.A.; Walsh, C.T. Assembly-line enzymology for polyketide and nonribosomal peptide antibiotics: logic, machinery, and mechanisms. *Chem. Rev.* **2006**, *106*, 3468-3496.

Fleming, A. On the antibacterial action of cultures of a *Penicilium*, with special reference to their use in the isolation of *B. influenzal*. *Br. J. Exp. Pathol.* **1929**, *10*, 226-236.

Fox, E.M.; Howlett, B.J. Secondary metabolism: regulation and role in fungal biology. *Curr. Opin. Microbiol.* **2008**, *11*, 1-7.

Frisvad, J.C. Physiological criteria and mycotoxin production as aids in identification of common asymmetric penicillia. *Appl. Environ. Microbiol.* **1981**, *41*, 568-579

Frisvad, J.C.; Filtenborg, O. Classification of terverticillate penicillia based on profiles of mycotoxins and other secondary metabolites. *Appl. Environ. Microbiol.* **1983**, *46*, 1301-1310.

Frisvad 1987, J.C.; Thrane, U. Standardized high-performance liquid chromatography of 182 mycotoxins and other fungal metabolites based on alkylphenone retention indices and UV-VIS spectra (diode array detection). *J. Chromatogr.* **1987**, *404*, 195-214.

Frisvad, J.C.; Samson, R.A. Polyphasic taxonomy of *Penicillium* subgenus *Penicillium*. A guide to identification of the food air-borne terverticillate Penicillia and their mycotoxins. *Stud. Mycol.* **2004a**, *49*, 1-173.

Frisvad, J.C.; Smedsgaard, J.; Larsen, T.O.; Samson, R.A. Mycotoxin, drugs and other extrolites produced by species in *Penicillium* subgenus *Penicillium*. *Stud. Mycol.* **2004b**, *49*, 201-241.

Frisvad, J.C.; Smedsgaard, J.; Samson, R.A.; Larsen, T.O.; Thrane, U. Fumonisin B_2 production by *Aspergillus niger*. *J. Agric. Food Chem.* **2007**, *55*, 9727-9732.

Fuchser, J.; Zeeck, A. Aspinolides and aspinonene/aspyrone co-metabolites, new pentaketides produced by *Aspergillus ochraceus*. *Liebigs Ann./Recueil* **1997**, 87-95.

Fujita, M.; Yamada, M.; Nakajima, S.; Kawai, K.-I.; Nagai, M. *O*-methylation effect on the carbon-13 nuclear magnetic resonance signals of *ortho*-disubstituted phenols and its application to structure determination of new phthalides from *Aspergillus silvaticus*. *Chem. Pharm. Bull.* **1984**, *32*, 2622-2627.

Fukuyama, K.; Kawai, H.; Tsukihara, T.; Tsukihara, K.; Katsure, Y.; Hamasaki, T.; Hatsuda, Y.; Kuwano, H. A structure analysis of a bromo derivative of parasiticolide A by the X-ray diffraction method. *Bull. Chem. Soc. Jpn.* **1975**, *48*, 2949-2950.

Galagan, J.E; Calvo, S.E, Cuomo, C.; Ma, L.-J.; Wortman, J.R.; Batzoglou, S.; Lee, S.-I.; Bastürkmem, M.; Spevak, C.C.; Clutterbuck, J.; Kapitonov, V.; Jurka, J.; Scazzocchio, C.; Farman, M.; Butler, J.; Purcell, S.; Harris, S.; Braus, G.H.; Draht, O.; Busch, S.; D'Enfert, C.; Bouchier, C.; Goldman, G.H.; Bell-Pedersen, D.; Griffiths-Jones, S.; Doonan, J.H.; Yu, J.; Vienken, K.; Pain, A.; Freitag, M.; Selker, E.U.; Archer, D.B.; Peñalva, M.Á.; Oakley, B.R.; Momany, M.; Tanaka, T.; Kumagai, T.; Asai, K.; Machida, M.; Nierman, W.C.; Denning, D.W.; Caddick, M.; Hynes, M.; Paoletti, M.; Fischer, R.; Miller, B.; Dyer, P.; Sachs, M.S.; Osmani, S.A.; Birren, B.W. Sequencing of *Aspergillus nidulans* and comparative analysis with *A. fumigatus* and *A. oryzae*. *Nature* **2005**, *438*, 1105-1115.

Gallagher, R.T.; Wilson, B.J. Aflatrem, the tremorgenic mycotoxin from *Aspergillus flavus*. *Mycopathologia* **1978**, *66*, 183-185.

Gallagher, R.T.; Clardy, J. Aflatrem, a tremorgenic toxin from *Aspergillus flavus*. *Tetrahedron Lett.* **1980**, *21*, 239-242.

Gao, W.; Yang, H.; Qi, L.-W.; Liu, E.H.; Ren, M.-T.; Yan, Y.T.; Chen, J.; Li, P. Unbiased metabolite profiling by liquid chromatography-quadrupole time-of-flight mass spectrometry and multivariate data analysis for herbal authentication: classification of seven *Lonicera* species flower buds. *J. Chromatogr. A* **2012**, *1245*, 109-116.

Geiser, D.M.; Pitt, J.I.; Taylor, J.W. Cryptic speciation and recombination in the aflatoxin-producing fungus *Aspergillus flavus*. *Proc. Natl. Acad. Sci. USA* **1998**, *95*, 399-393.

Geiser, D.M.; Dorner, J.W.; Horn, B.W.; Taylor, J.W. The phylogenetics of mycotoxin and sclerotium production in *Aspergillus flavus* and *Aspergillus oryzae*. *Fungal Genet. Biol.* **2000**, *31*, 169-179.

Gelderblom, W.C.; Jaskiewicz, K.; Marasas, W.F.; Thiel, P.G.; Horak, R.M.; Vleggaar, R.; Kriek, N.P. Fumonisin – novel mycotoxins with cancer-promoting activity produced by *Fusarium moniliforme*. *Appl. Environ. Microbiol.* **1988**, *54*, 1806-1811.

Gelderblom, W.C.A.; Cawood, M.E.; Snyman, S.D.; Vleggaar, R.; Marasas, W.F.O. Structure-activity relationships of fumonisins in short-term carcinogenesis and cytotoxicity assays. *Fd. Chem. Toxic.* **1993**, *31*, 407-414.

Geris, R.; Simpson, T.J. Meroterpenoids produced by fungi. *Nat. Prod. Rep.* **2009**, *26*, 1063-1094.

Gilbert, L.I.; Granger, N.A.; Roe, R.M. The juvenile formones: historical facts and speculations on future research directions. *Insect Biochem. Molec.* **2000**, *30*, 617-644.

Gill, G. SUMO and ubiquitin in the nucleus: different functions, similar mechanisms? *Genes. Dev.* **2004**, *18*, 1105-1115.

Gloer, J.B.; TePaske, M.R.; Sima, J.S. Antiinsectan aflavinine derivatives from the sclerotia of *Aspergillus flavus*. *J. Org. Chem.* **1988**, *53*, 5457-5460.

Gloer, J.B.; Rinderknecht, B.L. Nominine: a new insecticidal indole diterpene from the sclerotia of *Aspergillus nomius*. *J. Org. Chem.* **1989**, *54*, 2530-2532.

Gould, R.O.; Simpson, T.J.; Walkinshaw, M.D. Isolation and X-ray crystal structures of astellolides A and B, sesquiterpenoid metabolites of *Aspergillus variecolor*. *Tetrahedron Lett.* **1981**, *22*, 1047-1050.

Gross, H. Strategies to unravel the function of orphan biosynthesis pathways: recent examples and future prospects. *Appl. Microbiol. Biotechnol.* **2007**, *75*, 267-277.

Hamasaki, T. Kuwano, H.; Isono, K.; Hatsuda, Y.; Fukuyama, K.; Tsukihara, T.; Katsube, Y. A new metabolite, parasiticolide A, from *Aspergillus parasiticus*. *Agr. Biol. Chem.* **1975**, *39*, 749-751.

Hansen, B.G.; Salomonsen, B.; Nielsen, M.T.; Nielsen, J.B.; Hansen, N.B.; Nielsen, K.F.; Regueira, T.B.; Nielsen, J.; Patil, K.R.; Mortensen, U.H. Versatile enzyme expression and characterization system for *Aspergillus nidulans*, with the *Penicillium brevicompactum* polyketide synthase gene from the mycophenolic acid gene cluster as a test case. *Appl. Environ. Microbiol.* **2011**, *77*, 3044-3051.

Heneghan, M.N.; Yakasai, A.A.; Williams, K.; Kadir, K.A.; Wasil, Z.; Bakeer, W.; Fisch, K.M.; Bailey, A.M.; Simpson, T.J.; Cox, R.J. The programming role of *trans*-acting enoyl reductases during the biosynthesis of highly reduced fungal polyketides. *Chem. Sci.* **2011**, *2*, 972-979.

Henrikson, J.C.; Hoover, A.R.; Joyner, P.M.; Cichewicz, R.H. A chemical epigenetics approach for engineering the *is situ* biosynthesis of a cryptic natural product from *Aspergillus niger*. *Org. Biomol. Chem.* **2009**, *7*, 435-438.

Henry, K.M.; Townsend, C.A. Ordering the reductive and cytochrome P450 oxidative steps in demethylsterigmatocystin formation yields general insights into the biosynthesis of aflatoxin and related fungal metabolites. *J. Am. Chem. Soc.* **2005**, *127*, 3724–3733.

Hertweck, C. The biosynthetic logic of polyketide diversity. *Angew. Chem. Int. Ed.* **2009**, *48*, 4688-4716.

Hoffmeister, D.; Keller, N.P. Natural products of filamentous fungi: enzymes, genes and their regulation. *Nat. Prod. Rep.* **2007**, *24*, 393-416.

Höfs, R.; Walker, M.; Zeeck, A. Hexacyclinic acid, a polyketide from *Streptomyces* with a novel carbon skeleton. *Angew. Chem. Int. Ed.* **2000**, *39*, 3259-3261.

Hornby, J.M.; Jensen, E.C.; Lisec, A.D.; Taste, J.J.; Jahnke, B.; Shoemaker, R.; Dussault, P.; Nickerson, K.W. Quorum sensing in the dimorphic fungus *Candida albicans* is mediated by fornesol. **2001**, *67*, 2982-2992.

Iizuka, H.; Iida, M. Maltoryzine, a new toxic metabolite produced by a strain if *Aspergillus oryzae* var. *microspores* isolated from the poisonous malt sprout. *Nature* **1962**, *196*, 681-682.

Ishikawa, Y.; Morimoto, K.; Hamasaki, T. Flavogaulin, a metabolite of *Eurotium chevalieri*, its antioxidation and synergism with tocopherol. *J. Am. Oil Chem. Soc.* **1984**, *61*, 1864-1868.

Jenuwein, T.; Allis, C.D. Translating the histone code. *Science* **2001**, *293*, 1074-1080.

Jin, F.J.; Takahashi, T.; Utsushikawa, M.; Furukido, T.; Nishida, M.; Ogawa, M.; Tokuoka, M.; Koyama, Y. A trial of minimization of chromosome 7 in *Aspergillus oryzae* by multiple chromosomal deletions. *Mol. Genet. Genimics* **2010**, *283*, 1-12.

Johnson, E.S. Proteinmodification by SUMO. *Annu. Rev. Biochem.* **2004**, *73*, 355-382.

Kato, N.; Brooks, W.; Calvo, A.M. The expression of sterigmatocystin and penicillin genes in *Aspergillus nidulans* is controlled by *veA*, a gene required for sexual development. *Eukaryot. Cell* **2003**, *2*, 1178-1186.

Kawahara, N.; Nozawa, K.; Nakajima, S.; Kawai, K.-I. Studies on fungal products. Part 15. Isolation and structure determination of arugosin E from *Aspergillus silvaticus* and cycloisoemericellin from *Emericella striata*. *J. Chem. Soc. Perkin Trans. I* **1988a**, 907-911.

Kawahara, N.; Nozawa, K.; Nakajima, S.; Udagawa, S.-I.; Kawai, K.-I. Studies on fungal products XVI. New metabolites related to 3-methylorsellinate from *Aspergillus silvaticus*. *Chem. Pharm. Bull.* **1988b**, *36*, 398-400.

Käfer, E. Origins of translocations in *Aspergillus nidulans*. *Genetics* **1965**, *52*, 217-232.

Kelkar, H.S.; Keller, N.P.; Adams, T.H. *Aspergillus nidulans stcP* encodes an *O*-methyltransferase that is required for sterigmatocystin biosynthesis. *Appl. Environ. Microbiol.* **1996**, *62*, 4296–4298.

Kelkar, H.S.; Skloss, T.W.; Haw, J.F.; Keller, N.P.; Adams, T.H. *Aspergillus nidulans stcL* encodes a putative cytochrome P-450 monooxygenase required for bisfuran desaturation during aflatoxin/sterigmatocystin biosynthesis. *J. Biol. Chem.* **1997**, *272*, 1589–1594.

Keller, N.P.; Kantz, N.J.; Adams, T.H. *Aspergillus nidulans verA* is required for production of the mycotoxin sterigmatocystin. *Appl. Environ Microbiol*. **1994**, *60*, 1444–1450.

Keller, N.P.; Segner, S.; Bhatnagar, D.; Adams, T.H. *stcS*, a putative P-450 monooxygenase, is required for the conversion of versicolorin A to sterigmatocystin in *Aspergillus nidulans*. *Appl. Environ. Microbiol.* **1995**, *61*, 3628–3632.

Keller, N.P.; Watanabe, C.M.H.; Kelkar, H.S.; Adams, T.H.; Townsend, C.A. Requirement of monooxygenase-mediated steps for sterigmatocystin biosynthesis by *Aspergillus nidulans*. *Appl. Environ. Microbiol.* **2000**, *66*, 359–362.

Keller, N.P.; Turner, G.; Bennett, J.W. Fungal secondary metabolism – from biochemistry to genomics. *Nat. Rev. Microbiol*. **2005**, *3*, 937-947.

Kempken, F.; Rohlfs, M. Fungal secondary metabolite biosynthesis – a chemical defence strategy against antagonistic animals? *Fungal Ecol.* **2010**, *3*, 107-114.

Klausmeyer, P.; McCloud, T.G.; Tucker, K.D.; Cardellina II, J.H.; Shoemaker, R.H. Aspirochlorine class compounds from *Aspergillus flavus* inhibit azole-resistant *Candida albicans*. *J. Nat. Prod.* **2005**, *68*, 1300-1302.

Knaggs A.R. The biosynthesis of shikimate metabolites. *Nat. Prod. Rep.* **2003**, *20*, 119-136.

Kobayashi, T.; Abe, K.; Asai, K.; Gomi, K.; Juvvadi, P.R.; Kato, M.; Kitamoto, K.; Takeuchi, M.; Machida, M. Genomics of *Aspergillus oryzae*. *Biosci. Biotechnol. Biochem.* **2007**, *71*, 646-670.

Koglin, A.; Walsh, C.T. Structural insights into nonribosomal peptide enzymatic assembly lines. *Nat. Prod. Rep.* **2009**, *26*, 987-1000.

Kralj, A. Kehraus, S.; Krick, A.; Eguerva, E.; Kelter, G.; Maurer, M.; Wortmann, A.; Fiebig, H.H.; König, G.M. Arugosin G and H: prenylated polyketides from the marine-derived fungus *Emericella nidulans* var. *acristata*. *J. Nat. Prod.* **2006**, *69*, 995-1000.

Kroken, S.; Glass, N.L.; Taylor, J.W.; Yoder, O.C.; Turgeon, B.G. Phylogenomic analysis of type I polyketide synthase genes in pathogenic and saprobic ascomycetes. *Proc. Natl. Acad. Soc. USA* **2003**, *100*, 15670-15675.

Kuhnz, W.; Rembold, H. Carbon-13 nuclear magnetic resonance spectra of juvenile hormone III, some of its derivatives, and of analogous compounds. *Org. Magn. Resonance* **1981**, *16*, 138-140.

Laatsch, H. AntiBase 2010. Available online: http://www.wiley-vch.de/stmdata/antibase2010.php (accessed on May 30th 2012).

Lamb, H.K.; van den Hombergh, J.P.T.W,: Newton, G.H.; Moore, J.D.; Roberts, C.F.; Hawkins, A.R. Differential flux through the quinate and shikimate pathways. *Biochem. J.* **1992**, *284*, 181-187.

Lee, Y.H.; Tominaga, M.; Hayashi, R.; Sakamoto, K.; Yamada, O.; Akita, O. *Aspergillus oryzae* strains with a large deletion of the aflatoxin biosynthetic homologous gene cluster differentiated by chromosomal breakage. *Appl. Microbiol. Biotechnol.* **2006**, *72*, 339-345.

Liu, T.; Chiang, Y.-M.; Somoza, A.D.; Oakley, B.R.; Wang, C.C.C. Engineering of an “unnatural” natural product by swapping polyketide synthase domains in *Aspergillus nidulans*. *J. Am. Chem. Soc.* **2011**, *133*, 13314-13316.

Lo, H.-C.; Entwistle, R.; Gou, C.-J.; Ahuja, M.; Szewczyk, E.; Hung, J.-H.; Chiang, Y.M.; Oakley, B.R.; Wang, C.C.C. Two separate gene clusters encode the biosynthetic pathway for the meroterpenoids, austinol and dehydroaustinol in *Aspergillus nidulans*. *J. Am. Chem. Soc.* **2012**, *134*, 4709-4720.

Longland, C.L.; Dyer, J.L.; Michelangeli, F. The mycotoxin paxillin inhibits the cerebellar inositol 1,4,5-triphosphate receptor. *Eur. J. Pharmacol.* **2000**, *408*, 219-225.

Machida, M.; Asai, K.; Sano, M.; Tanaka, T.; Kumagai, T.; Terai, G.; Kusumoto, K.I.; Arima, T.; Akita, O.; Kashiwaga, Y.; Abe, K.; Gomi, K.; Horiuchi, H.; Kitamoto, K.; Kobayashi, T.; Takeuchi, M.; Denningm D.W.; Galagan, J.E.; Nierman, W.C.; Yu, J.; Archer, D.B.; Bennett, J.W.; Bhatnagar, D.; Cleveland, T.E.; Fedorova, N.D.; Gotoh, O.; Horikawa, H.; Hosoyama, A.; Ichinomiya, M.; Igarashi, R.; Iwashita, K.; Juvvadi, P.R.; Kato, M.; Kato, Y.; Kin, T.; Kokubun, A.; Maeda, H.; Maeyama, N.; Maruyama, J.; Nagaski, H.; Nakajima, T.; Oda, K.; Okada, K.; Paulsen, I.; Sakamoto, K.; Sawano, T.; Takahashi, M.; Takase, K.; Terabayashi, Y.; Wortman, J.R.; Yamada, O.; Yamagata, Y.; Anazawa, H.; Hata, Y.; Koide, Y.; Komori, T.; Koyama, Y.; Minetoki, T.; Suharnan, S.; Tanaka, A.; Isono, K.; Kuhara, S.; Ogasawara, N.; Kikuchi, H. Genome sequencing and analysis of *Aspergillus oryzae*. *Nature* **2005**, *438*, 1157-1161.

Machida, M.; Yamada, O., Gomi, K. Genomics of *Aspergillus oryzae*: learning from the history of koji mold and exploration of its future. *DNA Res.* **2008a**, *15*, 173-183.

Machida, M.; Terabayashi, Y.; Sano, M.; Yamene, N.; Tamano, K.; Payne, G.A.; Yu, J.; Cleveland, T.E.; Nierman, W.C. Genomics of industrial Aspergilli and comparison with toxigenic relatives. *Food Addit. Contam. Part A* **2008b**, *25*, 1147-1151.

MacKenzie, S.E.; Savard, M.E.; Blackwell, B.A.; Miller, J.D.; ApSimon, J.W. Isolation of a new fumonisin from *Fusarium moniliforme* grown in liquid culture. *J. Nat. Prod.* **1998**, *61*, 367-369.

MacPherson, S.; Larochelle, M.; Turcotte, B. A fungal family of transcriptional regulators: the zinc cluster proteins. *Microbiol. Biol. Rev.* **2006**, *70*, 583-604.

Manabe, M.; Tanaka, K.; Goto, T.; Matsuura, S. Producing capability if kojic acid and aflatoxin by koji mold. In: *Toxigenic Fungi – Their Toxins and Health Hazards*; Kurata, H., Ueno, Y., Eds.; Elsevier: Amsterdam, The Netherlands, **1984**; Volume 7, pp. 4-14.

Manske, R.H.F.; Holmes, H.L. The alkaloids of fumariaceous plants. XXXIX. The constitution of capaurine. *J. Am. Chem. Soc.* **1945**, *67*, 95-98.

Marin, S.; Magan, N.; Ramos, A.J.; Sanchis, V. Fumonisim-producing strains of *Fusarium*: a review of their ecophysiology. *J. Food Prot.* **2004**, *67*, 1792-1805.

Márquez-Fernández, O.; Trigos, Á.; Ramos-Balderas, J.L.; Viniegra-González, G.; Deising, H.B.; Aguirre, J. Phosphopantetheinyl transferase CfwA/NpgA is required for *Aspergillus nidulans* secondary metabolism and asexual development. *Eukaryot. Cell* **2007**, *6*, 710-720.

Matthias, S.; Tanovic, A.; Marahiel, M.A. Nonribosomal peptide synthetases: structure and dynamics. *Curr. Opin. Struc. Biol.* **2010**, *20*, 234-240.

McDonald, T.; Hammond, T.; Noordermeer, D.; Zhang, Y.-Q.; Keller, N. The sterigmatocystin cluster revisited: lessons from a genetic model. In *Food science and technology/Aflatoxin and food safety*; Abbas, H.K., Ed.; CRC Press: Boca Raton, FL, USA, **2005**: pp. 117–136.

Meyer, V. Genetic engineering of filamentous fungi – progress, obstacles and future trends. *Biotechnol. Adv.* **2008**, *26*, 177-185.

Miziorko, H.M. Enzymes of the mevaloate pathway of isoprenoid biosynthesis. *Arch. Biochem. Biophys.* **2011**, *505*, 131-143.

Moreau, A.; Couture, A.; Deniau, E.; Grandclaudon, P.; Lebrun, S. First total synthesis of cichorine and zinnimidine. *Org. Biomol. Chem.* **2005** *3*, 2305-2309.

Monti, F.; Ripamonti F.; Hawser, S.P.; Islam, K. Aspirochlorine: a highly selective and potent inhibitor of fungal protein synthesis. *J. Antibiot*. **1999**, *52*, 311-318.

Movassaghi, M.; Schmidt, M.A.; Ashenhurst, J.A. Concise total synthesis of (+)-WIN 64821 and (-)-ditryptophenaline. *Angew. Chem. Int. Ed.* **2008**, *47*, 1485-1487.

Nagaraju, G.P.C. Is methyl farnesoate a crutecean hormone? *Aquaculture* **2007**, *272*, 39-54.

Nahlik, K.; Dumkow, M.; Bayram, Ö.; Helmstaedt, K.; Bunsch, S.; Valerius, O.; Gerke, J.; Hoppert, M.; Schwier, E.; Opitz, L.; Westermann, M.; Grond, S.; Feussner, K.; Geobel, C.; Kaever, A.; Meinicke, P.; Feussner, I.; Brais, G.H. The COP9 signal medieates transcriptional and metabolic response to hormones, oxidative stress protection and cell wall rearrangement during fungal development. *Mol. Microbial.* **2010**, *78*, 964-979.

Nayak, T.; Szewczyk, E.; Oakley, C.E.; Osmani, A.; Ukil, L.; Murray, S.L.; Hynes, M.J.; Osmani, S.A.; Oakley, B.R. A versatile and efficient gene-targeting system for *Aspergillus nidulans*. *Genetics* **2006**, *172*, 1557-1566.

NCBI *A. kawachii* genome statistics. **2012a**. Avaliable at: http://www.ncbi.nlm.nih.gov/genome/genomes/10858 (accessed June 17th 2012)

NCBI *A. sojae* genome statistics. **2012b**. Avaliable at: http://www.ncbi.nlm.nih.gov/genome/genomes/10858 (accessed June 17th 2012)

Nesbitt, B.F.; Okelly, J.; Sheridan, A.; Sargeant, K. Toxic metabolites of *Aspergillus flavus*. *Nature* **1962**, *195*, 1062-1063.

Newman, D.J.; Cragg, G.M. Natural products as sources of new drugs over the 30 years from 1981-to 2010. *J. Nat. Prod.* **2012**, *75*, 311-335.

Nicholson, T.P.; Rudd, B.A.M.; Dawson, M.; Lazarus, C.M.; Simpson, T.J.; Cox, R.J. Design and utility of oligonucleotide gene probes for fungal polyketide synthases. *Chem. Biol.* **2001**, *8*, 157-178.

Nicholson, M.J.; Koulman, A.; Monahan, B.J.; Pritchard, B.L.; Payne, G.A.; Scott, B. Identification of two aflatrem biosynthesis gene loci in *Aspergillus flavus* and metabolic engineering of *Penicillium paxilli* to elucidate their function. *Appl. Environ. Microbiol.* **2009**, *75*, 7469-7481.

Nielsen, M.L.; Albertsen, L.; Lettier, G.; Nielsen, J.B.; Mortensen, U.H. Efficient PCR-based gene targeting with a recyclable marker for *Aspergillus nidulans*. *Fung. Genet. Biol.* **2006**, *43*, 54-64.

Nielsen, J.B.; Nielsen, M.L.; Mortensen, U.H. Transient disruption of non-homologous end-joining facilitates targeted genome manipulations in the filamentous fungus *Aspergillus nidulans*. *Fungal genet. Biol.* **2008**, *45*, 165-170.

Nielsen, K.F.; Mogensen, J.; Johansen, M.; Larsen, T.O.; Frisvad, J.C. Review of secondary metabolites and mycotoxins from the *Aspergillus niger* group. *Anal. Bioanal. Chem.* **2009**, *395*, 1225-1242.

Nielsen, M.L.; Nielsen, J.B.; Rank, C.; Klejnstrup, M.L.; Holm, D.K.; Brogaard, K.H.; Hansen, B.G.; Frisvad, J.C.; Larsen, T.O.; Mortensen, U.H. A genome-wide polyketide synthase deletion library uncovers novel genetic links to polyketides and meroterpenoids in *Aspergillus nidulans*. *FEMS Microbiol. Lett.* **2011**, *321*, 157-166.

Nierman, W.C.; Pain, A.; Anderson, M.J.; Wortman, J.R.; Kim, H.S.; Arroyo, J.; Berriman, M.; Abe, K.; Archer, D.B.; Bermejo, C.; Bennett, J.; Bowyer, P.; Chen, D.; Collins, M.; Coulsen, R.; Davies, R.; Dyer, P.S.; Farman, M.; Fedorova, N.; Fedorova, N.; Feldblyum, T.V.; Fischer, R.; Fosker, N.; Fraser, A.; García, J.L.; García, M.J.; Goble, A.; Goldman, G.H.; Gomi, K.; Griffith-Jones, S.; Gwilliam, R.; Haas, B.; Haas, H.; Harris, D.; Horiuchi, H.; Huang, J.; Humphray, S.; Jiménez, J.; Keller, N.; Khouri, H.; Kitamoto, K.; Kobayashi, T.; Konzack, S.; Kulkarni, R.; Kumagao, T.; Lafton, A.; Latgé, J.-P.; Li, W.; Lord, A.; Lu, C.; Majoros, W.H.; May, G.S.; Miller, B.L.; Mohamoud, Y.; Molina, M.; Monod, M.; Mouyna, I.; Mulligan, S.; Murphy, L.; O'Niel, S.; Paulsen, I.; Peñalva, M.A.; Pertea, M.; Price, C.; Pritchard, B.L.; Quail, M.A.; Rabinowitsch, E.; Rawlins, N.; Rajandream, M.A.; Reichard, B.L.; Renauld, H.; Robson, G.D.; de Córdoba, S.R.; Rodríguez-Penã, J.M.; Ronning, C.M.; Rutter, S.; Salzberg, S.L.; Sanchez, S.; Takeuchi, M.; Tekaia, F.; Turner, G.; de Aldana, C.R.V.; Weidman, J.; White, O.; Woodward, J.; Yu, J.-H.; Fraser, C.; Galagan, J.E.; Asai, K.; Machida, M.; Hall, N.; Barrell, B.; Denning, D.W. Genomic sequence of the pathogenic and allergenic filamentous fungus *Aspergillus fumigatus*. *Nature* **2005**, *438*, 1151-1156.

Nowrousian, M.; Stajich, J.E.; Chu, M.; Engh, I.; Espagne, E.; Halliday, K.; Kamerewerd, J.; Kempken, F.; Knab, B.; Kuo, H.C.; Osiewacz, H.D.; Poggeler, S.; Read, N.D.; Seiler, S.; Smith, K.M.; Zickler, D.; Kuck, U.; Freitag, M. *De novo* assembly of a 40 Mb eukaryotic genome from short sequence reads: *Sordaria macrospora*, a model organism for fungal morphogenesis. *PLoS Genet*. **2010**, *6*, e1000891.

Nützmann, H.-W.; Reyes-Dominguez, Y.; Scherlach, K.; Schroeckh, V.; Horn, F.; Gacek, A.; Schümann, J.; Hertweck, C.; Strauss, J.; Brakhage, A. Bacteria-induced natural product formation in the fungus *Aspergillus nidulans* requires Saga/Ada-mediated histone acetylation. *Proc. Natl. Acad. Soc. USA* **2011**, *108*, 14282-14287.

Noonim, P.; Mahakarnchanakul, W.; Nielsen, K.F.; Frisvad, J.C.; Samson, R.A. Fumonisin B_2 production by *Aspergillus niger* from Thai coffee beans. *Food Addit. Contam., Part A* **2009**, *26*, 94-100.

Nozawa, K.; Seyea, H.; Nakajima, S.; Udagawa, S.-I.; Kawai, K.-I. Studies on fungal products. Part 10. Isolation and structures of novel bicoumarins, desertorins A, B, and C, from *Emericella desertorum*. *J. Chem. Soc. Perkin Trans. I* **1987**, 1735-1738.

Oldfield, E., Lin, F.Y. Terpene biosynthesis: modularity rules. *Angew. Chem. Int. Ed.* **2012**, *51*, 1124-1137.

Oleynek, J.J.; Sedlock, D.M.; Barrow, C.J.; Appell, K.C.; Casiano, F.; Haycock, D.; Ward, S.J.; Kaplita, P.; Gillum, A.M. WIN 94821, a novel neurokinin antagonist produced by an *Aspergillus* sp. II. Biological activity. *J. Antibiot.* **1994**, *47*, 399-410.

Orth, R. Mycotoxins of *Aspergillus oryzae* strains for use in the food industry as starters and enzyme producing molds. *Ann. Nutr. Alim*. **1977**, *31*, 617-624.

Palmer, J.M.; Keller, N.P. Secondary metabolism in fungi: does chromosomal location matter? *Curr. Opin. Microbiol.* **2010**, *13*, 1-6.

Payne, G.A.; Nierman, W.C.; Wortman, J.R.; Pritchard, B.L.; Brown, D.; Dean, R.A.; Bhatnagar, D.; Cleveland, T.E.; Machida, M.; Yu, J. Whole genome comparison of *Aspergillus flavus* and *A. oryzae*. *Med. Mycol.* **2006**, *44*, S9-S11.

Pel, H.J.; de Winde, J.H.; Archer, D.B.; Dyer, P.S.; Hofmann, G.; Schaap, P.J.; Turner, G.; de Vries, R.P.; Albang, R.; Albermann, K.; Andersen, M.R.; Bendtsen, J.D.; Benen, J.A.E.; van den Berg, M.; Breestraat, S.; Caddick, M.X.; Contreras, R.; Cornell, M.; Coutinho, P.M.; Danchin, E.G.J.; Debets, A.J.M.; Dekker, P.; van Dijck, P.W.M.; van Dijk, A.; Dijkhuizen, L.; Driessen, A.J.M.; d'Enfert, C.; Geysens, S.; Goosen, C.; Groot, G.S.P., de Groot, P.W.J.; Guillemette, T.; Henrissat, B.; Herweijer, M.; van der Hombergh, J.P.T.W.; van den Hondel, C.A.M.J.; van der Heijden, R.T.J.M.; van der Kaaij, R.M.; Klis, F.M.; Kools, H.J.; Kubicek, C.P.; van Kuyk, P.A.; Lauber, J.; Lu, X.; van der Maarel, M.J.E.C.; Meulenberg, R.; Menke, H.; Mortimer, M.A.; Nielsen, J.; Oliver, S.G.; Olsthoorn, M.; Pal, K.; van Peij, N.N.M.E.; Ram, A.F.J.; Rinas, U.; Roubos, J.A.; Sagt, C.M.J.; Schmool, M.; Sun, J.B.; Ussery, D.; Varga, J.; Vervecken, W.; de Vondervoort, P.J.J.V.; Wedler, H.; Wösten, H.A.B.; Zeng, A.-P.; van Ooyen, A.J.J.; Visser, J.; Stam, H. Genome sequencing and analysis of the versatile cell *Aspergillus niger* CBS 513.88. *Nat. Biotechnol.* **2007**, *25*, 221-231.

Perrone, G.; Susca, A.; Cozzi, G.; Ehrlich, K.; Varga, J.; Frisvad, J.C.; Meijer, M.; Noonim, P.; Mahakarnchanakul, W.; Samson, R.A. Biodiversity of *Aspergillus* species in some important agricultural products. *Stud. Mycol.* **2007**, *59*, 53-66.

Pfefferle, W.; Anke, H.; Bross, M.; Steffan, B.; Vianden, R.; Steglich, W. Asperfuran, a novel antifungal metabolite from *Aspergillus oryzae*. *J. Antibiot.* **1990**, *43*, 648-654.

Pickens, L.B.; Tang, Y.; Chooi, Y.-H. Metabolic engineering for the production of natural products. *Annu. Rev. Chem. Biomol. Eng.* **2011**, *2*, 211-236.

Pildain, M.B.; Frisvad, J.C.; Vaamonde, G.; Cabral, D.; Varga, J.; Samson, R.A. Two novel aflatoxin-producing *Aspergillus* species from Argentinean peanuts. *Int. J. Syst. Evol. Microbiol.* **2008**, *58*, 725-735:

Pontecorvo, G.; Roper, J.A.; Hemmons, L.M.; MacDonald, K.D.; Bufton, A.W.J. The genetics of *Aspergillus nidulans*. *Adv. Genet. Incorp. Mol. Genet. Med*. **1953**, *5*, 141-238.

Price, M.S.; Yu, J.; Nierman, W.C.; Kim, H.S.; Pritchard, B.; Jacobus, C.A.; Bhatnagar, D.; Cleveland, T.E.; Payne, G.A. The aflatoxin pathway regulator AflR induces gene transcription inside and outside of the aflatoxin biosynthetic cluster. *FEMS Microbiol. Lett.* **2006**, *255*, 275-279.

Punt, P.J.; van Biezen, N.; Conesa, A.; Albersm A.; Mangnus, J.; van den Hondel, C. Filamentous fungi as cell factories for heterologous protein production. *Trends Biotechnol.* **2002**, *20*, 200-206.

Rank, C.; Nielsen, K.F.; Larsen, T.O.; Varga, J.; Samson, R.A.; Frisvad, J.C. Distribution of sterigmatocystin in filamentous fungi. *Fungal Biol.* **2011**, *115*, 406-420.

Raper, K.B.; Fennell, D.I. *The genus Aspergillus*; Williams & Wilkins: Baltimore, MD, USA, **1965**.

Rheeder, J.P.; Marasas, W.F.O.; Vismer, H.F. Production of fumonisin analogs by *Fusarium* species. *Appl. Environ. Microbiol.* **2002**, *68*, 2101-2105.

Robert, M.; Barbier, M.; Lederer, E.; Roux, L.; Bieman, K.; Vetter, W. Two new natural phytotoxins – aspergillomarasmines A and B and their identity to lycomarasmine and its derivatives. *Bulletin de la Societe Chimique de France* **1962**, 187-188.

Rohlfs, M.; Churchill, A.C.L. Fungal secondary metabolites as modulators of interactions with insects and other arthropods. *Fungal Genet. Biol.* **2011**, *48*, 23-34.

Rohmer, M. From molecular fossils of bacterial hopanoids to the formation of isoprene units: discovery and elucidation of the methylerythritol phosphate pathway. *Lipids* **2008**, *43*, 1095-1107.

Rokas, A. Payne, G.; Fedorova, N.D.; Baker, S.E.; Machida, M.; Yu, J.; Georgianne, D.R.; Dean, R.A.; Bhatnagar, D.; Cleveland, T.E.; Wortman, J.R.; Maiti, R.; Joardar, V.; Amedeo, P.; Denning, D.W.; Nierman, W.C. What can comparative genimocs tell us about species concepts in the genus *Aspergillus*? *Stud. Mycol.* **2007**, *59*, 11-17.

Sabater-Vilar, M.; Nijmeijer, S.; Fink-Gremmels, J. Genotoxicity assessment of five tremorgenic mycotoxins (fumitremorgen B, paxilline, penitrem A, verruculogen, and verrucosidin) produced by molds isolated from fermented meats. *J. Food Protec.* **2003**, *66*, 2123-2129.

Sakata, K.; Masago, H.; Sakurai, A.; Takahashi, N. Isolation of aspirochlorine (=antibiotic A30641) possessing a novel dithiodiketopiperazine structure from *Aspergillus flavus*. *Tetrahedron Lett.* **1982**, *23*, 2095-2098.

Sakata, K.; Kuwatsuka, T.; Sakurai, A.; Takahashi, N.; Tamura, G. Isolation of aspirochlorine (=antibiotic A30641) as a true antimicrobial constituent of the antibiotic, oryzachlorin, from *Aspergillus oryzae*. *Agric. Biol. Chem.* **1983**, *47*, 2673-2674.

Sakata, K.; Maruyama, M. Structural revision of aspirochlorine (=antibiotic A30641), a novel epidithiopiperazine-2,5-dione produced by *Aspergillus* spp. *Tetrahedron Lett.* **1987**, *28*, 5607-5610.

Sakuno, E.; Yabe, K.; Nakajima, H. Involvement of two cytosolic enzymes and a novel intermediate 5'-oxoaverantin in the pathway from 5'-hydroxyaverantin to averufin in aflatoxin biosynthesis. *Appl. Environ. Microbiol.* **2003**, *69*, 6418–6426.

Sanchez, J.F.; Chiang, Y.-M.; Szewczyk, E.; Davidson, A.D.; Ahuja, M.; Oakley, C.E.; Bok, J.W.; Keller, N.; Oakley, B.R.; Wang, C.C.C. Molecular genetic analysis of the orsellinic acid/F9775 gene cluster of *Aspergillus nidulans*. *Mol. BioSyst.* **2010**, *6*, 587-593.

Sanchez, J.F.; Entwistle, R.; Hung, J.-H.; Yaegashi, J.; Jain, S.; Chiang, Y.-M.; Wang, C.C.C.; Oakley, B.R. Genome-based deletion analysis reveals the prenyl xanthone biosynthesis pathway in *Aspergillus nidulans*. *J. Am. Chem. Soc.* **2011**, *133*, 4010-4017.

Sanchez, J.F.; Somoza, A.D.; Keller, N.P.; Wang, C.C.C. Advances in *Aspergillus* secondary metabolite research in the post-genomic era. *Nat. Prod. Rep.* **2012**, *29*, 351-371.

Savard, M.E.; Blackwell, B.A. Spectral characteristics of secondary metabolites from *Fusarium* fungi. In: *Mycotoxins in grain: compounds other than aflatoxin*; Miller, J.D.; Trenholm, H.L., Eds.; Eagan Press: St. Paul, MN, USA, **1994a**; pp. 59-260.

Savard, M.E.; Miller, J.D.; Blais, L.A.; Seifert, K.A.; Samson, R.A. Secondary metabolites of *Penicillium bilaii* strain PB-50. *Mycopathologia* **1994b**, *127*, 19-27.

Scherlach, K.; Hertweck, C. Discovery of aspoquinolones A-D, prenylated quinolone-2-one alkaloids from *Aspergillus nidulans*, motivated by genome mining. *Org. Biomol. Chem.* **2006**, *4*, 3517-3520.

Scherlach, K.; Hertweck, C. Triggering cryptic natural product biosynthesis in microorganisms. *Org. Biomol. Chem.* **2009**, *7*, 1753-1760.

Scherlach, K.; Schuemann, J.; Dahse, H.-M.; Hertweck, C. Aspernidine A and B, prenylated isoindolinone alkaloids from the model fungus *Aspergillus nidulans*. *J. Antibiot.* **2010**, *63*, 375-377.

Scherlach, K.; Sarkar, A.; Schroeckh, V.; Dahse, H.-M.; Roth, M.; Brakhage, A.A.; Horn, U.; Hertweck, C. Two induced fungal polyketide pathways converge into antoproliferative spiroanthrones. *ChemBioChem* **2011**, *12*, 1836-1839.

Schiewe, H.-J.; Zeeck, A. Cineromycins, γ-Butyrolactones and ansamycins by analysis of the secondary metabolite pattern created by a single strain if *Streptomyces*. *J. Antibiot*. **1999**, *52*, 635-642.

Schneider, P.; Weber, M.; Hoffmeister, D. The *Aspergillus nidulans* enzyme TdiB catalyzes prenyltransfer to the precursor of bioactive asterriquinones. *Fungal Genet. Biol.* **2008**, *45*, 302-309.

Schroeckh, V.; Scherlach, K.; Nützmann, H.-W.; Shelest, E.; Schmidt-Heck, W.; Schuemann, J.; Martin, K.; Hertweck, C.; Brakhage, A.A. Intimate bacterial-fungal interaction triggers biosynthesis of archetypal polyketides in *Aspergillus nidulans*. *Proc. Natl. Acad. Soc. USA* **2009**, *106*, 14558-14563.

Schuster, E.; Dunn-Coleman, N.; Frisvad, J.C.; van Dijck, P.W.M. On the safety of *Aspergillus niger* – a review. *Appl. Microbiol. Biotechnol.* **2002**, *59*, 426-435.

Scott, F.E.; Simpson, T.J.; Trimble, L.A.; Vederas, J.C. Biosynthesis of the meroterpenoid Austin by *Aspergillus ustus*: synthesis and incorporation of ^{13}C, ^{18}O-labelled ethyl 3,5-dimethylorsellinate. *J.C.S. Chem. Comm.* **1986**, *3*, 214-215.

Sheehan, J.J.; Benedetti, B.L.; Barth, A.L. Anticonvulsant effects of the BK-channel antagonist paxilline. *Epilepsia* **2009**, *50*, 711-720.

Shiomi, K.; Hatae, K.; Yamaguchi, Y.; Masuma, R.; Tomoda, H.; Kobayashi, S.; Omura, S. New antibiotics miyakamides produced by a fungus. *J. Antibiot.* **2002**, *55*n 952-961.

Shwab, E.K.; Bok, J.W.; Tribus, M.; Galehr, J.; Graessle, S.; Keller, N.P. Histone deacetylase activity regulates chemical diversity in *Aspergillus*. *Eukaryot. Cell* **2007**, *6*, 1656-1664.

Silva, J.C.; Minto, R.E.; Barry, C.E., III; Holland, K.A.; Townsend, C.A. Isolation and characterization of the versicolorin B synthase gene from *Aspergillus parasiticus*. *J. Biol. Chem.* **1996**, *271*, 13600–13608.

Simpson, T.J.; Stenzel, D.J. Biosynthesis of austin, a polyketide – terpenoid metabolite of *Aspergillus ustus*. *J.C.S. Chem. Comm.* **1981**, *20*, 1042-1043.

Simpson, T.J.; Stenzel, D.J. Studies on fungal metabolites. Part 3. ^{13}C N.m.r. spectral and structural studies on Austin and new related meroterpenoids from *Aspergillus ustus*, *Aspergillus variecolor*, and *Penicillium diversum*. *J. Chem. Soc. Perkin Trans. I* **1982**, *11*, 2687-2692.

Simpson, T.J. Genetic and biosynthetic studies of the fungal prenylated xanthone shamixanthone and related metabolites in *Aspergillus spp.* revisited. *ChemBioChem* **2012**, doi: 10.1002/cbic.201200012 (ahead of print)

Smedsgaard, J. Micro-scale extraction procedure for standardized screening of fungal metabolite production in cultures. *J. Chromatogr. A* **1997**, *760*, 264-270.

Springer, J.P.; Clardy, J. The structure of paxilline, a tremorgenic metabolite of *Penicillium paxilli* Bainier. *Tetrahedron Lett.* **1975**, *30*, 2531-2534.

Springer, J.P.; Büchi, G. The structure of ditrytophenaline – a new metabolite of *Aspergillus flavus*. *Tetrahedron Lett.* **1977**, *28*, 2403-2406.

Staub, G.M.; Gloer, J.B.; Wicklow, D.T.; Dowd, P.F. Aspernomine: a cytotoxic antiinsectan metabolite with a novel ring system from the sclerotia of *Aspergillus nomius*. *J. Am. Chem. Soc.* **1992**, *114*, 1015-1017.

Staub, G.M.; Gloer, K.B.; Gloer, J.B. New paspalinine derivatives with antiinsectan activity from the sclerotia of *Aspergillus nomius*. *Tetrahedron Lett.* **1993**, *34*, 2569-2572.

Steyn, P.S.; Vleggaar, R. Tremorgenic mycotoxins. *Fortschritte der chemie Organischer Naturstoffe* **1985**, *48*, 1-80.

Stierle, A.; Hershenhorn, J.; Strobel, G. Zinniol-related phytotoxins from *Alternaria cichorii*. *Phytochemi*. **1993**, *32*, 1145-1149.

Strauss, J.; Reyes-Dominguez, Y. Regulation of secondary metabolism by chromatin structure and epigenetic codes. *Fungal. Genet. Biol.* **2011**, *48*, 62-69.

Szewczyk, E.; Chiang, Y.-M.; Oakley, C.E.; Davidson, A.D.; Wang, C.C.C.; Oakley, B.R. Identification and characterization of the asperthecin gene cluster of *Aspergillus nidulans*. *Appl. Environ. Microbiol.* **2008**, *74*, 7607-7612.

Tanaka, S.; Wade, K.; Marumo, S.; Hattori, H. Structure of sporogen-AO 1, a sporogenic substance of *Aspergillus oryzae*. *Tetrahedron Lett.* **1984a**, *25*, 5907-5910.

Tanaka, S.; Wada, K.; Katayama, M.; Marumo, S. Isolation of sporogen-AO1, a sporogenic substance from *Aspergillus oryzae*. *Agric. Biol. Chem.* **1984b**, *48*, 3189-3191.

Tepaske, M.R.; Gloer, J.B. Three new aflavinines from the sclerotia of *Aspergillus tubingensis*. *Tetrahedron* **1989a**, *45*, 4961-4968.

Tepaske, M.R.; Gloer, J.B. The structure of tubingensin B: a cytotoxic carbazole alkaloid from the sclerotia of *Aspergillus tubingensis*. *Tetrahedron Lett.* **1989b**, *30*, 5965-5968.

Tepaske, M.R.; Gloer, J.B. Aflavazole: a new antiinsectan carbazole metabolite from the sclerotia of *Aspergillus flavus*. *J. Org. Chem.* **1990**, *55*, 5299-5301.

Tepaske, M.R.; Gloer, J.B. Aflavarin and β-aflatrem: new anti-insectan metabolites from the sclerotia of *Aspergillus flavus*, *J. Nat. Prod.* **1992**, *55*, 1080-1086.

Tian, Y.; He, J.; Zhang, R.; Lv, H.; Ma, S.; Chen, Y.; Yu, S.; Chen, X.; Wu, Y.; He, W.; Abliz, Z. Integrated rapid resolution liquid chromatography-tandem mass spectrometric approach for screening and identification of metabolites of the potential anticancer agent 3,6,7-trimethoxyphenanthroindolizidine in rat urine. *Anal. Chim. Acta.* **2012**, *731*, 60-67.

Toh, D.-F; New, L.-S.; Koh, H.-L.; Chan, E.C.-Y. Ultra-high performance liquid chromatography/time of flight mass spectrometry (UHPLC/TOFMS) for time-depending profiling of raw and steamed *Panax notoginseng*. *J. Pharmaceut. Biomed.* **2010**, *52*, 43-50.

Tokuoka, M.; Seshime, Y.; Fujii, I.; Kitamoto, K.; Takahashi, T.; Koyama, Y. Identification of a novel polyketide synthase-nonribosomal peptide synthetase (PKS-NRPS) gene required for the biosynthesis of cyclopiazonic acid. *Fungal Genet. Biol.* **2008**, *45*, 1608-1615.

Tominaga, M.; Lee, Y.-H.; Hayashi, R.; Suzuki, Y.; Yamada, O.; Sakamoto, K.; Gotoh, K.; Akita, O. Molecular analysis of an inactive aflatoxin biosynthesis gene cluster in *Aspergillus oryzae* RIK strains. *Appl. Environ. Microbiol.* **2006**, *72*, 484-490.

Trail, F.; Chang, P.-K.; Cary, J.; Linz, J.E. Structural and functional analysis of the *nor-1* gene involved in the biosynthesis of aflatoxins by *Aspergillus parasiticus*. *Appl. Environ. Microbiol.* **1994**, *60*, 4078–4085.

Verger, A.; Perdomo, J.; Crossley, M. Modification with SUMO. A role in transcriptional regulation. *EMBO Rep.* **2003**, *4*, 137-143.

Walsh, C.T. Combinatorial biosynthesis of antibiotics: challenges and opportunities. *ChemBioChem* **2002**, *3*, 124-134.

Walsh, C.T.; Fischbach, M.A. Natural products version 2.0: connecting genes to molecules. *J. Am. Chem. Soc.* **2010**, *132*, 2469-2493.

Watanabe, A.; Ono, Y.; Fujii, I.; Sankawa, U.; Mayorga, M.E.; Timberlake, W.E.; Ebizuka, Y. Product identification of polyketide synthase coded by *Aspergillus nidulans wA* gene. *Tetrahedron Lett.* **1998**, *39*, 7733-7736.

Watanabe, A.; Fujii, I.; Sankawa, U.; Mayorga, M.E.; Timberlake, W.E.; Ebizuka, Y. Re-identification of *Aspergillus nidulans wA* gene to code for a polyketide synthase of naphthopyrone. *Tetrahedron Lett.* **1999**, 40, 91-94.

Watanabe, C.M.H.; Townsend, C.A. Initial characterization of a type I fatty acid synthase and polyketide synthase multienzyme complex NorS in the biosynthesis of aflatoxin B_1. *Chem. Biol.* **2002**, *9*, 981–988.

Wicklow, D.T.; Cole, R. Tremorgenic indole metabolites and aflatoxins in sclerotia of *Aspergillus flavus*: an evolutionary perspective. *Can. J. Bot.* **1982**, *60*, 525-528.

Wicklow, D.T.; McAlpin, C.E.; Yeoh, Q.L. Diversity of *Aspergillus oryzae* genotypes (RFLP) isolated from traditional soy sauce production within Malaysia and Southeast Asia. *Mycoscience* **2007**, *48*, 373-380.

Williams, R.B.; Henrikson, J.C.; Hoover, A.R.; Lee, A.E.; Cichewicz, R.H. Epigenetic remodeling of the fungal secondary metabolome. *Org. Biomol. Chem.* **2008**, *6*, 1895-1897.

Wilson, B.J.; Wilson, C.H. Toxin from *Aspergillus flavus*: production on food materials of a substance causing tremors in mice. *Science* **1964**, *144*, 177-178.

Wilson, B.J. Toxins other than aflatoxin produced by *Aspergillus flavus*. *Bacteriol. Rev.* **1966**, *30*, 478-484.

Wilson, T.G. The molecular site of action of juvenile hormone and juvenile hormone insecticides during metamorphosis: how these compounds kill insects. *J. Insect. Physiol.* **2004**, *50*, 111-121.

Winter, J.M.; Behnken, S.; Hertweck, C. Genomics-inspired discovery of natural products. *Curr. Opin. Chem. Biol.* **2011**, *15*, 22-31.

Wong, K.H.; Todd, R.B.; Oakley, B.R.; Oakley, C.E.; Hynes, M.J.; Davis, M.A. Sumoylation in *Aspergillus nidulans*: *sumO* inactivation, overexpression and live-cell imaging. *Fungal Genet. Biol.* **2008**, *45*, 728-737.

Wong, F.T.; Khosla, C. Combinatorial biosynthesis of polyketides – a perspective. *Curr. Opin. Chem. Biol.* **2012**, *16*, 117-123.

Yabe, K.; Nakamura, Y.; Nakajima, H.; Ando, Y.; Hamasaki, T. Enzymatic conversion of norsolorinic acid to averufin in aflatoxin biosynthesis. *Appl. Environ. Microbiol*. **1991**, *57*, 1340–1345.

Yabe, L.; Matsuyama, Y.; Ando, Y.; Nakajima, H.; Hamasaki, T. Stereochemistry during aflatoxin biosynthesis: Conversion of norsolorinic acid to averufin. *Appl. Environ. Microbiol.* **1993**, *59*, 2486–2492.

Yabe, K.; Nakajima, H. Enzyme reactions and genes in aflatoxin biosynthesis. *Appl. Microbiol. Biotechnol. **2004**, 64, 745–755.*

Yadav, G.; Gokhale, R.S.; Mohanty, D. Towards prediction of metabolic products of polyketide synthases: an *In Silico* analysis. *PLoS Comp. Biol.* **2009**, *5*, e1000351:1-e1000351:14.

Yaoita, Y.; Danbara, K.; Kikuchi, M. Two new aromatic compounds from *Hericium erinaceum* (Bull.; Fr.) Pers. *Chem. Pharm. Bull.* **2005**, *53*, 1202-1203.

Yeh, H.-H.; Chiang, Y.-M.; Entwistle, R.; Ahuja, M.; Lee, K.H.; Bruno, K.S.; Wu, T.-K.; Oakley, B.R.; Wang, C.C.C. Molecular genetic analysis reveals that a nonribosomal peptide synthetase-like (NRPS-like) gene in *Aspergillus nidulans* is responsible for microperfuranone biosynthesis. *Appl. Microbiol. Biotechnol.* **2012** Ahead of print.

Yin, W.; Keller, N.P. Transcriptional regulatory elements in fungal secondary metabolism. *J. Microbiol* **2011**, *49*, 329-339.

Yu, J.-H.; Leonard, T.J. Sterigmatocystin biosynthesis in *Aspergillus nidulans* requires a novel type I polyketide synthase. *J. Bacteriol.* **1995**, *177*, 4792–4800.

Yu, J.; Chang, P.-K.; Ehrlich, K.C.; Cary, J.W.; Bhatnagar, D.; Cleveland, T.E.; Payne, G.A.; Linz, J.E.; Woloshuk, C.P.; Bennett, J.W. Clustered pathway genes in aflatoxin biosynthesis. *Appl. Environ. Microbiol.* **2004**, *70*, 1253–1262.

Yu, J.-H.; Keller, N. Regulation of secondary metabolism in filamentous fungi. *Annu. Rev. Phytopathol*. **2005a**, *43*, 437-458.

Yu, J.; Cleveland, T.E.; Nierman, W.C.; Bennett, J.W. *Aspergillus flavus* genomics: gateway to human and animal health, food safety, and crop resistance to diseases. *Rev. Iberoam. Micol.* **2005b**, *22*, 192-202.

Yu, J.; Payne, G.A.; Nierman, W.C.; Machida, M.; Bennett, J.W.; Campbell, B.C.; Robens, J.F.; Bhatnagar, D.; Dean, R.A.; Cleveland, T.E. *Aspergillus flavus* genomics as a tool for studying the mechanism of aflatoxin formation. *Food Addit. Contam. Part A* **2008**, *25*, 1153-1157.

Paper 1

"Genetics of polyketide metabolism in *Aspergillus nidulans*"

ML Klejnstrup, RJN Frandsen, DK Holm, MT Nielsen, UH Mortensen, TO Larsen, and JB Nielsen

Accepted in Metabolites, *2*, 100-133 (2012)

Metabolites **2012**, *2*, 100-133; doi:10.3390/metabo2010100

OPEN ACCESS

metabolites

ISSN 2218-1989

www.mdpi.com/journal/metabolites/

Review

Genetics of Polyketide Metabolism in *Aspergillus nidulans*

Marie L. Klejnstrup [1], Rasmus J. N. Frandsen [2], Dorte K. Holm [2], Morten T. Nielsen [2], Uffe H. Mortensen [2], Thomas O. Larsen [1] and Jakob B. Nielsen [2,*]

[1] Department of Systems Biology, Center for Microbial Biotechnology, Technical University of Denmark, Søltofts Plads B221, DK-2800 Kgs. Lyngby, Denmark;
E-Mails: marlk@bio.dtu.dk (M.L.K.); tol@bio.dtu.dk (T.O.L)

[2] Department of Systems Biology, Center for Microbial Biotechnology, Technical University of Denmark, Søltofts Plads B223, DK-2800 Kgs. Lyngby, Denmark; E-Mails: rasf@bio.dtu.dk (R.J.N.F.); dmkp@bio.dtu.dk (D.K.H.); motni@bio.dtu.dk (M.T.N.); um@bio.dtu.dk (U.H.M.)

* Author to whom correspondence should be addressed; E-Mail: jbn@bio.dtu.dk;
Tel.: +45-4525-2657; Fax: +45-4588-4148.

Received: 1 November 2011; in revised form: 23 December 2011 / Accepted: 17 January 2012 / Published: 30 January 2012

Abstract: Secondary metabolites are small molecules that show large structural diversity and a broad range of bioactivities. Some metabolites are attractive as drugs or pigments while others act as harmful mycotoxins. Filamentous fungi have the capacity to produce a wide array of secondary metabolites including polyketides. The majority of genes required for production of these metabolites are mostly organized in gene clusters, which often are silent or barely expressed under laboratory conditions, making discovery and analysis difficult. Fortunately, the genome sequences of several filamentous fungi are publicly available, greatly facilitating the establishment of links between genes and metabolites. This review covers the attempts being made to trigger the activation of polyketide metabolism in the fungal model organism *Aspergillus nidulans*. Moreover, it will provide an overview of the pathways where ten polyketide synthase genes have been coupled to polyketide products. Therefore, the proposed biosynthesis of the following metabolites will be presented; naphthopyrone, sterigmatocystin, aspyridones, emericellamides, asperthecin, asperfuranone, monodictyphenone/emodin, orsellinic acid, and the austinols.

Keywords: secondary metabolites; polyketides; polyketide synthases; gene clusters; biosynthesis; *Aspergillus nidulans*

---

1. Introduction

Aspergillus nidulans, teleomorph *Emericella nidulans*, is one of the most significant biological model systems in the fungal kingdom. This was pioneered by Pontecorvos' [1] work in the middle of the last century, which demonstrated that *A. nidulans*, in addition to the asexual state, also proliferate via sexual and parasexual life cycles, hence, offering an ideal platform for genetic studies. Related species in the genus *Aspergillus* include important industrial cell factories, *A. niger* and *A. oryzae*, species that cause allergic diseases, *A. clavatus*, as well as opportunistic pathogens, such as *A. fumigatus*.

A common feature of aspergilli and filamentous fungi in general is their capacity to produce secondary metabolites (SMs). As opposed to the primary metabolites, SMs are not essential for cellular growth, but provide fungi, as well as bacteria and plants, with a competitive advantage in nature, e.g., by serving as agents for chemical warfare or as signal molecules. Hence, an impressive range of compounds with broad ranging bioactivities has evolved. SMs can be divided into four main chemical classes: Polyketides (PK), terpenoids, shikimic acid derived compounds, and non-ribosomal peptides (NRP). Moreover, hybrid metabolites composed of moieties from different classes are common, as in the meroterpenoids, which are fusions between PKs and terpenes. Hybrid molecules significantly add to the complexity and variety of the fungal metabolomes.

In addition to their likely important ecological roles in their natural biological niches, SMs also have a considerable impact on human life. For instance aflatoxins, ochratoxins, and fumonisins act as mycotoxins by having a detrimental effect on humans and livestock, whereas others are beneficial and serve as food additives, pigments, cholesterol-lowering drugs, immunosuppressants, antibiotics and anticancer agents. The different aspects of SM action and application have spurred a tremendous interest in fungal secondary metabolites, which is further underlined by the fact that around 63% of all small molecule drugs, which reached the market from 1981–2006 were inspired by natural products or derivatives thereof [2].

In filamentous fungi, the competitive race in SM development and the cost of producing and secreting complex compounds have resulted in the evolution of a multifaceted regulation of SM biosynthesis to avoid unnecessary use of resources. This hampers their discovery since production of most SMs is not induced under laboratory conditions. Analysis of full genome sequences of eight different aspergilli have demonstrated that for the majority of genes that putatively encode enzymes for SM production, the product is not known or detected. In this review, we will provide highlights of the use of genome mining, sophisticated molecular biological and chemical tools to trigger the production of SMs from cryptic gene clusters and discuss how these techniques have accelerated our understanding of PK production and regulation in *A. nidulans*.

1.1. Polyketide Biosynthesis in A. nidulans

PKs in fungi are synthesized by the use of acyl-CoA units. They act as the general substrates for large multi-domain enzymes named polyketide synthases (PKSs), which resemble eukaryotic fatty-acid synthases (FASs) in domain architecture. PKSs are divided into three types of PKSs based on their catalytic organization, however, only the iterative type I PKS (iPKS) has been reported in *A. nidulans*. The iPKS repeat the use of a single module containing several catalytic domains until the growing

chain of acyl-CoA units block further elongation. For descriptions of PKSs in general, excellent reviews by Crawford [3], Hertweck [4] and Cox [5] can be consulted. The most commonly encountered catalytic activities in fungal PKSs will be addressed as a general introduction to fungal PKSs in the following three paragraphs.

Three fundamental domains are found in all iPKSs in *A. nidulans* like in filamentous fungi in general; β-ketosynthase (KS), acyltransferase (AT), and the acyl carrier protein (ACP). The KS catalyzes the C–C bond formation via decarboxylation reactions through Claisen condensations between thioesters. The ACP domain is responsible for transiently holding the growing acyl chain, hereby allowing the loading of malonyl extender units. The acyl groups are transferred from CoA by AT onto KS and ACP. The iterative use of the three domains results in a non-reduced PK, a β-keto thioester. Additional domains can be present in the PKS allowing the introduction of further chemical complexity.

iPKSs in fungi can, based on their catalytic domains, be classified as non-reducing (NR-PKSs), partially reducing (PR-PKSs), or highly reducing (HR-PKSs) [6]. This is based on their ability to reduce the β-keto carbon. In PR- and HR-PKSs, reduction occurs through the β-ketoreductase (KR) domain that converts the β-ketone to a hydroxyl group. The resulting hydroxyl can go all the way to saturation by elimination of water through the dehydratase (DH) domain followed by hydrogenation by enoyl reductase (ER). In addition, reducing PKSs can also possess a methyltransferase domain (MT) responsible for C-methylation of the growing PK chain, using S-adenosylmethionine (SAM) as a carbon-donor. The degree of modifications and their position in the PK product is always the same for the individual PKSs. However, it is presently unknown how deployment of the various modifying domains is programmed into the PKS enzyme.

NR-PKSs differ in domain architecture from reducing PKS by not having any of the reducing domains and by having an N-terminal starter unit-ACP transacylase (SAT) domain and an internal product template (PT) domain. The SAT domain is responsible for selecting the starter unit to be extended by the enzyme [7], while the PT domain is responsible for folding and cyclization of the non-reduced PK backbone [3,8]. The number of iterations within the PKS and thereby the display of functional groups and the size of the final product is likely determined by the size of the active site cavity in the iPKS [9]. Once the length of the final product has been achieved, the PK chain is released from the PKS, catalyzed by either a thioesterase (TE), a Claisen cyclase (CLC) domain if present, or by accessory enzymes. A more detailed discussion on PKS release mechanisms is reviewed by Du and Lou [10].

It should be noted that it currently is impossible to reliably predict the product of iPKSs based on their amino acid sequences and domain architecture. This is in part due to the inability to predict the number of iterations performed by the iPKS and in part due the lack of understanding of how deployment of tailoring domains in individual iterations are programmed into the enzyme.

Interestingly, the PKS encoding gene tends to reside in clusters of genes coding for a broad range of enzymatic activities. The compound coming directly from the PKS rarely seem to be the final product in the biosynthesis, but usually undergoes further modifications by tailoring enzymes from small decorations to drastic and large intervention and couplings.

Through inspection of the genome sequence (genome mining), the latest estimate of genes encoding PKSs in *A. nidulans* is 32 open reading frames (ORFs) [11] (Figure 1), indicating that the number of PK containing end products in *A. nidulans* should count at least 32 plus stable intermediates. The compounds detected under a given condition do not necessarily reflect the final outcome of a PK

pathway, since the presence of intermediates and shunt products depends on other downstream enzymes and regulation.

Figure 1. An overview of the relative distribution of the 32 putative polyketide synthases (PKS) open reading frames (ORFs) on the eight chromosomes of *A. nidulans*. Green and red AN numbers represent assigned and unassigned PKS genes, respectively. Dark grey circles and ends symbolize centromeric and telomeric regions, respectively, and should not be considered to scale.

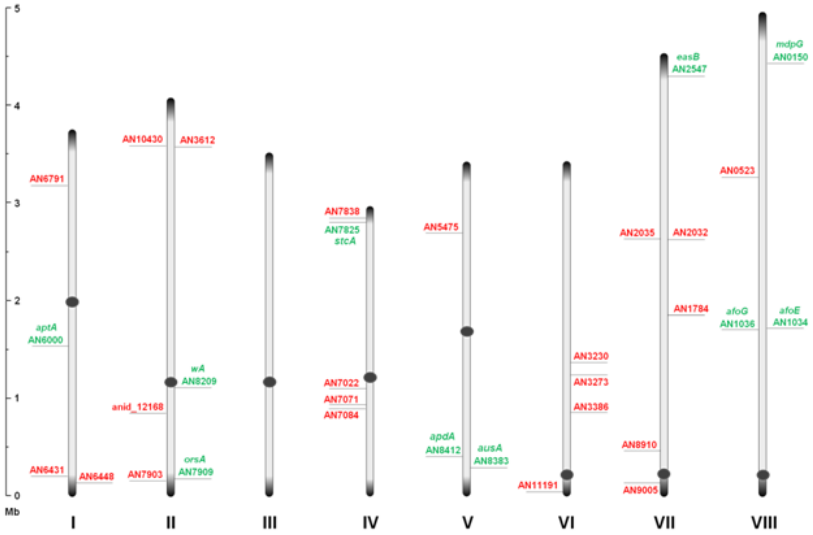

At present, a total of nine PKS genes have been coupled to the polyketome (collection of PKs and their synthesis) in *A. nidulans*, and numerous endeavors are currently attempting to unveil the mechanisms of PK metabolism in this model fungus. The pathways described in this review will follow in chronological order with respect to the discovery from PK to genes. For each of the PK gene clusters that have been linked to products so far we will focus on the PK compounds, their discovery, genetics as well as their biosynthetic pathway: Naphthopyrone, sterigmatocystin, aspyridones, emericellamides, asperthecin, asperfuranone, monodictyphenone (emodin), orsellinic acid, and the austinols.

2. Naphthopyrone

Spores from *A. nidulans* are characterized by a dark grey-green macroscopic appearance. This is due to deposition of pigments in the conidial wall as shown by ultrastructure studies using transmission electron microscopy (TEM) [12]. The responsible pigment is based on the PK-naphthopyrone YWA1 and the function of the pigment layer has been shown to include quenching of reactive oxygen species [13] and increased resistance to UV radiation [14]. The work on naphthopyrone synthesis in *A. nidulans* has paved the way for understanding iPKS domain structure.

The study of conidial pigmentation in *A. nidulans* has been extremely valuable for genetic screens. The first pigment mutant recorded in literature was the spontaneous white alba (w_a) strain reported by

Yuill in 1939 [15]. In addition to the white mutant class, *yA*$^{-}$ mutants producing yellow conidia were discovered. These available color variants served as easy recognizable markers (green, white, and yellow) that allowed the establishment of fundamental genetic tools in *A. nidulans* [1]. Interestingly, sexual crossing showed that the *wA*$^{-}$ mutation masked the effect of the *yA*$^{-}$ mutation (epistatic) [1,16]. Clutterbuck and co-workers [16] proposed that WA synthesized the yellow pigment that was observed in *yA* mutants and that the YA enzyme converted this compound into the green conidial pigment. In 1967, Agnihotri and co-workers [17] found that the wild type strains if grown under copper limiting conditions could mimic the yellow phenotype of the *yA*$^{-}$ strain. *yA* (AN6635) and *wA* (AN8209) were isolated and mapped to loci, chromosome I and II respectively, by complementation of a cosmid based library in 1989 and 1990, respectively [18,19]. Later, cross-feeding experiments performed by Clutterbuck [16] revealed that the *yA* phenotype was caused by the lack of a copper dependent extracellular laccase (p-diphenol oxidase). The *wA* functionality in pigment formation was confirmed by gene-deletion studies [19]. The lack of clustering of the two *A. nidulans* conidial pigment genes also became evident by their different expression patterns and the finding that they are controlled by different regulatory systems [20,21]. The *yA* gene is expressed in phialide cells and primary sterigmata (metulae) [18], and controlled by BrlA and AbaA [21], while *wA* is expressed only in phialides [22] and controlled by WetA [20]. Interestingly, none of the genes are expressed in the conidia. Characterization of the WA PKS was accomplished by Northern blotting, which revealed that *wA* encoded a 7.5 kb large transcript [19], and sequencing of the locus [22]. Re-sequencing of the 3′ region in 1998 led to a revised gene model of the PKS with the following domain structure KS-AT-ACP-CLC. This novel CLC domain [23] catalyzed release of the product and cyclization of the second aromatic ring of YWA1 via a Claisen condensation reaction [24].

Heterologous expression of *wA* in *A. oryzae* resulted in the production of the yellow compound, as observed in *yA*$^{-}$ mutants, which was identified to be the heptaketide naphthopyrone named YWA1 [25]. In 2002, *wA* was used for constructing a collection of chimeric PKSs (cPKS) by mixing its domains with those of *Colletotrichum lagenarium pks1*, known to produce the tetraketide 1,3,6,8-tetrahydroxynaphthalene (T4HN). One of the resulting cPKSs, SW-B, produced several new compounds including both *tetra*- and pentaketides [26]. The results prompted a reanalysis of the two PKSs, which revealed the existence of two previously overlooked conserved domains; an N-terminal and a central domain. These domains were later identified as a SAT and PT domain, respectively, thus providing the full domain structure SAT-KS-AT-PT-ACP-CLC [3,7,8]. With the organization within WA in mind, the biosynthetic pathway can be envisioned as condensations of an acetyl-CoA with six malonyl-CoA units in six successive reactions resulting in the formation of YWA1 [25] (Figure 2).

Figure 2. Biosynthetic pathway for formation green conidial pigment in *A. nidulans*

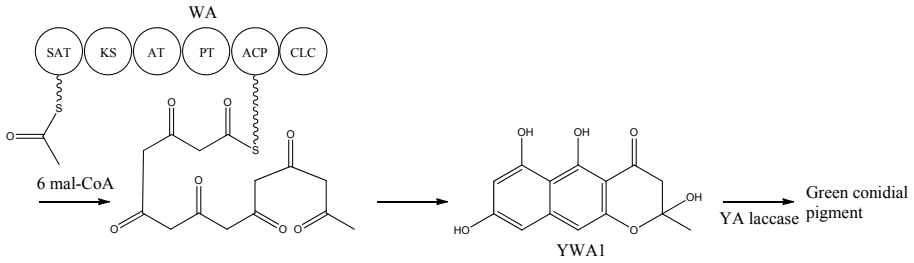

YWA1 is then believed to be dimerized or polymerized by the YA laccase into the green conidial pigment(s) via phenolic oxidative coupling. However, to date no one has succeeded in characterizing the chemical structure of the green conidial pigmentation in detail. As the final product remains elusive, it is impossible to predict if other tailoring enzymes further modify the YWA1 backbone or reactions occur with other metabolites or cellular components, e.g., the cell wall.

3. Sterigmatocystin

Sterigmatocystin, a PK, was first partially purified from a *Sterigmatocytis* sp. in 1948 by Nekam and Polgar [27]. Hatsuda and co-workers [28,29] successfully isolated sterigmatocystin in 1954 from *A. versicolor*. The correct relative structure was determined in 1962 by Bullock *et al.* [30]. By performing degradative experiments it was shown that the stereochemistry of sterigmatocystin was the same as that of aflatoxin [31], which had the absolute stereochemistry determined in 1967 [32]. The absolute stereochemistry of sterigmatocystin was confirmed via crystallography [33,34].

The aflatoxins are among the most carcinogenic mycotoxins and the research in aflatoxin and sterigmatocystin intensified with the Turkey X disease caused by aflatoxins in the middle of the last century [35]. Aflatoxins are reported to be produced only by a few aspergilli. *A. nidulans* does not produce aflatoxins, as the biosynthesis stops at sterigmatocystin, a late, yet stable precursor of the pathway. Sterigmatocystin is a powerful mycotoxin, though it is estimated to be 150 times less carcinogenic than the most potent aflatoxin, B_1 [36]. Fungi that are able to produce aflatoxins and/or sterigmatocystin are common contaminants of food, feed, and indoor environments and may be mammalian and plant pathogens [37,38]. Due to the high toxicity and prevalence of sterigmatocystin and aflatoxins, they are likely the most extensively studied examples of secondary metabolism in fungi both in terms of biosynthesis and biological function, and there are several excellent and comprehensive reviews for further reading on aflatoxin biosynthesis [39,40]. Studies on the biosynthesis of aflatoxin and sterigmatocystin have been carried out in several fungi (*A. flavus*, *A. nidulans* and *A. parasiticus*) and some of the assigned gene functions in *A. nidulans* are proposed based on gene homology to these two other species.

The biosynthetic cluster of sterigmatocystin in *A. nidulans* was first characterized by Brown and co-workers in 1996 [41]. They identified a 60 kb region in the *A. nidulans* genome responsible for the synthesis of sterigmatocystin. The cluster contains 27 genes named s*tcA-X* (Figure 3), reflecting their order of appearance on the chromosome [41].

Figure 3. The sterigmatocystin gene cluster. The black arrows are predicted *stc* ORFs, while light grey arrows are genes with unassigned functions.

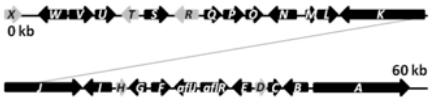

The PKS catalyzing the production of the PK backbone of sterigmatocystin was identified by Yu and co-workers in 1995 [42] and originally named *pksST*, but was later renamed to *stcA* by Brown *et al.* [41] to simplify nomenclature. Besides the PKS, the *stc* gene cluster is predicted to contain two transcription factors (*aflR*, *aflJ*), six monoxygenases (*stcB*, *stcC*, *stcF*, *stcL*, *stcM*, *stcS*, *stcW*), two dehydrogenases (*stcG*, *stcV*), an esterase (*stcI*), an O-methyltransferase (*stcP*), two ketoreductases (*stcE*, *stcU*), a VERB synthase (*stcN*), an oxidase (*stcO*), a monooxydase/oxidase (*stcQ*), a Baeyer-Villiger oxidase (*stcR*), a fatty acid synthase composed by the two subunits HexA and HexB (encoded by *stcJ* and *stcK*, respectively), and five unassigned genes (*stcD*, *stcH*, *stcR*, *stcT*, *stcX*), which may also be part of the cluster [39–41,43–47].

The *stc* cluster is a relatively large gene cluster, and studying the gene regulation has led to important discoveries. The two TFs were found to be present within the cluster. The AflR is a Zn_2Cys_6 TF that regulates transcription of the *stc* locus in *A. nidulans* [41,48], while AflJ (also named AflS) have been shown to have a role in the regulation of aflatoxin biosynthesis in *A. flavus* and is likely to have a similar function in *A. nidulans* [49]. Interestingly, Bok and Keller [50] discovered a novel regulator (LaeA) of secondary metabolism in *A. nidulans* in a mutant screen for loss of *aflR* expression. Deletion of *laeA* resulted in a significantly decreased production of different classes of SMs like sterigmatocystin and penicillin. LaeA, a putative methyl transferase was moreover acting in a feedback loop with AflR since overexpression of *aflR* downregulates *laeA* expression, and overexpression of *laeA* could not increase production of sterigmatocystin [50]. LaeA was shown to be a part of the conserved Velvet complex, which is important for regulation of fungal development and secondary metabolism [51]. Another hint on chromatin regulated gene expression came from the deletion of a histone deacetylase, *hdaA*Δ, which led to significant increase in the expression of two *stc* cluster genes, *stcU* and *aflR* compared to the reference [52].

Applying this strategy of deleting and overexpressing genes encoding global epigenetic regulators has paved the way for novel discoveries in secondary metabolism. Moreover the alternative of utilizing a chemical epigenetic approach through epigenetic modifier molecules has proven successful in activating gene clusters in *A. niger* [53].

The first step in the biosynthesis of sterigmatocystin (Figure 4) is the production of hexanoate by the FAS units, StcJ and StcK [41]. Watanabe and Townsend [54] showed that the hexanoyl-CoA is not an intermediate freed from the complex, indicating that hexanoate is transferred directly to the SAT domain of the PKS. The PK backbone is assembled by StcA by condensation of the starter unit, hexanoyl-CoA and seven malonyl-CoA extender units followed by cyclization and release of norsolorinic acid anthrone [42]. The oxidation of norsolorinic acid anthrone to norsolorinic acid may be catalyzed by *stcM*, a monooxygenase ortholog to *hypC* that converts norsolorinic acid anthrone to norsolorinic acid in *A. parasiticus* [43]. Norsolorinic acid is the first stable intermediate in the biosynthesis of sterigmatocystin and is converted into averantin by StcE, reducing the hexanoate ketone to an alcohol [41,55,56].

Figure 4. Proposed biosynthesis of sterigmatocystin. StcA contains starter unit-ACP transacylase (SAT), β-ketosynthase (KS), acyltransferase (AT), product template (PT), acyl carrier protein (ACP) and thioesterase/claisen cyclase (TE/CLC) domains. *Indicates a proposed, but not confirmed, enzyme. Multiple arrows indicate that the number of enzymatic steps is unknown.

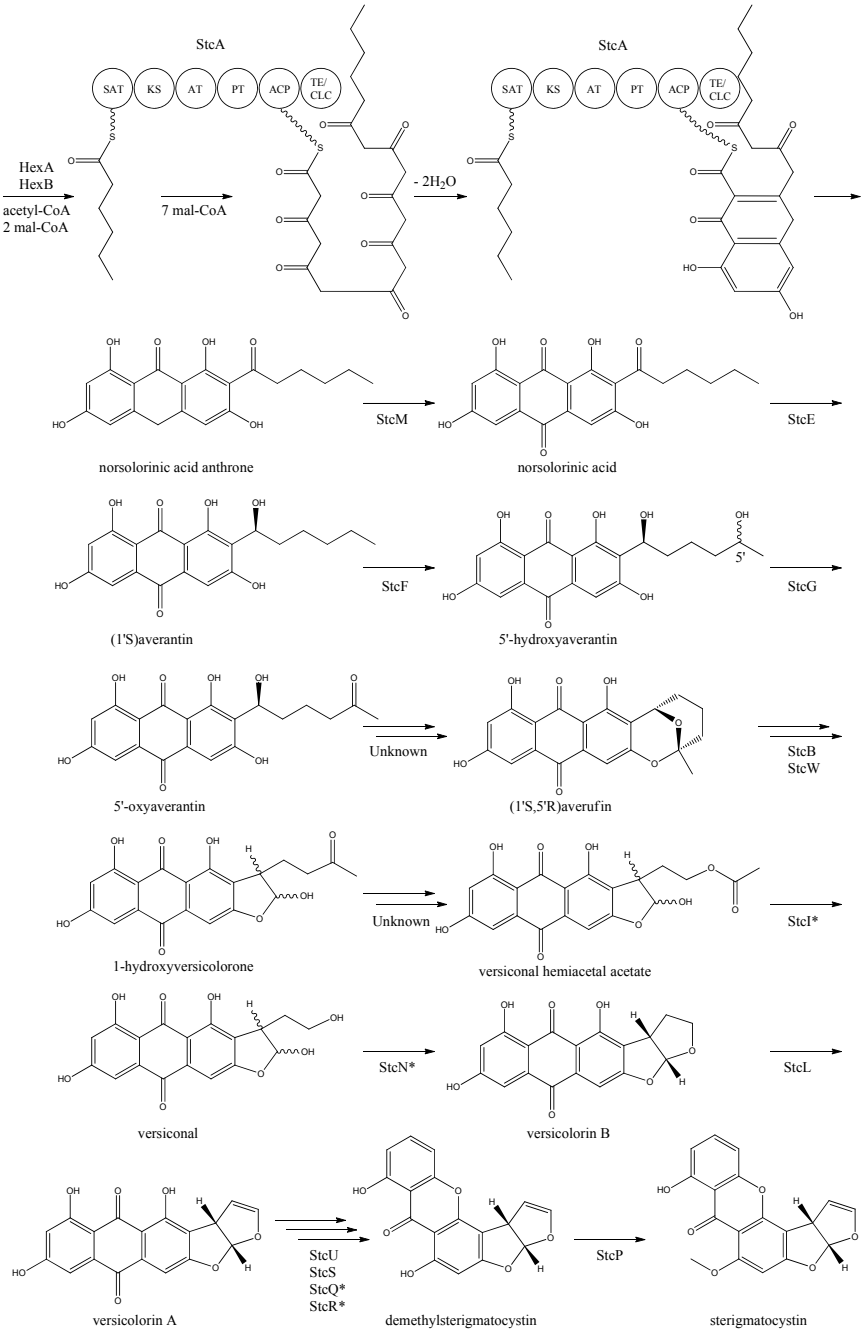

Yabe *et al.* [55] showed that 5′-hydroxyaverantin is a step towards aflatoxin in *A. parasiticus* and a later study showed that the oxidation of averantin into 5′-hydroxyaverantin is catalyzed by StcF [57]. The conversion of 5′-hydroxyaverantin to 5′-oxyaverantin is likely catalyzed by StcG [39,44]. In a study in *A. parasiticus* by Yabe and co-workers it was shown that both (1′*S*, 5′*S*)- and (1′*S*, 5′*R*)-hydroxyaveratin are formed in the conversion of averatin to 5′-oxyaveratin [58]. Disruption of *aflH* in *A. parasiticus* resulted in the accumulation of 5′-hydroxyaverantin, however, small amounts of *O*-methylsterigmatocystin present suggested that other enzymes may be involved in the reaction [44,59]. The gene(s) responsible for the conversion of 5′-oxyaverantin to averufin have not been identified [39,60].

Individual disruption of StcB and StcW resulted in elimination of sterigmatocystin and accumulation of averufin, indicating that both enzymes catalyze the conversion of averufin to 1-hydroxyversicolorone [57]. It was not possible for the authors to determine why two monooxygenases were required for this reaction step [57]. No gene products have been identified as being responsible for the conversion of 1-hydroxyversicolorone to versiconal hemiacetal acetate. StcI is thought to catalyze the reaction from 1-hydroxyversicolorone to versiconal based on studies of the ortholog AflJ in *A. parasiticus*, though other genes capable of this reaction may be present in *A. nidulans* [44,61].

Deletion of *stcN* did not result in the production of sterigmatocystin or other intermediates [44]. However, StcN show homology to AflK and the versicolorin B synthase, Vbs, in *A. parasiticus*, indicating that the biosynthetic step from versiconal to versicolorin B may be catalyzed by StcN [39,44,62]. StcL was shown by Kelkar *et al.* [63] to catalyze the conversion of versicolorin B to versicolorin A. Inactivation of *stcL* resulted in accumulation of dihydrosterigmatocystin, leading to a branching of the sterigmatocystin biosynthesis as seen in the aflatoxin biosynthesis. Addition of versicolorin A to the mutant gave production of sterigmatocystin, and that indicated that this enzyme functions before versicolorin A [63].

Keller and co-workers [64,65] showed that StcU and StcS are involved in the conversion of versicolorin A to demethylsterigmatocystin. Individual disruption of *stcU* and *stcS* led to the accumulation of versicolorin A and eliminated production of sterigmatocystin in *A. nidulans* [64,65]. Henry and Townsend [45] studied the same step in the aflatoxin biosynthesis in *A. parasiticus* and proposed an oxidation-reduction-oxidation mechanism, involving at least a ketoreductase AflM and a monooxygenase AflN, orthologs to *stcU* and *stcS*, respectively. Ehrlich *et al.* [46] and Cary *et al.* [47] identified two enzymes, AflY, a Baeyer-Villiger oxidase and AflX, an oxidoreductase, to be involved in the conversion of versicolorin A to demethylsterigmatocystin in *A. parasiticus* and *A. flavus*, respectively. *aflX* and *aflY* are homologous to *stcQ* and *stcR*, which suggests that these genes might be involved in the biosynthetic step from versicolorin A to demethylsterigmatocystin [46,47].

The final step in the biosynthesis of sterigmatocystin is the methylation of demethylsterigmatocystin catalyzed by StcP [66]. The conversion of sterigmatocystin to aflatoxin involves two additional biosynthetic steps; an *O*-methylation of sterigmatocystin by *aflP* followed by involvement of *aflQ* to produce aflatoxin [39]. Slot and Rokas have recently showed that the sterigmatocystin gene cluster in *Podospora anserina* was horizontally transferred from *Aspergillus*, which shows that transfer of large metabolite clusters between fungi are possible [67].

4. Aspyridone

Aspyridone is a PK-NRP hybrid and a fascinating example on how PK-NRP compounds in *A. nidulans* can be assembled from the activity of a single fusion enzyme. The aspyridones have shown to display moderate cytotoxicity [68]. The responsible gene cluster was discovered by Bergmann and co-workers [68] using a genome mining approach. Using the *Aspergillus* genome sequence, they identified a SM gene cluster, which contained a putative TF (AN8414/*apdR*) that the authors hypothesized could trigger activation of the genes in the cluster. Accordingly, the authors overexpressed the TF under the control of an inducible *alcA* promoter by integrating it randomly in the genome. In agreement with the hypothesis, it was demonstrated by Northern blot analysis that six of the nearest neighbor genes were up-regulated in this strain on inductive medium, and that the aspyridones and two intermediates or shunt products could also be detected. Prediction of the catalytic potential for the six upregulated genes (*apdA, apdB*, *apdC*, *apdD*, *apdE,* and *apdG*) combined with the structure of the accumulating compounds allowed the authors to propose a model for the biosynthesis of aspyridones including an assignment of the involved enzymes (Figure 5).

Figure 5. Proposed biosynthesis of aspyridone A and B. (**a**) Based on proposed biosynthesis by [68,72,73]; (**b**) Based on results by Halo *et al.* [78] Multiple arrows indicate that the number of enzymatic steps is unknown.

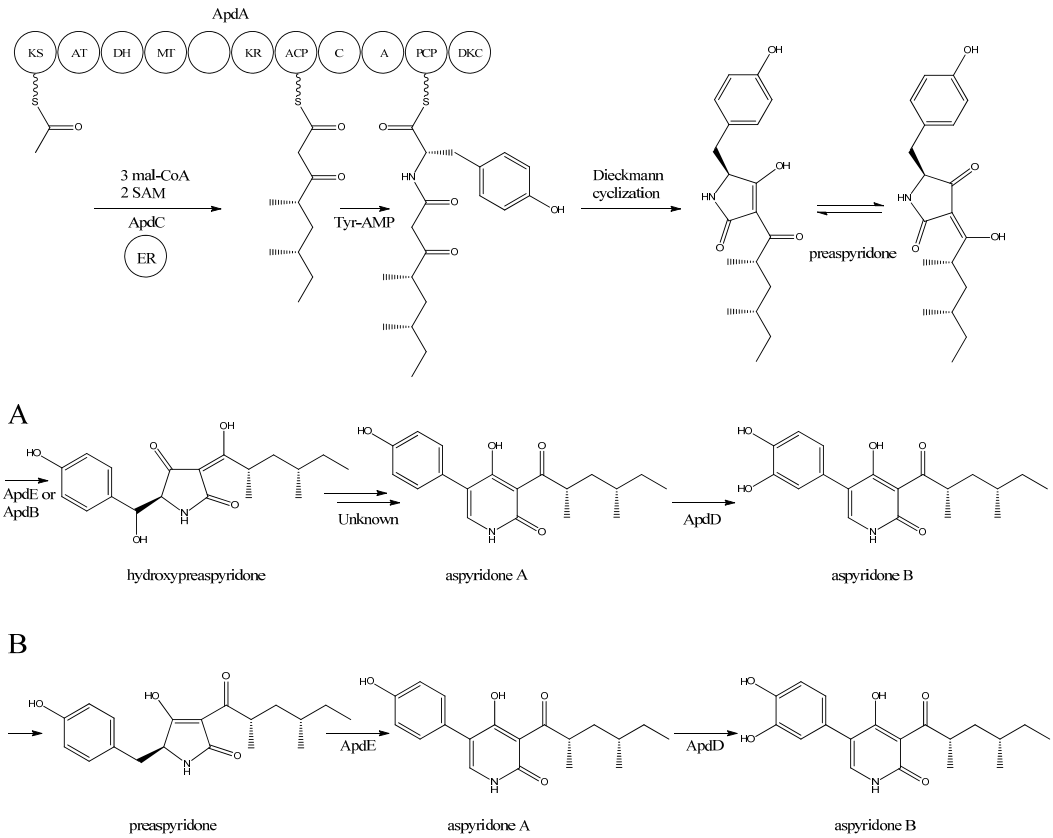

apdA was deleted by Chiang *et al.* [69] and confirmed to be involved in aspyridone biosynthesis as reported by Bergmann *et al.* [68].

The structure of aspyridone A and B suggested that their synthesis involved both PKS and NRPS activity. Indeed, analysis of the AN8412 structure revealed domains characteristic for a HR-PKS as well as NRPS in one ORF spanning more than 11 kb. This is a special subclass of reducing PKSs, where the PKS has been directly fused with a single NRPS module at the C′-terminal end. This architecture allows for the incorporation of amino acids or carboxylic acids into the carboxylic end of the growing PK chain. Only one of these fusion enzymes has been found in *A. nidulans*, but has been reported in other fungi [70,71]. Since AN8412 is the first enzyme to act in the pathway, the gene was named *apdA*. ApdA catalyzes the assembly of the PK-amino acid backbone of the aspyridones by three Claisen condensations of malonyl-CoA, and KR-DH-ER-MT carries out full reduction of the β-keto and the methylations, which are required. However, as ApdA lacks a functional ER domain, the ER activity is most likely provided by ApdC, a homolog to an enoyl reductase (LovC) from the lovastatin biosynthetic gene cluster [68]. The resulting triketide is transferred to the NRPS module, where it is linked to tyrosine [68]. Bergmann and co-workers listed the domains through protein homology in the NRPS as condensation (C), adenylation (A), peptidyl carrier protein (PCP) and reductase domain (RED).The release of the PKS-NRPS hybrid product was proposed to be a NADPH-dependent reductive release followed by an intramolecular Knoevenagel condensation and enzymatic oxidation [68]. Biochemical studies of the role of ApdA and ApdC in the biosynthetic pathway of the aspyridones have been performed by Liu *et al.* [72] and Xu *et al.* [73]. Liu and co-workers [72] defined the NRPS module as C-A-T-R with the latter two being thiolation and reductase, which is an alternative to the more frequent C-A-T-TE found in these modules. However, this reductase domain (R*) in the NRPS module of ApdA is not the standard SDR superfamily dehydrogenase since tyrosine in the Ser-Tyr-Lys catalytic triad is mutated suggesting a redox-independent condensation reaction and the release of a tautomer of preaspyridone from ApdA by a Dieckmann cyclization, which was first shown by Halo and co-workers [74]. This result has been confirmed by Xu *et al.* who expressed the *apdA* and *apdC* genes in *Saccharomyces cerevisiae* and *Escherichia coli*, respectively [73]. The purified enzymes (ApdA and ApdC) were incubated in the presence of cofactors and building blocks and the predominant product was preaspyridone [73].

The formation of preaspyridone into aspyridone A and B was proposed by Bergmann *et al.* [68], (and outlined in Figure 5a) using the predicted functions of the remaining genes of the *apd* gene cluster. The proposed biosynthesis involved ApdB and ApdE which shows similarity to cytochrome P450 oxygenases and cytochrome P450 alkane hydroxylases, respectively, and were believed to catalyze the formation of hydroxypreaspyridone [68]. Based on the study of pyridone rearrangement in metabolites related to aspyridone it was suggested that ApdE or ApdB were involved in the pyridone rearrangement [68,75–77]. Moreover, aspyridone A was hypothesized to be converted into aspyridone B by ApdD, a putative FAD-dependent monooxygenase, which is related to other ring hydroxylases [68]. Aspyridone has a similar structure to other pyridines isolated from fungi, e.g., tenellin whose biosynthetic gene cluster also has been identified [75,76]. The proposed biosynthesis of aspyridone was, as described above, based on predicted gene functions and not isolated intermediates. However, a study on the biosynthesis of the related metabolite tenellin by Halo and co-workers [78] showed that the suggested biosynthesis may be incorrect and an alternative biosynthesis was suggested (as shown

in Figure 5b). In this biosynthesis preaspyridone is not converted into hydroxyaspyridone but ring expanded by ApdE to aspyridone A similar to the biosynthesis of tenellin [78]. Halo *et al.* also showed that the hydroxylated metabolite of pretenellin is a shunt metabolite as it could not be converted into tenellin.

5. Emericellamides

The emericellamides are other examples of hybrid compounds that are formed between PKs and NRPs. In this case the biosynthesis requires a PKS and a NRPS rather than a fusion PKS-NRPS as used in the production of the aspyridones. Emericellamides are cyclic depsipeptides and a total of five variants, A, C–F, of these metabolites have been found in *A. nidulans*. Initially, emericellamide A and B were isolated and described from an unidentified marine-derived *Emericella* strain in a screen due to their antibacterial activity against methicillin-resistant *Staphylococcus aureus* [79].

In order to discover novel natural products, Chiang and co-workers [69] searched the genome sequence of *A. nidulans* for NRPS gene candidates. Subsequently, six of these genes were randomly chosen and deleted by gene targeting. One of the resulting mutants, AN2545Δ, showed a metabolite profile where emericellamide A was missing. Furthermore, HPLC profiles and dereplication using mass spectrometry and database searches revealed four additional compounds, which disappeared in the mutant metabolite profile. Since these compounds had not previously been described in *A. nidulans*, they were purified and their structures solved by NMR analysis revealing that they were novel analogues of emericellamide A and B, thus named emericellamide C–F [69].

To investigate whether AN2545, now called *easA*, defines a gene cluster encoding all necessary enzymatic activities in the emericellamide biosynthetic pathway, the genes from AN2542 to AN10325, a total of ten, were deleted [69]. Most of these gene deletions did not affect emericellamide production as judged by LC-MS analysis, demonstrating that they do not participate in the biosynthesis. However, the emericellamides were absent in four of the deletion strains, now named *easA*-*easD*, indicating that these genes are involved in the pathway.

Bioinformatic analysis of the three additional genes suggested that they all encode activities that are relevant for emericellamide biosynthesis. Specifically, *easB* (AN2547), a PKS, *easC* (AN2548), an acyl transferase, and *easD* (AN2549), an acyl-CoA ligase. Based on these putative activities, the authors proposed a biosynthetic pathway for emericellamide production (Figure 6). In this model, the biosynthesis is initiated by EasB, a HR-PKS composed of the domains KS-AT-MT-DH-ER-KR-ACP. Since the PK component of the different emericellamide variants differ with respect to chain length and methylation pattern, it indicates that iterativity of this PKS is flexible [69].

Next, the PK carboxylic acid is converted to a CoA thioester by the acyl-CoA ligase, EasD, loaded onto the acyltransferase EasC, and then transferred to the thiolation (T) domain of EasA. This NRPS is a multi-modular enzymatic assembly containing 18 domains grouped into five modules. Among those, the authors propose that the first T domain is responsible for accepting the incoming PK from EasC (Figure 6). Moreover, the remaining domains fit well with the fact that five amino acids are incorporated into emericellamides. The authors note that this NRPS does not contain a TE domain at the end of module 5, indicating that this enzymatic activity is not necessary for cyclization of the emericellamides [69].

Figure 6. Proposed biosynthesis of the emericallamides. The order of the methyltransferase (MT) and dehydratase (DH) domain as suggested by Chiang *et al.* [69], however a BLASTp analysis suggests a swapping of the MT and DH domains. The NRPS, EasA, contains 18 (T, E (epimerization), C, A) domains grouped into five modules.

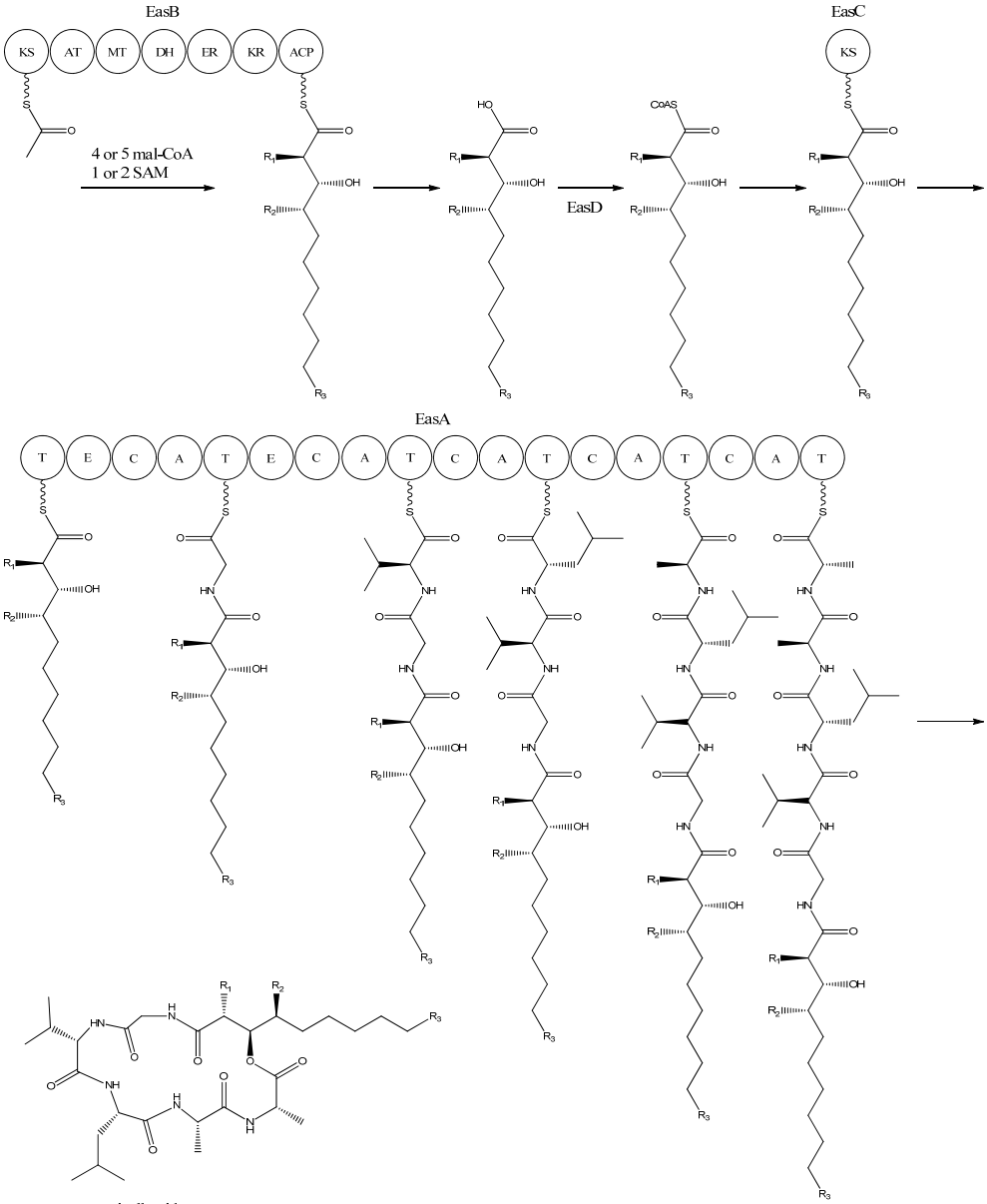

6. Asperthecin

Asperthecin is a PK compound that was first isolated from *A. quadrilineatus* by Howard and Raistrick in 1955 [80], however, the structure was not fully determined until six years later [81]. Initially, various chemical derivatizations and spectroscopic data determined a partial structure of asperthecin [80]. Neelakantan and co-workers [82] reduced the number of possible structures to two, and further derivatizations of asperthecin by Birkinshaw and Gourlay resulted in the final structure [81]. *A. quadrilineatus* is a member of the *A. nidulans* group, therefore Howard and Raistrick [80] extended the search of asperthecin to additional members of the *A. nidulans* group. No other was as rich in asperthecin production as *A. quadrilineatus*, yet small amounts of crystallized asperthecin could be obtained from cultures of *A. nidulans* and *A. rugulosus* indicating that production of asperthecin was possible in other aspergilli [80].

About 50 years later, Szewczyk and co-workers [83] used a molecular genetics approach to find the gene cluster responsible for the production of asperthecin in *A. nidulans*. Since many aspects of the regulation in the polyketome were unknown, the authors speculated whether sumoylation had an effect. SUMO is a small ubiquitin-like protein which is post-translationally added to proteins in the cell, as it plays a role in regulating transcription. *A. nidulans* contains one SUMO encoding gene, *sumO* [84], deletion of which led to a decrease in the production of SMs such as austinol, dehydroaustinol, and sterigmatocystin, and an increase in the production of a metabolite identified to be asperthecin, whereas the production of emericellamides were not affected [83]. Due to the aromatic structure of asperthecin, Szewczyk *et al.* [83] studied the domain prediction in 27 putative PKS-protein sequences using the *A. nidulans* genome sequence and available tools, in order to identify potential producers of non-reduced PKs. Ten NR-PKSs were identified and a deletion series of all NR-PKS genes was performed in the *sumO*Δ background [83]. While nine of the PKS-deletion strains still produced asperthecin, the AN6000 (*aptA*) PKS-deletion strain failed to synthesize asperthecin [83]. With the notion that most end compounds in PK biosynthesis are made by a clustered gene collective, six candidate genes surrounding *aptA* were picked in an attempt to identify the *apt* biosynthetic cluster. Two of these genes, *aptB* (AN6001) and *aptC* (AN6002), were found to be required for asperthecin production [83]. One strain (AN5999Δ) had a significantly lower production of asperthecin compared to the reference strain, but asperthecin was still present in the metabolite extracts, and as the strain showed poor growth, it was not included in the *apt* gene cluster.

Interestingly, AptA was shown to have SAT-KS-AT-PT-ACP domains, but lack a TE/CLC domain [83,85–88]. Independent groups have used this case as a model system to study the mode of PK release, and two alternating mechanisms for the biosynthesis of asperthecin are shown in Figure 7 [86,87]. The first model suggests the formation of the PK backbone by condensations of one acetyl-CoA and seven malonyl-CoA units [86], with the β-lactamase AptB releasing the octaketide from AptA [83]. This assumption was based on a study by Awakawa and co-workers [85] in *A. terreus*, where there was a release of atrochrysone carboxylic acid from the atrochrysone carboxylic acid synthase (ACAS) lacking a TE/CLC domain, in the presence of the atrochrysone carboxylic ACP thioesterase (ACTE), a member of the β-lactamase superfamily [85]. The unstable atrochrysone carboxylic acid then undergoes a series of reactions; decarboxylation, dehydration, and various oxidations where the monooxygenase AptC is believed to be involved, and in the end yielding asperthecin [86].

Figure 7. Proposed biosynthesis of asperthecin (**a**) As suggested by Chiang *et al.* [86]; (**b**) Based on proposed biosynthesis by Li *et al.* [87]. AptA contains SAT, KS, AT, PT and ACP domains. Multiple arrows indicate that the number of enzymatic steps is unknown.

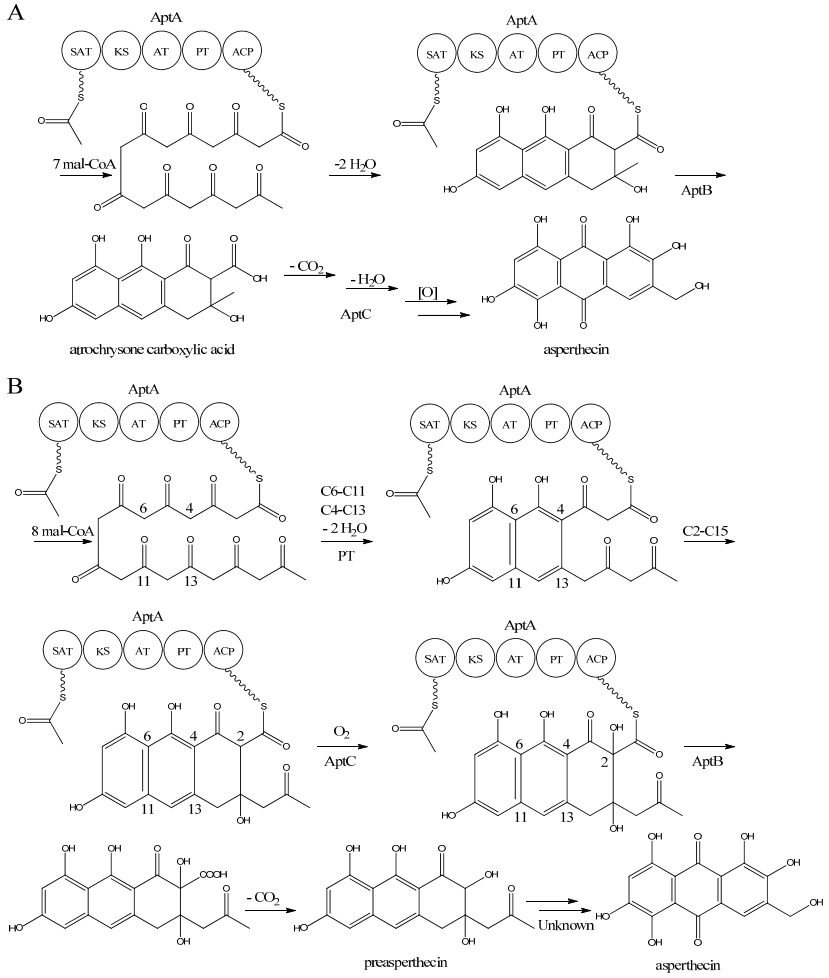

In another approach, Li *et al.* [87] introduced *aptA*, *aptB*, and *aptC* into *S. cerevisiae*, which resulted in the production of a nonaketide (here called preasperthecin), and not the octaketide as proposed by Chiang *et al.* [86]. Expressing *aptA* and *aptB* without *aptC* resulted in a product identical to preasperthecin except for the lack of C2-OH, confirming that AptC is responsible for this step [87]. Expression of *aptA* and *aptC* alone did not lead to the production of preasperthecin or any other traceable compounds, confirming that AptB is needed for release of the PK from AptA [87]. These results were confirmed by an *in vitro* assay after expressing *aptA*, *aptB* and *aptC* in *E. coli* [87]. Further insight into AptA functionality came from expressing the AptA-PT domain in *E. coli*, and combining it with the *Gibberella fujikuroi* PKS4, which can produce nonaketide products *in vitro* [88]. The experiment revealed that AptA-PT can catalyze C6-C11 cyclization, and most likely also the C4-C13 cyclization. Further, a spontaneous C2-C15 cyclization was followed by a C1-C17

esterification [88]. The *apt* gene cluster appears likely to consist of additional genes, which are responsible for the conversion of preasperthecin into asperthecin.

7. Asperfuranone

Asperfuranone is an example of a novel PK metabolite discovered through genetic mining in *A. nidulans*, as this compound had not previously been reported in the literature before Chiang and co-workers [89] in 2009. Asperfuranone was later shown to possess bioactive properties as it inhibited proliferation of human non-small A549 cancer cells [90]. Investigating the loci containing putative PKS gene clusters, Chiang and co-workers [89] noticed that a NR-PKS gene (AN1034, *afoE*) and a HR-PKS gene (AN1036, *afoG*) were located close to each other on chromosome VIII. Since no products had ever been detected from activity of this locus, and due to the rare constellation of two neighbor PKSs, the authors speculated whether a novel metabolite could be revealed. A putative transcriptional activator (AN1029, *afoA*) was found near the PKS and the authors replaced the upstream sequence of *afoA*, estimated to be the native promoter, with the inducible *alcA* promoter [89]. This indeed turned on the expression of the cluster, since asperfuranone and a precursor metabolite were detected. The structure of asperfuranone was determined based on one- and two-dimensional NMR experiments and the absolute configuration by a modified Mosher's method, whereas the precursor preasperfuranone had already been determined in the literature [89,91]. With these two compounds being identified, a gene-deletion strategy was performed to map the other genes assigned to the *afo* gene cluster, which involved twelve surrounding genes including the two PKSs [89]. Four deletion strains *afoD*Δ, *afoE*Δ, *afoF*Δ, and *afoG*Δ fully eliminated asperfuranone production whereas *afoB*Δ and *afoC*Δ strongly reduced production of asperfuranone [82]. The deletions confirmed that both *afoE* and *afoG* were responsible for the production of asperfuranone, and that the deletion of *afoD*, encoding a putative hydroxylase, resulted in the production of preasperfuranone [89]. Deletion of *afoB* reduced the production of asperfuranone and due to a high homology to efflux pumps, Chiang and co-workers [89] suggested that it was responsible for the transport of asperfuranone out of the cell.

With the gene cluster and predicted functionalities of the gene products defined, a biosynthetic pathway of asperfuranone was proposed (Figure 8) [89]. The assembly of the primary reduced tetraketide is synthesized by AfoG from one acetyl-CoA, three malonyl-CoA, and two SAM. The tetraketide is transferred to the SAT domain of AfoE and extended with four malonyl-CoA and one SAM [89]. The octaketide is released from AfoE after aldol condensation and reductive release from a C-terminal reductase (R) domain, which resembles a reductive release mechanism to generate the aldehydes described by Bailey *et al.* [92], forming the aldehyde preasperfuranone [89]. The biosynthetic steps from preasperfuranone to asperfuranone are uncharacterized and the suggestions are not based on identified metabolites [89]. Accumulation of preasperfuranone in the *afoD*Δ suggested AfoD to be the next enzyme in the biosynthesis of asperfuranone. The deletions of *afoF*, encoding a putative FAD/FMN-dependent oxygenase and *afoC*, initially believed to code for a homologue to citrinin biosynthesis oxidoreductase, did not reveal any intermediates, the order of reactions and the exact enzymatic functions for AfoF and AfoC have not been determined. In *afoC*Δ, the production of asperfuranone was not fully eliminated, which Chiang and co-workers [89] suggested could be due to other enzymes catalyzing the reaction, however less efficiently.

Figure 8. Proposed biosynthesis of asperfuranone. The highly reducing (HR)-PKS, AfoG, contains KS, AT, DH, CM, ER, KR, and ACP domains whereas the NR-PKS, AfoE, contains SAT, KS, AT,PT, ACP, CM , and R domains. The only intermediate isolated in the biosynthesis is preasperfuranone [89]. Multiple arrows indicate that the number of enzymatic steps and reaction order is unknown.

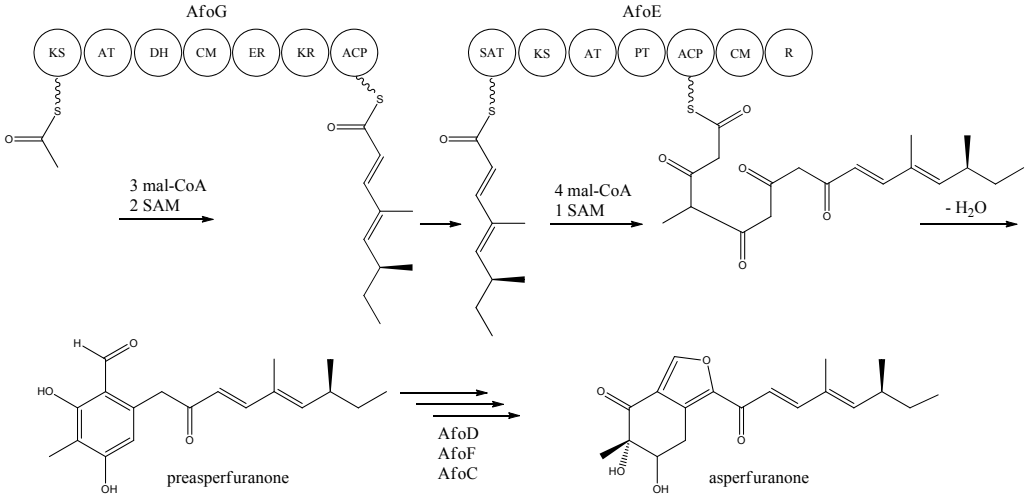

Other puzzling discoveries have been made in connection to the asperfuranone production. When trying to activate a cryptic NRPS gene cluster containing two NRPSs, *inpA* (AN3495) and *inpB* (AN3496), by overexpression of a regulatory gene, *scpR* (AN3492), Bergmann *et al.* [93] also activated asperfuranone. This is an interesting example of a regulatory gene located on chromosome II that activates the *afo* cluster located on chromosome VIII [93]. Lui *et al.* [94] have attempted to engineer the production of a new metabolite by swapping the SAT domain of AfoE with the StcA-SAT. This led to the production of a new metabolite though having the same length as the native AfoE product, asperfuranone [94].

8. Monodictyphenone/Emodin

The PK monodictyphenone was first reported in *A. nidulans* in 2005 [95] and the genes behind the production of monodictyphenone were mapped four years later [96]. This discovery not only enabled the establishment of a biosynthesis model for monodictyphenone in *A. nidulans*, it has subsequently revealed that more than ten different stable products among different classes of related polyketides can be linked to monodictyphenone biosynthesis [11,96–98]. These metabolites count monodictyphenone, emodin and the emodin derivates 2-hydroxyemodin, 2-aminoemodin, ω-hydroxy emodin, and emodic acid. Moreover, the arugosins and prenyl-xanthones are also coupled to the pathway [11,98]. The compound emodin has been studied for more than a century [99], and is an anthraquinone found in a wide array of both plants and fungi [100,101]. Emodin and several derivatives (e.g. emodic acid) have been shown to possess anti-bacterial and cancer preventive properties [102–106].

The presence of the SM clusters in silent areas of chromosomes, e.g. near telomeres and centromeres, suggests that chromatin remodeling factors can influence the expression of genes responsible for SMs. As rationalized by Bok and co-workers [96], removal of histone-tail methylation could open heterochromatic regions for transcription. The authors deleted an ortholog, *cclA*, to the yeast *BRE2* gene, encoding an enzyme partner of the COMPASS transcriptional regulator complex conserved in eukaryotes, which rendered *A. nidulans* defective in di- and trimethylation of lysine 4 of the histone 3 tails (H3K4). The *cclA* deletion was established in a mutant strain, *stcJ*Δ, to avoid interference of high amounts of sterigmatocystin in purification of other metabolites. The effect was striking as the loss of CclA in HPLC analysis showed an altered chemical landscape compared to the *stcJ*Δ reference [96].

As the compounds appearing were UV-active suggesting high conjugation likely due to aromaticity, the ten NR-PKSs investigated in the asperthecin and asperfuranone studies were individually deleted in the *cclA*Δ *stcJ*Δ double deletion background. This screen revealed six products that all were linked to one PKS, AN0150 (*mdpG*) [96]. Delineation of the cluster was achieved by inspecting the genome sequence for possible cluster candidates followed by Northern blotting for gene-expression analysis in the *cclA*Δ *stcJ*Δ, where the products were detected. The cluster was found to span 12 putative ORFs (AN10021-AN10023 (*mdpA-L*)) [97] of which two genes AN0147 (*mdpD*) and AN10035 (*mdpI*), did not show altered expression from the reference [96,97]. The *mdp*-cluster candidates were also deleted in the *cclA*Δ *stcJ*Δ mutant strain to confirm the expression analysis data and to draw the borders of the cluster [97]. The authors suggest that two transcriptional activators are present within the cluster; MdpE as a main activator (homologue to AflR) and that MdpA is a co-activator. The *mdp* locus is located near the telomere of chromosome VIII, and activation of the genes in the *cclA*Δ strain supports the hypothesis of epigenetic regulation in these areas through chromatin remodeling [96].

Two groups cultivated *A. nidulans* on complex growth media, which revealed six additional metabolites. First Sanchez *et al.* [98] discovered that emericillin, variecoxanthone A, shamixanthone, and epi-shamixanthone were also products of the *mdp* cluster, and subsequently Nielsen and co-workers [11] added arugosin A and H to the pathway. Since these PKs are prenylated, a BLAST search of the *A. nidulans* genome sequence was performed and pathway-candidate genes were deleted. Two prenyl transferases encoded by *xptA* and *xptB*, and one neighbor GMC oxidoreductase encoded by *xptC*, were found to be involved in the pathway, though they were located on other chromosomes than the *mdp* cluster (for cluster overview see Sanchez *et al.* [98]). This is an intriguing example of SM-cluster members located on more than one chromosome, however, prenyl transferases are known to have broad substrate specificity, and it is currently not known whether they are involved in other processes than prenyl-xanthone formation [98].

MdpG synthesizes the main PK backbone. Since MdpG lacks a CLC/TE domain, MdpF, a putative zinc dependent hydrolase, is believed to catalyze the release of the PK from MdpG [97]. The mechanism is believed to follow the case of ACAS and ACTE as introduced previously in the asperthecin section. Awakawa and co-workers [85] demonstrated that the direct product of the ACAS/ACTE is not emodin anthrone as proposed earlier [107,108], but more likely atrochrysone carboxylic acid (Figure 9). Atrochrysone carboxylic acid was not observed *in vitro*, instead the decarboxylated product atrochrysone was the major product in the assays and therefore proposed to be an intermediate to emodin, as suggested by Couch and Gautier [109]. Conversion of atrochrysone to

emodin requires dehydration (forming emodin anthrone) and a final oxidation (Figure 9), however, Awakawa and co-workers [85] observed small amounts of both emodin anthrone and emodin *in vitro* showing that these reactions may occur non-enzymatically. Based on these observations, Chiang and co-workers [97] proposed that *mdpH* encodes a decarboxylase, catalyzing the conversion of atrochrysone carboxylic acid to atrochrysone. The deletion of *mpdH* resulted in accumulation of a shunt product endocrocin produced via endocrocin anthrone. Enzymes responsible for dehydration of atrochrysone or modification of emodin into the observed derivatives have not yet been identified.

Figure 9. Proposed biosynthesis of emodin. MdpG contains SAT, KS, AT, PT, and ACP domains.

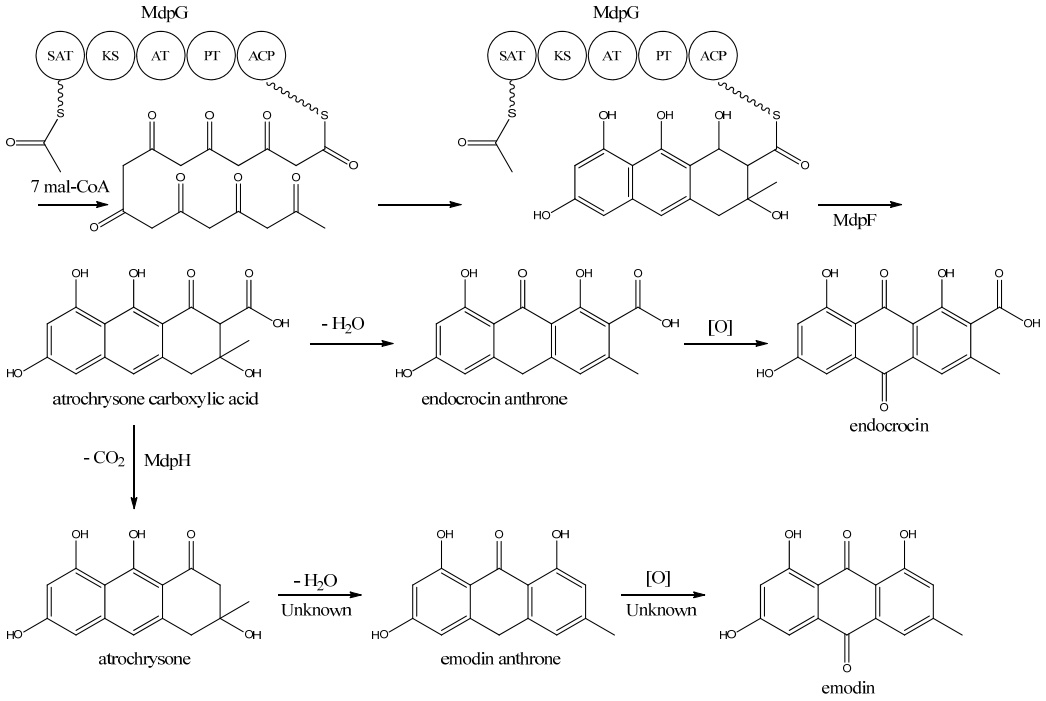

The first stable intermediate following emodin towards the prenyl-xanthones is monodictyphenone [97,98], and gene-deletion studies points to at least the five following enzymes are involved; a dehydratase (MdpB), a ketoreductase (MdpC), a glutathione S transferase (MdpJ), an oxidoreductase (MdpK), and a Baeyer-Villiger oxidase (MdpL) [97]. The mechanism has been proposed to be analogous to the conversion of versicolorin A to demethylsterigmatocystin which is known to proceed through oxidation-reduction-oxidation catalyzed by a cytochrome P450 monooxygenase (VerA) and a ketoreductase (StcU) [45,65,110]. However, none of the above mentioned Mdp enzymes appear to be homologous to VerA, and the role of the individual enzymes has not been investigated further [97].

The biosynthesis of the six monodictophenone derived metabolites is based on hydroxylation (MdpD), C-prenylation (XptA), *O*-prenylation (XptB), and carboxylic acid reduction (unidentified enzyme) [11,98]. Central in the pathway is the hydroxylation of C2 in monodictyphenone accompanied by reduction of the carboxylic acid. The carboxylic acid is suggested by Sanchez and co-workers [98] to be reduced to a hydroxy group, the B-ring is closed by dehydration and the

intermediate is O-prenylated at C2 to yield variecoxanthone A, which in turn is C-prenylated to emericillin (Figure 10). The final known step in prenyl-xanthone biosynthesis gives rise to the stereoisomers shamixanthone and epishamixanthone and is catalyzed by XptC [98]. Alternatively, Nielsen and co-workers include synthesis of arugosins by partially reducing the carboxylic acid to an aldehyde, followed by C-prenylation, yielding arugosin H and O-prenylation to give arugosin A. Subsequent reduction of the aldehyde to a hydroxyl group, and ring closure by dehydration then gives emericillin and shamixanthones [11].

Figure 10. Suggested biosynthesis of the shamixanthons from emodin. Multiple arrows indicate that the number of enzymatic steps are unknown.

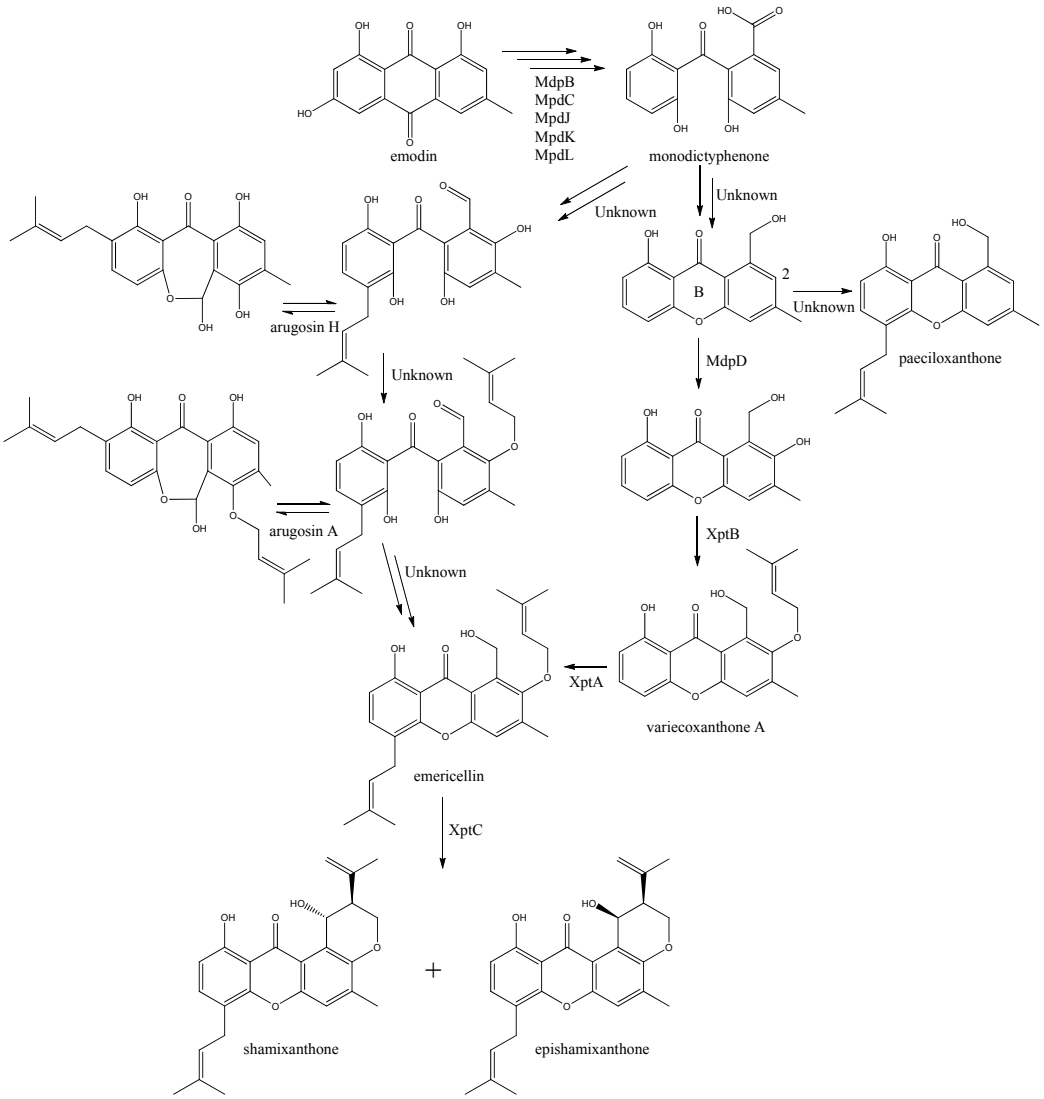

9. Orsellinic Acid

In addition to the *mdp* cluster, the loss of CclA also led to the discovery of another gene cluster driven by an NR-PKS [96]. Two PK products, the cathepcin K inhibitors F-9775A and F-9775B, first isolated from *Paecilomyces carneus* [111], were detected and mapped to AN7909. Following this discovery, Schroeckh and co-workers [112] found the primary metabolite from AN7909 (*orsA*) to be orsellinic acid, an archetypal metabolite [113]. Moreover, the metabolite lecanoric acid typically found in lichens and produced by mycobiots such as *Umbilicaria antarctica* [114] was linked to OrsA [112]. Following the initial observations, the number of detected metabolites from the *orsA* gene cluster has expanded to gerfelin, a C10-deoxy-gerfelin, diorcinol, orcinol, cordyol C, and violaceol I and II [115,116]. The biosynthetic activities of the *orsA* cluster are as yet not elucitated, and this illustrates the need for applying different eloquent strategies to trigger production of these metabolites.

The deficiency in methylation of H3K4 in the *cclA*Δ strain resulted in activation of both *mdp* and *ors* gene clusters. Expression analysis revealed that the annotated ORFs from AN7909-AN7915 were possible cluster members, hereby indicating candidates for a gene cluster [96]. The *ors* gene cluster, *orsB-orsE*, was identified by Schroeckh and co-workers [112] as four additional ORFs spanning AN7911-AN7914, which was confirmed by Sanchez *et al.* [115], who deleted all genes from AN7901 to AN7915. Interestingly, the neighbor PKS to the *ors* locus, AN7903, was deleted by Nielsen *et al.* [11] and the resulting strain failed to produce F-9775A and B like AN7909Δ under the conditions tested. Schroeckh and co-workers [112] defined *orsA-E* using gene-expression analysis through both an *Aspergillus* secondary metabolism array (ASMA) and relative expression analysis in quantitative reverse-transcriptase PCR (qRT-PCR). The induction of *orsA* was achieved by co-cultivating with a soil bacterium, *Streptomyces rapamycinicus* (initially named *S. hygroscopicus*) and extracting mRNA from the fungus [112]. This response on SM level was further investigated by Nützmann and co-workers [117]. Since the loss of H3K4 methylation induced gene expression in *ors* locus [96], the rationale was that the transcriptional activation of silent secondary-metabolism genes by acetylation of lysines on histone tails, especially H3K9, is equally important and the search for histone acetyl transferases (HATs) in the genome sequence was commenced [117]. Forty HATs were found and deleted, and only four proved to be essential. Of the 36 deletions of nonessential HATs in *A. nidulans*, the deletions of *gcnE* and *adaA*, both essential core parts of the multi-subunit Saga/Ada complex, an important complex for HAT activity in *A. nidulans*, significantly lowered the *ors* transcripts investigated [117]. Thus, Saga/Ada plays a role in the response to *S. rapamycinicus* and loss of this complex downregulated orsellinic acid metabolites, as well as sterigmatocystin, terrequinone, and penicillin [117].

Four additional orsellinic acid derived compounds were found in a defect COP9 signalosome (CSN) mutant strain [116]. The multiunit CSN complex is found in higher eukaryotes, albeit with different functional roles depending on the tissues. In *A. nidulans* the CSN is required for fruiting body formation and is not essential for asexual growth. By deleting *csnE*; orcinol, cordyol C, and violaceol I+II were produced, and the genes *orsA-orsE* were shown to be differentially expressed [116]. The link of the violaceol metabolites to *ors* was confirmed by Nielsen and co-workers [11] who applied an OSMAC strategy on their reference strain and compared this to their deletion library.

Very little is known about the biosynthesis of the metabolites of the *ors* locus. One acetyl-CoA and three malonyl-CoA units can yield a C8 aldol intermediate, and as proposed by Nielsen *et al.* [11], this can lead to the tetraketide orsellinic acid through loss of water and enolization and to the C7 compound orcinol by decarboxylation and enolization. Oxidation of orcinol in the para position then leads to 5-methyl-benzene-1,2,3-triol which is believed to either dimerize with the loss of water to give violaceol I and II, Figure 11, or to give F-9775A+B, Figure 12, in an unknown series of synthesis steps. Another outcome is the formation of lecanoric acid by dimerization of orsellinic acid. Though the steps in the pathway have been hypothesized, most steps are not accounted for. It has been reported that OrsA having the domains SAT-KS-AT-PT-ACP-TE is responsible solely to form orsellinic acid. OrsA, OrsB, and OrsC seem to be sole responsible for F-9775A+B formation. Moreover, it has been shown that gerfelin and a C10-deoxy derivative of gerfelin accumulate in *orsB*Δ, whereas diorcinol was found in high amounts in the *orsC*Δ strain [115]. Gerfelin, C10-deoxy gerfelin and cordyol C are all dimers built up of two of the three suggested monomer units, orsellinic acid, orcinol and 5-methylbenzene-1,2,3-triol.

Recently Scherlach and co-workers [118] continuously cultivated *A. nidulans* under nitrogen-limitation and carbon-limitation. At nitrogen limiting conditions in continuous cultivations two novel products, denoted as spiroanthrones, were found. They could not be detected at batch cultivation. The metabolites were based on anthraquinone and orsellinic acid derived phenols. The induced expression of both *mdpG* and *orsA* confirmed increased activity under the N-limiting continuous cultivation conditions.

10. Austinol and Dehydroaustinol

The meroterpenoids austinol and the related compound dehydroaustin were first isolated from *A. ustus* by Simpson and co-workers in 1982 [119], where the structure of austinol was elucidated by ^{1}H and ^{13}C NMR. Austinol and dehydroaustinol are just two examples out of many meroterpenoids that are derived from 3,5-dimethyl orsellinic acid as presented in the excellent review by Geris and Simpson [120].

The two austinols were detected for the first time in *A. nidulans* four years ago [121], where it was further substantiated that austinol was indeed of partly PK origin. Deletion of the phosphopantheteinyl transferase (PPTase) *cfwA*/*npgA* in *A. nidulans* resulted in a strain that among many other compounds did not produce austinol and dehydroaustinol [121]. The PPTase is responsible for attaching the phosphopantetheine moiety to the acyl carrier domain of the PKSs and NRPSs, thus it is an activator of the enzyme complexes. Hence, the abolition of austinol and dehydroaustinol production in the PPTase deficient strain strongly suggests a PK origin of these compounds.

In 2011, Nielsen and co-workers [11] discovered the PKS responsible for synthesis of the PK part of austinol and dehydroaustinol in *A. nidulans*. A deletion library of all 32 putative PKS genes in *A. nidulans* was created and screened using an OSMAC approach [122] to enable activation of different clusters on different media. One single strain deleted in AN8383 (*ausA*) failed to produce austinol and dehydroaustinol [11]. This discovery was supported by the introduction of a point mutation at the phosphopantetheine attachment site, thus abolishing activation of the enzyme by the PPTase to ensure the loss of austinols was not an indirect effect e.g., at chromatin level. The *ausA*Δ

strain was complemented by re-introducing the *ausA* gene into the deletion strain. Introducing the gene under control of the inducible *alcA* promoter revealed that 3,5-dimethyl orsellinic acid (3,5-MOA) was indeed the precursor for austinol and dehydroaustinol in *A. nidulans*, as shown experimentally via labeling studies by Simpson and co-workers 20 years earlier [11,123,124].

Figure 11. Proposed biosynthesis of orsellinic acid and its derivatives of orsellinic acid. The enzymes that catalyze the individual reactions in the biosynthesis of the metabolites are so far unknown and biosynthesis is proposed based on the observed metabolites.

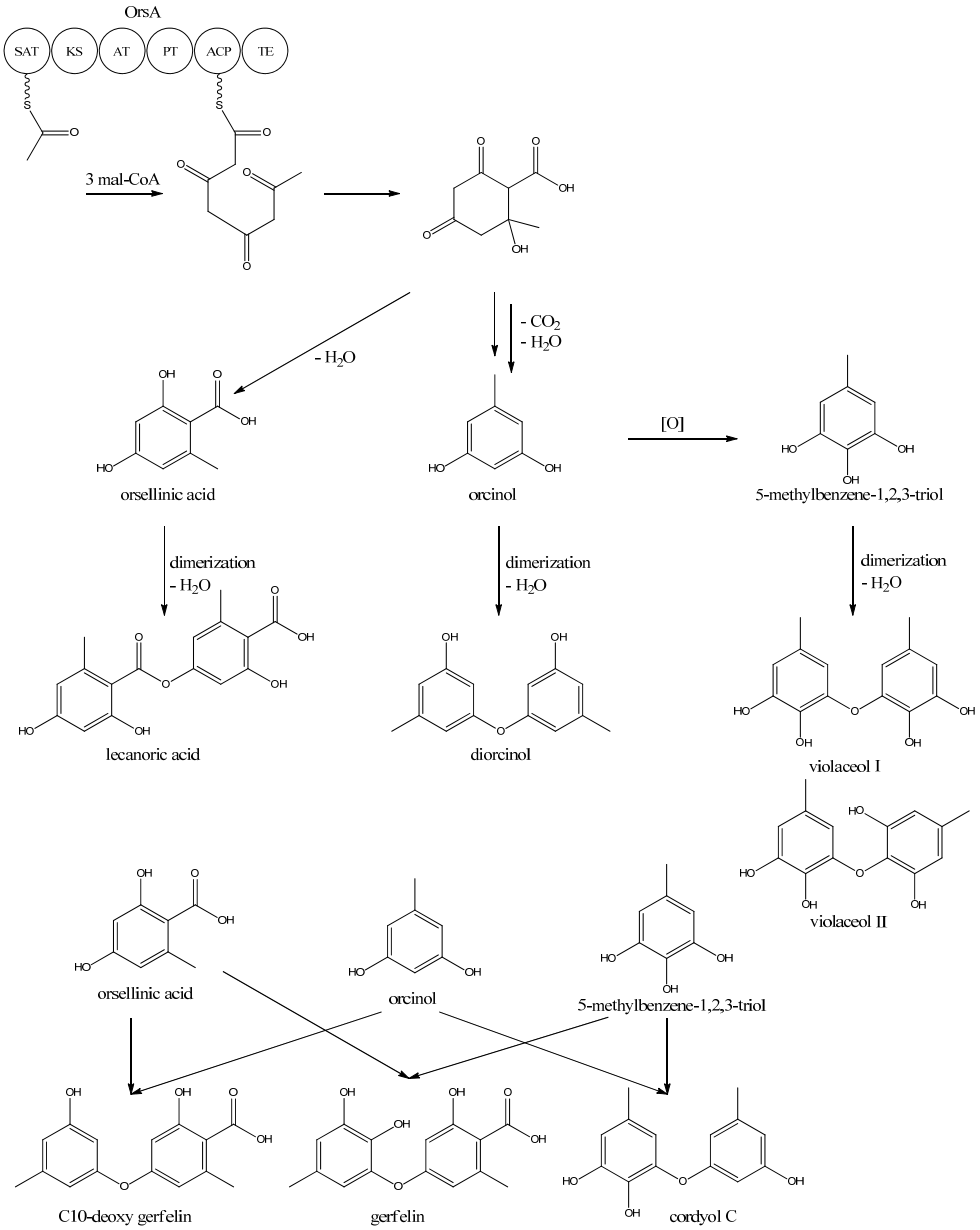

Figure 12. The proposed enzymes involved in the biosynthesis of F-9775A and F-9775B of the figure here.

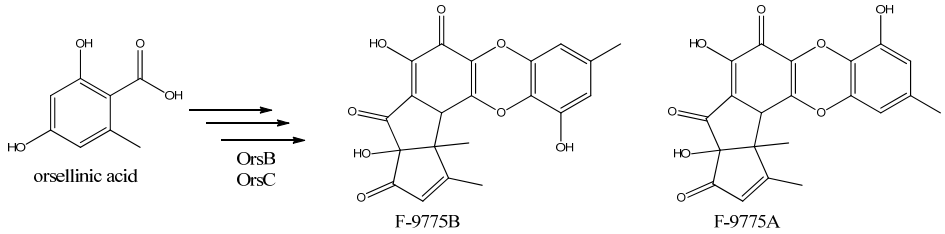

A more detailed understanding of the biosynthesis of the austinols has not been established yet. However, it is well established that 3,5-dimethyl orsellinic acid is synthesized from condensation of an acetyl-CoA unit with 3 malonyl-CoA units to form the PK backbone, which is methylated twice, catalyzed by AusA. The PK part is then alkylated with farnesyl pyrophosphate to form a transient intermediate (Figure 13), which can then act as a precursor for several similar meroterpenoids, such as andibenins, austin, berkeleyones and andrastins [120]. Recently we tentatively identified neoaustin and austinolide in *A. nidulans* extracts by LC-MS analysis (unpublished data), which makes us hypothesize that the biosynthesis towards the austinols involves (i) oxidation and acyl shift in the D ring (ii) lactonization from the substituent groups of the D ring, a Baeyer-Villiger type oxidation and 1,2 alkyl shift in the A ring to give neoaustin. Neoaustin is subsequently oxidized in the D ring by another Baeyer-Villiger type oxidation to give austinolide that upon further oxidation and ring condensation leads to austinol and dehydroaustinol, Figure 13.

11. Concluding Remarks

Secondary metabolism represents chemical diversity and span in biological functionality to the extreme. As shown above, individual compound classes can even form hybrid molecules to other compound classes. There is a high commercial interest in discovery and utilization of SMs in general as drugs or additives, or to avoid mycotoxins in food and feeds. Mapping PK biosynthesis to genes in *A. nidulans* as presented in this review involves great complexity. One challenge is to find and activate the genes required to produce the compounds. As shown, it takes in-depth understanding of fungal biology, nutrient sensing, chromatin remodeling, as well as analysis on all levels from DNA to metabolites to unveil cryptic gene clusters and their products. Moreover, the majority of the pathways described in this review have been elucidated in a relatively short time span. This has been possible due to bioinformatics. The availability of the genome sequence, as well as resources and tools in, e.g., *Aspergillus* Comparative Database (ACD), *Aspergillus* Genome Database (AspGD), and the Central *Aspergillus* REsource (CADRE) have been key aids to perform the extensive genome mining.

The ability to predict enzymatic function based on gene sequences has proven fruitful in characterization of secondary metabolism, since this has revealed the location of e.g., PKS genes. Additionally, the presence of gene cluster specific TFs was utilized in activation of silent SM clusters both in the case of aspyridones and asperfuranone. The asperfuranone biosynthesis is moreover an example of a previously unknown compound, with a potential to be a novel drug, has been found in a

well-known filamentous fungus. Another case of a metabolite with attractive properties is emodin, which has been known for more than a century, but just recently had the biosynthetic machinery uncovered in *A. nidulans*. Both asperthecin and the emericellamides were firstly discovered and isolated from less well described aspergilli, however, after the compounds were observed in *A. nidulans*, the candidates for responsible genes in biosynthesis were found in a few months. The study of conidial pigment biosynthesis in *A. nidulans* has contributed to our basic understanding of fungal development and PKS organization, and provided researchers with an easy assayable marker system for genetic studies. Interestingly, the structure of the final pigment(s) still remains unknown after more than 70 years of research, underlining the difficulties in elucidating structures of highly polymerized PKs.

Figure 13. Proposed biosynthesis of austinol and dehydroaustinol. All genes in the biosynthesis of austinol and dehydroaustinol, except AusA, are unknown.

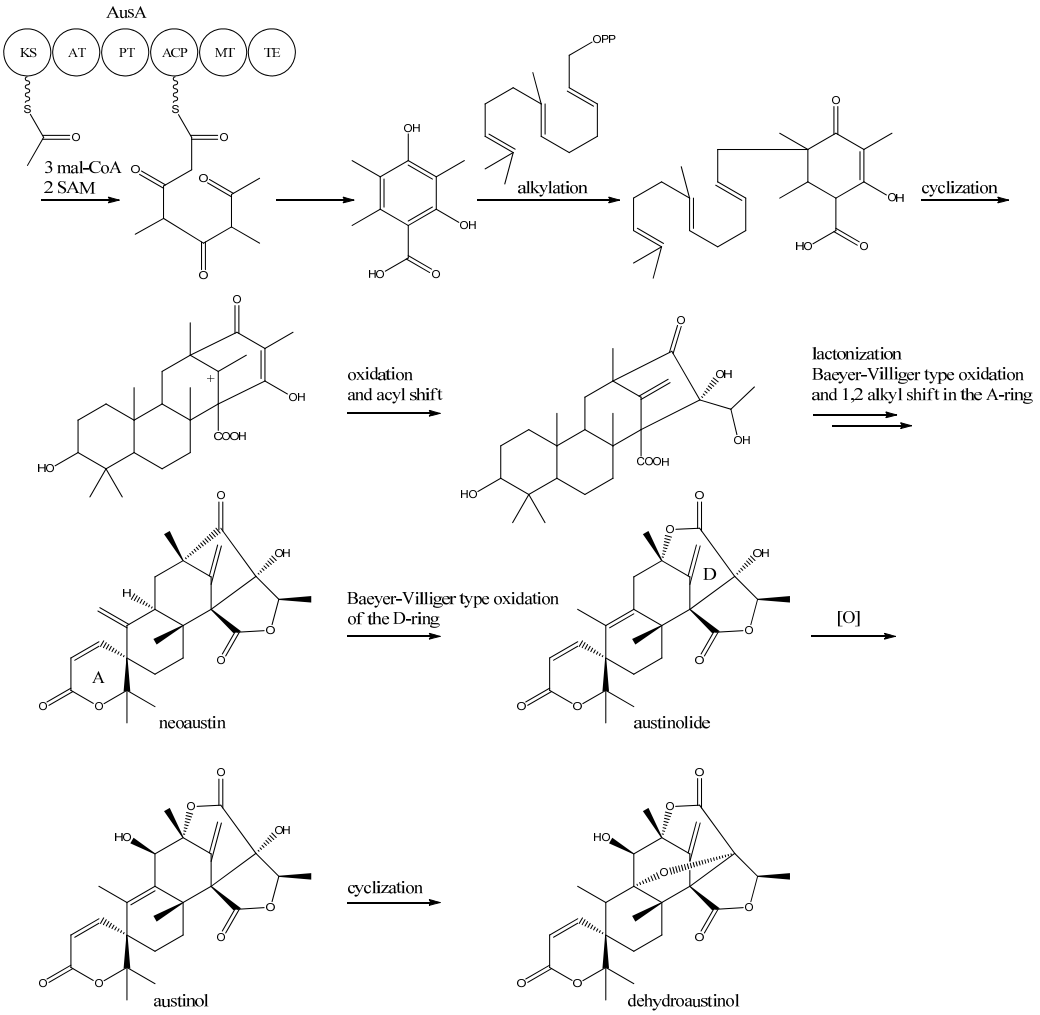

Epigenetic regulation through chromatin remodeling has shown to be involved in activation of several SM gene clusters. Conserved chromatin remodeling factors have influenced both local activation of some SM clusters and more global responses within the genome. Gene clusters producing sterigmatocystin, orsellinic acid, emodins, and austinols have shown to respond to specific factors. The presence of SM producing genes outside gene clusters, e.g., in prenyl-xanthone production, is probably more common than observed so far. Moreover, cross-talk between pathways is frequently observed, as more pathways become known. This can open a discussion whether common pools of intermediates or enzymes can exist. In addition, the compartmentalization of SM production is an area to be explored. Furthermore, controlling compartmentalization of production as well as secretion will influence yields and downstream applications which are important factors for exploiting SM production commercially. Existing compounds can be modified genetically to add/remove chemical groups on existing drugs, mix moieties from different SM classes or species by for example domain swapping, and to considerably increase/abolish a specific production.

Altogether the recent uncovering of secondary metabolism in *A. nidulans* is an illustrative example of strong interdisciplinary efforts requiring strong expertise within chemistry, biology, microbiology, molecular genetics, protein chemistry, computer science, and engineering. Ultimately, the efforts described in this review can form the basis for uncovering of the specific biological roles of the chemical arsenal in the fungus.

Acknowledgments

This work was supported by the Danish Research Agency for Technology and Production grant # 09-064967, FOBI, DTU, and Novozymes. Additionally, we thank Maria Månsson for critical proof reading of the manuscript and for suggestions.

Conflict of Interest

The authors declare no conflict of interest.

References and Notes

1. Pontecorvo, G.; Roper, J.A.; Hemmons, L.M.; MacDonald, K.D.; Bufton, A.W.J. The genetics of *Aspergillus nidulans*. *Adv. Genet. Incorp. Mol. Genet. Med.* **1953**, *5*, 141–238.
2. Newman, D.J.; Cragg, G.M. Natural products as sources of new drugs over the last 25 years. *J. Nat. Prod.* **2007**, *70*, 461–477.
3. Crawford, J.M.; Townsend, C.A. New insights into the formation of fungal aromatic polyketides. *Nat. Rev. Microbiol.* **2010**, *8*, 879–889.
4. Hertweck, C. The biosynthetic logic of polyketide diversity. *Angew. Chem. Int. Ed.* **2009**, *48*, 4688–4716.
5. Cox, R.J. Polyketides, proteins and genes in fungi: Programmed nano-machines begin to reveal their secrets. *Org. Biomol. Chem.* **2007**, *5*, 2010–2026.
6. Bingle, L.E.H.; Simpson, T.J.; Lazarus, C.M. Ketosynthase domain probes identify two subclasses of fungal polyketide synthase genes. *Fun. Gen. Biol.* **1999**, *26*, 209–223.

7. Crawford, J.M.; Vagstad, A.L.; Ehrlich, K.C.; Townsend, C.A. Starter unit specificity directs genome mining of polyketide synthase pathways in fungi. *Bioorg. Chem.* **2008**, *36*, 16–22.
8. Crawford, J.M.; Thomas, P.M.; Scheerer, J.R.; Vagstad, A.L.; Kelleher, N.L.; Townsend, C.A. Deconstruction of iterative multidomain polyketide synthase function. *Science* **2008**, *320*, 243–246.
9. Yadav, G.; Gokhale, R.S.; Mohanty, D. Towards prediction of metabolic products of polyketide synthases: An *in silico* analysis. *PLoS Comp. Biol.* **2009**, *5*, e1000351:1–e1000351:14.
10. Du, L.; Lou, L. PKS and NRPS release mechanisms. *Nat. Prod. Rep.* **2010**, *27*, 255–278.
11. Nielsen, M.L.; Nielsen, J.B.; Rank, C.; Klejnstrup, M.L.; Holm, D.K.; Brogaard, K.H.; Hansen, B.G.; Frisvad, J.C.; Larsen, T.O.; Mortensen, U.H. A genome-wide polyketide synthase deletion library uncovers novel genetic links to polyketides and meroterpenoids in *Aspergillus nidulans*. *FEMS Microbiol. Lett.* **2011**, *321*, 157–166.
12. Chung, Y.S.; Kim, J.M.; Han, D.M.; Chae, K.S.; Jahng, K.Y. Ultrastructure of the cell wall of a null pigmentation mutant, *npgA1*, in *Aspergillus nidulans*. *J. Microbiol.* **2003**, *41*, 224–231.
13. Jahn, B.; Boukhallouk, F.; Lotz, J.; Langfelder, K.; Wanner, G.; Brakhage, A.A. Interaction of human phagocytes with pigmentless *Aspergillus* conidia. *Infect. Immun.* **2000**, *68*, 3736–3739.
14. Wright, P.J.; Pateman, J.A. Ultraviolet-light sensitive mutants of *Aspergillus nidulans*. *Mutation Res.* **1970**, *9*, 579–587.
15. Yuill, E. Two new Aspergillus mutants. *J. Bot.* **1939**, *77*, 174–175.
16. Clutterbuck. A.J. Absence of laccase from yellow-spored mutants of *Aspergillus nidulans*. *J. Gen. Microbial.* **1972**, *70*, 423–435.
17. Agnihotri, V.P. Role of trace elements in the growth and morphology of five ascosporic *Aspergillus* species. *Can. J. Bot.* **1967**, *45*, 73–79.
18. O'Hara, E.B.; Timberlake, W.E. Molecular characterization of the *Aspergillus nidulans yA* locus. *Genetics* **1989**, *121*, 249–254.
19. Mayorga, M.E.; Timberlake, W.E. Isolation and molecular characterization of the *Aspergillus nidulans w*A gene. *Genetics* **1990**, *126*, 73–79.
20. Marshall, M.A.; Timberlake, W.E. *Aspergillus nidulans wetA* activates spore-specific gene expression. *Mol. Cell. Biol.* **1991**, *11*, 55–62.
21. Adams, T.H.; Wieser, J.K.; Yu, J.H. Asexual sporulation in *Aspergillus nidulans*. *Microbiol. Mol. Biol. Rev.* **1998**, *62*, 35–54.
22. Mayorga, M.E.; Timberlake, W.E. The developmentally regulated *Aspergillus nidulans w*A gene encodes a polypeptide homologous to polyketide and fatty acid synthases. *Mol. Gen. Genet.* **1992**, *235*, 205–212.
23. Watanabe, A.; Ono, Y.; Fujii, I.; Sankawa, U.; Mayorga, M.E.; Timberlake, W.E.; Ebizuka, Y. Product identification of polyketide synthase coded by *Aspergillus nidulans w*A gene. *Tetrahedron Lett.* **1998**, *39*, 7733–7736.
24. Fujii, I.; Watanabe, A.; Sankawa, U.; Ebizuka, Y. Identification of Claisen cyclase domain in fungal polyketide synthase WA, a naphthopyrone synthase of *Aspergillus nidulans*. *Chem. Biol.* **2001**, *8*, 189–197.
25. Watanabe, A.; Fujii, I.; Sankawa, U.; Mayorga, M.E.; Timberlake, W.E.; Ebizuka, Y. Re-identification of *Aspergillus nidulans w*A gene to code for a polyketide synthase of naphthopyrone. *Tetrahedron Lett.* **1999**, *40*, 91–94.

26. Watanabe, A.; Ebizuka, Y. A novel hexaketide naphthalene synthesized by a chimeric polyketide synthase composed of fungal pentaketide and heptaketide synthase. *Tetrahedron Lett.* **2002**, *43*, 843–846.
27. Nekam, L.; Polgar, P. The inhibitory effect of a mold upon *Staphylococcus*. *Urol. Cutan. Rev.* **1948**, *52*, 372–373.
28. Hatsuda, Y.; Kuyama, S. Studies on the metabolic products of *Aspergillus versicolor*. Part 1. Cultivation of *Aspergillus versicolor*, isolation and purification of metabolic products. *J. Agric. Chem. Soc. Jpn*. **1954**, *28*, 989–991.
29. Hatsuda, Y.; Kuyama, S.; Terashima, N. Studies on the metabolic products of *Aspergillus versicolor*. Part 2. Physical and chemical properties and the chemical structure of sterigmatocystin. *J. Agric. Chem. Soc. Jpn*. **1954**, *28*, 992–998.
30. Bullock, E.; Underwood, J.G.V.; Roberts, J.C. Studies in mycological chemistry. 11. Structure of isosterigmatocystin and an amended structure for sterigmatocystin. *J. Chem. Soc.* **1962**, *10*, 4179–4183.
31. Holker, J.S.E.; Mulheirn, L.J. Biosynthesis of sterigmatocystin. *Chem. Comm.* **1968**, *24*, 1574–1579.
32. Brechbühler, S.; Buchi, G.; Milne, G. Absolute configuration of aflatoxins. *J. Org. Chem.* **1967**, 2641–2642.
33. Fukuyama, K.; Hamada, K.; Tsukihara, T.; Katsube, Y.; Hamasaki, T.; Hatsuda, Y. Crystalstructures of sterigmatocystin and *O*-methylsterigmatocystin, metabolites of genus *Aspergillus*. *Bull. Chem. Soc. Jpn.* **1976**, *49I*, 1153–1154.
34. Fukuyama, K.; Tsukihara, T.; Katsube, Y.; Tanaka, N.; Hamasaki, T.; Hatsuda, Y. Crystal and molecular structure of *p*-bromobenzoate of sterigmatocystin. *Bull. Chem. Soc. Jpn.* **1975**, *48*, 1980–1983.
35. Blount, W.P. Turkey "X" disease. *Turkey* **1961**, *61*, 55–58.
36. Terao, K. Sterigmatocystin—A masked potent carcinogenic mycotoxin. *J. Toxicol. Toxin Rev.* **1983**, *2*, 77–110.
37. Bennett, J.W.; Klinch, M. Mycotoxins. *Clin. Microbiol. Rev.* **2003**, *16*, 497–516.
38. Bhatnager, D.; Yu, J.; Ehrlich, K.C. Toxins of filamentous fungi. *Chem. Immunol*. **2002**, *81*, 167–206.
39. Yu, J.; Chang, P.K.; Ehrlich, K.C.; Cary, J.W.; Bhatnagar, D.; Cleveland, T.E.; Payne, G.A.; Linz, J.E.; Woloshuk, C.P.; Bennett, J.W. Clustered pathway genes in aflatoxin biosynthesis. *Appl. Environ. Microbiol.* **2004**, *70*, 1253–1262.
40. Yabe, K.; Nakajima, H. Enzyme reactions and genes in aflatoxin biosynthesis. *Appl. Microbiol. Biotechnol.* **2004**, *64*, 745–755.
41. Brown, D.W.; Yu, J.H.; Kelkar, H.S.; Fernandes, M.; Nesbitt, T.C.; Keller, N.P.; Adams, T.H.; Leonard, T.J. Twenty-five coregulated transcripts define a sterigmatocystin gene cluster in *Aspergillus nidulans*. *Proc. Natl. Acad. Sci. USA* **1996**, *93*, 1418–1422.
42. Yu, J.H.; Leonard, T.J. Sterigmatocystin biosynthesis in *Aspergillus nidulans* requires a novel type I polyketide synthase. *J. Bacteriol.* **1995**, *177*, 4792–4800.
43. McDonald, T.; Hammond, T.; Noordermeer, D.; Zhang, Y.Q.; Keller, N. The sterigmatocystin cluster revisited: lessons from a genetic model. In *Food Science and Technology/Aflatoxin and Food Safety*; Abbas, H.K., Ed.; CRC Press: Boca Raton, FL, USA, 2005; pp. 117–136.

44. Ehrlich, K.C.; Li, P.; Scharfenstein, L.; Chang, P.K. HypC, the anthrone oxidase involved in aflatoxin biosynthesis. *Appl. Environ. Microbiol.* **2010**, *76*, 3374–3377.
45. Henry, K.M.; Townsend, C.A. Ordering the reductive and cytochrome P450 oxidative steps in demethylsterigmatocystin formation yields general insights into the biosynthesis of aflatoxin and related fungal metabolites. *J. Am. Chem. Soc.* **2005**, *127*, 3724–3733.
46. Ehrlich, K.C.; Montalbano, B.; Boué, S.M.; Bhatnagar, D. An aflatoxin biosynthesis cluster gene encodes a novel oxidase required for conversion of versicolorin A to sterigmatocystin. *Appl. Environ. Microbiol.* **2005**, *71*, 8963–8965.
47. Cary, J.W.; Ehrlich, K.C.; Bland, J.M.; Montalbano, B.G. The aflatoxin biosynthesis cluster gene, *aflX*, encodes an oxidoreductase involved in conversion of versicolorin A to demethylsterigmatocystin. *Appl. Environ. Microbiol.* **2006**, *72*, 1096–1101.
48. Yu, J.H.; Butchko, R.A.E.; Fernandes, M.; Keller, N.P.; Leonard, T.J.; Adams, T.H. Conservation of structure and function of the aflatoxin regulatory gene *aflR* from *Aspergillus nidulans* and *A. flavus*. *Curr. Genet.* **1996**, *29*, 549–555.
49. Meyers, D.M.; Obrian, G.; Du, W.L.; Bhatnagar, D.; Payne, G.A. Characterization of *aflJ*, a gene required for conversion of pathway intermediates to aflatoxin. *Appl. Environ. Microbiol.* **1998**, *64*, 3713–3717.
50. Bok, J.W.; Keller, N.P. LeaA, a regulator of secondary metabolism in *Aspergillus* spp. *Eukaryot. Cell* **2004**, *3*, 527–535.
51. Bayram, Ö.; Krappmann, S.; Ni, M.; Bok, J.W.; Helmstaedt, K.; Valerius, O.; Braus-Stromeyer, S.; Kwon, N.J.; Keller, N.P. VelB/VeA/LaeA complex coordinates light sighal with fungal development and secondart metabolism. *Science* **2008**, *320*, 1504–1506.
52. Shwab, E.K; Bok, J.W.; Tribus, M.; Galehr, J.; Graessle, S.; Keller, N.P. Histone deacetylase activity regulates chemical diversity in *Aspergillus*. *Eukaryot. Cell* **2007**, *6*, 1656–1664.
53. Fisch, K.M.; Gillaspy, A.F.; Gipson, M.; Henrikson, J.C.; Hoover, A.R.; Jackson, L.; Najar, F.Z.; Wägele, H.; Cichewicz, R.H. Chemical induction of silent biosynthetic pathway transcription in *Aspergillus niger*. *J. Ind. Microbiol. Biotechnol*. **2009**, *36*, 1199–1213.
54. Watanabe, C.M.H.; Townsend, C.A. Initial characterization of a type I fatty acid synthase and polyketide synthase multienzyme complex NorS in the biosynthesis of aflatoxin B_1. *Chem. Biol.* **2002**, *9*, 981–988.
55. Yabe, K.; Nakamura, Y.; Nakajima, H.; Ando, Y.; Hamasaki, T. Enzymatic conversion of norsolorinic acid to averufin in aflatoxin biosynthesis. *Appl. Environ. Microbiol*. **1991**, *57*, 1340–1345.
56. Trail, F.; Chang, P.K.; Cary, J.; Linz, J.E. Structural and functional analysis of the *nor-1* gene involved in the biosynthesis of aflatoxins by *Aspergillus parasiticus*. *Appl. Environ. Microbiol.* **1994**, *60*, 4078–4085.
57. Keller, N.P.; Watanabe, C.M.H.; Kelkar, H.S.; Adams, T.H.; Townsend, C.A. Requirement of monooxygenase-mediated steps for sterigmatocystin biosynthesis by *Aspergillus nidulans*. *Appl. Environ. Microbiol.* **2000**, *66*, 359–362.
58. Yabe, L.; Matsuyama, Y.; Ando, Y.; Nakajima, H.; Hamasaki, T. Stereochemistry during aflatoxin biosynthesis: Conversion of norsolorinic acid to averufin. *Appl. Environ. Microbiol.* **1993**, *59*, 2486–2492.

59. Chang, P.K.; Yu, J.; Ehrlich, K.C.; Boue, S.M.; Montalbano, B.G.; Bhatnagar, D.; Cleveland, T.E. *adhA* in *Aspergillus parasiticus* is involved in conversion of 5′-hydroxyaverantin to averufin. *Appl. Environ. Microbiol.* **2000**, *66*, 4715–4719.
60. Sakuno, E.; Yabe, K.; Nakajima, H. Involvement of two cytosolic enzymes and a novel intermediate 5'-oxoaverantin in the pathway from 5′-hydroxyaverantin to averufin in aflatoxin biosynthesis. *Appl. Environ. Microbiol.* **2003**, *69*, 6418–6426.
61. Chang, P.K.; Yabe, K.; Yu, J. The *Aspergillus parasiticus estA*-encoded esterase converts versiconal hemiacetal acetate to versiconal and versiconol acetate to versiconol in aflatoxin biosynthesis. *Appl. Environ. Microbiol.* **2004**, *70*, 3593–3599.
62. Silva, J.C.; Minto, R.E.; Barry, C.E., III; Holland, K.A.; Townsend, C.A. Isolation and characterization of the versicolorin B synthase gene from *Aspergillus parasiticus*. *J. Biol. Chem.* **1996**, *271*, 13600–13608.
63. Kelkar, H.S.; Skloss, T.W.; Haw, J.F.; Keller, N.P.; Adams, T.H. *Aspergillus nidulans stcL* encodes a putative cytochrome P-450 monooxygenase required for bisfuran desaturation during aflatoxin/sterigmatocystin biosynthesis. *J. Biol. Chem.* **1997**, *272*, 1589–1594.
64. Keller, N.P.; Kantz, N.J.; Adams, T.H. *Aspergillus nidulans verA* is required for production of the mycotoxin sterigmatocystin. *Appl. Environ Microbiol*. **1994**, *60*, 1444–1450.
65. Keller, N.P.; Segner, S.; Bhatnagar, D.; Adams, T.H. *stcS*, a putative P-450 monooxygenase, is required for the conversion of versicolorin A to sterigmatocystin in *Aspergillus nidulans*. *Appl. Environ. Microbiol.* **1995**, *61*, 3628–3632.
66. Kelkar, H.S.; Keller, N.P.; Adams, T.H. *Aspergillus nidulans stcP* encodes an *O*-methyltransferase that is required for sterigmatocystin biosynthesis. *Appl. Environ. Microbiol.* **1996**, *62*, 4296–4298.
67. Slot, J.C.; Rokas, A. Horizontal transfer of a large and highly toxic secondary metabolic gene cluster between fungi. *Curr. Biol.* **2011**, *21*, 134–139.
68. Bergmann, S.; Schümann, J.; Scherlach, K.; Lange, C.; Brakhage, A.A.; Hertweck, C. Genomics-driven discovery of PKS-NRPS hybrid metabolites from *Aspergillus nidulans*. *Nat. Chem. Biol.* **2007**, *3*, 213–217.
69. Chiang, Y.M.; Szewczyk, E.; Nayak, T.; Davidson, A.D.; Sanchez, J.F; Lo, H.C.; Ho, W.Y.; Simityan, H.; Kuo, E.; Praseuth, A.; *et al.* Molecular genetic mining of the *Aspergillus* secondary metabolome: Discovery of the emericellamide biosynthetic pathway. *Chem. Biol.* **2008**, *15*, 527–532.
70. Sims, J.W.; Fillmore, J.P.; Warner, D.D.; Schmidt, E.W. Equisetin biosynthesis in *Fusarium heterosporum*. *Chem. Commun.* **2005**, 186–188.
71. Song, Z.; Cox, R.J.; Lazarus, C.M.; Simpson, T.J. Fusarin C biosynthesis in *Fusarium moniliforme* and *Fusarium venenatum*. *ChemBioChem* **2004**, *5*, 1196–1203.
72. Liu, X.; Walsh, C.T. Cyclopiazonic acid biosynthesis in *Aspergillus* sp.: Characterization of a reductase-like R* domain in cyclopiazonate synthetase that forms and releases *cyclo*-acetoacetyl-L-tryptophan. *Biochemistry* **2009**, *48*, 8746–8757.
73. Xu, W.; Cai, X.; Jung, M.E.; Tang, Y. Analysis of intact and dissected fungal polyketide synthase-nonribosomal peptide synthetase *in vitro* and in *Saccharomyces cerevisiae*. *J. Am. Chem. Soc.* **2010**, *132*, 13604–13607.

74. Halo, L.M.; Marshall, J.W.; Yakasai, A.A., Song, Z.; Butts, C.P.; Crump, M.P.; Heneghan, M.; Bailey, A.M.; Simpson, T.J.; Lazarus, C.M.; Cox, R.J. Authentic heterologous expression of the tenellin iterative polyketide synthase nonribosomal peptide synthetase requires coexpression with an enoyl reductase. *ChemBioChem* **2008**, *9*, 585–594.
75. Eley, K.L.; Halo, L.M.; Song, Z.; Powles, H.; Cox, R.J.; Bailey, A.M.; Lazarus, C.M.; Simpson, T.J. Biosynthesis of the 2-pyridone tenellin in the insect pathogenic fungus *Beauveria bassiana*. *ChemBioChem* **2007**, *8*, 289–297.
76. Fujita, Y.; Oguri, H.; Oikawa, H. Biosynthetic studies on the antibiotics PF1140: a novel pathway for a 2-pyridone framework. *Tetrahedron Lett.* **2005**, *46*, 5885–5888.
77. McInnes, A.G.; Smith, D.G.; Wat, C.K. Tenellin and Bassianin, Metabolites of *Beauveria* Species. Structure elucidation with ^{15}N- and doubly ^{13}C-enriched compounds using ^{13}C nuclear magnetic resonance spectroscopy. *J. Chem. Soc. Chem. Commun.* **1974**, *8*, 281–282.
78. Halo, L.M.; Heneghan, M.N.; Yakasai, A.A.; Song, Z.; Williams, K.; Bailey, A.M.; Cox, R.J.; Lazarus, C.M.; Simpson, T.J. Late stage oxidations during the biosynthesis of the 2-pyridone tenellin in the entomopathogenic fungus *Beauveria bassiana*. *J. Am. Chem. Soc.* **2008**, *130*, 17988–17996.
79. Oh, D.C.; Kauffman, C.A; Jensen, P.R.; Fenical, W. Induced production of emericellamides A and B from the marine-derived fungus *Emericella* sp. in competing co-culture. *J. Nat. Prod.* **2007**, *70*, 515–520.
80. Howard, B.H.; Raistrick, H. Studies in the biochemistry of micro-organism. 94. The colouring matters of species in the *Aspergillus nidulans* group. Part I. Asperthecin, a crystailline colouring matter of *Aspergillus quadrilineatus* Thom & Raper. *Biochem. J.* **1955**, *59*, 475–484.
81. Birkinshaw, J.H.; Gourlay, R. Studies in the biochemistry of micro-organisms. 109. The structure of asperthecin. *Biochem. J.* **1961**, *81*, 618–622.
82. Neelakantan, S.; Pocker, A.; Raistrick, H. Studies in the biochemistry of micro-organisms. 101. The colouring matters of species in the *Aspergillus nidulans* group. Part 2. Further observations on the structure of asperthecin. *Biochem. J.* **1957**, *66*, 234–237.
83. Szewczyk, E.; Chiang, Y.M.; Oakley, C.E.; Davidson, A.D.; Wang, C.C.C; Oakley, B.R. Identification and characterization of the asperthecin gene cluster of *Aspergillus nidulans*. *Appl. Environ. Microbiol.* **2008**, *74*, 7607–7612.
84. Wong, K.H.; Todd, R.B.; Oakley, B.R.; Oakley, C.E.; Hynes, M.J.; Davis, M.A. Sumoylation in *Aspergillus nidulans*: *sumO* inactivation, overexpression and live-cell imaging. *Fungal Genet. Biol.* **2008**, *45*, 728–737.
85. Awakawa, T.; Yokota, K.; Funa, N.; Doi, F.; Mori, N.; Watanabe, H.; Horinouchi, S. Physically discrete β-lactamase-type thioesterase catalyzes product release in atrochrysone synthesis by iterative type I polyketide synthase. *Chem. Biol.* **2009**, *16*, 613–623.
86. Chiang, Y.M.; Oakley, B.R.; Keller, N.P.; Wang, C.C.C. Unraveling polyketide synthesis in members of the genus *Aspergillus*. *Appl. Microbiol. Biotechnol.* **2010**, *86*, 1719–1736.
87. Li, Y.; Chooi, Y.H.; Sheng, Y.; Valentine, J.S.; Tang, Y. Comparative characterization of fungal anthracenone and naphthacenedione biosynthetic pathways reveals an α-hydroxylation-dependent claisen-like cyclization catalyzed by a dimanganese thioesterase. *J. Am. Chem. Soc.* **2011**, *133*, 15773–15785.

88. Li, Y.; Xu, W.; Tang, Y. Classification, prediction, and verification of the regioselectivity of fungal polyketide synthase product template domains. *J. Biol. Chem.* **2010**, *285*, 22764–22773.
89. Chiang, Y.M.; Szewczyk, E.; Davidson, A.D.; Keller, N.; Oakley, B.R.; Wang, C.C.C. A gene cluster containing two fungal polyketide synthases encodes the biosynthetic pathway for a polyketide, asperfuranone, in *Aspergillus nidulans*. *J. Am. Chem. Soc.* **2009**, *131*, 2965–2970.
90. Wang, C.C.C; Chiang, Y.M.; Praseuth, M.B.; Kuo, P.L.; Liang, H.L.; Hsu, Y.L. Asperfuranone from *Aspergillus nidulans* inhibits proliferation of human non-small cell lung cancer A549 cells via blocking cell cycle progression and inducing apoptosis. *Basic Clin. Pharmacol. Toxicol.* **2010**, *107*, 583–589.
91. Matsuzaki, K.; Tahara, H.; Inokoshi, J.; Tanaka, H.; Masuma, R.; Omura, S. New brominated and halogen-less derivatives and structure-activity relationship of azaphilones inhibiting gp120-CD4 binding. *J. Antibiot.* **1998**, *51*, 1004–1011.
92. Bailey, A.M.; Cox, R.J.; Harley, K.; Lazarus, C.M.; Simpson, T.J.; Skellam, E. Characterisation of 3-methylorcinaldehyde synthase (MOS) in *Acremonium strictum*: First observation of a reductive release mechanism during polyketide biosynthesis. *Chem. Commun.* **2007**, *39*, 4053–4055.
93. Bergmann, S.; Funk, A.N.; Scherlach, K.; Schroeckh, V.; Shelest, E.; Horn, U.; Hertweck, C.; Brakhage, A.A. Activation of a silent fungal polyketide biosynthesis pathway through regulatory cross talk with a cryptic nonribosomal peptide synthetase gene cluster. *Appl. Environ. Microbiol.* **2010**, *76*, 8143–8149.
94. Liu, T.; Chiang, Y.M.; Somoza, A.D.; Oakley, B.R.; Wang, C.C.C. Engineering of an "unnatural" natural product by swapping polyketide synthase domains in *Aspergillus nidulans*. *J. Am. Chem. Soc.* **2011**, *133*, 13314–13316.
95. Lu, P.; Zhang, A.; Dennis, L.M.; Dhal-Roshak, A.M.; Xia, Y.Q.; Arison, B.; An, Z.; Tkacz, J.S. A gene (*pks2*) encoding a putative 6-methylsalicylic acid synthase from *Glarea lozoyensis*. *Mol. Gen. Genomics* **2005**, *273*, 207–216.
96. Bok, J.W.; Chiang, Y.M.; Szewczyk, E.; Reyes-Dominguez, Y.; Davidson, A.D.; Sanchez, J.F.; Lo, H.C.; Watanabe, K.; Strauss, J.; Oakley, B.R.; *et al.* Chromatin-level regulation of biosynthetic gene clusters. *Nat. Chem. Biol.* **2009**, *5*, 462–464.
97. Chiang, Y.M.; Szewczyk, E.; Davidson, A.D.; Entwistle, R.; Keller, N.P.; Wang, C.C.C.; Oakley, B.R. Characterization of the *Aspergillus nidulans* monodictyphenone gene cluster. *Appl. Environ. Microbiol.* **2010**, *76*, 2067–2074.
98. Sanchez, J.F.; Entwistle, R.; Hung, J.H.; Yaegashi, J.; Jain, S.; Chiang, Y.M.; Wang, C.C.C.; Oakley, B.R. Genome-based deletion analysis reveals the prenyl xanthone biosynthesis pathway in *Aspergillus nidulans*. *J. Am. Chem. Soc.* **2011**, *133*, 4010–4017.
99. Jowett, H.A.D.; Potter, C.E. CXXVII—The constitution of chrysophante acid and of emodin. *J. Chem. Soc. Trans.* **1903**, *83*, 1327–1334.
100. Beal, G.D.; Okey, R. The qualitative identification of the drugs containing emodin. *J. Am. Chem. Soc.* **1917**, *39*, 716–725.
101. Gatenbeck, S. Incorporation of labelled acetate in emodin in *Penicillum islandicum*. *Acta Chem. Scand.* **1958**, *12*, 1211–1214.

102. Basu, S.; Ghosh, A.; Hazra, B. Evaluation of the antibacterial activity of *Ventilago madraspatana* Gaertn., *Rubia cordifolia* Linn. and *Lantana camara* Linn.: Isolation of emodin and physcion as active antibacterial agents. *Phytother. Res.* **2005**, *19*, 888–894.
103. Chen, J.; Zhang, L.; Zhang, Y.; Zhang, H.; Du, J.; Ding; J.; Guo, Y.; Jiang, H.; Shen, X. Emodin targets the β-hydroxyacyl carrier protein dehydratase from *Helicobactor pylori*: Enzymatic inhibition assay with crystal structural and thermodymamic characterization. *BMC Microbiol.* **2009**, *9*, 91:1–91:12.
104. Huang, Q.; Lu, G.; Shen, H.M.; Chung, M.C.M.; Ong, C.N. Anti-cancer properties of anthraquinones from rhubarb. *Med. Res. Rev.* **2007**, *27*, 609–630.
105. Srinivas, G.; Babykutty, S.; Sathiadevan, P.P.; Srinivas, P. Molecular mechanism of emodin action: Transition from laxative ingredient to an antitumor agent. *Med. Res. Rev.* **2007**, *27*, 591–608.
106. Zargar, B.A.; Masoodi, M.H.; Ahmed, B.; Ganie, S.A. Phytoconstituents and therapeutic uses of *Rheum emodi* wall. Ex Meissn. *Food Chem.* **2011**, *128*, 585–589.
107. Chen, Z.G., Fujii, I.; Ebizuka, Y.; Sankawa, U. Purification and characterization of emodinanthrone oxygenase from *Aspergillus terreus*. *Phytochemistry* **1995**, *38*, 299–305.
108. Huang, K.X.; Fujii, I.; Ebizuka, Y.; Gomi, K.; Sankawa, U. Molecular cloning and heterologous expression of the gene encoding dihydroheodin oxidase, a multicopper blue enzyme from *Aspergillus terreus*. *J. Biol. Chem.* **1995**, *270*, 21495–21502.
109. Couch, R.D.; Gaucher, G.M. Rational elimination of *Aspergillus terreus* sulochrin production. *J. Biotech.* **2004**, *108*, 171–178.
110. Henry, K.M.; Townsend, C.A. Synthesis and fate of *o*-carboxybenzophenones in the biosynthesis of aflatoxin. *J. Am. Chem. Soc.* **2005**, *127*, 3300–3309.
111. Sato, S.; Morishita, T.; Hosoya, T.; Ishikawa, Y. Novel pentacyclec compounds, F-9775A and F-9775B, their manufacture with *Paecilomyces carneus*, and their use for treatment of osteoporosis. Japan Pat. JP11001480A 19990106, 1999.
112. Schroeckh, V.; Scherlach, K.; Nützmann, H.W.; Shelest, E.; Schmidt-Heck, W.; Schuemann, J.; Martin, K.; Hertweck, C.; Brakhage, A.A. Intimate bacterial-fungal interaction triggers biosynthesis of archetypal polyketides in *Aspergillus nidulans*. *Proc. Natl. Acad. Soc. USA* **2009**, *106*, 14558–14563.
113. Gaucher, G.M.; Sherpherd, M.G. Isolation of orsellinic acid synthase. *Biochem. Biophys. Res. Commun.* **1968**, *32*, 664–671.
114. Leo, H.; Yamamoto, Y.; Kim, J.A.; Jung, J.S.; Koh, Y.J.; Hur, J.S. Lecanoric acid, a secondary lichen substance with antioxidant properties from *Umbilicaria antarctica* in maritime Antarctica (King George Island). *Polar Biol.* **2009**, *32*, 1033–1040.
115. Sanchez, J.F.; Chiang, Y.M.; Szewczyk, E.; Davidson, A.D.; Ahuja, M.; Oakley, C.E.; Bok, J.W.; Keller, N.P.; Oakley, B.R.; Wang, C.C.C. Molecular genetic analysis of the orsellinic acid/F9775 gene cluster of *Aspergillus nidulans*. *Mol. BioSyst.* **2010**, *6*, 587–593.
116. Nahlik, K.; Dumkow, M.; Bayram, Ö.; Helmstaedt, K.; Busch, S.; Valerius, O.; Gerke, J.; Hoppert, M.; Schwier, E.; Opitz, L.; *et al.* The COP9 signalosome mediates transcriptional and metabolic response to hormones, oxidative stress production and cell wall rearrangement during fungal development. *Mol. Microbiol.* **2010**, *78*, 964–979.

117. Nützmann, H.W.; Reyes-Doninguez, Y.; Scherlach, K.; Schroeckh, V.; Horn, F.; Gacek, A.; Schümann, J.; Hertweck, C.; Strauss, J.; Brakhage, A.A. Bacteria-induced natural product formation in the fungus *Aspergillus nidulans* requires Saga/Ada-mediated histone acetylation. *Proc. Natl. Acad. Soc. USA* **2011**, *108*, 14282–14287.
118. Scherlach, K.; Sarkar, A.; Schroeckh, V.; Dahse, H.M.; Roth, M.; Brakhage, A.A.; Horn, W.; Hertweck, C. Two induced fungal polyketide pathways converge into antoproliferative spiroanthrones. *ChemBioChem* **2011**, *12*, 1836–1839.
119. Simpson, T.J.; Stenzel, D.J.; Bartlett, A.J.; O'Brien, E.; Holker, J.S.E. Studies on fungal metabolites. Part 3. ^{13}C-NMR spectral and structural studies on Austin and new related meroterpenoids from *Aspergillus ustus*, *Aspergillus variecolor*, *Penicillum diversum*. *J. Chem. Soc. Perkin Trans. I* **1982**, *11*, 2687–2692.
120. Geris, R.; Simpson, T.J. Meroterpenoids produced by fungi. *Nat. Prod. Rep.* **2009**, *26*, 1063–1094.
121. Márquez-Fernández, O.; Trigos, Á.; Ramos-Balderas, J.L.; Viniegra-González, G.; Deising, H.B.; Aguirre, J. Phosphopantetheinyl transferase CfwA/NpgA is required for *Aspergillus nidulans* secondary metabolism and asexual development. *Eukaryot. Cell* **2007**, *6*, 710–720.
122. Bode, H.B.; Bethe, B.; Höfs, R.; Zeeck, A. Big effects from small changes: possible ways to explore nature's chemical diversity. *ChemBioChem* **2002**, *3*, 619–627.
123. Simpson, T.J.; Stenzel, D.J. Biosynthesis of austin, a polyketide-terpenoid metabolite of *Aspergillus ustus*. *JCS Chem. Commun.* **1981**, *20*, 1042–1043.
124. Scott, F.E.; Simpson, T.J.; Trimble, L.A.; Vederas, J.C. Biosynthesis of the meroterpenoid austin by *Aspergillus ustus*: Synthesis and incorporation of ^{13}C, ^{18}O-labelled ethyl 3,5-dimethylorsellinate. *J.C.S. Chem. Comm.* **1986**, *3*, 214–215.

© 2012 by the authors; licensee MDPI, Basel, Switzerland. This article is an open access article distributed under the terms and conditions of the Creative Commons Attribution license (http://creativecommons.org/licenses/by/3.0/).

Paper 2

"Comparative chemistry of *Aspergillus oryzae* (RIB40) and *A. flavus* (NRRL 3357)"

C Rank and ML Klejnstrup (joint 1st author), LM Petersen, S Kildgaard, JC Frisvad, CH Gotfredsen, and TO Larsen

Accepted in Metabolites, *2*, 39-56 (2012)

Metabolites **2012**, *2*, 39-56; doi:10.3390/metabo2010039

OPEN ACCESS

metabolites

ISSN 2218-1989

www.mdpi.com/journal/metabolites/

Article

Comparative Chemistry of *Aspergillus oryzae* (RIB40) and *A. flavus* (NRRL 3357)

Christian Rank [1,†], Marie Louise Klejnstrup [1,†], Lene Maj Petersen [1], Sara Kildgaard [1], Jens Christian Frisvad [1], Charlotte Held Gotfredsen [2] and Thomas Ostenfeld Larsen [1,*]

[1] Department of Systems Biology, Center for Microbial Biotechnology, Technical University of Denmark, Søltofts Plads B221, DK-2800 Kgs. Lyngby, Denmark;
E-Mails: christian.rank@gmail.com (C.R.); marlk@bio.dtu.dk (M.L.K.);
lmape@bio.dtu.dk (L.M.P.); sarakildgaard@hotmail.com (S.K.); jcf@bio.dtu.dk (J.C.F.)

[2] Department of Chemistry, Technical University of Denmark, Kemitorvet B201, DK-2800 Kgs. Lyngby, Denmark; E-Mail: chg@kemi.dtu.dk

[†] These authors contributed equally to this work.

[*] Author to whom correspondence should be addressed; E-Mail: tol@bio.dtu.dk;
Tel.: +45-4525-2632; Fax: +45-4588-4148.

Received: 18 November 2011; in revised form: 14 December 2011 / Accepted: 22 December 2011 / Published: 5 January 2012

Abstract: *Aspergillus oryzae* and *A. flavus* are important species in industrial biotechnology and food safety and have been some of the first aspergilli to be fully genome sequenced. Bioinformatic analysis has revealed 99.5% gene homology between the two species pointing towards a large coherence in the secondary metabolite production. In this study we report on the first comparison of secondary metabolite production between the full genome sequenced strains of *A. oryzae* (RIB40) and *A. flavus* (NRRL 3357). Surprisingly, the overall chemical profiles of the two strains were mostly very different across 15 growth conditions. Contrary to previous studies we found the aflatrem precursor 13-desoxypaxilline to be a major metabolite from *A. oryzae* under certain growth conditions. For the first time, we additionally report *A. oryzae* to produce parasiticolide A and two new analogues hereof, along with four new alkaloids related to the *A. flavus* metabolites ditryptophenalines and miyakamides. Generally the secondary metabolite capability of *A. oryzae* presents several novel end products likely to result from the domestication process from *A. flavus*.

Keywords: *Aspergillus oryzae*; (RIB40); *Aspergillus flavus*; (NRRL 3357); parasiticolide; ditryptoleucine; oryzamide

1. Introduction

Aspergillus oryzae is one of industry's most used "workhorses" and has been used for centuries in food fermentation for the production of e.g., sake, soy sauce and other traditional Asian foods [1]. *A. oryzae* is also a widely used organism for production of amylase, lipases and proteases and more recently also for heterologous expression of secondary metabolite genes and non-fungal proteins [2–4]. For many years, *A. oryzae* has been suspected to be a domesticated form of *A. flavus*, a plant and mammalian pathogenic saprophyte, capable of producing some of the most carcinogenic compounds known: the aflatoxins. Genetic work and subsequent genome sequencing of strains of both species have verified the tight link between the species [1,5–8].

The relationship of the two species has resulted in extensive screening of the toxic potential of *A. oryzae*, but no genuine evidence of aflatoxin production in validated *A. oryzae* isolates has ever been shown. Other important toxins, known from *A. flavus*, have on the other hand been shown in *A. oryzae*: 3-Nitropropionic acid [9] and cyclopiazonic acid (CPA) [10] along with kojic acid [11,12] (Figure 1). Additional metabolites previously reported from *A. oryzae* are asperfuran [13], sporogen AO1 [14,15], maltoryzine [16], and aspergillomarasmine A [17,18]. Aspirochlorine has been found in *A. flavus*, *A. oryzae* and *A. tamarii* [19–23] (Figure 1). For reviews on the safety and taxonomy of *A. oryzae*, see [7,24–26].

Figure 1. Known compounds from *Aspergillus flavus* or *A. oryzae.*

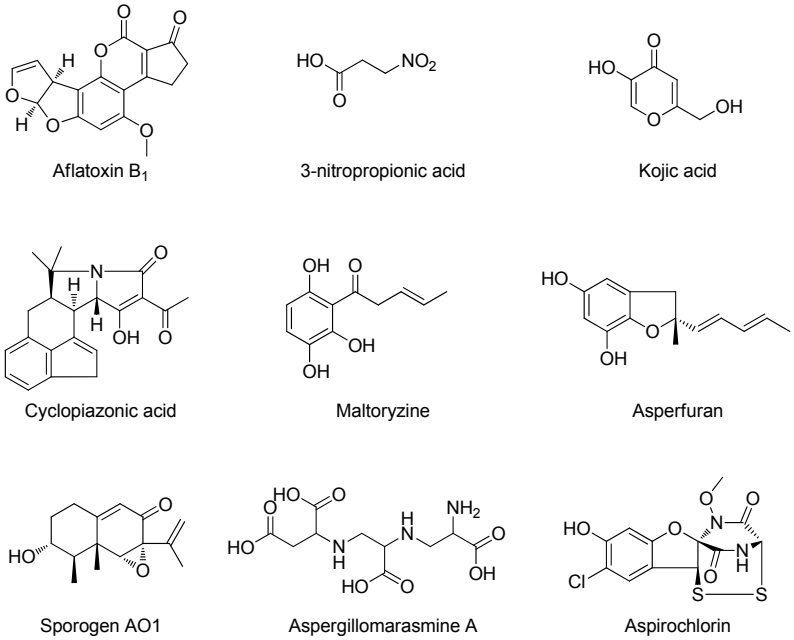

The few predicted differences between the genomes of *A. oryzae* and *A. flavus* (ca. 99.5% genome homology and 98% at the protein level for RIB40/ATCC 42149 and NRRL 3357 [27]), could lead one to expect *A. oryzae* to produce most of the metabolites found in *A. flavus* [1,28–31], but published metabolic data indicates a very low chemical correlation [32]. It is with reference to the established genetic heritage of *A. oryzae* from *A. flavus* remarkable that maltoryzine, sporogen AO1, asperfuran and aspergillomarasmine A have never been unambigously identified in *A. flavus*. Though research on *A. flavus* chemistry has focused primarily on toxic compounds, one would expect that these metabolites should be part of its chemical potential as they are for the domesticated *A. oryzae*. The preliminary bioinformatic studies in conjunction with the genome sequencing shows roughly the same number of predicted genes: 32 Polyketide synthases (PKSs) and 28 non-ribosomal synthases (NRPSs) for *A. flavus* and 32 PKSs and 27 NRPSs for *A. oryzae* with 2 NRPSs apparently unique for each strain [33]. The exclusiveness of these genes in terms of end product has yet to be verified chemically.

Most of the predicted genes for secondary metabolites of *A. oryzae* (or *A. flavus*) have not been mapped to specific metabolic products, despite the genome sequencing of RIB40 in 2005 [27]. Only genes of the most important toxins: Aflatoxin [31,34,35], CPA [36,37] and aflatrem [38] have been fully annotated in both species, which leaves much to be explored. The full chemical potential of either species is unknown and epigenetic modifiers [39–43] may be necessary, alongside with the use of different growth conditions to aid triggering the full potential of secondary metabolite expression in these two closely related species.

The aim of the current work has been to perform an initial comparative investigation of the chemistry from the two genome sequenced strains of *A. oryzae* (RIB40) and *A. flavus* (NRRL 3357), in order to get further insights into possible homologies and differences in secondary metabolite production for these two important species.

2. Results and Discussion

2.1. De-Replication of A. oryzae RIB40

For the analysis of *A. oryzae* RIB40 chemistry, we investigated a series of solid media (YES, YESBEE, DRYES, CYA, CYAS, CY20, CY40, DUL, GAK, GMMS, MEA, OAT, PDA, TGY, WATM (see Methods and Materials for explanation) cultivations with micro-scale extractions [44,45] and subsequently analyzed with HPLC-DAD-MS for selection of optimal conditions. The different media were tested on a collection of *A. oryzae* (RIB40, IBT 28103) and *A. flavus* (NRRL 3357, IBT 23106, IBT 3642) and these strains were cultivated at 25 °C in the dark for 7 and 14 days. The media screening for *A. oryzae* and *A. flavus* indicated the greatest chemodiversity and metabolite production from CYA, YES and WATM agar for our purpose.

The comparison of the secondary metabolite profiles of the two strains, NRRL 3357 and RIB40, exposed a surprisingly high degree of chemical difference on all media as illustrated in Figure 2 and Table 1 for the WATM medium. The major metabolite repetitions between the two genome sequenced strains were merely kojic acid and ergosterol, like a number of minor metabolites (not analyzed here) seemed to be shared between the two strains. Altogether, this is in sharp contrast to the high gene homology, particularly for the secondary metabolite genes.

Figure 2. ESI+ BPC chromatogram of 7 day micro scale extract from WATM, bottom: *A. oryzae* RIB40, top: *A. flavus* NRRL 3357. Besides kojic acid (shown in box) and analogues in the beginning of chromatogram and ergosterol in the end (not shown), there are very few identical compounds between the genetically almost identical strains. Note that aspirochlorine is only detectable in negative ionization, and therefore not visible in this chromatogram.

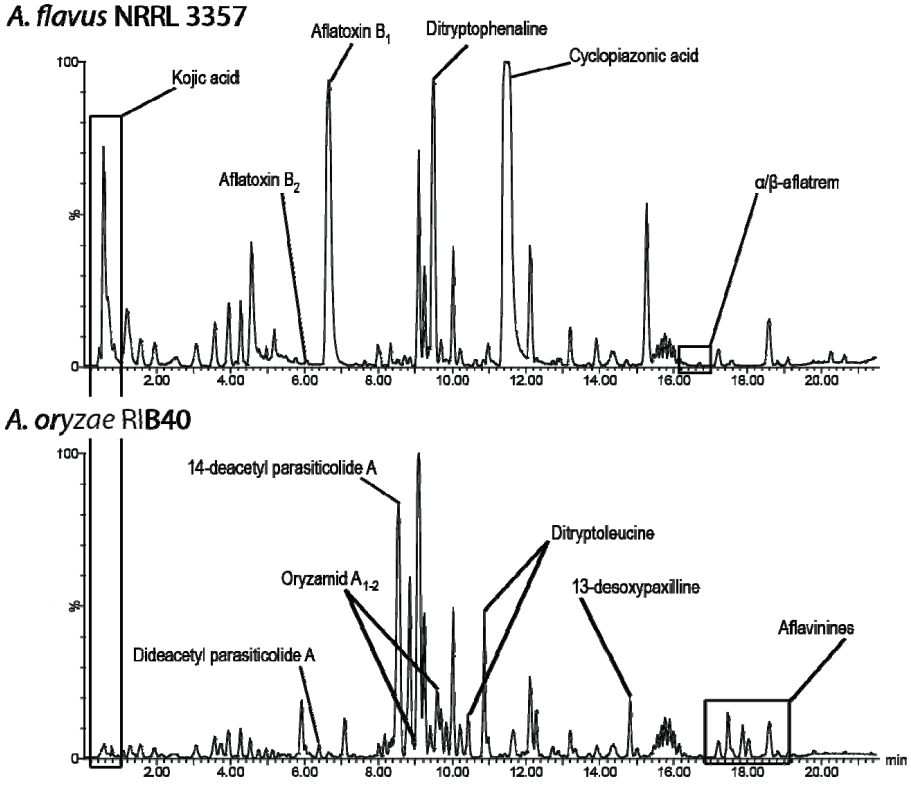

Table 1. LC-MS de-replication of some of the important secondary metabolite pathways from the two full genome sequenced siblings, *A. flavus* (NRRL 3357) and *A. oryzae* (RIB40). Based on 7 day fermentation on solid WATM agar in the dark. (+) indicates the presence of these types of compounds in *A. flavus* based on UV spectroscopic analysis. * New compounds reported here for the first time.

Metabolite	***A. flavus* NRRL 3357**	***A. oryzae* RIB40**
Kojic acid	+	+
Aflatoxin	+	-
Aflavinines	(+)	+
Aflatrem	+	13-desoxypaxilline
Miyakamides	(+)	Oryzamides *
Aspirochlorine	-	+
Cyclopiazonic acid	+	-
Ditryptophenaline	+	Ditryptoleucine *
Parasiticolide A	-	14-deacetyl parasiticolide A *

Known metabolites to *A. oryzae* were de-replicated and we found that the RIB40 strain did not produce detectable levels (LC-MS) of CPA (as also noted by Tokuoka *et al.* [36]), asperfuran, sporogen AO1, maltoryzine or aspergillomarasmine under these growth conditions. It did, however, produce kojic acid and aspirochlorine and a series of potentially new metabolites of which some were isolated, structurally characterized and reported here.

2.2. New Metabolites to A. oryzae RIB40

During fermentation of the chemically potent RIB40 strain, we have been interested in the tremorgenic compounds, allegedly coupled to fungal sclerotia [46–54] and whether these could be found in *A. oryzae* as they have been in *A. flavus*. The RIB40 strain produces large and abundant sclerotia, especially on WATM agar, a fact not widely announced in literature although sclerotia have been observed in *A. oryzae* sporadically [55–57]. No sclerotia were observable after 14 days on YES agar, but although these metabolites are often characterized as sclerotial metabolites, there is not a strict correlation between the biosynthesis of these metabolites and the formation of sclerotia, as also noted by Wilson [58], and this extract was used for the described isolations.

Here, we report the discovery of the aflatrem precursor 13-desoxypaxilline (13-dehydroxypaxilline) in *A. oryzae* RIB40, originally isolated from *Penicillium paxilli* [59–63]. Aflatrem is known from *A. flavus* and was discovered by Wilson and Wilson in 1964 [64] and structure elucidated by Gallagher *et al.* in 1978 and 1980 [65,66]. 13-desoxypaxilline was present in YES, CYA, OAT and WATM agar 7 day old micro-scale extracts. From the 14 days old YES 200 plate extract used for isolation, 13-desoxypaxilline was recovered as an intermediate metabolite. LC-MS, LC-MS/MS and NMR data analysis (Supplementary Material) confirmed the structure. Naturally the prospect of finding aflatrem itself was investigated, though no apparent peak was visible in HPLC-DAD data files. The use of a LC-MS/MS method further confirmed 13-desoxypaxilline as an end-product of *A. oryzae* RIB40 for the above cultivation conditions, since none of the proposed intermediate steps towards aflatrem could be detected (LC-MS/MS) and only one sample (WATM, 7d) showed traces of paspaline, a precursor for 13-desoxypaxilline (Figure 3).

Figure 3. The final steps in the proposed biosynthesis of aflatrem (in *A. flavus*). *A. oryzae* RIB40 biosynthesis stops at 13-desoxypaxilline [38].

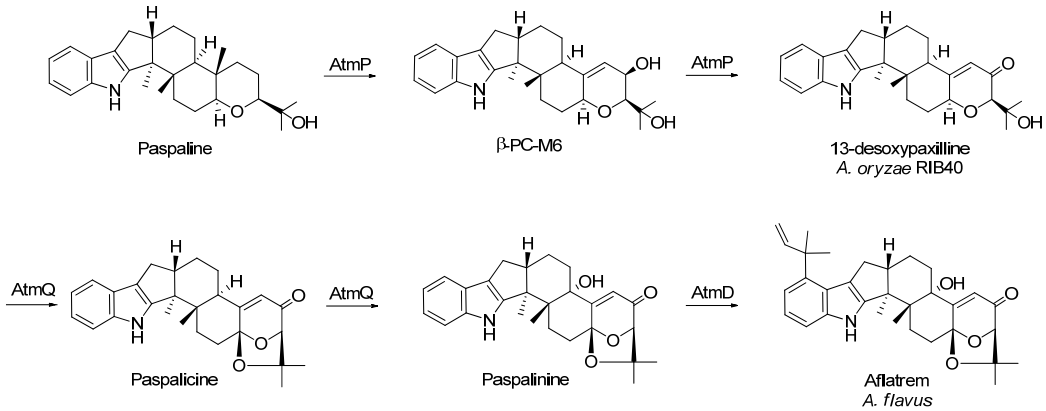

A second extract was made from 100 plates of a 14-day old *A. oryzae* RIB40 culture grown on WATM agar with abundant sclerotia formation to validate the findings from the YES extract. The analysis of the WATM extract showed 13-desoxypaxilline as a major metabolite alongside other sclerotium-related metabolites, such as aflavinines (based on UV-data not shown). The discovery of 13-desoxypaxilline as the apparent end-product of *A. oryzae* RIB40 is in agreement with the analysis of Nicholson *et al.* [38], who showed that a frameshift mutation in the *atmQ* gene presumably accounts for 13-desoxypaxilline not being converted into paspalicine and paspalinine. This mutation is therefore likely responsible for terminating the aflatrem biosynthesis in RIB40 prematurely, short of the acetal ring closure, C-13 hydroxylation and isoprene attachment. Nicholson *et al.* [38] demonstrated that AtmQ is a multifunctional cytochrome P450 monooxygenase likely to catalyze the several oxidative steps needed for biosynthesis of the acetal ring present in the structures of paspalicine, paspalinine and aflatrem, altogether pointing towards a more complex biosynthesis than shown here. Contrary to our discovery, Nicholson *et al.* did not find the aflatrem gene cluster of RIB40 to be transcribed during their fermentations [38].

The isolated 13-desoxypaxilline is a member of the paspalitrem tremorgens, a widely distributed group of metabolites that have been isolated from several genera: *Penicillium*, *Eupenicillium*, *Claviceps*, *Emericella*, *Aspergillus* and *Phomopsis* [67–69]. Besides the tremorgenic activity in animals, these metabolites have been shown to be insecticides [68], which is believed to be their ecological function together with aflatoxin and CPA for protection of the sclerotia against fungivorous insects [46,47].

In addition to 13-desoxypaxilline, two new analogues of parasiticolide A were also isolated and are here reported for the first time. The metabolites showed to be dide- and 14-deacetoxy analogues, and are most likely precursors to the sesquiterpene parasiticolide A (= astellolide A) (see Figure 4). The metabolites were present in CYA, YES and WATM extracts and isolated from the same 14 day old YES extract as 13-desoxypaxilline, and the dide- and 14-deacetyl analogues were also found in the sclerotia enriched WATM extract. Again the metabolites were analyzed using LC-MS and NMR. Several different extraction procedures were tested to verify the correctness of the compounds as genuine metabolites and not as *in vitro* degraded parasiticolide A products, but all samples showed only dide- and 14-deacetyl parasiticolide A and no traceable (LC-MS) levels of parasiticolide A itself, even with different non-acidic extractions. Parasiticolide A have been isolated from *A. flavus* var. *columnaris* (FKI-0739) once [71] and was originally isolated and characterized from *A. parasiticus* (IFO 4082) [72,73] and later also from a mutant of *Emericella variecolor* (= *A. stellatus* Curzi) [74]. Recently parasiticolides have been detected in the newly described species *A. arachidicola* (CBS 117610) and *A. minisclerotigenes* (CBS 117635) [75]. There have to our knowledge not been published any toxic studies on the parasiticolides, but the related peniopholides from the fungus *Peniophora polygonia* have been reported to have antifungal properties [76].

Figure 4. Structures of dide- and 14-deacetyl parasiticolide A and parasiticolide A.

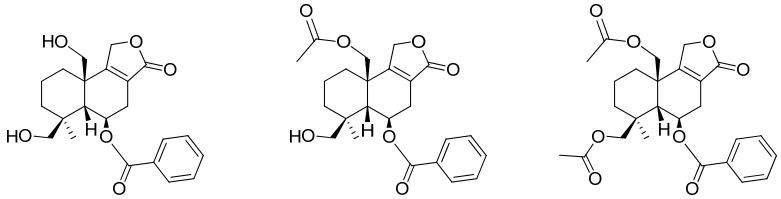

In our observations parasiticolides are more often detectable metabolites of *A. oryzae* than of *A. flavus* under the same fermentation conditions, suggesting that the pathway is partly silenced for *A. flavus* and may need epigenetic modification to be expressed under otherwise normal growth conditions. It is interesting that parasiticolide A is scarcely observed in *A. flavus*, when it is an important product of *A. oryzae* and also of *A. parasiticus*. As for 13-desoxypaxilline, dide- and 14-deacetyl parasiticolide A are almost certainly products of a prematurely ended biosynthesis, here parasiticolide A. We also isolated and elucidated a third parasiticolide A analogue; a formyl variant of parasiticolide A, but it was not possible to exclude the possibility of in vitro chemistry due to the formic acid added during the ethyl acetate extraction, so the correctness of this metabolite remains tentative. (Hamasaki *et al.* used benzene to extract parasiticolide A [77]). All paraciticolide analogues were structure elucidated by NMR and shift values correlated with the published data for parasiticolide A, except for the missing signals of the acetate units and their minor influence on the chemical shifts values of adjacent protons and carbons (See Supplementary Material for NMR data).

To further verify these observations, a MS/MS method was used to analyze several different microscale extracts of RIB40 for parasiticolide A itself. Trace amounts of parasiticolide A was found under these conditions and compared to an isolate of *A. parasiticus* (IBT 4387) capable of producing parasiticolide A. In the *A. parasiticus* isolate no dide- or 14-deacetyl parasiticolide A could be measured, indicating a complete transformation into the end-product (Figure 4). The small amount of parasiticolide A in RIB40 (roughly 1:1.000 ratio compared to 14-acetyl parasiticolide A, presuming the same response factor) might be the result of spontaneous acetylation involving the first acetylating enzyme. When the gene cluster of this metabolite is mapped, it is likely that the gene responsible for the last (specific) acetylation will be found to be mutated. Except for the section *Nidulantes* member *Emericella variecolor*, all other producers of these metabolites have been members of section *Flavi*. No indication points to these metabolites being part of the previously mentioned sclerotium metabolites since they are not found in selective sclerotium extracts, but are found for example in *A. arachidicola*, which is not known to produce sclerotia.

Four new *A. flavus* related NRPS compounds were also isolated from *A. oryzae* RIB40 and characterized based on standard interpretation of ^{1}H, COSY, HMQC and HMBC NMR data (see Supplementary Material). The compounds showed to be two isomeric metabolites named ditryptoleucine related to the ditryptophenalines [78–81] and the two indole-enamides named oryzamides $A_{1\text{-}2}$ (*cis*- and *trans*-forms) structurally similar to the antibiotic miyakamide $B_{1\text{-}2}$ [71] (Figure 5).

Figure 5. Structure of the new *A. oryzae* metabolites: Ditryptoleucine and oryzamide A_{1-2}.

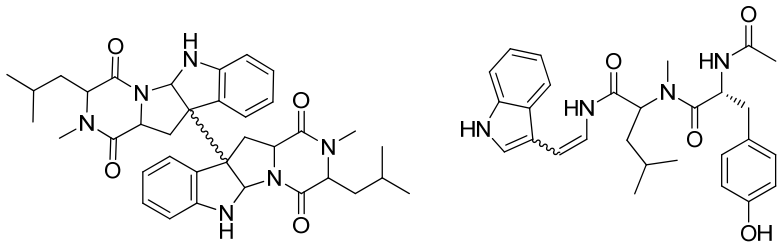

It proved difficult to unambiguously isolate the *cis*- and *trans*-isomer of oryzamide A in a pure form due to isomerization around the double bond. Due to this the structure elucidation has been performed on mixtures of compounds. It is evident from the structure elucidation that oryzamides A_{1-2} only differ in the configuration around the double bond of the enamine as evident from the size of the coupling constant. Marfey analysis of the amino acid derived compounds only established the presence of L-tyrosine in the oryzamides. NMR structural data on the trans isomer (A_1) is present in the supporting material.

Intriguingly, these *A. oryzae* metabolites have apparently exchanged phenylalanine with leucine compared to the similar *A. flavus* metabolites, indicating either a common trait in the domestication process or a coupling between the two pathways. The diketopiperazine ditryptoleucine was isolated in two variants with ^{1}H-NMR shifts varying around the C-C dimeric bond, but with the same base structure. This unspecific dimerization is in line with previously isolated compounds. A hybrid between the ditryptophenaline and ditryptoleucine was isolated from an *Aspergillus* sp. as WIN 64745, with both a phenylalanine and leucine moiety, but with no *N*-methylation [79]. These compounds were tested and proved antagonistic against substance P at the NK1 receptor [82]. The oryzamides A_{1-2} are variants of the miyakamides B_{1-2} [71]. The exchanged phenylalanine has been substituted with leucine between a tryptophan and a tyrosine in the oryzamides. However this exchange of phenylalanine and leucine has often been found for compounds produced within the same species. *Penicillium polonicum* (= *P. fructigenum*) [83-85] produces both fructigenine A = puberuline = rugulosuvine A, containing phenylalanine and fructigenine B = verrucofortine, containing leucine. We could also detect two slightly later eluting compounds in the *A. oryzae* RIB40 extracts likely to be two further indole-enamides having phenylalanine incorporated instead of tyrosine as evident from LC-DAD-MS analysis (data not shown) as also seen for the miyakamides [71].

3. Experimental

General procedures and methods for analysis are described in [43,44,86].

Mass spectrometric analysis was performed using a Agilent HP 1100 liquid chromatograph with a DAD system (Waldbronn, Germany) on a LCT oaTOF mass spectrometer (Micromass, Manchester, UK) with a Z-spray ESI source and a LockSpray probe. For general procedures see [87]; method 1 for

LC-DAD-TOF was used in this study. All solvents used were HPLC grade from Sigma-Aldrich (St. Louis, MO, USA).

3.1. Fungal Material and Fermentation

A. oryzae RIB40 (IBT28103); *A. flavus* NRRL3357 (IBT3696), (IBT15934), NRRL 13462; *A. parvisclerotigenus* IBT16807 and *A. minisclerotigenes* IBT13353 were obtained from the IBT Culture Collection at DTU Systems Biology, Technical University of Denmark. The RIB40 isolate used for isolation of 13-dehydroxypaxilline was cultured for 14 days at 25 °C in the dark on 200 Petri dishes with Yeast Extract Sucrose agar (YES). All strains were grown for 1 week at 25 °C on YES, Czapek Yeast Autolysate (CYA), Wickerhams Antibiotic Test Medium (WATM) agar [88], YESBEE [89] (YES+50 g Bee pollen Type III, granulate, Sigma, P-8753, pr. 1 L medium), DRYES (Dichloran rose Bengal chloramphenicol agar), AFPA (*Aspergillus flavus*, *A. parasiticus* agar), CYAS (CYA + 50 g NaCl pr. 1 L medium), CY20 (CYA + 170 g sucrose pr. 1 L), CY40 (CYA with added 370 g sucrose pr. 1 L medium), DUL (Dulaney's medium for Penicillin), GAK (Potato-carrot agar), GMMS (Glucose minimal media (GMM) + 2% sorbitol), MEA (Malt extract agar), OAT (Oat meal agar), PDA (Potato-dextrose agar). For medium formulations see Samson *et al.* [90].

3.2. Extraction and Isolation of Pure Compounds

13-Desoxypaxilline. The plates were homogenized using a Stomacher and 100 mL EtOAc with 1% HCO_2H pr. 10 plates. The extract was filtered and dried down on a freeze drier. The crude extract was separated on a KP-C18-HS 60 g SNAP column using a Biotage Isolera One (Biotage, Uppsala, Sweden), resulting in a 22 mg fraction. The fraction was segmented with a 10 g ISOL Diol column, using 12 steps of stepwise Heptane-dichloromethane-EtOAc-MeOH. 13-desoxypaxilline was predominant in a 100% EtOAc fraction (6 mg), and purified on a Waters HPLC W600/996PDA (Milford, MA, USA) and a RP column (Phenomenex Luna C18(2), 250 × 10 mm, 5 µm, Torrance, CA, USA) using a gradient of 80% MeCN (H_2O–Milli-Q (Millipore, MA, USA)) to 90% over 10 min. with 50 ppm TFA added to the solvents. The collection was concentrated on a rotary evaporator (Büchi V-855/R-215, Flawil, Switzerland) and dried under N_2 to yield 0.5 mg of white, amorphous 13-desoxypaxilline.

Dideacetyl-, 14-deacetyl-, and 18-formyl parasiticolide A. From the same fermentation described for 13-desoxypaxilline a more polar, 90 mg fraction was fractionated with a 10 g ISOL Diol column, using 12 steps of stepwise Heptane-dichloromethane-EtOAc-MeOH. The parasiticolide A-analogues were predominant in a 100% EtOAc fraction (10 mg), and purified on a Waters HPLC W600/996PDA (Milford, MA, USA) and a RP column (Phenomenex Luna C18(2), 250 × 10 mm, 5 µm, Torrance, CA, USA) using a gradient of 72% MeCN (H_2O–Milli-Q (Millipore, MA, USA)) to 87% over 15 min. with 50 ppm TFA. The collection was concentrated on a rotary evaporator (Büchi V-855/R-215) and dried under N_2 to yield 0.3, 1.0 and 0.8 mg of white, amorphous di-, 14-deactyl- and 18-formyl parasiticolide A, respectively. See Supplemental Material for NMR data.

Ditryptoleucine. 400 plates of *A. oryzae* RIB40 were cultured on YES medium. The plates were homogenized using a Stomacher and 100 mL EtOAc pr. 10 plates. The extract was filtered and dried

down on a freeze drier. The crude extract were separated into three phases by dissolving it in 9:1 MeOH:H_2O–Milli-Q and extracted into a heptan phase and afterwards a DCM phase. The DCM phase was separated on a KP-C18-HS SNAP column using a Biotage Isolera One (Biotage, Uppsala, Sweden) using a gradient of 10% MeOH (H_2O–Milli-Q (Millipore, MA, USA)) to 100% over 15 CVs (column volumes) resulting in a 402 mg fraction. The fraction was further separated on another KP-C18-HS SNAP column using a Biotage Isolera One (Biotage, Uppsala, Sweden) using a gradient of 10% MeOH (H_2O–Milli-Q (Millipore, Ma, USA)) to 25% over 2 CVs, 25% MeOH to 50% over 8 CVs and 50% to 100% over 4 CVs resulting in a 60.1 mg fraction. The fraction was fractionated on a LH-20 column using 100% MeOH. The ditryptoleucines were present in the earlier fractions and were purified on a Waters HPLC W600/996PDA (Milford, MA, USA) using a RP column (Phenomenex Luna C18(2), 250 × 10 mm, 5 µm, Torrance, CA, USA) using a gradient of 50% MeCN (H_2O–Milli-Q (Millipore, MA, USA)) to 100% over 20 min. with 50 ppm TFA and a flow of 4 mL/min. The collections were concentrated on a rotary evaporator (Büchi V-855/R-215) and dried under N_2 to yield 4.0 mg of the two isomers. See Supplemental Data for NMR data.

Oryzamides $A_{1\text{-}2}$. The remaining broth from the fermentation described for ditryptoleucine was extracted with EtOAc + 1% HCO_2H for 24 h. The extract was filtered and dried down on a freeze drier. The crude extract were separated into three phases by dissolving it in 9:1 MeOH:H_2O–Milli-Q and extracted into a heptan phase and afterwards a DCM phase. The DCM phase was separated on a KP-C18-HS SNAP column using a Biotage Isolera One (Biotage, Uppsala, Sweden) using a gradient of 10% MeOH (H_2O–Milli-Q (Millipore, MA, USA)) to 100% over 15 CVs (column volumes) resulting in a 654 mg fraction. The fraction was fractionated with a 10 g ISOL Diol column, using 13 steps of stepwise Hexane-dichloromethane-EtOAc-MeOH. The miyakamides were predominant in the 40:60 DCM:EtOAc and 20:80 DCM:EtOAc fractions (43.8 mg), and purified on a Waters HPLC W600/996PDA (Milford, MA, USA) and a RP column (Phenomenex Luna C18(2), 250 × 10 mm, 5µm, Torrance, CA, USA) using a gradient of 45% MeCN (H_2O–Milli-Q (Millipore, MA, USA)) to 62% over 15 min. with 50 ppm TFA. The collection was concentrated on a rotarvap (Büchi V-855/R-215) and dried down under N_2 to yield 4.0 and 2.0 mg of oryzamide A_1 and A_2, respectively. See Supplemental Data for NMR data.

3.3. Marfeys Method

100 µg of each peptide was hydrolysed with 200 µL 6 M HCl at 110 °C for 20 h. To the hydrolysis products (or 50 µL (2.5 µmol) solutions of standard D- and L-amino acids) was added 50 µL water, 20 µL 1 M $NaHCO_3$ solution and 100 µL 1% FDAA in acetone, followed by reaction at 40 °C for 1 h. The reaction mixture was removed from the heat, neutralized with 10 µL 2 M HCl and the solution was diluted with 820 µL MeOH to a total volume of 1 mL. The FDAA derivatives were analysed by UHPLC-DAD on a Dionex Ultimate 3000 RS DAD equipped with a Kinetex C18 column (2.6 µm, 150 × 2.10mm, Phenomenex). The analyses were run with a gradient elution of MeCN/H_2O–Mili-Q (Millipore, MA,USA) added 50 ppm TFA from 15 to 100% MeCN over 7 min (60 °C, 0.8 mL/min). The retention times of the FDAA derivatives were compared to retention times of the standard amino acid derivatives.

3.4. Selective Extraction of Sclerotium Metabolites

The selective extraction of sclerotia from IBT 15934, NRRL 13462, IBT 16807 and IBT 13353 was made from harvested sclerotia of a 7 day old cultivation on WATM and CYA agar (25 °C in dark). The sclerotia were washed several times with Milli-Q (Millipore, Millford, USA) 0.22 µm H_2O and dried. The sclerotia were transferred to a 2 mL Eppendorf tube together with three stainless steel balls (2 × 1 mm and 1 × 5 mm) and frozen with liquid N_2 before mechanical crushed. The pulverized sclerotia were suspended in 1mL methanol and transferred to a 2 mL vial with 1 mL of 1:2:3 methanol:dichloromethane:ethylacetate and left for evaporation overnight in a fume hood. The dried extract was resolved in 1 mL methanol in ultrasonicated for 10 min and then filtered with a 0.45 µm PTFE filter to a clean vial for analysis.

3.5. HPLC-DAD-TOF Method

Mass was measured using a Agilent HP 1100 liquid chromatograph with a DAD system (Waldbronn, Germany) on a LCT oaTOF mass spectrometer (Micromass, Manchester, UK) with a Z-spray ESI source and a LockSpray probe. For general procedures see [86], method 1.

3.6. NMR Instrumentation

NMR spectra were recorded on a Varian Unity Inova 500 MHz spectrometer equipped with a 5 mm probe using standard pulse sequences. The signals of the residual solvent protons and solvent carbons were used as internal references (δ_H 2.50 and δ_C 39.5 ppm for DMSO). In cases where higher field was needed the NMR spectra were recorded on a Bruker Avance 800-MHz spectrometer equipped with a 5-mm TCI Cryoprobe at the Danish Instrument Center for NMR Spectroscopy of Biological Macromolecules.

3.7. MS/MS Method Used for Aflatrem and Parasiticolide Screening

Liquid chromatography was performed on an Agilent (Torrence, CA, USA) 1100 HPLC system coupled to a triple-quadropole mass spectrometer (Waters-Micromass, Manchester, UK) with a Z-spray ESI operated in positive mode source using a flow of 700 L/h nitrogen desolvated at 350 °C. The hexapole was held at 50 V. The system was controlled by MassLynx v4.1 (Waters-Micromass). Nitrogen was used as collision gas, and the MS operated in MRM mode (dwell time = 100 ms) with the parameters listed in Table 2. Extracts of 2 µL were injected and separated on a Phenomenex Gemini C_6-phenyl, 3 µm, 2 × 50 mm column with a flow of 0.3 µL/min. Water contained 20 mM ammonium formate. Oven temperature 40 °C. Two different methods were applied to the aflatrem- and parasiticolide screen: Aflatrem inlet method: Linearly gradient from 50 to 100% MeCN over 5 min, increased to 0.5 µL/min over 1.5 min. The column was washed additionally 1.5 min with 100% MeCN at 0.5 µL/min, followed by a return to 50% MeCN over 2.5 min and kept at this level for another 1 min with a linearly decrease in flow to 0.3 µL/min, prior to the next sample. Standards used for analysis of this pathway were from Sigma-Aldrich Aldrich (St. Louis, MO, USA). Parasiticolides: linearly gradient from 20 to 90% MeCN over 15 min, increased to 0.5µL/min from 90 to 100% MeCN in additional 1 min. The column was washed from 2 min with 100% MeCN at 0.5 µL/min, followed by a return to

20% MeCN over 1.5 min and kept at this level for another 3.5 min with a linearly decrease in flow to 0.3 µL/min, before the next sample. Standards were internal standards from other extracts of the known parasiticolide A producer *A. parasiticus*: IBT 4387 (= CBS 260.67) and IBT 11863 (= CBS 115.37).

Table 2. MS/MS method including scan event, retention times, transition ions and the cone and collision energies used.

Compound	Scan event	RT (min)	Ion type	Transition (*m*/*z*) [a]	Cone (V)	Collision energy (eV)
Paxilline	1	4.0	Quantifier	436 → 130	25	30
			Qualifier	436 → 182	25	30
Paspalinine	2	4.3	Quantifier	434 → 130	25	20
			Qualifier	434 → 376	25	20
13-desoxypaxilline	3	4.8	Quantifier	420 → 182	25	30
			Qualifier	420 → 130	25	30
Aflatrem	4	5.2	Quantifier	502 → 198	25	20
			Qualifier	502 → 445	25	20
Paspaline	5	5.5	Quantifier	422 → 130	25	20
			Qualifier	422 → 275	25	20
Dideacetyl-parasiticolide A	1	7.0	Quantifier	387 → 217	30	40
			Qualifier	387 → 189	30	40
14-deacetyl parasiticolide A	2	8.7	Quantifier	429 → 217	30	40
			Qualifier	429 → 189	30	40
Parasiticolide A	3	10.4	Quantifier	488 → 229	30	30
			Qualifier	488 → 247	30	30

[a] All transitions were made from $[M+H]^+$, except for paraciticolide A: $[M+NH_4]^+$.

4. Conclusions

The tremorgenic 13-desoxypaxilline has been isolated from *A. oryzae* RIB40 and verified under several different growth conditions contrary to previous studies. We believe that 13-desoxypaxilline is the end-product of the aflatrem biosynthesis for the RIB40 strain since no aflatrem could be detected in any fermentation using LC-MS/MS as detection.

The new metabolites dide- and 14-deacetyl parasiticolide A were also found as genuine products from the RIB40 strain and the compounds were present in multiple fermentations, however parasiticolide A was only detected in trace amounts using a LC-MS/MS method. This indicates a defective acetylation of the 14-deacetyl parasiticolide A and the small amount of parasiticolide A in RIB40 could be the result of spontaneous acetylation in the cell cytosol. The mono-deacetylated analogue detected in both *A. flavus* and *A. oryzae* had same retention times, suggesting a selective acetylation.

The new NRPS compounds ditryptoleucine and oryzamides $A_{1\text{-}2}$ appear to be natural variants of known *A. flavus* metabolites. They share the exchange of a phenylalanine for a leucine, although they are believed to originate from two unrelated pathways.

Altogether, our findings contribute to understanding why the overall chemical profiles of *A. oryzae* (RIB40) and *A. flavus* (NRRL 3357) appear quite different since some of the end-products usually seen in *A. flavus* are apparently not reached in *A. oryzae*. Whether the different chemical profiles are merely

the result of different regulation that can be overcome by the use of epigenetic modifiers or are a result of genuine mutations remains to be settled. *A. oryzae* RIB40 is clearly a chemically potent strain, and as more of its chemistry is unfolded we believe that most of the biosynthetic pathways of *A. flavus* will be found to be more or less functional. Future research will reveal whether the many different *A. oryzae* strains that are used as industrial workhorses are as chemically potent as the RIB40 strain.

Supplementary Materials

Supplementary materials can be accessed at: http://www.mdpi.com/2218-1989/2/1/39/s1.

Acknowledgments

This work was funded by the Danish Research Agency for Technology and Production (Grant: 09-064967). We thank the Danish Instrument Center for NMR Spectroscopy of Biological Macromolecules at the Carlsberg Laboratory for 800 MHz NMR time.

Conflict of Interest

The authors declare no conflict of interest.

References and Notes

1. Machida, M.; Yamada, O.; Gomi, K. Genomics of *Aspergillus oryzae*: Learning from the history of koji mold and exploration of its future. *DNA Res.* **2008**, *15*, 173–183.
2. Punt, P.J.; Biezen, N.V.; Conesa, A.; Albers, A.; Mangnus, J.; van den Hondel, C. Filamentous fungi as cell factories for heterologous protein production. *Trends Biotechnol.* **2002**, *20*, 200–206.
3. Meyer, V. Genetic engineering of filamentous fungi—Progress, obstacles and future trends. *Biotechnol. Adv.* **2008**, *26*, 177–185.
4. Fisch, K.M.; Bakeer, W.; Yakasai, A.A.; Song, Z.; Pedrick, J.; Wasil, Z.; Bailey, A.M.; Lazarus, C.M.; Simpson, T.J.; Cox, R.J. Rational domain swaps decipher programming in fungal highly reducing polyketide synthases and resurrect an extinct metabolite. *J. Am. Chem. Soc.* **2011**, *133*, 16335–16641.
5. Geiser, D.M.; Pitt, J.I.; Taylor, J.W. Cryptic speciation and recombination in the aflatoxin-producing fungus *Aspergillus flavus*. *Proc. Natl. Acad. Sci. USA* **1998**, *95*, 388–393.
6. Geiser, D.M.; Dorner, J.W.; Horn, B.W.; Taylor, J.W. The phylogenetics of mycotoxin and sclerotium production in *Aspergillus flavus* and *Aspergillus oryzae*. *Fungal Genet. Biol.* **2000**, *31*, 169–179.
7. Abe, K.; Gomi, K.; Hasegawa, F.; Machida, M. Impact of *Aspergillus oryzae* genomics on industrial production of metabolites. *Mycopathologia* **2006**, *162*, 143–153.
8. Kobayashi, T.; Abe, K.; Asai, K.; Gomi, K.; Juvvadi, P.R.; Kato, M.; Kitamoto, K.; Takeuchi, M.; Machida M. Genomics of *Aspergillus oryzae*. *Biosci. Biotechnol. Biochem.* **2007**, *71*, 646–670.
9. Iwasaki, T.; Kosikowski, F.V. Production of beta-nitropropionic acid in foods. *J. Food Sci.* **1973**, *38*, 1162–1165.

10. Orth, R. Mycotoxins of *Aspergillus oryzae* strains for use in food-industry as starters and enzyme producing molds. *Annales de la Nutrition et de l'Alimentation* **1977**, *31*, 617–624.
11. Manabe, M; Tanaka, K.; Goto, T.; Matsuura, S. Production capabilities of kojic acid and aflatixin by koji mold. In *Toxigenic Fungi—Their Toxins and Health Hazards*; Kurata, H., Ueno, Y., Eds.; Elsevier: Amsterdam, The Netherlands, 1984; Volume 7, pp. 4–14.
12. Bentley, R. From miso, sake and shoyu to cosmetics: A century of science for kojic acid. *Nat. Prod. Rep.* **2006**, *23*, 1046–1062.
13. Pfefferle, W.; Anke, H.; Bross, M.; Steffan, B.; Vianden, R.; Steglich, W. Asperfuran, a novel antifungal metabolite from *Aspergillus oryzae*. *J. Antibiot.* **1990**, *43*, 648–654.
14. Tanaka, S.; Wada, K.; Katayama, M.; Marumo, S. Isolation of sporogen AO1, a sporogenic substance, from *Aspergillus oryzae*. *Agric. Biol. Chem.* **1984**, *48*, 3189–3191.
15. Tanaka, S.; Wada, K.; Marumo, S.; Hattori, H. Structure of sporogen AO1, a sporogenic substance of *Aspergillus oryzae*. *Tetrahedron Lett.* **1984**, *25*, 5907–5910.
16. Iizuka, H.; Iida, M. Maltoryzine, a new toxic metabolite produced by a strain of *Aspergillus oryzae* var. *microsporus* isolated from poisonous malt sprout. *Nature* **1962**, *196*, 681–682.
17. Barbier, M.; Vetter, W.; Bogdanov, D.; Lederer, E. Synthese und eigenschafgen eines analogen des lycomarasmins und der aspergillomarasmine. *Annalen der Chemie-Justus Liebig* **1963**, *668*, 132.
18. Robert, M.; Barbier, M.; Lederer, E.; Roux, L.; Bieman, K.; Vetter, W. Two new natural phytotoxins—Aspergillomarasmines A and B and their identity to lycomarasmine and its derivatives. *Bulletin de la Societe Chimique de France* **1962**, 187–188.
19. Monti, F.; Ripamonti, F.; Hawser, S.P.; Islam, K. Aspirochlorine: A highly selective and potent inhibitor of fungal protein synthesis. *J. Antibiot.* **1999**, *52*, 311–318.
20. Sakata, K.; Masago, H.; Sakurai, A.; Takahashi, N. Isolation of aspirochlorine (=antibiotic A30641) posessing a novel dithiodiketopiperazine structure from *Aspergillus flavus*. *Tetrahedron Lett.* **1982**, *23*, 2095–2098.
21. Sakata, K.; Kuwatsuka, T.; Sakurai, A.; Takahashi, N.; Tamura, G. Isolation of aspirochlorine (=antibiotic A30641) as a true anti-microbial constituent of the antibiotic, oryzachlorin, from *Aspergillus oryzae*. *Agric. Biol. Chem.* **1983**, *47*, 2673–2674.
22. Sakata, K.; Maruyama, M.; Uzawa, J.; Sakurai, A.; Lu, H.S.M.; Clardy, J. Structural revision of aspirochlorine (=antibiotic A30641), a novel epidithiopiperazine-2,5-dione produced by *Aspergillus* spp. *Tetrahedron Lett.* **1987**, *28*, 5607–5610.
23. Klausmeyer, P.; McCloud, T.G.; Tucker, K.D.; Cardellina, J.H.; Shoemaker, R.H. Aspirochlorine class compounds from *Aspergillus flavus* inhibit azole-resistant *Candida albicans*. *J. Nat. Prod.* **2005**, *68*, 1300–1302.
24. Barbesgaard, P.; Heldt-Hansen, H.P.; Diderichsen, B. On the safety of *Aspergillus oryzae*: A review. *Appl. Microbiol. Biotechnol.* **1992**, *36*, 569–572.
25. Tanaka, K.; Goto, T.; Manabe, M.; Matsuura, S. Traditional Japanese fermented foods free from mycotoxin contamination. *Jpn. Agric. Res. Quart.* **2002**, *36*, 45–50.
26. Varga, J.; Frisvad, J.C.; Samson, R.A. Two new aflatoxin producing species, and an overview of *Aspergillus* section Flavi. *Stud. Mycol.* **2011**, *69*, 57–80.

27. Rokas, A.; Payne, G.; Fedorova, N.D.; Baker, S.E.; Machida, M.; Yu, J.; Georgianna, D.R.; Dean, R.A.; Bhatnagar, D.; Cleveland, T.E. What can comparative genomics tell us about species concepts in the genus *Aspergillus*? *Stud. Mycol.* **2007**, *59*, 11–17.
28. Machida, M.; Asai, K.; Sano, M.; Tanaka, T.; Kumagai. T.; Terai., G.; Kusumoto, K.-I.; Arima, T.; Akita, O.; Kashiwagi, Y.; *et al.* Genome sequencing and analysis of *Aspergillus oryzae*. *Nature* **2005**, *438*, 1157–1161.
29. Machida, M.; Terabayashi, Y.; Sano, M.; Yamane, N.; Tamano, K.; Payne, G.A.; Yu, J.; Cleveland, T.E.; Nierman, W.C. Genomics of industrial aspergilli and comparison with toxigenic relatives. *Food Addit. Contam. Part A* **2008**, *25*, 1147–1151.
30. Payne, G.A.; Nierman, W.C.; Wortman, J.R.; Pritchard, B.L.; Brown, D.; Dean, R.A.; Bhatnagar, D.; Cleveland, T.E.; Machida, M.; Yu, J. Whole genome comparison of *Aspergillus flavus* and *A. oryzae*. *Med. Mycol.* **2006**, *44*, S9–S11.
31. Yu, J.; Payne, G.A.; Nierman, W.C.; Machida, M.; Bennett, J.W.; Campbell, B.C.; Robens, J.F.; Bhatnagar, D.; Dean, R.A.; Cleveland, T.E. *Aspergillus flavus* genomics as a tool for studying the mechanism of aflatoxin formation. *Food Addit. Contam. Part A* **2008**, *25*, 1152–1157.
32. Laatsch, H. AntiBase 2010. Available online: http://www.wiley-vch.de/stmdata/antibase2010.php (accessed on 27 December 2011).
33. Cleveland, T.E.; Yu, J.; Fedorova, N.; Bhatnagar, D.; Payne, G.A.; Nierman, W.C.; Bennett, J.W. Potential of *Aspergillus flavus* genomics for applications in biotechnology. *Trends Biotechnol.* **2009**, *27*, 151–157.
34. Lee, Y.-H.; Tominaga, M.; Hayashi, R.; Sakamoto, K.; Yamada, O.; Akita, O. *Aspergillus oryzae* strains with a large deletion of the aflatoxin biosynthetic homologous gene cluster differentiated by chromosomal breakage. *Appl. Microbiol. Biotechnol.* **2006**, *72*, 339–345.
35. Tominaga, M.; Lee, Y.H.; Hayashi, R.; Suzuki, Y.; Yamada, O.; Sakamoto, K.; Gotoh, K.; Akita, O. Molecular analysis of an inactive aflatoxin biosynthesis gene cluster in *Aspergillus oryzae* RIB strains. *Appl. Environ. Microbiol.* **2006**, *72*, 484–490.
36. Tokuoka, M.; Seshime, Y.; Fujii, I.; Kitamoto, K.; Takahashi, T.; Koyama, Y. Identification of a novel polyketide synthase-nonribosomal peptide synthetase (PKS-NRPS) gene required for the biosynthesis of cyclopiazonic acid in *Aspergillus oryzae*. *Fungal Genet. Biol.* **2008**, *45*, 1608–1615.
37. Chang, P.-K.; Horn, B.W.; Dorner, J.W. Clustered genes involved in cyclopiazonic acid production are next to the aflatoxin biosynthesis gene cluster in *Aspergillus flavus*. *Fungal Genet. Biol.* **2009**, *46*, 176–182.
38. Nicholson, M.J.; Koulman, A.; Monahan, B.J.; Pritchard, B.L.; Payne, G.A.; Scott, B. Identification of two aflatrem biosynthetic gene loci in *Aspergillus flavus* and metabolic engineering in *Penicillium paxilli* to elucidate gene function. *Appl. Environ. Microbiol.* **2009**, *75*, 7469–7481.
39. Shwab, E.K.; Bok, J.W.; Tribus, M.; Galehr, J.; Graessle, S.; Keller, N.P. Histone deacetylase activity regulates chemical diversity in *Aspergillus*. *Eukaryot. Cell* **2007**, *6*, 1656–1664.
40. Shwab, E.K.; Keller, N.P. Regulation of secondary metabolite production in filamentous ascomycetes. *Mycol. Res.* **2008**, *112*, 225–230.
41. Williams, R.B.; Henrikson, J.C.; Hoover, A.R.; Lee, A.E.; Cichewicz, R.H. Epigenetic remodeling of the fungal secondary metabolome. *Org. Biomol. Chem.* **2008**, *6*, 1895–1897.

42. Henrikson, J.C.; Hoover, A.R.; Joyner, P.M.; Cichewicz, R.H. A chemical epigenetics approach for engineering the in situ biosynthesis of a cryptic natural product from *Aspergillus niger*. *Org. Biomol. Chem.* **2009**, *7*, 435–438.
43. Yakasai, A.A.; Davison, J.; Wasil, Z.; Halo, L.M.; Butts, C.P.; Lazarus, C.M.; Bailey, A.M.; Simpson, T.J.; Cox, R.J. Nongenetic reprogramming of a fungal highly reducing polyketide synthase. *J. Am. Chem. Soc.* **2011**, *133*, 10990–10998.
44. Frisvad, J.C.; Thrane, U. Standardized high-performance liquid-chromatography of 182 mycotoxins and other fungal metabolites based on alkylphenone retention indexes and UV-Vis spectra (Diode-Array Detection). *J. Chromatogr. A* **1987**, *404*, 195–214.
45. Smedsgaard, J. Micro-scale extraction procedure for standardized screening of fungal metabolite production in cultures. *J. Chromatogr. A* **1997**, *760*, 264–270.
46. Wicklow, D.T.; Cole, R.J. Tremorgenic indole metabolites and aflatoxins in sclerotia of *Aspergillus flavus*—An evolutionary perspective. *Can. J. Bot.* **1982**, *60*, 525–528.
47. Gloer, J.B.; Tepaske, M.R.; Sima, J.S.; Wicklow, D.T.; Dowd, P.F. Antiinsectan aflavinine derivatives from the sclerotia of *Aspergillus flavus*. *J. Org. Chem.* **1988**, *53*, 5457–5460.
48. Gloer, J.B.; Rinderknecht, B.L.; Wicklow, D.T.; Dowd, P.F. Nominine—A new insecticidal indole diterpene from the sclerotia of *Aspergillus nomius*. *J. Org. Chem.* **1989**, *54*, 2530–2532.
49. Staub, G.M.; Gloer, J.B.; Wicklow, D.T.; Dowd, P.F. Aspernomine—A cytotoxic antiinsectan metabolite with a novel ring-system from the sclerotia of *Aspergillus nomius*. *J. Am. Chem. Soc.* **1992**, *114*, 1015–1017.
50. Staub, G.M.; Gloer, K.B.; Gloer, J.B.; Wicklow, D.T.; Dowd, P.F. New paspalinine derivatives with antiinsectan activity from the sclerotia of *Aspergillus nomius*. *Tetrahedron Lett.* **1993**, *34*, 2569–2572.
51. Tepaske, M.R.; Gloer, J.B.; Wicklow, D.T.; Dowd, P.F. The structure of tubingensin B—A cytotoxic carbazole alkaloid from the sclerotia of *Aspergillus tubingensis*. *Tetrahedron Lett.* **1989**, *30*, 5965–5968.
52. Tepaske, M.R.; Gloer, J.B.; Wicklow, D.T.; Dowd, P.F. 3 new aflavinines from the sclerotia of *Aspergillus tubingensis*. *Tetrahedron* **1989**, *45*, 4961–4968.
53. Tepaske, M.R.; Gloer, J.B.; Wicklow, D.T.; Dowd, P.F. Aflavazole—A new antiinsectan carbazole metabolite from the sclerotia of *Aspergillus flavus*. *J. Org. Chem.* **1990**, *55*, 5299–5301.
54. Tepaske, M.R.; Gloer, J.B.; Wicklow, D.T.; Dowd, P.F. Aflavarin and beta-aflatrem—New anti-insectan metabolites from the sclerotia of *Aspergillus flavus*. *J. Nat. Prod.* **1992**, *55*, 1080–1086.
55. Raper, K.B.; Fennell, D.I. *The genus Aspergillus*; Williams & Wilkins: Baltimore, MD, USA, 1965.
56. Wicklow, D.T.; Mcalpin, C.E.; Yeoh, Q.L. Diversity of *Aspergillus oryzae* genotypes (RFLP) isolated from traditional soy sauce production within Malaysia and Southeast Asia. *Mycoscience* **2007**, *48*, 373–380.
57. Jin, F.J.; Takahashi, T.; Utsushikawa, M.; Furukido, T.; Nishida, M.; Ogawa, M.; Tokuoka, M.; Koyama Y. A trial of minimization of chromosome 7 in *Aspergillus oryzae* by multiple chromosomal deletions. *Mol. Genet. Genomics* **2010**, *283*, 1–12.
58. Wilson, B.J. Toxins other than aflatoxins produced by *Aspergillus flavus*. *Bacteriol. Rev.* **1966**, *30*, 478–484.

59. Springer, J.P.; Clardy, J.C.; Wells, J.M.; Cole, R.J.; Kirksey, J.W. Structure of paxilline, a tremorgenic metabolite of *Penicillium paxilli* Bainier. *Tetrahedron Lett.* **1975**, 2531–2534.
60. Longland, C.L.; Dyer, J.L.; Michelangeli, F. The mycotoxin paxilline inhibits the cerebellar inositol 1,4, 5-trisphosphate receptor. *Eur. J. Pharmacol.* **2000**, *408*, 219–225.
61. Bilmen, J.G.; Wootton, L.L.; Michelangeli, F. The mechanism of inhibition of the sarco/ endoplasmic reticulum Ca2+ ATPase by paxilline. *Arch. Biochem. Biophys.* **2002**, *406*, 55–64.
62. Sabater-Vilar, M.; Nijmeijer, S.; Fink-Gremmels, J. Genotoxicity assessment of five tremorgenic mycotoxins (fumitremorgen B, paxilline, penitrem A, verruculogen, and verrucosidin) produced by molds isolated from fermented meats. *J. Food Protec.* **2003**, *66*, 2123–2129.
63. Sheehan, J.J.; Benedetti, B.L.; Barth, A.L. Anticonvulsant effects of the BK-channel antagonist paxilline. *Epilepsia* **2009**, *50*, 711–720.
64. Wilson, B.J.; Wilson, C.H. Toxin from *Aspergillus flavus*—Production on food materials of substance causing tremors in mice. *Science* **1964**, *144*, 177–178.
65. Gallagher, R.T.; Wilson, B.J. Aflatrem, the tremorgenic mycotoxin from *Aspergillus flavus*. *Mycopathologia* **1978**, *66*, 183–185.
66. Gallagher, R.T.; Clardy, J.C.; Wilson, B.J. Aflatrem, a tremorgenic toxin from *Aspergillus flavus*. *Tetrahedron Lett.* **1980**, *21*, 239–242.
67. Cole, R.J.; Dorner, J.W.; Springer, J.P.; Cox, R.H. Indole metabolites from a strain of *Aspergillus flavus*. *J. Agric. Food Chem.* **1981**, *29*, 293–295.
68. Steyn, P.S.; Vleggaar, R. Tremorgenic mycotoxins. *Fortschritte der Chemie Organischer Naturstoffe* **1985**, *48*, 1–80.
69. Bills, G.F.; Giacobbe, R.A.; Lee, S.H.; Peláez, F.; Tkacz, J.S. Tremorgenic mycotoxins, paspalitrem A and C, from a tropical *Phomopsis*. *Mycol. Res.* **1992**, *96*, 977–983.
70. Laakso, J.A.; Gloer, J.B.; Wicklow, D.T.; Dowd, P.F. A new penitrem analog with antiinsectan activity from the sclerotia of *Aspergillus sulphureus*. *J. Agric. Food Chem.* **1993**, *41*, 973–975.
71. Shiomi, K.; Hatae, K.; Yamaguchi, Y.; Masuma, R.; Tomoda, H.; Kobayashi, S.; Omura, S. New antibiotics miyakamides produced by a fungus. *J. Antibiot.* **2002**, *55*, 952–961.
72. Fukuyama, K.; Kawai, H.; Tsukihara, T.; Tsukihara, K.; Katsube, Y.; Hamasaki, T.; Hatsuda, Y.; Kuwano, H. Structure-analysis of a bromo derivative of parasiticolide A by X-ray-diffraction method. *Bull. Chem. Soc. Jpn*. **1975**, *48*, 2949–2950.
73. Ishikawa, Y.; Morimoto, K.; Hamasaki, T. Flavoglaucin, a metabolite of *Eurotium chevalieri*, its antioxidation and synergism with tocopherol. *J. Am. Oil Chem. Soc.* **1984**, *61*, 1864–1868.
74. Gould, R.O.; Simpson, T.J.; Walkinshaw, M.D. Isolation and X-ray crystal structures of astellolides A and B, sesquiterpenoid metabolites of *Aspergillus variecolor*. *Tetrahedron Lett.* **1981**, *22*, 1047–1050.
75. Pildain, M.B.; Frisvad, J.C.; Vaamonde, G.; Cabral, D.; Varga, J.; Samson, R.A. Two novel aflatoxin-producing *Aspergillus* species from Argentinean peanuts. *Int. J. Syst. Evol. Microbiol.* **2008**, *58*, 725–735.
76. Ayer, W.A.; Trifonov, L.S. Drimane sesquiterpene lactones from *Peniophora polygonia*. *J. Nat. Prod.* **1992**, *55*, 1454–1461.
77. Hamasaki, T.; Kuwano, H.; Isono, K.; Hatsuda, Y.; Fukuyama, K.; Tsukihara, T.; Katsube, Y. New metabolite, parasiticolide A, from *Aspergillus parasiticus*. *Agric. Biol. Chem.* **1975**, *39*, 749–751.

78. Springer, J.P.; Buchi, G.; Kobbe, B.; Demain, A.L.; Clardy, J.C. The structure of ditryptophenaline—New metabolite of *Aspergillus flavus*. *Tetrahedron Lett.* **1997**, *27*, 2403–2406.
79. Barrow, C.J.; Cai, P.; Snyder, J.K.; Sedlock, D.M.; Sun, H.H.; Cooper, R. WIN 64821, a new competitive antagonist to substance-P, isolated from an *Aspergillus* species—Structure determination and solution conformation. *J. Org. Chem.* **1993**, *58*, 6016–6021.
80. Oleynek, J.J.; Sedlock, D.M.; Barrow, C.J.; Appell, K.C.; Casiano, F.; Haycock, D.; Ward, S.J.; Kaplita, P.; Gillum, A.M. WIN-64821, a novel neurokinin antagonist produced by an *Aspergillus* sp .2. Biological-activity. *J. Antibiot.* **1994**, *47*, 391–398.
81. Barrow, C.J.; Sedlock, D.M. 1′-(2-Phenyl-ethylene)-ditryptophenaline, a new dimeric diketopiperazine from *Aspergillus flavus*. *J. Nat. Prod.* **1994**, *57*, 1239–1244.
82. Movassaghi, M.; Schmidt, M.; Ashenhurst, J. Concise total synthesis of (+)-WIN 64821 and (−)-ditryptophenaline. *Angew. Chem. Int. Ed. Engl.* **2008**, *47*, 1485–1487.
83. Arai, K.; Kimura, K.; Mushiroda, T.; Yamamoto, Y. Structures of fructigenines A and B, new alkaloids isolated from *Penicillium fructigenum* Takeuchi. *Chem. Pharm. Bull.* **1989**, *37*, 2937–2939.
84. Frisvad, J.C.; Samson, R.A. Polyphasic taxonomy of *Penicillium* subgenus *Penicillium*. A guide to identification of the food and air-borne terverticillate Penicillia and their mycotoxins. *Stud. Mycol.* **2004**, *49*, 1–173.
85. Frisvad, J.C.; Smedsgaard, J.; Larsen, T.O.; Samson, R.A. Mycotoxins, drugs and other extrolites produced by species in *Penicillium* subgenus *Penicillium*. *Stud. Mycol.* **2004**, **49**, 201–241.
86. Frisvad, J.C.; Skouboe, P.; Samson, R.A. Taxonomic comparison of three different groups of aflatoxin producers and a new efficient producer of aflatoxin B1, sterigmatocystin and 3-*O*-methylsterigmatocystin, *Aspergillus rambellii* sp nov. *Syst. Appl. Microbiol.* **2005**, *28*, 442–453.
87. Nielsen, K.F.; Mogensen, J.M.; Johansen, M.; Larsen, T.O.; Frisvad, J.C. Review of secondary metabolites and mycotoxins from the *Aspergillus niger* group. *Anal. Bioanal. Chem.* **2009**, *395*, 1225-1242.
88. Raper, K.B.; Thom, C. *Manual of the Penicillia*; Williams and Wilkins: Baltimore, MD, USA, 1949.
89. Medina, A.; Gonzalez, G.; Saez, J.M. Bee pollen, a substrate that stimulates ochratoxin A production by *Aspergillus ochraceus*. *Syst. Appl. Microbiol.* **2004**, *27*, 261–267.
90. Samson, R.A.; Hoekstra, E.S.; Frisvad, J.C. *Introduction to Food- and Airborne Fungi*. **7**; Centraalbureau voor Schimmelcultures: Utrecht, The Netherlands, 2004.

© 2012 by the authors; licensee MDPI, Basel, Switzerland. This article is an open access article distributed under the terms and conditions of the Creative Commons Attribution license (http://creativecommons.org/licenses/by/3.0/).

Supplementary Material

Comparative chemistry of *Aspergillus oryzae* (RIB40) and *A. flavus* (NRRL 3357)

Christian Rank [1,†], Marie Louise Klejnstrup [1,†], Lene Maj Petersen [1], Sara Kildgaard [1], Jens Christian Frisvad [1], Charlotte Held Gotfredsen [2] and Thomas Ostenfeld Larsen [1,*]

13-Desoxypaxilline

HRESIMS: *m/z* = 420.2551 $[M+H]^+$, calculated for $[C_{27}H_{33}NO_3+H]^+$: 420.2533.

NMR spectra were acquired in DMSO-d_6 on a Bruker Avance 800 MHz spectrometer using standard pulse sequences. ^{1}H-NMR (799.30 MHz, DMSO-d_6, 25 °C, 2.50 ppm): 0.88 (3H, s, H-23), 1.00 (3H, s, H-25), 1.16 (3H, s, H-29), 1.20 (3H, s, H-28), 1.52 (1H, ddd, *J* = 25.4, 12.8, 4.4 Hz, H-14a), 1.60 (1H, m, H-14b), 1.65 (1H, m, H-15a), 1.74 (1H, d, *J* = 12.2 Hz, H-15b), 1.81 (1H, ddd, *J* = 17.9, 13.8, 4.2 Hz, H-6a), 1.98 (1H, ddd, *J* = 13.8, 13.6, 4.2 Hz, H-5a), 2.07 (1H, m, H-5b), 2.22 (1H, m, H-6b), 2.32 (1H, dd, *J* = 12.8, 11.0 Hz, H-17a), 2.53 (1H, m, H-13), 2.62 (1H, dd, *J* = 12.8, 6.3 Hz, H-17b), 2.71 (1H, m, H-16), 3.74 (1H, d, *J* = 1.6 Hz, H-9), 4.34 (1H, br. s, 27-OH), 4.41 (1H, m, H-7), 5.73 (1H, s, H-11), 6.91 (1H, dd, *J* = 7.6, 7.6 Hz, H-21), 6.95 (1H, dd, *J* = 7.6, 7.6 Hz, H-22), 7.27 (1H, d, *J* = 7.6 Hz, H-23), 7.28 (1H, d, *J* = 7.6 Hz, H-20), 10.76 (1H, s, N-H).

^{13}C-NMR (201.00, DMSO-d_6, 25 °C, 39.5 ppm): 14.4 (C-25), 15.4 (C-26), 23.5 (C-15), 24.8 (C-14), 25.5 (C-28), 25.7 (C-29), 26.7 (C-17), 29.5 (C-6), 30.7 (C-5), 41.6 (C-13), 48.5 (C-16), 49.2 (C-3), 49.8 (C-4), 70.7 (C-27), 74.0 (C-7), 82.4 (C-9), 111.6 (C-23), 115.8 (C-18), 117.5 (C-20), 118.1 (C-21), 119.2 (C-22), 120.7 (C-11), 124.4 (C-19), 140.2 (C-24), 150.4 (C-2), 168.6 (C-12), 196.1 (C-10).

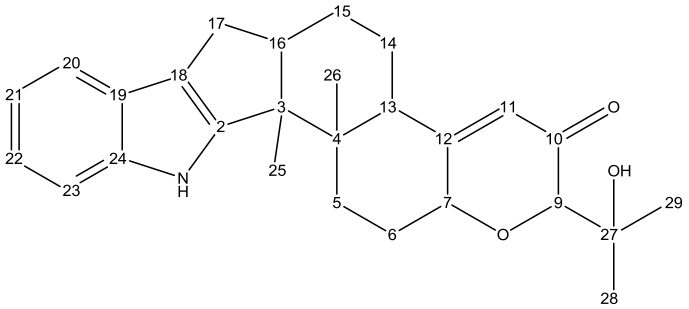

14-Deacetyl parasiticolide A

All NMR spectra of parasiticolide A analogues were acquired in DMSO-d_6 on a Varian Unity Inova 500 MHz spectrometer with 4 mm gHX Nano probe and with a spin rate of 2 kHz for all samples, using standard pulse sequences. The spectra were referenced to this solvent with resonances δ_H = 2.50 and δ_C = 39.5.

HRESIMS: *m/z* = 429.1901 $[M+H]^+$, calculated for $[C_{24}H_{28}O_7+H]^+$: 429.1908.

^{1}H-NMR (499.87 MHz, DMSO-d_6, 25 °C, 2.50 ppm): 0.96 (1H, td, J = 13.6, 3.7 Hz, H-3a), 1.01 (3H, s, H-13), 1.36 (1H, td, J = 13.3, 3.3 Hz, H-1a), 1.45 (1H, m, H-2a), 1.63 (1H, m, H-2b), 1.91 (1H, s, H-5), 1.97 (1H, m, H-3b), 2.08 (3H, s, H-17), 2.11 (1H, d, J = 13.2, H-1b), 2.36 (1H, d, J = 19.0 Hz, H-7a), 2.76 (1H, ddt, J = 19.0, 6.0, 3.1 Hz, H-7b), 3.14 (1H, d, J = 10.6, H-14a), 3.61 (1H, d, J = 10.6 Hz, H-14b), 4.67 (1H, d, J = 11.0 Hz, H-15a), 4.80 (1H, d, J = 11.0, H-15b), 4.96 (2H, m, H-11), 5.83 (1H, d, J = 6.0 Hz, H-6), 7.52 (2H, m, H-4′/6′), 7.67 (1H, tt, J = 7.3, 1.2 Hz, H-5′), 7.97 (2H, m, H-3′/7′).

^{13}C-NMR (125.70 MHz, DMSO-d_6, 25 °C, 39.5 ppm): 17.3 (C-2), 20.6 (C-17), 28.2 (C-7), 30.7 (C-1), 34.6 (C-3), 39.4 (C-4), 39.8 (C-10), 52.5 (C-5), 62.9 (C-14), 65.4 (C-15), 66.5 (C-6), 71.1 (C-11), 121.2 (C-8), 128.7 (4′/6′), 129.3 (3′/7′), 129.8 (C-2′), 133.5 (5′), 165.6 (C-1′), 166.8 (C-9), 170.5 (C-16), 173.2 (C-12).

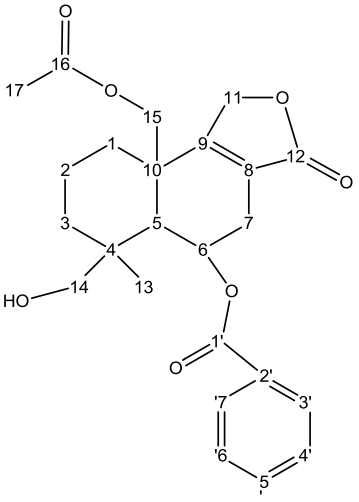

Dideacetyl parasiticolide A

HRESIMS: m/z = 387.1817 $[M+H]^+$, calculated for $[C_{22}H_{26}O_6+H]^+$: 387.1802.

^{1}H-NMR (499.87 MHz, DMSO-d_6, 25 °C, 2.50 ppm): 0.91 (1H, ddd, J = 13.4, 13.4, 3.7 Hz, H-3a), 0.99 (3H, s, H-13), 1.17 (1H, dd, J = 12.9, 3.5 Hz, H-1a), 1.42 (1H, m, H-2a), 1.65 (1H, m, H-2b), 1.81 (1H, s, H-5), 1.97 (1H, d, J = 13.4 Hz, H-3b), 2.28 (1H, d, J = 12.9 Hz, H-1b), 2.31 (1H, d, J = 19.3 Hz, H-7a), 2.73 (1H, m, H-7b), 3.09 (1H, dd, J = 10.5, 5.3 Hz), 3.60 (1H, dd, J = 10.5, 5.3 Hz, H-14b), 4.07 (1H, m, H-15a), 4.12 (1H, m, H-15b), 4.42 (1H, dd, J = 5.3, 5.3 Hz, 14-OH), 4.86 (1H, dd, J = 17.5, 2.0 Hz, H-11a), 5.06 (1H, dt, J = 17.5, 2.5 Hz, H-11b), 5.10 (1H, dd, J = 5.2, 5.2 Hz, 15-OH), 5.80 (1H, d, J = 5.8 Hz, H-6), 7.55 (2H, m, H-4′/6′), 7.67 (1H, m, H-5′), 7.90 (2H, m, H-3′/7′).

^{13}C-NMR (125.70 MHz, DMSO-d_6, 25 °C, 39.5 ppm): 17.6 (C-2), 27.3 (C-13), 28.5 (C-7), 30.5 (C-1), 34.9 (C-3), 39.4 (C-4), 42.9 (C-10), 52.7 (C-5), 62.4 (C-15), 63.1 (C-14), 66.9 (C-6), 72.0 (C-11), 119.5 (C-8), 128.9 (C-4′/6′), 129.0 (C-3′/7′), 129.8 (C-2′), 133.5 (C-5′), 165.7 (C-1′), 169.4 (C-9), 173.6 (C-12).

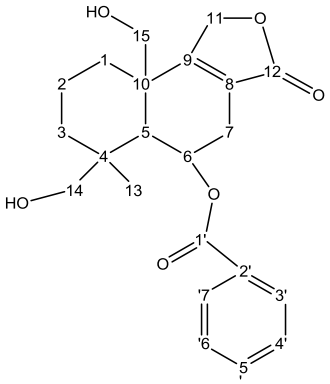

18-Formyl parasiticolide A

HRESIMS: *m/z* = 457.1889 $[M+H]^+$, calculated for $[C_{25}H_{28}O_8+H]^+$: 457.1857.

^{1}H-NMR (499.87 MHz, DMSO-d_6, 25 °C, 2.50 ppm): 1.10 (3H, s, H-13), 1.18 (1H, ddd, *J* = 13.7, 13.7, 3.3 Hz, H-3a), 1.43 (1H, ddd, *J* = 13.2, 13.2, 2.9 Hz, H-1a), 1.51 (1H, m, H-2a), 1.71 (1H, m, H-2b), 1.82 (1H, d, *J* = 13.7 Hz, H-3a), 2.06 (1H, s, H-5), 2.09 (3H, s, H-17), 2.16 (1H, d, *J* = 13.2 Hz, H-1b), 2.43 (1H, d, *J* = 19.3 Hz, H-7a), 2.80 (1H, m, H-7b), 3.99 (1H, d, *J* = 11.0 Hz, H-14a), 4.36 (1H, d, *J* = 11.0 Hz, H-14b), 4.71 (1H, d, *J* = 10.8 Hz, H-15a), 4.78 (1H, d, *J* = 10.8 Hz, H-15b), 4.98 (2H, m, H-11), 5.83 (1H, d, *J* = 5.6 Hz, H-6), 7.52 (2H, dd, *J* = 7.6, 7.6 Hz, H-4′/6′), 7.68 (1H, dd, *J* = 7.6, 7.6 Hz, H-5′), 7.98 (2H, d, *J* = 7.6 Hz, H-3′/7′), 8.06 (1H, s, H-18).

^{13}C-NMR (125.70 MHz, DMSO-d_6, 25 °C, 39.5 ppm): 16.9 (C-2), 20.5 (C-17), 26.6 (C-13), 27.9 (C-7), 30.5 (C-1), 35.4 (C-3), 36.9 (C-4), 39.6 (C-10), 52.1 (C-5), 65.0 (C-14), 65.1 (C-15), 66.5 (C-6), 71.1 (C-11), 121.0 (C-8), 128.6 (C-4′/6′), 129.0 (C-3′/7′), 129.2 (C-2′), 133.4 (C-5′), 161.6 (C-18), 165.1 (C-1′), 165.9 (C-9), 170.1 (C-16), 172.8 (C-12).

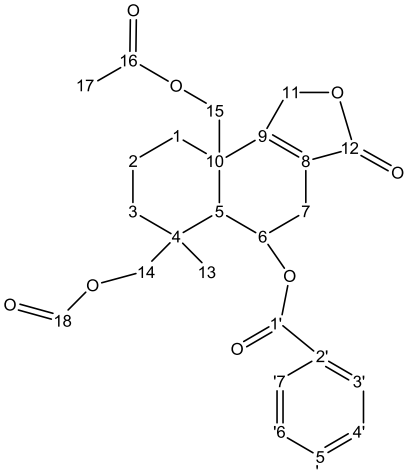

Ditryptoleucine A

HRESIMS: *m/z* = 625.3472 $[M+H]^+$, calculated for $[C_{36}H_{44}N_6O_4+H]^+$: 625.3497.

^{1}H-NMR (499.87 MHz, DMSO-*d*$_6$, 25 °C, 2.50 ppm): 0.81 (6H, d, *J* = 6.4 Hz, H-21), 0.83 (6H, d, *J* = 6.4 Hz, H-20), 1.42 (H2, m, H-18a), 1.48 (H2, m, H-18b), 1.58 (H2, m, H-19), 2.44 (H4, m, H-11), 2.80 (H6, s, H-17), 3.76 (H2, dd, *J* = 10.4, 3.8 Hz, H-12), 3.81 (H2, dd, *J* = 7.9, 6.0 Hz, H-15), 5.09 (H2, m, H-2), 6.61 (H2, d, *J* = 7.8, H-5), 6.66 (H2, t, *J* = 7.5, H-7), 6.68 (H2, s, H-3), 7.05 (H2, t, 7.8, H-6), 7.23 (H2, d, *J* = 7.8, H-8).

^{13}C-NMR (125.70 MHz, DMSO-*d*$_6$, 25 °C, 39.5 ppm): 21.9 (C-20), 22.6 (C-21), 23.7 (C-19), 31.8 (C-17), 36.1 (C-11), 39.4 (C-18), 56.7 (C-12), 57.9 (C-10), 61.6 (C-15), 76.7 (C-2), 108.7 (C-5), 117.2 (C-7), 124.6 (C-8), 126.7 (C-9), 129.0 (C-6), 150.9 (C-4), 165.0 (C-16), 166.1 (C-13).

Ditryptoleucine B

^{1}H-NMR (499.87 MHz, DMSO-*d*$_6$, 25 °C, 2.50 ppm): 0.81 (6H, d, *J* = 6.1 Hz, H-21), 0.83 (6H, d, *J* = 6.2 Hz, H-20), 1.42 (H2, m, H-18), 1.49 (H2, m, H-19), 2.45 (H2, dd, *J* = 13.5, 4.7, H-11a), 2.75 (H6, s, H-17), 3.13 (H2, m, H-11b), 3.33 (H2, s, H-2), 3.82 (H2, t, *J* = 6.9 Hz, H-15), 4.23 (H2, m, H-12), 6.58 (H2, d, *J* = 7.5, H-5), 6.65 (H2, t, *J* = 7.1, H-7), 6.70 (H2, s, H-3), 7.01 (H2, t, 7.2, H-6), 7.37 (H2, d, *J* = 7.1, H-8).

^{13}C-NMR (125.70 MHz, DMSO-*d*$_6$, 25 °C, 39.5 ppm): 21.5 (C-21), 22.5 (C-20), 23.6 (C-19), 31.6 (C-17), 37.0 (C-11), 38.0 (C-18), 55.3 (C-12), 60.8 (C-10), 61.7 (C-15), 76.3 (C-2), 108.5 (C-5), 117.4 (C-7), 124.0 (C-8), 130.2 (C-9), 128.3 (C-6), 149.6 (C-4) 166.9 (C-16), 166.6 (C-13).

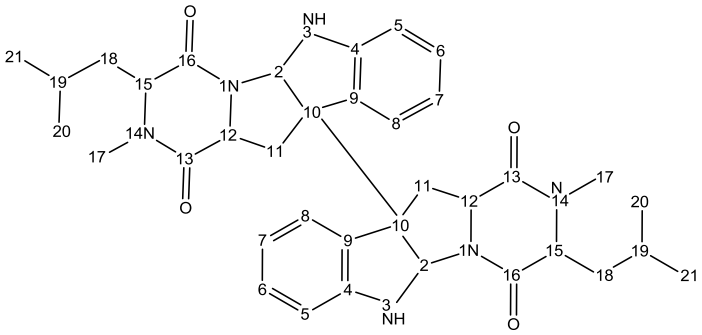

Oryzamide A$_1$

HRESIMS: *m/z* = 491.26526 $[M+H]^+$, calculated for $[C_{28}H_{34}N_4O_4+H]^+$: 491.26525.

^{1}H-NMR (499.87 MHz, DMSO-*d*$_6$, 25 °C, 2.50 ppm): 0.83 (3H, d, *J* = 6.5 Hz, H-5′), 0.88 (3H, d, *J* = 6.6 J, H-5′), 1.36 (1H, m, H-4′), 1.59 (2H, m, H-3′), 1.77 (3H, s, H-2‴), 2.67 (1H, m, H-3″), 2.83 (1H, m, H-3″), 2.87 (3H, s, N-CH), 4.76 (1H, m, H-2″), 5.02 (1H, m, H-2′), 6.47 (1H, d, *J* = 14.8, H-2), 6.61 (2H, d, *J* = 8.4 Hz, H-6″/8″), 7.01 (2H, d, *J* = 8.4 Hz, H-5″/9″), 7.05 (1H, m, H-8), 7.10

(1H, m, H-7), 7.26 (1H, m, H-1), 7.36 (1H, m, H-6), 7.41 (1H, s, H-4), 7.62 (1H, d, J = 7.9 Hz, H-9), 8.24 (1H, d, J = 8.0 Hz, 2″-NH), 9.16 (1H, s, 7″-OH), 9.84 (1H, d, J = 9.8 Hz, 1-NH), 11.11 (1H, s, 4-NH).

^{13}C-NMR (125.70 MHz, DMSO-d_6, 25 °C, 39.5 ppm): 21.6 (C-5′), 22.0 (C-2‴), 22.7 (C-5′), 24.1 (C-4′), 30.9 (C-N), 36.2 (C-3″), 36.9 (C-3′), 50.5 (C-2″), 54.2 (C-2′), 106.4 (C-2), 111.4 (C-3), 111.5 (C-6),114.6 (C-6″/8″), 118.5 (C-9), 118.8 (C-8), 119.2 (C-1), 121.1 (C-7), 123.1 (C-4), 125.0 (C-10), 127.4 (C-4″), 129.7 (C-5″/9″), 136.9 (C-5), 156.0 (C-7″), 167.7 (C-1′), 168.8 (C-1‴), 172.3 (C-1″).

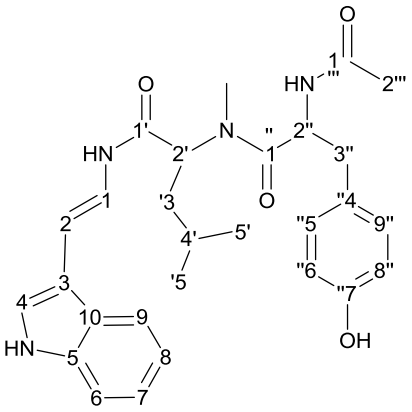

Paper 3

"Isolation and NMR characterization of fumonisin B_2 and a new fumonisin B_6 from *Aspergillus niger*"

M Månsson, ML Klejnstrup, RK Phipps, KF Nielsen, JC Frisvad, CH Gotfredsen, and TO Larsen

Accepted in Journal of Agricultural and Food Chemistry, *58*, 949-953 (2010)

JOURNAL OF AGRICULTURAL AND FOOD CHEMISTRY
ARTICLE

J. Agric. Food Chem. 2010, 58, 949–953 949
DOI:10.1021/jf902834g

Isolation and NMR Characterization of Fumonisin B_2 and a New Fumonisin B_6 from *Aspergillus niger*

Maria Månsson,[†] Marie Louise Klejnstrup,[†] Richard K. Phipps,[†] Kristian F. Nielsen,[†] Jens C. Frisvad,[†] Charlotte H. Gotfredsen,[‡] and Thomas O. Larsen*,[†]

[†]Department of Systems Biology, Center for Microbial Biotechnology, Technical University of Denmark, Building 221, DK-2800 Kgs. Lyngby, Denmark and [‡]Department of Chemistry, Kemitorvet, Technical University of Denmark, Build. 201, DK 2800 Kgs. Lyngby, Denmark

A new fumonisin, fumonisin B_6 (**1**), has been isolated by cation-exchange and reverse-phase chromatography, together with fumonisin B_2 (**2**), from stationary cultures of the fungus *Aspergillus niger* NRRL 326. Analysis of mass spectrometric and NMR data determined that FB_6 is a positional isomer of FB_1 and iso-FB_1, having hydroxyl functions at C3, C4, and C5. Analysis of the NMR data for FB_2 showed very similar chemical shift values when compared to an authentic *Fusarium* FB_2 standard, strongly indicating identical molecules despite that an absolute stereochemical assignment of FB_2 from *A. niger* was not possible.

KEYWORDS: Fumonisins; *Aspergillus niger*; mycotoxins; food safety; NMR

INTRODUCTION

Recently, our group was the first to report the production of the mycotoxin fumonisin B_2 (FB_2) from *Aspergillus niger* NRRL 3122, using HPLC−MS (*1*). The finding did not come as a great surprise, since others (*2*, *3*) had already reported a fumonisin-like gene cluster in the *A. niger* genome of two different strains of the species. Later, we also reported FB_4 from *A. niger*, generally produced in amounts around 10−25% of the FB_2 (*4*, *5*). Until these findings, fumonisin production has only been previously reported in certain species within the *Gibberella fujikuroi* and *Fusarium oxysporum* species complexes, which are common fungal contaminants of maize-based foods and feeds (*6*−*9*). The first fumonisins were described by Gelderblom et al. (*9*) from cultures of *F. verticillioides*. Since then, more than 25 fumonisins have been identified by NMR (*6*) and a further 25 have been putatively identified by LC−MS^n (*10*). The most abundant and most toxic fumonisins are the B-series analogues (*11*−*13*), which contain a terminal 2-amino-3-hydroxy motif on an eicosane backbone and two hydroxy groups esterified with tricarboxylic acids (TCA). In most Fusaria, FB_1 is predominant, usually representing some 70% of the total fumonisin content. FB_2 and FB_3 usually account for up to 15−25% and 3−8%, respectively, while FB_4 is normally present in insignificant amounts (*14*−*16*).

The recent documentation of fumonisin B-series production by *A. niger* has raised the question of whether fumonisins might be an overlooked health risk due to the ubiquitous presence of *A. niger* on a wide range of food stuffs not usually contaminated with *Fusarium* species (*17*). This includes grapes and thereby raisins and wine, peanuts, coffee, tea, and several other products (*1*). Moreover, one could be concerned that industrial products such as enzymes and fine chemicals could be contaminated with traces of fumonisins because of the wide application of *A. niger* as "workhorse" in industrial fermentations (*18*−*21*).

Our recent LC−HRMS based investigations of fumonisin production by *A. niger* and other black Aspergilli suggested that besides FB_2 and FB_4 *A. niger* can also produce an additional third fumonisin with the same elementel composition as FB_1 and iso-FB_1 but with a different retention time than the two latter compounds. The present study reports the isolation and characterization of this novel compound, which we named fumonisin B_6. In addition, we isolated and characterized FB_2 from *A. niger* by NMR in order to further validate that FB_2 from *A. niger* is indeed identical to that of FB_2 previously reported from several *Fusarium* species.

MATERIALS AND METHODS

Fungal Incubation. In a 10 L glass vessel, 2 L of still culture of 55% rice meal and 45% corn steep liquor (RC) medium was prepared according to Bullermann (*22*) but with a reduced amount of agar (1.5 g/L). It was inoculated with a spore suspension from 7 d old ex-type cultures of *A. niger* NRRL 326, ex-tannin-gallic acid fermentation (=IBT 27876 = ATCC 16888 = CBS 554.65) from CYA. After incubation for 14 d in darkness at 25 °C, the mycelia and media were homogenized with 2 L of MeCN/H_2O (50/50, v/v) and shaken overnight. After filtration the extract was concentrated on a rotary evaporator and freeze-dried.

Preparative Chromatography. The raw extract, 9.3 g, was initially subjected to flash chromatography on a 135 g, 50 μm C_{18} material (Phenomenex, Torrance, CA) which was eluted with H_2O−MeOH mixtures in steps of 10%, starting from 10% MeOH. The 70% MeOH fraction (163 mg) was further enriched for fumonisins on a 1000 mg, 33 μm Strata X-C mixed-mode RP-cation-exchange material (Phenomenex), which was washed with MeCN and eluted with MeCN−H_2O (containing 4% NH_4OH) in steps of 20% from 4% NH_4OH. The fumonisin-containing fraction (20% MeCN, 19 mg), was finally subjected

*To whom correspondence should be addressed. Phone: +4525 2632. Fax: +45 4588 4148. E-mail: tol@bio.dtu.dk.

© 2009 American Chemical Society

Published on Web 12/22/2009

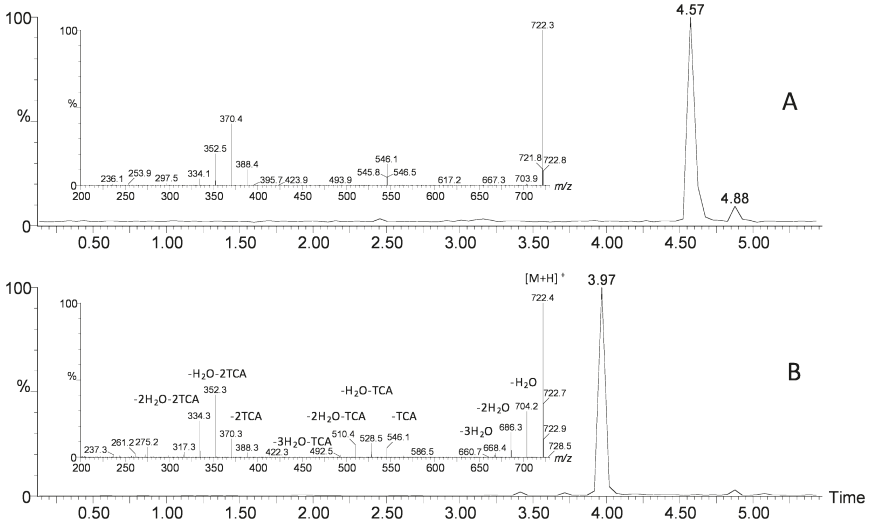

Figure 1. Daughter-ion chromatogram (*m/z* 722) showing FB_6 (4.57 min) and FB_1 (retention time = 3.97 min) and the corresponding daughter-ion spectra (25 eV) from the compound produced by *A. niger* (FB_6) sample (**A**) and an authentic FB_1 standard (**B**).

to RP separation on a 250 mm × 10 mm i.d., 5 μm Luna C_{18} (II) column (Phenomenex) using an MeCN−H_2O gradient (starting at 30% MeCN + 50 ppm TFA increasing to 70% over 15 min). Fractions were collected automatically every 20 s and pooled for each chromatographic run after analysis of the content of each fraction by LC−MS had shown which fractions contained fumonisin B_6 (1.8 mg) and fumonisin B_2 (4.2 mg).

Analytical LC−MS. LC−DAD-HRMS was performed as described by Frisvad et al. (*1*) or by LC−tandem MS (MS/MS) on an Agilent 1100 liquid chromatograph (Waldbronn, Germany) coupled to a Quattro Ultima triple mass spectrometer (Micromass, Manchester, U.K.) with an ESI source. The separation was performed on a 50 mm × 2 mm i.d., 3 μm Gemini C_6-phenyl (Phenomenex) column fitted with a security guard system using a linear gradient starting from 20% MeCN in H_2O (both with 20 mM formic acid) to 55% MeCN for 6 min at a flow rate of 300 μL/min. MS/MS was performed using nitrogen as collision gas and making daughter ion scans of the protonated molecular ions (*m/z* 722 and 706), using fragmentation potentials from 15 to 50 V. Solvents were HPLC grade, and all other chemicals were analytical grade unless otherwise stated. Fumonisin standards (FB_1 and FB_2 mixture 50 μg/mL) used for MS analysis were acquired from Biopure (Tulln, Austria). FB_3 was from Chiron (Trondheim, Norway). FB_2 used for NMR analysis was from Alexis Biochemicals (Lausen, Switzerland).

NMR Spectroscopy. NMR spectra were recorded on a Bruker Avance 800 MHz spectrometer with a 5 mm TCI cryoprobe at the Danish Instrument Center for NMR Spectroscopy of Biological Macromolecules. The 2D DQF-COSY, NOESY, gHSQC, gH2BC, and gHMBC spectra were acquired using standard pulse sequences. The NMR data used for the structural assignment of the fumonisins were acquired in CD_3OD (δ_H 3.31 ppm and δ_C 49.15 ppm).

RESULTS AND DISCUSSION

In the current study, the ex-type culture of *A. niger* was used, as it has been found to be a strong producer strain of fumonisins (*1*). With no published protocols for purification of fumonisins from *A. niger*, we chose to use mixed-mode RP cation-exchange for purification. This was done because *A. niger* produces high amounts of acidic naphtho-γ-pyrones and organic acids, which would likely also bind to a strong anion-exchanger (SAX), which is the usual way to purify fumonisins (*23*).

Analytical LC−MS was used to compare the retention times and daughter-ion spectra of the purified *A. niger* fumonisin analogues to those of authentic standards of FB_1, FB_2, and FB_3. The daughter-ion spectra of the FB_2 standard and FB_2 from *A. niger*, eluting at the same time, were identical and consistent with previously reported ESI-MS/MS data (*24*−*26*), with losses of H_2O and TCA groups from the alkyl backbone dominating the spectra. This confirmed the presence of FB_2 or an isomer thereof in the *A. niger* extract. LC−HRMS analyses also showed a peak with the same elemental composition as FB_1, however, eluting slightly later (**Figure 1**). LC−MS/MS also confirmed this and showed that it eluted 0.6 min after the authentic standard of FB_1 and 0.15 min before FB_2 on the C_6-phenyl column. Significant differences in the daughter-ion spectra clearly showed that *A. niger* produces an FB_1 analogue and not FB_1 (**Figure 1**). The same was observed in the crude *A. niger* extract; thus, the FB_1 analogue was not an artifact of the purification process but proved to be the novel analogue fumonisin B_6 (FB_6). FB_6 displayed significantly less abundant losses of H_2O than FB_1, which indicates the presence of adjacent hydroxyl groups blocking the hydrogens from detaching, thereby allowing the H_2O loss. This is in agreement with our previous findings during our studies of the fragmentation patterns of 474 microbial metabolites using LC−MS ESI^+ and ESI^- MS (*27*), where we have never observed H_2O losses unless a β-hydrogen could be lost because of double bond formation.

NMR Based Structural Investigations. To further validate that the FB_2 purified from *A. niger* is identical to that produced by *Fusarium*, 1D and 2D homo- and heteronuclear NMR spectra of the purified *A. niger* fumonisin FB_2 were carefully inspected and compared to those of an authentic standard of FB_2. The NMR data obtained in methanol-d_4 displayed comparable chemical shifts for the 34 expected ^{13}C NMR chemical shift values except for the resonances originating from the two TCA side chains and their sites of attachment to the fumonisin backbone. In this region, deviations in the ^{13}C NMR chemical shifts of between −1.8 to +0.3 ppm were observed. These results could be explained by a difference in the structural fold of the FB_2 between the two samples, likely to be caused by differences in pH and thereby overall level of protonation of the four carboxylic acid functionalities. The fact that FB_2 does have a unique globular

Table 1. NMR Data for Fumonisin B_6, B_1, and Iso-B_1

	fumonisin B_6				fumonisin B_1 (*16*)		fumonisin iso-B_1 (*29*)	
ID	H (ppm)	C (ppm)	HMBC[c]	H2BC[c]	H (ppm)	C (ppm)	H (ppm)	C (ppm)
1	1.34 (d, 7.0)	16.3	2, 3	2	1.27 (d, 6.7)	16.0	1.30 (d, 6.8)	14.2
2	3.67 (qd, 2.0, 7.0)	50.0	1, 3	1	3.14 (dq, 6.7, 6.8)	53.7	3.43 (dq, 4.3)	51.8
3	3.64 (dd, 2.0, 7.1)	71.8	1, 4		3.74 (ddd, 9.6, 6.8, 3.2)	70.3	3.55 (dd, 4.0)	73.2
4	3.46 (dd, 1.8, 7.1)	74.9	2, 5		1.55 (m)	41.7	3.65 (m)	72.2
5	3.71 (ddd, 1.8, 5.1, 8)	71.4			3.84 (m)	68.4	1.45	34.2
							1.55	
6	1.53 (m)	34.8			1.40−1.60	39.1	1.34 (br m)	30.6
	1.59 (m)							
7[b]	1.26−1.37	30.6	4, 8		1.30−1.50	26.6	1.38	26.3
							1.54	
8[b]	1.26−1.37	30.6			1.30−1.50	26.7	1.32	26.5
							1.52	
9[b]	1.26−1.37	30.6	10		1.40−1.60	39.0	1.4	38.9
10	1.25	27.5	9		3.62 (m)	69.8	3.62 (m)	70.0
11	1.04 (m)	36.1			1.15 (m)	44.6	1.08	44.5
	1.40 (m)				1.45 (m)		1.5	
12	1.50 (m)	29.9	15	21	1.81 (m)	26.9	1.83 (m)	27.0
13	1.43 (m)	36.1	14, 16, 21	12	1.55 (m)	36.6	1.45	37.0
	1.62 (m)			14	1.70 (m)		1.66	
14	5.18 (ddd,~3, ~4, 10.9)[a]	72.8			5.16 (ddd, 10.8, 3.7, 2.4)	72.8	5.16 (ddd, 11, 3, 4)	72.7
15	4.92 (dd, 3.5, 8.3)	78.7	13, 14, 16, 17, 22, 29		4.94 (dd, 8.1, 3.7)	78.7	4.94 (dd, 4, 8)	78.9
16	1.70 (m)	34.7	15	15, 22	1.70 (m)	34.8	1.70 (m)	34.9
17	1.09 (m)	32.9	16, 22		1.07 (m)	32.9	1.08	32.9
	1.44 (m)				1.44(m)		1.43	
18	1.18 (m)	29.5			1.18 (m)	29.5	1.18	29.8
	1.13 (m)				1.33 (m)		1.33	
19	1.31 (m)	23.7	17, 20	20	1.10 (m)	23.9	1.22	23.9
	1.26 (m)				1.40 (m)		1.38	
20	0.89 (t, 7.0)	14.2	18, 19		0.89 (t, 7.1)	14.4	0.89 (t, 7)	14.4
21	0.92 (d, 6.7)	20.8	12, 13	12	0.96 (d, 6.7)	20.8	0.96 (d, 6.7)	20.8
22	0.94 (d, 6.9)	15.7	14, 16	16	0.94 (d, 6.8)	16.0	0.93 (d, 6.8)	16.1
23		172.9				173.5		173.5
24	2.51 (dd, 6.7, 17.0)	36.3	23, 25, 26, 28		2.45 (dd, 16.7, 7.4)	37.1	2.45	37.3
	2.72 (dd, 7.2, 17.0)		25, 26, 27		2.71 (dd, 16.7, 7.4)		2.71	
25	3.15 (m)	38.7	23, 24, 28		3.10−3.20 (m)	39.6	3.14	39.7
26	2.55 (dd, 5.9, 17.0)	36.3	24, 25, 27		2.50 (dd, 16.5, 5.2)	37.8	2.48	38.0
	2.68 (dd, 7.5, 16.8)		25, 27		2.66 (dd, 16.5, 8.3)		2.64	
27		175.4				177.4		177.2
28		177.1				178.5		178.7
29		172.9				173.0		173.2
30	2.64 (dd, 6.3, 16.7)	36.3	29, 31, 32, 34		2.60 (dd, 16.6, 6.4)	36.9	2.59	37.0
	2.80 (dd, 7.2, 16.9)		29, 31, 32, 34		2.79 (dd, 16.6, 7.2)		2.79	
31	3.16 (m)	38.7	29, 30, 34		3.10−3.20 (m)	39.7	3.14	39.6
32	2.58 (dd, 6.2, 16.9)	36.1	30, 31, 33		2.52 (dd, 16.5, 6.0)	37.5	2.51	37.7
	2.74 (dd, 7.2, 16.9)		31, 33		2.72 (16.5, 7.5)		2.7	
33		175.2				177.0		176.7
34		176.8				178.0		178.2

[a] Only approximate *J* coupling constants (in Hz) due to overlap in the region. [b] Ambigous assignment due to total overlap in the region. [c] HMBC and H2BC connectivities are from the assigned proton to the indicated carbon atom(s).

folded structure has previously been addressed by Beier and Stanker (*28*). In order to ensure that the two samples had been subjected to the same purification protocol, the standard FB_2 sample was run over a cation exchange column, in the same way as the last purification step for the isolated *A. niger* FB_2 sample. This proved to be very important, since the spectra obtained for FB_2 from *Fusarium* after this procedure were now identical to those from *A. niger* FB_2, confirming that only minor changes in the sample preparation (e.g., pH) can have a large effect on the structural fold of the fumonisin molecules and thereby spectroscopic output. Comparisons of the *J* coupling constants for the protons in the amino terminal part of the FB_2 (C2−C5) and the attactments of the TCA side chains (C14 and C15), from *A. niger* and *Fusarium*, showed that they are of the same size, proving that the relative stereochemistry for these parts of the FB_2 backbone is the same for *Aspergillus* and *Fusarium*. On the other hand the stereochemistry at positions C12 and C16 could not be elucidated on the basis of the data available because of chemical shift overlaps. The optical rotation of FB_2 from *A. niger* ($[\alpha]_D^{20}$ −11.36 (*c* 1 mg/mL, MeOH)) was similar to that known from *Fusarium*; however, with several stereocenters in the molecule this is not a direct proof of identical stereochemistry for FB_2 originating from the two different genera.

Altogether, the presented data point toward identical stereochemistry of the two FB_2 molecules; however, a genetic comparison of the fumonisin gene cluster in the two different genera revealed several differences in the placement and orientation of the different involved synthase genes (*2*). This could lead to structural differences in the polyketide synthases and thereby the final stereochemistry of fumonisins produced by *A. niger*,

	M_r	R_1	R_2	R_3
FB_1	721.3884	H	OH	OH
Iso-FB_1	721.3884	OH	H	OH
FB_2 (**2**)	705.3935	H	OH	H
FB_3	705.3935	H	H	OH
FB_4	689.3986	H	H	H
FB_6 (**1**)	721.3884	OH	OH	H

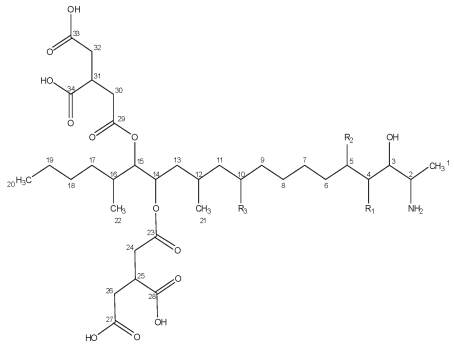

Figure 2. Fumonisin structures and numbering scheme.

which is why we conclude that further structural studies such as X-ray analysis need to be performed to establish the absolute stereochemistry of FB_2 from *A. niger*.

NMR studies of FB_6 substantiated the MS analyses, indicating a new fumonisin of the B type. Unambiguous assignments of the proton and carbon resonances of FB_6 could be obtained for most of the resonances. However, spectral overlap hampered some specific assignments in the alkane-like part of the molecule. The assignment was compared to literature values for fumonisins (*16*, *29*). A series of 2D DQF-COSY, HSQC, HMBC, and H2BC experiments established partial assignment of the backbone as well as the TCA side chains present in the structure. Thirty-four carbon resonances could be identified comprising four CH_3 groups, 14 CH_2 groups, 10 CH groups, and 6 carboxyl carbon resonances (**Table 1**). The two TCA side chains bound to the backbone structure could be assigned as two separate spin systems C23−C28 and C29−C34 (**Figure 2**) with only minor differences in their chemical shifts. The attachment of the C29−C34 TCA side chain to the backbone structure could be confirmed by the presence of an HMBC correlation between H15 and C29, whereas the position of the C23−C28 TCA side chain is based on the chemical shift of H14/C14 and comparison with the assignment obtained for FB_1 and iso-FB_1. Unambiguous assignments of the fragments C1−C6 and C10−C20 were obtained. In **Table 1**, a comparison of the chemical shifts of FB_6 to FB_1 and iso-FB_1 can be seen. Comparing the resonance assignment of FB_6 to FB_1 and iso-FB_1 showed only minor deviations between the structures except at the positions of OH attachment in the backbone structure. Where FB_1 and iso-FB_1 have OH groups attached to C3, C5, and C10 and to C3, C4, and C10, respectively, the new fumonisin FB_6 has OH groups at C3, C4, and C5 (**Figure 2**). The chemical shift values of 1.25 ppm for H10 and 27.5 ppm for C10, DQF-COSY connectivities from H 11 to H 10 and HMBC correlations from H 9 to C10 and from H 10 to C9, confirm that no OH group is bound at this position due to the large upfield shift of the resonances when compared to FB_1, where H 10 and C10 resonate at 3.62 and 69.8 ppm, respectively. In the amino terminal portion of the backbone structure, DQF-COSY connectivities can be traced along the chain from H3 at 3.64 ppm, H4 at 3.46 ppm, and H5 at 3.71 ppm to H6 at 1.53/1.59 ppm. In addition, HMBC correlations can be seen from H4 to C2/C5 and from H3 to C4, confirming the presence of the third OH group at C4 in the structure. The chemical shift obtained for H4/C4 of 3.46 ppm/74.9 ppm compared to 3.65 ppm/72.2 ppm as seen in iso-FB_1 and equivalently for H5/C5 of 3.71 ppm/71.4 ppm compared to 3.84 ppm/68.4 ppm for FB_1 is in agreement with the proposed structure for FB_6.

Altogether, the analysis of these data proves FB_6, with hydroxyl functionalities at C3, C4, and C5, to be a structural isomer of FB_1 and iso-FB_1. As can be seen in **Figure 2** FB_6 and iso-FB_1 have a hydroxyl at C4, which is rare for the B-series fumonisins and only previously seen for iso-FB_1 (*29*). As is the case for FB_2, the absolute stereochemistry of FB_6 still needs to be resolved, which is work that is ongoing in our laboratory. Analysis of several *A. niger* strains in our laboratory (results not shown) has shown that the frequencies of production of fumonisins in *A. niger* on average are 100% (FB_2), 10−25% (FB_4), and 5−10% (FB_6). Testing of the toxicological properties of not only FB_2 and FB_6 but also FB_4, including investigations of the different conformations that we have seen for these *A. niger* fumonisins, is also in progress in our laboratory.

ACKNOWLEDGMENT

We thank the Danish Instrument Center for NMR Spectroscopy of Biological Macromolecules for NMR time.

LITERATURE CITED

(1) Frisvad, J. C.; Smedsgaard, J.; Samson, R. A.; Larsen, T. O.; Thrane, U. Fumonisin B_2 production by *Aspergillus niger*. *J. Agric. Food Chem.* **2007**, *55*, 9727–9732.

(2) Baker, S. E. *Aspergillus niger genomics*: past, present and into the future. *Med. Mycol.* **2006**, *44*, S17–S21.

(3) Pel, H. J.; de Winde, J. H.; Archer, D. B.; Dyer, P. S.; Hofmann, G.; Schaap, P. J.; et al. Genome sequencing and analysis of the versatile cell factory *Aspergillus niger* CBS 513.88. *Nat. Biotechnol.* **2007**, *25*, 221–231.

(4) Nielsen, K. F.; Mogensen, J.; Johansen, M.; Larsen, T. O.; Frisvad, J. C. Review of secondary metabolites and mycotoxins from the *Aspergillus niger* group. *Anal. Bioanal. Chem.* **2009**, *395*, 1225–1242.

(5) Noonim, P.; Mahakarnchanakul, W.; Nielsen, K. F.; Frisvad, J. C.; Samson, R. A. Fumonisin B_2 production by *Aspergillus niger* from Thai coffee beans. *Food Addit. Contam., Part A* **2009**, *26*, 94–100.

(6) Rheeder, J. P.; Marasas, W. F. O.; Vismer, H. F. Production of fumonisin analogs by *Fusarium* species. *Appl. Environ. Microbiol.* **2002**, *68*, 2101–2105.

(7) Paepens, C.; De Saeger, S.; Van Poucke, C.; Dumoulin, F.; Van Calenbergh, S.; Van Peteghem, C. Development of a liquid chromatography/tandem mass spectrometry method for the quantification of fumonisin B-1, B-2 and B-3 in cornflakes. *Rapid Commun. Mass Spectrom.* **2005**, *19*, 2021–2029.

(8) Ross, P. F.; Nelson, P. E.; Richard, J. L.; Osweiler, G. D.; Rice, L. G.; Plattner, R. D.; Wilson, T. M. Production of fumonisins by *Fusarium moniliforme* and *Fusarium proliferatum* isolates associated with equine leukoencephalomalacia and a pulmonary-edema syndrome in swine. *Appl. Environ. Microbiol.* **1990**, *56*, 3225–3226.

(9) Thiel, P. G.; Marasas, W. F. O.; Sydenham, E. W.; Shephard, G. S.; Gelderblom, W. C. A.; Nieuwenhuis, J. J. Survey of fumonisin

production by *Fusarium* species. *Appl. Environ. Microbiol*. **1991**, *57*, 1089–1093.
(10) Bartok, T.; Szecsi, A.; Szekeres, A.; Mesterhazy, A.; Bartok, M. Detection of new fumonisin mycotoxins and fumonisin-like compounds by reversed-phase high-performance liquid chromatography/electrospray ionization ion trap mass spectrometry. *Rapid Commun. Mass Spectrom*. **2006**, *20*, 2447–2462.
(11) Bezuidenhout, S. C.; Gelderblom, W. C. A.; Gorstallman, C. P.; Horak, R. M.; Marasas, W. F. O.; Spiteller, G.; Vleggaar, R. Structure elucidation of the fumonisins, mycotoxins from *Fusarium moniliforme*. *J. Chem. Soc., Chem. Commun*. **1988**, *11*, 743–745.
(12) Gelderblom, W. C. A.; Cawood, M. E.; Snyman, S. D.; Vleggaar, R.; Marasas, W. F. O. Structure−activity-relationships of fumonisins in short-term carcinogenesis and cytotoxicity assays. *Food Chem. Toxicol*. **1993**, *31*, 407–414.
(13) Gutleb, A. C.; Morrison, E.; Murk, A. J. Cytotoxicity assays for mycotoxins produced by *Fusarium* strains: a review. *Environ. Toxicol. Pharmacol*. **2002**, *11*, 309–320.
(14) Musser, S. M.; Plattner, R. D. Fumonisin composition in cultures of *Fusarium moniliforme*, *Fusarium proliferatum*, and *Fusarium nygami*. *J. Agric. Food Chem*. **1997**, *45*, 1169–1173.
(15) Thiel, P. G.; Marasas, W. F. O.; Sydenham, E. W.; Shephard, G. S.; Gelderblom, W. C. A. The implications of naturally-occurring levels of fumonisins in corn for human and animal health. *Mycopathology* **1992**, *117*, 3–9.
(16) Miller, J., Trenholm, H. L., Eds. *Mycotoxins in Grain: Compounds Other Than Aflatoxin*; Eagan Press: St. Paul, MN, 1994.
(17) Bouras, N.; Mathieu, F.; Coppel, Y.; Strelkov, S. E.; Lebrihi, A. Occurrence of naphtho-gamma-pyrones- and ochratoxin A-producing fungi in French grapes and characterization of new naphtho-gamma-pyrone polyketide (aurasperone G) isolated from *Aspergillus niger* C-433. *J. Agric. Food Chem*. **2007**, *55*, 8920–8927.
(18) Schuster, E.; Dunn-Coleman, N.; Frisvad, J. C.; Van Dijck, P. W. On the safety of *Aspergillus niger* — a review. *Appl. Microbiol. Biotechnol*. **2002**, *59*, 426–435.
(19) Blumenthal, C. Z. Production of toxic metabolites in *Aspergillus niger*, *Aspergillus oryzae*, and *Trichoderma reesei*: Justification of mycotoxin testing in food grade enzyme preparations derived from the three fungi. *Regul. Toxicol. Pharmacol*. **2004**, *39*, 214–228.
(20) Goldberg, I.; Rokem, J. S.; Pines, O. Organic acids: old metabolites, new themes. *J. Chem. Technol. Biotechnol*. **2006**, *81*, 1601–1611.
(21) Karaffa, L.; Kubicek, C. P. *Aspergillus niger* citric acid accumulation: do we understand this well working black box? *Appl. Microbiol. Biotechnol*. **2003**, *61*, 189–196.
(22) Bullermann, L. B. A screening medium and method to detect several mycotoxins in mold cultures. *J. Milk Food Technol*. **1974**, *37*, 1–3.
(23) Hinojo, M. J.; Medina, A.; Valle-Algarra, F. M.; Gimeno-Adelantado, J. V.; Jimenez, M.; Mateo, R. Fumonisin production in rice cultures of *Fusarium verticillioides* under different incubation conditions using an optimized analytical method. *Food Microbiol*. **2006**, *23*, 119–127.
(24) Josephs, J. Detection and characterization of fumonisin mycotoxins by liquid chromatography electrospray ionization using ion trap and triple quadrupole mass spectrometry. *Rapid Commun. Mass Spectrom*. **1996**, *10*, 1333–1344.
(25) Sewram, V.; Mshicileli, N.; Shephard, G. S.; Vismer, H. F.; Rheeder, J. P.; Lee, Y. W.; Leslie, J. F.; Marasas, W. F. O. Production of fumonisin B and C analogues by several *Fusarium* species. *J. Agric. Food Chem*. **2005**, *53*, 4861–4866.
(26) Caldas, E. D.; Jones, A. D.; Winter, C. K.; Ward, B.; Gilchrist, D. G. Electrospray-ionization mass-spectrometry of sphinganine analog mycotoxins. *Anal. Chem*. **1995**, *67*, 196–207.
(27) Nielsen, K. F.; Smedsgaard, J. Fungal metabolite screening: database of 474 mycotoxins and fungal metabolites for dereplication by standardised liquid chromatography−UV−mass spectrometry methodology. *J. Chromatogr., A* **2003**, *1002*, 111–136.
(28) Beier, R. C.; Stanker, L. H. Molecular models for the stereochemical structures of fumonisin B_1 and B_2. *Arch. Environ. Contam. Toxicol*. **1997**, *33*, 1–8.
(29) MacKenzie, S. E.; Savard, M. E.; Blackwell, B. A.; Miller, J. D.; ApSimon, J. W. Isolation of a new fumonisin from *Fusarium moniliforme* grown in liquid culture. *J. Nat. Prod*. **1998**, *61*, 367–369.

Received for review August 13, 2009. Revised manuscript received November 27, 2009. Accepted November 27, 2009. We thank the Danish Food Industry Agency for financial support (Grant 3304-FVFP-07-730-01).

Paper 4

"A genome-wide polyketide synthase deletion library uncovers novel genetic links to polyketides and meroterpenoids in *Aspergillus nidulans*"

ML Nielsen, JB Nielsen, C Rank, ML Klejnstrup, DK Holm, KH Brogaard, BG Hansen, JC Frisvad, TO Larsen, and UH Mortensen

Accepted in Journal of FEMS Microbiology Letters, *321*, 157-166 (2011)

RESEARCH LETTER

A genome-wide polyketide synthase deletion library uncovers novel genetic links to polyketides and meroterpenoids in *Aspergillus nidulans*

Michael L. Nielsen, Jakob B. Nielsen, Christian Rank, Marie L. Klejnstrup, Dorte K. Holm, Katrine H. Brogaard, Bjarne G. Hansen, Jens C. Frisvad, Thomas O. Larsen & Uffe H. Mortensen

Department of Systems Biology, Center for Microbial Biotechnology, Technical University of Denmark, Lyngby, Denmark

Correspondence: Uffe H. Mortensen, Department of Systems Biology, Center for Microbial Biotechnology, Technical University of Denmark, Building 223, 2800 Kgs. Lyngby, Denmark. Tel.: +45 4525 2701; fax: +45 4588 4148; e-mail: um@bio.dtu.dk

Received 14 April 2011; revised 26 May 2011; accepted 27 May 2011.
Final version published online 27 June 2011.

DOI:10.1111/j.1574-6968.2011.02327.x

Editor: Richard Staples

Keywords
filamentous fungi; secondary metabolism; arugosin; austinol; violaceol; shamixanthone

Abstract

Fungi possess an advanced secondary metabolism that is regulated and coordinated in a complex manner depending on environmental challenges. To understand this complexity, a holistic approach is necessary. We initiated such an analysis in the important model fungus *Aspergillus nidulans* by systematically deleting all 32 individual genes encoding polyketide synthases. Wild-type and all mutant strains were challenged on different complex media to provoke induction of the secondary metabolism. Screening of the mutant library revealed direct genetic links to two austinol meroterpenoids and expanded the current understanding of the biosynthetic pathways leading to arugosins and violaceols. We expect that the library will be an important resource towards a systemic understanding of polyketide production in *A. nidulans*.

Introduction

It is well known that filamentous fungi produce a large number of bioactive secondary metabolites (Bérdy, 2005; Cox, 2007; Newman & Cragg, 2007). Polyketide (PK) compounds constitute a major part of these metabolites and have long been recognized as a valuable source of diverse natural compounds of medical importance, for example lovastatin (cholesterol lowering) (Lai *et al*., 2005), griseofulvin (antibiotic) (Chooi *et al*., 2010) and mycophenolic acid (immunosuppressant) (Bentley, 2000). However, polyketides also include many toxic compounds that pose a serious threat to human health, for example patulin, ochratoxins, fumonisins and aflatoxin (Frisvad *et al*., 2004; Månsson *et al*., 2010). Polyketides are biosynthesized by large multidomain polyketide synthases (PKSs), which besides acyl transferase, β-ketoacyl synthase and acyl carrier domains may also contain keto reductase, dehydratase, cyclization and methyl-transferase domains (Cox, 2007; Smith & Tsai, 2007; Hertweck, 2009). In fungi, the different catalytic activities often work in an iterative manner (fungal type I) and it is generally difficult to predict the exact product formed by a given PKS from its sequence alone (Keller *et al*., 2005). Product prediction is further complicated by the fact that the resulting polyketide structure may be decorated by tailoring enzymes. Such genes are often physically associated with the PKS gene in a gene cluster allowing for coordinated regulation (Schümann & Hertweck, 2006). The fact that natural products may be of mixed biosynthetic origin, combining elements such as polyketides with terpenes (meroterpenoids) and/or nonribosomal peptide units, adds to the complexity (Chang *et al*., 2009; Geris & Simpson, 2009; Hertweck, 2009; Scherlach *et al*., 2010).

As a consequence of their bioactivity, societal importance and also the prospect of reprogramming the biosynthetic machinery for drug development (Cox, 2007), there is tremendous interest in the discovery and understanding of fungal polyketide biosynthesis. The availability of full genome sequences of a number of filamentous fungi has provided a means to address the discovery of polyketides because the PKS genes are large and contain several conserved protein domains. Importantly, analysis of the

© 2011 Federation of European Microbiological Societies
Published by Blackwell Publishing Ltd. All rights reserved

genomic sequences from filamentous fungi (including *Aspergillus nidulans*, teleomorph, *Emericella nidulans*) predict numbers of individual PKS genes that exceeds significantly the number of polyketides that these fungi are known to produce (Galagan *et al.*, 2005). In fact, the genome of *A. nidulans* (Galagan *et al.*, 2005) appears to contain as many as 32 individual PKS genes (Nierman *et al.*, 2005; Szewczyk *et al.*, 2008; von Döhren, 2009), but until now only nine genes have been linked to eight polyketides (Yamazaki & Maebayas, 1982; Bergmann *et al.*, 2007; Chiang *et al.*, 2008; Szewczyk *et al.*, 2008; Bok *et al.*, 2009; Chiang *et al.*, 2009; Schroeckh *et al.*, 2009) (see Supporting Information, Fig. S1). This may reflect that many polyketides are either produced in small amounts, under special conditions, or in developmental stages that are rarely observed under laboratory conditions.

Towards a more complete genetic mapping of the secondary metabolism in *A. nidulans*, we first cultivated a reference strain on an array of different growth media to uncover polyketides that were not previously linked to a gene cluster. This analysis revealed several compounds, including austinols, violaceols, arugosins and prenylated xanthones. Next, genetic links to these compounds were established by constructing and screening an *A. nidulans* mutant library containing individual deletions of 32 putative PKS genes.

Materials and methods

Strains

The *A. nidulans* strain IBT29539 (*argB2*, *pyrG89*, *veA1*, *nkuA*Δ) (Nielsen *et al.*, 2008) was used as the reference strain and for deletion-strain constructions. *Escherichia coli* strain DH5α was used for cloning.

Media

Fungal minimal medium (MM) was as described in Cove (1966), but with 1% glucose, 10 mM $NaNO_3$ and 2% agar. Medium for *alcA* promoter induction consisted of MM supplemented with 100 mM L-threonine and 100 mM glycerol as carbon source instead of 1% glucose. Polyketide screening media variants CYA, CYAs, YES and RT were prepared as per Frisvad & Samson (2004). CY20 medium consisted of CYA with 170 g sucrose; RTO contained RT with 30 g organic oat meal; and YE was made as YES but without sucrose. All media variants were supplemented with 10 mM uridine, 10 mM uracil and/or 4 mM L-arginine where appropriate.

Construction of *A. nidulans* gene deletion library

Individual PKS gene deletions were carried out as described previously (Nielsen *et al.*, 2006), except that the targeting fragments were assembled using Gateway technology (Hartley *et al.*, 2000) (see Table S1 for PCR oligonucleotide and Fig. S2 for an overview of the procedure). The *A. nidulans* transformants were streak purified and rigorously screened through three complementing diagnostic PCRs. Subsequently, the *Aspergillus fumigatus pyrG* marker was eliminated from all strains by selecting on 5-fluoroorotic acid medium before final verification by two additional complementing diagnostic PCRs (see Fig. S3 and Table S2). All strains have been deposited in the IBT strain collection, DTU, (http://www.fbd.dtu.dk/straincollection/).

Construction of the *ausA*-S1660A strain

The amino acid substitution of serine to alanine, S1660A, in *ausA* (AN8383) was created by USER fusion (Geu-Flores *et al.*, 2007) according to the method described by Hansen *et al.* (2011). The allele was transferred to IBT29539 and the *pyrG* marker was eliminated by direct repeat recombination, creating strain IBT31032 containing only the desired point mutation. The strain was verified to contain the *ausA*-S1660A allele by sequencing (StarSEQ, Germany). See Table S3 for primer details.

Ectopic integration of *ausA* into IS1

The gene, *ausA*, was PCR amplified by USER fusion (Geu-Flores *et al.*, 2007) and inserted into both pU1111-1 and pU1211-1 (Hansen *et al.*, 2011) creating pDH23 (*gpdA* promoter) and pDH24 (*alcA* promoter), respectively. For both plasmids, the gene-targeting substrate was excised by NotI digestion and transformed into IBT28738 using *A. nidulans argB* as a selectable marker. Transformants were streak purified and verified for correct integration into the IS1 site (Hansen *et al.*, 2011) by two complementing diagnostic PCRs.

Chemical analysis of the mutants

Strains were inoculated as three point stabs on solid media and incubated for 7 days at 37 °C in the dark. Metabolite extraction was performed according to the micro extraction procedure (Smedsgaard, 1997). Extracts were analyzed by two methods: (1) Ultra-high performance liquid chromatography-diode array detection (UHPLC-DAD) analyses using a Dionex RSLC Ultimate 3000 (Dionex, Sunnyvale, CA) equipped with a diode-array detector. Separation of 1 μL extract was obtained on a Kinetex C_{18} column (150 × 2.1 mm, 2.6 μm; Phenomenex, Torrence, CA) at 60 °C using a linear water–acetonitrile gradient starting from 15% CH_3CN to 100% (50 ppm trifluoroacetic acid) over 7 min at a flow rate of 0.8 mL min^{-1}. (2) Exact mass, HPLC-DAD-HRMS, was performed on a 5 cm × 3 μm, Luna C18(2) column (Phenomenex) using a water–acetonitrile gradient from 15% CH_3CN to 100% over 20 min (20 mM formic acid). LC-DAD-MS analysis was performed on a LCT oaTOF mass spectrometer (Micromass,

© 2011 Federation of European Microbiological Societies
Published by Blackwell Publishing Ltd. All rights reserved

Manchester, UK) as in Nielsen & Smedsgaard (2003) and Nielsen *et al.* (2009).

Isolation and structure elucidation of secondary metabolites

3,5-Dimethylorsellinic acid and dehydroaustinol were purified from large-scale ethyl acetate extracts prepared from 100 MM agar plates after 4 days' cultivation in darkness at 37 °C. The compounds were purified using a 10 × 250 mm Phenomenex pentafluorophenyl column (5 μm particles) with a water–acetonitrile gradient from 15% to 100% CH_3CN in 20 min using a flow of 5 mL min^{-1}. Arugosin A was isolated from an ethyl acetate extract of the reference strain grown on 200 CYAs agar plates using a Waters 19 × 300 mm C18 Delta Pak column (15 μm particles), gradient from 80% to 90% CH_3CN in 10 min, and a flow of 30 mL min^{-1}. The NMR spectra were acquired on a Varian Unity Inova 500 MHz spectrometer using standard pulse sequences. Additional details about the compound identification can be found in the supporting information.

Results and discussion

Selecting media that support secondary metabolite production in *A. nidulans*

The principle of using different media and/or incubation conditions for fungal secondary metabolite production has often been promoted (Oxford *et al.*, 1935; Davis *et al.*, 1966; Pitt *et al.*, 1983; Bode *et al.*, 2002; Scherlach & Hertweck, 2006). Based on our previous experiences (Frisvad, 1981; Frisvad & Filtenborg, 1983; Filtenborg *et al.*, 1990; Frisvad *et al.*, 2007), eight different media, CYA, CYAs, CY20, MM, RT, RTO, YE and YES, were initially selected for the analysis (Fig. 1a). HPLC analyses revealed a large number of different secondary metabolites produced by the *A. nidulans* reference strain on CYA, CYAs, CY20, RT, RTO and YES (Fig. 1b) and these metabolites served as a source for further investigation.

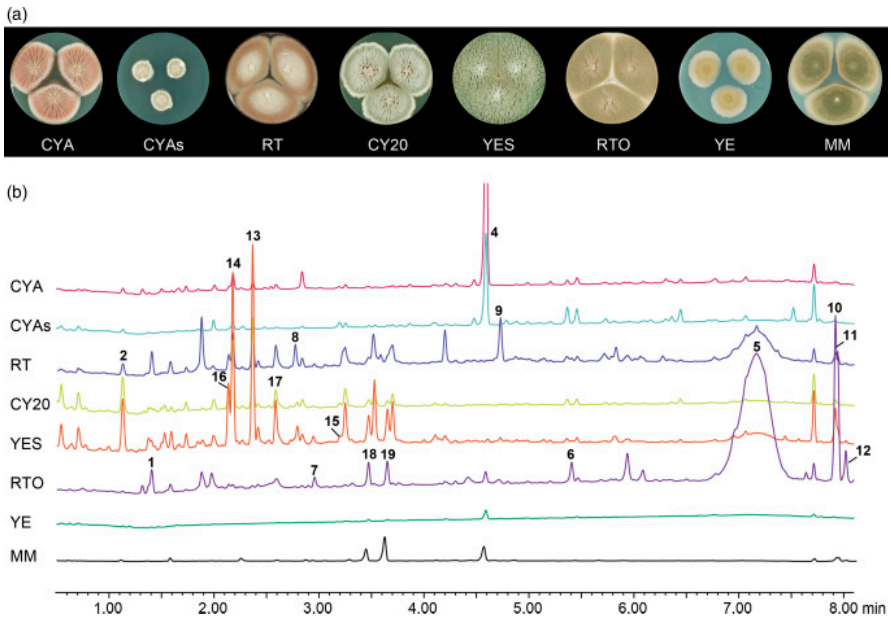

Fig. 1. (a) The appearance of the *Aspergillus nidulans* reference strain, IBT29539, cultivated on different media. (b) UV-chromatograms (210 nm) of extracts of the reference strain provides an excellent demonstration of the profound effect different media compositions have on production of secondary metabolites. From the bottom: minimal media (MM), yeast extract (YE), Raulin-Thom oatmeal (RTO), yeast extract sucrose (YES), Czapek yeast salt (CY20), Raulin-Thom (RT), Czapek yeast agar salt (CYAs), and Czapek yeast agar (CYA). The metabolite profiles on MM and YE media were considered to be redundant and these two media were therefore not used for further screening. Numbers above peaks correspond to compound identity as follows: monodictyphenone (**1**), orsellinic acid (**2**), sterigmatocystin (**4**), arugosin A (**5**), arugosin H (**6**), 2-ω-dihydroxyemodin (**7**), ω-hydroxyemodin (**8**), emodin (**9**), emericellin (**10**), shamixanthone (**11**), epi-shamixanthone (**12**), violaceol I (**13**), violaceol II (**14**), lecanoric acid (**15**), F9775A (**16**), F9775B (**17**), austinol (**18**) and dehydroaustinol (**19**).

© 2011 Federation of European Microbiological Societies
Published by Blackwell Publishing Ltd. All rights reserved

Construction and initial characterization of a genome-wide PKS gene deletion library

To investigate whether any of the compounds observed in Fig. 1 could be genetically linked to a PKS gene, we decided to take a global approach and individually deleted all 32 (putative and known) PKS genes in the *A. nidulans* genome (see Fig. S4), as defined from the annotation of the genome databases at the Broad Institute of Harvard and MIT and the *Aspergillus* Genome Database at Stanford (Arnaud *et al.*, 2010). All genes were individually deleted by replacing the entire ORFs using gene-targeting substrates based on the *pyrG* marker from *A. fumigatus* for selection. Before analyzing the deletion mutant strains, the *pyrG* marker was excised by direct repeat recombination (Nielsen *et al.*, 2006) in each case. This was carried out to ensure that the analyses of individual mutant strains were comparable to and not influenced by differences in the primary metabolism due to gene cluster-specific expression levels of the *pyrG* marker. All 32 deletion mutant strains (see Table S4) were viable and able to sporulate, showing that none of the 32 genes are essential for growth and that no polyketide product is essential for conidiation. As expected, the one strain carrying the *wA*Δ mutation formed white conidiospores as it fails to produce the naphthopyrone, YWA1, the precursor of green conidial pigment (Watanabe, 1998; Watanabe *et al.*, 1999).

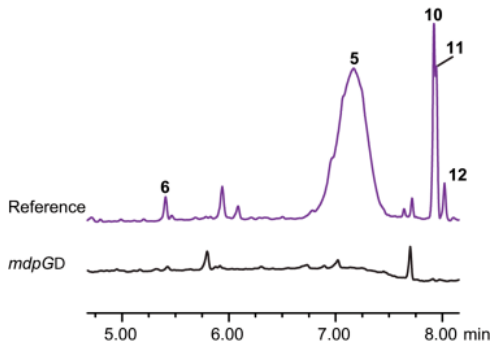

Fig. 2. The late portion of the UV-chromatogram (210 nm) of the *Aspergillus nidulans* reference strain and *mdpG*Δ on RTO medium. The deletion abolishes formation of arugosin A (**5**), arugosin H (**6**), emericellin (**10**), shamixanthone (**11**) and epi-shamixanthone (**12**) and a few unidentified peaks.

In addition to *wA*, eight additional PKS genes have previously been linked to metabolites. In our analysis, key compounds representing four of these gene clusters could be detected: monodictyphenone (**1**) (observed on RTO, YES and CY20), orsellinic acid (**2**) (observed on YES, CY20, RT, CYAs and CYA), emericellamide (A) (**3**) (observed on all media) and sterigmatocystin (**4**) (observed on RTO, CYAs and CYA). To verify the previously published gene links to these compounds, we individually compared the metabolic profiles of the reference strain to the corresponding profiles obtained with the single PKS gene deletion mutant strains. In agreement with previous analyses, these four compounds

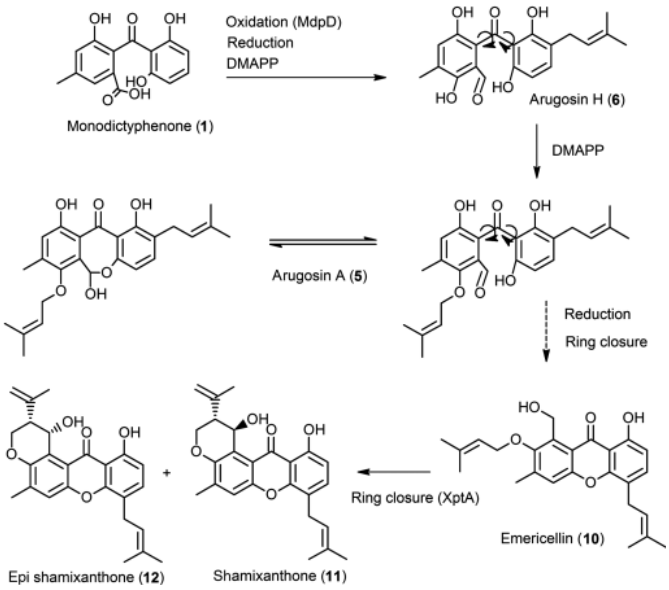

Fig. 3. Proposed biosynthetic route of the arogusins and shamixanthones. As seen in Fig. 2, arugosin A is produced in large amounts relative to the expected end products: emericellin (**10**) and shamixanthones (**11** and **12**). DMAPP, dimethylallylpyrophosphate. MdpG and XptA are enzymatic activities as proposed by Sanchez *et al.* (2011).

© 2011 Federation of European Microbiological Societies
Published by Blackwell Publishing Ltd. All rights reserved

disappeared in *mdpG* (Bok *et al*., 2009), *orsA* (Schroeckh *et al*., 2009), *easB* (Chiang *et al*., 2008) and *stcA* (Yu & Leonard, 1995) deletion strains of our library (Fig. S5). Compounds resulting from the remaining four PKS genes were identified by activating the gene clusters by controlled expression of the transcription factor gene in the cluster (Bergmann *et al*., 2007; Chiang *et al*., 2009) or by deleting *sumO* that influences regulation of biological processes at many different levels (Szewczyk *et al*., 2008). Expression from these clusters is apparently not triggered by growth on any of our media, and natural conditions provoking their activation remain to be discovered.

Next, we performed a comparison of the metabolite profiles from the 32 deletion mutants with those obtained with the reference strain with the aim of uncovering novel genetic links between PKS genes and polyketides. The most significant changes are described below.

mdpG is involved in the biosynthesis of arugosins

First we focused our attention on the most prominent compound produced on RTO, YES, CY20 and RT media, which eluted as a broad peak around 7.2 min. This compound completely disappeared in the *mdpG*Δ strain (Fig. 2 and Fig. S6). Moreover, it had a characteristic UV spectrum in the UHPLC analysis indicating an arugosin-like metabolite. MS analysis indicated the compound to be arugosin A (*m/z* 425 a.m.u. for $[M+H]^+$), which to our knowledge has not been reported before from *A. nidulans*. We therefore decided to confirm the structure of this compound (**5**). A large-scale extraction was performed and the metabolite was purified. The NMR data in dimethyl sulfoxide are in agreement with the literature (Kawahara *et al*., 1988) for the hemiacetal form of arugosin A except that the equilibrium was shifted completely to the open form (Fig. 3). In methanol, the NMR data showed that the compound exists in equilibrium between the closed and open ring form (data not shown), explaining the broad peak observed in Fig. 2. A minor peak could be assigned as a mono-prenylated arugosin as $[M+H]^+$ at *m/z* 357 a.m.u. The MS data of this compound did not indicate loss of a prenyl moiety, suggesting that it is arugosin H (**6**), a likely immediate precursor of arugosin A (Fig. 3). Hence, our data show that *mdpG*, which is known for its role in formation of monodictyphenone, is also involved in formation of arugosins.

It is not unusual that one PKS gene cluster is responsible for the biosynthesis of a family of structurally similar compounds (Walsch, 2002; Kroken *et al*., 2003; Frisvad *et al*., 2004; Amoutzias *et al*., 2008). In the original analysis of the *mdpG* gene cluster, it was activated due to remodeling of the chromatin landscape, which occurs in a *cclA* deletion strain (Chiang *et al*., 2010). That study genetically linked the *mdpG* gene cluster to eight emodin analogues, including several aminated species, which were detected and tentatively identified. In our analyses, we also detected several emodins including 2-ω-dihydroxyemodin (**7**), ω-hydroxyemodin (**8**) and emodin (**9**), as well as the more apolar compounds emericellin (**10**), shamixanthone (**11**) and epishamixanthone (**12**) (Fig. 1 and Fig. S7). Like in the original study, all emodins disappear in our *mpdG*Δ strain.

Recently, it was demonstrated that the polyketide part of prenylated xanthones also could be coupled to *mpdG* (Sanchez *et al*., 2011). Our finding that *mpdG* is involved in formation of arugosins indicates that these compounds serve as intermediates in the conversion of monodictyphenone into xanthones, Fig. 3. In agreement with this, previous studies have reported arugosins to be precursors for emericellin (**10**) and shamixanthones (**11**) and (**12**) (Ahmed *et al*., 1992; Kralj *et al*., 2006; Márquez-Fernández *et al*., 2007), but have not established a genetic link to *mpdG*.

AN7903 and *orsA* are involved in violaceol production

Our reference strain produces the antibiotic violaceol I (**13**) and II (**14**), in significant amounts (Fig. 4 and Fig. S8). These two diphenyl ethers have been identified in *Emericella*

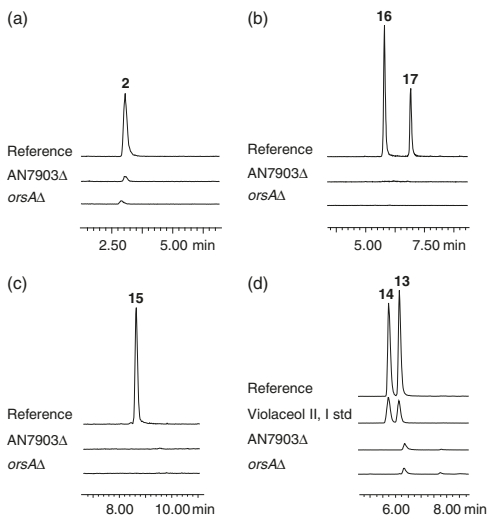

Fig. 4. Extracted ion chromatograms of metabolic extracts from the reference strain and the two mutants *orsA*Δ and AN7903Δ after cultivation on YES medium. Compounds shown are (a) *m/z* 167 $[M-H]^-$, orsellinic acid (**2**), (b) *m/z* 397 $[M+H]^+$, F9775A and B (**16** and **17**, respectively), (c) *m/z* 317 $[M-H]^-$, lecanoric acid (**15**) and (d) *m/z* 261 $[M-H]^-$, violaceol I and II (**13** and **14**). An extracted ion chromatogram of a violaceol I and II in house standard is included in (d).

© 2011 Federation of European Microbiological Societies
Published by Blackwell Publishing Ltd. All rights reserved

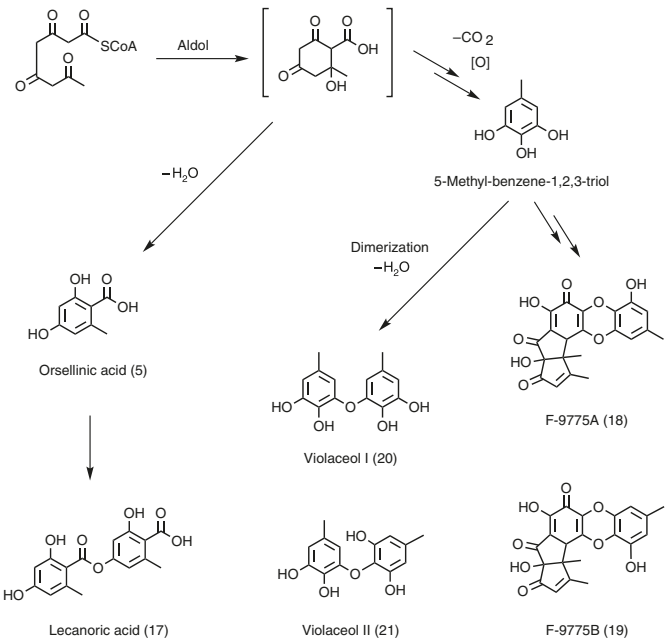

Fig. 5. Proposed biosynthetic pathways related to the *orsA* gene cluster. A common C_8 aldol intermediate, presented in the bracket, can by loss of water and enolization lead to orsellinic acid and by further esterification to lecanoric acid, or be decarboxylated and further oxidized to yield the C_7 compound 5-methyl-benzene-1,2,3-triol. This compound is the precursor of the two diphenyl ethers violaceol I and II and the pigments F-9775A and B.

violacea, *Aspergillus sydowi* and *Aspergillus funiculosus* (Taniguchi *et al*., 1978; Yamazaki & Maebayas, 1982) and recently also in *A. nidulans* (Nahlik *et al*., 2010). Our analysis now links the biosynthesis of the two violaceols to *orsA* as they disappear in our *orsA*Δ strain. It has previously been shown that *orsA* (AN7909) is involved in the formation of orsellinic acid (**2**), lecanoric acid (**15**), the two colored compounds F-9775A (**16**) and F-9775B (**17**), orcinol, diorcinol, gerfeldin and deoxy-gerfeldin. (Schroeckh *et al*., 2009; Sanchez *et al*., 2010). Our analysis confirms the link between orsellinic acid, lecanoric acid, diorcinol, F-9775A, F-9775B to *orsA* as these compounds are missing in the *orsA*Δ strain. However, we have not been able to detect the gerfeldins in any of our strains, and apparently our conditions favor violaceol and not gerfeldin formation.

The violaceols are formed by dimerization of two C_7 monomers of 5-methylbenzene-1,2,3-triol, a compound that we could tentatively detect as $[M\text{-}H]^-$ at *m/z* 139 in cultivation extracts. The C_7 backbone of 5-methylbenzene-1,2,3-triol, may conceivably be formed by decarboxylation of a C_8 aldol intermediate as suggested by Turner 40 years ago (Turner, 1971) (Fig. 5). This C_8 intermediate also serves as a branch point towards orsellinic acid.

Interestingly, the same compounds that disappear in the *orsA*Δ strain also disappear in AN7903Δ, a strain missing a PKS gene separated from *orsA* by only ~20 kb (Fig. 4). This result does not contradict the original assignment of *orsA* as the PKS gene responsible for production of orsellinic acid. Although the enzymes encoded by the two genes are predicted to share many of the same functional domains, AN7903 is larger by around 500 amino acid residues and contains a methyl-transferase domain, which is not required for orsellinic acid production. Moreover, we note that Schroeckh *et al*. (2009) observed that both AN7903 and *orsA* were upregulated when orsellinic acid was induced by co-cultivation with *Streptomyces hygroscopicus*, indicating cross-talk between the two clusters. Surprisingly, what appear to be trace amounts of orsellinic acid can be detected as *m/z* 167 $[M\text{-}H]^-$ in both the AN7903Δ and the *orsA*Δ strains (Fig. 4). The source of this residual orsellinic acid remains elusive, but it could possibly stem from unmethylated byproducts from the PKS, AN8383, that produces 3,5-dimethylorsellinic acid, see below.

AN8383 is responsible for austinol and dehydroaustinol biosynthesis

Interestingly, production of austinol (**18**) and dehydroaustinol (**19**) was observed in the reference strain on several media (Fig. 1). Despite the fact that the production of these compounds is known from *A. nidulans* (Szewczyk *et al*., 2008), they have not yet been assigned to a specific gene.

© 2011 Federation of European Microbiological Societies
Published by Blackwell Publishing Ltd. All rights reserved

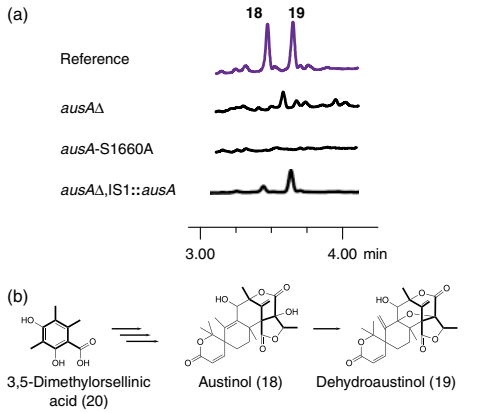

Fig. 6. (a) UV-chromatograms (210 nm) showing the presence of austinol (**18**) and dehydroaustinol (**19**) in the reference strain, *ausA*Δ and ausA-S1660A after growth on RTO medium. The lower trace (*ausA*Δ, IS1::*ausA*) is the *ausA*Δ mutant expressing *ausA* under control of the *gpdA* promoter from IS1 (IBT31281, cultured on MM) (b) Incorporation of 3,5-orsellinic acid (**20**) into the meroterpenoid austinol. The carbon skeleton of orsellinic acid is presented in bold.

Only the AN8383Δ strain failed to produce the two austinols on all the media, which triggered austinol production in the reference strain (Fig. 6a). This, phenotype could be rescued by inserting the structural gene of AN8383 under the control of the *gdpA* promoter into an ectopic locus, IS1 (Hansen *et al.*, 2011) (Fig. 6a). Moreover, a point mutant strain AN8383-S1660A also failed to produce austinols on these six media (Fig. 6a). In this strain, the DSL motif of the AN8383 PKS has been mutated to DAL, preventing the phosphopantetheine moiety of coenzyme A to attach to the acyl carrier protein domain of the PKS, thus disrupting polyketide synthesis (Evans *et al.*, 2008). The lack of austinols can thus be linked directly to an AN8383-encoded function rather than to silencing of another gene caused by chromatin changes provoked by the AN8383 deletion.

To confirm the role of AN8383 in austinol production, we constructed a new strain that expresses the AN8383 ORF controlled by the inducible *alcA* promoter from the ectopic locus, IS1 (Hansen *et al.*, 2011). On inductive medium, the subsequent LC-MS analysis showed a large novel peak eluting at ca. 6 min (see Fig. S9). The corresponding compound was purified and the structure was elucidated by NMR (Fig. S10), identifying 3,5-dimethylorsellinic acid (**20**), which is in good agreement with the route of synthesis previously proposed for austinol (Fig. 6b; Geris & Simpson, 2009). In a parallel analysis using a strain expressing AN8383 under the control of the constitutive *gpdA* promoter we obtained the same result (data not shown).

Together, the results strongly indicate that AN8383 encodes a PKS producing 3,5-dimethylorsellinic acid and that this compound serves as the first intermediate in the complex biosynthesis of austinol and dehydroaustinol that also involves a yet unidentified prenyl transferase(s). Based on these results, we have named the locus AN8383, *ausA*.

Concluding remarks

In the present study, we constructed a genome-wide PKS deletion library, which we screened for effects on polyketide production on a variety of media. This analysis has provided novel links between PKS genes and polyketide products demonstrating the strength of this approach. Many PKS genes still remain to be functionally connected to products, as many gene clusters have not yet been activated. As the repertoire of tools and methods to induce gene expression is rapidly increasing, new polyketide compounds will likely soon be uncovered in *A. nidulans*. To this end, the genome-wide PKS gene deletion library presented here will undoubtedly serve as a useful resource.

Acknowledgements

This work was supported by the Danish Research Agency for Technology and Production, grant # 09-064967. We thank Lisette Knoth-Nielsen for her dedicated and valuable technical assistance in the laboratory. In addition, we thank Rasmus John Normand Frandsen for suggestions and critical reading of the manuscript.

References

Ahmed SA, Bardshiri E, McIntyre CR & Simpson TJ (1992) Biosynthetic-studies on Tajixanthone and Shamixanthone, Polyketide Hemiterpenoid Metabolites of *Aspergillus variecolor*. *Aust J Chem* **45**: 249–274.

Amoutzias GD, Van de Peer Y & Mossialos D (2008) Evolution and taxonomic distribution of nonribosomal peptide and polyketide synthases. *Future Microbiol* **3**: 361–370.

Arnaud MB, Chibucos MC, Costanzo MC *et al.* (2010) The *Aspergillus* genome database, a curated comparative genomics resource for gene, protein and sequence information for the *Aspergillus* research community. *Nucleic Acids Res* **38**: D420–D427.

Bentley R (2000) Mycophenolic acid: a one hundred year Odyssey from antibiotic to immunosuppressant. *Chem Rev* **100**: 3801–3825.

Bérdy J (2005) Bioactive microbial metabolites. *J Antibiot (Tokyo)* **58**: 1–26.

Bergmann S, Schümann J, Scherlach K, Lange C, Brakhage AA & Hertweck C (2007) Genomics-driven discovery of PKS-NRPS hybrid metabolites from *Aspergillus nidulans*. *Nat Chem Biol* **3**: 213–217.

© 2011 Federation of European Microbiological Societies
Published by Blackwell Publishing Ltd. All rights reserved

Bode HB, Bethe B, Höfs R & Zeeck A (2002) Big effects from small changes: possible ways to explore nature's chemical diversity. *Chembiochem* **3**: 619–627.

Bok JW, Chiang YM, Szewczyk E *et al.* (2009) Chromatin-level regulation of biosynthetic gene clusters. *Nat Chem Biol* **5**: 462–464.

Chang P-K, Ehrlich KC & Fujii I (2009) Cyclopiazonic acid biosynthesis of *Aspergillus flavus* and *Aspergillus oryzae*. *Toxins* **1**: 74–99.

Chiang Y-M, Szewczyk E, Nayak T *et al.* (2008) Molecular genetic mining of the *Aspergillus* secondary metabolome: discovery of the emericellamide biosynthetic pathway. *Chem Biol* **15**: 527–532.

Chiang Y-M, Szewczyk E, Davidson AD, Keller N, Oakley BR & Wang CCC (2009) A gene cluster containing two fungal polyketide synthases encodes the biosynthetic pathway for a polyketide, asperfuranone, in *Aspergillus nidulans*. *J Am Chem Soc* **131**: 2965–2970.

Chiang Y-M, Szewczyk E, Davidson AD, Entwistle R, Keller N, Wang CCC & Oakley BR (2010) Characterization of the *Aspergillus nidulans* monodictyphenone gene cluster. *Appl Environ Microb* **76**: 2067–2074.

Chooi Y-H, Cacho R & Tang Y (2010) Identification of the viridicatumtoxin and griseofulvin gene clusters from *Penicillium aethiopicum*. *Chem Biol* **17**: 483–494.

Cove DJ (1966) The induction and repression of nitrate reductase in the fungus *Aspergillus nidulans*. *Biochim Biophys Acta* **113**: 51–56.

Cox RJ (2007) Polyketides, proteins and genes in fungi: programmed nano-machines begin to reveal their secrets. *Org Biomol Chem* **5**: 2010–2026.

Davis ND, Diener UL & Eldridge DW (1966) Production of aflatoxins B1 and G1 by *Aspergillus flavus* in a semisynthetic medium. *Appl Microbiol* **14**: 378–380.

Evans SE, Williams C, Arthur CJ, Burston SG, Simpson TJ, Crosby J & Crump MP (2008) An ACP structural switch: conformational differences between the apo and holo forms of the actinorhodin polyketide synthase acyl carrier protein. *ChemBioChem* **9**: 2424–2432.

Filtenborg O, Frisvad JC & Thrane U (1990) The significance of yeast extract composition on metabolite production in *Penicillium*. *Modern Concepts in Penicillium and Aspergillus Classification* (Samson RA & Pitt JI, eds), pp. 433–440. Plenum Press, New York.

Frisvad JC (1981) Physiological criteria and mycotoxin production as aids in identification of common asymmetric penicillia. *Appl Environ Microb* **41**: 568–579.

Frisvad JC & Filtenborg O (1983) Classification of terverticillate penicillia based on profiles of mycotoxins and other secondary metabolites. *Appl Environ Microb* **46**: 1301–1310.

Frisvad JC & Samson RA (2004) Polyphasic taxonomy of *Penicillium* subgenus *Penicillium*. A guide to identification of food and air-borne terverticillate Penicillia and their mycotoxins. *Stud Mycol* **49**: 1–173.

Frisvad JC, Smedsgaard J, Larsen TO & Samson RA (2004) Mycotoxins, drugs and other extrolites produced by species in *Penicillium* subgenus *Penicillium*. *Stud Mycol* **49**: 201–241.

Frisvad JC, Smedsgaard J, Samson RA, Larsen TO & Thrane U (2007) Fumonisin B(2) production by *Aspergillus niger*. *J Agr Food Chem* **55**: 9727–9732.

Galagan JE, Calvo SE, Cuomo C *et al.* (2005) Sequencing of *Aspergillus nidulans* and comparative analysis with *A. fumigatus* and *A. oryzae*. *Nature* **438**: 1105–1115.

Geris R & Simpson TJ (2009) Meroterpenoids produced by fungi. *Nat Prod Rep* **26**: 1063–1094.

Geu-Flores F, Nour-Eldin HH, Nielsen MT & Halkier BA (2007) USER fusion: a rapid and efficient method for simultaneous fusion and cloning of multiple PCR products. *Nucleic Acids Res* **35**: e55.

Hansen BG, Salomonsen B, Nielsen MT, Nielsen JB, Hansen NB, Nielsen KF, Regueira TB, Nielsen J, Patil KR & Mortensen UH (2011) A versatile gene expression and characterization system for *Aspergillus*: heterologous expression of the gene encoding the polyketide synthase from the mycophenolic acid gene cluster from *Penicillium brevicompactum* as a case study. *Appl Environ Microb.* **77**: 3044–3051.

Hartley JL, Temple GF & Brasch MA (2000) DNA cloning using *in vitro* site-specific recombination. *Genome Res* **10**: 1788–1795.

Hertweck C (2009) The biosynthetic logic of polyketide diversity. *Angew Chem Int Edit* **48**: 4688–4716.

Kawahara N, Nozawa K, Nakajima S & Kawai K (1988) Studies on fungal products. Part 15. Isolation and structure determination of arugosin E from *Aspergillus silvaticus* and cycloisoemericellin from *Emericella striata*. *J Chem Soc Perk Trans I* **1988**: 907–911.

Keller N, Turner G & Bennett J (2005) Fungal secondary metabolism – from biochemistry to genomics. *Nat Rev Microbiol* **3**: 937–947.

Kralj A, Kehraus S, Krick A, Eguereva E, Kelter G, Maurer M, Wortmann A, Fiebig HH & Konig GM (2006) Arugosins G and H: prenylated polyketides from the marine-derived fungus *Emericella nidulans* var. *acristata*. *J Nat Prod* **69**: 995–1000.

Kroken S, Glass NL, Taylor JW, Yoder OC & Turgeon BG (2003) Phylogenomic analysis of type I polyketide synthase genes in pathogenic and saprobic ascomycetes. *P Nat Acad Sci USA* **100**: 15670–15675.

Lai L-ST, Tsai T-H, Wang TC & Cheng T-Y (2005) The influence of culturing environments on lovastatin production by *Aspergillus terreus*. *Enzyme Microb Tech* **36**: 737–748.

Månsson M, Klejnstrup ML, Phipps RK, Nielsen KF, Frisvad JC, Gotfredsen CH & Larsen TO (2010) Isolation and NMR characterization of fumonisin B2 and a new fumonisin B6 from *Aspergillus niger*. *J Agr Food Chem* **58**: 949–953.

Márquez-Fernández O, Trigos A, Ramos-Balderas JL, Viniegra-González G, Deising HB & Aguirre J (2007) Phosphopantetheinyl transferase CfwA/NpgA is required for *Aspergillus nidulans* secondary metabolism and asexual development. *Eukaryot cell* **6**: 710–720.

© 2011 Federation of European Microbiological Societies
Published by Blackwell Publishing Ltd. All rights reserved

Nahlik K, Dumkow M, Bayram O *et al.* (2010) The COP9 signalosome mediates transcriptional and metabolic response to hormones, oxidative stress protection and cell wall rearrangement during fungal development. *Mol Microbiol* **78**: 964–979.

Newman DJ & Cragg GM (2007) Natural products as sources of new drugs over the last 25 years. *J Nat Prod* **70**: 461–477.

Nielsen JB, Nielsen ML & Mortensen UH (2008) Transient disruption of non-homologous end-joining facilitates targeted genome manipulations in the filamentous fungus *Aspergillus nidulans*. *Fungal Genet Biol* **45**: 165–170.

Nielsen KF & Smedsgaard J (2003) Fungal metabolite screening: database of 474 mycotoxins and fungal metabolites for dereplication by standardised liquid chromatography-UV-mass spectrometry methodology. *J Chromatogr A* **1002**: 111–136. ISI: 000183799200011.

Nielsen KF, Mogensen JM, Johansen M, Larsen TO & Frisvad JC (2009) Review of secondary metabolites and mycotoxins from the *Aspergillus niger* group. *Anal Bioanal Chem* **395**: 1225–1242.

Nielsen ML, Albertsen L, Lettier G, Nielsen JB & Mortensen UH (2006) Efficient PCR-based gene targeting with a recyclable marker for *Aspergillus nidulans*. *Fungal Genet Biol* **43**: 54–64.

Nierman WC, Pain A, Anderson MJ *et al.* (2005) Genomic sequence of the pathogenic and allergenic filamentous fungus *Aspergillus fumigatus*. *Nature* **438**: 1151–1156.

Oxford AE, Raistrick H & Simonart P (1935) Studies in the biochemistry of microorganisms. XLIV. Fulvic acid, a new crystalline yellow pigment, a metabolic product of *P. griseofulvum* Dierckx, *P. flexuosum* Dale and *P. brefeldianum* Dodge. *Biochem J* **29**: 1102–1115.

Pitt JI, Hocking AD & Glenn DR (1983) An improved medium for the detection of *Aspergillus flavus* and *A. parasiticus*. *J Appl Bacteriol* **54**: 109–114.

Sanchez JF, Chiang YM, Szewczyk E, Davidson AD, Ahuja M, Elizabeth Oakley C, Woo Bok J, Keller N, Oakley BR & Wang CC (2010) Molecular genetic analysis of the orsellinic acid/F9775 gene cluster of *Aspergillus nidulans*. *Mol Biosyst* **6**: 587–593.

Sanchez JF, Entwistle R, Hung J, Yaegashi J, Jain S, Chiang Y, Wang C & Oakley B (2011) Genome-based deletion analysis reveals the prenyl xanthone biosynthesis pathway in *Aspergillus nidulans*. *J Am Chem Soc* **133**: 4010–4017.

Scherlach K & Hertweck C (2006) Discovery of aspoquinolones A-D, prenylated quinoline-2-one alkaloids from *Aspergillus nidulans*, motivated by genome mining. *Org Biomol Chem* **4**: 3517–3520.

Scherlach K, Schuemann J, Dahse HM & Hertweck C (2010) Aspernidine A and B, prenylated isoindolinone alkaloids from the model fungus *Aspergillus nidulans*. *J Antibiot (Tokyo)* **63**: 375–377.

Schroeckh V, Scherlach K, Nützmann HW, Shelest E, Schmidt-Heck W, Schuemann J, Martin K, Hertweck C & Brakhage AA (2009) Intimate bacterial-fungal interaction triggers biosynthesis of archetypal polyketides in *Aspergillus nidulans*. *P Natl Acad Sci USA* **106**: 14558–14563.

Schümann J & Hertweck C (2006) Advances in cloning, functional analysis and heterologous expression of fungal polyketide synthase genes. *J Biotechnol* **124**: 690–703.

Smedsgaard J (1997) Micro-scale extraction procedure for standardized screening of fungal metabolite production in cultures. *J Chromatogr A* **760**: 264–270.

Smith S & Tsai S-C (2007) The type I fatty acid and polyketide synthases: a tale of two megasynthases. *Nat Prod Rep* **24**: 1041–1072.

Szewczyk E, Chiang Y-M, Oakley C, Davidson A, Wang C & Oakley B (2008) Identification and characterization of the asperthecin gene cluster of *Aspergillus nidulans*. *Appl Environ Microb* **74**: 7607–7612.

Taniguchi M, Kaneda N, Shibata K & Kamikawa T (1978) Isolation and biological activity of a self-growth- inhibitor from *Aspergillus sydowi*. *Agr Biol Chem* **42**: 1629–1630.

Turner WB (1971) *Fungal Metabolites*, Academic Press, London, pp. 1–446.

von Döhren H (2009) A survey of nonribosomal peptide synthetase (NRPS) genes in *Aspergillus nidulans*. *Fungal Genet Biol* **46** (suppl 1): S45–S52.

Walsch CT (2002) Combinatorial biosynthesis of antibiotics: challenges and opportunities. *ChemBioChem* **3**: 124–134.

Watanabe A, Ono Y, Fujii I, Sankawa U, Mayorga ME, Timberlake WE & Ebizuka Y (1998) Product identification of polyketide synthase coded by *Aspergillus nidulans wA* gene. *Tetrahedron Lett* **39**: 7733–7736.

Watanabe A, Fujii I, Sankawa U, Mayorga M, Timberlake W & Ebizuka Y (1999) Re-identification of *Aspergillus nidulans wA* gene to code for a polyketide synthase of naphthopyrone. *Tetrahedron Lett* **40**: 91–94.

Yamazaki M & Maebayashi Y (1982) Structure determination of violaceol-I and -II, new fungal metabolites from a strain of *Emericella violacea*. *Chem Pharm Bull (Tokyo)* **30**: 514–518.

Yu JH & Leonard TJ (1995) Sterigmatocystin biosynthesis in *Aspergillus nidulans* requires a novel type-I polyketide synthase. *J Bacteriol* **177**: 4792–4800.

Supporting Information

Additional Supporting Information may be found in the online version of this article:

Fig. S1. Eight known metabolites that have been linked to specific PKS genes in *Aspergillus nidulans*.
Fig. S2. A graphical illustration of the procedure used to make the gene targeting fragments for the PKS deletions.
Fig. S3. Procedure for diagnostic PCR.
Fig. S4. Chromosome map showing the position of the 32 PKS genes.
Fig. S5. Verification that the polyketide is absent in selected deletion mutants.

© 2011 Federation of European Microbiological Societies
Published by Blackwell Publishing Ltd. All rights reserved

Fig. S6. Positive mode extracted ion chromatograms for the *mdpG*Δ strain cultivated on RTO.
Fig. S7. Additional polyketides that were detected in metabolite extracts in this study.
Fig. S8. The mutants *orsA*Δ and AN7903Δ lack production of violaceols.
Fig. S9. Extracted ion chromatograms of metabolic extracts from the reference and *ausA*Δ strains.
Fig. S10. ^{1}H NMR spectrum of 3,5-dimethylorsellinic acid in dimethyl sulfoxide-d_6.
Fig. S11. ^{1}H NMR spectrum of dehydroaustinol in $CDCl_3$.
Fig. S12. ^{1}H NMR spectrum of arugosin A open form in dimethyl sulfoxide-d_6.
Table S1. PCR primers for Gateway assembly.
Table S2. Oligonucleotide primers for diagnostic PCR.
Table S3. Additional oligonucleotides used in the study.
Table S4. The constructed *Aspergillus nidulans* strains have been deposited into the IBT Culture Collection.

Please note: Wiley-Blackwell is not responsible for the content or functionality of any supporting materials supplied by the authors. Any queries (other than missing material) should be directed to the corresponding author for the article.

© 2011 Federation of European Microbiological Societies
Published by Blackwell Publishing Ltd. All rights reserved

A Genome-wide Polyketide Synthase Deletion Library uncovers Novel Genetic Links to Polyketides and Meroterpenoids in *Aspergillus nidulans*

Michael L. Nielsen, Jakob B. Nielsen, Christian Rank, Marie L. Klejnstrup, Dorte M. K. Holm, Katrine H. Brogaard, Bjarne G. Hansen, Jens C. Frisvad, Thomas O. Larsen and Uffe H. Mortensen

Supporting Information

Additional Supporting Information may be found in the online version of this article:

Figures (page 3)

Supporting Information

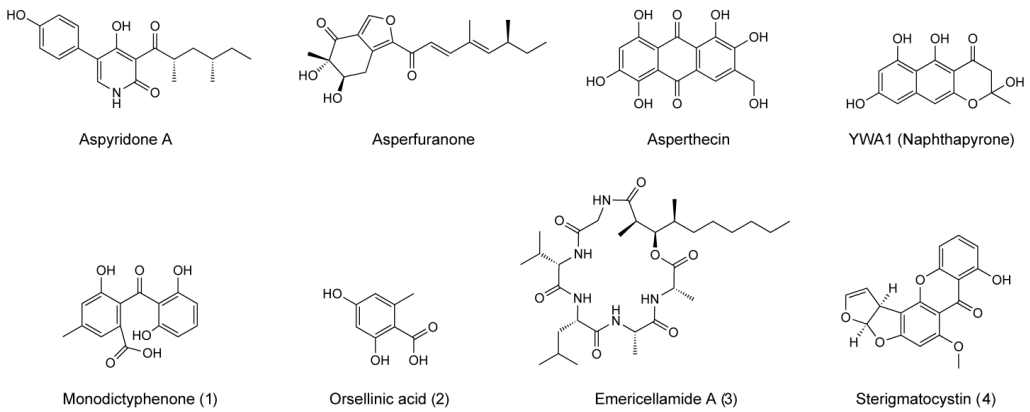

Fig. S1. Eight known metabolites that have been linked to specific PKS genes in *A. nidulans*. Aspyridone (*adpA*), asperfuranone (*afoE/G*), asperthecin (*aptA*), YWA1 (*wA*), (**1**) monodictypheonone (*mdpG*), (**2**) orsellinic acid (*orsA*), (**3**) emericellamide (A) (*easB*) and (**4**) sterigmatocystin (*stcA*).

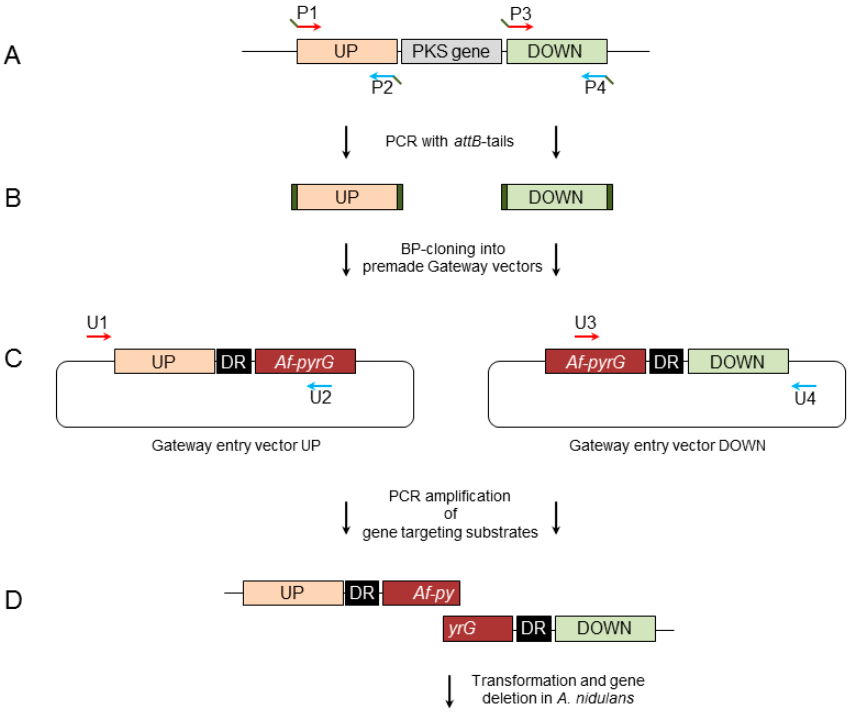

Fig. S2. A graphical illustration of the procedure employed to make the gene targeting fragments for the PKS deletions. Genomic DNA serves as template for two separate PCR reactions (A) that amplify the UP-stream and DOWN-stream regions of the PKS gene targeted for deletion. The oligonucleotide pairs contain approx. 20 nucleotide *attB* sequences that allow BP-recombination according to the Gateway cloning system (Invitrogen). (B) The PCR products with the specific *attB* sequences are incorporated into donor vectors (C) that contain *A. fumigatus pyrG* flanked by a sequence (DR) that serves as a direct repeat in the final mutant. The resulting plasmids (D) are purified from *E. coli*, and used as template to amplify gene-targeting substrates by PCR. Universal oligonucleotides U1 & U2 are used to amplify the UP-stream targeting fragments; and D1 and D2 are used to amplify DOWN-stream targeting fragments. The final targeting substrates (E) are co-transformed as bipartite gene-targeting substrates.

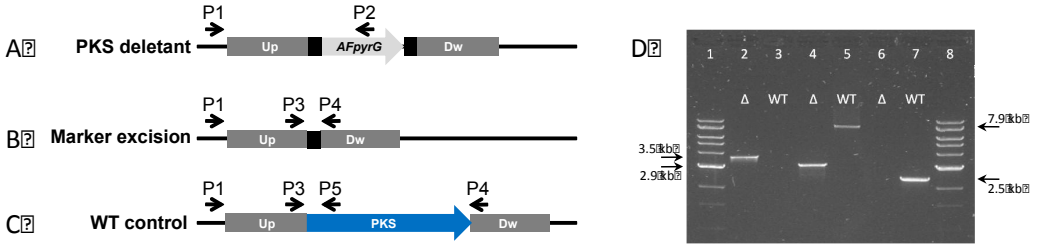

Fig. S3. Illustration of the diagnostic PCR procedure. A standard repertoire of PCR reactions were used in the analysis of PKS deletion mutant strains. (A) shows PCR check of a targeting event for a given PKS locus. Up and Dw depicts the up- and downstream flanks of the PKS, respectively. The forward primer, P1, anneals outside the targeting sequence and the reverse primer, P2, is placed within the *A. fumigatus pyrG* (*AFpyrG*) marker gene. (B) the marker gene has been excised from the locus and the primer pair, P1 or P3 with P4, binds on either side of the remaining direct repeat sequence. The reaction can also occur on reference strain genomic DNA template, but in this case to produce a significantly larger fragment as illustrated in (C). In addition to this, a PCR reaction (C) using P1 or P3 with P5 positioned inside the PKS gene, identifies false positives. The PKS gene is shown as a blue arrow, the marker gene as a light grey arrow and the direct repeat as black squares. Drawing is not to scale. A control PCR reaction with reference strain genomic DNA as template is always included. (D) shows a typical agarose gel result for the PCR verification of a deletion strain (AN0150 (*mdpG*) in this case). Lanes are indicated by numbers 1-8 below the wells. Lane 1 & 8, 1 kb ladder from New England Biolabs. Lane 2 shows the test for correct replacement of *mdpG* with the AF*pyrG* marker by P1 & P2 (test A) in the deletion strain candidate giving the 3.5 kb band, and the expected absence of a band in the WT control reaction in lane 3. Lanes 4 and 5, confirms marker loss after counter-selecting on 5-FOA via primers P1 and P4 (test B), the pop-out event is verified by the 2.9 kb band in lane 4 whereas WT gave the expected larger 7.9 kb band. Lane 6 and 7 with primers P1 & P5 confirm that the deletion strain is pure and does not contain WT nuclei (intact *mdpG* sequence). All spore PCR reactions were run in triplicates.

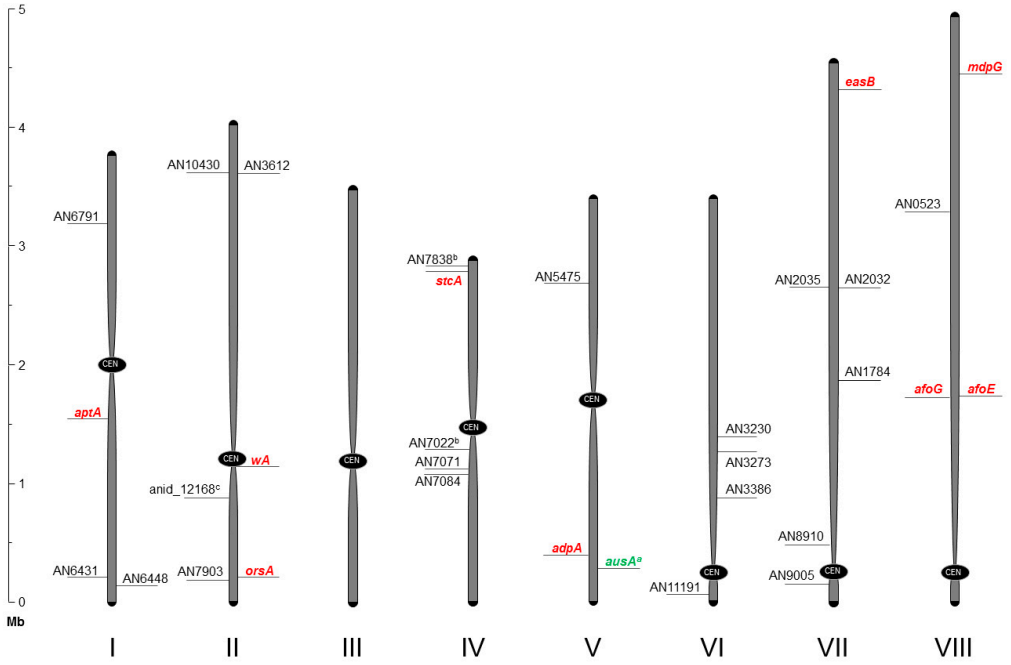

Fig. S4. Chromosome map showing the position of the 32 PKS genes on the eight chromosomes of *A. nidulans*. The map was generated based mainly on information from the *Aspergillus* Genome Database at Stanford. The approximate location of the centromere is shown for each of the eight chromosomes. Telomeres are indicated as black tips and are not to scale. PKS genes that have previously been linked to polyketide compounds have been marked in red with the corresponding gene names. The scale bar on the left indicates size in mega bases (Mb). [a] In the present study, we name the PKS gene AN8383, *ausA*, (marked in green) due to its role in the biosynthesis of austinols. [b] These ORFs have been removed from the genome annotation of the *Aspergillus* Genome Database at Stanford during preparation of Version 5. We have made the deletions according to Version 4 of annotation. [c] The annotation of this gene was taken from the genome databases at the Broad Institute of Harvard and MIT.

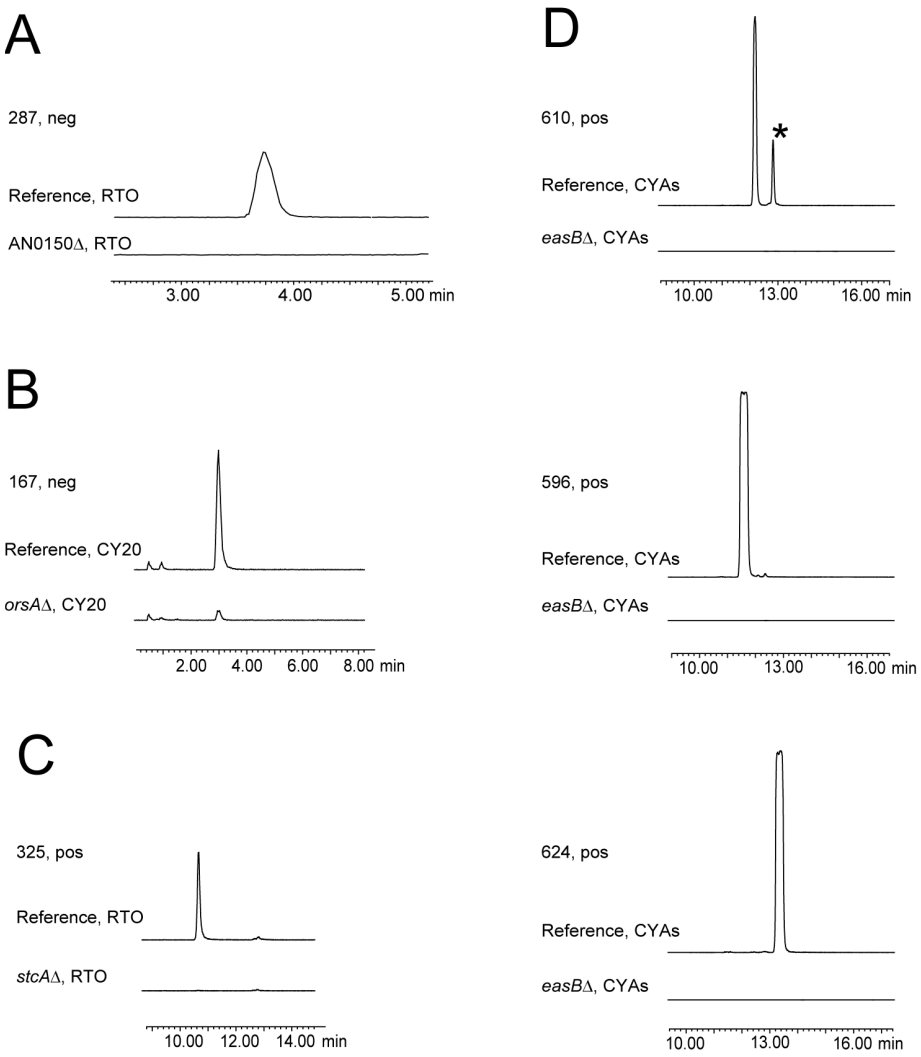

Fig. S5. Verification that the polyketide is absent in selected deletion mutants by either positive or negative mode extracted ion chromatograms. The *mdpG*Δ, *orsA*Δ, *easB*Δ and *stcA*Δ mutants are compared to the reference strain for the mass corresponding to the metabolites these genes are known to be involved in. (A) Monodictyphenone *m/z* 287 $[M-H]^-$, (B) orsellinic acid *m/z* 167 $[M-H]^-$, (C) sterigmatocystin *m/z* 325 $[M+H]^+$ and (D) emericellamide A *m/z* 610 $[M+H]^+$, emericellamide C/D *m/z* 596 $[M+H]^+$, emericellamide E/F *m/z* 624 $[M+H]^+$. * Chiang et al, (Chiang et al. 2008) also observed a minor compound with the same mass.

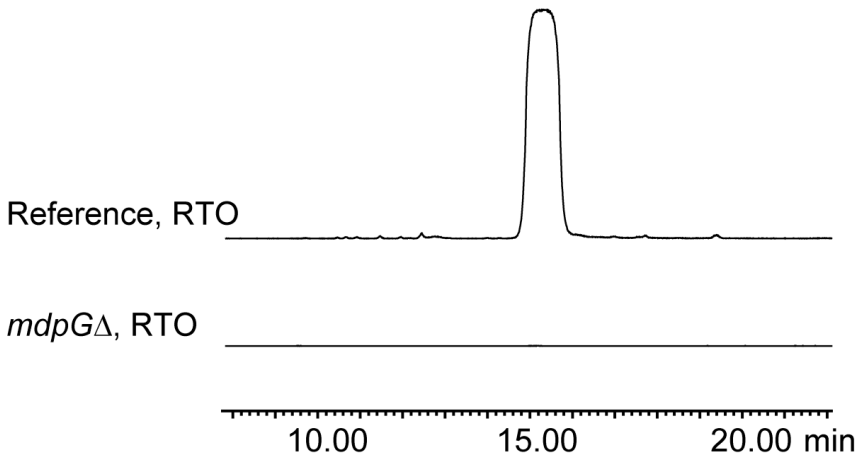

Fig. S6. Positive mode extracted ion chromatograms for the *mdpG*Δ strain cultivated on RTO, identifying arugosin A *m/z* 425 $[M+H]^+$.

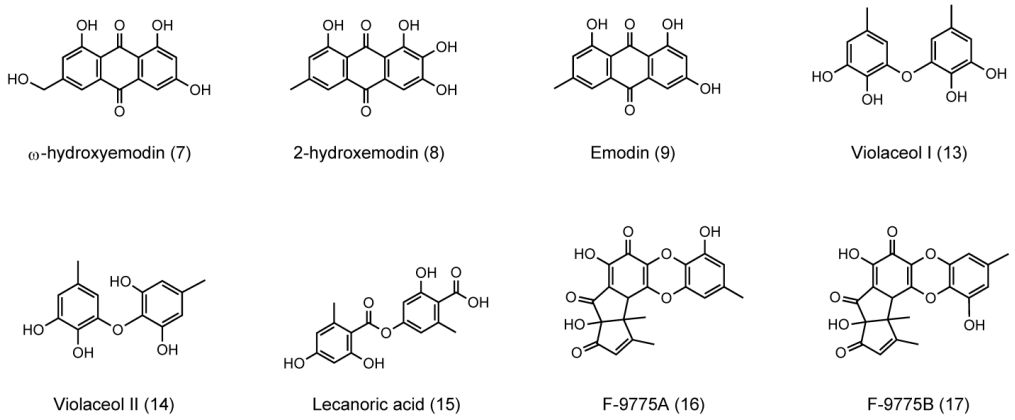

Fig. S7. Additional polyketides that were detected in metabolite extracts in this study.

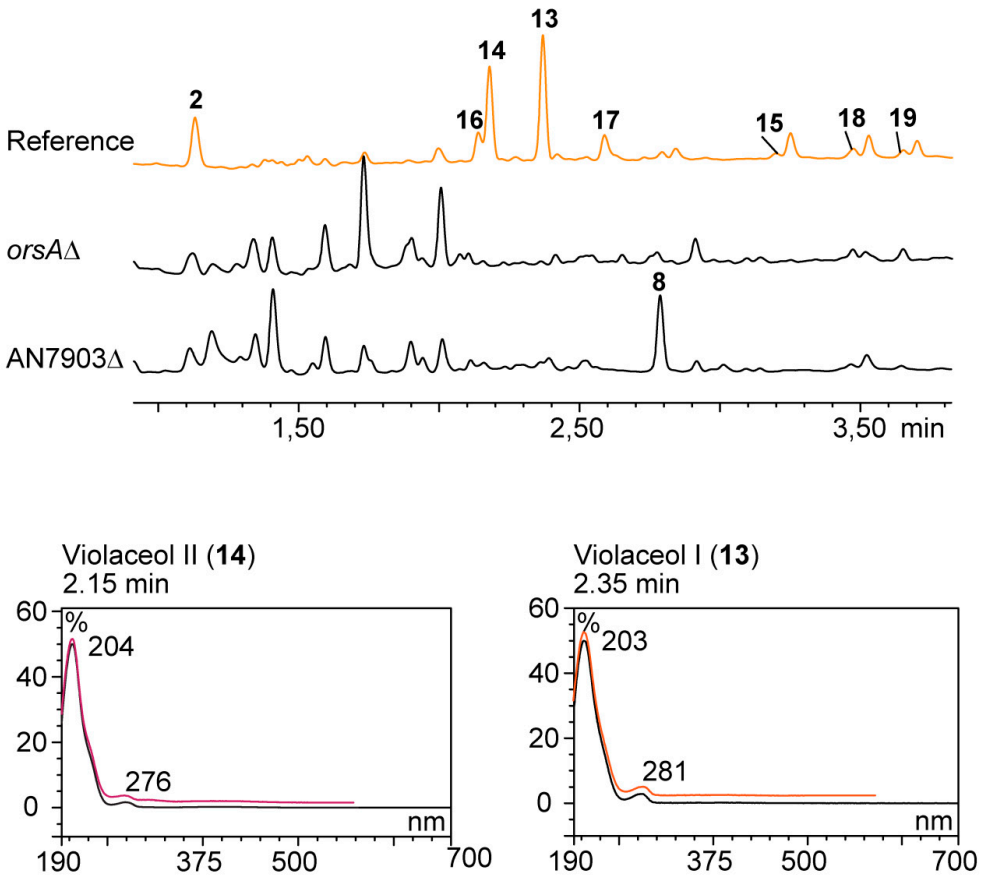

Fig. S8. (A) UHPLC profiles (UV 210 nm) of *orsA*Δ, AN7903Δ compared to the reference strain. The peaks are numbered as follows: orsellinic acid (**2**), ω-hydroxyemodin (**8**), violaceol I (**13**), violaceol II (**14**), lecanoric acid (**15**), F9775A (**16**), F9775B (**17**), austinol (**18**), dehydroaustinol (**19**). (B) UV-spectra of violaceol I (left panel) and II (right panel) standard are shown in black, with an overlay shown in red of the UV-spectra of the sample representing peak 14 (left panel) and peak 13 (right panel). There is agreement between standards and samples.

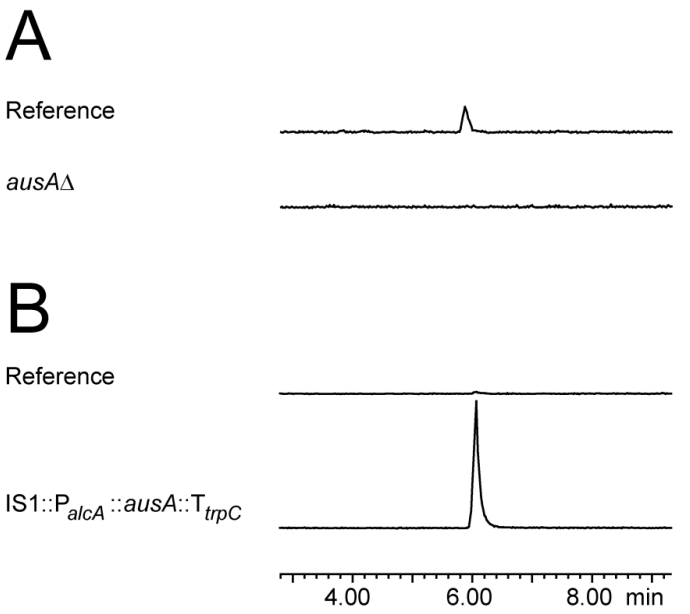

Fig. S9. Extracted ion chromatograms (detection of 3,5-dimethyl orsellinic acid as $[M-H]^-$ at *m/z* 195) of metabolic extracts from (A) the reference strain and the *ausA*Δ (AN8383Δ) strain on RTO medium and (B) the reference and the *ausA* overexpression strain on induction medium (glycerol with threonine).

92

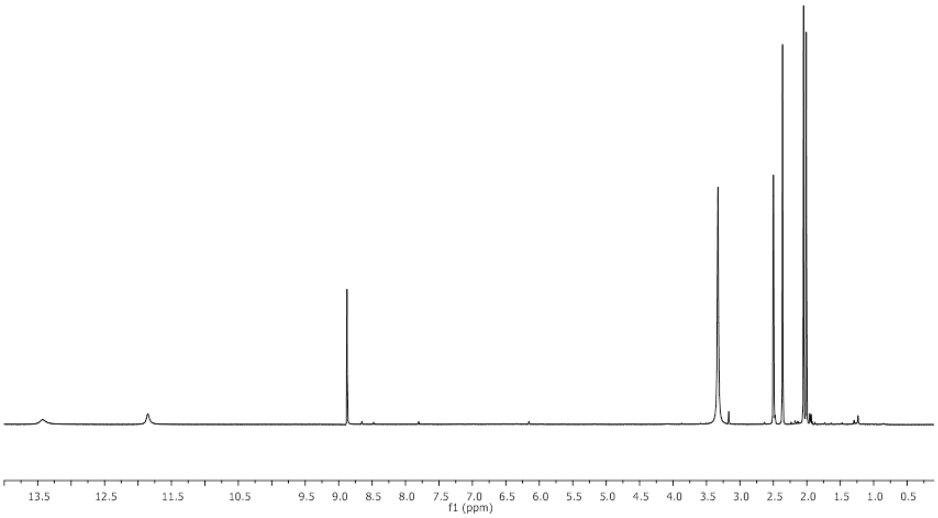

93

94 Fig. S10. ^{1}H NMR spectrum of 3,5-dimethyl orsellinic acid in DMSO-d_6.

95

96

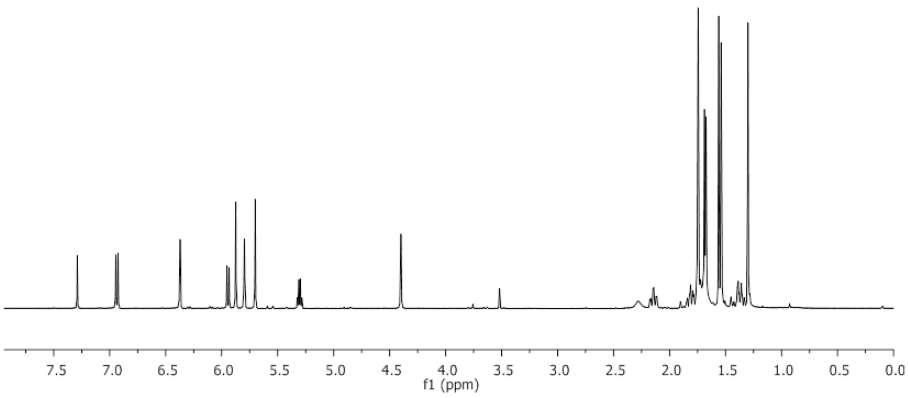

97

98 Fig. S11. ^{1}H NMR spectrum of dehydroaustinol in $CDCl_3$.

99

100

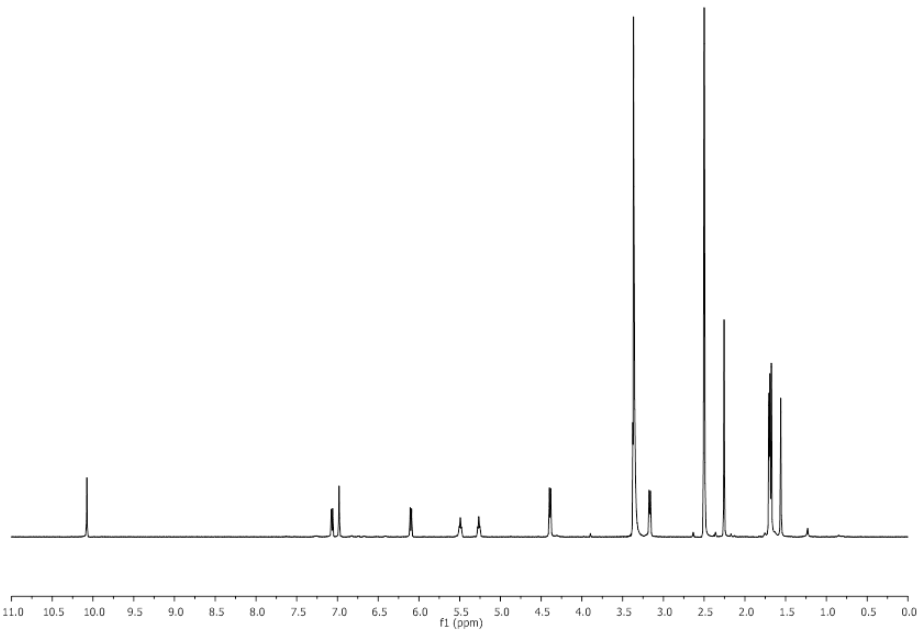

101

102 Fig. S12. ^{1}H NMR spectrum of arugosin A open form in DMSO-d_6.

Text S1. Details about compound identification.

Compound Identification

3,5-dimethyl orsellinic acid. yellow/brownish powder; High resolution electron spray ionization mass spectra, HRESIMS, *m/z* 197.0818 $[M+H]^+$, calculated for $[C_{10}H_{12}O_4+H]^+$: 197.0814. ^{1}H NMR (DMSO-d_6): δ (ppm) = 2.01 (3H, s), 2.05 (3H, s), 2.36 (3H, s), 8.89 (1H, s), 11.85 (1H, s), 13.43 (1H, s); ^{13}C (DMSO-d_6): δ (ppm) = 8.7, 12.0, 18.1, 106.0, 108.2, 115.7, 136.4, 157.5, 158.9, 173.9. These ^{1}H and ^{13}C NMR data are in good agreement with published data (Hirota et al., 1997; Andres et al., 1967) (see supplemental Fig. S10).

Dehydroaustinol. Pale reddish compound; HRESIMS *m/z* 457.1867 $[M+H]^+$, calculated for $[C_{25}H_{28}O_8+H]^+$: 457.1857. ^{1}H NMR ($CDCl_3$): δ (ppm) = 6.89 (1H, d, *J* = 9.8 Hz*), 6.32 (1H, s), 5.89 ((1H, d, *J* = 9.8 Hz), 5.83 (1H, s), 5.75 (1H, s), 5.65 (1H, s), 5.26 (1H, q, *J* = 6.8), 4.35 (s, 1H), 2.30 (1H, br. s), 2.10 (1H, ddd, *J* = 13.8, 13.8, 3.8 Hz*), 1.77 (1H, ddd, *J* = 13.8, 13.8, 3.8 Hz*), 1.72 (1H, m), 1.71 (3H, s), 1.63 (3H, d, *J* = 6.8 Hz), 1.51 (3H, s), 1.49 (3H, s), 1.32 (1H, ddd, *J* = 3.8, 13.8, 13.8 Hz), 1.24 (3H, s). These ^{1}H NMR data are in good agreement with published data (Márquez-Fernández et al., 2007) except for the coupling constants reported for protons resonating at 6.89 ppm, 1.71 ppm and 2.10 ppm that were 2, 27.7 and 27.7 Hz, respectively (the discrepancy is indicated by asterisk above). A coupling constant of 27.7 Hz is not possible due to Karplus equation and dihedral angles, and upon closer inspection, we observed that the signals for protons at 1.71 and 2.10 ppm should have been listed as a ddd, not a dt, thus making the third coupling constant equivalent to the second one. The coupling constant listed in (Márquez-Fernández et al., 2007) for 6.89 ppm does not match up with that given for its partner at 5.89 ppm, both of which should be around 10 Hz, due to *cis* coupling (see supplemental Fig. S11), indicating that our data is correct.

Arugosin A open form. Yellow compound; HRESIMS *m/z* 425.1936 $[M+H]^+$, calculated for $[C_{25}H_{28}O_6+H]^+$: 425.1959. ^{1}H NMR (DMSO-d_6): δ (ppm) = 10.08 (1H, s), 7.07 (1H, d, *J* = 8.3 Hz), 6.98 (1H, s), 6.10 (1H, d, *J* = 8.3 Hz), 5.49 (1H, t, *J* = 7.0 Hz), 5.29 (1H, t, *J* = 7.1 Hz), 4.39 (2H, d, *J* = 7.0 Hz), 3.17 (2H, d, *J* = 7.0 Hz), 2.26 (3H, s), 1.71 (3H, s), 1.70 (3H, s), 1.68 (3H, s), 1.56 (3H, s); ^{13}C (DMSO-d_6): δ (ppm) =

15.3, 17.4, 17.6, 25.3, 25.3, 26.7, 71.6, 105.4, 110.3, 118.4, 119.1, 122.5, 124.0, 126.9, 128.5, 131.1, 132.5, 135.7, 139.3, 148.6, 152.3, 158.4, 160.5, 190.1, 201.4 (see supplemental Fig. S12).

Violaceol I and II. De-replicated and validated against in-house standards of both compounds. HRESIMS *m/z* 263.0886 $[M+H]^+$, calculated for $[C_{14}H_{14}O_5 +H]^+$: 263.0914.

Table S1. PCR primers for Gateway assembly.

Primer name	Oligonucleotide sequence[a]
AN0150-U-1	GGGGACAAGTTTGTACAAAAAAGCAGGCTggactgaagtagactgtaatctgcg
AN0150-U-2	GGGGACAACTTTGTATAGAAAAGTTGGGTAACAACAGGAttctgaggcgatggaaccacc
AN0150-D-3	GGGGACAACTTTGTATAATAAAGTTGggcagtatgttaaccggtagtgaaaggg
AN0150-D-4	GGGGACCACTTTGTACAAGAAAGCTGGGTcaatccacgtgaatggaaccatgacgat
AN0523-U-1	GGGGACAAGTTTGTACAAAAAAGCAGGCTctgtatggtggggacgaaaa
AN0523-U-2	GGGGACAACTTTGTATAGAAAAGTTGGGTctaccccggcacattcgata
AN0523-D-3	GGGGACAACTTTTCTATACAAAGTTGgctgcgtgtttttactgttg
AN0523-D-4	GGGGACAACTTTATTATACAAAGTTGTgtactaagtcatcagcaggc
AN1034-U-1	GGGGACAAGTTTGTACAAAAAAGCAGGCTcagctaagcaagtacgccat
AN1034-U-2	GGGGACAACTTTGTATAGAAAAGTTGGGTggagggtagctaggtagttg
AN1034-D-3	GGGGACAACTTTTCTATACAAAGTTGgatgcaggggctaacaggaa
AN1034-D-4	GGGGACAACTTTATTATACAAAGTTGTgttcaggagggaggacatta
AN1036-U-1	GGGGACAAGTTTGTACAAAAAAGCAGGCTcatcacctacctccagcaca
AN1036-U-2	GGGGACAACTTTGTATAGAAAAGTTGGGTGtgccttgtggatggggatt
AN1036-D-3	GGGGACAACTTTTCTATACAAAGTTGggtttgtagtttgctctgg
AN1036-D-4	GGGGACAACTTTATTATACAAAGTTGttttatcttcttccctgccc
AN10430-U-1	GGGGACAAGTTTGTACAAAAAAGCAGGCTcggccttcgttgtgtcattt
AN10430-U-2	GGGGACAACTTTGTATAGAAAAGTTGGGTGgcgagtagggtgtcaatggt
AN10430-D-3	GGGGACAACTTTTCTATACAAAGTTGagcatgtaatgagtcagtgg
AN10430-D-4	GGGGACAACTTTATTATACAAAGTTGatatatagagcgcgtctcgt
AN11191-U-1	GGGGACAAGTTTGTACAAAAAAGCAGGCTCGGAACCATCCTCAAGCAC
AN11191-U-2	GGGGACAACTTTGTATAGAAAAGTTGGGTCCTGGAGGGTTTTGCTTGGAG
AN11191-D-3	GGGGACAACTTTGTATAATAAAGTTGGATTTTGGCTATACCACATGGC
AN11191-D-4	GGGGACCACTTTGTACAAGAAAGCTGGGTGAACGGAGGTCTTCTGCAC
AN1784-U-1	GGGGACAAGTTTGTACAAAAAAGCAGGCTGACGCCATGAAGACCATGAC
AN1784-U-2	GGGGACAACTTTGTATAGAAAAGTTGGGTGGTGGGCCGATATTTGCAG
AN1784-D-3	GGGGACAACTTTGTATAATAAAGTTGACATTCATCGAGTCTCTCTTTCG
AN1784-D-4	GGGGACCACTTTGTACAAGAAAGCTGGGTGCTGTCTCGTTGGCGGAG
AN2032-U-1	GGGGACAACTTTGTATAGAAAAGTTGGGTgacgcaatatctttcgcgcagaagg
AN2032-U-2	GGGGACAAGTTTGTACAAAAAAGCAGGCTtacctccagtggtacatctggccca
AN2032-D-3	GGGGACAACTTTATTATACAAAGTTGaactggctgagtattgtaagacgagggagca
AN2032-D-4	GGGGACAACTTTTCTATACAAAGTTGtctctgatatgtatgtttctgggtagccgac
AN2035-U-1	GGGGACAAGTTTGTACAAAAAAGCAGGCTtatatgggagtgggggcttg
AN2035-U-2	GGGGACAACTTTGTATAGAAAAGTTGGGTGaggtagaagtagagtggatgg
AN2035-D-3	GGGGACAACTTTTCTATACAAAGTTGaccctaccctctgattcaaact
AN2035-D-4	GGGGACAACTTTATTATACAAAGTTGcatgcctcgaacacctcaaac
AN2547-U-1	GGGGACAAGTTTGTACAAAAAAGCAGGCTatcccacaaattccagatagcc
AN2547-U-2	GGGGACAACTTTGTATAGAAAAGTTGGGTAACAACACGTatctcttggatgctcacacatg
AN2547-D-3	GGGGACAACTTTGTATAATAAAGTTGaggtacggctaatcgttgaccgtctg
AN2547-D-4	GGGGACCACTTTGTACAAGAAAGCTGGGTtgatgcgctgaaataccaggtgctt
AN3230-U-1	GGGGACAACTTTGTATAGAAAAGTTGGGTgggagggtagaattaaagagcggaaggatggca

AN3230-U-2	GGGGACAAGTTTGTACAAAAAAGCAGGCTtaactgtggcgactggagggctc
AN3230-D-3	GGGGACAACTTTATTATACAAAGTTGaaggctgcaatttctacgctgagc
AN3230-D-4	GGGGACAACTTTTCTATACAAAGTTGagtgggccattctggccttgc
AN3273-U-1	GGGGACAAGTTTGTACAAAAAAGCAGGCTcgaaaagccgaacaaggaca
AN3273-U-2	GGGGACAACTTTGTATAGAAAAGTTGGGTcccggataccgtcacactct
AN3273-D-3	GGGGACAACTTTTCTATACAAAGTTGtgctaagacgacgatactgt
AN3273-D-4	GGGGACAACTTTATTATACAAAGTTGTcgcgaggaagggagtatttt
AN3386-U-1	GGGGACAAGTTTGTACAAAAAAGCAGGCTccatgttgatgttcgctcgt
AN3386-U-2	GGGGACAACTTTGTATAGAAAAGTTGGGTcgtaactggcttggatctca
AN3386-D-3	GGGGACAACTTTTCTATACAAAGTTGcgcaaaaggctggagacgag
AN3386-D-4	GGGGACAACTTTATTATACAAAGTTGTgcgccgtctactatccaagc
AN3612-U-1	GGGGACAAGTTTGTACAAAAAAGCAGGCTGCTCCTGTTGGAGAAGCTGG
AN3612-U-2	GGGGACAACTTTGTATAGAAAAGTTGGGTGACAGAAAACAGCAGGTTTGAGC
AN3612-D-3	GGGGACAACTTTGTATAATAAAGTTGCGGAAAATATGGAGGATCGGC
AN3612-D-4	GGGGACCACTTTGTACAAGAAAGCTGGGTGAAGACGGCAGCAAGGATG
AN5475-U-1	GGGGACAAGTTTGTACAAAAAAGCAGGCTacagtacttgaagaatcgaagtcctgccacc
AN5475-U-2	GGGGACAACTTTGTATAGAAAAGTTGGGTgtaccgactctgggagaagcaagccca
AN5475-D-3	GGGGACAACTTTTCTATACAAAGTTGcgtggctcaccgcctaagca
AN5475-D-4	GGGGACAACTTTATTATACAAAGTTGatcagagaacacaacacagccctacc
AN6000-U-1	GGGGACAAGTTTGTACAAAAAAGCAGGCTtcaatgcgaaaaagctgggagaacc
AN6000-U-2	GGGGACAACTTTGTATAGAAAAGTTGGGTggagggcaaaatgcccgcac
AN6000-D-3	GGGGACAACTTTTCTATACAAAGTTGggtgttatggtatacagagtgctcgactcg
AN6000-D-4	GGGGACAACTTTATTATACAAAGTTGagcggttcatttgcacaccgagg
AN6431-U-1	GGGGACAAGTTTGTACAAAAAAGCAGGCTCAAGGTGGAGGAGGCAGC
AN6431-U-2	GGGGACAACTTTGTATAGAAAAGTTGGGTCTTCACGATCTCTACCTCTGGTC
AN6431-D-3	GGGGACAACTTTGTATAATAAAGTTGGTGAAGGGCTTGGTCGGAC
AN6431-D-4	GGGGACCACTTTGTACAAGAAAGCTGGGTGTGGTCACCTACCTGCGTG
AN6448-U-1	GGGGACAAGTTTGTACAAAAAAGCAGGCTgaaacccgttcagccaacca
AN6448-U-2	GGGGACAACTTTGTATAGAAAAGTTGGGTgaaaggactgaacgaccggg
AN6448-D-3	GGGGACAACTTTTCTATACAAAGTTGagaggagataccacgaagat
AN6448-D-4	GGGGACAACTTTATTATACAAAGTTGTgaacaattgggggtctaac
AN6791-U-1	GGGGACAAGTTTGTACAAAAAAGCAGGCTcacgccatgagacggatggcac
AN6791-U-2	GGGGACAACTTTGTATAGAAAAGTTGGGTgaagtacctcccggataggggctcc
AN6791-D-3	GGGGACAACTTTTCTATACAAAGTTGgacctgatatacattgccactaacgaaccca
AN6791-D-4	GGGGACAACTTTATTATACAAAGTTGatcagaaggcgactgcgaagc
AN7022-U-1	GGGGACAACTTTGTATAGAAAAGTTGGGTggggaattcagactgggtggtgttgtgc
AN7022-U-2	GGGGACAAGTTTGTACAAAAAAGCAGGCTtcgatccagacgttcattctgttcggaggagg
AN7022-D-3	GGGGACAACTTTATTATACAAAGTTGacgcattgatttctgcgcgaggactgg
AN7022-D-4	GGGGACAACTTTTCTATACAAAGTTGggacacgtcaacagtattggcattcagg
AN7071-U-1	GGGGACAACTTTGTATAGAAAAGTTGGGTgtcgcagatgtctcccatctcgcca
AN7071-U-2	GGGGACAAGTTTGTACAAAAAAGCAGGCTttactcgtcgcccttctgggctg
AN7071-D-3	GGGGACAACTTTATTATACAAAGTTGaaccccaatctcactgcagacctc
AN7071-D-4	GGGGACAACTTTTCTATACAAAGTTGccgtctatcaatggaataacacggatgccca
AN7084-U-1	GGGGACAACTTTGTATAGAAAAGTTGGGTgagactgaggtccaactccgacg

AN7084-U-2	GGGGACAAGTTTGTACAAAAAAGCAGGCTccgtctctgagcgtgctggaa
AN7084-D-3	GGGGACAACTTTATTATACAAAGTTGagggttacctgtgccggagac
AN7084-D-4	GGGGACAACTTTTCTATACAAAGTTGccctcgtaaccaaatcacaccactcc
AN7825-U-1	GGGGACAAGTTTGTACAAAAAAGCAGGCTtcatcccagatactcggattgcgctgaa
AN7825-U-2	GGGGACAACTTTGTATAGAAAAGTTGGGTAACAACCAGTagctaacggtgagattcagattgcct
AN7825-D-3	GGGGACAACTTTGTATAATAAAGTTGggttctcaggtattctgtgtcgagtgc
AN7825-D-4	GGGGACCACTTTGTACAAGAAAGCTGGGTagtggtcaggccatatttctgggcgat
AN7838-U-1	GGGGACAAGTTTGTACAAAAAAGCAGGCTgacactgaaagatgggacgagtgtgcga
AN7838-U-2	GGGGACAACTTTGTATAGAAAAGTTGGGTgtggtgaaggaggagacctgagtgca
AN7838-D-3	GGGGACAACTTTTCTATACAAAGTTGcgcgactgtttagtaagtagtgctgtaggcga
AN7838-D-4	GGGGACAACTTTATTATACAAAGTTGactgctaacgaggaaaagctgtgtggctc
AN7903-U-1	GGGGACAAGTTTGTACAAAAAAGCAGGCTggctctactcgagctgacgt
AN7903-U-2	GGGGACAACTTTGTATAGAAAAGTTGGGTAACAACAATGgtgatcgaactgatcatggccgtcaata
AN7903-D-3	GGGGACAACTTTGTATAATAAAGTTGcggccattaaggctactcctgcagacaa
AN7903-D-4	GGGGACCACTTTGTACAAGAAAGCTGGGTtgatatggcctcggatgagcttgtcgta
AN7909-U-1	GGGGACAACTTTGTATAGAAAAGTTGGGTgtgccgtgaagagtcaagctccgtg
AN7909-U-2	GGGGACAAGTTTGTACAAAAAAGCAGGCTgagatgcttccctatatgctcgaacgagcca
AN7909-D-3	GGGGACAACTTTATTATACAAAGTTGaaatagtcgcggcggcatttcc
AN7909-D-4	GGGGACAACTTTTCTATACAAAGTTGgcatgcgacatagttgggggacc
AN8209-U-1	GGGGACAAGTTTGTACAAAAAAGCAGGCTacccaaggttgacaacacgatatctgc
AN8209-U-2	GGGGACAACTTTGTATAGAAAAGTTGGGTAACAACGAGAgactgcatctaagtgttcagccacaa
AN8209-D-3	GGGGACAACTTTGTATAATAAAGTTGaatacgccgcgatcttctatgagcag
AN8209-D-4	GGGGACCACTTTGTACAAGAAAGCTGGGTggctagacggaacattccatcttacg
AN8383-U-1	GGGGACAAGTTTGTACAAAAAAGCAGGCTGCGATCTCTCTGGCGAAAG
AN8383-U-2	GGGGACAACTTTGTATAGAAAAGTTGGGTGGAATGAGACACAGTCGCTTA
AN8383-D-3	GGGGACAACTTTGTATAATAAAGTTGGTTCCTGCGAAGACACGTTG
AN8383-D-4	GGGGACCACTTTGTACAAGAAAGCTGGGTGGGTGTTGACTGAGGAGC
AN8412-U-1	GGGGACAAGTTTGTACAAAAAAGCAGGCTaagacggtgcgctttcatagatgtcagc
AN8412-U-2	GGGGACAACTTTGTATAGAAAAGTTGGGTAACAACGCGCagctggtacctatactgcatcaccaagg
AN8412-D-3	GGGGACAACTTTGTATAATAAAGTTGatcaccgctctgatctacagtagctgc
AN8412-D-4	GGGGACCACTTTGTACAAGAAAGCTGGGTgtcggcttcatcattctcggggtcatgt
AN8910-U-1	GGGGACAAGTTTGTACAAAAAAGCAGGCTcccaagacggactacgcagc
AN8910-U-2	GGGGACAACTTTGTATAGAAAAGTTGGGTggtgcaggatacgcggaggac
AN8910-D-3	GGGGACAACTTTGTATAATAAAGTTGgtcctcgatggggtcatagtaagccaacagtg
AN8910-D-4	GGGGACCACTTTGTACAAGAAAGCTGGGTatgggctgcgtacccgagagaa
AN9005-U-1	GGGGACAAGTTTGTACAAAAAAGCAGGCTgccatatctgggaagcggagga
AN9005-U-2	GGGGACAACTTTGTATAGAAAAGTTGGGTggaccaaacacttcctttgcggggtacaa
AN9005-D-3	GGGGACAACTTTTCTATACAAAGTTGgtgcagtaagggtttgtggttgaggga
AN9005-D-4	GGGGACAACTTTATTATACAAAGTTGaacgaagaagacatacctgcggctg
anid_12168-U-1	GGGGACAAGTTTGTACAAAAAAGCAGGCTggaggacgctttggtgaagg
anid_12168-U-2	GGGGACAACTTTGTATAGAAAAGTTGGGTcaccggcaagaacacacaat
anid_12168-D-3	GGGGACAACTTTTCTATACAAAGTTGctgcccgcaaatcggaatat
anid_12168-D-4	GGGGACAACTTTATTATACAAAGTTGTcccttatcagctttgctctc
Uni-U1[b]	cttttgctggccttttgctc

Uni-U2[b]	tgctgtccaagcttatctcc
Uni-D1[c]	tacatcgccgtcatcaag
Uni-D2[c]	gattttgagacacgggccag

[a] For each oligonucleotide, the *attB* sequence required for Gateway recombination is capitalized.

[b] Oligonucleotide for amplifying the final upstream gene targeting substrate from the Gateway upstream plasmid . These oligonucleotides are labeled U1 and U2 in Fig. S2, respectively.

[c] Oligonucleotide for amplifying the final downstream gene targeting substrate from the Gateway downstream plasmid. These oligonucleotides are labeled D1 and D2 in Fig. S2, respectively.

Table S2. Oligonucleotide primers for diagnostic PCR.

Gene	External Forward[a]	Gap Check Forward[b]	Gap Check Reverse[b]	Internal Reverse[c]
AN0150	GAGTTCGGGGTGGTATAG	CGACCGGGGATCTAGTATTC	GTTGCTGGGGGATTGGGAGT	ACTACCTCGGCACCAATAAC
AN0523	GAGAGACGCATCGGGAAGAA	CCGCATGGTGGATTCTTTAG	GTGGCGATTGATTTCGTGTG	TGCTTTTCCAGTTCCGCCAG
AN1034	CAATTCTATCCGCTCTCTCC	CCTTAATCTCCGGCTCCAAT	GAGGACTGGTACGGCGAATG	TCTCGTCCTCCTGTTTCTGG
AN1036	CATCAGCGACGAGCCGTAC	GCATTTCAAGCCCTCCCTCT	CACTGAGCCAGAAAGGGCAA	TAGACGGAGGTGTTGGTGCC
AN10430	GAGGAGCTGGAGCAACTG	CTCTTTCGGTTTGACGTTCT	GTCAAGACCGCCAAACAACT	CTTGCCGTCTTGATTGATGC
AN11191	CCGGTTCTCGCTCTCCTTC	GCCAATCTTACATGCTCCAG	CTTTCTCCAATGGTTTGTCC	CCTAGCGAGTGAGTATGCGT
AN1784	CGAGCTTCTGCTTCATCC	CCGTGACAAACCTACCATCA	GAACTGGGGCTCTGCATGAT	GCCCGTTGCCCTAATAACAC
AN2032	CAAGTGGCCGTTGTCGGC	CCACCATATCGTCTGCCTTA	GATATCCTTCCTTTCGGGGG	TAGCTCGGGAGTCGTCAAGG
AN2035	GAACTGGGTGGATTCGTCG	GTAGGGCTAGGGATTAGGGA	GTGAAGGGATGGTGCTAGTT	GACAGCATTCCCAGTGACCC
AN2547	GGGTGCTGTTGGGAAGTT	GCGCTGCAGGAAATGAAAGT	GAGGATTCGAGGTATGGAGC	CCACTGACCGACGTATACAC
AN3230	GGCTCCGTGAAATCAAACAT	GCTCGGGATTTTGCTGTCAG	CCTCCAAACTTCCCATTACT	GTTTCCCTGCAGCTCTTGCC
AN3273	GACGACGCTGAGCAACAG	GGAGGAATGGTGGCAGTAGG	CCGCAACTGACATATCACCA	CTCGAGATGGTGTGGCCTTG
AN3386	GTGACTGCTGGCCTAGAAC	CAGTCCCCATTTGTTCCATC	CACCCTCCCAGATCGCTTCT	CACCGCTTCATCCCCATCTC
AN3612	CTGCCTGCTAGCCACCTA	GGCGCTCCCTGACTGAAGTT	GTTCTTTTTCCTGAGCTCGT	CTCCAGCCCCAGATACATTC

AN5475	CAACGACAGTGCACATGG	GCAGGAGACGGAACCACTAA	CCTCTTTTGCTGCATTGCTA	CCAGCCAATCCTCTCCGAAG
AN6000	CTGACGAATCGCGACCTAC	GTGCGTCGAGTCTGTAATAT	GGACCAACCCAAGAAACCGT	CCGATACTCAAGCCAGCAAG
AN6431	CTGATCCGTCGCTGCAGG	GAGGTTTTTATGTGCGCGCT	GTGGTATGGTGTCAAGTGGT	AGCAGCCTATCTTTTCGCCC
AN6448	GTGCGCAGAGCTGAGAGA	CGGTGCTTAGCCTGTGTTTT	CATTGGAAGACTGAGCTGGT	TCTTACACCAGGGAATTGCG
AN6791	GGAAGATAGCTCTGGAGTAC	GATGAGGTCAAACGGGGTGG	CCCCTTGTTCTGTGCTGTGT	GTTCGTGAGGGTCAATTGGG
AN7022	GTGCGCACCTATTCCATTAG	CTCCTGTTCTGGGTGACATC	GCAGTGGTGTCTTGTACAGT	TGCTCCGCGTCTATAGAGTG
AN7071	CCTATCGATACTTTCAACTCTC	GGCTTTTGATCTGCTCGCTG	CCTTGGGTGGTAGAGTTGTT	CATTTGCACCAGGGCTTTCT
AN7084	GGCCAGCGTCGTTACGAC	GTCGATTTTGAAAGGGGTGT	GGAAGATGGAAATGAGGCGG	CCTCATACACGACCTCCAAC
AN7825	CTTGGCTTGGTCAGTGATTC	GCAATCAGAGGGGGACAATC	CTTGGAATTGCTGACGCTAC	CTGTGTTTGGTTGGTTTCGG
AN7838	TCTCTCTGGACAGAGACTTG	GCTGCAGTAACCCCTCTTGA	GGATGCTGCTCTTACAATGA	TGGGTCCTGAAGATGTGTGG
AN7903	GTGTGTATTCCTCTCTCCC	GGGAGGCGGATTACTTGACA	CATTTTCGAGGGCGGATCCA	AGAATTCCAAGACGCACTGA
AN7909	GCCGTTTCCAGAATATACG	GGGGCTCTATCAGATGTGTA	CTCATTGTAGCGCGTTGGTT	CCAGGCCCAAGTTGACTATC
AN8209	CAACCATTTTCCGAGGCCAC	GAATCGACCAAATAGGAGCC	GGTTTCTTGGGCCTCTTTCC	GAGACTCACATTTCGGCGGG
AN8383	GCTCCTGTCCAAATGCGC	GCTGCAGTAACCCCTCTTGA	GTCGGACAAAACCCAGCTTC	GCAAGGAACAAGCAGCACTG
AN8412	GACGACATCCCCCTTACGGA	CGTTGTGGGTATCGCTTGGA	GGACTTAGGGATTCGGGGCT	ATCCTTGTCCCACATCCTCG
AN8910	AGACTCTACTAGCCCTAGG	CACTATTGATCAAGCAGCCA	GGGTAGCCTGGTAATGAAAG	GTGCATTCCTAGCCCTTGTG
AN9005	GGAAGTCTAGCTGGAGAAG	GCGCATCAGCAGACATAAAG	CCGGGAGTTATCGAGTAGTG	ACCTCACAAACACCATTTCG
Anid_12168	CTTTTAATGACTCGGCTGCT	GAGCTAGAGTTGGGGTTGGG	CCCGCAGCATCTGAATCAAA	CACTTAGCATAACGCCCTTC

AF*pyrG*[d]	–	–	–	GGAAGAGAGGTTCACACC

[a] These oligonucleotides anneal upstream of the "upstream targeting sequence" for each PKS gene. Labeled "P1" in Fig. S3.

[b] These oligonucleotide pairs, "Gap Check" forward and reverse anneal on either side of the targeted gene in the upstream and downstream targeting sequences, respectively. Labeled "P3" and "P4" in Fig. S3.

[c] These oligonucleotides anneal to the open reading frame of the targeted gene in reverse direction. Labeled "P5" in Fig. S3 (except AF*pyrG*).

[d] This oligonucleotide anneals to the *A. fumigatus pyrG*, priming in reverse direction. Labeled "P2" in Fig. S3.

Table S3. Additional oligonucleotides used in the study.

Purpose	Name	Oligonucleotide sequence[a]
Construction of pU4002	BGHA195	gggtttaaUtaagtcctcagcggatcctctagaccgtggagtt
	BGHA196	ggtcttaaUtaatgcctcagcacaaagggaaaaccttgacga
Construction of *ausA*-S1660A	BGHA600	gggtttaaUgaatgatcggtcatagctttgg
	BGHA601	ataagagcgUcgacaccgatatcgccg
	BGHA602	acgctcttaUgagcactgaagtcttaaccgaaat
	BGHA603	ggtcttaaUggattacctgtctggatgtcagat
	BGHA604	ggcattaaUgaatgatcggtcatagctttgg
	BGHA605	ggacttaaUggattacctgtctggatgtcagat
Integration of ausA into IS1	FW-AN8383-1	agagcgaUatggggtcccttgatgataata
	RV-AN8383-1	aaattgUatgcgatatgctgcacgg
	FW-AN8383-2	acaattUggcacggaagcagaaccgagatatg
	RV-AN8383-2	attgtgaUttcggtctcgacggcccc
	FW-AN8383-3	atcacaaUcacagaccgagagccaaa
	RV-AN8383-3	tctgcgaUttataagccaacgtgtcttcg
Sequencing of *ausA*	BGHA576	ttgtgcaacactcacgcaag
	BGHA577	tcaacagcgacaaagccaaca
	BGHA578	ctgtgtattccaactacgagcc
	BGHA579	gatacatcaccgacggcattt
	BGHA580	gcacaggaggaacgaccaat
	BGHA581	ctctacaacacaagggacggat

[a] The uracil base necessary for USER cloning is indicated by a "U" in the oligonucleotide sequence.

Table S4. The constructed *A. nidulans* strains have been deposited into the IBT Culture Collection.

IBT Strain	Genotype [a]
29539 [b]	*argB2, pyrG89, nkuA*Δ
28738[c]	*argB2, pyrG89, nkuA-trS::AFpyrG*
30995	*argB2, pyrG89, nkuA*Δ, *mpdG*Δ
30996	*argB2, pyrG89, nkuA*Δ, AN0523Δ
30997	*argB2, pyrG89, nkuA*Δ, *afoE*Δ
30998	*argB2, pyrG89, nkuA*Δ, *afoG*Δ
30999	*argB2, pyrG89, nkuA*Δ, AN10430Δ
31000	*argB2, pyrG89, nkuA*Δ, AN11191Δ
31001	*argB2, pyrG89, nkuA*Δ, AN1784Δ
31002	*argB2, pyrG89, nkuA*Δ, AN2032Δ
31003	*argB2, pyrG89, nkuA*Δ, AN2035Δ
31004	*argB2, pyrG89, nkuA*Δ, *easB*Δ
31005	*argB2, pyrG89, nkuA*Δ, AN3230Δ
31006	*argB2, pyrG89, nkuA*Δ, AN3273Δ
31007	*argB2, pyrG89, nkuA*Δ, AN3386Δ
31008	*argB2, pyrG89, nkuA*Δ, AN3612Δ
31009	*argB2, pyrG89, nkuA*Δ, AN5475Δ
31010	*argB2, pyrG89, nkuA*Δ, *aptA*Δ
31011	*argB2, pyrG89, nkuA*Δ, AN6431Δ
31012	*argB2, pyrG89, nkuA*Δ, AN6448Δ
31013	*argB2, pyrG89, nkuA*Δ, AN6791Δ
31014	*argB2, pyrG89, nkuA*Δ, AN7022Δ
31015	*argB2, pyrG89, nkuA*Δ, AN7071Δ
31016	*argB2, pyrG89, nkuA*Δ, AN7084Δ
31017	*argB2, pyrG89, nkuA*Δ, *stcA*Δ
31018	*argB2, pyrG89, nkuA*Δ, AN7838Δ
31019	*argB2, pyrG89, nkuA*Δ, AN7903Δ

31020	*argB2, pyrG89, nkuA*Δ, *orsA*Δ
31021	*argB2, pyrG89, nkuA*Δ, *wA*Δ
31022[d]	*argB2, pyrG89, nkuA*Δ, *ausA*Δ
31023	*argB2, pyrG89, nkuA*Δ, *adpA*Δ
31024	*argB2, pyrG89, nkuA*Δ, AN8910Δ
31025	*argB2, pyrG89, nkuA*Δ, AN9005Δ
31026[e]	*argB2, pyrG89, nkuA*Δ, anid_12168Δ
31030[f]	*argB2, pyrG89,* IS1*::*P_{alcA}*::ausA::*T_{trpC}*::argB*
31031[g]	*argB2, pyrG89,* IS1*::*P_{gpdA}*::ausA::*T_{trpC}*::argB*
31032[h]	*argB2, pyrG89, nkuA*Δ, *ausA*-S1660A
31281[i]	*argB*2, *pyrG*89, *nkuA*Δ, *ausA*Δ, IS1*::*P_{gpdA}*::ausA::*T_{trpC}*::argB*

[a] all strains carry the *veA1* mutation

[b] *nkuA*Δ deletion strain (Nielsen et al., 2008)

[c] transient small repeat in *nkuA* (Nielsen et al., 2008)

[d] AN8383 was designated *ausA* in this study

[e] The annotation of this gene was from the *Aspergillus* Comparative Sequencing Project, Broad Institute of Harvard and MIT

[f] Strain contains inducible expression (*alcA* promoter) of *ausA* in IS1

[g] Strain constitutive expression (*gpdA* promoter) of *ausA* in IS1

[h] Strain contains a point mutation in *ausA* with S166A (serine to alanine)

[i] The *ausA* deletion (strain, IBT31022) was complemented by the expression of *ausA* from IS1

Supporting References

Andres, W, Kunstmann, M, & Mitscher, L (1967) Isolation and structure of 2, 4-dihydroxy-3, 5, 6-trimethylbenzoic acid from *Mortierella ramanniana*. *Cell Mol Life Sci* 23: 703–704.

Chiang, Y-M et al. (2008) Molecular genetic mining of the *Aspergillus* secondary metabolome: Discovery of the emericellamide biosynthetic pathway. *Chem Biol* 15: 527-532.

Hirota, A, Morimitsu, Y, & Hojo, H (1997) New antioxidative indophenol-reducing phenol compounds isolated from the *Mortierella* sp. fungus. *Biosci Biotechnol Biochem* 61: 647–650.

Márquez-Fernández, O, Trigos, A, Ramos-Balderas, JL, Viniegra-González, G, Deising, HB, & Aguirre, J (2007) Phosphopantetheinyl transferase CfwA/NpgA is required for *Aspergillus nidulans* secondary metabolism and asexual development. *Eukaryot cell.* 6: 710-20.

Nielsen, JB, Nielsen, ML, & Mortensen, UH (2008) Transient disruption of non-homologous end-joining facilitates targeted genome manipulations in the filamentous fungus *Aspergillus nidulans*. *Fungal Genet Biol* 45: 165-170.

Paper 5

"Characterization of the *Aspergillus nidulans* 3-methylorsellinic acid gene cluster"

JB Nielsen and ML Klejnstrup (joint 1st author), P Khorsand-Jamal, DK Holm, A Kabat, ML Nielsen, JC Frisvad, CH Gotfredsen, TO Larsen, and UH Mortensen

Manuscript in preparation

Introduction. Filamentous fungi are reservoirs of bioactive natural products, i.e. secondary metabolites that are classified into groups such as polyketides, nonribosomal peptides, terpenoids, and hybrid molecules mixing moieties of these classes. The selection of secondary metabolites produced by one fungus inevitably pinpoints to the environmental niche and the challenges it faces. As these products display high chemical diversity, the bioactivities are similarly broad ranged, in extremes ranging from harmful mycotoxins to beneficial drugs. This fuels the interest to link secondary metabolites to their corresponding genes often residing in gene clusters to ultimately map the full biosynthetic pathway. This task has however shown to be cumbersome due to the expression of most gene clusters responsible for secondary metabolite production has been challenging to stimulate under lab conditions. Even in a well-studied fungus as *Aspergillus nidulans*, the biosynthetic pathways of many clusters are still unidentified regarding if they are active at all. Moreover, in several cases only a few metabolites have been coupled to a specific PKS and the remaining products remains to be found (Ahuja 2012).

In *A. nidulans* at least four PKSs have been shown to produce variants based on an orsellinic acid backbone, namely orsellinic acid (OrsA; Schroeckh 2009), 3,5-dimethylorsellinic acid (3,5-DMOA, AusA; Nielsen 2011), 3-methylorsellinic acid (3-MOA; Hansen 2011; Ahuja 2012) and orsellinic acid aldehyde (PkfA; Ahuja 2012) . Moreover, Hansen and co-workers showed that 5-MOA could be heterologously produced by transferring the PKS, *mpaC*, the first step in mycophenolic acid production from *Penicillium brevicompactum* (Hansen 2011). Furthermore, Nielsen et al. reported that small amounts of orsellinic acid were still present in extracts of *orsA*Δ (Nielsen 2011). This could indicate that synthesis of orsellinic acid variants as potentially leaky, which could complicate characterization of these pathways. Recently, 3-MOA and cichorine were reported to be produced by AN6448, PkbA (Ahuja 2012). We set out to map and characterize the biosynthetic activities present in the *pkbA* gene cluster. In addition to determining several of the biochemical steps, we found that nitrogen was incorporated by a to our knowledge novel mechanism by the NRPS-like enzyme AN6444. Moreover a novel carbon skeleton was discovered in the metabolites cichonidulol/demethylcichonidulol.

Results and Discussion

Ectopic overexpression of the putative transcription factor AN6446 results in production of 3-MOA and associated metabolites. 32 putative PKS ORFs were deleted and challenged in an OSMAC approach by Nielsen et al., 2011. Through analysis of the data we also found loss of 3-methylorsellinic acid production in the *pkbA*Δ mutant strain grown on CYA, CY20 and RT compared to the reference strain by UHPLC-MS analysis employing a 3-MOA standard, see Fig 1 for comparison on CYA. All of the remaining 31 PKS deletion strains produced 3-MOA under these conditions (data not shown). Our observation corresponds to the finding recently published by Ahuja et al (Ahuja 2012) that the PKS encoding *pkbA* is required to produce 3-MOA. The complete loss of 3-MOA production also showed that 3-MOA cannot be derived from the three other orsellinic acid producing gene clusters in *A. nidulans*, *ors, pkf* and *aus* under the tested conditions.

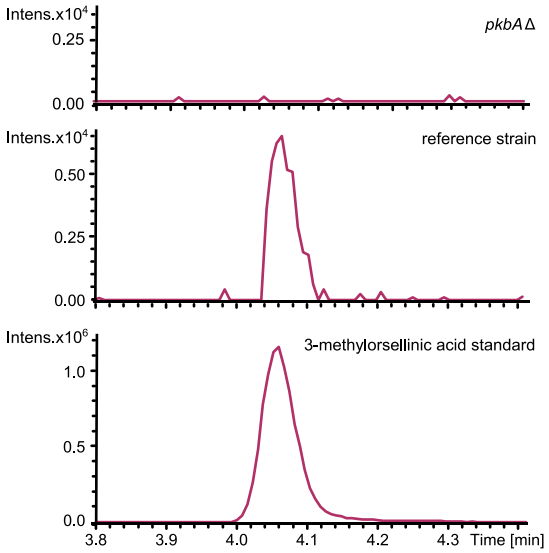

Figure 1 Extracted ion chromatograms of 3-methylorsellinic acid $[M+H]^+$ (calc. *m/z* 183.06483±0.001) of a standard, the reference strain and *pkbAΔ* strains on CYA medium cultivated for seven days at 37°C.

As 3-MOA production was relatively low in the reference strain extracts and no other metabolites were found to be significantly differentiated in the *pkbA*Δ extracts compared to the reference, we decided to induce production of potential metabolites from PkbA, and searched the genome sequence for neighbor ORFs predicted to encompass transcriptional regulator activity. AN6446 was predicted to have a DNA binding domain of the Myb/SANT family both associated with transcriptional regulation, e.g. the SANT domain is present in numerous chromatin remodeling enzymes. We speculated that AN6446 could be a cluster-specific activator or repressor, and thus constructed an AN6446 overexpression strain (AN6446-Oex) based on ectopic expression from the IS1 site (Hansen 2011). The overexpression of AN6446 clearly had an effect on *A. nidulans*, since the AN6446-Oex compared to the reference displayed a decrease in pigmentation of conidia to a dusty green appearance and a light brown center of the colony after seven days growth on MM, see Fig 2.

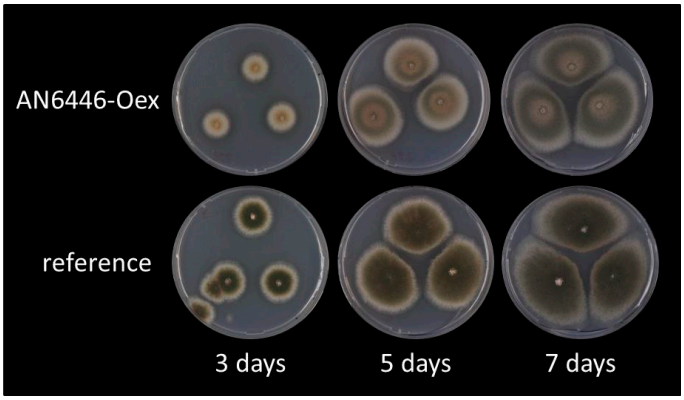

Figure 2. The reference strain compared to the AN6446-Oex strain cultivated on MM at 37°C for three, five and seven days.

UHPLC-TOF-MS analysis revealed several new peaks appearing in the AN6446-Oex strain compared to the reference indicating that the overexpression had indeed turned on the likely 3-MOA biosynthetic pathway. 3-MOA was, as in the reference strain, present in trace amounts in the AN6446-Oex strain.

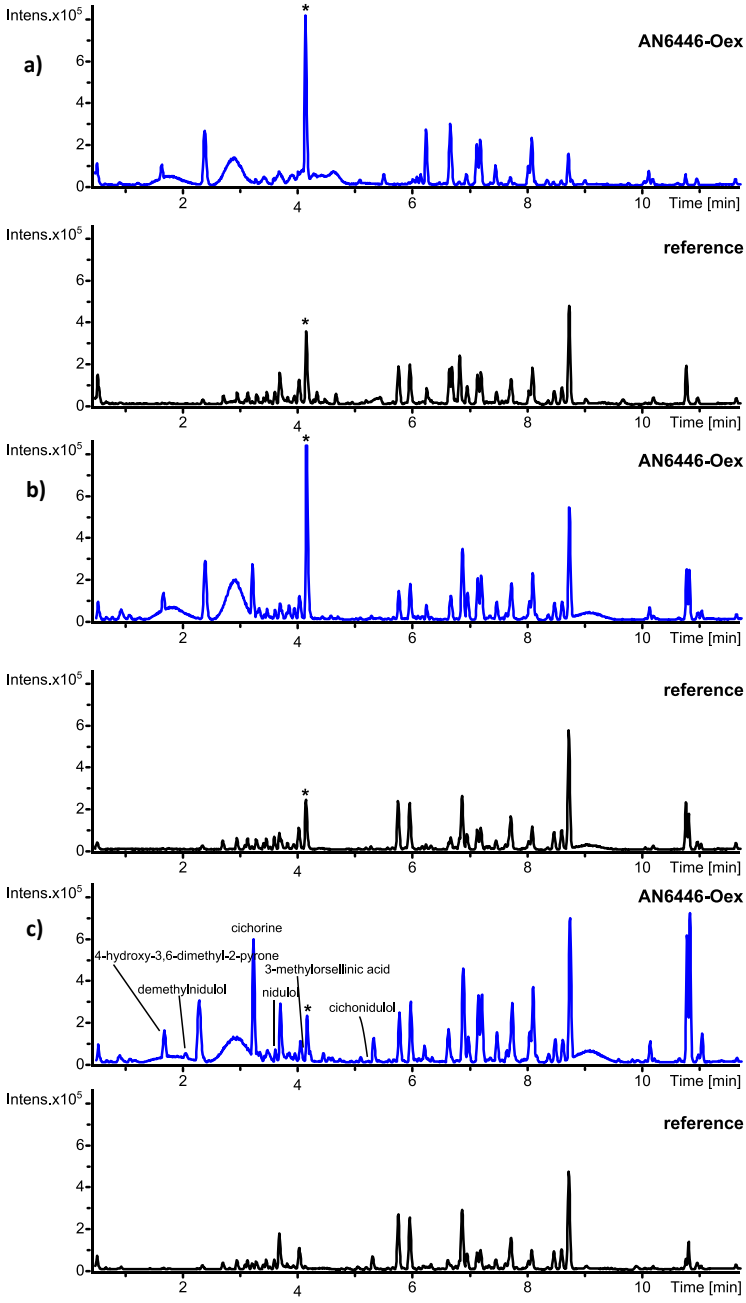

Figure 3 UHPLC-TOFMS ESI$^+$ BPC of the micro-extracts of the reference (black) and AN6446-Oex (blue) strains cultivated on MM media at 37°C for **a)** three, **b)** five, and **c)** seven days.

Extracts of the AN6446-Oex strain cultivated for three different periods, i.e. 3, 5 and 7 days, displayed highly similar metabolite profiles, albeit some metabolite were not visible before 5 days. Consequently, the strains were grown for seven days throughout the study. Moreover this showed that MM medium was a suited growth medium for isolation of candidate metabolites under the artificial conditions encountered in the overexpression strain.

Overexpression of AN6446 resulted in production of two dimers having a novel carbonskeleton

A large-scale extract of 200 MM dishes cultivating the AN6446-Oex strain was prepared for isolation and structure elucidation of several metabolites. In figure 3, the UHPLC-TOF-MS ESI$^+$ BPC of the large-scale extract versus the micro-extracts showed that several of the peaks were not present in the large extracts. Sample preparations and cultivation conditions of a large number of plates could influence this loss of metabolites observed, however further analysis revealed more compounds than visible in the chromatogram as cichorine eluting at 3.2 min was in high concentrations.

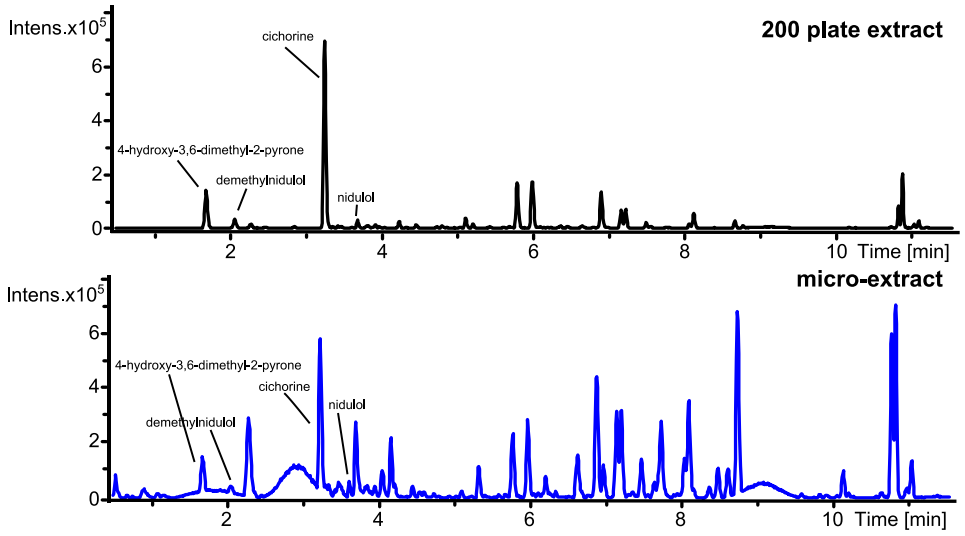

Figure 4 UHPLC-TOF-MS ESI$^+$ BPC of the micro-extract (bottom) and 200 plate extract (top) of the overexpression of AN6446-Oex strain cultivated on MM medium for seven days at 37°C.

Isolation and structure elucidation by NMR revealed the presence of several metabolites; cichorine, demethylnidulol and 4-hydroxy-3,5-dimethyl-2-pyrone and two dimers of cichorine and nidulol/demethylnidulol, named cichonidulol and demethylcichonidulol, see figure 5. Although present in the extract of AN6446-Oex, nidulol was isolated from the singular deletion mutant strain, AN6444Δ. Both cichorine and nidulol have been reported previously in literature. Cichorine have been isolated from *A. silvaticus* (Kawahara 1988), *Alternaria cichorii* (Stierle 1993) and *A. nidulans* (Ahuja 2012) whereas nidulol have been reported from *A. nidulans* (Aucamp 1968), *A. silvaticus* (Fujita 1984), and *Emericella desertorum* (Nozawa 1987).

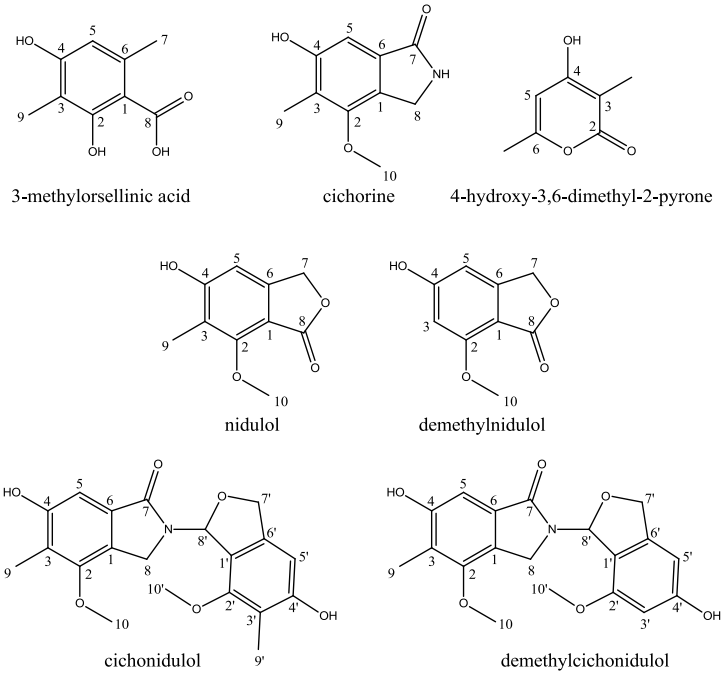

Figure 5 Structures of metabolites isolated and elucidated throughout this study. 3-methylorsellinic acid, cichorine, demethylcichorine, nidulol, demethylnidulol, cichonidulol, demethylcichonidulol, 4-hydroxy-3,6-dimethyl-2-pyrone.

The structures were elucidated using 2D NMR-spectra, where especially heteronuclear HSQC and HMBC spectra were extensively used due to the absence of proton-proton couplings and low proton density of the metabolites. In addition the results were in accordance with chemical shift values reported in literature for

cichorine (Monreau 2005), 3-methylorsellinic acid (Ahuja 2012), demethylnidulol (El-Feraly 1985), and 4-hydroxy-3,6-dimethyl-2-pyrone (Savard 1994).

The resemblance of the molecular formulas of cichorine ($C_{10}H_{11}NO_4$) and nidulol ($C_{10}H_{10}O_4$) and initial comparison of the ^{1}H-spectra suggested that these metabolites could be related. The main issue in structure elucidation of these two metabolites was whether the carbonyl was situated on C_7 or C_8. This problem was solved by comparison of the carbon chemical shift of cichorine to the shifts reported in the obtained after total synthesis of cichorine (Moreau 2005). For all the metabolites key HMBC correlations from H_5 the C_7 and/or C_8 and from H_7/H_8 to the carbons present in the aromatic ring, figure 6, aided in the structure elucidation. A NOESY correlation between H_8 and H_{10} in cichorine which were missing in nidulol confirmed the difference in the two structures

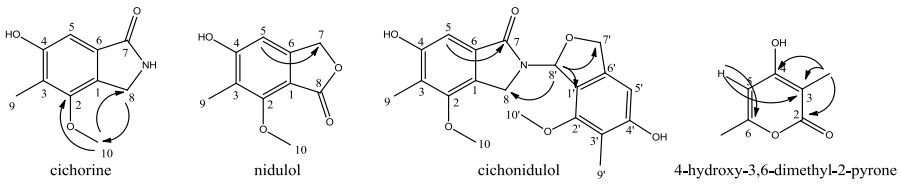

Figure 6 Key HMBC correlations of cichorine, nidulol, cichonidulol and 4-hydroxy-3,6-dimethyl-2-pyrone.

The UV spectrum of demethylnidulol was identical to the one of nidulol and the molecular formula $C_9H_8O_4$ showed that the difference between the two metabolites was a carbon and two protons. Through analysis of the NMR-spectra it was confirmed that the two metabolites were related and that the difference was a demethylation of C_3 in nidulol which gave demethylnidulol.

Through the analysis of the large-scale AN6446-Oex extract we noticed two small peaks eluting around five minutes which had UV-spectra that resembled the ones of nidulol and cichorine. These metabolites were present in small amounts in the large extract and based on the molecular formular of these metabolites $C_{20}H_{21}NO_6$ and $C_{19}H_{19}NO_6$ we speculated whether they could be dimers of cichorine, 3-MOA, nidulol or demethylnidulol through condensation and the formation of e.g. an ester as seen with the formation of lecanoric acid in the orsellinic acid pathway (Schroeckh 2009). 2.0 mg of $C_{20}H_{21}NO_6$ and 0.6 mg of

$C_{19}H_{19}NO_6$ were isolated from the extract and the structure of $C_{19}H_{19}NO_6$ were elucidated based on 2D NMR analysis to be a dimer of cichorine and nidulol, named cichonidulol. Analysis of the HMBC spectrum, key HMBC couplings of cichonidulol shown in figure 6, revealed that the link of the two molecules was not through an ester formation but interestingly through a C-N bond formed at the carbonyl position in nidulol. A search of the literature showed that cichonidulol and demethylnidulol were novel metabolites with a new carbon skeleton. The metabolite which showed the closest resemblance was the plant metabolite, capaurine, which contains the C-N condensation bond between two ringsystems; however, the nitrogen containing ring is a six membered ring and the substitution patterns of are quite different (Manske 1945).

Table 1 ^{13}C-chemical shifts (ppm) of 3-methylorsellinic acid, cichorine, nidulol, demethylnidulol, cichonidulol and demethylcichonidulol. All data obtained in DMSO-d_6 (referenced to 39.5 ppm)

ID	3-MOA	Cichorine	Nidulol	Demethyl-nidulol	Cichonidulol	Demethylcichonidulol
1/1’	103.7/-	123.1/-	107.2/-	92.9/-	121.3/116.1	
2/2’	163.0/-	153.6/-	157.5/-	159.6/-	153.6/153.8	
3/3’	107.7/-	118.9/-	117.5/-	101.1/-	120.5/115.3	
4/4’	159.7/-	156.3/-	162.7/-	168.8/-	156.9/158.1	
5/5’	109.9/-	102.9/-	103.0/-	103.2/-	103.4/102.4	
6/6’	139.4/-	131.9/-	148.6/-	151.4/-	131.0/139.5	
7/7’	23.4/-	169.8/-	68.2/-	66.9/-	167.1/71.7	
8/8’	173.8/-	43.1/-	168.5/-	178.1/-	43.2/83.5	
9/9’	7.9/-	9.1/-	8.2/-	-/-	9.3/8.6	
10/10’	-/-	58.9/-	53.9/-	53.9/-	59.0/59.2	

Table 4.1 lists the ^{13}C-chemical shifts of the above mentioned isolated metabolites where it is seen that the largest differences in shift values occur around at C_1 and C_6 differs depending on the position of the carbonyl.

The amount of $C_{19}H_{19}NO_6$ isolated was not sufficient for full 2D analysis; however, comparison of the ^1H-specrum to the one of cichonidulol revealed the only difference between the two were a demethylation in nidulol on C_3 thereby generating a dimer of cichorine and demethylnidulol, named demethylcichonidulol.

The final metabolite isolated was 4-hydroxy-3,6-dimethyl-2-pyrone whose chemical shifts were in close resemblance to those in the literature (Savard 1994). This metabolite is different from the above mentioned compounds having a completely different carbon skeleton. We therefore speculated if this metabolite was a product of *pkbA* or we could have activated another PKS encoding gene. We overexpressed *pkbA* and extracts of *pkbA*-Oex grown on MM showed high production of both 3-MOA and 4-hydroxy-3,6-dimethyl-2-pyrone (data not shown). Moreover, screening the data from all the PKS deletion strain grown on CYA medium revealed that only the *pkbA*Δ strain lost the ability to produce 4-hydroxy-3,6-dimethyl-2-pyrone.

Delineation of the cluster by gene expression analysis in overexpression and deletion strains of AN6446.

To verify that AN6446p had an activator effect on the surrounding genes, relative gene expression measurement by qRT-PCR analysis was performed. A deletion of AN6446, which displayed the same phenotype, as the reference was added to the analysis with the hypothesis that this would have the inverse effects from the overexpression strain minimizing the risk of picking false cluster members. Moreover, none of the peaks observed as an effect of the overexpression strains were present in the extracts of AN6446Δ (data not shown).

RNA was extracted from the reference strain as well as the deletion and overexpression strain of AN6446 grown on MM for four days. Relative gene expression levels were monitored by qRT-PCR on all 25 ORFs ranging from AN6435 to AN6457 both included. In Figure 7 the average fold change (fc) of the three runs

for all genes in the AN6446 overexpression and deletion strains compared to the reference are shown. A level of 1 in fc denotes unaltered expression in respect to the reference strain. One criterion for genes to be a putative cluster member was for AN6446-Oex to have fc above 1 coupled to fc close to 0 for AN6446Δ. As shown in Figure 7, the two levels of AN6446 expression had dramatic effects on the expression of numerous genes in the study. However, based on fc criteria as stated above the number of candidates was narrowed down to six genes besides AN6446: AN6444, AN6447, AN6448, AN6449, AN6450, AN6451. AN6445 and AN6452 both have fc's close to 1 for AN6446-Oex considering the standard deviation, and will thus not be considered cluster members, though they both have fcs close to 0 for the AN6446Δ, which could reflect local organization in the chromatin. In both mutant strains, the expression of distant neighbor genes were influenced, since only AN6435, AN6440, AN6441 and AN11921 were unchanged from the wild type with fc=1 in both mutant strains. AN6453 and AN6454 were significantly downregulated in respect to the reference strain. AN6438 to AN6439 were increased 4-6 fold in fc AN6446-Oex, but did not respond to the deletion of the AN6446-Oex. These examples indicate that the genetic alterations did affect the expression in the locus, and therefore some changes could be artifacts and not cluster specific reactions. Taken together the qRT-PCR data suggests the action of seven gene products.

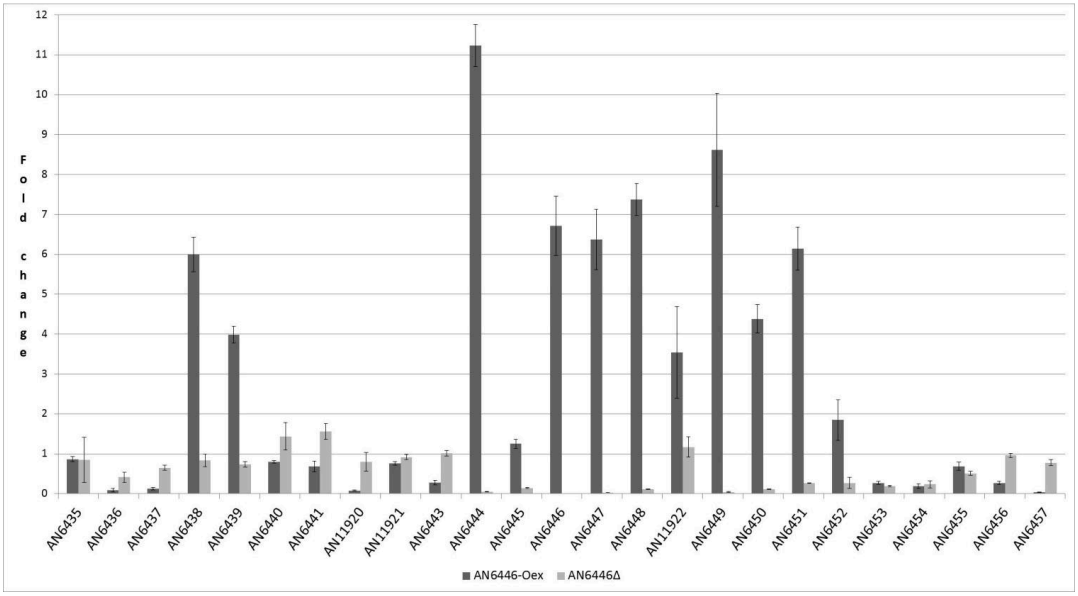

Figure 7 Results of the qRT-PCR analysis of AN6446-Oex and AN6446Δ on the genes from AN6435-AN6457 compared to the reference strain. An expression of 1 means unaltered expression, over 1 means higher expression and below 1 means lower expression. These data show that AN6444, AN6446, AN6447, AN6448, AN6449, AN6450 and AN6451 are upregulated in the overexpression strain and downregulated in the deletionstrain indicating that the *pkbA* cluster contains these genes.

Deletion of all genes spanning AN6435-AN6457 to confirm results from gene expression analysis

Gene deletions of all the 25 initial candidate genes were performed in the AN6446-Oex background to confirm the conclusions obtained from qRT-PCR and to elucidate on the biosynthetic role of the gene products. The six most distant genes in each side of the cluster were deleted in triplets (AN6435-AN6437; AN6438-AN6440; AN6452-AN6454; AN6455-AN6457) and the gene in between as singular deletion mutants.

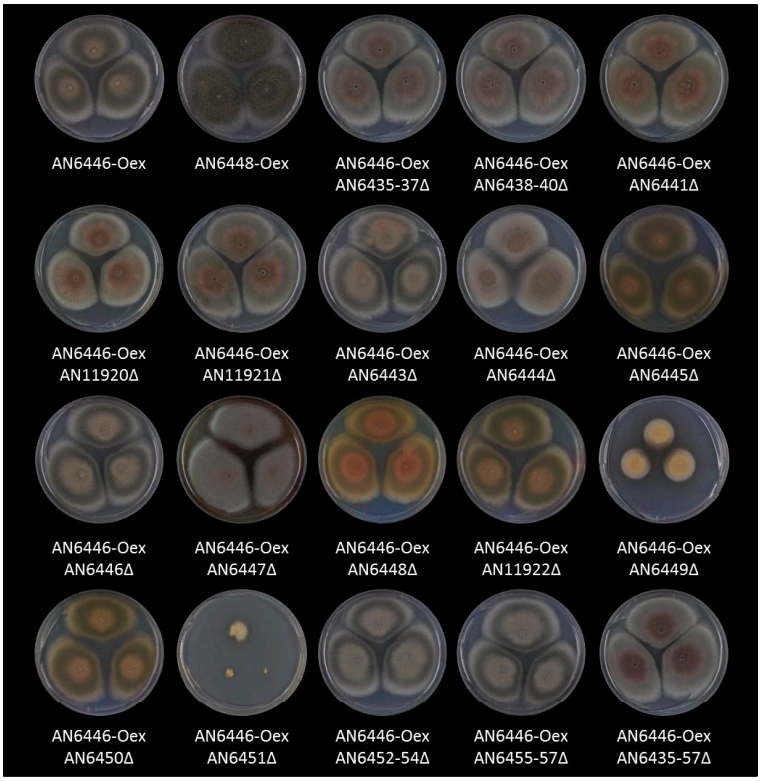

Figure 8 The phenotypes of the AN6446-Oex, *pkbA*-Oex, AN6446-Oex AN6435-6437Δ, AN6446-Oex AN6438-6440Δ, AN6446-Oex AN6441Δ, AN6446-Oex AN11920Δ, AN6446-Oex AN11921Δ, AN6446-Oex AN6443Δ, AN6446-Oex AN6444Δ, AN6446-Oex AN6445Δ, AN6446-Oex AN6446Δ, AN6446-Oex AN6447Δ, AN6446-Oex AN6448Δ, AN6446-Oex AN11922Δ, AN6446-Oex AN6449Δ, AN6446-Oex AN6450Δ, AN6446-Oex AN6451Δ, AN6446-Oex AN6452-6454Δ, AN6446-Oex AN6455-6457Δ and AN6446-Oex AN6435-6457Δ strains cultivated on MM medium for seven days at 37°C.

To see whether AN6446 had regulatory effects on secondary metabolite production outside the cluster, a full cluster deletion (AN6435-AN6457) in the overexpression strain was constructed as well. The phenotypes can be compared in figure 8, and the loss of genes, predicted to form the gene cluster of PkbA, indeed stood out from the others in the phenotype display. The phenotypes varied greatly, indicating altered metabolism in the respective strains. To investigate which metabolites originated from this cluster and if correlated with the phenotype of the mutant strains plug micro-extraction was performed (Frisvad 1987, Smedsgaard 1997) and the extracts were analyzed by UHPLC-TOF-MS. In figure 9, 10 and 11 ESI^+ BPC of all the extracts can be seen, and they are grouped based on their metabolic patterns.

Interestingly, in figure 9, a number of deletion strains, from AN6435 to AN11921, are displayed where all the key metabolites appearing in the AN6446-Oex strain had disappeared. Since the qRT-PCR data did not support that these genes belonged to the cluster, we speculated that this effect links to local chromosomal aberration due to change in the strain. Inactivating one or some of the genes instead with point mutations would test this hypothesis. In the whole cluster deletion strain, AN6446-Oex AN6435-AN6457Δ, all metabolite production is eliminated including 4-hydroxy-3,6-dimethyl-2-pyrone strongly indicating that this metabolite is a product of the cluster. However, the eliminated production may reflect the deletions of AN6435 to AN11921. A cluster deletion from AN6444 to AN6451 would be an alternative. Moreover, the phenotypes of these strains were very similar as the metabolic profiles were. The strains all showed the same differences from the reference strain, namely the massive production of the siderophore triacetylfusarinine.

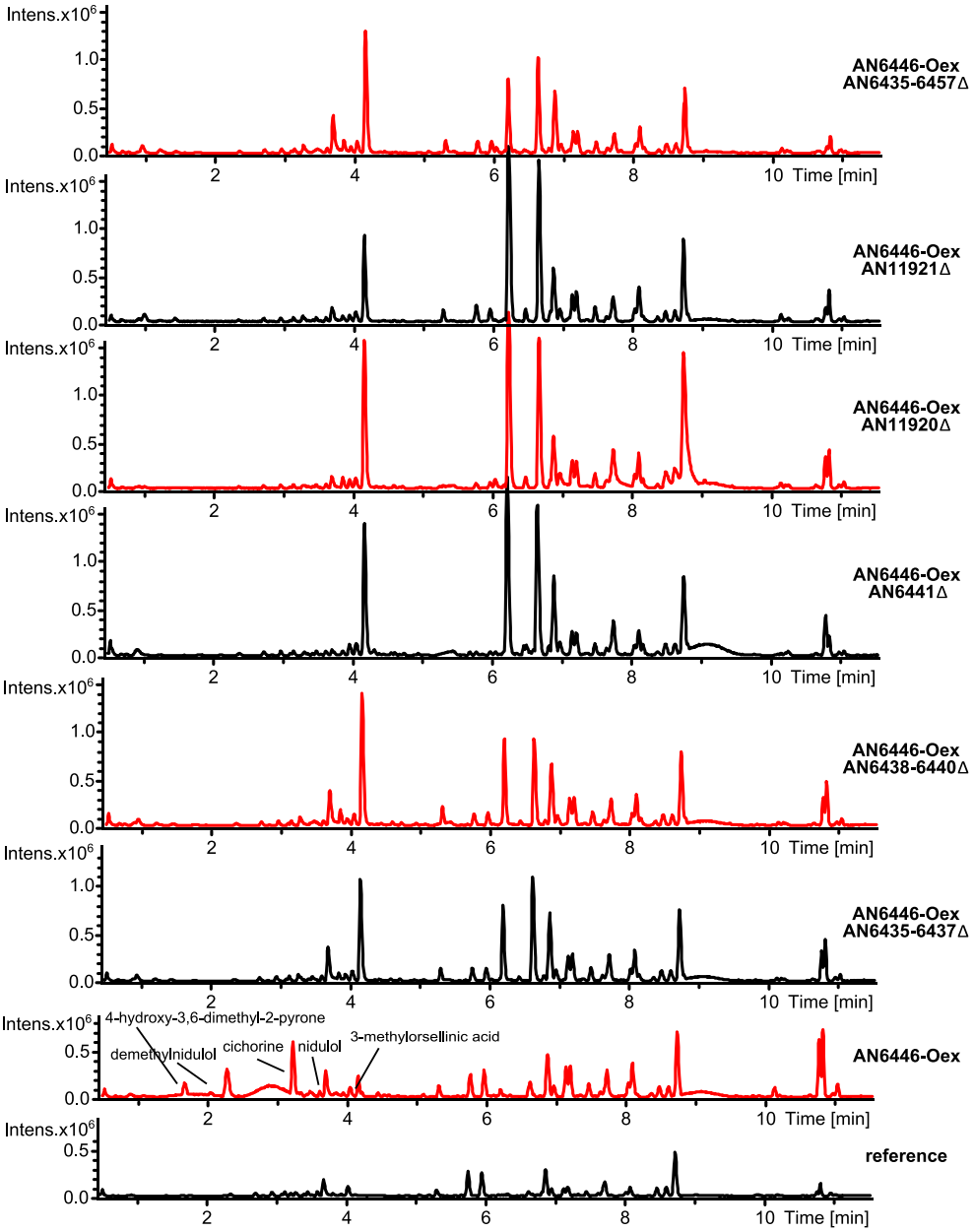

Figure 9 UHPLC-TOF-MS ESI$^+$ BPC of the micro-extracts of the (from bottom to top) reference, AN6446-Oex, AN6446-Oex AN6435-6437Δ, AN6446-Oex AN6438-6440Δ, AN6446-Oex AN6441Δ, AN6446-Oex AN11920Δ, AN6446-Oex AN11921Δ, AN6446-Oex AN6435-6457Δ strains cultivated on MM medium for seven days at 37°C.

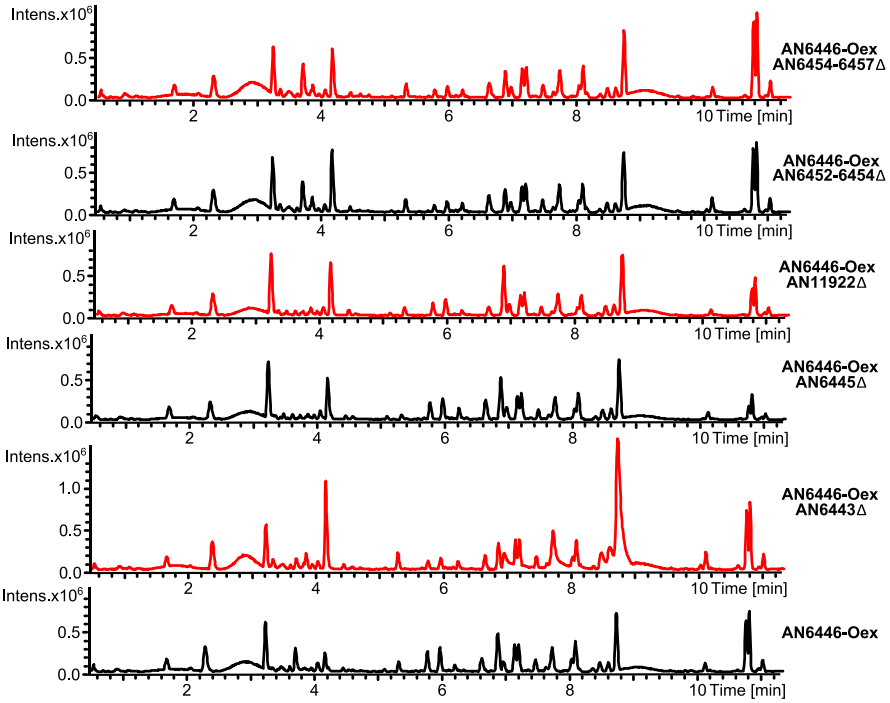

Figure 10 UHPLC-TOF-MS ESI$^+$ BPC of the micro-extracts of the (from bottom to top) AN6446-Oex, AN6446-Oex AN6443Δ, AN6446-Oex AN6445Δ, AN6446-Oex AN11922Δ, AN6446-Oex AN6452-6454Δ, AN6446-Oex AN6454-6457Δ strains cultivated on MM medium for seven days at 37°C. The figure illustrates that these genes are not involved in the *pkbA* gene cluster in agreement with the qRT-PCR data.

The ESI$^+$ BPC chromatograms of the micro-extracts of the second group of strains are collected in figure 10. These mutant strains all have chromatograms mimicking the profile of AN6446-Oex. In this group, the colonies of the strains in figure 8 resembled the overexpression strain, and these results are in agreement with the qRT-PCR data, which excluded these genes to be part of 3-MOA gene cluster.

The last group of mutant strains collected in figure 11 as BPC chromatograms of the micro-extracts, actually constitute the strains pointing out from the gene expression analysis as belonging to the cluster as depicted in figure 12. The metabolites isolated in this study are listed in table 1 if present in the extracts of mutant strains. There are also other peaks appearing in the chromatograms, however no metabolite have been assigned to these at the present time.

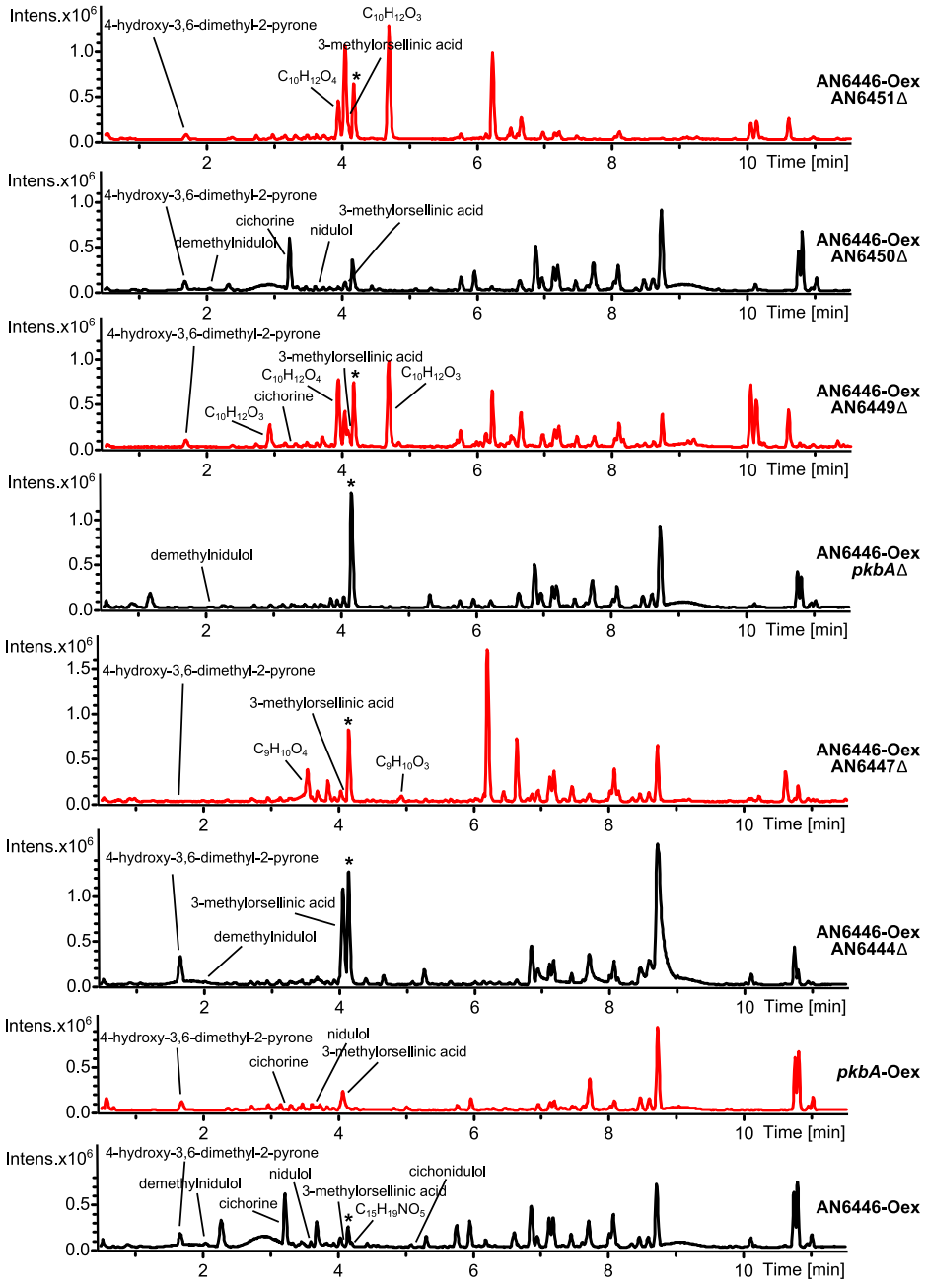

Figure 11 UHPLC-TOF-MS ESI$^+$ BPC of the micro-extracts of the AN6446-Oxe, AN6448-Oex, AN6446-Oex AN6444Δ, AN6446-Oex AN6446Δ, AN6446-Oex AN6447Δ, AN6446-Oex *pkbA*Δ, AN6446-Oex AN6449Δ, AN6446-Oex AN6450Δ and AN6446-Oex AN6451Δ strains cultivated on MM medium for seven days at 37°C.

Table 2 Detection of metabolites (through EIC^{+}) in the micro-extracts of the deletion and overexpression strains constructed and identified as belonging to the 3-methylorsellinic clusters in this study; (from bottom to top) AN6446-Oex, AN6448-Oex, AN6446-Oex AN6444Δ, AN6446-Oex AN6447Δ, AN6446-Oex *pkbA*Δ, AN6446-Oex AN6449Δ, AN6446-Oex AN6450Δ, AN6446-Oex AN6451Δ. Parenthesis indicates the metabolites are present in trace amounts. *A metabolite eluting close to cichorine with a small mass difference makes further analysis needed for clarification. *A metabolite eluting close to cichorine with a small mass difference makes further analysis needed for clarification.**Eluting at 2.9 minutes.***Eluting at 4.7 minutes

Metabolite	AN6446-Oex	*pkbA* -Oex	AN6444Δ[a]	AN6447Δ[a]	*pkbA*Δ[a]	AN6449Δ[a]	AN6450Δ[a]	AN6451Δ[a]
3-methyl-orsellinic acid	(+)	+	+	+	-	+	(+)	+
Cichorine*	+	+	-	-	-	-	+	-
Nidulol	+	+	-	-	-	-	+	-
Demethyl-nidulol	+	-	+	-	(+)	-	+	-
Cichonidulol	(+)	-	-	-	-	-	-	-
Demethyl-cichonidulol	-	-	-	-	-	-	-	-
4-hydroxy-3,6-dimethyl-2-pyrone	+	+	+	(+)	-	+	+	+
$C_9H_{10}O_3$	-	-	-	+	-	-	-	-
$C_9H_{10}O_4$	-	-	-	+	-	(+)	-	(+)
$C_{10}H_{12}O_3$**	-	-	-	-	-	+	-	-
$C_{10}H_{12}O_3$***	+	-	-	-	-	+	-	+
$C_{10}H_{12}O_4$	-	-	-	-	-	+	-	+
$C_{15}H_{19}NO_5$	+	(+)	-	-	-	+	+	-

[a] strain having AN6446-Oex allele

In the deletion of *pkbA* in the AN6446-Oex strain the isolated metabolites are all, except demethylnidulol, missing confirming that these metabolites are part of the 3-MOA gene cluster. Demethylnidulol were detected in trace amount and could be due to the conversion of orsellinic acid into the product, however this metabolite cannot be detected in several of the mutants.

AN6450 is predicted to encode an oxidoreductase, and showed in the qRT-PCR analysis to be regulated by AN6446, however the metabolite profile of AN6446-Oex AN6450Δ was equal to that of AN6446-Oex indicating that either it does not take part in the biosynthesis, or the product this enzymatic step was not detected.

Figure 12. The 3-MOA, *pkbA*, gene cluster and the nearest neighbor genes. Arrows in black denotes cluster members and grey are genes not supported by data to be cluster members.

Interestingly, AN6451 is predicted to be a transporter of the Major Facilitator Superfamily (MFS) having close to full sequence coverage and more than 50 % sequence identity to transporters from other fungi, e.g. the CtnC transporter of the citrinin biosynthesis in *Monascus purpureus*, and this deletion mutant is heavily impaired in growth. This indicates that some compartmentalization of the biosynthesis may occur and failure to transport either 3-MOA or 4-hydroxy-3,6-dimethyl-2-pyrone, or even other products in the pathway can be toxic, at least under the artificial conditions that overexpression of AN6446 offers.

Table 3 Predicted function of the genes identified as belonging to the 3-methylorsellinic acid cluster.

Gene	Predicted function
AN6444	NRPS-like
AN6446	Transcription factor
AN6447	*O*-methyltransferase
pkbA	PKS
AN6449	Cytochrome P450
AN6450	Oxidoreductase
AN6451	Transporter

Based on the metabolic profile of the deletion strains a biosynthetic pathway from 3-methylorsellinic acid to cichonidulol is proposed, figure 13. 4-hydroxy-3,6-dimethyl-2-pyrone disappears in the AN6446-Oex *pkbA*Δ strain and are only present in trace amounts in the AN6446-Oex AN6447Δ strain. As opposed to 3-methylorsellinic acid the polyketide backbone seems to be C_6 and not C_8 and may be a shunt product of PkbA. If the methylation pattern in the assembly of the polyketide backbones of 3-methylorsellinic acid and

4-hydroxy-3,6-dimethyl-2-pyrone were the same one would expect the latter to be methylated at C_5 and not C_3 as is observed. This shows that there are several differences between the assembly of the two metabolites. Other metabolites with the same UV-spectrum as 4-hydroxy-3,6-dimethyl-2-pyrone were detected in the deletion strains but have not yet been isolated. Ahuja and co-workers (Ahuja 2012) isolated two products of the PkgA enzyme, dehydrocitreoisocoumarin and 6,8-dihydroxy-3-(2-oxopropyl)-isocoumarin where the difference of the polyketide backbone also was the incorporation of one malonyl-CoA less in the latter.

The first step of the biosynthesis is likely to be oxidation and reduction of 3-MOA. The proposed intermediates are the 3-MOA in which the carboxylic acid has been reduced to an aldehyde ($C_9H_{10}O_3$) and the 6-methyl oxidated ($C_9H_{10}O_3$). Due to the appearance of metabolites identified to have these molecular formulas in the AN6447Δ strain the next step is proposed to be *O*-methylation of the 2-OH catalyzed by the enzyme encoded by AN6447. This metabolite could then undergo ring closure to form nidulol. The C_7-carbonyl of nidulol, silvaticol, has also been reported in the literature isolated from *A. silvaticus* (Fujita 1984) and Kawahara and co-workers (Kawahara 1988) suggest quadrilineatin as the intermediate before ring closure thereby explaining that both metabolites nidulol and silvaticol are present in *A. silvaticus*. Neither silvaticol nor quadrilineatin have been detected in any of the examined extracts yet.

The metabolic profile of the AN6446-Oex AN6449Δ and AN6446-Oex AN6451Δ appear to be similar. Several peaks appear in these two deletions where the molecular formula for one of these is equal to the proposed methylated product of AN6447 ($C_{10}H_{12}O_4$) indicating that these enzymes are involved in the next steps of the biosynthesis. The roles for these two enzymes in the biosynthesis are still unknown but identification of the intermediates could provide helpful answers. AN6449 encodes for a cytochrome P450 which could be responsible for the oxidation of the $C_{10}H_{12}O_4$ to a quadrilineatin proposed in figure 13 which could then undergo further modifications to cichorine.

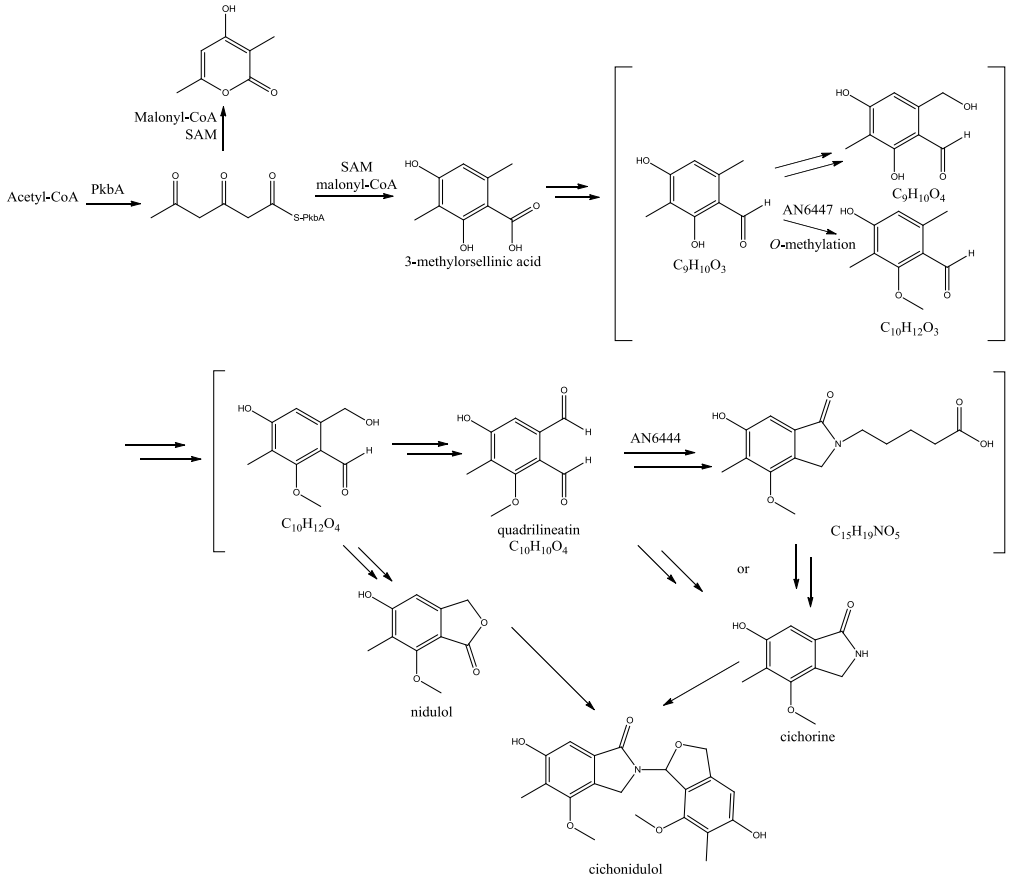

Figure 13 Proposed biosynthetic route of the elucidated metabolites of the *pkbA* cluster. The metabolites in boxes have all been identified through NMR-analyses, whereas the metabolites in brackets are proposed intermediates which have been detected through MS-analysis and the rest have not been detected.

In the AN6444Δ strain the production of several metabolites have terminated including cichorine and other nitrogen containing metabolites for example a metabolite eluding at 4.2 minutes with the molecular formula $C_{15}H_{19}NO_5$ (identified through LC-TOF-MS). The role of AN6444 strongly indicates contribution of the nitrogen to the molecule and ring closure. As no new intermediates were detected in the extracts the exact role of the enzyme remains elusive. The nitrogen incorporated in the structure could arise from either transamination as seen in the biosynthesis of amino acids or from an amino acid which reacts with the dialdehyde. This reaction could yield a lactam where the rest of the amino acid is still attached to the

nitrogen followed by decarboxylation as seen for erinacerin A, figure 14, where the residual part of decarboxylated phenyalalanine is attached to the lactam-*N* (Yaoita 2005). The above mentioned metabolite, $C_{15}H_{19}NO_5$, which was present in the AN6446-Oex and AN6446-Oex AN6449Δ strains could indeed resemble the product, figure 14, of these reactions if the amino acid was 2-aminoadipic acid. Bioinformatic analysis of AN6444 supports this hypothesis since predicts the adenylation domain of AN6444 to encode for this amino acid. This amino acid residue would then have to be cleaved from the molecule to reach cichorine. A way to test this hypothesis is to do feeding experiments with labeled 2-aminoadipic acid. Aspernidine A and B (not detected in these extracts) are two other metabolites reported from *A. nidulans* by Scherlach and co-workers (Scherlach 2010) where nitrogen is incorporated into aromatic part of the structure and is proposed to be derived from an orsellinic acid. The nitrogen of these metabolites could also arise from AN6444 or other NRPS-like enzymes.

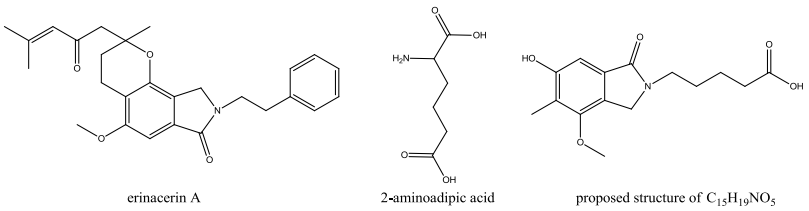

Figure 4.32 The structure of erinacerin A, 2-aminoadipic acid and proposed structure of $C_{15}H_{19}NO_5$.

It remains unknown whether the dimers, cichonidulol and demethylcichonidulol, were catalyzing by an enzyme or the dimerization occurred non-enzymatic. Due to the small production of the metabolites in the overexpression strain the data obtained is not sufficient for identifying the enzyme.

This study has through qRT-PCR and subsequent chemical analysis identified the genes belonging to the 3-methylorsellinic acid gene cluster. Several metabolites have been isolated, structure elucidated and linked to the gene cluster e.g. nidulol, cichonidulol, demethylcichonidulol and 4-hydroxy-3,6-dimethyl-2-pyrone. The function of AN6447 has been shown to be *O*-methylation and data strongly suggests that AN6444 is involved in the incorporation of a nitrogen atom into the structure which might occur through an aminoadipic intermediate. Several interesting intermediates have been identified through QTOF-MS analysis and remain

to be isolated and structure elucidated to shed more light over the biosynthesis. A shunt product of the PKS has been identified and through analysis of the PKS deletion library and data of the strains constructed in this work it have been linked to PkbA.

Materials and methods

Strains and media. The *A. nidulans* strain IBT29539, *nkuA*Δ, (*argB2*, *pyrG89*, *veA1*, *nkuA*Δ) was used for overexpressing AN6446, and the IBT28738 (*nkuA-trS*) was used as reference in qRT-PCR experiments as well as a control in metabolite analysis (*argB2*, *pyrG89*, *veA1*, *nkuA-trS*::AF*pyrG*) (Nielsen 2008). In table 1, all strains available and constructed in this study are listed. *Escherichia coli* strain DH5α was used for cloning.

Fungal minimal medium (MM) was as described in (Cove 1966), but with 1% glucose, 10 mM $NaNO_3$ and 2% agar (Sorbigel, Hendaye, France), when necessary supplemented with 10 mM uridine (Uri), 10 mM uracil (Ura) and 4 mM L-arginine (Arg). Elimination of the *pyrG* marker was done on 5-FOA (1.3 mg/ml) supplemented MM, as previously described in Nielsen (2006). All chemicals were from Sigma-Aldrich (St. Louis, Mo, USA) unless otherwise stated.

Table 4. List of strains used in this study

Strain	Genotype
***nkuA*Δ**[a]	*nkuA*Δ
nkuA-trS[a]	*nkuA-trS*::AF*pyrG*
AN6444Δ	*nkuA*Δ, AN6444Δ
AN6445Δ	*nkuA*Δ, AN6445Δ
AN6446Δ	*nkuA*Δ, AN6446Δ
AN6446-Oex	*nkuA*Δ, IS1::PgpdA-AN6446-TtrpC::AF*pyrG*
AN6446-Oex AN6451Δ	*nkuA*Δ, IS1::PgpdA-AN6446-TtrpC, AN6451Δ::AF*pyrG*
AN6446-Oex AN6450Δ	*nkuA*Δ, IS1::PgpdA-AN6446-TtrpC, AN6450Δ::AF*pyrG*
AN6446-Oex AN6449Δ	*nkuA*Δ, IS1::PgpdA-AN6446-TtrpC, AN6449Δ::AF*pyrG*

AN6446-Oex AN11922Δ	*nkuA*Δ, IS1::PgpdA-AN6446-TtrpC, AN11922Δ::AF*pyrG*
AN6446-Oex AN6448Δ	*nkuA*Δ, IS1::PgpdA-AN6446-TtrpC, AN6448Δ::AF*pyrG*
AN6446-Oex AN6447Δ	*nkuA*Δ, IS1::PgpdA-AN6446-TtrpC, AN6447Δ::AF*pyrG*
AN6446-Oex AN6446Δ	*nkuA*Δ, IS1::PgpdA-AN6446-TtrpC, AN6446Δ::AF*pyrG*
AN6446-Oex AN6445Δ	*nkuA*Δ, IS1::PgpdA-AN6446-TtrpC, AN6445Δ::AF*pyrG*
AN6446-Oex AN6444Δ	*nkuA*Δ, IS1::PgpdA-AN6446-TtrpC, AN6444Δ::AF*pyrG*
AN6446-Oex AN6443Δ	*nkuA*Δ, IS1::PgpdA-AN6446-TtrpC, AN6443Δ::AF*pyrG*
AN6446-Oex AN11921Δ	*nkuA*Δ, IS1::PgpdA-AN6446-TtrpC, AN11921Δ::AF*pyrG*
AN6446-Oex AN11920Δ	*nkuA*Δ, IS1::PgpdA-AN6446-TtrpC, AN11920Δ::AF*pyrG*
AN6446-Oex AN6441Δ	*nkuA*Δ, IS1::PgpdA-AN6446-TtrpC, AN6441Δ::AF*pyrG*
AN6446-Oex AN6457-55Δ	*nkuA*Δ, IS1::PgpdA-AN6446-TtrpC, AN6457-AN6455Δ::AF*pyrG*
AN6446-Oex AN6454-52Δ	*nkuA*Δ, IS1::PgpdA-AN6446-TtrpC::AF*pyrG*, AN6454-AN6452Δ::AF*pyrG*
AN6446-Oex AN6440-38Δ	*nkuA*Δ, IS1::PgpdA-AN6446-TtrpC::AF*pyrG*, AN6440-AN6438Δ::AF*pyrG*
AN6446-Oex AN6437-35Δ	*nkuA*Δ, IS1::PgpdA-AN6446-TtrpC::AF*pyrG*, AN6437-AN6435Δ::AF*pyrG*
AN6446-Oex AN6437-57Δ	*nkuA*Δ, IS1::PgpdA-AN6446-TtrpC::AF*pyrG*, AN6437-AN6457Δ::AF*pyrG*
***pkbA*-Oex**	*nkuA*Δ, IS1::PgpdA-*pkbA*-TtrpC::*argB*

[a] Strain from Nielsen et al., 2008

Primers used in this study

USER Deletion Primers	
AN6451-DL-Up-FU	GGGTTTAAUTGTCAGAGAAGCGAGGAAC
AN6451-DL-Up-RU	GGACTTAAUGGCCGGCGAACAATAGATA
AN6451-DL-Dw-FU	GGCATTAAUCCTCGGTTCTTGACAACG
AN6451-DL-Dw-RU	GGTCTTAAUCACATTCTCCATCGCTCTC
AN6450-DL-Up-FU	GGGTTTAAUAGAGTGATCAGTTGGAGGAT
AN6450-DL-Up-RU	GGACTTAAUGAGACTGCTACGCCTGATAT
AN6450-DL-Dw-FU	GGCATTAAUGGCTGTTCATCTTCGTACTC
AN6450-DL-Dw-RU	GGTCTTAAUTCTAGCCATCGTTCTGGTC
AN6449-DL-Up-FWD	GGGTTTAAUGGCTATATTGTTGGTGGTGT
AN6449-DL-Up-RU	GGACTTAAUGAGTACGAAGATGAACAGCC
AN6449-DL-Dw-FU	GGCATTAAUGGTTGATGAAGTAGTCTGAG
AN6449-DL-Dw-RU	GGTCTTAAUCCAATATAGAAGCGACGGTC
AN11922-DL-Up-FU	GGGTTTAAUCATCCACTGTTTCGTCTCAT
AN11922-DL-Up-RU	GGACTTAAUAGGCGAAGACACATTGATG

AN11922-DL-Dw-FU	GGCATTAAUGGCCAATCATCCATACAGTG
AN11922-DL-Dw-RU	GGTCTTAAUTGGCTCGACTACTTCTGGAA
AN6448-DL-Up-FU	GGGTTTAAUCGGCTAGACTCCACTTACAA
AN6448-DL-Up-RU	GGACTTAAUGGCTCGAACACACCTATGAA
AN6448-DL-Dw-FU	GGCATTAAUAGAGGAGATACCACGAAGAT
AN6448-DL-Dw-RU	GGTCTTAAUACAGACTCCTTGATATGACG
AN6447-DL-Up-FU	GGGTTTAAUTAGACTGAATTGAACGACGC
AN6447-DL-Up-RU	GGACTTAAUAAGAATGCTTGGAGTGGACA
AN6447-DL-Dw-FU	GGCATTAAUGGTGTCTGTCCACTTGTTG
AN6447-DL-Dw-RU	GGTCTTAAUGTACTGGTAATGGTTGAGGTG
AN6446-DL-Up-FU	GGGTTTAAUCCAGCTCCGATATATTGTGC
AN6446-DL-Up-RU	GGACTTAAUTTGGAGGTATTCTGGAAGGT
AN6446-DL-Dw-FU	GGCATTAAUGTTCTTGGTGTCGTGTCGTA
AN6446-DL-Dw-RU	GGTCTTAAUCATCGAAGACAGCATACCT
AN6445-DL-Up-FU	GGGTTTAAUGGTGGCAAGAACAATCGTAT
AN6445-DL-Up-RU	GGACTTAAUAGATGATGAAGCTGTAGTGTG
AN6445-DL-Dw-FU	GGCATTAAUGAGAGGAGATAGAAGGCTTG
AN6445-DL-Dw-RU	GGTCTTAAUTCATCCTTCATCGCCATTCA
AN6444-DL-Up-FU	GGGTTTAAUGGATACCATAACGCTCAAGA
AN6444-DL-Up-RU	GGACTTAAUTCTCACGCGATCTGACACTA
AN6444-DL-Dw-FU	GGCATTAAUCGGTTGCTAGACGTTATCT
AN6444-DL-Dw-RU	GGTCTTAAUGCGGTCCAAGAGATGTGA
AN6443-DL-Up-FU	GGGTTTAAUTCCGACCAGAAGATTCGT
AN6443-DL-Up-RU	GGACTTAAUAATAGCCTTGACGTGGAC
AN6443-DL-Dw-FU	GGCATTAAUTTGGAACAGCTGAAGACTC
AN6443-DL-Dw-RU	GGTCTTAAUCTCGTCTTCTCTTAACCTCG
AN6441-DL-Up-FU	GGGTTTAAUTGGGTTAGCCACGCTCAG
AN6441-DL-Up-RU	GGACTTAAUGGCTCTAGAAGTTGAAGACTGCTG
AN6441-DL-Dw-FU	GGCATTAAUGTGGTTTGGCGTCTTGAGTGG
AN6441-DL-Dw-RU	GGTCTTAAUCAGAGTGTCAGGGGCTGAG
AN11921-DL-Up-FU	GGGTTTAAUCAGCTGAGGCATGCAGAG
AN11921-DL-Up-RU	GGACTTAAUGGGGTTGTTGAAATCGAGTGTTGG
AN11921-DL-Dw-FU	GGCATTAAUGTATGAGTCATAGCGCGCG
AN11921-DL-Dw-RU	GGTCTTAAUGTCACGTGCGCAAGCTAATCG
AN11920-DL-Up-FU	GGGTTTAAUCGCCGCCCTTACCCAACG
AN11920-DL-Up-RU	GGACTTAAUCGTCCAGAACCGCATAGTCTAGC
AN11920-DL-Dw-FU	GGCATTAAUGAGACTGGAGAATGGGTCTGG
AN11920-DL-Dw-RU	GGTCTTAAUGTCTAATTCGGTTTGGAACAGCTG
Fusion PCR Deletion Primers	
AN6457-DL-Dw-Fad	aattccagctgaccaccatgGCGTACACGCTGCGCGGAC
AN6457-DL-Dw-R	GCTGACCAGGCCGTATCTTCC
AN6454-DL-Dw-Fad	aattccagctgaccaccatgGCGAGATGATGGGCAGGA
AN6454-DL-Dw-Rad	gatccccgggaattgccatgGCTCTGTTGGACCCCACCT
AN6452-DL-Up-F	GCTGATTGCAGTCTGCCTG
AN6452-DL-Dw-Rad	gatccccgggaattgccatgCGAGGGGGATGTAAACAGC
AN6440-DL-Dw-Fad	aattccagctgaccaccatgGCAAGCAAGGCAGCTGTTC
AN6440-DL-Dw-R	GACACGAGCCTCCACGATG
AN6438-DL-Up-F	GCAGCGTCTCTATCGGATG
AN6438-DL-Up-Rad	gatccccgggaattgccatgGCCATCACTCGGTATGAGC
AN6437-DL-Dw-Fad	aattccagctgaccaccatgGCATGTGCATATGAAAGCTCT
AN6437-DL-Dw-R	GCTGTGAACCAGCGTGTC
AN6435-DL-Up-F	GCCATTCTTGCTTGGAAGC
AN6435-DL-Up-Rad	gatccccgggaattgccatgCGTTTCAAGGTCAGACCCTG

Check Primers	
AN64TT-CHK-F	GCCGATTCAAGCACTCTGC
AN64TT-CHK-R	GCGTCTGCCTTCACTTGC
AN6457-CHK-Int-R	GCAAGCAAGGACAACTCG
AN6455-CHK-Dw-F	GCTGCAGATCGTCTGCTCAG
AN6455-CHK-Dw-R	CCTGCAGAAGCGCCCAGT
AN6454-CHK-F	GGCGTATACGACCGAGAAGC
AN6454-CHK-Int-R	GCTCCCGTGGACGAACC
AN6453-CHK-F	GCGAGGTTACATCGACATGG
AN6452-CHK-F	GCACCAGTGATGAGAGCGAC
AN6451-CHK-F	TGTGAATCGTGTGGGCTCTA
AN6451-CHK-R	CTGCGATTCATGAGCTTTG
AN6450-CHK-F	GGGTGCGGGTAAAGTAGAAA
AN6450-CHK-R	GGCGTAGCAGTCTCCCAGTG
AN6450-CHK-R	CAATCTGCAGCCGTCACTA
AN6449-CHK-F	TGGCCGCACTAAAGACTGA
AN6449-CHK-R	GAGGTAAAGCAAGGCGTAT
AN6448-CHK-F	GCAGAGACCGAACTTGCGG
AN6448-CHK-R	GCCGCCACCATATGCAGAG
AN6448-CHK-F	TAATCGACATCATCGCCAGA
AN6448-CHK-R	GAATTTCGCCCATTGTACTG
AN6447-CHK-F	TGGGCTCTGAAGTCTGTATT
AN6447-CHK-R	GACACGACACCAAGAACTT
AN6446-CHK-F	GCAACTGACGACTTAGACT
AN6446-CHK-R	TAAGTGACGAGAGCTGGAAT
AN6445-CHK-F	GCACACCAATCTCAAACTG
AN6445-CHK-R	TACAACTTGGCGGACATCA
AN6445-CHK-F	GCGTCTAGCAGGGATGAAGG
AN6445-CHK-R	GCACCAGAGACCGAGGGC
AN6444-CHK-F	TTGTATTGTCTTTGCGCCTC
AN6444-CHK-R	CACGGCATAAGTCAGAAAGG
AN6443-CHK-F	CTCTCACTGTCTGCTCTCT
AN6443-CHK-R	TCAGGCTCAGTGTTACATC
AN11922-CHK-F	ATGGGAGTTGCTAACGAAAG
AN11922-CHK-R	TGTCAAACCTCGTCTCGTT
AN11920-CHK-F	GCTCAACGGATACGCCAGAG
AN11920-CHK-R	GCCGACGATCGTCTCCTG
AN6441-CHK-F	GCAGCGAACGTGACTGTGTG
AN6441-CHK-R	GCCAACAGCCGCGGAG
AN6439-CHK-Int-F	GCCTATACGCATCCTTTGC
AN6438-CHK-F	GCACCTTACAGACACGGACTGG
AN6436-CHK-R	GCGCCTGGACGAGACTC
AN6435-CHK-F	GCCAGCTGCACACCACTC
qRT-PCR Primers	
AN6457-3-qRT-F	CCTCCAAGAAGACGAACCCTG
AN6457-3-qRT-R	CTTGATCCGCTCAGAGCCC
AN6456-3-qRT-F	GCGACATGGGAGCAAAGAAGG
AN6456-3-qRT-R	GAATACTGGTGTAGGGGCTGG
AN6455-3-qRT-F	CCTATCCTCACCGTCTTCACC
AN6455-3-qRT-R	CCACACTGGCCCCAACCATATTC
AN6454-3-qRT-F	CAGCCGATATCATAGACGCC
AN6454-3-qRT-R	CCTCACCCTTACCCTGCTC
AN6453-3-qRT-F	CGAGAAGTCGGCAGTTGCG

AN6453-3-qRT-R	GGACAAAAGGCTTGAGGGGG
AN6452-3-qRT-F	CACGACAATCATCCTCGCG
AN6452-3-qRT-R	CCTTTCAGTCCCACTAGCCC
AN6451-3-qRT-F	CGCCCATGTACCATCGACT
AN6451-3-qRT-R	CAACTTGCGGACCCTCTCG
AN6450-3-qRT-F	CTTCCTGAACGGCAAGTCAGAC
AN6450-3-qRT-R	GTCCCGAAACCCAGCTGC
AN6449-3-qRT-F	CAAGACGCTGTACAACTCGTTGC
AN6449-3-qRT-R	CCACCGGTTCTCCAAGTGC
AN11922-3-qRT-F	CCAACACCGCACGATTCTCC
AN11922-3-qRT-R	CACTGTCGTCAGCAGTCAAATCC
AN6448-3-qRT-F	GTCCCTACGCGCAGATCC
AN6448-3-qRT-R	CTTCCCAGACACCTCCTCCTTC
AN6447-3-qRT-F	TACATGCGGTACCCGCAC
AN6447-3-qRT-R	GCCAATCTCCACAATCCCAACC
AN6446-3-qRT-F	GGAGATACCAGACTGGACGG
AN6446-3-qRT-R	GGTACTGGTAATGGTTGAGGTGG
AN6445-3-qRT-F	GATGAGATCGTCGAGTGGCTG
AN6445-3-qRT-R	CTGGGGGAAGGAAAGGCATG
AN6444-3-qRT-F	GACAACCCAGCGAAGAAACTCC
AN6444-3-qRT-R	CTTCAACCACCCAATCTCCTTCCA
AN6443-3-qRT-F	GTATTGCGCATCGACTGAAGAC
AN6443-3-qRT-R	CTCCACCTGTCCGACAATATCC
AN11921-3-qRT-F	CTGCTCTCCATTTCCTCTTCGC
AN11921-3-qRT-R	CCACGAGTGTCACGACACC
AN11920-3-qRT-F	CCTGTTCTACCTCCACCATGC
AN11920-3-qRT-R	CACCAGCCCGTTCATCCAC
AN6441-3-qRT-F	GGCGATGGATATACCTGCGG
AN6441-3-qRT-R	GAGGCAGCTGAGGCTTGAG
AN6440-3-qRT-F	CCGACACAATCAGCTGCC
AN6440-3-qRT-R	CCGCCTTCGATATCCTATCCAC
AN6439-3-qRT-F	CCAGTACCTATATTTGCCGCCC
AN6439-3-qRT-R	GTCATCCATCGCAGGCAC
AN6438-3-qRT-F	CAGACTCGGATCATAGCATCC
AN6438-3-qRT-R	CCAGTCCTGGCTCCTCTTG
AN6437-3-qRT-F	CACCCGTACCTCGCACAC
AN6437-3-qRT-R	CCAGAGACTGCAGCCCTC
AN6436-3-qRT-F	GAGAGCGAGCAAGTGGTGC
AN6436-3-qRT-R	GGTTCACCAGGTCGTAGTAGTG
AN6435-qRT-3-F	GCCTCAACGTATTTCCCCTGG
AN6435-qRT-3-R	GAGCCCCTTCTTTGCGCC
Overexpression Primers	
AN6446-Oex-FU	AGAGCGAUATGAACGACACTTCTGGTCGAC
AN6446-Oex-RU	TCTGCGAUTCAGGACCCCGTGTTGTAC
AN6448-Oex-5-FU	AGAGCGAUATGGCTCCGGCACCATCC
AN6448-Oex-5-RU	AGCGGGAGAACUCGGCCGCTGTTTTAGTGTC
AN6448-Oex-3-FU	AGTTCTCCCGCUTTGGCCGCCTGGTAAGCA
AN6448-Oex-3-RU	TCTGCGAUTTACTTCCCAGACACCTCCTC

PCR and DNA substrate construction.

The annotation of AspGD was used for retrieving gene sequence information. Oligonucletides were produced by IDT (Integrated DNA Technologies Inc, Coralville, IA, USA) or Sigma-Aldrich, see table x for list. The PfuX7 polymerase (Nørholm, 2010) was used in all PCR reactions as described in Hansen et al. (Hansen 2011). All DNA fragments for gene deletion and overexpression were assembled into transformation ready cassettes via the USER cloning technology as presented in Hansen et al., 2011, except for the triplet gene deletions, which were constructed by fusion-PCR as described in Nielsen et al., 2008. Overexpression construct for AN6446 were propagated in pU2111 having AsiSI/Nb.BtsI USER cassettes and AF*pyrG* flanked by direct repeats (Hansen 2011). The pU2002A vector designed to incorporate gene-targeting sequences flanking DR-AF*pyrG*-DR was digested with PacI/Nt.BbvCI prior to mixing with appropriate PCR fragments and USER cloning. All gene-targeting substrates were liberated from their vector backbone with SwaI (1U/µl). Overexpression of *pkbA* was established in a modified pU1111 vector employing *A. nidulans argB* as genetic marker (Hansen et al., 2011), pDH57. The pDH57 vector carries the *ccdB* suicide gene from the Gateway™ cloning system (Invitrogen, Carlsbad, CA, USA), allowing elimination of background from uncut plasmid from the USER™ cloning reaction. The *ccdB*::*camR* cassette was amplified from pDONR (Invitrogen) using primers containing USER tails that were designed to restore the AsiSI/Nb.BtsI cassette. Furthermore, a silent point mutation was introduced in order to eliminate an Nb.BtsI nicking site in *ampR*. Primers for *pkbA*-Oex construct, split in two parts for USER fusion, were designed using the PHUSER program (Olsen 2011). The transformation substrate was excised from the vector by NotI digestion after manufacturer's protocol.

USER mix, restriction and nicking enzymes were purchased from New England Biolabs, Ipswich, MA, USA. Protoplasting and gene-targeting procedures were performed as described previously (Johnstone 2005, Nielsen 2006). Gene targeting events were verified by diagnostic spore-PCR in 40 µL reaction volume applying 20 min of initial denaturation.

Relative gene expression by qRT-PCR. The AN6446-Oex, AN6446Δ and the reference strain were inoculated as three-points on MM+Arg for 5 days in the dark at 37 °C. Cultivations for plug extraction were done in parallel to confirm that the levels of gene expression also were resulting in appearance or absence of

metabolites as expected. Total RNA from the three strains was isolated with Qiagen Plant RNAeasy kit (Qiagen, Hilden, Germany). The samples were disrupted by a TissueLyser LT (Qiagen) using 45 Hz for 1 min. 10 µg of RNA was DNAse I (Qiagen) treated after manufacturer's protocol, with addition of 10U of RNAguard RNAse inhibitor (Amersham Biosciences, Nassau, NY, USA). 1 µg of DNAse I treated RNA samples were used in cDNA synthesis by the Phusion RT-PCR Kit (Finnzymes, Vantaa, Finland) according to manufacturer's protocol. The subsequent qRT-PCR was performed in a Chromo 4TM Detector/PTC-200 (MJ Research, St. Bruno, Canada) using the SYBR® Green JumpStart Taq ReadyMix (Sigma). *hhtA* (AN0733) encoding histone protein H3 was chosen as internal standard for normalization of expression levels. Only one of them, *hhtA,* was used for the fold change calculations. Primer combinations for the qPCR and sequences are listed in Supplementary table1. Moreover, two types of control samples were initially included for the qPCR; the DNAse treated RNA sample used for the reverse transcriptase reaction, and a template-free reaction to test for primer-dimer influence on the overall fluorescence. The final individual cDNA samples were added to the reactions as 5 times diluted samples. Samples were run in triplicates. The program was 94 °C for 2 min and cycling conditions 40 times; 94 °C for 10 s, 60 °C for 15 s, 72 °C for 30 s. A melting curve from 65 °C to 95 °C with reads every 0.2 min was ending the program to evaluate the purity of the reaction products. The fluorescence threshold values, C(t), was determined through the OpticonMonitor 3.1 software (MJ Research). The relative expression levels was approximated by $2^{-\Delta\Delta C(t)}$ as $\Delta\Delta C(t) = \Delta C(t)\text{normalized} - \Delta C(t)\text{calibrator}$. The $\Delta C(t)\text{normalized} = \Delta C(t)\text{target gene} - \Delta C(t)\text{internal\_std}$ and the calibrator C(t) values were the corresponding values from the reference strain.

Chemical characterization of mutant strains by LC-DAD-MS: All strains were grown as three point inoculations for 7 days at 37 degrees in the dark on solid media. Extraction of metabolites were performed by the agar plug extraction method (Smedsgaard 1997) using three 6mm agar plugs/extract. Extracts were analyzed by LC-HRMS. LC-HRMS analysis were made on a MaXis 3G QTOF (Bruker Daltronics) coupled to a Dionex Ultimate 3000 UHPLC system equipped with a 100 x 2.0 mm, 2.6 μm, Kinetex C-18 column. The separation column was held at a temperature of 40°C and a gradient system composed of A: 20 mM formic acid in water, and B: 20 mM formic acid in acetonitrile was used. The flow was 0.4 ml/min, 85% A graduating to 100% B in 0-10 min, 100% B 10-13 min, 85% A 13.1-15 minutes. For calibration, a mass spectrum of sodium formate was recorded at the beginning of each chromatogram using the divert valve (0.3-0.4 min). Samples were analyzed both in positive and negative ionization mode. De-replication of induced compounds were performed by comparison of accurate mass to the metabolite database Antibase2009 (Laatsch 2010) as well as comparison of UV spectra to published data.

Isolation of 3-methylorsellinic acid

AN6444Δ was cultured on 100 MM plates for 7 days at 37°C in the dark. The plates were homogenized using a Stomacher and 100 mL ethyl acetate (EtOAc) + 1% formic acid (FA) pr. 10 plates. The extract was filtered after 1 hour and the remaining broth was extracted with EtOAc + 1% FA for 24 hours. The extract was filtered and the two fractions pooled and dried down on a freeze drier. The crude extract were separated into three phases by dissolving it in 9:1 MeOH:H_2O – Milli-Q and extracted into a heptane phase followed by addition of H_2O-Milli-Q to 1:1 methanol(MeOH):H_2O – Milli-Q and extracted into a dicloromethane (DCM) phase and a aqueous phase. The aqueous phase was separated on a KP-C18-HS SNAP column using a Biotage Isolera One (Biotage, Uppsala, Sweden) using a gradient of 10% MeOH (H_2O-Milli-Q (Millipore, MA, USA)) to 100% over 15 CVs (column volumes) resulting in 22 fractions. Fraction 17 contained 9.2 mg of pure 3-methylorsellinic acid and were concentrated on a rotarvap (Büchi V-855/R-215) and dried down under N_2(g).

Isolation of cichorine (X1)

AN6446-Oex was cultured on 200 MM plates for 7 days at 37°C in the dark. The plates were homogenized using a Stomacher and 100 mL EtOAc + 1% FA pr. 10 plates. The extract was filtered after 1 hour and the remaining broth was extracted with EtOAc + 1% FA for 24 hours. The extract was filtered and the two fractions pooled and dried down on a freeze drier. The crude extract were separated into three phases by dissolving it in 9:1 MeOH:H_2O – Milli-Q and extracted into a heptane phase followed by addition of H_2O-Milli-Q to 1:1 MeOH:H_2O – Milli-Q and extracted into a DCM phase and a aqueous phase. The DCM phase

was separated on a KP-C18-HS SNAP column using a Biotage Isolera One (Biotage, Uppsala, Sweden) using a gradient of 10% MeOH (H_2O-Milli-Q (Millipore, MA, USA)) to 100% over 15 CVs (column volumes) resulting in 22 fractions. Cichorine was present in fractions 12 and 13 and was purified on a Waters HPLC W600/996PDA (Milford, MA, USA) using a RP column (Phenomenex Luna C18(2), 250 x 21.20 mm, 5 µm, Torrance, CA, USA) using an isocratic gradient of 20% MeCN (H_2O – Milli-Q (Millipore, MA, USA)) over 20 minutes with a flow of 15 mL/min. The collections were concentrated on a rotarvap (Büchi V-855/R-215) and dried down under N_2(g) to yield 9.3 mg of cichorine.

Isolation of nidulol

AN6445Δ was cultured on 100 MM plates for 7 days at 37°C in the dark. The plates were homogenized using a Stomacher and 100 mL EtOAc + 1% FA pr. 10 plates. The extract was filtered after 1 hour and the remaining broth was extracted with EtOAc + 1% FA for 24 hours. The extract was filtered and the two fractions pooled and dried down on a freeze drier. The crude extract were separated into three phases by dissolving it in 9:1 MeOH:H_2O – Milli-Q and extracted into a heptane phase followed by addition of H_2O-Milli-Q to 1:1 MeOH:H_2O – Milli-Q and extracted into a DCM phase and a aqueous phase. The DCM and MeOH:H_2O phases were separated seperately on a KP-C18-HS SNAP column using a Biotage Isolera One (Biotage, Uppsala, Sweden) using a gradient of 10% MeOH (H_2O-Milli-Q (Millipore, MA, USA)) to 100% over 15 CVs (column volumes) resulting in 22 fractions each. Nidulol was present in fraction 17 of both the phases and was purified on a Waters HPLC W600/996PDA (Milford, MA, USA) using a RP column (Phenomenex Luna C18(2), 250 x 10 mm, 5 µm, Torrance, CA, USA) using a gradient of 15% MeCN (H_2O – Milli-Q (Millipore, MA, USA)) to 30% MeCN over 5 min followed by 15 minutes of isocratic flow of 30% MeCN with 50 ppm TFA added to the solvents and a flow of 5 mL/min. The collections were concentrated on a rotarvap (Büchi V-855/R-215) and dried down under N_2(g) to yield 1.2 mg of nidulol.

Isolation of demethylnidulol

The MeOH:H_2O phase of the extract of the AN6446-Oex described for the isolation of cichorine was separated on a KP-C18-HS SNAP column using a Biotage Isolera One (Biotage, Uppsala, Sweden) using a gradient of 10% MeOH (H_2O-Milli-Q (Millipore, MA, USA)) to 100% over 15 CVs (column volumes) resulting in 22 fractions. Demethylnidulol was present in fractions 12 and was purified on a Gilson 322 liquid chromatograph with a 215 liquid handler/injector (BioLab, Risskov, Denmark) using a RP column (Phenomenex Luna C18(2), 250 x 10 mm, 5 µm, Torrance, CA, USA) using a flow of 15% MeCN (H_2O – Milli-Q (Millipore, MA, USA)) over 10 minutes followed by a gradient from 15% to 95% MeCN with a flow of 5

mL/min. The collections were concentrated on a rotarvap (Büchi V-855/R-215) and dried down under N_2(g) to yield 1.0 mg of cichorine.

Isolation of cichonidulol

Cichonidulol was present in fraction 18 of the separated DCM phase described in the isolation of cichorine and was purified on a Gilson 322 liquid chromatograph with a 215 liquid handler/injector (BioLab, Risskov, Denmark) using a RP column (Phenomenex Luna C18(2), 250 x 10 mm, 5 µm, Torrance, CA, USA) using a flow of 15% MeCN (H_2O – Milli-Q (Millipore, MA, USA)) over 10 minutes followed by a gradient from 15 % to 95 % MeCN over 30 minutes with a flow of 5 mL/min. The collections were concentrated on a rotarvap (Büchi V-855/R-215) and dried down under N_2(g) to yield 2.0 mg of cichonidulol.

Isolation of demethylcichonidulol

One of the fractions from the last purification step of cichonidulol contained demethylcichonidulol and was purified on a Gilson 322 liquid chromatograph with a 215 liquid handler/injector (BioLab, Risskov, Denmark) using a RP column (Phenomenex Luna C18(2), 250 x 10 mm, 5 µm, Torrance, CA, USA) using a flow of 15% MeCN (H_2O – Milli-Q (Millipore, MA, USA)) over 10 minutes followed by a gradient from 15 % MeCH to 95 % MeCN over 20 minutes with a flow of 5 mL/min. The collections were concentrated on a rotarvap (Büchi V-855/R-215) and dried down under N_2(g) to yield 0.6 mg of demethylcichonidulol.

Isolation of 4-hydroxy-3,6-dimethyl-2-pyrone

4-hydroxy-3,6-dimethyl-2-pyrone was present in an earlier fraction than demethylnidulol in the purification procedure described previously. The collections were concentrated on a rotarvap (Büchi V-855/R-215) and dried down under N_2(g) to yield 1.0 mg of cichorine.

NMR studies and structure elucidation: NMR spectra were acquired in DMSO-d_6 on a Varian Unity Inova 500 MHz spectrometer for cichorine, 3-methylorsellinic acid, nidulol and 4-hydroxy-3,6-dimethyl-2-pyrone and on a Bruker Avance 800 MHz spectrometer at the Danish Instrument Center for NMR Spectroscopy of Biological Macromolecules for demethylnidulol, cichonidulol and demethylcichonidulol using standard pulse sequences. The spectra were referenced to this solvent with resonances δ_H = 2.49 and δ_C = 39.5.

Characterization data of 3-methylorsellinic acid. ^{1}H NMR (500 MHz, DMSO-d_6): δ 13.06 (1H, br. s, 8-OH), 9.98 (1H, s, 4-OH), 6.23 (1H, s, H-5), 2.38 (3H, s, H-7), 1.91 (3H, s, H-9); ^{13}C NMR (125 MHz): δ 173.8 (C-8),

163.0 (C-2), 159.7 (C-4), 139.4 (C-6), 109.9 (C-5), 107.7 (C-3), 103.7 (C-1), 23.4 (C-7), 7.9 (C-9). HRMS (*m/z*): $[M+H]^+$ calcd. for $C_9H_{11}O_4$, 183.0652; found, 183.0648.

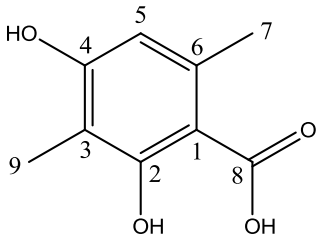

NMR-table:

Number	^{1}H (ppm)	^{13}C (ppm)	Multiplicity (J/Hz)	Integral	HMBC
1	-	103.7	-	-	-
2	-	163.0	-	-	-
3	-	107.7	-	-	-
4	-	159.7	-	-	-
4-OH	9.98	-	s	1	
5	6.23	109.9	s	1	1, 3, 4, 7 ,8 ,9
6	-	139.4	-	-	-
7	2.38	23.4	s	3	1, 2, 5 , 6, 8
8	-	173.8	-	-	-
9	1.91	7.9	s	3	2, 3, 4, 6
8-OH	13.06	-	br. s	1	-

Characterization data of cichorine. ^{1}H NMR (500 MHz, DMSO-d_6): δ 9.71 (1H, s, 4-OH), 8.41 (1H, s, N-H), 6.81 (1H, s, H-5), 4.40 (2H, s, H-8), 3.84 (3H, s, H-10), 2.05 (3H, s, H-9); ^{13}C NMR (125 MHz): δ 169.8 (C-7), 156.3 (C-4), 153.6 (C-2), 131.9 (C-6), 123.1 (C-1), 118.9 (C-3), 102.9 (C-5), 58.9 (C-10), 9.1 (C-9). HRMS (*m/z*): $[M+H]^+$ calcd. for $C_{10}H_{12}NO_3$, 194.08117; found, 194.08123.

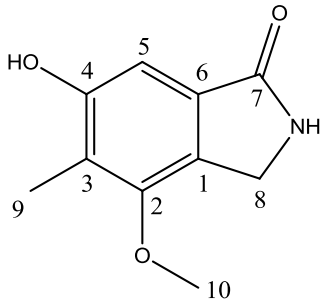

Number	^{1}H (ppm)	^{13}C (ppm)	Multiplicity (J/Hz)	Integral	HMBC
1	-	123.1	-	-	-
2	-	153.6	-	-	-
3	-	118.9	-	-	-
4	-	156.3	-	-	-
4-OH	9.71	-	s	1	3, 4
5	6.81	102.9	s	1	1, 2, 3, 4, 6, 7, 9
6	-	131.9	-	-	-
7	-	169.8	-	-	-
8	4.40	43.1	s	2	1, 2, 4, 5, 6, 7, 10
9	2.05	9.1	s	3	1, 2, 3, 4, 5, 6
10	3.84	58.9	s	3	2, 8
N-H	8.41	-	s	1	1, 6, 7, 8

Characterization data of nidulol. ^{1}H NMR (500 MHz, DMSO-d_6): δ 10.72 (1H, s, 4-OH), 6.73 (1H, s, H-5), 5.17 (2H, s, H-7), 3.87 (3H, s, H-10), 2.05 (3H, s, H-9); ^{13}C NMR (125 MHz): δ 168.5 (C-8), 162.7 (C-4), 157.5 (C-2), 148.6 (C-6), 117.5 (C-3), 107.2 (C-1), 103.0 (C-5), 68.2 (C-7), 61.1 (C-10), 8.2 (C-9). HRMS (*m/z)*: $[M+H]^{+}$ calcd. for $C_{10}H_{11}O_4$, 195.0652; found, 195.0652.

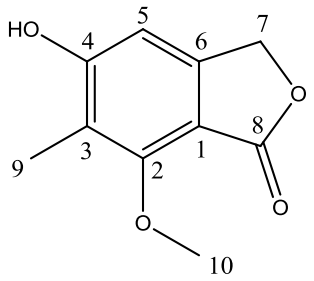

NMR-table:

Number	^{1}H (ppm)	^{13}C (ppm)	Multiplicity (J/Hz)	Integral	HMBC
1	-	107.2	-	-	-
2	-	157.5	-	-	-
3	-	117.5	-	-	-
4	-	162.7	-	-	-
4-OH	10.72	-	s	1	3, 4
5	6.73	103.0	s	1	1, 3, 7
6	-	148.6	-	-	-
7	5.17	68.2	s	2	1, 6, 8
8	-	168.5	-	-	-
9	2.02	8.2	s	3	2, 3, 4
10	3.87	61.1	s	3	2

Characterization data of demethylnidulol: ^{1}H NMR (800 MHz, DMSO-d_6): δ 5.67 (1H, s, H-5), 5.64 (1H, s, H-3), 4.82 (2H, s, H-7), 3.61 (3H, s, H-10); ^{13}C NMR (200 MHz): δ 178.1 (C-8), 168.8 (C-4), 159.6 (C-2), 151.4 (C-6), 103.2 (C-5), 101.1 (C-3), 92.9 (C-1), 66.9 (C-7), 53.9 (C-10). HRMS (*m/z*): $[M+H]^+$ calcd. for $C_9H_9O_4$, 181.0495; found, 181.0497.

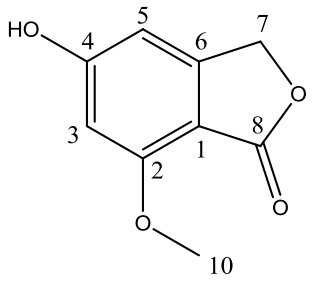

NMR-table:

Number	^{1}H (ppm)	^{13}C (ppm)	Multiplicity (J/Hz)	Integral	HMBC
1	-	92.9	-	-	-
2	-	159.6	-	-	-
3	5.64	101.1	s	1	5, 6
4	-	168.8	-	-	-
5	5.67	103.2	s	1	3, 6
6	-	151.4	-	-	-
7	4.82	66.9	s	2	1, 2, 4, 5, 6, 8
8	-	178.1	-	-	-
10	3.61	53.9	s	3	2, 3

Characterization data of cichonidulol. ^{1}H NMR (800 MHz, DMSO-d_6): δ 9.74-10.11 (1H, br. s), 7.21 (1H, d, J = 1.8 Hz, H-8'), 6.91 (1H, s, H-5), 6.59 (3H, s, H-5'), 5.17 (1H, d, J = 12.3 Hz, H-7'b), 4.88 (1H, d, J = 12.3 Hz, 7'a), 4.28 (1H, d, J = 16.3 Hz, H-8b), 3.75 (1H, d, J = 16.3 Hz, H-8a), 3.70 (3H, s, H-10), 3.56 (3H, s, H-10'), 2.05 (3H, s, H-9), 1.98 (3H, s, H-9'); ^{13}C NMR (200 MHz): δ 167.1 (C-7), 158.1 (C-4'), 156.9 (C-4), 153.8 (C-2'), 153.6 (C-2), 139.5 (C-6'), 131.0 (C-6), 121.3 (C-1), 120.5 (C-3), 116.1 (C-1'), 115.3 (C-3'), 103.4 (C-5), 102.4 (C-5'), 83.5 (C-8'), 71.7 (C-7'), 95.2 (C-10'), 59.0 (C-10), 43.2 (C-8), 9.3 (C-9), 8.6 (C-9'). HRMS (*m/z)*: $[M+H]^+$ calcd. for $C_{20}H_{22}NO_6$, 372.1442; found, 372.1441.

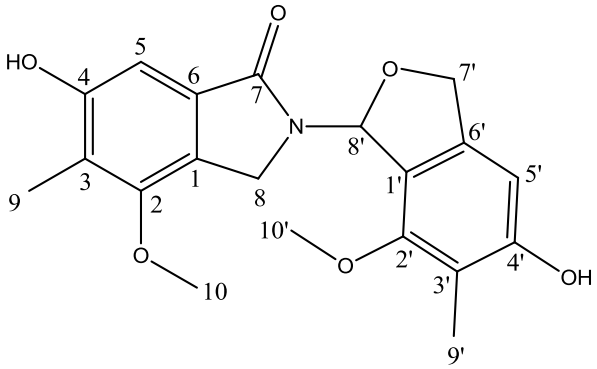

NMR-table:

Number	^{1}H (ppm)	^{13}C (ppm)	Multiplicity (J/Hz)	Integral	HMBC	DQF-COSY
1	-	121.3	-	-	-	-
2	-	153.6	-	-	-	-
3	-	120.5	-	-	-	-
4	-	156.9	-	-	-	-
5	6.91	103.4	s	1	1, 4, 7	-
6	-	131.0	-	-	-	-
7	-	167.1	-	-	-	-
8a	3.75	43.2	d (16.3)	1	1, 6	8b
8b	4.28	43.2	d (16.3)	1	1, 6	8a
9	2.05	9.3	s	3	2, 3, 4	-
10	3.70	59.0	s	3	2	-
1’	-	116.1	-	-	-	-
2’	-	153.8	-	-	-	-
3’	-	115.3	-	-	-	-
4’	-	158.1	-	-	-	-
5’	6.59	102.4	s	1	1’, 4’, 7’	-
6’	-	139.5	-	-	-	-
7’a	4.88	71.7	d (12.3)	1	1’, 6’, 8’	7’b
7’b	5.17	71.7	d (12.3)	1	6’	7’a, 8’
8’	7.21	83.5	d (1.8)	1	1’, 7’, 8	7’b

9′	1.98	8.6	s	3	2′, 3′, 4′, 5′	-
10′	3.56	59.2	s	3	2′	-

Characterization data of demethylcichonidulol. ^{1}H NMR (500 MHz, DMSO-d_6): δ HRMS (*m/z)*: 6.97 (1H, d, J = 2.2, H-8′), 6.90 (1H, s, H-5), 6.35 (1H, s, H-3′ or H-5′), 6.34 (1H, s, H-3′ or H-5′), 5.16 (1H, dd, J =12.8, 2.2 Hz, H-7′a), 4.86 (1H, d, J = 12.8 Hz, H-7′b), 4.25 (1H, d, J = 16.0 Hz, H-8a), 3.78 (1H, d, J = 16 Hz, H-8b), 3.71 (3H, s, H-10), 3.63 (3H, s, H-10′), 2.05 (3H, s, H-9). HRMS (*m/z*): $[M+H]^+$ calcd. for $C_{19}H_{20}O_6$, 358.1285; found 358.1283.

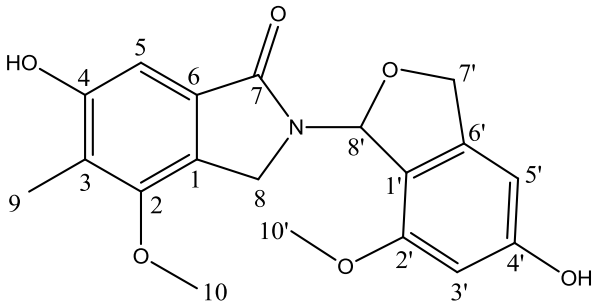

Characterization data of 4-hydroxy-3,6-dimethyl-2-pyrone. ^{1}H NMR (500 MHz, DMSO-d_6): δ 5.46 (1H, s, H-5), 1.93 (3H, s, 3-CH_3), 1.56 (3H, s, 6-CH_3); ^{13}C NMR (125 MHz): δ 174.9 (C-4), 166.0 (C-2), 156.0 (C-6), 106.6 (C-5), 91.0 (C-3), 19.0 (6-CH_3), 9.1 (3-CH_3). HRMS (*m/z)*: $[M+H]^+$ calcd. for $C_7H_9O_3$, 141.0546; found, 141.0543.

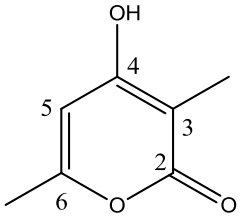

NMR-table:

Number	^{1}H (ppm)	^{13}C (ppm)	Multiplicity (J/Hz)	Integral	HMBC
2	-	166.0	-	-	-
3	-	91.0	-	-	-

4	-	174.9	-	-	-
5	5.46	106.0	s	1	3, 6, 6-CH_3
6	-	156.0	-	-	-
6-CH_3	1.93	19.1	s	3	5, 6
3-CH_3	1.56	9.1	s	3	3, 4, 5

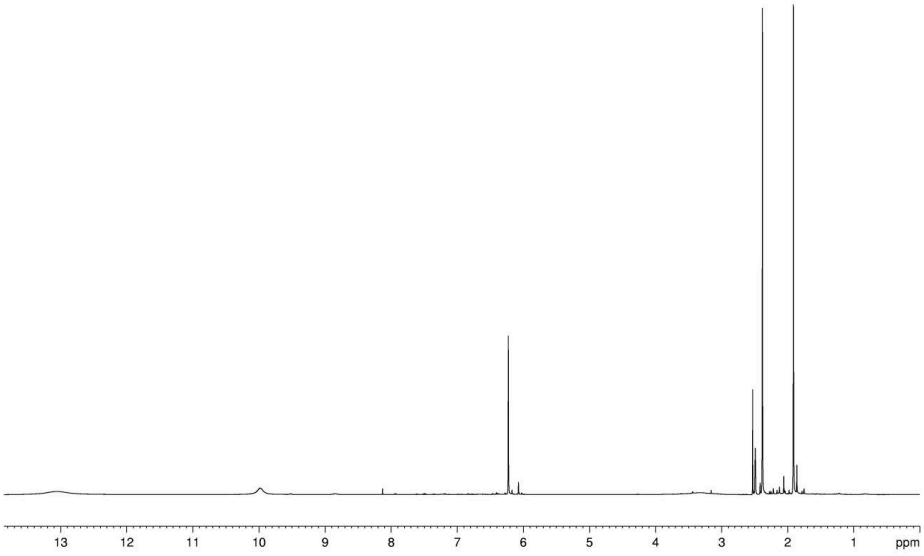

^{1}H NMR spectrum 3-methylorsellinic acid in DMSO-d_6

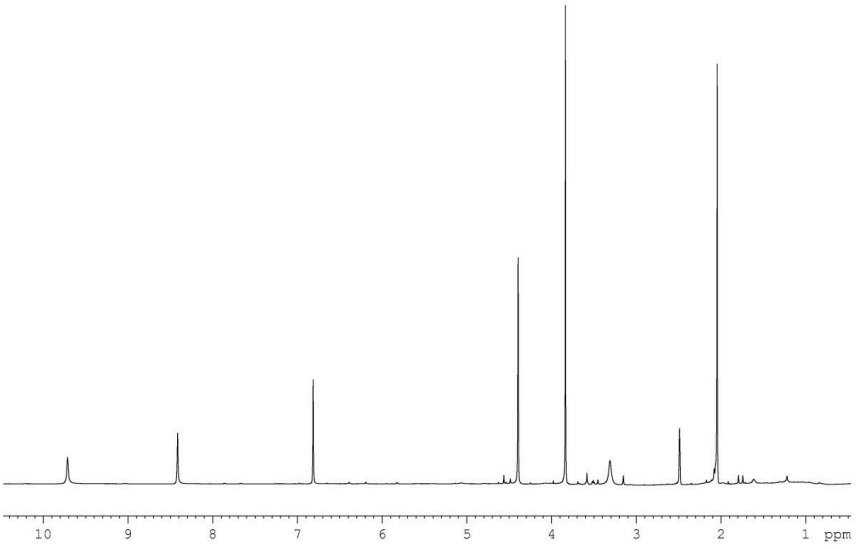

^{1}H NMR spectrum cichorine in DMSO-d_6

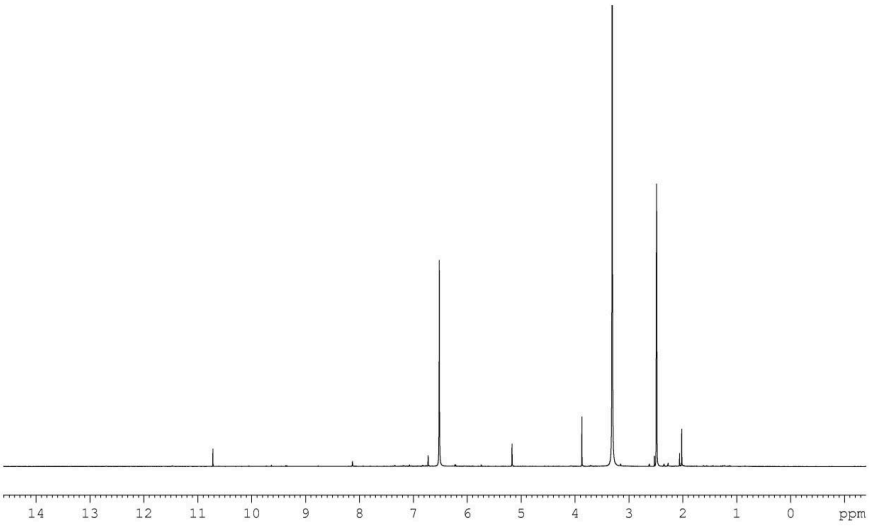

^{1}H NMR spectrum nidulol in DMSO-d_6

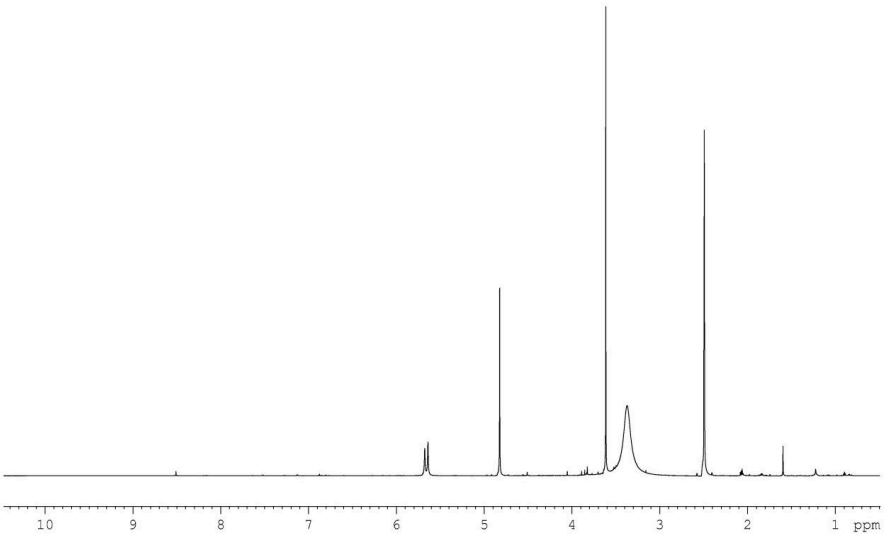

^{1}H NMR spectrum demethylnidulol in DMSO-d_6

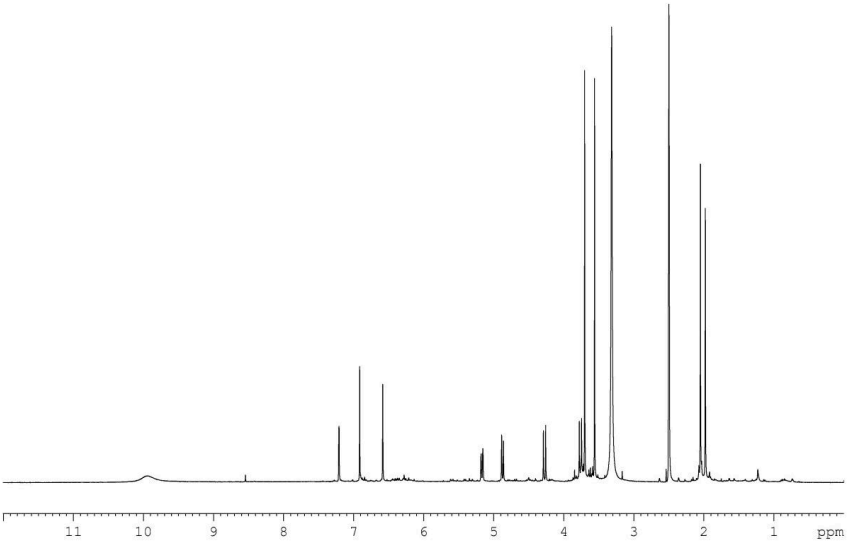

^{1}H NMR spectrum cichonidulol in DMSO-d_6

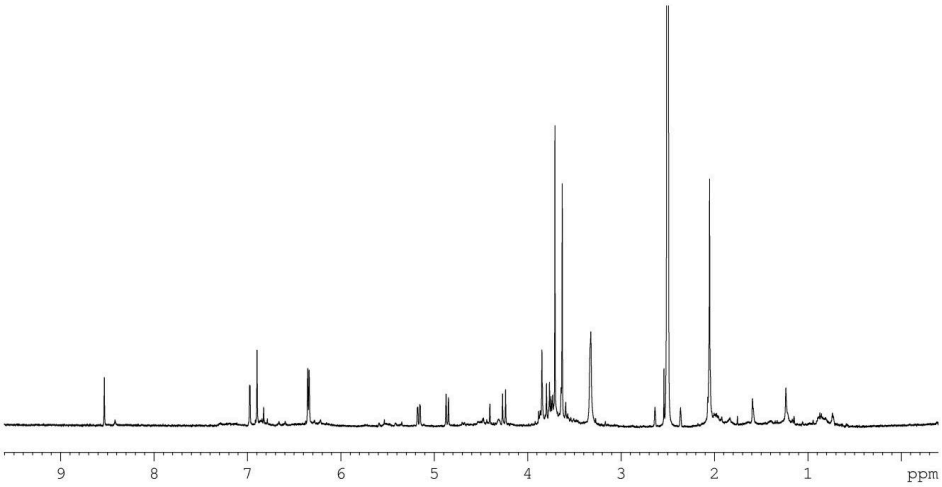

^{1}H NMR spectrum demethylcichonidulol in DMSO-d_6

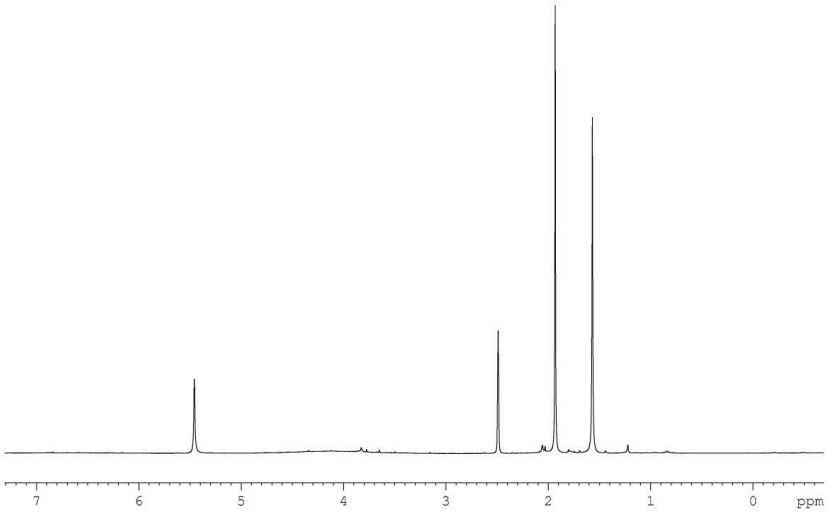

^{1}H NMR spectrum 4-hydroxy-3,6-dimethyl-2-pyrone in DMSO-d_6

References

Ahuja, M.; Chiang, Y.M.; Chang, S.L.; Praseuth, M.B.; Entwistle, R.; Sanchez, J.F.; Lo, H.H.; Oakley, B.R.; Wang, C.C.C. Illuminating the diversity of aromatic polyketide synthases in *Aspergillus nidulans*. *J. Am. Chem. Soc.* **2012**, *134*, 8212-8221.

Aucamp, P.J.; Holzapfel, C.W. The constution of nidulol (5-hydroxy-7-methoxy-6-methylphthalide), a metabolic product of *Aspergillus nidulans* (Eidam) Wint. *J. S. Afr. Chem. I.* **1968**, *21*, 26-32.

Cove, D.J. The induction and repression of nitrate reductase in the fungus *Aspergillus nidulans*. *Biochim. Biophys. Acta* **1966**, *113*, 51-56

El-Feraly, F.S.; Cheatham, S.F.; McChesney, J.D. Total synthesis of notholaenic acid. *J. Nat. Prod.* **1985**, *48*, 293-298.

Frisvad 1987, J.C.; Thrane, U. Standardized high-performance liquid chromatography of 182 mycotoxins and other fungal metabolites based on alkylphenone retention indices and UV-VIS spectra (diode array detection). *J. Chromatogr.* **1987**, *404*, 195-214.

Fujita, M.; Yamada, M.; Nakajima, S.; Kawai, K.-I.; Nagai, M. *O*-methylation effect on the carbon-13 nuclear magnetic resonance signals of *ortho*-disubstituted phenols and its application to structure determination of new phthalides from *Aspergillus silvaticus*. *Chem. Pharm. Bull.* **1984**, *32*, 2622-2627.

Hansen, B.G.; Salomonsen, B.; Nielsen, M.T.; Nielsen, J.B.; Hansen, N.B.; Nielsen, K.F.; Regueira, T.B.; Nielsen, J.; Patil, K.R.; Mortensen, U.H. Versatile enzyme expression and characterization system for *Aspergillus nidulans*, with the *Penicillium brevicompactum* polyketide synthase gene from the mycophenolic acid gene cluster as a test case. *Appl. Environ. Microbiol.* **2011**, *77*, 3044-3051.

Johnstone, I.L.; Hughes, S.G.; Clutterbuck, A.J. Cloning an *Aspergillus nidulans* developmental gene ny transformation. *EMBO J.* **1985**, *4*, 1307-1311.

Kawahara, N.; Nozawa, K.; Nakajima, S.; Udagawa, S.-I.; Kawai, K.-I. Studies on fungal products XVI. New metabolites related to 3-methylorsellinate from *Aspergillus silvaticus*. *Chem. Pharm. Bull.* **1988b**, *36*, 398-400.

Laatsch, H. AntiBase 2010. Available online: http://www.wiley-vch.de/stmdata/antibase2010.php (accessed on May 30th 2012).

Manske, R.H.F.; Holmes, H.L. The alkaloids of fumariaceous plants. XXXIX. The constitution of capaurine. *J. Am. Chem. Soc.* **1945**, *67*, 95-98.

Moreau, A.; Couture, A.; Deniau, E.; Grandclaudon, P.; Lebrun, S. First total synthesis of cichorine and zinnimidine. *Org. Biomol. Chem.* **2005** *3*, 2305-2309.

Nielsen, M.L.; Albertsen, L.; Lettier, G.; Nielsen, J.B.; Mortensen, U.H. Efficient PCR-based gene targeting with a recyclable marker for *Aspergillus nidulans*. *Fung. Genet. Biol.* **2006**, *43*, 54-64.

Nielsen, J.B.; Nielsen, M.L.; Mortensen, U.H. Transient disruption of non-homologous end-joining facilitates targeted genome manipulations in the filamentous fungus *Aspergillus nidulans*. *Fungal genet. Biol.* **2008**, *45*, 165-170.

Nielsen, M.L.; Nielsen, J.B.; Rank, C.; Klejnstrup, M.L.; Holm, D.K.; Brogaard, K.H.; Hansen, B.G.; Frisvad, J.C.; Larsen, T.O.; Mortensen, U.H. A genome-wide polyketide synthase deletion library uncovers novel genetic links to polyketides and meroterpenoids in *Aspergillus nidulans*. *FEMS Microbiol. Lett.* **2011**, *321*, 157-166.

Nozawa, K.; Seyea, H.; Nakajima, S.; Udagawa, S.-I.; Kawai, K.-I. Studies on fungal products. Part 10. Isolation and structures of novel bicoumarins, desertorins A, B, and C, from *Emericella desertorum*. *J. Chem. Soc. Perkin Trans. I* **1987**, 1735-1738.

Nørholm 2010

Savard, M.E.; Miller, J.D.; Blais, L.A.; Seifert, K.A.; Samson, R.A. Secondary metabolites of *Penicillium bilaii* strain PB-50. *Mycopathologia* **1994**, *127*, 19-27

Scherlach, K.; Schuemann, J.; Dahse, H.M.; Hertweck, C. Aspernidine A and B, prenylated isoindolinone alkaloids from the model fungus *Aspergillus nidulans*. *J. Antibiot.* **2010**, *63*, 375-377.

Schroeckh, V.; Scherlach, K.; Nützmann, H.-W.; Shelest, E.; Schmidt-Heck, W.; Schuemann, J.; Martin, K.; Hertweck, C.; Brakhage, A.A. Intimate bacterial-fungal interaction triggers biosynthesis of archetypal polyketides in *Aspergillus nidulans*. *Proc. Natl. Acad. Soc. USA* **2009**, *106*, 14558-14563.

Smedsgaard, J. Micro-scale extraction procedure for standardized screening of fungal metabolite production in cultures. *J. Chromatogr. A* **1997**, *760*, 264-270.

Stierle, A.; Hershenhorn, J.; Strobel, G. Zinniol-related phytotoxins from *Alternaria cichorii*. *Phytochemi*. **1993**, *32*, 1145-1149.

Yaoita, Y.; Danbara, K.; Kikuchi, M. Two new aromatic compounds from *Hericium erinaceum* (Bull.; Fr.) Pers. *Chem. Pharm. Bull.* **2005**, *53*, 1202-1203.

Olsen, L.R.; Hansen, N.B.; Bonde, M.T.; Genee, H.J.; Holm, D.K.; Carlsen, S.; Hansen, B.G.; Patil, K.R.; Mortensen, U.H.; Wernersson, R. PHUSER (Primer Help for USER): a novel tool for USER fusion primer design. *Nucleic Acids Res.* **2011**, *39*, W61-67.

Paper 6

"A combined genetic and multi medium approach reveals new secondary metabolites of *Aspergillus nidulans*"

ML Klejnstrup, MT Nielsen, JB Nielsen, JC Frisvad, CH Gotfredsen, UH Mortensen and TO Larsen

Rough draft

A combined genetic and multi medium approach reveals new secondary metabolites of *Aspergillus nidulans*

Marie Louise Klejnstrup[1], Morten Thrane Nielsen[1,2], Jakob Blæsbjerg Nielsen[1], Jens Christian Frisvad[1], Charlotte Held Gotfredsen[3], Uffe Hasbro Mortensen[1], Thomas Ostenfeld Larsen[1]

Affiliation

[1] Center for Microbial Biotechnology, Department of Systems Biology, Technical University of Denmark, 2800 Kgs Lyngby, Denmark.

[2] Current address: Novo Nordisk Foundation Center for Biosustainability, Technical University of Denmark, Fremtidsvej 3, 2970 Hoersholm, Denmark.

[3] Department of Chemistry, Technical University of Denmark, 2800 Kgs Lyngby, Denmark.

Introduction

The construction of a deletion library of 32 putative PKS encoding genes constructed in our group by Nielsen *et al.* (Nielsen 2011) made us look into the production of polyketides in other strains of *A. nidulans* to identify candidates to isolate, structure elucidate and, if possible, link to their synthase genes. Linking of metabolites present in small quantities in the reference strain could be possible due to the possibility of comparison with an isolated standard. In the search of new secondary metabolites of *A. nidulans* we investigated the IBT culture collection at CMB. The strain chosen for the study IBT24909 produced, among others, four metabolites of which three, asperugin B, nidubenzal A, and B were isolated and structure elucidated and the last, asperugin A were putatively identified through LC-MS analysis. These metabolites were detected in trace amounts in the reference strains of the above mentioned deletion study and candidates were chosen for a deletion study in a *cclA*Δ strain which also produced these metabolites. Asperugin A and B were linked to the PKS encoding gene AN3230, *pkfA*, which have been shown by Ahuja and co-workers (Ahuja 2012) to catalyze the production of orsellinaldehyd. The biosynthetic origin of the novel metabolites nidubenzal A and B remains to be clarified.

Materials and methods

Strains

Nine strains of *A. nidulans* strains were used in a *cclA* deletion series, see supplementary table 1. Protoplasting and genetic transformation was as described in Johnstone et al. (Johnstone 1985) and Nielsen et al. (Nielsen 2006). IBT28738 was used as reference strain for chemical analysis (*argB2*, *pyrG89*, *veA1*, *nkuA-trS*::AF*pyrG*) (Nielsen 2008). *Escherichia coli* strain DH5α was used for cloning. The IBT24909 was used for isolation of aspuridone B and nidubenzal A and B.

Media

Fungal minimal medium (MM) was as described in (Cove 1966), but with 1% glucose, 10 mM $NaNO_3$ and 2% agar (Sorbigel, Hendaye, France), when necessary supplemented with 10 mM uridine (Uri), 10 mM uracil (Ura) and 4 mM L-arginine (Arg). For transformation medium, glucose was replaced with 1 M sucrose. Elimination of the *Aspergillus fumigatus pyrG* marker was done on 5-FOA (1.3 mg/ml) supplemented MM, as previously described by Nielsen et al. 2006 (Nielsen 2006). All chemicals were from Sigma-Aldrich (St. Louis, Mo, USA) unless otherwise stated. CYA, CYAs, YES, RT, CY20, RTO, and YE were prepared as described in Nielsen *et al.* (Nielsen 2011).

PCR and DNA substrate construction

The *Aspergillus* genome database (AspGD) was used for retrieving gene sequence information. Oligonucletides were produced by IDT (Integrated DNA Technologies Inc, Coralville, IA, USA) or Sigma-Aldrich, see supplementary table 2 for list. The PfuX7 polymerase (Nørholm, 2010) was used in all PCR reactions as described in Hansen et al., 2011. Deletion of *qutC* was based on bipartite gene targeting substrates by fusion-PCR and the recyclable AF*pyrG* marker with direct repeats (Nielsen et al., 2006; 2008), whereas the *cclA*Δ DNA substrate for the deletion series was based on the USER technology. The pU2002A vector designed to incorporate gene-targeting sequences flanking the AF*pyrG* marker with direct repeats was digested with PacI/Nt.BbvCI prior to mixing with appropriate PCR fragments and USER cloning. The *cclA*Δ deletion substrate was linearized prior to transformation with SwaI (1U/µl) according to manufacturer's protocol. USER mix, restriction and nicking enzymes were from New England Biolabs, Ipswich, MA, USA.

Chemical analysis

All *cclA*Δ strains were grown as three point inoculations for 7 days at 37 degrees in the dark on solid media. Extraction of metabolites were performed by the agar plug extraction method (Smedsgaard 1997) using three 6mm agar plugs/extract. Extracts were analyzed by UHPLC-DAD and LC-HRMS. UHPLC-DAD analysis was performed on a Dionex RSLC Ultimate 3000 (Dionex, Sunnyvale, CA) equipped with a diode-array detector. Separation was performed at 60°C on a 150 mm × 2.1 mm ID, 2.6 µm Kinetex C_{18} column (Phenomenex, Torrence, CA) using a linear water/MeCN (both buffered with 50 ppm tri-fluoroacetic acid (TFA)) gradient starting from 15% MeCN to 100% over 7 min at a flow rate of 0.8 mL min^{-1}. LC-HRMS analysis were made on a MaXis 3G QTOF (Bruker Daltronics) coupled to a Dionex Ultimate 3000 UHPLC system equipped with a 100 x 2.0 mm, 2.6 µm, Kinetex C-18 column. The separation column was held at a temperature of 40°C and a gradient system composed of A: 20 mM formic acid in water, and B: 20 mM formic acid in acetonitrile was used. The flow vas 0.4 ml/min, 85% A graduating to 100% B in 0-10 min, 100% B 10-13 min, 85% A 13.1-15 min. For calibration, a mass spectrum of sodium formate was recorded at the beginning of each chromatogram using the divert valve (0.3-0.4 min). Samples were analyzed both in positive and negative ionization mode. De-replication of induced compounds were performed by comparison of accurate mass to the metabolite database Antibase2010 (Laatsch 2010) as well as comparison of UV spectra to published data.

The IBT24909 extract was analyzed by a HPLC-DAD-HRMS on a 5 cm x 3 µm, Luna C_{18} (2) column (Phenomenex) using a water-acetonitrile gradient from 15 % CH_3CN to 100 % over 20 minutes (20 mM

formic acid). LC-DAD-MS analysis was performed on a LCT oaTOF mass spectrometer (Micromass, Manchester, UK) as in Nielsen *et al.* (Nielsen 2003, Nielsen 2009)

Isolation of nidubenzal A and B

IBT24909 was cultured on 200 CYAs plates for 13 days at 25°C in the dark. The plates were homogenized using a Stomacher and 100 mL ethyl acetate (EtOAc) + 1% formic acid (FA) pr. 10 plates. The extract was filtered after 1 hour and the remaining broth was extracted with EtOAc + 1% FA for 24 hours. The extract was filtered and the two fractions pooled and dried down on a freeze drier. The extract was separated on a KP-C18-HS SNAP column using a Biotage Isolera One (Biotage, Uppsala, Sweden) using a gradient of 10% MeOH (H_2O-Milli-Q (Millipore, MA, USA)) to 100% over 15 CVs (column volumes) resulting in 27 fractions. Asperugin B was present in fractions 20 to 23 which were pooled and purified on a Waters HPLC W600/996PDA (Milford, MA, USA) using a RP column (Phenomenex Luna C18(2), 250 x 10 mm, 5 µm, Torrance, CA, USA) using a gradient of 80% MeCN (H_2O – Milli-Q (Millipore, MA, USA)) to 100 % over 20 minutes with a flow of 4 mL/min. The collections were concentrated on a rotarvap (Büchi V-855/R-215) and dried down under N_2(g) to yield 3.7 mg of nidubenzal A/B.

Isolation of asperugin B

Asperugin was collected in a later fraction than nidubenzal A/B in the last purification step described above. The collections were concentrated on a rotarvap (Büchi V-855/R-215) and dried down under N_2(g) to yield 4.3 mg of asperugin.

NMR studies and structure elucidation

NMR spectra were acquired in DMSO-d_6 on a Varian Unity Inova 500 MHz spectrometer for asperugin B and on a Bruker Avance 800 MHz spectrometer at the Danish Instrument Center for NMR Spectroscopy of Biological Macromolecules for nidubenzal A/B using standard pulse sequences. The spectra were referenced to this solvent with resonances δ_H = 2.49 and δ_C = 39.5.

Characterization data of nidubenzal A

^{1}H NMR (800 MHz, DMSO-*d_6*): δ 9.72 (1H, s, H-7), 7.38 (1H, m, H-6), 7.36 (1H, m, H-2), 6.92 (1H, d, J = 7.9 Hz, H-5), 5.42 (1H, t, J = 6.2 Hz, H-2'), 5.06 (1H, m, H-6'), 5.03 (1H, m, H-10'), 4.61 (2H, d, J = 6.2 Hz, H-1'), 2.06 (2H, m, H-5'), 2.03 (2H, m, H-4'), 1.98 (2H, m, H-9'), 1.89 (2H, t, J = 7.3 Hz, H-8'), 1.71 (3H, s, H-15'), 1.61 (3H, s, H-12'), 1.54 (3H, s, H-14'), 1.53 (3H, s, H-13'); ^{13}C NMR (200 MHz): δ 190.9 (C-7), 153.7 (C-4), 147.1 (C-3), 140.0 (C-3'), 130.4 (C-11'), 128.2 (C-1), 125.8 (C-6), 123.8 (C-10'), 119.5 (C-2'), 115.4 (C-5), 112.3 (C-2), 64.9 (C-1'), 38.7 (C-4'), 25.4 (C-5'), 25.3 (C-12'), 17.3 (C-13'), 16.1 (15'), 15.5 (C-14'). HRMS (*m/z)*: $[M+H]^+$ calcd. for $C_{24}H_{32}O_5$, 343.2268; found, 343.2267.

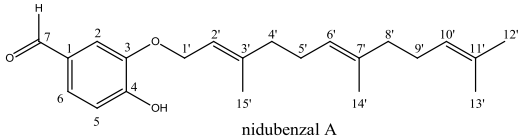

nidubenzal A

Number	^{1}H (ppm)	^{13}C (ppm)	Multiplicity (J/Hz)	Integral	HMBC	DQF-COSY	H2BC
1	-	128.2	-	-	-	-	-
2	7.36	112.3	m	1	3, 4, 6, 7	6	-
3	-	147.1	-	-	-	-	-
4	-	153.7	-	-	-	-	-
5	6.92	115.4	d (J = 7.9 Hz)	1	1, 3, 4	6	6
6	7.38	125.8	m	1	2, 4, 7	2, 5	5
7	9.72	190.9	s	1	1, 2, 3, 6	-	1
1’	4.61	64.9	d (J = 6.2 Hz)	2	3, 2’, 3’, 4’, 5’, 15’	2’	2’
2’	5.42	119.5	t (J = 6.2 Hz)	1	1’, 4’, 5’, 15’	1’	1’
3’	-	140.0	-	-	-	-	-
4’	2.03	38.7	m	2	2’, 3’, 5’, 15’	5’	5’
5’	2.06	25.4	m	2	3’, 4’, 6’, 7’	4’, 6’	4’, 6’
6’	5.06	123.3	m	1	5’, 8’, 14’	5’	5’
7’	-	134.5	-	-	-	-	-
8’	1.89	39.0	t (J = 7.3 Hz)	2	6’, 7’, 9’, 14’	9’	9’
9’	1.98	26.0	m	2	7’, 8’, 10’, 11’	8’, 10’	8’, 10’
10’	5.03	128.8	m	1	12’, 13’	9’	9’
11’	-	130.4	-	-	-	-	-
12’	1.61	25.3	s	3	8’, 9’, 10’, 11’, 13’	-	-
13’	1.53	17.3	s	3	10’, 11’, 12’	-	-
14’	1.54	15.5	s	3	6’, 7’, 8’	-	-
15’	1.71	16.1	s	3	1’, 2’, 3’, 4’	-	-

Characterization data of nidubenzal B

^{1}H NMR (800 MHz, DMSO-d_6): δ 9.72 (1H, s, H-7), 7.35 (1H, d, J = 1.7 Hz, H-6), 7.24 (1H, d, J = 1.8 Hz, H-2), 7.09 (1H, d, J = 8.2 Hz, H-5), 5.42 (1H, t, J = 6.2 Hz, H-2’), 5.06 (1H, m, H-6’), 5.03 (1H, m, H-10’), 4.66 (2H, d, J = 6.2 Hz, H-1’), 2.06 (2H, m, H-5’), 2.03 (2H, m, H-4’), 1.98 (2H, m, H-9’), 1.89 (2H, t, J = 7.3 Hz, H-8’), 1.71 (3H, s, H-15’), 1.61 (3H, s, H-12’), 1.54 (3H, s, H-14’), 1.53 (3H, s, H-13’); ^{13}C NMR (200 MHz): δ 191.4 (C-7), 152.4 (C-4), 147.0 (C-3), 140.0 (C-3’), 130.4 (C-11’), 129.6 (C-1), 124.0 (C-6), 123.8 (C-10’), 119.5 (C-2’), 115.4

(C-5), 112.3 (C-2), 64.9 (C-1'), 38.7 (C-4'), 25.4 (C-5'), 25.3 (C-12'), 17.3 (C-13'), 16.1 (15'), 15.5 (C-14'). HRMS (*m/z*): $[M+H]^+$ calcd. for $C_{24}H_{32}O_5$, 343.2268; found, 343.2267.

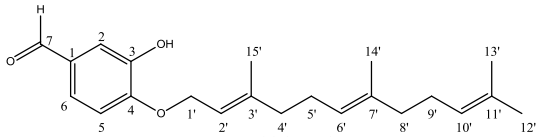

nidubenzal B

Number	^{1}H (ppm)	^{13}C (ppm)	Multiplicity (J/Hz)	Integral	HMBC	DQF-COSY	H2BC
1	-	129.6	-	-	-	-	-
2	7.24	113.4	d (J = 1.8 Hz)	1	3, 4, 6, 7	6	-
3	-	147.0	-	-	-	-	-
4	-	152.4	-	-	-	-	-
5	7.09	112.6	d (J = 8.2 Hz)	1	1, 3, 4	6	6
6	7.35	124.0	m	1	2, 4, 7	2, 5	5
7	9.74	191.4	s	1	1, 2, 3, 6	-	-
1’	4.66	65.0	d (J = 6.2 Hz)	2	4, 2’, 3’, 4’	2’	2’
2’	5.42	119.5	t (J = 6.2 Hz)	1	1’, 4’, 5’, 15’	1’	1’
3’	-	140.0	-	-	-	-	-
4’	2.03	38.7	m	2	2’, 3’, 5’, 15’	5’	5’
5’	2.06	25.4	m	2	3’, 4’, 6’, 7’	4’, 6’	4’, 6’
6’	5.06	123.3	m	1	5’, 8’, 14’	5’	5’
7’	-	134.5	-	-	-	-	-
8’	1.89	39.0	t (J = 7.3 Hz)	2	6’, 7’, 9’, 14’	9’	9’
9’	1.98	26.0	m	2	7’, 8’, 10’, 11’	8’, 10’	8’, 10’
10’	5.03	128.8	m	1	12’, 13’	9’	9’
11’	-	130.4	-	-	-	-	-
12’	1.61	25.3	s	3	8’, 9’, 10’, 11’, 13’	-	-
13’	1.53	17.3	s	3	10’, 11’, 12’	-	-
14’	1.54	15.5	s	3	6’, 7’, 8’	-	-
15’	1.71	16.1	s	3	1’, 2’, 3’, 4’	-	-

Characterization data of asperugin A

HRMS (*m/z)*: $[M+H]^+$ calcd. for $C_{24}H_{32}O_5$, 401.2322; found, 401.2314.

Characterization data of asperugin B

^{1}H NMR (500 MHz, DMSO-d_6): 10.49 (1H, s, H-7), 10.16 (1H, s, H-8), 6.99 (1H, s, H-3), 5.46 (1H, t, J = 7.1 Hz, H-2'), 5.03 (1H, m, H-10'), 5.02 (1H, m, H-6'), 4.62 (2H, d, J = 7.1, H-1'), 1.99 (2H, m, H-5'), 1.98 (2H, m, H-9'), 1.95 (2H, m, H-4'), 1.89 (2H, t, J = 7.6 Hz, H-8'), 1.62 (3H, s, H-13'), 1.58 (3H, s, H-15'), 1.54 (3H, s, H-12'), 1.52 (3H, s, H-14'); ^{13}C NMR (125 MHz): δ 193.1 (C-7), 192.5 (C-8), 157.6 (C-6), 157.0 (C-4), 141.4 (C-3'), 136.9 (C-5), 134.6 (C-7'), 133.3 (C-2), 130.7 (C-11'), 124.1 (C-10'), 123.6 (C-6'), 119.9 (C-2'), 113.7 (C-1), 112.6 (C-3), 68.0 (C-1'), 39.2 (C-8'), 39.1 (C-4'), 26.2 (C-9'), 25.8 (C-5'), 25.5 (C-13'), 17.6 (C-12'), 16.1 (C-15'), 15.7 (C-14'). HRMS (*m/z)*: $[M+H]^+$ calcd. for $C_{23}H_{30}O_5$, 387.2166; found, 387.2154.

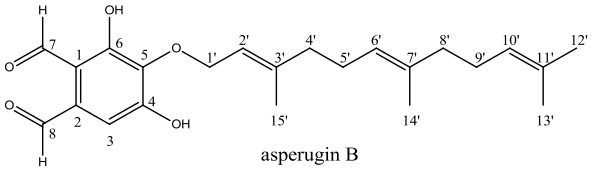

asperugin B

Number	^{1}H (ppm)	^{13}C (ppm)	Multiplicity (J/Hz)	Integral	HMBC	DQF-COSY
1	-	113.7	-	-	-	-
2	-	133.3	-	-	-	-
3	6.99	112.6	s	1	1, 2, 4, 5, 8	-
4	-	157.0	-	-	-	-
5	-	136.9	-	-	-	-
6	-	157.6	-	-	-	-
7	10.49	193.1	s	1	1, 2, 5, 6	-
8	10.16	195.5	s	1	1, 2, 5, 6	-
1'	4.62	68.0	d (J = 7.1 Hz)	2	5, 2', 3', 4', 5'	2'
2'	5.46	119.9	m	1	1', 4', 15'	1'
3'	-	141.4	-	-	-	-
4'	1.95	39.1	m	2	2', 3', 5', 6', 15'	5'
5'	1.99	25.8	m	2		4', 6'
6'	5.02	123.6	m	1	5', 8', 14'	5'
7'	-	134.6	-	-	-	-

8’	1.89	26.2	m	2	overlap	9’
9’	1.98	26.2	m	2	overlap	8’, 10’
10’	5.03	124.1	m	1	12’, 13’	9’
11’	-	130.7	-	-	-	-
12’	1.54	17.6	s	3	8’, 10’, 11’, 13’	-
13’	1.62	25.5	s	3	8’, 10’, 11’, 12’	-
14’	1.52	15.7	s	3	6’, 7’, 8’	-
15’	1.58	16.1	s	3	2’, 3’, 4’	-

Results and discussion

The strain chosen for this study was IBT24909 which was cultivated on 200 plates of CYAs for 13 days at 25°C for optimal production of **1**, **2**, and **3**. The LC-DAD chromatogram at 210 nm of the extract can be seen in figure 1.

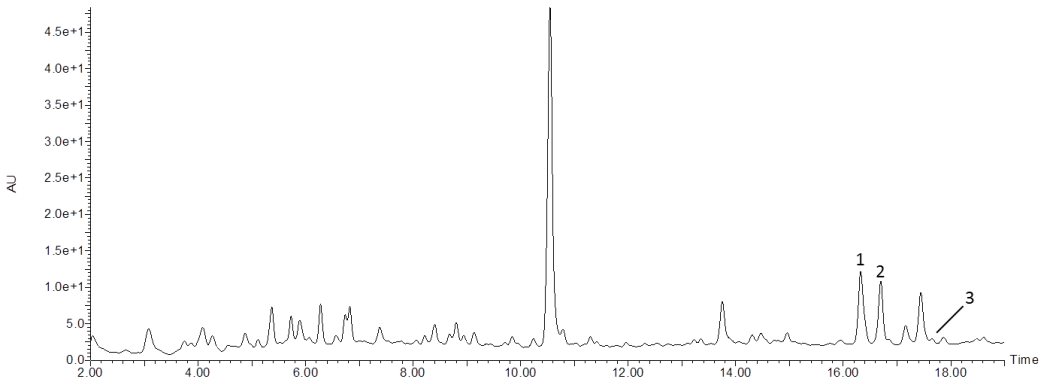

Figure 1 LC-DAD chromatogram (210 nm) of 200 plate extract of IBT24909 cultivated on CYAs for 13 days. The two peaks **1** and **2** were identified as potential PKs. The large peak at 10.5 minutes is sterigmatocystin.

After inspection of the chromatogram two rather large peaks, **1** and **2**, were identified as putative PKs based on their UV-spectra which had absorption maxima at wavelengths over 300 nm indicating that the metabolite or part of it contained a highly conjugated system.

The metabolites were isolated and structure elucidated by 2D NMR (DQF-COSY, HSQC, HMBC, H2BC and NOESY).

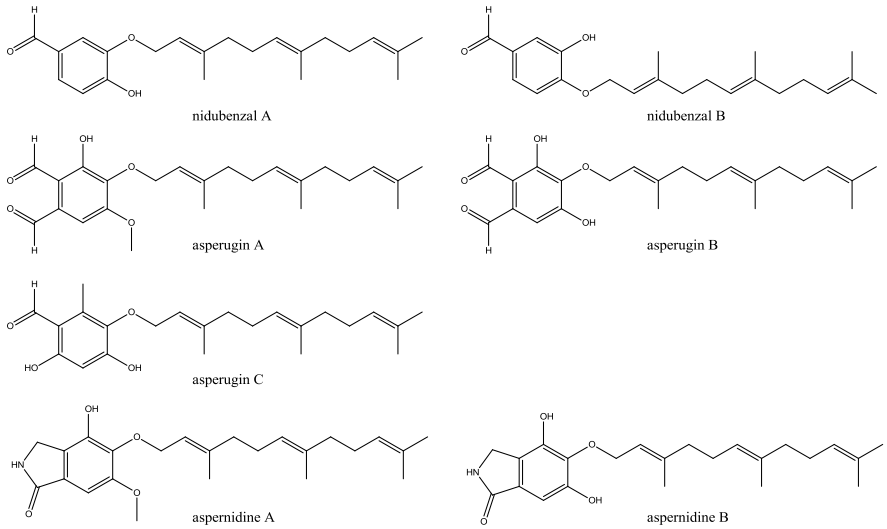

Figure 2 Structures of nidubenzal A and B (**1**), asperugin A, B (**2**), and C, and aspernidine A and B

NMR analysis of **A** revealed that two isomers, that we named nidubenzal A and B, figure 2, were present in the solution in a 5:1 ratio. The difference of the chemical shift values of the two isomers were small and only visible for H_1'/C_1' and in the aromatic moiety of the molecule.

The structure of the farnesyl side chain was deduced based on DQF-COSY, HSQC, HMBC and H2BC correlations and comparison with literature data from the related structures aspernidine A and B (Scherlach 2010). The attachment of the farnesyl side chain to the two isomers was based on HMBC correlations of H_1' to C_3 and C_4 for nidubenzal A and B, respectively. Nidubenzal A has been reported in a synthetic screening library (Aurora Fine Chemicals LLC); however, neither nidubenzal A nor B has previously been reported from nature.

The structure of **2** was also solved through 2D-NMR analysis (DQF-COSY, HSQC, and HMBC) which showed that it was asperugin B a metabolite previously isolated from the related fungus *A. rugulosus* (Ballantine 1967). Two other asperugins, A and C, have been isolated from *A. rugulosus* (Ballantine 1964, 1965, and 1971) and through LC-TOF-MS-analysis we tentatively identified asperugin A (**3**) but not asperugin C in the *A. nidulans* IBT24909 extract. We have not yet been able to isolate asperugin A in quantities sufficient for NMR-analysis. In 2005 An *et al.* (An 2005) reported production of asperugin A and B (also with B as the major product), as well as violaceol, in a strain where cosmid-size DNA from slow growing fungi was cloned and introduced into *A. nidulans*. During the course of this study Scherlach *et al*. reported the characterization of aspernidine A and B isolated from *A. nidulans* (Scherlach 2010); however, we were not able to trace these metabolites through LC-TOF-MS analysis of our extract.

All the isolated metabolites, nidubenzal A and B, asperugin A-C and the related aspernidines, seem to be hybrid metabolites which consist of a farnesyl side chain and an aromatic moiety, which may be of PK origin. The aromatic nature of the metabolites indicated that the pathway could be initiate with formation of a NR-PK catalyzed by a NR-PKS. The products of the NR-PKS could be orsellinic acid or even more likely orsellinaldehyde, figure 3, which have, just recently, been shown to be a metabolite of *A. nidulans* from the AN3230 (PkfA) NR-PKS (Ahuja 2012). The only difference between the aromatic part of asperugin A and B, and aspernidine A and B, are an O-methylation indicating that the two metabolites in each group are derived from the same biosynthetic pathway. Scherlach *et al.* (Scherlach 2010) suggests that the aspernidines are formed by either orsellinic acid or the corresponding aldehyde which traps ammonia nitrogen in an intermediary aldehyde, where oxidoreduction and condensation steps leads to the isoindolinone moiety. The precursor of the aromatic moiety of asperugin C could also be orsellinaldehyde which, in a shunt pathway, will be methylated instead of oxidated. The two new metabolites nidubenzal A and B differs in the aromatic moiety which containing seven carbons instead of the eight of the backbone of the other metabolites. This could indicate a different biosynthetic pathway or a decarboxylation from a C_8-PK product. We speculated whether these metabolites might be a product of the shikimic acid pathway since the substitution pattern resembles protocatechuic acid, figure 3, a shunt product from the biosynthesis of shikimic acid, differing only by the aldehyde in the place of the carboxylic acid.

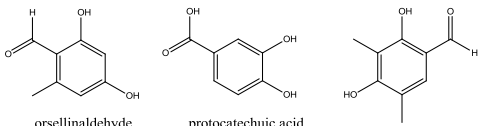

Figure 3 Structures of orsellinaldehyde, protocatechuic acid and 2-ethyl-4,6-dihydroxy-3,5-dimethylbenzaldehyde

Since the metabolites might be of PK origin we went back to the reference strain of the PKS deletion library (Nielsen 2011) to see if we could trace the metabolites through extracted ion chromatograms (EICs) on any of the media used in the study.

Nidubenzal A and B were present in small quantities on the CYAs medium so we went back to the deletion library to see whether we could identify a possible PKS to link to these metabolites. In two of the PKS deletions, *ausA*Δ and AN11191Δ, the production seemed to have been abolished; however, due to the small quantities of metabolites present in the extract it was, in some cases, difficult to determine the presence of the metabolites.

Asperugin A could not be detected in any of the strains whereas asperugin B could be traced. The same procedure for identification of putative PKSs as for the nidubenzals was done and six PKS candidates were identified, AN0523 (*pkdA*), AN11191, AN3230 (*pkfA*), *ausA*, AN6791, and AN9005. It has recently been reported that AN3230 produces orsellinaldehyde and AN0523 2-ethyl-4,6-dihycroxy-3,5-dimethylbenzaldehyde, figure 4.37 (Ahuja 2012). *ausA*, *pkfA* and *pkdA* are NR-PKSs whereas AN11191, AN6791 and AN9005 are PR-PKSs (Sanchez 2012). These results gave several possible genes so we were not able to link the metabolites to their synthase genes.

At the same time as this study we were also working on a strain where the *cclA* gene had been deleted which activated the production of the asperugins and nidubenzals. It had already been shown that this deletion strain increased the production of secondary metabolites in *A. nidulans* (Bok 2009). We wanted to investigate whether challenging the *cclA*Δ strain on complex media could activate even more secondary metabolite production.

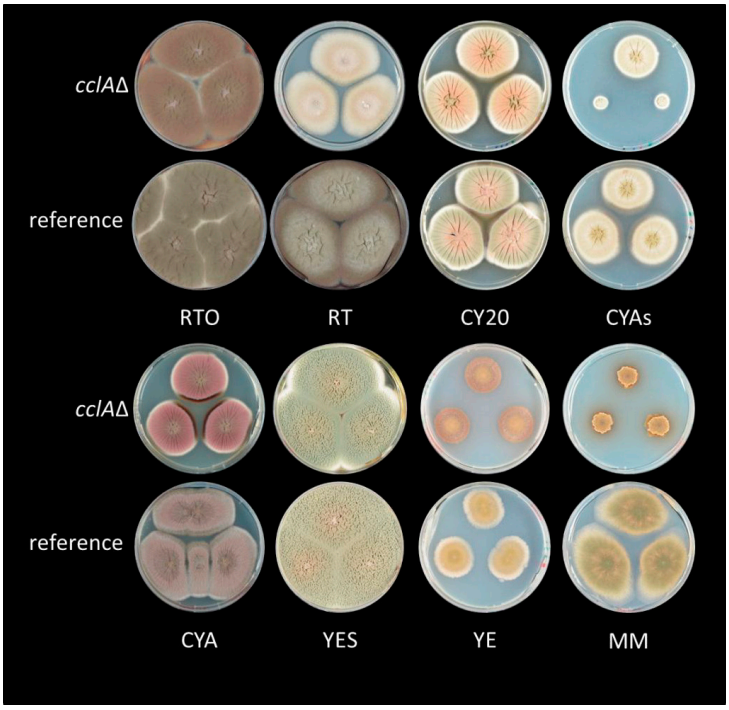

Figure 4 The appearance of the reference strain compared to the *cclA*Δ strain cultivated for seven days at 37°C on RTO, RT, CY20. CYAs, CYA, YES, YE, and MM medium.

Figure 4 show the phenotypical appearance of the *cclA*Δ strain compared to the reference strain when grown on the same eight media as used initially in the deletion study. It is evident that the fungus was affected by the deletion and as the reference strain it responded differently to the different medium conditions. Generally it seems that the *cclA*Δ strains grow slower than the reference. To analyze the metabolite production micro-extraction was performed (Frisvad 1987, Smedsgaard 1997) and the extracts were analyzed by both UHPLC-DAD and UHPLC-TOF-MS. The UHPLC analysis revealed a diverse and different production of secondary metabolites on the eight media compared to the reference strain, figure 5.

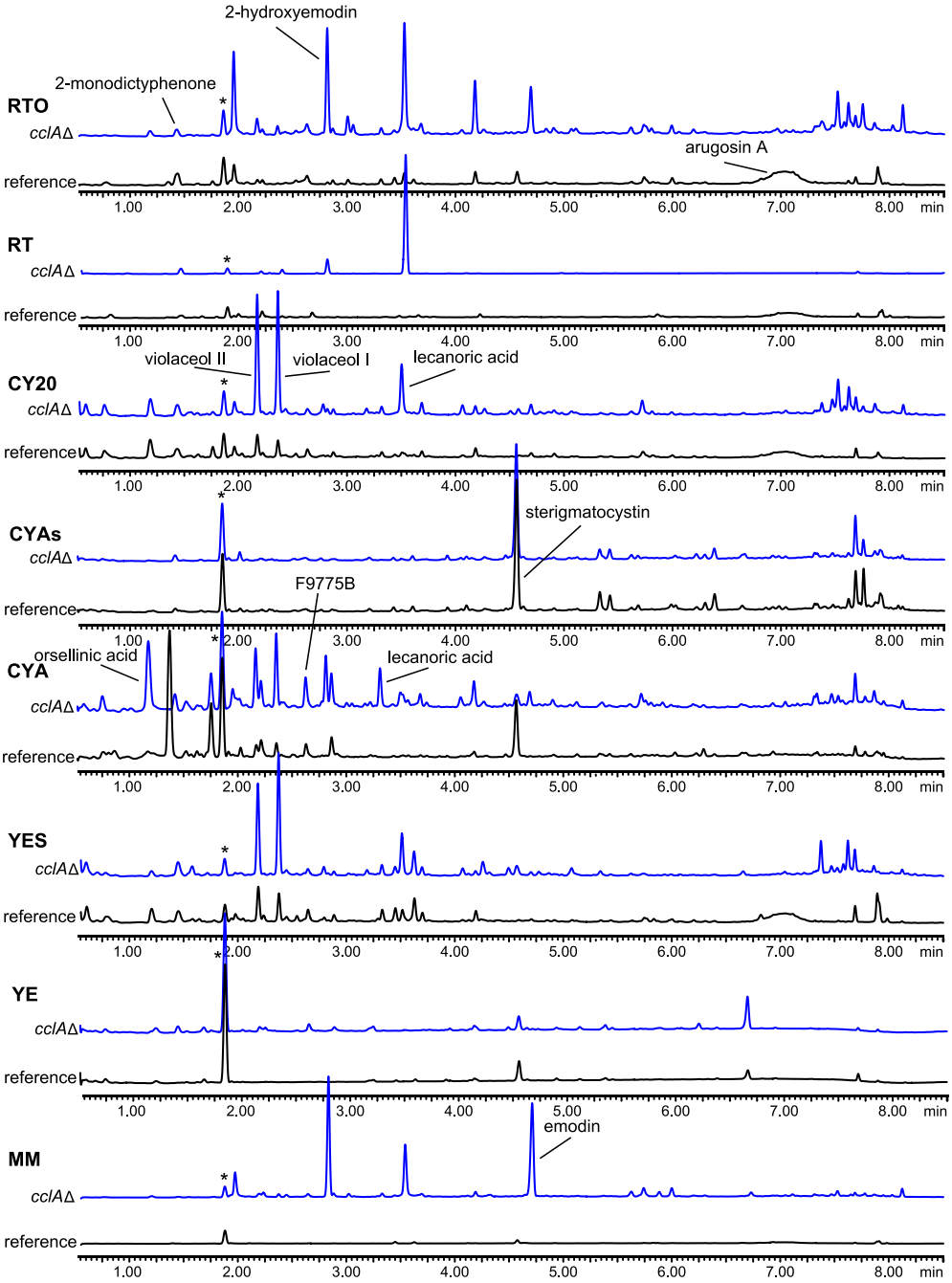

Figure 5 UHPLC-DAD chromatograms (210 nm) of micro-extracts of the *cclA*Δ strain cultivated on eight different media compositions for seven days at 37°C compared to the reference strain. From top to bottom RTO, RT, CY20, CYAs, CYA, YES, YE and MM.*This peak corresponds to an internal standard of chloroamphenicol added to the extracts. The

concentration of chloroamphenicol is the same in all the samples. Metabolites were identified through comparison with standards or based on exact mass and UV-data.

In all of the media except YE and CYAs there seemed to be an activation of secondary metabolite production. It was especially noticeable that many of the metabolites produced in the *cclA*Δ strain are derived from the orsellinic acid and monodictyphenone pathway, which was also the gene clusters activated by Bok *et al.* (Bok 2009). Arugosin A which was linked to the monodictyphenone pathway in section 4.3.1.2 seemed to disappear in the *cclA*Δ strain whereas intermediates in this pathway, for example emodin, seemed to accumulate. Most noticeable for our study, and what is focused on in this section, was the increased production of asperugin A and B as well as nidubenzal A and B on several of the media; YES, CY20, CYAs, CYA, RTO and MM, figure 6.

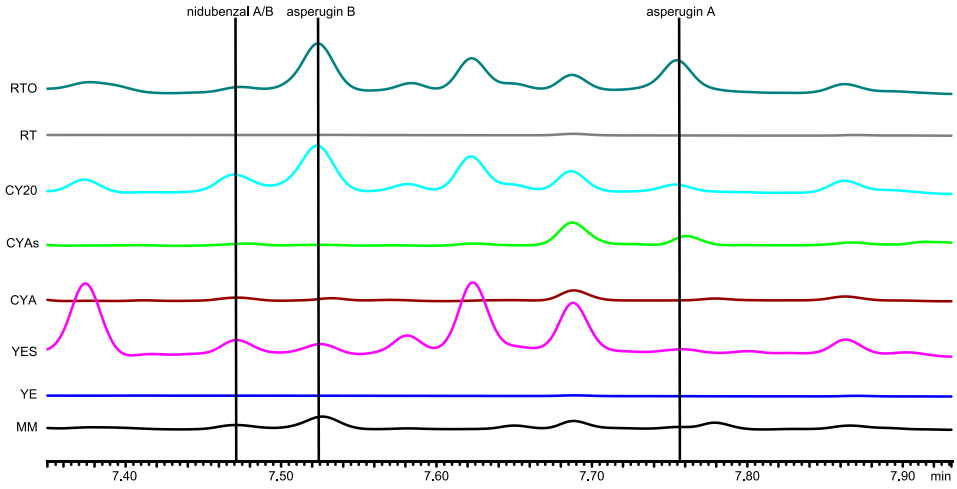

Figure 6 UHPLC-DAD chromatograms (210 nm) from seven to eight minutes of micro-extracts of the *cclA*Δ on the eight different media. From top to bottom: RTO, RT, CY20, CYAs, CYA, YES, YE and MM.

The increased production of asperugin A and B, and nidubenzal A and B in this strain allowed for creating double deletions of *cclA* and the putative candidate PKS genes in order to understand the changes in production of the metabolites. Therefore *cclA* was deleted in the respective PKS gene deletions identified previously. We included both the NR- and PR-PKSs in the study since it seemed like they might have an effect on asperugin production. Since it was originally thought that these products could be derived from orsellinic acid, and due to the activation of several orsellinic acid derived metabolites in the *cclA*Δ strain, a deletion of *cclA* in *orsA*Δ was also created to see if there were an effect on the production of the nidubenzals and asperugins. As described previously we wondered whether the nidubenzal A and B could be shikimic derived so we also made a deletion mutant of the *qutC* gene which has been shown to encode for an enzyme, dehydroshikimic acid dehydratase that catalyzes the production of protocatechius acid from 3-dehydroshikimic acid in *A. nidulans* (Lamb 1992).

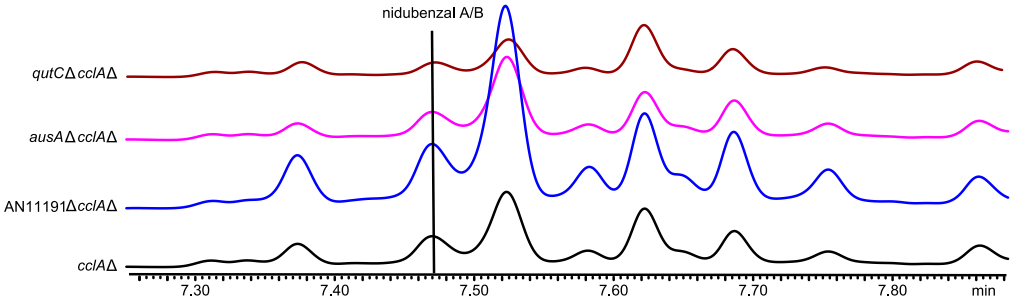

Figure 7 UHPLC chromatograms (210 nm) of micro-extracts of the *qutC*Δ*cclA*Δ, *ausA*Δ*cclA*Δ, AN11191Δ*cclA*Δ and *cclA*Δ strains after cultivation for seven days at 37°C on CY20 medium. The other parts of the chromatogram were also identical.

The double deletion mutants made were analyzed on both UHPLC-DAD and UHPLC-TOF-MS on all eight media. As seen in figure 7 nidubenzal A and B were present in all the deletion strains and on the different media; however, spore-PCR analysis of the AN11191Δ*cclA*Δ strain showed presence WT AN11191 nuclei indicating this strain was not suited for analysis. A new double deletion based on the original confirmed AN11191Δ strain is in progress of being constructed. As the *qutC*Δ*cclA*Δ strain also produced nidubenzal A and B it indicates that they are derived from either AN11191 or an alternative route to protocatechuic acid exists in *A. nidulans*.

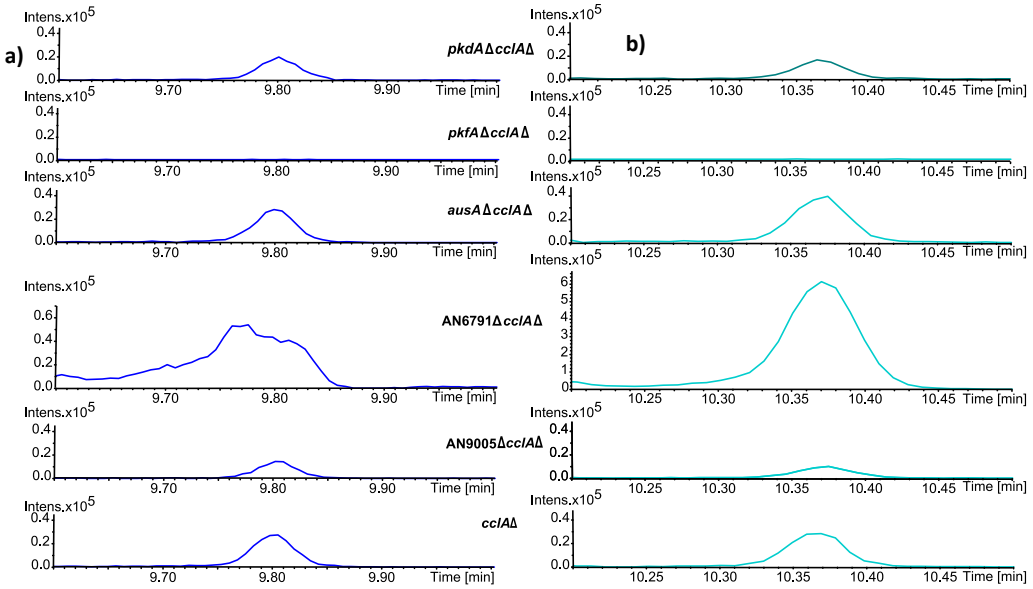

Figure 8 EIC of **a)** asperugin A (calc. $[M-H]^-$ 401.23225±0.002]) and **b)** asperugin B (calc. $[M+H]^+$ 387.21660±0.002]) of micro-extracts of the (from top to bottom) *pkdA*Δ*cclA*Δ, *pkfA*Δ*cclA*Δ, *ausA*Δ*cclA*Δ, AN6791Δ*cclA*Δ, AN9005Δ*cclA*Δ and *cclA*Δ strains after cultivation on CY20 medium for seven days at 37°C.

The extracted ion chromatograms (EIC) of asperugin A and B in the double deletion mutants and the reference strain can be seen in figure 8. As the AN11191Δ*cclA*Δ strain was not correct it have been removed from the study, however a correct strain will be included in the analysis for the presence of the asperugins. As can be seen on the figure production of asperugin A and B are abolished in the *pkfA*Δ*cclA*Δ strain and this was consistent on the eight analyzed media. Ahuja *et al.* (Ahuja 2012) recently showed that overexpression of this PKS with an inducible promoter led to the production of orsellinaldehyde. Further biosynthesis of orsellinaldehyde to the asperugins would require several tailoring enzymes catalyzing oxidation of a methyl to an aldehyde, oxidation of the aromatic ring, a terpene synthase and an *O*-methyltransferase. As suggested by Scherlach *et al.* (Scherlach 2010) further modifications to the aromatic moiety of the metabolites could lead to the biosynthesis of the aspernidines. This biosynthetic pathway resembles in some ways the proposed biosynthesis of the cichorine gene cluster. Preliminary bioinformatics studies indicated the presence of *O*-methyltransferase, prenyltransferase, oxidase, cytochrome P450, and monooxidase enzymatic functions surrounding the *pkfA* gene. Construction of the double deletions of *cclA* and the surrounding genes to determine the biosynthetic pathway of these metabolites including identifying intermediates are ongoing. In the AN6791Δ*cclA*Δ stain it appears that the production of asperugin A and B have increased compared to the other strains. This is interesting due to the fact that the deletion was constructed based on analysis of the deletion library where the metabolites were missing in the single deletion strain, AN6791Δ. This phenomena is seen in several media (YES, CY20, CYAs and MM); however, the reason for this apparently increase in production is so far unknown.

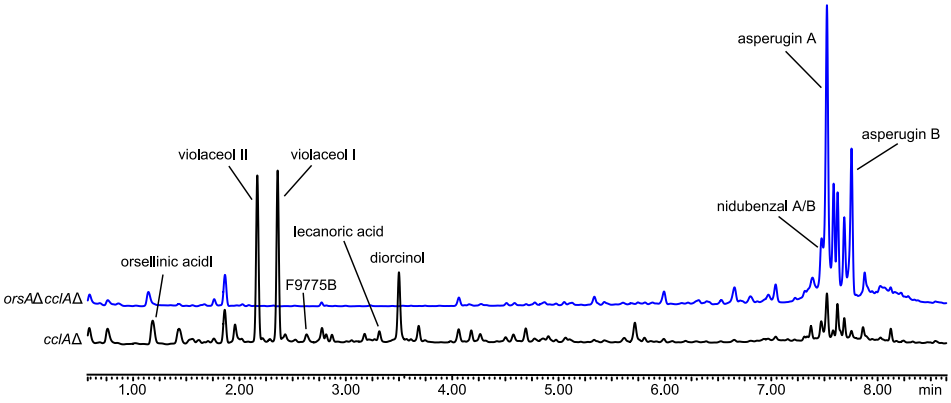

Figure 9 UHPLC chromatograms (210 nm) of micro-extracts of the *orsA*Δ*cclA*Δ strain compared to the *cclA*Δ strain on CY20 medium.

Due to the orsellinic acid like nature of asperugins we included a double deletion of *orsA* and *cclA* in the study. As seen from figure 9 the deletions did not abolish the production of the asperugins; however, the metabolites which have been shown to be derived from the orsellinic acid biosynthetic pathway were indeed absent in the double deletion strain (Bok 2009, Schroeckh 2009, Sanchez 2010, Nahlik 2010).

References:

Ahuja, M.; Chiang, Y.M.; Chang, S.L.; Praseuth, M.B.; Entwistle, R.; Sanchez, J.F.; Lo, H.H.; Oakley, B.R.; Wang, C.C.C. Illuminating the diversity of aromatic polyketide synthases in *Aspergillus nidulans*. *J. Am. Chem. Soc.* **2012**, *134*, 8212-8221.

An, Z.; Harris, G.H.; Zink, D.; Giacobbe, R.; Lu, P.; Sangari, R.; Svetnik, V.; Gunter, B.; Liaw, A.; Masurekar, P.S.; Liesch, J.; Gould, S.; Strohl, W. Expression of cosmid-size DNA of slow-growing fungi in *Aspergillus nidulans* for secondary metabolite screening. In *Mycology series: Handbook of industrial mycology* (ed Bills, G.) **2005**, *22*, 167-186.

Ballantine, J.A.; Hassall, C.H.; Jones, G. Asperugin, a ,etabolite associated with abnormal morphology of *Aspergillus rugulosus*. *Tetrahedron Lett.* **1964**, *49*, 3739-3740.

Ballantine, J.A.; Hassall, C.H.; Jones, G. The biosynthesis of phenols. Part IX. Asperugin, a metabolic product of *Aspergillus rugulosus*. *J. Chem. Soc.* **1965**, 4672-4678.

Ballantine, J.A.; Hassall, C.H.; Jones, B.D.; Jones, G. The biosynthesis of phenols XII. Asperugin B, a metabolite of *Aspergillus rugulosus*. *Phytochem.* **1967**, *6*, 1157-1159.

Ballantine, J.A.; Ferrito, V.; Hassall, C.H. The biosynthesis of asperugin in *Aspergillus rugulosus*. *Phytochem.* **1971**, *10*, 1309-1313.

Bok, J.W.; Chiang, Y.M.; Szewczyk, E.; Reyes-Domingez, Y.; Davidson, A.D.; Sanchez, J.F.; Lo, H.C.; Watanabe, K.; Strauss, J.; Oakley, B.R.; Wang, C.C.C.; Keller, N.P. Chromatin-level regulation of biosynthetic gene clusters. *Nat. Chem. Biol.* **2009**, *5*, 462-464.

Cove, D.J. The induction and repression of nitrate reductase in the fungus *Aspergillus nidulans*. *Biochim. Biophys. Acta* **1966**, *113*, 51-56.

Frisvad 1987, J.C.; Thrane, U. Standardized high-performance liquid chromatography of 182 mycotoxins and other fungal metabolites based on alkylphenone retention indices and UV-VIS spectra (diode array detection). *J. Chromatogr.* **1987**, *404*, 195-214.

Johnstone, I.L.; Hughes, S.G.; Clutterbuck, A.J. Cloning an *Aspergillus nidulans* developmental gene ny transformation. *EMBO J.* **1985**, *4*, 1307-1311.

Laatsch, H. AntiBase 2010. Available online: http://www.wiley-vch.de/stmdata/antibase2010.php (accessed on May 30th 2012).

Lamb, H.K.; van den Hombergh, J.P.T.W,: Newton, G.H.; Moore, J.D.; Roberts, C.F.; Hawkins, A.R. Differential flux through the quinate and shikimate pathways. *Biochem. J.* **1992**, *284*, 181-187.

Nahlik, K.; Dumkow, M.; Bayram, Ö.; Helmstaedt, K.; Bunsch, S.; Valerius, O.; Gerke, J.; Hoppert, M.; Schwier, E.; Opitz, L.; Westermann, M.; Grond, S.; Feussner, K.; Geobel, C.; Kaever, A.; Meinicke, P.; Feussner, I.; Brais, G.H. The COP9 signal medieates transcriptional and metabolic response to hormones,

oxidative stress protection and cell wall rearrangement during fungal development. *Mol. Microbial.* **2010**, *78*, 964-979.

Nielsen, K.F.; Smedsgaard, J. Fungal metabolite screening: database of 474 mycotoxins and fungal metabolites for dereplication by standardised liquid chromatography-IV-mass spectrometry methodology. *J. Chromatogr. A.* **2003**, *1002*, 111-136.

Nielsen, M.L.; Albertsen, L.; Lettier, G.; Nielsen, J.B.; Mortensen, U.H. Efficient PCR-based gene targeting with a recyclable marker for *Aspergillus nidulans*. *Fung. Genet. Biol.* **2006**, *43*, 54-64.

Nielsen, J.B.; Nielsen, M.L.; Mortensen, U.H. Transient disruption of non-homologous end-joining facilitates targeted genome manipulations in the filamentous fungus *Aspergillus nidulans*. *Fungal genet. Biol.* **2008**, *45*, 165-170.

Nielsen, K.F.; Mogensen, J.; Johansen, M.; Larsen, T.O.; Frisvad, J.C. Review of secondary metabolites and mycotoxins from the *Aspergillus niger* group. *Anal. Bioanal. Chem.* **2009**, *395*, 1225-1242.

Nielsen, M.L.; Nielsen, J.B.; Rank, C.; Klejnstrup, M.L.; Holm, D.K.; Brogaard, K.H.; Hansen, B.G.; Frisvad, J.C.; Larsen, T.O.; Mortensen, U.H. A genome-wide polyketide synthase deletion library uncovers novel genetic links to polyketides and meroterpenoids in *Aspergillus nidulans*. *FEMS Microbiol. Lett.* **2011**, *321*, 157-166.

Nørholm, M.H.H. A mutant Pfu DNA polymerase designed for advanced uracil-excision DNA engineering. *BMC Biotechnol.* **2010**, *10*, 21.

Sanchez, J.F.; Chiang, Y.M.; Szewczyk, E.; Davidson, A.D.; Ahuja, M.; Oakley, C.E.; Bok, J.W.; Keller, N.; Oakley, B.R.; Wang, C.C.C. Molecular genetic analysis of the orsellinic acid/F9775 gene cluster of *Aspergillus nidulans*. *Mol. BioSyst.* **2010**, *6*, 587-593.

Sanchez, J.F.; Somoza, A.D.; Keller, N.P.; Wang, C.C.C. Advances in *Aspergillus* secondary metabolite research in the post-genomic era. *Nat. Prod. Rep.* **2012**, *29*, 351-371.

Scherlach, K.; Schuemann, J.; Dahse, H.M.; Hertweck, C. Aspernidine A and B, prenylated isoindolinone alkaloids from the model fungus *Aspergillus nidulans*. *J. Antibiot.* **2010**, *63*, 375-377.

Schroeckh, V.; Scherlach, K.; Nützmann, H.W.; Shelest, E.; Schmidt-Heck, W.; Schuemann, J.; Martin, K.; Hertweck, C.; Brakhage, A.A. Intimate bacterial-fungal interaction triggers biosynthesis of archetypal polyketides in *Aspergillus nidulans*. *Proc. Natl. Acad. Soc. USA* **2009**, *106*, 14558-14563.

Smedsgaard, J. Micro-scale extraction procedure for standardized screening of fungal metabolite production in cultures. *J. Chromatogr. A* **1997**, *760*, 264-270.

Supplementary material

Supplementary table 1: Strains used for deletions of *cclA*

Strain	Genotype	Reference
IBT29539	*argB2*, *pyrG89*, *veA1*, *nkuA*Δ	Nielsen et al., 2008
IBT30996	*argB2*, *pyrG89*, *veA1*, *nkuA*Δ, AN0523Δ	Nielsen et al., 2011
-	*argB2*, *pyrG89*, *veA1*, *nkuA*Δ, *qutC*Δ	This study
IBT31005	*argB2*, *pyrG89*, *veA1*, *nkuA*Δ, *pkfA*Δ	Nielsen et al., 2011
IBT31013	*argB2*, *pyrG89*, *veA1*, *nkuA*Δ, AN6791Δ	Nielsen et al., 2011
IBT31020	*argB2*, *pyrG89*, *veA1*, *nkuA*Δ, *orsA*Δ	Nielsen et al., 2011
IBT31022	*argB2*, *pyrG89*, *veA1*, *nkuA*Δ, *ausA*Δ	Nielsen et al., 2011
IBT31025	*argB2*, *pyrG89*, *veA1*, *nkuA*Δ, AN9005Δ	Nielsen et al., 2011
IBT31000	*argB2*, *pyrG89*, *veA1*, *nkuA*Δ, AN11191Δ	Nielsen et al., 2011

Supplementary table 2: Primers used in this study

ANqutC-DL-Up-F	CTTACAGCCCTAGTCATTCC	Deletion fragment Up
ANqutC-DL-Up-Rad	gatccccgggaattgccatgGAGCTGATTGAGTTGAAGAC	Deletion fragment Up
ANqutC-DL-Dw-Fad	aattccagctgaccaccatgGGTAATGATGGCTCATGCACG	Deletion fragment Dw
ANqutC-DL-Dw-R	GATGTTGACGGTGCTGGATATTG	Deletion fragment Dw
ANqutC-CHK-Up-F	CACCACTAGAACAACTACATACGG	Strain verification
ANqutC-CHK-Dw-R	GTGCTGGGGAAATTTTGGGTG	Strain verification
ANcclA-DL-Up-FU	GGGTTTAAUGTGATCACTTCGCAGGGTAG	Deletion fragment Up
ANcclA-DL-Up-RU	GGACTTAAUCCTTTGCGGATAGGTATTTCAC	Deletion fragment Up
ANcclA-DL-Dw-FU	GGCATTAAUCAGCTGGGTCATGGATTGG	Deletion fragment Dw
ANcclA-DL-Dw-RU	GGTCTTAAUGACGGAGCTTGAGCTTTACG	Deletion fragment Dw

ANcclA-CHK-Up-F	CGGTTTCTCTCTGTGTCTCC	Strain verification
ANcclA-CHK-Dw-R	CGCCTCACATCCGACTAC	Strain verification

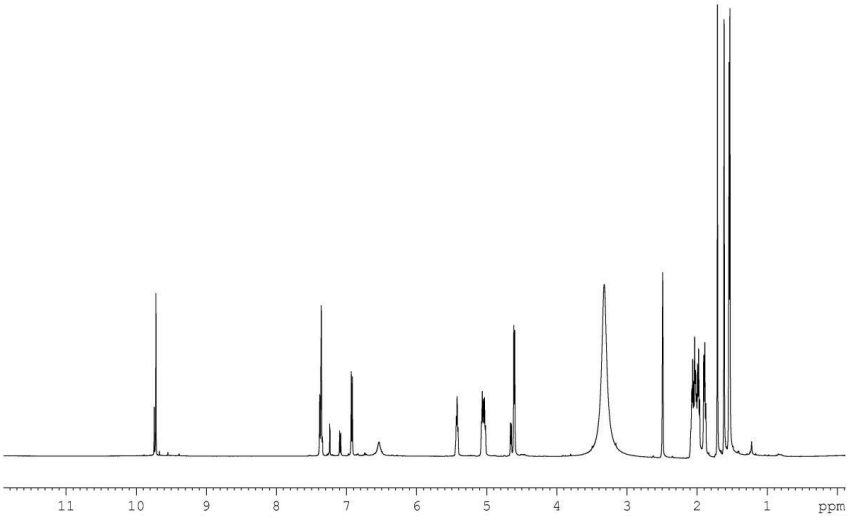

^{1}H NMR of nidubenzal A and B in DMSO-d_6

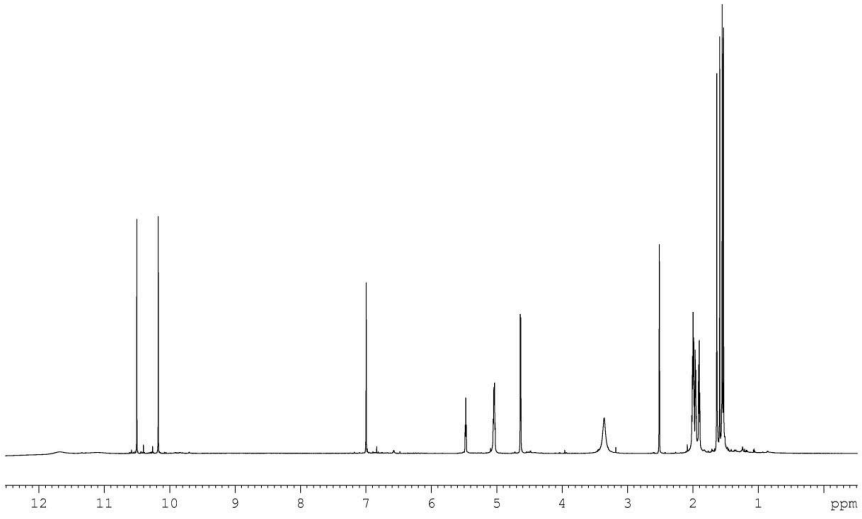

^{1}H NMR of asperugin B in DMSO-d_6

Paper 7

"A regulatory protein from *Aspergillus niger* induces juvenile hormones upon heterologous expression in *A. nidulans*"

MT Nielsen and ML Klejnstrup (joint 1st author), CH Gotfredsen, MR Andersen, BG Hansen, UH Mortensen, and TO Larsen

Submitted to PLoS ONE – under revision

Title

A regulatory protein from *Aspergillus niger* induces juvenile hormones upon heterologous expression in *A. nidulans*.

Authors

Nielsen, M.T.[1,2,3], Klejnstrup, M.L.[1,2], Gotfredsen, C.H. [4], Andersen, M.R.[1], Hansen, B.G.[1,5], Mortensen, U.H. [1*] and Larsen, T. O. [1*]

Affiliation

[1] Center for Microbial Biotechnology, Department of Systems Biology, Technical University of Denmark, 2800 Kgs Lyngby, Denmark.

[2] These authors contributed equally to the work.

[3] Current address: Novo Nordisk Foundation Center for Biosustainability, Technical University of Denmark, Fremtidsvej 3, 2970 Hoersholm, Denmark.

[4] Department of Chemistry, Technical University of Denmark, 2800 Kgs Lyngby, Denmark.

[5] Current address: Novozymes A/S, Krogshoejvej 36, 2880 Bagsvaerd, Denmark.

* Authors to whom correspondence should be addressed (um@bio.dtu.dk; tol@bio.dtu.dk)

Abstract

Fungal natural products are considered a rich, underexplored resource of bioactive compounds. A combined heterologous expression and growth condition variation approach using *Aspergillus nidulans* as model induced insect juvenile hormone III and methyl farnesoate, essential developmental hormones previously unobserved in fungi. The approach is of general relevance in endeavors to uncover metabolites produced by silent gene clusters while the finding of juvenile hormones is of ecological relevance.

Introduction

Filamentous fungi are capable of synthesizing a wide range of bioactive molecules important for growth in a complex and competitive ecological niche. These compounds have been found to have diverse pharmaceutical applications [1]. With the release of full genome sequences of several filamentous fungi it became apparent that the number of predicted secondary metabolite synthases by far exceeds the number of known metabolites [2, 3]. These observations hints that specific environmental stimuli are required for induction of the majority of secondary metabolites, thus coining the terms silent and orphan synthases [4]. Despite attempts to identify or mimic these stimuli in order to unravel the secondary metabolism of the model organism *Aspergillus nidulans*, the majority of predicted synthases are still considered silent [5, 6]. Genetic approaches have been somewhat successful through manipulation of histone methylation [7] or specific regulators [8]. The latter approach is particularly attractive as it is a targeted approach and therefore promises rapid linking of induced metabolites to genes. Moreover, as biosynthetic pathways towards secondary metabolites tend to be clustered in the genome [2, 3], specific regulators may be identified by genomic co-localization. However, the number of successful applications of this approach is limited, possibly because far from all predicted gene clusters contain regulatory proteins. We decided to investigate whether induction of secondary metabolites could be achieved through heterologous expression of regulatory genes from other filamentous fungi using *A. niger* as test case. A selection of putative pathway specific regulators was constitutively expressed individually from a defined locus [9]. This genetic approach was combined with a screen of several complex media recently demonstrated to influence *A. nidulans*

secondary metabolism [10]. The combinatorial approach resulted in the identification of one regulatory protein that strongly induced metabolites not previously reported from *A. nidulans*. Among the induced metabolites were insect juvenile hormone III and methyl farnesoate, sesquiterpene hormones crucial for correct development of insects and crustaceans respectively [11-13]. To the best of our knowledge, this is the first observation of juvenile hormones in fungi as well as the first example of transcriptional activation of secondary metabolism between distantly related species.

Materials & Methods:

Strains and media. *Escherichia coli* strain DH5α was used to propagate all plasmids. All *A. niger* genes were amplified from strain ATCC1015. The *A. nidulans* strain NID74 (*argBΔ, veA1, pyrG89, nkuAΔ*) were used as background strain for all transformations as it allows gene targeting with the *argB* marker due to a complete deletion of the *A. nidulans argb*-open reading frame. NID74 was generated from NID1 using the fusion PCR technique essentially as described previously [14]. NID545 (argBΔ, pyrG89, veA1, nkuAΔ IS1::pgpdA-LacZ-TtrpC::argB) were used as reference strain for metabolite analysis. Genotypes of all strains are summarized in supplementary table 2. All *A. nidulans* strains were propagated on solid glucose minimal medium (MM) (1 % glucose, 10 mM NaNO3, 1x salt solution, 2 % agar (Bie & Berntsen, BBB 10030,SO-BI-GEL,Agar)), supplemented with 10 mM uridine (Uri), 10 mM uracil (Ura). Complex media used for chemical analysis were prepared as described by Frisvad and Samson [15] and supplemented with 10 mM Uri and 10mM Ura:

- *CYAs* (Yeast extract 5,0 g/l (Biokar, A1202HA), Czapek dox broth 35,0 g/l (Difco, 233810), NaCl 50,0 g/l (J.T Baker, 0277), 1x trace metals, 1,5 % agar(Bie & Berntsen, BBB 10030,SO-BI-GEL,Agar)).
- *OAT* (Oatmeal 30g/l, 1x trace metals, 1,5 % agar(Bie & Berntsen, BBB 10030,SO-BI-GEL,Agar)).
- *RTO* (Oatmeal 30g/l, (NH_4) H_2PO_4 0,4 g/l (Merck, 1126), K_2CO_3 0,4 g (Merck, 4928), $ZnSO_4$,$7H_2O$ 0,06 g/l (Merck, 8883), $FeSO_4$,$7H_2O$ 0,06 g (Merck, 3965), $(NH_4)_2SO_4$ 0,16 g/l (Merck, 1217), $MgCO_3$ 0,25 g (Riedel-de Haën, 13118), Tartaric acid ($C_4H_6O_6$) 2,6 g (Merck, 804), di-Ammonium tartrate ($C_4H_{12}N_2O_6$) 2,6 g (Merck,

1222), Glucose (D+) 50,0 g (BHD, 10117), 1x trace metals, 2 % agar (Bie & Berntsen, BBB 10030,SO-BI-GEL,Agar)),

- *YES* (Yeast extract 20 g/l (Biokar, A1202HA), Sucrose 150 g/l (Fluka, 84100), $MgSO_4,7H_2O$ 0,5 g/l (Merck, 5886), 1x trace metals, 2 % agar (Bie & Berntsen, BBB 10030,SO-BI-GEL,Agar)

PCR, USER cloning and *A. nidulans* strain construction. USER cloning compatible PCR products were amplified with 30 PCR cycles in 50 µl reaction mixtures using proof-reading PfuX7 polymerase [16]. USER vectors are denoted according to the nomenclature introduced by Hansen et al [9]. Putative *A. niger* genes were USER cloned into pU1111-IS*1* and transformed into *A. nidulans* as described previously [9]. In order to generate the NID545 reference strain the *E. coli lacZ* was cloned into a pU1014-IS*1* vector generating pU1011-IS*1*:*LacZ* which was transformed to an pU1110-*IS1-LacZ* vector by insertion of *A. nidulans gpdA* promoter in the AsiSI/Nb.BtsI cassette. DNA sequences of *LacZ* and all inserted *A. niger* ORFs were verified by sequencing of the corresponding expression plasmids. Gene targeting events were verified in all *A. nidulans* transformants by analytical PCR as described previously [9]. Supplementary table 3 summarizes the PCR primers used in this study.

Chemical characterization of mutant strains by LC-DAD-MS: All strains were grown as three point inoculations for 7 days at 37 degrees in the dark on solid media. Extraction of metabolites were performed by the agar plug extraction method [17] using three 6mm agar plugs/extract. Extracts were analyzed by UHPLC-DAD and LC-HRMS. UHPLC-DAD analysis was performed on a Dionex RSLC Ultimate 3000 (Dionex, Sunnyvale, CA) equipped with a diode-array detector. Separation was performed at 60°C on a 150 mm × 2.1 mm ID, 2.6 µm Kinetex C_{18} column (Phenomenex, Torrence, CA) using a linear water/MeCN (both buffered with 50 ppm tri-fluoroacetic acid (TFA)) gradient starting from 15% MeCN to 100% over 7 min at a flow rate of 0.8 mL min^{-1}. LC-HRMS analysis were made on a MaXis 3G QTOF (Bruker Daltronics) coupled to a Dionex Ultimate 3000 UHPLC system equipped with a 100 x 2.0 mm, 2.6 µm, Kinetex C-18 column. The separation

column was held at a temperature of 40°C and a gradient system composed of A: 20 mM formic acid in water, and B: 20 mM formic acid in acetonitrile was used. The flow vas 0.4 ml/min, 85% A graduating to 100% B in 0-10 min, 100% B 10-13 min, 85% A 13.1-15 min. For calibration, a mass spectrum of sodium formate was recorded at the beginning of each chromatogram using the divert valve (0.3-0.4 min). Samples were analyzed both in positive and negative ionization mode. De-replication of induced compounds were performed by comparison of accurate mass to the metabolite database Antibase2009 [18] as well as comparison of UV spectra to published data.

Chemical characterization of mutant strains by GC-MS: Volatile metabolites were collected during days 5-7 for the strains inoculated in CYAs. To collect the volatiles, a stainless steel Petri dish lid with a standard 1/4 Swagelock™ replaced the usual lid [19]. This lid possessed a standard 1/4 Swagelok fitting with PTFE insert in the centre that is used to hold a charcoal tube (SKC, 226-01). The collected volatiles were extracted from the charcoal tube with 0.3 mL of ether (Sigma Aldrich). The samples were concentrated to approximately 0.1 mL using a nitrogen flow in a GC vial and analysed using a Finnigan Focus GC coupled to a Finnigan Focus DSQ mass selective detector. The separation of the volatiles was done on a Supelco SLB™-5 MS capillary column, using He as carrier gas, at 1.2 mL/min. The injection and detection temperature was set to 220 °C. One microlitre of each sample was injected into the GC–MS system. Chromatographic conditions were set to an initial temperature of 35 °C for 1 min, raised at 6 °C/min to 220 °C and then 20 °C/min to 260 °C for 1 min. The separated compounds were characterized by their mass spectra generated by electron ionization (EI) at 70 eV at a scan range from *m*/*z* 35–300.

Isolation of methyl (2E,6E)-10,11-dihydroxy-3,7,11-trimethyl-2,6-dodecadienoate (X1).

NID477 was cultured on 100 CYAs plates for 7 days at 37°C in the dark. The plates were homogenized using a Stomacher and 100 mL ethyl acetate (EtOAc) + 1% formic acid (FA) pr. 10 plates. The extract was filtered

after 1 hour and the remaining broth was extracted with EtOAc + 1% FA for 24 hours. The extract was filtered and the two fractions pooled and dried down on a freeze drier. The crude extract were separated into three phases by dissolving it in 9:1 MeOH:H_2O – Milli-Q and extracted into a heptane phase followed by a dicloromethane (DCM) phase. The DCM phase was fractionated with a 10g ISOL Diol column, using 13 steps of stepwise Hexane-dichloromethane-EtOAc-MeOH. X1 was present in the DCM fraction (9.5 mg) and was purified on a Waters HPLC W600/996PDA (Milford, MA, USA) using a RP column (Phenomenex Luna C18(2), 250 x 10 mm, 5 µm, Torrance, CA, USA) using a gradient of 40% MeCN (H_2O – Milli-Q (Millipore, MA, USA)) to 100% over 20 min. with 50 ppm TFA and a flow of 4 mL/min. The collections were concentrated on a rotarvap (Büchi V-855/R-215) and dried down under N_2(g) to yield 2.0 mg of X1. 1 and 2D NMR characterization (1H, DQF-COSY, H2BC, HMBC and HSQC) of the compound showed that the compound present is a 2:3 mixture of X1a:X1b. The NMR data of X1 indicated that two diastereomers were present in the sample. The ^{1}H- and ^{13}C-chemical shifts differ most in the reduced end of X1 where a stereocenter (C_{10}) is present. The chemical shifts of H_1/C_1 to H_5/C_5 are identical. The difference of chemical shifts of the two methyl groups (H_{12}/C_{12} and H_{13}/C_{13}) and the two CH_2 groups next to the stereocenter are due to the presence of the chiral center. The two diastereomers present in the X1 solution must be due to the presence of X1 in both the *E*- and *Z*-conformation at the C_6 and C_7 double bond. The presence of both an *E* and a *Z* double bond conformation could a result from chemical modifications due to the presence of formic acid in the extraction process. The carbon shifts are in good agreement with published data [20]

Isolation of methyl (2E,6E)-10-hydroxy-11-formyl-3,7,11-trimethyl-2,6-dodecadienoate (X2).

X2 was present in the 60:40 DCM:EtOAc fraction (13.1 mg) of the Diol fractionation as described above and was purified on a Waters HPLC W600/996PDA (Milford, MA, USA) using a RP column (Phenomenex Luna C18(2), 250 x 10 mm, 5 µm, Torrance, CA, USA) using a gradient of 40% MeCN (H_2O – Milli-Q (Millipore, MA, USA)) to 100% over 20 min. with 50 ppm TFA and a flow of 4 mL/min. The collections were concentrated on a rotarvap (Büchi V-855/R-215) and dried down under N_2(g) to yield 2.6 mg of X2.

Isolation of methyl (2E,6E)-10,11-epoxid-3,7,11-trimethyl-2,6-dodecadienoate (JH III). JH-III was present in the 46:60 DCM:EtOAc fraction (26.2 mg) of the Diol fractionation as described for X1 and was purified on a Waters HPLC W600/996PDA (Milford, MA, USA) using a RP column (Phenomenex Luna C18(2), 250 x 10 mm, 5 µm, Torrance, CA, USA) using a gradient of 55% MeCN (H_2O – Milli-Q (Millipore, MA, USA)) to 65% over 20 min. with 50 ppm TFA and a flow of 4 mL/min. The collections were concentrated on a rotarvap (Büchi V-855/R-215) and dried down under N_2(g) to yield 1.4 mg of JH-III.

NMR studies and structure elucidation: NMR spectra were acquired in DMSO-d_6 on a Varian Unity Inova 500 MHz spectrometer for X1 and JH-III and on a Bruker Avance 800 MHz spectrometer at the Danish Instrument Center for NMR Spectroscopy of Biological Macromolecules for X2 using standard pulse sequences. The spectra were referenced to this solvent with resonances δ_H = 2.49 and δ_C = 39.5.

Characterization data of methyl (2E,6E)-10,11-dihydroxy-3,7,11-trimethyl-2,6-dodecadienoate (X1). NMR data for X1a: ^{1}H NMR (500 MHz, DMSO-*d_6*): δ 5.65 (s, 1 H), 5.07 (m, 1 H), 4.25 (d, J = 5.6 Hz, 1 H), 4.01 (s, 1 H), 3.57 (s, 3 H), 3.02 (ddd, J = 10.0, 5.6, 2.5 Hz, 1 H), 2.15 (m, 2 H), 2.15-2.11 (m, 2 H), 2.09 (s, 3 H), 1.87 (m, 2 H), 1.60 (m, 1 H), 1.56 (s, 3 H), 1.15 (m, 1 H), 1.02 (s, 3 H), 0.97 (s, 3 H); ^{13}C NMR (125 MHz): δ 166.1, 159.7, 135.9, 122.2, 114.7, 76.6, 71.5, 50.4, 39.7, 36.2, 29.4, 26.1, 25.1, 24.2, 18.2, 15.7. NMR data for X1b: ^{1}H NMR (500 MHz, DMSO-*d_6*): δ 5.65 (s, 1 H), 5.08 (m, 1 H), 3.74 (dd, J = 10.0, 3.0 Hz, 1 H), 3.57 (s, 3 H), 2.15 (m, 2 H), 2.15-2.11 (m, 2 H), 2.10 (m, 1 H), 2.09 (s, 3 H), 1.96 (m, 1 H), 1.57 (s, 3 H), 1.48 (m, 1 H), 1.41 (m, 1 H), 1.21 (s, 3 H), 1.08 (s, 3 H); ^{13}C NMR (125 MHz): 166.1, 159.7, 134.9, 123.0, 114.7, 82.6, 79.4, 50.4, 39.7, 35.7, 29.2, 27.7, 25.1, 22.8, 18.2, 15.6. HRMS (*m/z)*: $[M+H]^+$ calcd. For $C_{16}H_{29}O_4$, 285.2060; found, 285.2025; $[M+Na]^+$ calcd. For $C_{16}H_{28}O_4Na$, 307.1885; found, 307.1887; $[\alpha]_D$ = 0.0 (MeOH).

Characterization data of methyl (2E,6E)-10-hydroxy-11-formyl-3,7,11-trimethyl-2,6-dodecadienoate (X2).

^{1}H NMR (800 MHz, DMSO-d_6): δ 8.23 (s, 1 H), 5.65 (q, J = 1.0 Hz, 1H), 5.05 (t, J = 6.9, 1 H), 4.62 (s, 1 H), 4.52 (d, J = 10.2 Hz, 1 H), 3.57 (s, 3 H), 2.15 (m, 2 H), 2.11 (m, 2 H), 2.09 (d, J = 1 Hz, 3 H), 1.93 (m, 1 H), 1.84 (m, 1 H), 1.75 (m, 1 H), 1.55 (s, 3 H), 1.46 (m, 1 H), 1.04 (s, 3 H), 1.03 (s, 3 H); ^{13}C NMR (200 MHz): δ 166.2, 162.3, 159.9, 134.6, 123.4, 114.7, 79.7, 70.2, 50.4, 39.6, 35.7, 26.9, 25.2, 25.1, 25.1, 18.3, 15.6; HRMS (*m/z)*: $[M+H]^+$ calcd. for $C_{17}H_{29}O_5$, 313.2010; found, 313.2010. $[M+Na]^+$ calcd. for $C_{17}H_{28}O_5Na$, 335.1828; found, 335.1831.

Characterization data of methyl (2E,6E)-10,11-epoxid-3,7,11-trimethyl-2,6-dodecadienoate (JH III). ^{1}H NMR data of purified compound in DMSO-d_6 showed that the compound had degraded. HRMS (*m/z)*: $[M+H]^+$ calcd. for $C_{16}H_{27}O_3$, 267.1955; found, 267.1957.; $[M+Na]^+$ calcd. For $C_{16}H_{26}O_3Na$, 289.1780; found,289.1774.

Characterization data of methyl (2, 6, 10) -3,7,11-trimethyl-2,6-dodecadienoate (MF).

HRMS (*m/z)*: $[M+H]^+$ calcd. for $C_{16}H_{27}O_2$, 251.2006; found, 251.2007.

Authentic standard of JH-III was purchased from Sigma Aldrich (J2000-10MG)

Results and discussion

Selection of candidate pathway specific regulators was based on genomic co-localization of gene clusters. We utilized a collection of microarray experiments from *A. niger* grown under diverse conditions to identify regulatory genes associated with predicted secondary metabolite gene clusters using a local co-expression algorithm. Seven candidate genes associated with predicted gene clusters containing either polyketide synthases or non-ribosomal peptide synthases, were identified (supplementary table 1). All seven putative

transcription factors belonged to the binuclear zinc finger class, a class often associated with secondary metabolism in fungi [21]. BLAST analysis using the predicted protein sequences against the annotated *A. nidulans* genome (Aspergillus Comparative Database, BROAD Institute) revealed that only one candidate (fge1_pg_C_4000037) had a potential ortholog (ANID_06396, 62% amino acid identity, supplementary table 1). All seven putative regulators were expressed individually in *A. nidulans* under control of the strong constitutive *pgpdA*-promoter from the defined loci Integration Site-1 [9]. The resulting mutant strains were grown on minimal glucose media as well as four complex media representing diverse physiological conditions. Metabolites profiles were analyzed with LC-HRMS as well as UHPLC-DAD and compared to a reference strain constitutively expressing the *Escherichia coli* β-galactosidase from the same locus. Of all combinations of candidate genes and growth media, only *est_fge1_pg_C_150220* (annotation from *Aspergillus Comparative Database, BROAD institute)* grown under high salt conditions had a significant impact on secondary metabolism resulting in increased accumulation of several metabolites not previously reported to be produced by *A. nidulans* (figure 1A). Hence we renamed est_fge1_pg_C_150220 Secondary Metabolism associated Regulatory protein A (SmrA). Two of the induced metabolites, X1 and X2 had similar UV spectra indicating a biosynthetic relationship. The two compounds were isolated and identified by NMR analysis as a methyl (2E,6E)-10,11-epoxid-3,7,11-trimethyl-2,6-dodecadienoate (X1) [20] and its formylated analogue (X2) (figure 1B). The formylation, however, was subsequently demonstrated to occur during the extraction procedure thus X2 is a derivative of X1. The NMR data of X1 indicated that two diastereomers were present in the sample. The ^{1}H- and ^{13}C-chemical shifts differ most in the reduced end of X1 where a stereocenter (C_{10}) is present. The chemical shifts of H_1/C_1 to H_5/C_5 are identical. The difference of chemical shifts of the two methyl groups (H_{12}/C_{12} and H_{13}/C_{13}) and the two CH_2 groups next to the stereocenter are due to the presence of the chiral center. The two diastereomers present in the X1 solution must be due to the presence of X1 in both the *E*- and *Z*-conformation at the C_6 and C_7 double bond. The presence of both an *E* and a *Z* double bond conformation could a result from chemical modifications due to the presence of formic acid in the extraction process. The sesquiterpene X1 closely resemble the Insect Juvenile Hormone

(JH-III), a well-established hormone thought to be unique for insects with essential developmental roles and hence an important target of insecticides [12, 13]. The finding of X1 prompted us to search for related induced metabolites. The accurate mass of JH-III and the related crustacean hormone methyl-farnesoate (MF) [11] were used as input for targeted LC-HRMS analysis. Indeed, both searches revealed the presence of a single induced metabolite with accurate mass practically identical to the predicted mass of JH-III and MF, respectively (JH-III HRMS (*m/z)*: $[M+H]^+$ calculated. 267.1955; found, 267.1957, MF HRMS (*m/z)*: $[M+H]^+$ calculated 251.2006; found, 251.2007 supplementary figure 1). Identification of these metabolites as JH-III and MF (figure 1B) was established by comparison of retention time and mass spectra with an authentic standard (supplementary figure 1) or the metabolite database of the Xcalibur software package (Thermo Scientific), respectively. The strongest metabolite induction was observed when *A. nidulans* was grown under high salt conditions, however, close inspection of the LC-HRMS data of the remaining media revealed the presence of JH-III as well as increased levels of X1 in the *SmrA* expressing strain on rich yeast extract based media (supplementary figure 2). In order to establish whether the newly discovered terpenes were retained intracellularly or released to the environment we analyzed the composition of collected volatiles as well as the growth media. In the volatile fraction, MF constituted a major metabolite in the *SmrA* expressing strain as well as the reference (supplementary figure 3), whereas JH-III and X1 undetectable. None of the three terpenes were detectable in the growth media. The discovery of JH-III and MF represent to our knowledge the first report of production of juvenile hormones in fungi. It is tempting to speculate that accumulation of JH-III and release of MF may serve as a defense strategy against insect competitors or predators. Fungal secondary metabolites are known to play an important role in fungal/insect interactions [22, 23] and JHs constitute attractive targets due to their critical role in insect development and the fact that both absence and overexposure are detrimental [12]. Previous examples of both JH biosynthesis inhibition and overexposure as defense strategies are known as *Penicillium brevicompactum* synthesize the JH biosynthesis inhibitor brevioxime [24], whereas the plant *Cyperus iria* synthesize JH-III and MF [25]. As *A. nidulans* is generally believed to inhabit a great variety of ecological niches, among those dead plant

materials, it is most likely that competing or predating insects will be part of the natural environment. However, it cannot be excluded that X1, JH-III and/or MF could also serve hormonal functions in *A. nidulans.* A similar dual purpose has been demonstrated for the JH-III precursor farnesol [26] in *C. albicans,* as it regulate the transition from yeast to filamentous growth [27] as well as induce apoptosis in competing fungal species [28]. Clarification of the distribution of JHs in fungi and their biological function in *A. nidulans* will improve our understanding of fungal/insect interactions and perchance fungal morphology regulation. Moreover, the finding that heterologous expression of transcription factors may influence secondary metabolism is of general relevance for characterization of secondary metabolites. As the genomes of a large number of fungal species are currently being sequenced (www.genomesonline.org) a similar approach may be undertaken for these species using well-characterized regulatory proteins to induce previously uncharacterized metabolites.

Achknowledgements:

This work was supported by the Danish Research Agency for Technology and Production, grant # 09-064967. The authors would like to acknowledge the Danish Instrument Center for NMR Spectroscopy of Biological Macromolecules for the use of NMR facilities, Malene Møller Jensen, Susanne Hannibal, Hanne Jakobsen and Jesper Mogensen for technical assistance, and the Research School for Biotechnology at the faculty of Life Sciences, University of Copenhagen for funding.

Competing interests

The authors declare no competing interests.

Reference List

1. Newman,D.J. & Cragg,G.M. Natural products as sources of new drugs over the last 25 years. *Journal of Natural Products* **70**, 461-477 (2007).

2. Galagan,J.E. *et al.* Sequencing of Aspergillus nidulans and comparative analysis with A-fumigatus and A-oryzae. *Nature* **438**, 1105-1115 (2005).

3. Pel,H.J. *et al.* Genome sequencing and analysis of the versatile cell factory Aspergillus niger CBS 513.88. *Nat Biotech* **25**, 221-231 (2007).

4. Gross,H. Strategies to unravel the function of orphan biosynthesis pathways: recent examples and future prospects. *Applied Microbiology and Biotechnology* **75**, 267-277 (2007).

5. Brakhage,A.A. & Schroeckh,V. Fungal secondary metabolites - Strategies to activate silent gene clusters. *Fungal Genetics and Biology* **48**, 15-22 (2011).

6. Chiang,Y.M., Chang,S.L., Oakley,B.R., & Wang,C.C.C. Recent advances in awakening silent biosynthetic gene clusters and linking orphan clusters to natural products in microorganisms. *Current Opinion in Chemical Biology* **15**, 137-143 (2011).

7. Bok,J.W. *et al.* Chromatin-level regulation of biosynthetic gene clusters. *Nature Chemical Biology* **5**, 462-464 (2009).

8. Bergmann,S. *et al.* Activation of a Silent Fungal Polyketide Biosynthesis Pathway through Regulatory Cross Talk with a Cryptic Nonribosomal Peptide Synthetase Gene Cluster. *Applied and Environmental Microbiology* **76**, 8143-8149 (2010).

9. Hansen,B.G. *et al.* Versatile Enzyme Expression and Characterization System for Aspergillus nidulans, with the Penicillium brevicompactum Polyketide Synthase Gene from the Mycophenolic Acid Gene Cluster as a Test Case. *Applied and Environmental Microbiology* **77**, 3044-3051 (2011).

10. Nielsen,M.L. *et al.* A genome-wide polyketide synthase deletion library uncovers novel genetic links to polyketides and meroterpenoids in Aspergillus nidulans. *Fems Microbiology Letters* **321**, 157-166 (2011).

11. Nagaraju,G.P.C. Is methyl farnesoate a crustacean hormone? *Aquaculture* **272**, 39-54 (2007).

12. Wilson,T.G. The molecular site of action of juvenile hormone and juvenile hormone insecticides during metamorphosis: how these compounds kill insects. *Journal of Insect Physiology* **50**, 111-121 (2004).

13. Gilbert,L.I., Granger,N.A., & Roe,R.M. The juvenile hormones: historical facts and speculations on future research directions. *Insect Biochemistry and Molecular Biology* **30**, 617-644 (2000).

14. Nielsen,M.L., Albertsen,L., Lettier,G., Nielsen,J.B., & Mortensen,U.H. Efficient PCR-based gene targeting with a recyclable marker for Aspergillus nidulans. *Fungal Genetics and Biology* **43**, 54-64 (2006).

15. Frisvad,J.C. & Samson,R.A. Polyphasic taxonomy of *Penicillium* subgenus *Penicillium*. A guide to identification of food and air-borne terverticillate *Penicilia* and their mycotoxons. *Studies in Mycology* **49**, 1-173 (2004).

16. Norholm,M.H.H. A mutant Pfu DNA polymerase designed for advanced uracil-excision DNA engineering. *Bmc Biotechnology* **10**, 10.1186/1472-6750-10-21 (2010).

297 17. Smedsgaard,J. Micro-scale extraction procedure for standardized screening of fungal
298 metabolite production in cultures. *Journal of Chromatography A* **760**, 264-270 (1997).

299 18. Laatsch,H. *AntiBase 2009. The natural compound identifier*(Wiley-VCH GmpH & Co,
300 Weinheim, Germany.,2009).

301 19. Larsen,T.O. & Frisvad,J.C. A Simple Method for Collection of Volatile Metabolites from Fungi
302 Based on Diffusive Sampling from Petri Dishes. *Journal of Microbiological Methods* **19**, 297-305
303 (1994).

304 20. Kuhnz,W. & Rembold,H. C-13 Nuclear Magnetic-Resonance Spectra of Juvenile Hormone-Iii,
305 Some of Its Derivatives, and of Analogous Compounds. *Organic Magnetic Resonance* **16**, 138-140
306 (1981).

307 21. MacPherson,S., Larochelle,M., & Turcotte,B. A fungal family of transcriptional regulators: The
308 zinc cluster proteins. *Microbiology and Molecular Biology Reviews* **70**, 583-604 (2006).

309 22. Kempken,F. & Rohlfs,M. Fungal secondary metabolite biosynthesis - a chemical defence
310 strategy against antagonistic animals? *Fungal Ecology* **3**, 107-114 (2010).

311 23. Rohlfs,M. & Churchill,A.C.L. Fungal secondary metabolites as modulators of interactions with
312 insects and other arthropods. *Fungal Genetics and Biology* **48**, 23-34 (2011).

313 24. Moya,P. *et al.* Brevioxime: A new juvenile hormone biosynthesis inhibitor isolated from
314 Penicillium brevicompactum. *Journal of Organic Chemistry* **62**, 8544-8545 (1997).

315 25. Toong,Y.C., Schooley,D.A., & Baker,F.C. Isolation of Insect Juvenile Hormone-Iii from A Plant.
316 *Nature* **333**, 170-171 (1988).

26. Cao,L., Zhang,P., & Grant,D.F. An insect farnesyl phosphatase homologous to the N-terminal domain of soluble epoxide hydrolase. *Biochemical and Biophysical Research Communications* **380**, 188-192 (2009).

27. Hornby,J.M. *et al.* Quorum sensing in the dimorphic fungus Candida albicans is mediated by farnesol. *Applied and Environmental Microbiology* **67**, 2982-2992 (2001).

28. Dinamarco,T.M., Goldman,M.H.S., & Goldman,G.H. Farnesol-induced cell death in the filamentous fungus Aspergillus nidulans. *Biochemical Society Transactions* **39**, 1544-1548 (2011).

Figure legends:

Figure 1: Induction of metabolites by SmrA

Top panel: UHPLC-QTOFMS extracted ion chromatogram of m/z 251 (MF, $[M+H]^+$), 289 (JH-III, $[M+Na]^+$), 307 (X1, $[M+H]^+$) and 335 (X2, $[M+H]^+$) recorded in positive mode of extracts from the strain constitutively expressing *SmrA* (top) and reference (bottom) grown under high salt conditions. Chromatograms are normalized by intensity. Bottom panel: Structures of X1+2, JH-III and MF.

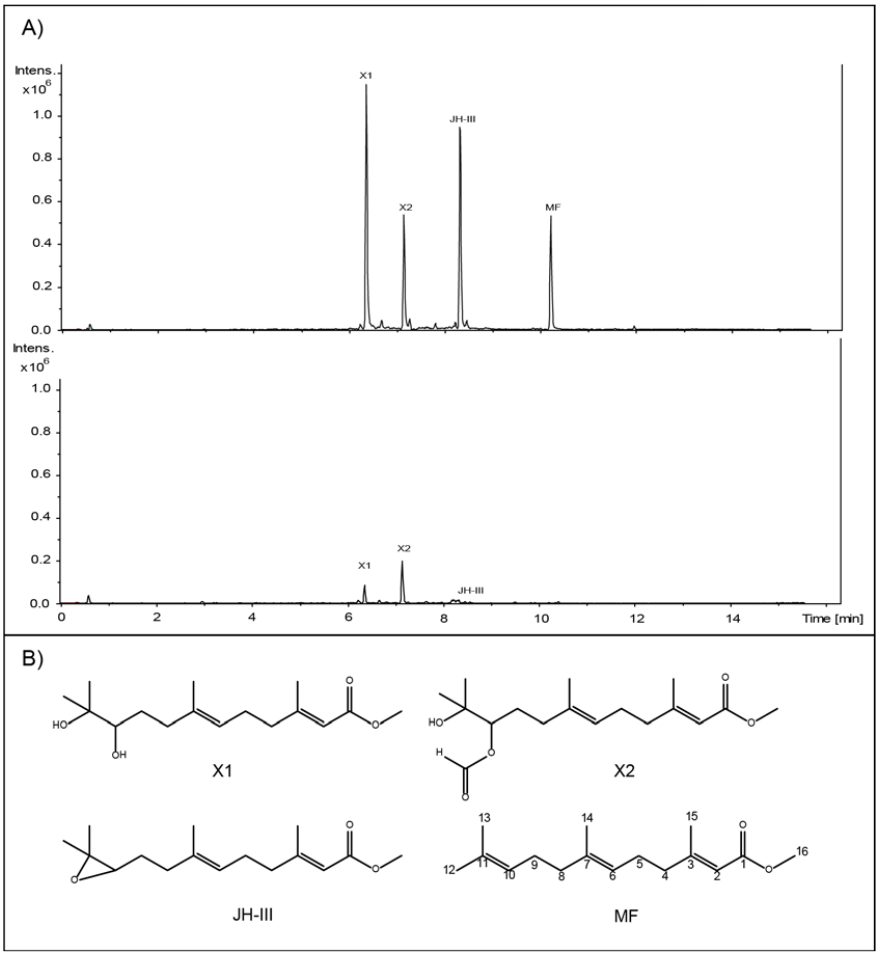

Title

A regulatory protein from *Aspergillus niger* induces juvenile hormones upon heterologous expression in *A. nidulans*.

Authors

Nielsen, M.T.[1,2,3], Klejnstrup, M.L.[1,2], Gotfredsen, C.H.[4], Andersen, M.R.[1], Hansen, B.G.[1,5], Mortensen, U.H.[1] and Larsen, T. O.[1*]

Affiliation

[1] Center for Microbial Biotechnology, Department of Systems Biology, Technical University of Denmark, 2800 Kgs Lyngby, Denmark.

[2] These authors contributed equally to the work.

[3] Current address: Novo Nordisk Foundation Center for Biosustainability, Technical University of Denmark, Fremtidsvej 3, 2970 Hoersholm, Denmark.

[4] Department of Chemistry, Technical University of Denmark, 2800 Kgs Lyngby, Denmark.

[5] Current address: Novozymes A/S, Krogshoejvej 36, 2880 Bagsvaerd, Denmark.

* Author to whom correspondence should be addressed (tol@bio.dtu.dk)

Supplementary figure legends:

Supplementary figure 1 Targeted LC-MS analysis of induced metabolites.

Extracted ion chromatogram traces of the accurate mass and corresponding mass spectra of X1, X2, JH-III and MF in the mutant strain constitutively expressing *SmrA* as well as the authentic JH-III standard(65% pure) purchased from Sigma Aldrich. Note that the standard contains several impurities.

Supplementary figure 2 Detection of induced metabolites on Yeast based media

Extracted ion chromatogram of X1 or JH-III of SmrA (top) and refenrece (bottom) grown on YES media. MS spectra of the 8.3 area are embedded. Characteristic ions from JH-III are m/z $[M+H]^+$ 267.1957 & $[M+Na]^+$ 289.1774 Da.

Supplementary figure 3 Excretion of MF by A. nidulans.

(top) Total MS chromatogram of the collected volatiles from the SmrA expressing strain and the reference. (bottom) mass spectrum of the compound eluting at 26.19 minutes. The compound was identified as MF by comparison to the metabolite library of the Xcalibur software package (Thermo Scientific).

Supplementary table 1: Candidate genes from A. niger.

Referred name	Strain #	Broad annotation	Transcript ID	Nidulans enzymes	Identity percentage
Candidate #1	**NID357**	**fge1_pg_C_4000037**	**38716**	ANID_06396, ANID_03269	62%, 27%
Candidate #2	**NID358**	**e_gw1_4.316**	**178503**	ANID_07346	26%
Candidate #3	**NID360**	**e_gw1_11.945**	**188323**	ANID_08894	25%
Candidate #4	**NID366**	**gw1_10.247**	**123782**	None	-
Candidate #5	**NID367**	**fge1_pg_C_19000192**	**45823**	ANID_11683, ANID_07921	43%, 22%
Candidate #6	**NID476**	**e_gw1_8.296**	**184613**	ANID_04485	30%
SmrA	**NID477**	**est_fge1_pg_C_150220**	**54836**	None	-

Supplementary table 2: Name and description of fungal strains used in this work

Strain #	Genotype	Description	Reference
NID74	*argBΔ, pyrG89, veA1, nkuAΔ*	Parental strain with permanent deletion of *nkuA* to facilitate gene targeting	This study
NID545	*argBΔ, pyrG89, veA1, nkuAΔ IS1::pgpdA-LacZ-TtrpC::argB*	Reference strain with E.coli LacZ integrated in IS1.	This study
NID357	*argBΔ, pyrG89, veA1, nkuAΔ, IS1:pgpdA:fge1_pg_C_4000037::argB*	Constitutive expression of putative binuclear zinc finger transcrption factor fge1_pg_C_4000037 integrated in IS1	This study
NID358	*argBΔ, pyrG89, veA1, nkuAΔ, IS1:pgpdA:e_gw1_4.316::argB*	Constitutive expression of putative binuclear zinc finger transcrption factor e_gw1_4.316 integrated in IS1	This study
NID360	*argBΔ, pyrG89, veA1, nkuAΔ, IS1:pgpdA::e_gw1_11.945::argB*	Constitutive expression of putative binuclear zinc finger transcrption factor e_gw1_11.945 integrated in IS1	This study
NID366	*argBΔ, pyrG89, veA1, nkuAΔ, IS1:pgpdA:gw1_10.247::argB*	Constitutive expression of putative binuclear zinc finger transcrption factor gw1_10.247 integrated in IS1	This study
NID367	*argBΔ, pyrG89, veA1, nkuAΔ, IS1:pgpdA:fge1_pg_C_19000192::argB*	Constitutive expression of putative binuclear zinc finger transcrption factor fge1_pg_C_19000192 integrated in	This study
NID476	*argBΔ, pyrG89, veA1, nkuAΔ, IS1:pgpdA::e_gw1_8.296::argB*	Constitutive expression of putative binuclear zinc finger transcrption factor e_gw1_8.296 integrated in IS1	This study
NID477	*argBΔ, pyrG89, veA1, nkuAΔ, IS1:pgpdA::SmrA::argB*	Constitutive expression of *SmrA (est_fge1_pg_C_150220)* integrated in IS1	This study

Supplementary table 3: PCR primers used in this study

Upper case letters indicate annealing nucleotides, lower case indicate tails for user cloning

PCR product	Primer pair (fw/rv)	Forward primer	Reverse Primer	Description
1	JBN2QQ/3QQ	GCCAAGTGGTGGAATGCG	gatcccgggaattgccatgCAACACTATCGC ATACTCTCC	Amplifies 2kb upstream region from AN-ArgB (AN_04409) for fusion PCR
2	JBN4QQ/5QQ	aattccagctgaccaccatgCCGATCACGTAAAAGCCTGTTA G	CAGGGCGTGGGAGATAGC	Amplifies 2kb downstream region from AN-ArgB (AN_04409) for fusion PCR
3	JBN5A/JBN2K	catggcaattcccggggatcTGGATAACCGTATTACCGCC	GGAAGAGAGGTTCACACC	Amplifies 5' AFpyrG sequence including 300bp direct repeat and native promoter for fusion PCR
4	JBN4Q/2B	TGATACAGGTCTCGGTCCC	catggtggtcagctggaattTGCCAAGCTTAAC GCGTACC	Amplifies 3' AFpyrG sequence including 300bp direct repeat and native terminator for fusion PCR
5	JBN2QQ/2K	GCCAAGTGGTGGAATGCG	GGAAGAGAGGTTCACACC	Amplifies AN-ArgB (AN_04409)::AFpyrG upstream gene targeting fragment
6	JBN4Q/5QQ	TGATACAGGTCTCGGTCCC	CAGGGCGTGGGAGATAGC	Amplifies AN-ArgB (AN_04409)::AFpyrG downstream gene targeting fragment
7	Motni165/185	cgtgcgauGCAGTGAGAGCGATCGCAGACACTGCATG ACCATGATTACGGATTC	cacgcgauTTATTTTTGACACCAGACCA	Amplifies the E. coli lacZ ORF for cloning into an AsiSI/Nb.BsmI casette. SP introduces an upstream AsiSi/Nb.BtsI casette
8	Motni355/354	agagcgauTAAGCTCCCTAATTGGCCC	tctgcgauGCGGTAGTGATGTCTGCTCA	Amplifies 0,5kb pgpdA promoter for cloning into an AsiSI/Nb.BtsI
9	287/288	agagcgauATGTTCGTCGCTCCGACGCTT	tctgcgauTCAGAATAAATTGCTTGGAAC	Amplifies the putative ORF of A.niger gene fge1_pg_C_4000037 (Broad Comparative Aspergillus Database annotation)/Transcription ID:38716 (Aspergillus niger v3.0 annotation)
10	289/290	agagcgauATGCGCCATCGACTCACAAA	tctgcgauTTAATAGAGAGCCCATCGC	Amplifies the putative ORF of A.niger gene e_gw1_4.316 (Broad Comparative Aspergillus Database annotation)/Transcription ID:178503 (Aspergillus niger v3.0 annotation)
11	297/298	agagcgauATGAGATCCTCCCAGTCCAA	tctgcgauTCAGCATCCATGCACATGAG	Amplifies the putative ORF of A.niger gene e_gw1_8.296 (Broad Comparative Aspergillus Database annotation)/Transcription ID:184613 (Aspergillus niger v3.0 annotation)
12	299/300	agagcgauATGAGTCCCGTGTCTGGCCA	tctgcgauTTACATATTCCATGCAAACGA	Amplifies the putative ORF of A.niger gene e_gw1_11.945 (Broad Comparative Aspergillus Database annotation)/Transcription ID:188323 (Aspergillus niger v3.0 annotation)
13	303/304	agagcgauATGGTCTACTGCGGTCGCC	tctgcgauCTATCCACTTAATGGTGGAC	Amplifies the putative ORF of A.niger gene est_fge1_pg_C_150220 (Broad Comparative Aspergillus Database annotation)/Transcription ID:54836 (Aspergillus niger v3.0 annotation)
14	305/306	agagcgauATGAACAGTGAACGAAAGCT	tctgcgauCTATGGATTGGCCATAACCT	Amplifies the putative ORF of A.niger gene gw1_10.247(Broad Comparative Aspergillus Database annotation)/Transcription ID:123782 (Aspergillus niger v3.0 annotation)
15	307/308	agagcgauATGGATTTGAAACAGAAAGTG	tctgcgauCTATCCTTCGAGAACCTCTT	Amplifies the putative ORF of A.niger gene fge1_pg_C_19000192 (Broad Comparative Aspergillus Database annotation)/Transcription ID:45823 (Aspergillus niger v3.0 annotation)
16	BGHA163/ BGHA502	GGTCTACTCCCCTGCGTCTA	AGGGAGGCCTTGTCGGTCTT	Check primers for integration in IS-1. Amplifies the junction between A. nidulans chromosome 1 and the pgpdA promoter
17	BGHA98/ BGHA162	GGTTTCGTTGTCAATAAGGGAA	GTTCAGGGTGACGGTGAGAG	Check primers for integration in IS-1. Amplifies the junction between A. nidulans chromosome 1 and the ArgB marker gene

Supplementary figure 1:

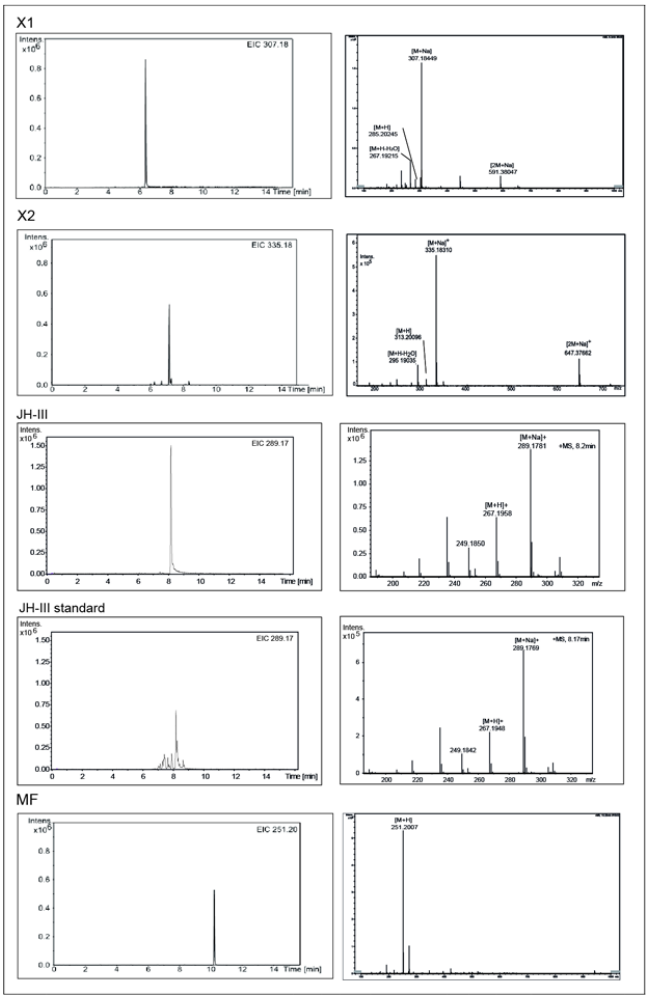

Supplementary figure 2:

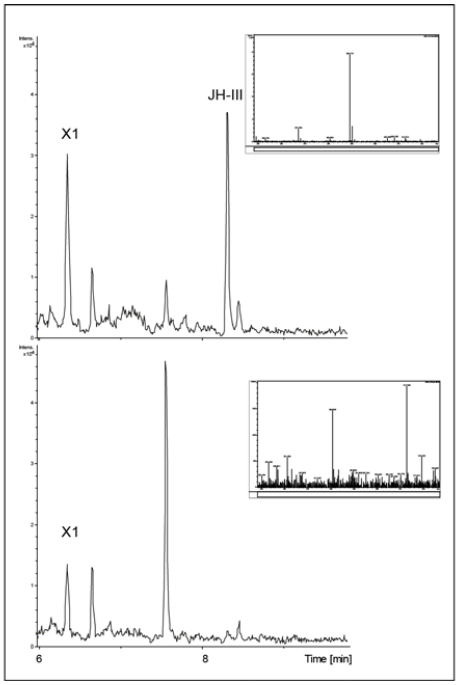

Supplementary figure 3:

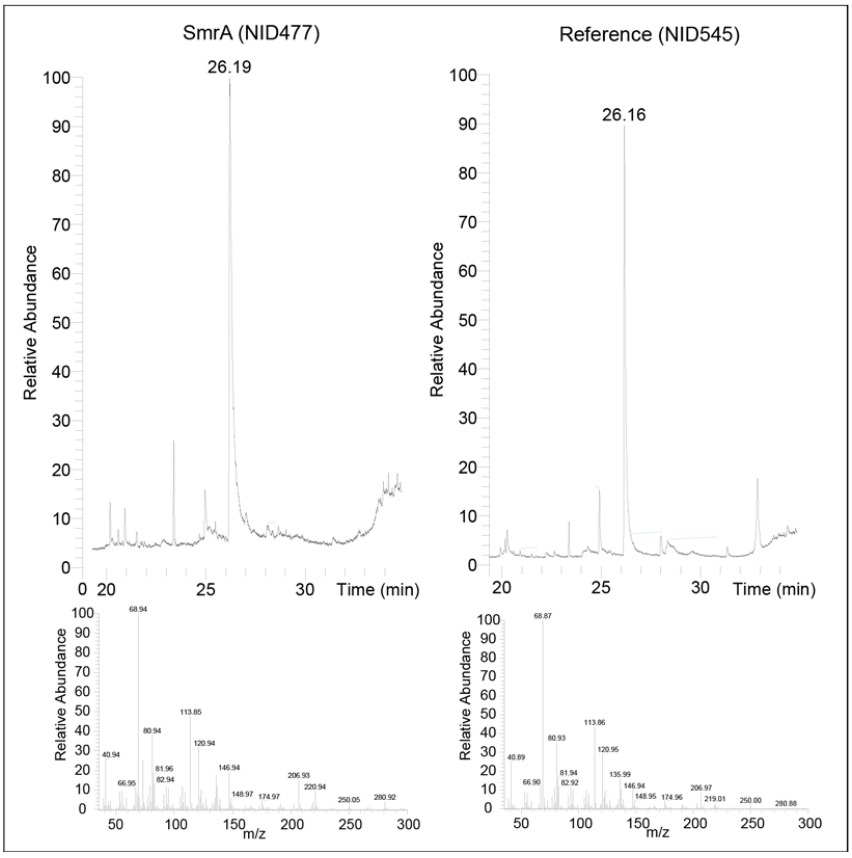
SmrA (NID477)
26.19
Relative Abundance
Time (min)
68.94
40.94
66.95
80.94
81.96
82.94
113.85
120.94
146.94
148.97
174.97
206.93
220.94
250.05
280.92
m/z
Reference (NID545)
26.16
Relative Abundance
Time (min)
68.87
40.89
66.90
80.93
81.94
82.92
113.86
120.95
135.99
146.94
148.95
174.96
206.97
219.01
250.00
280.88
m/z

CMB is an Engineering Center of Excellence funded by the Danish Research Agency. It is a collaboration between an acknowledged research manager, his/her institute and university, and the Research Agency. An Engineering Center of Excellence is a research institute of first-class quality with tradition for cooperation with industry.

Center for Microbial Biotechnology
Department of Systems Biology
Technical University of Denmark
Building 223
DK-2800 Kgs. Lyngby
Denmark

Phone: +45 4525 2525
Fax: +45 4588 4148

www.cmb.dtu.dk

ISBN-nr: 978-87-91494-17-8